frontiers | Research Topics

Surviving and thriving: how crops perceive and respond to temperature stress

Edited by
Zemin Wang, Yi Wang and Darren Wong

Published in
Frontiers in Plant Science

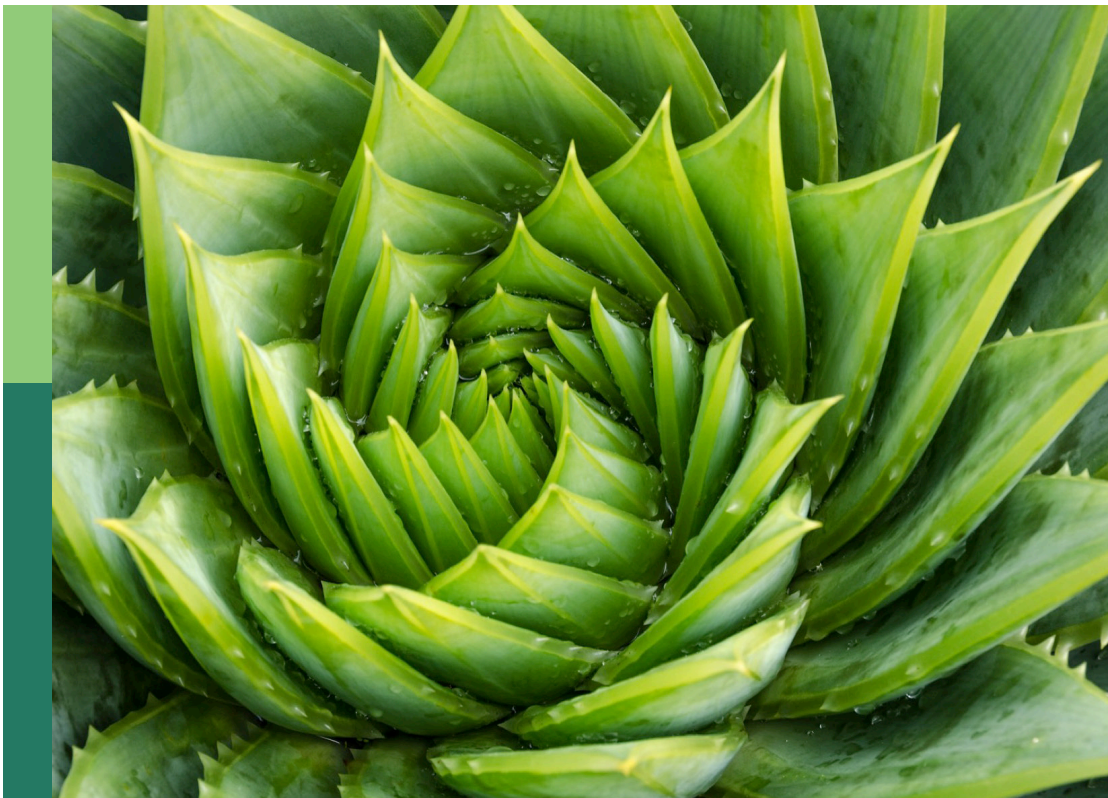

ISSN 1664-8714
ISBN 978-2-8325-5943-7
DOI 10.3389/978-2-8325-5943-7

About Frontiers

Frontiers is more than just an open access publisher of scholarly articles: it is a pioneering approach to the world of academia, radically improving the way scholarly research is managed. The grand vision of Frontiers is a world where all people have an equal opportunity to seek, share and generate knowledge. Frontiers provides immediate and permanent online open access to all its publications, but this alone is not enough to realize our grand goals.

Frontiers journal series

The Frontiers journal series is a multi-tier and interdisciplinary set of open-access, online journals, promising a paradigm shift from the current review, selection and dissemination processes in academic publishing. All Frontiers journals are driven by researchers for researchers; therefore, they constitute a service to the scholarly community. At the same time, the *Frontiers journal series* operates on a revolutionary invention, the tiered publishing system, initially addressing specific communities of scholars, and gradually climbing up to broader public understanding, thus serving the interests of the lay society, too.

Dedication to quality

Each Frontiers article is a landmark of the highest quality, thanks to genuinely collaborative interactions between authors and review editors, who include some of the world's best academicians. Research must be certified by peers before entering a stream of knowledge that may eventually reach the public - and shape society; therefore, Frontiers only applies the most rigorous and unbiased reviews. Frontiers revolutionizes research publishing by freely delivering the most outstanding research, evaluated with no bias from both the academic and social point of view. By applying the most advanced information technologies, Frontiers is catapulting scholarly publishing into a new generation.

What are Frontiers Research Topics?

Frontiers Research Topics are very popular trademarks of the *Frontiers journals series*: they are collections of at least ten articles, all centered on a particular subject. With their unique mix of varied contributions from Original Research to Review Articles, Frontiers Research Topics unify the most influential researchers, the latest key findings and historical advances in a hot research area.

Find out more on how to host your own Frontiers Research Topic or contribute to one as an author by contacting the Frontiers editorial office: frontiersin.org/about/contact

Surviving and thriving: how crops perceive and respond to temperature stress

Topic editors

Zemin Wang — Gansu Agricultural University, China

Yi Wang — Beijing Botanical Garden, Institute of Botany, Chinese Academy of Sciences (CAS), China

Darren Wong — Australian National University, Australia

Citation

Wang, Z., Wang, Y., Wong, D., eds. (2025). *Surviving and thriving: how crops perceive and respond to temperature stress*. Lausanne: Frontiers Media SA. doi: 10.3389/978-2-8325-5943-7

Table of contents

05 Editorial: Surviving and thriving: how crops perceive and respond to temperature stress
Zemin Wang, Yi Wang and Darren Chern Jan Wong

09 Transcriptomic profiling of wheat stem during meiosis in response to freezing stress
Danyu Yao, Juan Wang, Wentao Peng, Bowen Zhang, Xiaolan Wen, Xiaoneng Wan, Xiuyuan Wang, Xinchun Li, Jian Ma, Xiaofen Liu, Yinglun Fan and Guozhong Sun

25 *StMAPK1* functions as a thermos-tolerant gene in regulating heat stress tolerance in potato (*Solanum tuberosum*)
Xi Zhu, Huimin Duan, Guodong Zhang, Hui Jin, Chao Xu, Shu Chen, Chuanmeng Zhou, Zhuo Chen, Jinghua Tang and Yu Zhang

36 Heat responsive gene *StGATA2* functions in plant growth, photosynthesis and antioxidant defense under heat stress conditions
Xi Zhu, Huimin Duan, Hui Jin, Shu Chen, Zhuo Chen, Shunwei Shao, Jinghua Tang and Yu Zhang

51 Genome-wide analysis of the TIFY family and function of *CaTIFY7* and *CaTIFY10b* under cold stress in pepper (*Capsicum annuum* L.)
Xiaodi Wang, Ning Li, Tianxiang Zan, Kai Xu, Shenghua Gao, Yanxu Yin, Minghua Yao and Fei Wang

66 Heat stress during male meiosis impairs cytoskeletal organization, spindle assembly and tapetum degeneration in wheat
Attila Fábián, Barbara Krárné Péntek, Vilmos Soós and László Sági

87 Optimization of soybean physiochemical, agronomic, and genetic responses under varying regimes of day and night temperatures
Chuanbo Ding, Fahad Alghabari, Muhammad Rauf, Ting Zhao, Muhammad Matloob Javed, Rahma Alshamrani, Abdel-Halim Ghazy, Abdullah A. Al-Doss, Taimoor Khalid, Seung Hwan Yang and Zahid Hussain Shah

101 *GhBRX.1*, *GhBRX.2*, and *GhBRX4.3* improve resistance to salt and cold stress in upland cotton
Wei Wei, Jisheng Ju, Xueli Zhang, Pingjie Ling, Jin Luo, Ying Li, Wenjuan Xu, Junji Su, Xianliang Zhang and Caixiang Wang

116 *StMAPKK5* responds to heat stress by regulating potato growth, photosynthesis, and antioxidant defenses
Xi Zhu, Wei Li, Ning Zhang, Hui Jin, Huimin Duan, Zhuo Chen, Shu Chen, Qihua Wang, Jinghua Tang, Jiannan Zhou, Yu Zhang and Huaijun Si

130 Genome-wide characterization of the GRF transcription factors in potato (*Solanum tuberosum* L.) and expression analysis of *StGRF* genes during potato tuber dormancy and sprouting
Danni Cui, Yin Song, Weihao Jiang, Han Ye, Shipeng Wang, Li Yuan and Bailin Liu

144 Comparing time-series transcriptomes between chilling-resistant and -susceptible rice reveals potential transcription factors responding to chilling stress
Rui Zhang, XiaoHui Xi, XinYi Chen, Yi Wang and Ming Zhou

156 Identification of key genes and molecular pathways regulating heat stress tolerance in pearl millet to sustain productivity in challenging ecologies
Swati Singh, Aswini Viswanath, Animikha Chakraborty, Neha Narayanan, Renuka Malipatil, Jinu Jacob, Shikha Mittal, Tara C. Satyavathi and Nepolean Thirunavukkarasu

181 Identification of autophagy-related genes ATG18 subfamily genes in potato (*Solanum tuberosum* L.) and the role of *StATG18a* gene in heat stress
Xi Zhu, Wei Li, Ning Zhang, Huimin Duan, Hui Jin, Zhuo Chen, Shu Chen, Jiannan Zhou, Qihua Wang, Jinghua Tang, Yasir Majeed, Yu Zhang and Huaijun Si

frontiers | Frontiers in Plant Science

TYPE Editorial
PUBLISHED 10 January 2025
DOI 10.3389/fpls.2024.1550257

OPEN ACCESS

EDITED AND REVIEWED BY
Luisa M. Sandalio,
Spanish National Research Council (CSIC), Spain

*CORRESPONDENCE
Zemin Wang
wzm406433254@126.com

RECEIVED 23 December 2024
ACCEPTED 30 December 2024
PUBLISHED 10 January 2025

CITATION
Wang Z, Wang Y and Wong DCJ (2025) Editorial: Surviving and thriving: how crops perceive and respond to temperature stress. *Front. Plant Sci.* 15:1550257. doi: 10.3389/fpls.2024.1550257

Editorial: Surviving and thriving: how crops perceive and respond to temperature stress

Zemin Wang[1,2,3]*, Yi Wang[4] and Darren Chern Jan Wong[5,6]

[1]State Key Laboratory of Aridland Crop Science, Gansu Agricultural University, Lanzhou, China, [2]College of Life Science and Technology, Gansu Agricultural University, Lanzhou, China, [3]State Key Laboratory of Efficient Production of Forest Resources, Yinchuan, China, [4]Beijing Key Laboratory of Grape Science and Enology, and Chinese Academy of Sciences (CAS) Key Laboratory of Plant Resources, Institute of Botany, Chinese Academy of Sciences, Beijing, China, [5]Division of Ecology and Evolution, Research School Research of Biology, The Australian National University, Acton, ACT, Australia, [6]School of Agriculture, Food, and Wine, Waite Research Precinct, University of Adelaide, Adelaide, Australia

KEYWORDS

abiotic & biotic stress, transcript factor, tolerance, extreme temperature stress, crop

Editorial on the Research Topic
Surviving and thriving: how crops perceive and respond to temperature stress

Climate change-driven temperature fluctuations pose a significant threat to crop productivity, emphasizing the crucial need to elucidate how plants mitigate temperature stress-induced cellular damage to ensure agricultural sustainability and food security (Jin et al., 2024; Ding and Yang, 2022; Shi et al., 2018, 2015; Zhu, 2016). In this Research Topic, "*Surviving and Thriving: How Crops Perceive and Respond to Temperature Stress*," 12 original research articles have presented new and valuable insights into the genetic basis of temperature extremes (e.g. cold/freezing and/or high heat) in a wide range of cereal (e.g. wheat, rice, pearl millet), vegetable (i.e. pepper), legume (e.g. soybean), and fiber (e.g. cotton) crops, paving the way for enhancing crop resilience and contributing to global food security, with potential biotechnological applications ranging from textiles to biofuels. We briefly summarize these contributions below.

Frost-tolerant wheat varieties reveal key molecular pathways conferring cold tolerance

Spring frost poses a serious threat to wheat production and grain quality, however, the molecular mechanisms conferring frost tolerance remain poorly understood. By taking advantage of a frost-tolerant wheat cultivar and subjecting it to freezing stress at the meiotic stage, Yao et al. revealed that key phenotypic changes (e.g. reduction in plant height, seed setting rate, and cell wall thickening in the stem vascular tissue) coincide with transcriptomic changes impacting hormone signaling, cell wall biosynthesis, and transcription factor regulation pathways.

Machine learning prioritizes key cold tolerance genes in rice

By leveraging comparative transcriptomic analysis of chilling stress and recovery in resistant and susceptible rice cultivars, Zhang et al. successfully inferred various time-series weighted gene co-expression networks associated with chilling resistance and susceptibility. Several biological processes, including abscisic acid responses, water deprivation responses, protein metabolism, and transcription regulation, were significantly enriched. Using machine learning methods, five genes (e.g. C-repeat binding factor, OsCBF3) were further prioritized to be pivotal for chilling resistance in rice.

BREVIS RADIX genes: evolution and function in upland cotton's abiotic stress tolerance

Genome-wide analysis of the plant-specific BREVIS RADIX (BRX) family in upland cotton revealed 12, 6, and 6 BRX candidate genes in *Gossypium hirsutum*, *G. raimondii* and *G. arboreum*, respectively (Wei et al.). Chromosomal localization and collinearity analysis suggest that segmental duplications were the primary driver of BRX gene amplification. Silencing of abiotic-stress responsive GhBRX.1, GhBRX.2, and GhBRXL4.3 further confirmed their pivotal roles in plant tolerance to salt and low-temperature stress, extending their function beyond root and shoot growth (Beuchat et al., 2010).

TIFY TFs mediate cold stress responses via ROS signaling in pepper

Plant-specific TIFY transcription factors (TFs), characterized by a conserved TIFY domain, are known to regulate growth, development, and stress tolerance (Vanholme et al., 2007). In this Research Topic, Wang et al. identified 16 TIFY plant transcription family candidate genes dispersed across seven subgroups in pepper (Capsicum annuum L.). In particular, *CaTIFY7* and *CaTIFY10b* were highly induced in leaves during cold stress. Knockdown of *CaTIFY7* and *CaTIFY10b* compromised cold tolerance, while their overexpression enhanced it, by influencing many cold-responsive and reactive oxygen species (ROS)-related genes.

New insights into temperature management strategies for improved soybean production

Ding et al. investigated the impact of five physiologically relevant day/night temperature regimes in two thermotolerant and thermosensitive genotypes. A comprehensive evaluation of physiological, biochemical, and genetic analyses revealed that 35/27°C (T_4) was the optimal regime for growth and yield in their study system. At this temperature, plants showed enhanced photosynthesis, antioxidant activity, and upregulation of key heat stress-responsive genes.

Comparative genomics reveals the evolution of heat tolerance mechanisms in pearl millet

Singh et al. performed a multi-tissue comparative transcriptomic analysis and revealed distinct genotype (tolerant vs sensitive)- and tissue (root vs leaf)-specific heat-responsive expression. Enrichment of heat shock proteins (HSPs), ROS scavenging, diverse TF families, and secondary metabolism pathways were observed. Interestingly, foxtail millet shared a high degree of collinearity with pearl millet in specific heat-responsive HSP and TF genes, compared to other cereal grains.

New insights on the mechanism of meiotic heat sensitivity in the wheat male gametophyte

Fábián et al. used cutting-edge histochemical and transcriptomic methods to compare the responses of heat-tolerant and heat-sensitive wheat cultivars to heat stress during male meiosis. Their study revealed pivotal structural and temporal alterations of wheat male meiocytes and tapetal cells and their transcriptional responses triggered by meiosis-timed heat stress. Notably, the heat-tolerant cultivar maintained cytoskeletal integrity and upregulated genes involved in stress response and meiosis, whereas the heat-sensitive cultivar displayed cytoskeletal disruption, impaired meiotic division, and aberrant tapetum development.

Growth-regulating factors in potato: multi-faceted roles in development and stress responses

Growth-regulating factors (GRFs) are a plant-specific TF family with diverse roles including regulation of plant growth under stress conditions (Omidbakhshfard et al., 2015). In this Research Topic, 12 candidate GRF genes were identified in potatoes (Cui et al.) A systematic analysis of *StGRF* promoter regions identified numerous cis-acting elements associated with plant growth, development, abiotic stress, and hormone responses. Transcriptomic data supported the tissue-specific expression (e.g. stamens, roots, and young tubers) and differential expression of *StGRFs* under abiotic/biotic stress (e.g. heat and *Phytophthora infestans* infection) and hormone treatment.

Molecular mechanisms of heat stress tolerance mediated by mitogen-activated protein kinase modules in potato

In plants, mitogen-activated protein kinase (MAPK) modules (MAPKKK-MAPKK-MAPK) are activated by various environmental cues, including heat and cold stress, triggering a cascade of cellular signaling events (Bigeard and Hirt, 2018; Manna et al., 2023) In this Research Topic, Zhu et al.; Zhu et al. screened MAPK and MAPKK gene expression in potato (*Solanum tuberosum*) plants cultivated under mild (30°C) and/or acute (35°C) heat stress conditions, revealing that *StMAPK1* and *StMAPKK5* exhibited highly induced and sustained expression profiles. Overexpression of *StMAPK1* modified photosynthesis and preserves membrane stability in response to heat stress by inducing the expression of heat stress genes (*StHSP90*, *StHSP70*, *StHSP20*, and *StHSFA3*) and regulating multiple redox balance and turgor maintenance pathways. Similarly, *StMAPKK5* overexpression/silencing significantly affected both morphological (plant weight/height) and physiological (photosynthesis, transpiration) traits under heat stress by modulating various stress-responsive and antioxidant enzyme genes and associated biochemical defenses.

New roles of GATA transcription factors and autophagy-related genes in potato heat stress response

Plant GATA (TFs) regulate diverse developmental processes and organ development (e.g. photomorphogenesis, chlorophyll biosynthesis, stomata formation), however, their role in abiotic stress remains relatively unexplored in plants (Schwechheimer et al., 2022). Zhu et al. screened over 50 potato GATA transcription factor (TF) genes for heat stress response and found that StGATA2 was among the few exhibiting strong and prolonged induction. A deeper understanding of autophagy-related genes (ATG) in potatoes were also gained in this Research Topic (Zhu et al.). A systematic analysis of phylogenetic relationships, chromosome distribution, gene structure, interspecific collinearity, and organ- (e.g. leaf, flower, stem, root, stolon, petiole, and tuber) and stress- (i.e. heat) responsive expression was performed on six putative ATG18 subfamily members identified in the potato genome. *StATG18a* emerged to be highly induced by heat stress in several organs. *StGATA2*- and *StATG18a*-overexpression also elicited comparable phenotypic, biochemical, and genetic responses to heat stress atypical to transgenic potato lines overexpressing *StMAPK1* and *StMAPKK5*.

Author contributions

ZW: Writing – original draft, Writing – review & editing. YW: Writing – review & editing. DW: Writing – review & editing.

Funding

The author(s) declare financial support was received for the research, authorship, and/or publication of this article. This Research Program was financially supported by The Research Program Sponsored by State Key Laboratory of Aridland Crop Science, Gansu Agricultural University (No. GSCS-2022-03 and GSCS-2023-04); The Undergraduate Scientific Research Training (SIETP) Program (202411034 and 202411035); the National Natural Science Foundation of China (32260518); and The Scientific Research Start-up Fund by Gansu Agricultural University (GAU-KYQD-2019-06 and GAUKYQD2020-26).

Conflict of interest

The authors declare that the research was conducted in the absence of any commercial or financial relationships that could be construed as a potential conflict of interest.

The author(s) declared that they were an editorial board member of Frontiers, at the time of submission. This had no impact on the peer review process and the final decision.

Publisher's note

References

Beuchat, J., Scacchi, E., Tarkowska, D., Ragni, L., Strnad, M., and Hardtke, C. S. (2010). BRX promotes Arabidopsis shoot growth. *New Phytol.* 188, 23–29. doi: 10.1111/j.1469-8137.2010.03387.x

Bigeard, J., and Hirt, H. (2018). Nuclear signaling of plant MAPKs. *Front. Plant Sci.* 9. doi: 10.3389/fpls.2018.00469

Ding, Y., and Yang, S. (2022). Surviving and thriving: How plants perceive and respond to temperature stress. *Dev. Cell* 57, 947–958. doi: 10.1016/j.devcel.2022.03.010

Jin, X., Wang, Z., Li, X., Ai, Q., Wong, D. C. J., Zhang, F., et al. (2024). Current perspectives of lncRNAs in abiotic and biotic stress tolerance in plants. *Front. Plant Sci.* 14. doi: 10.3389/fpls.2023.1334620

Manna, M., Rengasamy, B., and Sinha, A. K. (2023). Revisiting the role of MAPK signalling pathway in plants and its manipulation for crop improvement. *Plant Cell Environ.* 46, 2277–2295. doi: 10.1111/pce.14606

Omidbakhshfard, M. A., Proost, S., Fujikura, U., and Mueller-Roeber, B. (2015). Growth-regulating factors (GRFs): A small transcription factor family with

important functions in plant biology. *Mol. Plant* 8, 998–1010. doi: 10.1016/j.molp.2015.01.013

Schwechheimer, C., Schröder, P. M., and Blaby-Haas, C. E. (2022). Plant GATA factors: their biology, phylogeny, and phylogenomics. *Annu. Rev. Plant Biol.* 73, 123–148. doi: 10.1146/annurev-arplant-072221-092913

Shi, Y., Ding, Y., and Yang, S. (2015). Cold signal transduction and its interplay with phytohormones during cold acclimation. *Plant Cell Physiol.* 56, 7–15. doi: 10.1093/pcp/pcu115

Shi, Y., Ding, Y., and Yang, S. (2018). Molecular regulation of CBF signaling in cold acclimation. *Trends Plant Sci.* 23, 623–637. doi: 10.1016/j.tplants.2018.04.002

Vanholme, B., Grunewald, W., Bateman, A., Kohchi, T., and Gheysen, G. (2007). The tify family previously known as ZIM. *Trends Plant Sci.* 12, 239–244. doi: 10.1016/j.tplants.2007.04.004

Zhu, J. K. (2016). Abiotic stress signaling and responses in plants. *Cell* 167, 313–324. doi: 10.1016/j.cell.2016.08.029

frontiers | Frontiers in Plant Science

TYPE Original Research
PUBLISHED 12 January 2023
DOI 10.3389/fpls.2022.1099677

OPEN ACCESS

EDITED BY
Darren Wong,
Australian National University, Australia

REVIEWED BY
Olive Onyemaobi,
Commonwealth Scientific and Industrial Research Organization (CSIRO), Australia
Jing Cang,
Northeast Agricultural University, China
Klára Kosová,
Crop Research Institute (CRI), Czechia

*CORRESPONDENCE
Guozhong Sun
sunguozhong@caas.cn

†These authors have contributed equally to this work

SPECIALTY SECTION
This article was submitted to Plant Abiotic Stress, a section of the journal Frontiers in Plant Science

RECEIVED 16 November 2022
ACCEPTED 19 December 2022
PUBLISHED 12 January 2023

CITATION
Yao D, Wang J, Peng W, Zhang B, Wen X, Wan X, Wang X, Li X, Ma J, Liu X, Fan Y and Sun G (2023) Transcriptomic profiling of wheat stem during meiosis in response to freezing stress.
Front. Plant Sci. 13:1099677.
doi: 10.3389/fpls.2022.1099677

Transcriptomic profiling of wheat stem during meiosis in response to freezing stress

Danyu Yao[1†], Juan Wang[1†], Wentao Peng[1,2†], Bowen Zhang[1,3], Xiaolan Wen[1,4], Xiaoneng Wan[1], Xiuyuan Wang[1,2], Xinchun Li[1], Jian Ma[3], Xiaofen Liu[4], Yinglun Fan[2] and Guozhong Sun[1*]

[1]National Engineering Laboratory of Crop Molecular Breeding, Institute of Crop Science, Chinese Academy of Agricultural Sciences, Beijing, China, [2]College of Agricultural Science and Engineering, Liaocheng University, Liaocheng, Shandong, China, [3]College of Agronomy, Jilin Agricultural University, Changchun, Jilin, China, [4]College of Landscape and Ecological Engineering, Hebei University of Engineering, Handan, Hebei, China

Low temperature injury in spring has seriously destabilized the production and grain quality of common wheat. However, the molecular mechanisms underlying spring frost tolerance remain elusive. In this study, we investigated the response of a frost-tolerant wheat variety Zhongmai8444 to freezing stress at the meiotic stage. Transcriptome profiles over a time course were subsequently generated by high-throughput sequencing. Our results revealed that the prolonged freezing temperature led to the significant reductions in plant height and seed setting rate. Cell wall thickening in the vascular tissue was also observed in the stems. RNA-seq analyses demonstrated the identification of 1010 up-regulated and 230 down-regulated genes shared by all time points of freezing treatment. Enrichment analysis revealed that gene activity related to hormone signal transduction and cell wall biosynthesis was significantly modulated under freezing. In addition, among the identified differentially expressed genes, 111 transcription factors belonging to multiple gene families exhibited dynamic expression pattern. This study provided valuable gene resources beneficial for the breeding of wheat varieties with improved spring frost tolerance.

KEYWORDS

***Triticum aestivum*, spring frost injury, transcriptome, hormone signal transduction, transcription factor, cell wall**

Introduction

Wheat (*Triticum aestivum* L.) is one of the most widely grown staple crops worldwide. The spring frost injury has become the limiting factor of wheat production because it has dramatically influenced the yield, quality, and the geographical distribution of wheat (Chen et al., 2020). The Yellow and Huai River Valley Winter Wheat Zone

(YHVWWZ) is the major producing area of China's winter wheat. Frost damage in spring generally occurs from February to April, when the plants are at the jointing to the booting stage of wheat growth. At this time, the wheat tissues are tender and contain a lot of water, so they are easy to get damaged (Frederiks et al., 2015). Exposure to low temperature may cause the damage of leaf, stem and young spike, which could result in the decrease in the grain number and quality. From 2001 to 2021, the frequency of spring frost injury in the YHVWWZ was as high as 40% (Liu et al., 2021). In 2018, it has caused the yield losses of 3,000 kg per hectare in wheat varieties with weak freezing tolerance when compared to freezing-resistant varieties (Ou and Wang, 2019). Therefore, breeding and promoting freezing-tolerant wheat varieties is an important approach to deal with the disaster of spring frost injury in YHVWWZ. However, at present, knowledge of the physiological mechanisms underlying the freezing tolerance is still elusive, limiting the genetic improvement of wheat varieties.

Low temperature stress includes both cold/chilling stress (>0°C) and freezing stress (<0°C). When exposed to low temperature, plants can perceive the signal and induce a series of complex changes in their morphological structure, internal substances and photosynthesis (Ding et al., 2019). The accumulation of soluble sugar and amino acid was observed in many plant species (Nakabayashi and Saito, 2015). A series of mechanisms are initiated to protect and maintain the normal metabolism and growth of plants, so as to avoid or minimize the damage of low temperature. During this complex biological process, a large number of genes are activated and play an important role for plants to survive. For instance, transcription factors (TFs) are thought to control many cold responsive genes through direct binding to cis-acting elements in the promoter regions. Regulation of cold-regulated (*COR*) genes by CRT/DRE-binding factors (CBFs) constitutes the predominant cold signaling pathway and was found to be conserved in both dicots and monocots (Park et al., 2015). In diploid *Triticum monococcum*, three *CBF* genes (*CBF12, CBF14, CBF15*) have been identified to be highly associated with frost tolerance (Knox et al., 2008). Overexpression of *CBF14* and *CBF15* from winter wheat resulted in the enhanced frost tolerance in spring barley (Soltész et al., 2013). The CBF transcription factors belong to the APETALA2/Ethylene response element binding protein (AP2/EREBP) family. Other transcription factors including MYB, NAC, bZIP, and WRKY TFs have also been identified to be linked to the tolerance of low temperature stress (Su et al., 2010; Mao et al., 2012).

In addition, phytohormone always acts as a crucial signal to modulate multiple plant processes and has been reported to play an essential role for plant to cope with low temperature stress. A key hormone is abscisic acid (ABA), which not only controls the internal water deficiency by regulating stomatal conductance but also regulates the transcriptome of downstream stress-related genes. It has been shown that CBF transcription factors induced the biosynthesis of ABA, which subsequently stimulated the expression of *COR* genes (Sharabi-Schwager et al., 2010; Wang et al., 2016). The exogenous application of ABA significantly improved the low-temperature tolerance of tomato (Kim et al., 2002), pepper (Guo et al., 2012), magnolia liliiflora (Yang et al., 2016) and wheat (Yu et al., 2020). Moreover, accumulating evidence indicated that jasmonic acid (JA) could mediate the responses to low temperature stress with other hormones, such as ABA, auxin, ethylene, and gibberellin (Hu et al., 2017). Wang et al. (2016) reported that JA could activate the ABA-dependent CBF signaling pathway and positively modulate the reactions to cold stress in tomato. Blocking of JA biosynthesis and signaling caused the hypersensitivity to freezing stress (Hu et al., 2013). In Arabidopsis, it has been reported that ethylene and gibberellin (GA) negatively regulated plant cold tolerance (Shi et al., 2012; Richter et al., 2013). For instance, a GA-deficient mutant showed increased expression level of cold-responsive genes and enhanced resistance to cold stress (Richter et al., 2013). These studies indicate the complex nature of plant's responses to low temperature.

It has been suggested that properties of cell wall strongly influence the frost resistance of plants. When subjected to freezing, ice crystallization takes place in the intercellular space which could lead to the dehydration and mechanical damage of cells. Plasma membrane and cell wall work together to perceive the external signal of freezing stress and in turn cause the corresponding changes in cell wall content, composition and structure. This phenomenon has been observed in multiple plant species such as Arabidopsis, winter wheat, maize and tobacco (Sugiyama and Shimazaki, 2007; Bilska-Kos et al., 2016; Willick et al., 2017; Parrotta et al., 2019; Takahashi et al., 2019). There is increasing evidence showing that cell wall genes were involved in the regulation of plant low temperature tolerance. A transcriptomic study performed by Le et al. (2015) showed that several cell wall genes were dramatically up regulated in Arabidopsis accessing to sub-zero temperatures. Mutant lacking *XTH19* gene, which encode a xyloglucan endotransglucosylase/hydrolase, showed hypersensitivity to low-temperature stress compared to wild-type plants (Takahashi et al., 2021). In addition, a novel frost tolerant gene, *SENSITIVE-TO-FREEZING8* (*SFR8*), has been cloned and demonstrated to influence pectin fucosylation (Panter et al., 2019).

Large-scale analysis of gene expression pattern by transcriptome techniques provides a cost-effective strategy for elucidating the molecular mechanisms underlying physiological processes and it can substantially increase the efficiency of identifying genes of interest. A range of plant species such as Arabidopsis, rice, wheat, maize, and cotton have been extensively subjected to transcriptional programming in response to different stresses (Jian et al., 2014; Huang et al., 2019; Sga et al., 2019; Wang et al., 2019). Zhao et al. (2019) integrated transcriptome and metabolome analyses for understanding how wheat plants respond to low temperature.

29,066 DEGs were identified, and pathways of phytohormone signaling and proline biosynthesis were shown to be significantly modulated under freezing treatment.

The objective of this study is to investigate the phenotypic changes as well as transcriptome dynamics of wheat cultivar zhongmai8444 in response to freezing temperature at the meiosis stage. Our results will provide valuable insights into understanding molecular mechanisms underlying the frost tolerance and help identify new gene resource that is beneficial for genetic improvement of spring frost tolerance in wheat.

Materials and methods

Plant materials, freezing treatment, and seed setting measurement

Zhongmai8444 is a spring wheat variety breed in our lab. It showed great freezing tolerance since it could survive in the winter of Beijing (-5°C to 2°C) by field trials for five consecutive years. Zhongmai8444 was grown in a growth chamber maintaining at 22°C during the day, 15°C during the night, 16-h light, 8-h dark, 80% humidity and a PPFD of 450 μmol m^{-2} s^{-1}. Three plants were grown in each pot and their growth stages were recorded according to the Zadoks scale (Zadoks et al., 1974). Developmental stages of pollen mother cells from immature anthers were examined following Draeger and Moore (2017). When the distance from flag leaf to the adjacent leaf was around 2-3 cm (Supplemental Figure S1), Zhongmai8444 was verified to be at meiotic stage and subjected to freezing treatment shown in Supplemental Figure S2. Wheat plants grown at 22°C (normal temperature growth) prior to freezing were set as the control group (time point T1). Temperature in growth chamber was gradually decreased from 22°C to -2.5°C using 6 h (time point T2) and then maintained at -2.5°C for 48 h (time point T4). Plants were also harvested after frozen at −2.5°C for 24 h (time point T3). Finally, temperature gradually increased from -2.5°C to 22°C (time point T5) and plants were collected as recovery group. Samples were named as J1 to J5 according to the time points (T1 to T5). Stem tissues from six individual plants were pooled (with three replications) and immediately frozen in liquid nitrogen for subsequent RNA extraction. In addition, another set of plants were treated with freezing (-2.5°C for 48 h) during meiosis as described above and transferred to normal growth condition for continuing growth. Plants that were maintained at normal growth condition were used as the control. The seed setting rate was analyzed using the equation: seed setting rate=grain number each spike/flower number each spike × 100%.

Cell wall thickness measurement

To investigate the cell wall morphology of stem tissue after freezing treatment, xylem cells from three individual plants were selected for further measurement. Thin cross-sections were cut from the base of wheat stem using a sterile razor blade and were subsequently incubated in 0.02% toluidine blue solution for 2 min at room temperature. After thoroughly washing, respective stem cross-sections were mounted in water prior to imaging on an OLYMPIC CX41RF microscope equipped with an EOS 450D camera (Canon). Cell wall morphology and thickness of the xylem cells were subsequently analyzed using the Image J software (National Institutes of Health; http://rsb.info.nih.gov/ij/). The cell wall thickness was analyzed from at least 20 xylem cells collected from three individual plants. For the observation by a transmission electron microscope (TEM), samples were prepared following Vigani et al. (2018) with some modifications. Briefly, stem tissues were fixed overnight in 3% (v/v) glutaraldehyde at room temperature and subsequently post fixed with 1% (w/v) osmium tetroxide for 2 h at 4°C. After dehydration in a graded ethanol series, samples were embedded in resin for ultrathin sectioning and visualization with a H-7500 TEM (HITACH, Japan) at 80 kV.

RNA extraction and sequencing

Total RNA was extracted from stem tissues using an RNAprep Pure Plant Kit (Tiangen) according to the manufacturer's instructions and its quantity, quality, and integrity were evaluated using an Agilent 2100 Bioanalyzer system (Agilent Technologies, Palo Alto, CA, USA). Purified RNA was sent to Novogene (https://cn.novogene.com/) for RNA sequencing using Illumina NovaSeq platform and 150 bp paired-end reads were generated. Clean reads were obtained by removing reads with adapters sequences, reads with poly-N and low-quality reads using in house scripts. Then, the reads after quality control were mapped to the wheat reference genome (https://urgi.versailles.inra.fr/download/iwgsc/IWGSC_RefSeq_Assemblies/v1.0/) using Hisat2 v2.0.5 (Kim et al., 2015). Wheat gene annotation was obtained from https://urgi.versailles.inra.fr/download/iwgsc/IWGSC_RefSeq_Annotations/v1.0/iwgsc_refseqv1.0_HighConf_2017Mar13.gff3.zip.

Gene expression levels were quantified as Fragments Per Kilobase of transcript sequence per million mapped fragments (FPKM) using the featureCounts v1.5.0-p3 program (Yang et al., 2014). Principal component analysis (PCA) was performed to evaluate the reproducibility of different samples under the same treatment.

Differential expression analysis

Differential gene expression analysis was performed using the DESeq2 (Love et al., 2014) package in R (1.20.0). The Benjamini and Hochberg method was used to adjust P-values to control the false discovery rate (FDR). Differentially expressed

genes were identified according to the threshold of |log2FoldChange| > 1 and FDR < 0.05. Gene Ontology (GO) and Kyoto Encyclopedia of Gene and Genomes (KEGG) pathways enrichment analysis of the DEGs were performed using clusterProfiler R package (Yu et al., 2012).

Real-time quantitative PCR

Real-time quantitative PCR was performed on the stem tissues to examine expression patterns of selected genes. Samples were run in triplicate with SuperReal SYBR Green PreMix Plus (Tiangen) on a Bio-Rad CFX96 Touch Real-Time PCR Detection System. The PCR reactions were performed under the following conditions: 95°C for 15 min, followed by 40 cycles of 95°C for 10 s, 58°C for 20 s, and 72°C for 30 s. Relative quantities were calculated and normalized to the actin gene, which was used as an internal control, using the $2^{-\Delta\Delta Ct}$ algorithm. The data are shown as means ± standard errors (SE) and primers used for qRT-PCR analysis are listed in Supplementary Table S4.

Results

Phenotypic analysis of Zhongmai8444 after freezing treatment

In previous study, we have demonstrated that Zhongmai8444 was extremely sensitive to freezing stress at the meiotic stage/phase by evaluating the damage of freezing on plant stems, leaves, spikes and other organs during the reproductive development (Wang et al., 2022). Consistently, the injury of stems (Supplementary Figure S3) and cell wall thickening in the vascular tissue were observed after Zhongmai8444 was treated with -2.5°C for 48 h (Figures 1A–C). Cell walls were found to be severely damaged when plants were recovered to normal room temperature (Figures 1D, E). In addition, plant height, grain number per spike and seed setting rate were quantified after the plants were treated with freezing stress or grown in normal growth conditions. Results indicated that Zhongmai8444 exhibited significantly reduced height, grain number and seed setting rate after -2.5°C freezing treatment for 48 h at the meiotic stage (Figures 1F, G; Table 1). To further understand the molecular mechanism underlying wheat frost tolerance, we performed RNA sequencing of the stem to identify differentially expressed genes responsive to freezing stress.

Mapping of RNA-Seq data to wheat genome

Utilizing the paired-end Illumina sequencing technology, the extracted RNA from stem tissue was sequenced to compare gene expression at different time points under freezing stress, samples were named as J1 to J5 accordingly. After quality control, sequencing data yield approximately 70 million high-quality clean reads per library shown in Supplemental Table S1. The clean reads shared a GC content of approximately 55% and the alignment rate uniquely mapped to the Chinese Spring iwgsc_refseqv1.0 reference genome (https://urgi.versailles.inra.fr/download/iwgsc/IWGSC_RefSeq_Assemblies/v1.0/) was ranged from 88.96% to 90.76%. In addition, Pearson correlation analysis (PCA) and principal component analysis were performed to determine the quality of biological replications of each sample (Supplemental Figure S4, Figure S5). Results showed that the sample J3-2 was relatively dispersed from the other two biological replicates and removed for further analysis. All the other samples had good repeatability with ePearson coefficient higher than 0.87 (Supplemental Figure S4).

Identification of differentially expressed genes under freezing

To systematically investigate the dynamics of transcriptome profiles of wheat stem, we identified genes that were differentially expressed by at least twofold (|log2FoldChange| > 1 and padj < 0.05) with -2.5°C freezing treatment. A clear difference was observed in the number of up-regulated and repressed DEGs at the indicated time points compared to control plants (Figure 2A). A total of 2016 up-regulated and 994 down-regulated genes were detected in stem tissue after 6-h-cooling (J2 vs J1). An increase in the number of significantly up-regulated (5058 to 7000) and down-regulated (6985 to 11778) DEGs was observed with the extended duration of freezing stress (from T2 to T4), which suggested the ongoing adaptation of plants to low temperature conditions. However, there was a small change in the number of DEGs when plants were recovered at 22°C after freezing stress (J5 vs J1). We subsequently constructed the Venn analysis to investigate the number of up-regulated and down-regulated genes that were commonly shared at different time points (Figures 2B, C respectively). Results showed that respectively 1010 up-regulated and 230 down-regulated genes were detected common at all time points.

Gene ontology clustering of DEGs

To functionally characterize the identified DEGs, a GO analysis was performed to classify them into the three categories: molecular function (MF), cellular component (CC) and biological process (BP). Significantly enriched GO terms identified at different time points with freezing treatment (J2 vs J1, J3 vs J1 and J4 vs J1 comparisons) were determined. The top 4 GO terms from each category were respectively presented in Figure 3 and highly overlap among samples collected from different time points. For instance, in the biological process

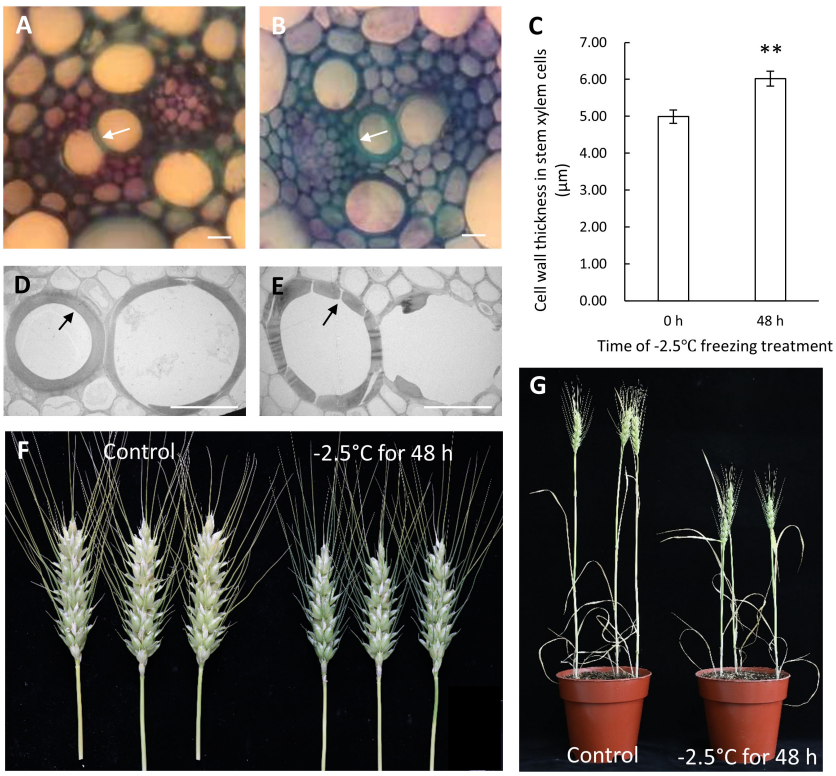

FIGURE 1
The phenotypic reactions of Zhongmai8444 treated with freezing stress at meiotic stage. **(A)** Morphology of cell walls in xylem cells when plants were grown in normal growth condition. **(B)** Cell wall thickening was observed in plants treated with -2.5°C for 48 h. **(C)** Bar graph represents the cell wall thickness of xylem cells in control and freezing-treated plants. Data are mean ± SE calculated from three biological replicates. ** indicates a significant difference (p-value < 0.01) using a Student's t-test. **(D)** TEM imaging showed that the cell walls of xylem cells were not disturbed in plants grown in normal growth condition. **(E)** Cell walls of xylem cells were severely damaged when plants were treated with -2.5°C for 48 h and recovered at room temperature. **(F)** Spike length and seed setting were dramatically reduced in plants treated with -2.5°C for 48 h (on the right) compared to plants grown in normal growth condition (on the left). **(G)** Freezing stress at meiotic stage leads to reduced plant height. Scale bars represent 20 μm.

category, the GO term "response to auxin", "response to endogenous stimulus", "response to hormone" were significantly enriched in all samples, suggesting an involvement of genes participated in the signal perception and transduction pathway. Similarly, under the cellular component and molecular function category, the most enriched GO terms "extracellular region", "apoplast", "cell wall" and "protein heterodimerization activity" were also detected in all samples. However, the "cell periphery" and "calcium ion binding" were only shared in the samples treated with 24 h or 48 h freezing stress. In addition, in the 48 h freezing treated samples, the other term "xyloglucan:xyloglucosyl transferase activity" and "glucosyltransferase activity" were also related to the cell wall metabolism and consistent with the detected phenotype of cell wall thickening. Therefore, we hypothesized that hormone signal transduction and cell wall biosynthesis process may be modulated to promote plant resistance to freezing.

Pathways enrichment analysis of DEGs

The KEGG analysis of DEGs in stem was also performed to identify pathways displaying significant changes (padj ≤ 0.05) in response to freezing (Table 2). "Plant hormone signal

TABLE 1 Effect of 48 h freezing stress (FS) on plant height and seed setting of Zhongmai8444.

	Plant height (cm)	Number of grains per spike	Seed setting rate (%)
Control	43.60 ± 0.78	24.83 ± 1.45	70.63 ± 2.82
48 h FS	31.58 ± 2.41**	18.33 ± 1.05**	56.57 ± 1.83**

Data are mean ± SE calculated from six biological replicates. ** indicates a significant difference (p-value < 0.01) using a Student's t-test.

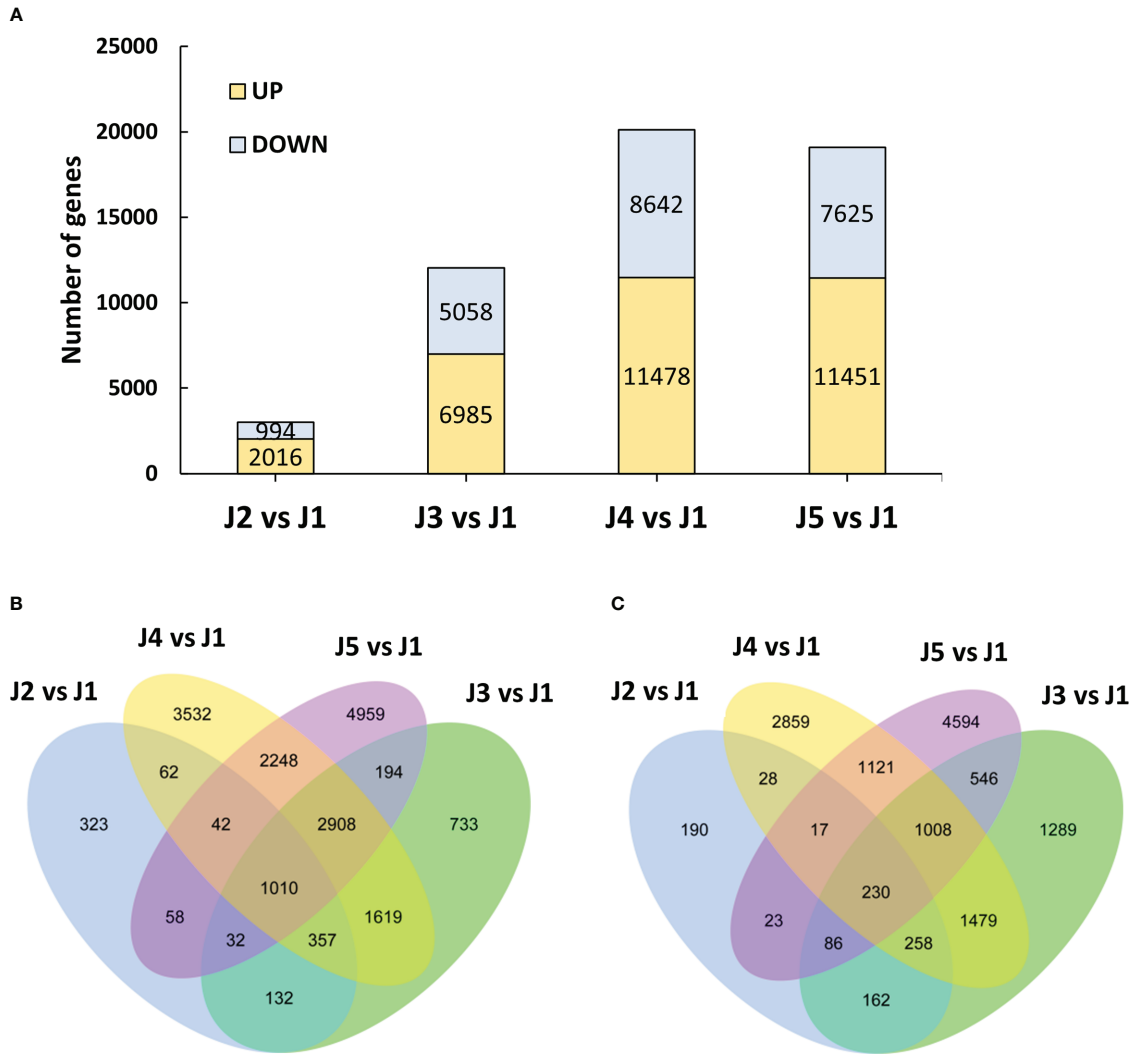

FIGURE 2
Overview of the transcriptome analysis. **(A)** Differentially expressed genes at each timepoint compared to control plants. **(B)** Venn diagram for the up-regulated genes shared by each time point after -2.5°C freezing treatment. **(C)** Venn diagram for the down-regulated genes shared by each time point after -2.5°C freezing treatment.

transduction" pathway was significantly enriched at every time point. In addition to this pathway, "circadian rhythm-plant" was also enriched after 6-h-cooling (J2 vs J1). In 24 h freezing treated samples (J3 vs J1), four pathways significantly changed including "plant-pathogen interaction", "plant hormone signal transduction", "MAPK signaling pathway-plant", and "phenylpropanoid biosynthesis". In addition, analysis revealed that DEGs in 48 h freezing treated samples (J4 vs J1) were associated with "plant-pathogen interaction", "plant hormone signal transduction", "phenylpropanoid biosynthesis", "circadian rhythm-plant", "photosynthesis-antenna proteins", "MAPK signaling pathway-plant", and "starch and sucrose metabolism" pathways. After samples were recovered after freezing treatment (J5 vs J1), the "photosynthesis-antenna proteins", "photosynthesis", "plant hormone signal transduction", and "MAPK signaling pathway-plant" pathways were significantly enriched among DEGs. Consistent with the GO analysis, our results emphasized the involvement of plant hormone in the response of wheat to freezing.

Representative mostly up-regulated and down-regulated DEGs

Venn analysis identified 1010 up-regulated and 230 down-regulated genes shared by all time points. We listed the expression of top 20 (ranked by the padj value of J4 vs J1 comparison) up-regulated (Table 3) and down-regulated DEGs (Table 4). We observed several low temperature related genes that have been significantly up regulated, including the

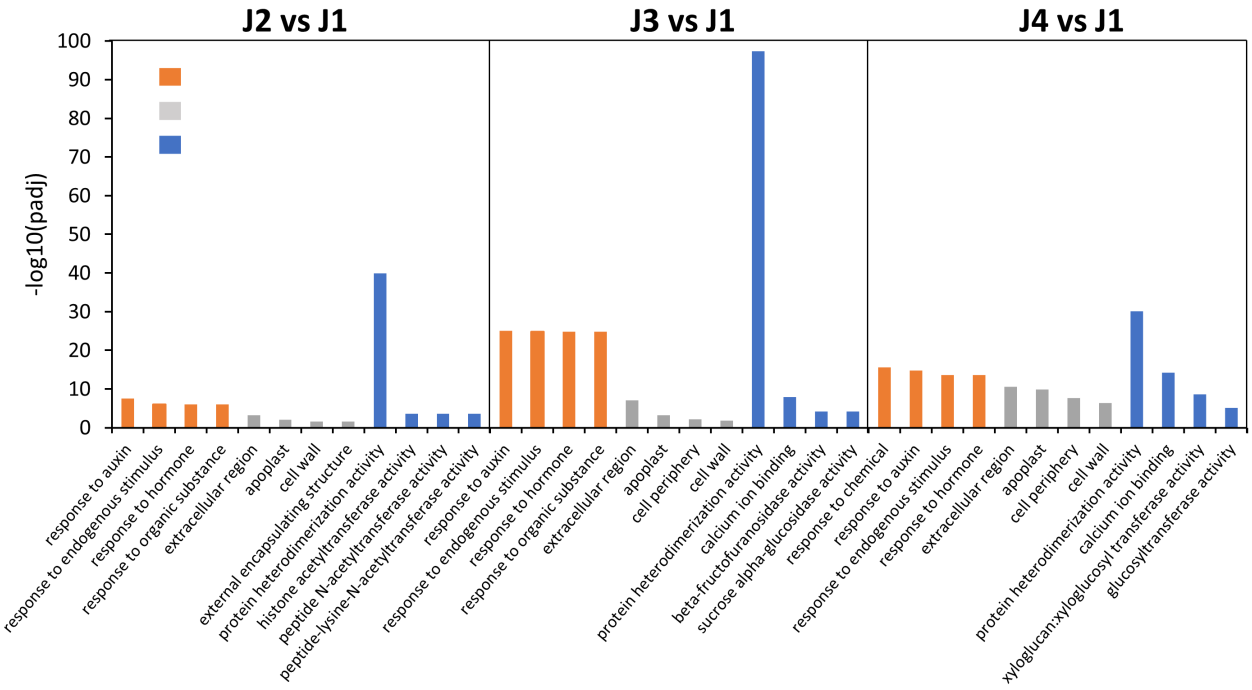

FIGURE 3
Histogram showing the most significantly enriched GO term from samples collected at each time point during freezing treatment. Color bars represent different functional classifications, including biological process (orange bars), cellular components (grey bars) and molecular function (blue bars).

abscisic acid (ABA) responsive protein (TraesCS5B01G502200, TraesCS5A01G488500), dehydrin (TraesCS4B01G228000, TraesCS6B01G383200) and late embryogenesis abundant (LEA) proteins (TraesCS1A01G423800, TraesCS3D01G158600, TraesCS3A01G175400). In addition, expression levels of genes involved in diverse biosynthesis process of cell wall, carbohydrates, amino acids, cytoskeleton, and other metabolites were also significantly affected. Few genes encoding the transcription factor were also identified, including those containing GRAM domain, NAC domain, and Myb-like DNA-binding domain. These results indicated that widespread genes showed substantial changes in expression level following freezing temperatures.

Identification of genes involved in hormone and signal transduction

The GO and KEGG enrichment analyses of the DEGs both highlighted that the plant hormone signal transduction pathway (dosa04075) was particularly affected by the freezing treatment (Figure 3; Table 2). Among the 1240 DEGs shared by all time points, many genes encoding a protein kinase and probably involved in the signal transduction were detected (Supplemental Table S2). More than 40 genes predicted to encode a protein kinase were differentially expressed under freezing treatment. Most of the genes were up regulated while only 6 genes were down regulated by

TABLE 2 Significantly enriched gene pathways at each time point following the low temperature treatment.

	Pathway	Gene ratio	padj	KEGG ID
J2 vs J1	Plant hormone signal transduction	16/98	0.000167	dosa04075
	Circadian rhythm-plant	6/98	0.002644	dosa04712
J3 vs J1	Plant-pathogen interaction	42/458	1.01E-05	dosa04626
	Plant hormone signal transduction	38/458	0.002092	dosa04075
	MAPK signaling pathway-plant	23/458	0.005750	dosa04016
	Phenylpropanoid biosynthesis	23/458	0.026783	dosa00940
J4 vs J1	Plant-pathogen interaction	71/797	2.30E-12	dosa04626

(Continued)

TABLE 2 Continued

	Pathway	Gene ratio	padj	KEGG ID
	Plant hormone signal transduction	57/797	1.71E-05	dosa04075
	Phenylpropanoid biosynthesis	40/797	2.91E-05	dosa00940
	Circadian rhythm-plant	17/797	3.45E-05	dosa04712
	Photosynthesis-antenna proteins	11/797	8.35E-05	dosa00196
	MAPK signaling pathway-plant	30/797	0.002174	dosa04016
	Starch and sucrose metabolism	33/797	0.002789	dosa00500
J5 vs J1	Photosynthesis-antenna proteins	16/944	6.24E-07	dosa00196
	Photosynthesis	23/944	3.74E-05	dosa00195
	Plant hormone signal transduction	63/944	0.004824	dosa04075
	MAPK signaling pathway-plant	37/944	0.008353	dosa04016

TABLE 3 Representative mostly up-regulated genes shared in all time points, shown as log2 value of fold changes.

Gene ID	Description	J2 vs J1	J3 vs J1	J4 vs J1	J5 vs J1
TraesCS5B01G502200	GRAM domain-containing protein/ABA-responsive	4.87	9.72	11.64	10.47
TraesCS6D01G403400	tRNA-2-methylthio-N (6)-dimethylallyladenosine synthase	4.61	7.51	9.66	8.34
TraesCS5B01G069300	HVA22-like protein	2.97	6.53	8.09	5.88
TraesCS7D01G358000	Cysteine-rich/transmembrane domain A-like protein	2.44	7.62	9.21	8.34
TraesCS5D01G481200	NAC domain-containing protein, putative	3.99	7.45	8.52	6.95
TraesCS1A01G423800	Late embryogenesis abundant protein	1.25	6.30	7.69	7.21
TraesCS4B01G228000	Senescence/dehydration-associated protein-like protein	2.72	6.97	7.97	6.84
TraesCS2D01G598500	Acetyl-coenzyme A synthetase	3.47	6.60	8.53	7.51
TraesCS5B01G491500	Actin depolymerizing factor	2.97	5.17	6.61	5.34
TraesCS5A01G488500	GRAM domain-containing protein/ABA-responsive	3.17	6.91	8.95	8.26
TraesCS5D01G491900	Actin depolymerizing factor	2.92	4.93	6.49	4.88
TraesCS1D01G218000	Beta-amylase	5.45	5.85	7.06	4.53
TraesCS3D01G158600	Late embryogenesis abundant protein	6.04	11.19	12.80	12.16
TraesCS3B01G422300	BAG family molecular chaperone regulator 2	2.33	6.54	7.63	6.71
TraesCS5A01G471700	LURP-one-like protein	2.62	5.45	7.12	5.57
TraesCS2A01G295400	Cell wall invertase	2.22	4.98	7.42	7.43
TraesCS5B01G356400	Nudix hydrolase-like protein	1.38	5.48	6.96	4.36
TraesCS6B01G383200	Dehydrin	6.73	12.09	13.96	11.90
TraesCS7A01G065000	Seed maturation protein	5.14	7.86	9.54	7.40
TraesCS3A01G175400	Late embryogenesis abundant protein	4.49	8.29	9.99	8.99

freezing stress. Genes encoding a receptor-like protein kinase constituted the largest group and may play key roles in mediating stress-associated signaling pathway, such as the leucine-rich repeat receptor-like protein kinase (Yang et al., 2022). KEGG analysis of the DEGs suggested that genes encoding protein phosphatase 2C (TraesCS3A01G362200 and TraesCS5A01G183600), which was associated in the carotenoid and ABA biosynthesis, were induced at all time points under freezing condition. The expression of

TABLE 4 Representative mostly down-regulated genes common in all time points, shown as log2 value of fold changes.

Gene ID	Description	J2 vs J1	J3 vs J1	J4 vs J1	J5 vs J1
TraesCS2A01G206700	Transmembrane protein	-1.27	-3.32	-5.25	-3.89
TraesCS7D01G078900	Homeobox-leucine zipper family protein	-1.38	-5.56	-6.80	-2.33
TraesCS2B01G233900	Transmembrane protein	-1.18	-2.56	-4.70	-3.65
TraesCS4D01G275000	DUF1677 family protein	-1.43	-4.35	-4.40	-3.66
TraesCS7D01G478900	Cyclin-dependent kinase inhibitor	-1.76	-4.67	-7.28	-3.31
TraesCS5A01G329900	MYB transcription factor	-1.07	-4.20	-4.06	-1.82
TraesCS6A01G401600	Histone H2A	-1.11	-1.00	-2.83	-3.15
TraesCS4A01G030500	Histone H2B	-1.17	-1.55	-4.14	-1.72
TraesCS5A01G534300	Tubulin beta chain	-1.22	-1.89	-3.94	-2.97
TraesCS7B01G432600	Rotundifolia-like protein	-1.23	-5.36	-6.73	-1.15
TraesCS3B01G451100	DUF868 family protein	-1.31	-2.90	-4.17	-3.24
TraesCS6A01G249300	Expansin protein	-1.15	-3.50	-3.72	-3.29
TraesCS5D01G110600	Histone H2A	-1.58	-0.93	-4.79	-1.89
TraesCS7A01G160200	Histidinol dehydrogenase	-1.07	-3.80	-3.99	-3.60
TraesCS1D01G029700	HXXXD-type acyl-transferase family protein	-1.39	-3.56	-6.89	-3.90
TraesCS4A01G096300	Rotundifolia-like protein	-1.80	-2.74	-8.02	-1.17
TraesCS2A01G291400	Unknown protein	-1.46	-2.58	-3.00	-2.70
TraesCS4A01G067900	Glucan endo-1,3-beta-glucosidase, putative	-1.12	-1.91	-3.62	-3.24
TraesCS5D01G222600	Auxin responsive SAUR protein	-2.19	-10.29	-6.27	-2.71
TraesCS7A01G337300	Leucine-rich repeat receptor-like protein kinase	-1.24	-1.71	-2.42	-4.32

TraesCS3A01G362200 was rapidly up-regulated after 6-h cooling and progressively up-regulated by 5.2 and 10 folds after maintaining at -2.5°C for 24 h and 48 h, respectively, compared to that in control group. The other gene TraesCS5A01G183600 showed similar expression pattern and 8 folds up-regulated expression at time point T4. In addition, 66 DEGs associated with the biosynthesis or signal transduction of the phytohormones like ethylene, auxin, ABA or GA were listed in Supplemental Table S2. All the ethylene related genes were induced upon freezing treatment and determined to encode AP2/ERF domain-containing TFs. *ERF* genes are critical for multiple plant species to deal with low temperature stress. In Arabidopsis, *ERF105* has been suggested to operate in conjunction with the well-known CBF regulon (Bolt et al., 2017).

Identification of transcription factors in response to freezing stress

Numerous families of TFs are known to play an important role when plants are challenged with various abiotic stresses. In current study, 111 putative TFs were identified to be differentially expressed (|log2FoldChange| > 1 and padj < 0.05) at all time points with freezing treatment (Table 5; Supplemental Table S3). Genes encode AP2/ERF domain-containing proteins constituted the largest group, followed by zinc finger proteins, NAC domain-containing proteins, MYB TFs, heat shock TFs, WRKY TFs, GRAS TFs, Growth-regulating factors, Homeobox domain TFs, bZIP proteins and ethylene insensitive 3 TF (Table 5). The identified TFs were classified into five subgroups based on their expression patterns (Figure 4). The expression level of TFs in Subgroup I declined immediately after cooling and became more dramatically reduced after continuous freezing treatment. In contrast, the transcript abundance of TFs in Subgroup II was significantly induced at the early time point and then decreased upon the duration of freezing treatment, which suggests that they play roles in early transduction of the low-temperature signal. Subgroup III TFs were active after freezing but showed a peak of expression when plants were recovered in normal growth condition. Subgroup IV and V, the two largest subgroups, were characterized by genes showing the highest expression after 24-h and 48-h freezing treatment, respectively. In addition, we listed the 10 most highly induced TF genes in stem tissue commonly shared in all time points (Table 6). Four genes encoding AP2 domain containing proteins and three NAC domain containing TF genes were identified. The transcript

TABLE 5 Classification of transcription factor genes differentially expressed at all time points (|log2FoldChange| > 1 and padj < 0.05) upon freezing stress.

Class	Gene number
AP2/ERF domain containing transcription factor	44
Zinc finger transcription factor	19
NAC domain-containing transcription factor	13
MYB transcription factor	13
Heat shock transcription factor	6
WRKY transcription factor	5
GRAS transcription factor	3
Growth-regulating factor	3
Homeobox domain transcription factor	2
bZIP transcription factor	2
Ethylene insensitive 3 transcription factor	1

level of two NAC TF encoded genes (TraesCS5D01G481200 and TraesCS5B01G480900) was most significant enhanced subjected to 24-h-freezing which showed the log2 value of fold changes as 8.52 and 7.48, respectively (Table 6). These two genes were confirmed to be the homologue of *TaNAC2-5A* which has been reported to play a role in plant freezing tolerance (Mao et al., 2012). Further experiments could be carried out to verify the functional role of other candidate TFs listed in Table 6.

Identification of genes associated with cell wall biosynthesis and modification

When subjected to freezing, plants could form a thick cell wall to resist low temperature stress. The GO analysis in our study also indicated that the expression of cell wall related genes was significantly modulated by freezing (Figure 3). Therefore, we have selected genes with a putative role in cell wall remodeling shared by J3 vs J1 and J4 vs J1 comparisons (Table 7). These genes were participated in the biosynthesis or modification of major cell wall components, such as cellulose, hemicellulose, and pectin. For instance, several genes encoding cellulose synthetic enzymes such as cellulose synthase and cellulose synthase-like proteins, endoglucanases, chitinase-like proteins and cobra-like proteins were identified differentially expressed (Table 7). In addition, genes encoding hemicellulose biosynthetic enzyme xyloglucan endo-transglycosylase constituted a large group and have been reported to play an important role in frost tolerance in Arabidopsis (Takahashi D, 2021). Our study indicated that the increased amounts of enzymes involved in cell wall biosynthesis and modification is in accordance with the cell wall thickening observed in wheat stem upon freezing.

Validation of gene expression by real time quantitative PCR analysis

We also performed qRT-PCR analysis to verify the accuracy and reproducibility of transcriptome profiles. According to the literature, six genes potentially involved in low temperature tolerance were selected for the analysis, such as zinc finger proteins (TraesCS6B01G246500 and TraesCS3A01G107200), protein kinase (TraesCS5B01G381500), actin depolymerizing factor (TraesCS5A01G478500), beta-amylase (TraesCS1A01G215500) and ABA-responsive protein (TraesCS5D01G503400) (Peng et al., 2015; Byun et al., 2021; Zhang et al., 2022). Our data showed that the expression pattern of selected genes obtained by qRT-PCR was highly consistent with RNA-Seq data, with the correlation coefficients (R^2) > 0.8 (Figure 5). These results support the reliability of the RNA-Seq analysis.

Discussion

Freezing injury during the reproductive phase of wheat frequently happens in spring, which has become the limiting factor of wheat production in China. To investigate the effect of freezing stress on wheat growth and reproduction, we performed the freezing treatment on Zhongmai8444 at the meiotic stage in a controlled growth condition. Transcriptomic analysis was subsequently carried out to elucidate the molecular mechanism underlying the frost tolerance of wheat plants.

Consistent with our previous study, Zhongmai8444 showed hypersensitivity to freezing stress at the meiotic stage (Wang et al., 2022). At this time, the developing pollen mother cells were at the meiosis phase and freezing temperature may cause the increase frequency of cellular abnormality of pollen cells. Therefore, wheat plants showed a decrease in seed setting after treated with freezing (Figure 1F, Table 1). Consistently, it has been reported that Australian wheat cultivars exhibited significant reduction in fertility when subjected to prolonged chilling temperature during meiosis (Barton et al., 2014). The decrease of grain number per spike and 1000-grain weights was observed when winter wheats were exposed to low temperature stress at booting stage (Zhang et al., 2019; Zhang et al., 2021). Results showed that altered sucrose metabolism and inhibited starch biosynthesis in young ear may lead to the reduction of yield. In addition, low temperature stress during floral development is known to cause yield losses in different crop plants such as rice (Li et al., 2022), sorghum (Wood et al., 2006), maize (Tranel et al., 2009), bell pepper (Mercado et al., 1997) and garlic (Shemesh Mayer et al., 2013). Stem injury and reduced plant height were also obvious in freezing-treated plants (Supplemental Figure S3, Figure 1G, Table 1). Vascular tissues in stem play an important role in transporting water, minerals and product of photosynthesis throughout the plants. Injury of stem and vascular tissue would inhibit the transportation of nutrients

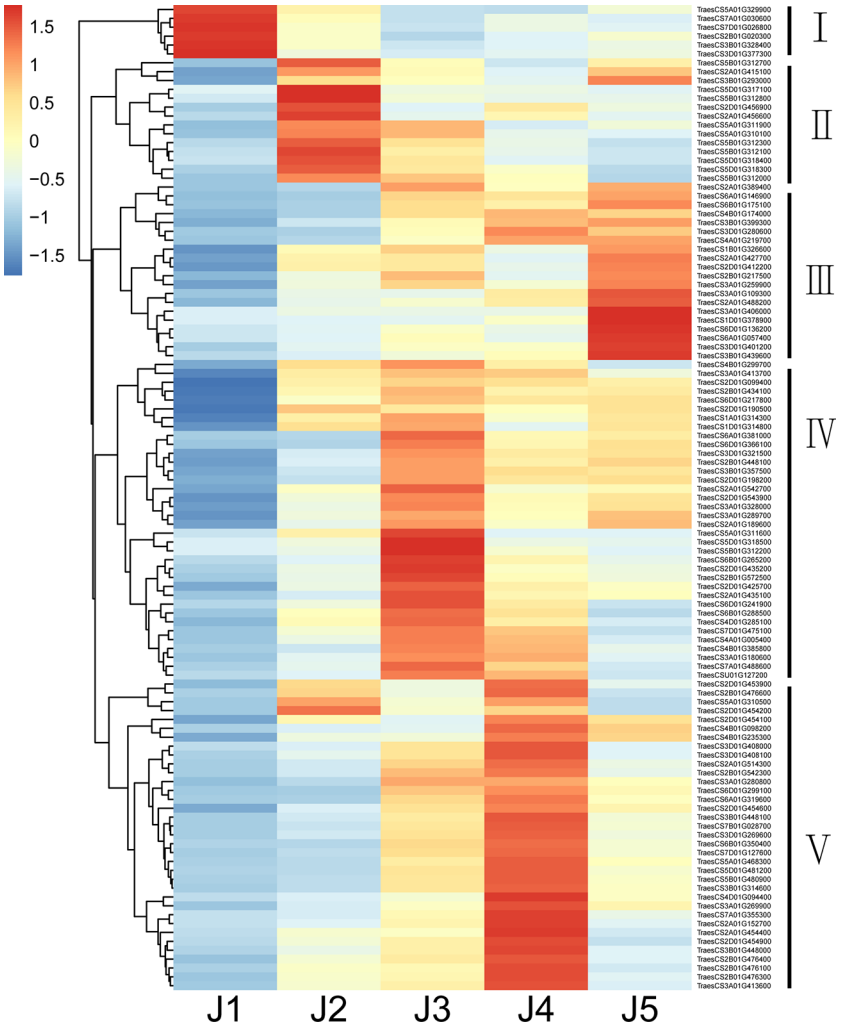

FIGURE 4
A heat map Showing the expression pattern of differentially expressed TF genes under freezing stress at different time points. Columns and rows in the heat map respectively represent the five time points of freezing treatment and common differentially expressed TFs. Color bars represent scaled FPKM of each TF gene.

required for plant growth and development. As a result, wheat plants exhibited reduced height and production.

Cell wall provides the structural integrity as well as the flexibility to a plant cell (Lampugnani et al., 2018). Our findings provide evidence supporting the remodeling of wheat cell wall under freezing stress. Under low temperature conditions, cell wall could help the dehydrated cells maintain the morphology by enhancing its mechanical strength and reduce the rate of cell dehydration by adjusting its structure (Johnson et al., 2018). Previous study demonstrated that chilling stress led to an increase of total cell wall amount as well as structural and compositional changes in cell wall during both cold acclimation and sub-zero acclimation (Takahashi et al., 2019). We identified a range of cell wall associated genes to be dramatically up regulated upon freezing stress by transcriptome analysis (Table 7). These genes were implicated in the metabolic events related to major cell wall component biosynthesis and may be critical for plant to resist freezing stress. For instance, Takahashi et al. (2021) suggested a potential role of Arabidopsis xyloglucan endotransglucosylase/hydrolase XTH19 in cell wall remodeling which influenced the freezing tolerance after low temperature acclimation.

To understand the molecular mechanism underlying freezing tolerance, we performed GO and KEGG enrichment analyses on identified DEGs. Our results showed that the plant hormone signal transduction was particularly affected by -2.5°C treatment, suggesting a critical role of phytohormone in conferring response of wheat to the freezing stress. Phytohormones are known to play a significant role in a wide range of adaptive responses to abiotic stresses (Peleg and Blumwald, 2011). When subjected to stresses, accumulation of

TABLE 6 Representative mostly up-regulated TFs common at all time points, shown as log2 value of fold changes.

Gene ID	Description	J2 vs J1	J3 vs J1	J4 vs J1	J5 vs J1
TraesCS5D01G481200	NAC domain-containing protein	3.99	7.45	8.52	6.95
TraesCS5B01G480900	NAC domain-containing protein	3.43	6.38	7.48	6.02
TraesCS6A01G146900	WRKY DNA-binding domain	3.95	6.95	7.13	7.50
TraesCS2D01G454900	Zinc-finger of the FCS-type	4.75	5.18	6.61	2.10
TraesCS7D01G127600	Ethylene-responsive transcription factor	2.70	5.28	6.18	4.67
TraesCS7B01G028700	Ethylene-responsive transcription factor	1.86	3.73	4.70	3.20
TraesCS4D01G094400	NAC domain-containing protein, putative	2.04	2.96	5.06	3.43
TraesCS3A01G280800	Heat shock factor	3.53	6.11	6.41	5.54
TraesCS6D01G299100	Ethylene-responsive transcription factor	6.60	12.28	12.90	11.97
TraesCS3D01G321500	Ethylene-responsive factor-like transcription factor	3.71	5.02	4.83	4.95

TABLE 7 Classification of cell wall related genes differentially expressed (|log2FoldChange| > 1 and padj < 0.05) under 24 h and 48 h freezing treatment.

Gene group	Gene function	Number
Glucan endo-1,3-beta-glucosidase	Beta-1,3-glucan degradation	34
Cellulose synthase and cellulose synthase-like protein	Cell wall biosynthesis	28
Xyloglucan endo-transglycosylase	Xyloglucan metabolism	14
Galactosyltransferase	Galactose biosynthesis	10
Cell wall invertase	Cell wall biosynthesis	10
Endoglucanase	Cellulose crystallization	9
Chitinase-like protein	Cellulose biosynthesis	5
Glucuronoxylan 4-O-methyltransferase-like protein	Xylan biosynthetic process	4
Pectin lyase-like protein	Pectin degradation	3
Cobra-like protein	Cellulose biosynthesis	3
Sucrose synthase	Cell wall biosynthesis	3
Beta-xylosidase	Xylan degradation	2
Alpha-L-arabinofuranosidase	Lignocellulose degradation	1
Endo-1,4-beta-xylanase	Xylan degradation	1
Rhamnogalacturonate lyase	Pectin degradation	1
Callose synthase	Callose biosynthesis	1
Xyloglucan fucosyltransferase	Xyloglucan biosynthesis	1

ABA could promote stomatal closure, enhance water balance, and induce antioxidant defense systems to alleviate oxidative injury (Lee and Luan, 2012). It has been reported that ABA regulated several ICE-CBF pathway-dependent genes, promoting plant's resistance to freezing (Knight et al., 2004). Furthermore, the involvement of ethylene signaling in low-temperature-stress response has been implicated in several studies (Zhang and Huang, 2010; Shi et al., 2012; Catalá et al., 2014), though its effect is debated. Other hormone such as GA also plays a role in plant responses to low-temperature stress and multiple phytohormones may crosstalk in modulating the expression of cold-responsive genes (Richter et al., 2013).

As the key regulator of transcription, TFs always play a critical role in mediating abiotic stress responses. In current study, we

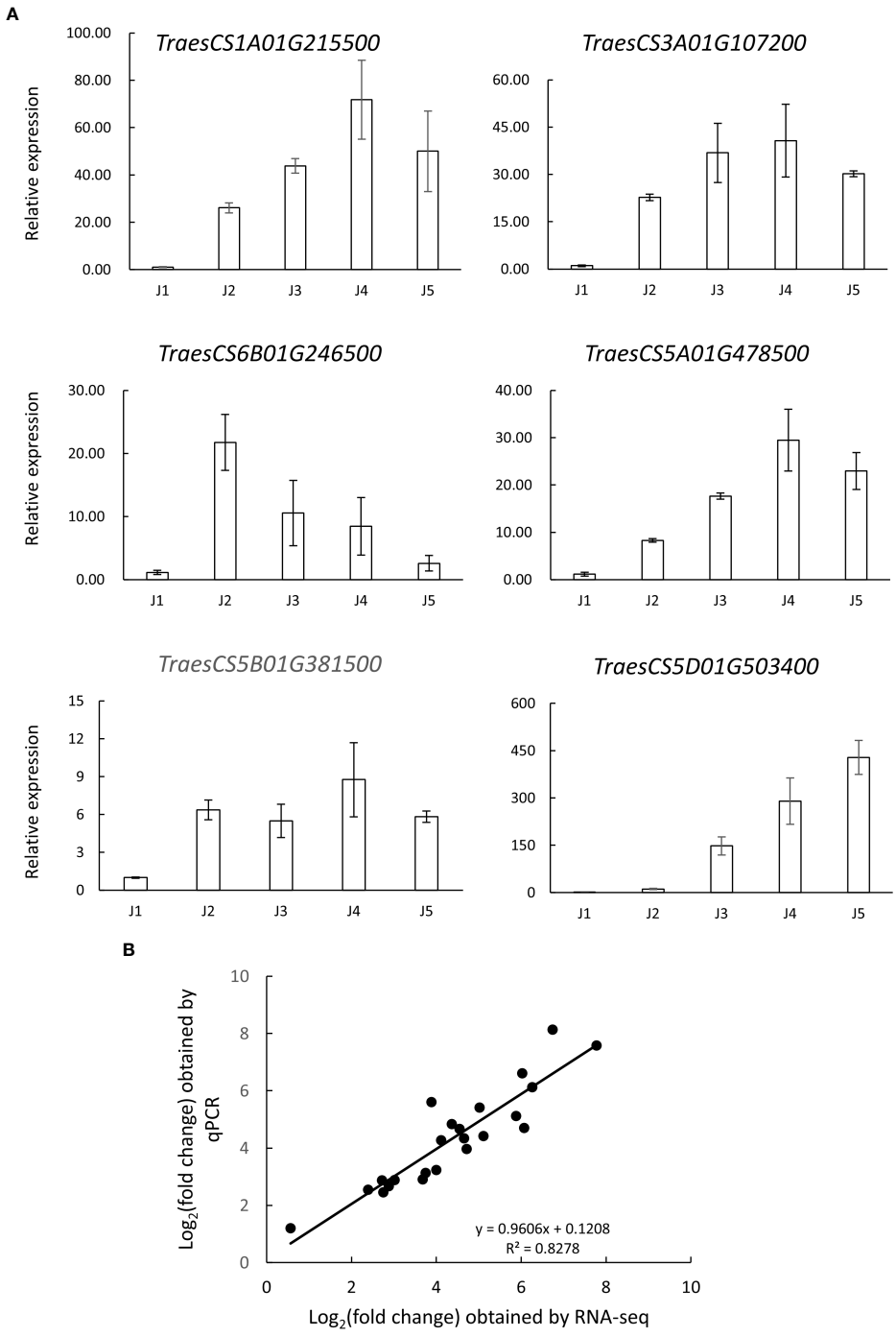

FIGURE 5
Verification of the expression pattern of selected genes *via* qRT-PCR analysis. **(A)** transcript levels of 6 selected genes in samples collected at different time points (J1-J5). The data are shown as means ± standard errors (SE) in three replicates. **(B)** Correlation analysis of the log2 of gene expression ratios obtained from RNA-seq data and qRT-PCR analysis.

demonstrated that most differentially expressed TF genes belong to AP2/ERF, Zinc finger and NAC family groups (Table 5, Table 6). The CBF transcription factors belong to the AP2/ERF superfamily and regulate a spectrum of cold-regulated (*COR*) genes. CBFs mediated signaling has been proposed to constitute the predominant cold signaling pathway in many plant species though it has not been well characterized (Park et al., 2015). In wheat, CBF14 and CBF15 TFs were identified to be linked to the frost-tolerance locus Fr-A2 and

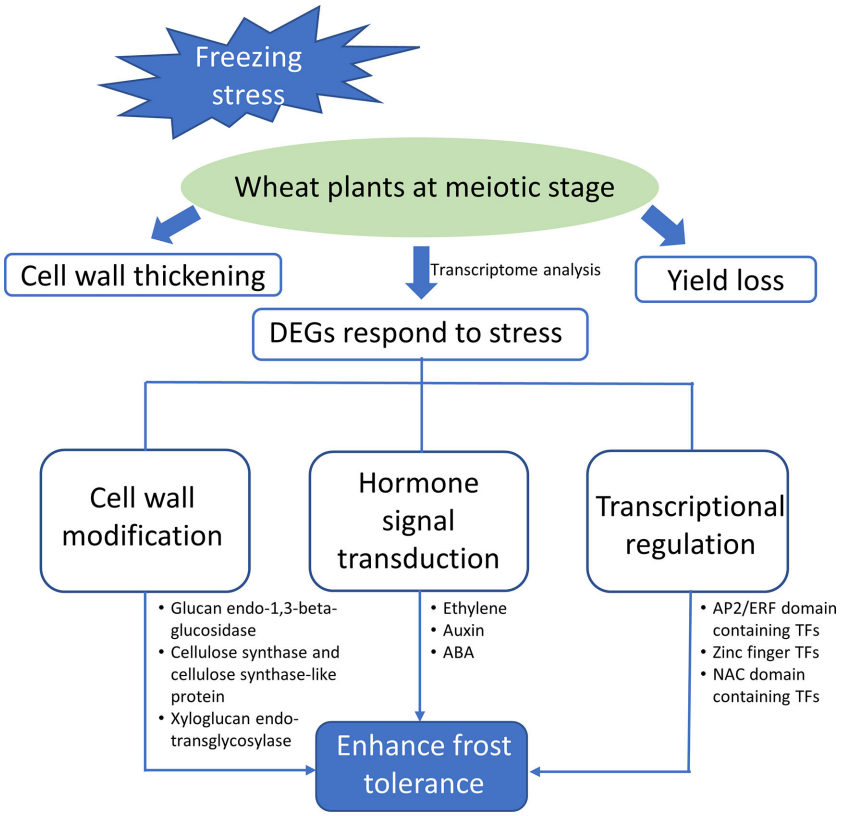

FIGURE 6
Schematic diagram showing the freezing induced changes of gene expression in wheat stems during meiosis. DEGs were mainly participated in pathways of cell wall modification, hormone signal transduction and transcriptional regulation to promote the freezing tolerance of plants.

positively regulate low-temperature-stress responses (Knox et al., 2008; Soltész et al., 2013). Zinc finger and NAC TFs play essential roles in response to various abiotic stresses and have been implicated in the resistance of freezing stress (Hao et al., 2011; Zhang et al., 2016). It has been reported that a C2H2-type zinc finger protein PhZFP1 could regulate cold stress tolerance in Petunia hybrida by modulating galactinol synthesis activity (Zhang et al., 2022). Overexpression of wheat *TaNAC2* gene in Arabidopsis resulted in the enhanced tolerance to multiple abiotic stress (Mao et al., 2012).

Furthermore, based on the listed mostly up-regulated and down-regulated DEGs (Table 3; Table 4), we proposed several other genes were also participated in freezing responsive process, such as genes encoding dehydrins, actin depolymerizing factors, LEA proteins and beta-amylase. Dehydrins are a distinct group of LEA proteins that exhibited high hydrophilicity and were proved to be an important factor to regulated plant freezing tolerance (Ndong et al., 2002). Overexpression of a dehydrin gene *ShDHN* resulted in the improved freezing tolerance in tomato (Liu et al., 2015). As the best characterized LEA protein, COR15A resided at the membrane surface during dehydration and stabilized cell membranes under freezing stress (Bremer et al., 2017a; Bremer et al., 2017b). In addition, it has been suggested that the actin depolymerizing factor protein may be required for the cytoskeletal arrangement during cold acclimation and important for plants to tolerate freezing (Byun et al., 2021). Our results provide the potential candidates associated with several metabolic pathways involved in freezing responses. Further research is needed to verify the functional roles of these predicted genes and employ them in future breeding program.

In this study, we evaluated the effect of freezing stress on wheat growth and development during meiosis phase. A model for wheat plants respond to freezing is proposed (Figure 6). Once subjecting to sub-zero temperature, a series of stress-related genes become active to minimize the damage of freezing and maintain plant's normal growth, including those encoding TFs, hormone signaling elements, and enzymes associated with cell wall remodeling. The functional validation of these candidate genes will help us better understand the mechanism underlying freezing tolerance and hold great potential for molecular breeding in spring freezing-tolerant wheat varieties.

Data availability statement

The datasets presented in this study can be found in online repositories. All the raw data have been deposited in the NCBI

Sequence Read Archive (SRA) database under BioProject accession number PRJNA901148.

Author contributions

Conceptualization and supervision, GS, JM, XLiu and YF; methodology, JW and WP; investigation, JW, WP, BZ, XLW, XNW, XYW; bioinformatic analyses, DY and JW; data curation, DY; manuscript preparation, DY, JW and WP; writing-review and editing, GS and DY. All authors contributed to the article and approved the submitted version.

Funding

This project was supported by the National Natural Science Foundation of China (32201806), the China Agriculture Research System of MOF and MARA (CARS-03), and the National Key R & D Program of China (2021YFD12006).

Conflict of interest

The authors declare that the research was conducted in the absence of any commercial or financial relationships that could be construed as a potential conflict of interest.

Publisher's note

All claims expressed in this article are solely those of the authors and do not necessarily represent those of their affiliated organizations, or those of the publisher, the editors and the reviewers. Any product that may be evaluated in this article, or claim that may be made by its manufacturer, is not guaranteed or endorsed by the publisher.

Supplementary material

The Supplementary Material for this article can be found online at: https://www.frontiersin.org/articles/10.3389/fpls.2022.1099677/full#supplementary-material

References

Barton, D. A., Cantrill, L. C., Law, A. M., Phillips, C. G., Sutton, B. G., and Overall, R. L. (2014). Chilling to zero degrees disrupts pollen formation but not meiotic microtubule arrays in T riticum aestivum l. *Plant Cell Environ.* 37, 2781–2794. doi: 10.1111/pce.12358

Bilska-Kos, A., Solecka, D., Dziewulska, A., Ochodzki, P., Jończyk, M., Bilski, H., et al. (2016). Low temperature caused modifications in the arrangement of cell wall pectins due to changes of osmotic potential of cells of maize. *Protoplasma* 254, 713–724. doi: 10.1007/s00709-016-0982-y

Bolt, S., Zuther, E., Zintl, S., Hincha, D. K., and Schmülling, T. (2017). ERF105 is a transcription factor gene of arabidopsis thaliana required for freezing tolerance and cold acclimation. *Plant Cell Environ.* 40, 108–120. doi: 10.1111/pce.12838

Bremer, A., Kent, B., Hauß, T., Thalhammer, A., Yepuri, N. R., Darwish, T. A., et al. (2017a). Intrinsically disordered stress protein COR15A resides at the membrane surface during dehydration. *Biophys. J.* 113, 572–579. doi: 10.1016/j.bpj.2017.06.027

Bremer, A., Wolff, M., Thalhammer, A., and Hincha, D. K. (2017b). Folding of intrinsically disordered plant LEA proteins is driven by glycerol-induced crowding and the presence of membranes. *FEBS J.* 284, 919–936. doi: 10.1111/febs.14023

Byun, M. Y., Cui, L. H., Lee, A., Oh, H. G., Yoo, Y.-H., Lee, J., et al. (2021). Abiotic stress-induced actin-depolymerizing factor 3 from deschampsia antarctica enhanced cold tolerance when constitutively expressed in rice. *Front. Plant Sci.* 12. doi: 10.3389/fpls.2021.734500

Catalá, R., López-Cobollo, R., Mar Castellano, M., Angosto, T., Alonso, J. M., Ecker, J. R., et al. (2014). The arabidopsis 14-3-3 protein RARE COLD INDUCIBLE 1A links low-temperature response and ethylene biosynthesis to regulate freezing tolerance and cold acclimation. *Plant Cell* 26, 3326–3342. doi: 10.1105/tpc.114.127605

Chen, X., Lin, T., Lin, F., Zhang, Y., Su, H., Hu, Y., et al. (2020). Research progress on damage mechanism and prevention and control measures of late spring coldness of wheat in huanghuai region. *J. Triticeae Crops* 40, 243–250. doi: 10.7606/ji.ssn.1009-1041.2020.02.14. (In Chinese with English abstract).

Ding, Y., Shi, Y., and Yang, S. (2019). Advances and challenges in uncovering cold tolerance regulatory mechanisms in plants. *New Phytol.* 222, 1690–1704. doi: 10.1111/nph.15696

Draeger, T., and Moore, G. (2017). Short periods of high temperature during meiosis prevent normal meiotic progression and reduce grain number in hexaploid wheat (*Triticum aestivum l.*). *Theor. Appl. Genet.* 130, 1785–1800. doi: 10.1007/s00122-017-2925-1

Frederiks, T. M., Christopher, J. T., Sutherland, M. W., and Borrell, A. K. (2015). Post-head-emergence frost in wheat and barley: Defining the problem, assessing the damage, and identifying resistance. *J. Exp. Bot.* 66, 3487–3498. doi: 10.1093/jxb/erv088

Guo, W. L., Chen, R. G., Gong, Z. H., Yin, Y. X., Ahmed, S. S., and He, Y. M. (2012). Exogenous abscisic acid increases antioxidant enzymes and related gene expression in pepper (Capsicum annuum) leaves subjected to chilling stress. *Genet. Mol. Res.* 11, 4063–4080. doi: 10.4238/2012.September.10.5

Hao, Y. J., Wei, W., Song, Q. X., Chen, H. W., Zhang, Y. Q., Wang, F., et al. (2011). Soybean NAC transcription factors promote abiotic stress tolerance and lateral root formation in transgenic plants. *Plant J.* 68, 302–313. doi: 10.1111/j.1365-313X.2011.04687.x

Huang, J., Zhao, X., and Chory, J. (2019). The arabidopsis transcriptome responds specifically and dynamically to high light stress. *Cell Rep.* 29, 4186–4199, e4183. doi: 10.1016/j.celrep.2019.11.051

Hu, Y., Jiang, Y., Han, X., Wang, H., Pan, J., and Yu, D. (2017). Jasmonate regulates leaf senescence and tolerance to cold stress: crosstalk with other phytohormones. *J. Exp. Bot.* 68, 1361–1369. doi: 10.1093/jxb/erx004

Hu, Y., Jiang, L., Wang, F., and Yu, D. (2013). Jasmonate regulates the inducer of CBF expression-c-repeat binding factor/DRE binding factor1 cascade and freezing tolerance in arabidopsis. *Plant Cell* 25, 2907–2924. doi: 10.1105/tpc.113.112631

Jian, C., Zeng, B., Zhang, M., Shaojun, X., and Wang, G. (2014). Dynamic transcriptome landscape of maize embryo and endosperm development. *Plant Physiol.* 166, 252–264. doi: 10.1104/pp.114.240689

Johnson, K. L., Gidley, M. J., Bacic, A., and Doblin, M. S. (2018). Cell wall biomechanics: a tractable challenge in manipulating plant cell walls 'fit for purpose'! *Curr. Opin. Biotechnol.* 49, 163–171. doi: 10.1016/j.copbio.2017.08.013

Kim, T. E., Kim, S. K., Han, T. J., Lee, J. S., and Chang, S. C. (2002). ABA and polyamines act independently in primary leaves of cold-stressed tomato (Lycopersicon esculentum). *Physiol. Plant* 115, 370–376. doi: 10.1034/j.1399-3054.2002.1150306.x

Kim, D., Langmead, B., and Salzberg, S. L. (2015). HISAT: A fast spliced aligner with low memory requirements. *Nat. Methods* 12, 357–360. doi: 10.1038/nmeth.3317

Knight, H., Zarka, D. G., Okamoto, H., Thomashow, M. F., and Knight, M. R. (2004). Abscisic acid induces CBF gene transcription and subsequent induction of cold-regulated genes *via* the CRT promoter element. *Plant Physiol.* 135, 1710–1717. doi: 10.1104/pp.104.043562

Knox, A. K., Li, C., Vágújfalvi, A., Galiba, G., Stockinger, E. J., and Dubcovsky, J. (2008). Identification of candidate CBF genes for the frost tolerance locus fr-a m 2 in triticum monococcum. *Plant Mol. Biol.* 67, 257–270. doi: 10.1007/s11103-008-9316-6

Lampugnani, E. R., Khan, G. A., Somssich, M., and Persson, S. (2018). Building a plant cell wall at a glance. *J. Cell. Sci.* 131, jcs207373. doi: 10.1242/jcs.207373

Le, M. Q., Pagter, M., and Hincha, D. K. (2015). Global changes in gene expression, assayed by microarray hybridization and quantitative RT-PCR, during acclimation of three arabidopsis thaliana accessions to sub-zero temperatures after cold acclimation. *Plant Mol. Biol.* 87, 1. doi: 10.1007/s11103-014-0256-z

Lee, S. C., and Luan, S. (2012). ABA signal transduction at the crossroad of biotic and abiotic stress responses. *Plant Cell Environ.* 35, 53–60. doi: 10.1111/j.1365-3040.2011.02426.x

Liu, F., Wan, Y., Cao, W., Zhang, Q., Li, Y., Li, Y., et al. (2021). Advances on identification of wheat cold tolerance in spring. *J. Plant Genet. Res.* 22, 1193–1199. doi: 10.13430/j.cnki.jpgr.20210113001

Liu, H., Yu, C., Li, H., Ouyang, B., Wang, T., Zhang, J., et al. (2015). Overexpression of ShDHN, a dehydrin gene from solanum habrochaites enhances tolerance to multiple abiotic stresses in tomato. *Plant Sci.* 231, 198–211. doi: 10.1016/j.plantsci.2014.12.006

Li, J., Zhang, Z., Chong, K., and Xu, Y. (2022). Chilling tolerance in rice: Past and present. *J. Plant Physiol.* 268, 153576. doi: 10.1016/j.jplph.2021.153576

Love, M. I., Huber, W., and Anders, S. (2014). Moderated estimation of fold change and dispersion for RNA-seq data with DESeq2. *Genome Biol.* 15, 550. doi: 10.1186/s13059-014-0550-8

Mao, X., Zhang, H., Qian, X., Li, A., Zhao, G., and Jing, R. (2012). TaNAC2, a NAC-type wheat transcription factor conferring enhanced multiple abiotic stress tolerances in arabidopsis. *J. Exp. Bot.* 63, 2933–2946. doi: 10.1093/jxb/err462

Mercado, J., Mar Trigo, M., Reid, M., Valpuesta, V., and Quesada, M. (1997). Effects of low temperature on pepper pollen morphology and fertility: evidence of cold induced exine alterations. *J. Horti. Sci.* 72, 317–326. doi: 10.1080/14620316.1997.11515518

Nakabayashi, R., and Saito, K. (2015). Integrated metabolomics for abiotic stress responses in plants. *Curr. Opin. Plant Biol.* 24, 10–16. doi: 10.1016/j.pbi.2015.01.003

Ndong, C., Danyluk, J., Wilson, K. E., Pocock, T., Huner, N. P., and Sarhan, F. (2002). Cold-regulated cereal chloroplast late embryogenesis abundant-like proteins. molecular characterization and functional analyses. *Plant Physiol.* 129, 1368–1381. doi: 10.1104/pp.001925

Ou, X., and Wang, Y. (2019). Preliminary study on wheat breading for late spring coldness tolerance in south of huanghuai region. *J. Trit. Crops* 39, 560–566. doi: 10.7606/j.issn.1009-1041.2019.05.07

Panter, P. E., Kent, O., Dale, M., Smith, S. J., Skipsey, M., Thorlby, G., et al. (2019). MUR1-mediated cell-wall fucosylation is required for freezing tolerance in arabidopsis thaliana. *New Phytol.t* 224, 1518–1531. doi: 10.1111/nph.16209

Park, S., Lee, C. M., Doherty, C. J., Gilmour, S. J., Kim, Y., and Thomashow, M. F. (2015). Regulation of the arabidopsis CBF regulon by a complex low-temperature regulatory network. *Plant J.* 82, 193–207. doi: 10.1111/tpj.12796

Parrotta, L., Faleri, C., Guerriero, G., and Cai, G. (2019). Cold stress affects cell wall deposition and growth pattern in tobacco pollen tubes. *Plant Sci.* 283, 329–342. doi: 10.1016/j.plantsci.2019.03.010

Peleg, Z., and Blumwald, E. (2011). Hormone balance and abiotic stress tolerance in crop plants. *Curr. Opin. Plant Biol.* 14, 290–295. doi: 10.1016/j.pbi.2011.02.001

Peng, T., Zhu, X., Duan, N., and Liu, J. H. (2015). PtrBAM1, a β-amylase-coding gene of poncirus trifoliata, is a CBF regulon member with function in cold tolerance by modulating soluble sugar levels. *Plant Cell Environ.* 37, 2754–2767. doi: 10.1111/pce.12384

Richter, R., Bastakis, E., and Schwechheimer, C. (2013). Cross-repressive interactions between SOC1 and the GATAs GNC and GNL/CGA1 in the control of greening, cold tolerance, and flowering time in arabidopsis. *Plant Physiol.* 162, 1992–2004. doi: 10.1104/pp.113.219238

Sga, B., Quan, X. A., Dm, A., Wz, A., Zx, A., Mz, A., et al. (2019). Transcriptomics profiling in response to cold stress in cultivated rice and weedy rice. *Gene* 685, 96–105. doi: 10.1016/j.gene.2018.10.066

Sharabi-Schwager, M., Samach, A., and Porat, R. (2010). Overexpression of the CBF2 transcriptional activator in arabidopsis suppresses the responsiveness of leaf tissue to the stress hormone ethylene. *Plant Biol.* 12, 630–638. doi: 10.1111/j.1438-8677.2009.00255.x

Shemesh Mayer, E., Winiarczyk, K., Błaszczyk, L., Kosmala, A., Rabinowitch, H. D., and Kamenetsky, R. (2013). Male Gametogenesis and sterility in garlic (Allium sativum l.): barriers on the way to fertilization and seed production. *Planta* 237, 103–120. doi: 10.1007/s00425-012-1748-1

Shi, Y., Tian, S., Hou, L., Huang, X., Zhang, X., Guo, H., et al. (2012). Ethylene signaling negatively regulates freezing tolerance by repressing expression of CBF and type-a ARR genes in arabidopsis. *Plant Cell* 24, 2578–2595. doi: 10.1105/tpc.112.098640

Soltész, A., Smedley, M., Vashegyi, I., Galiba, G., Harwood, W., and Vágújfalvi, A. (2013). Transgenic barley lines prove the involvement of TaCBF14 and TaCBF15 in the cold acclimation process and in frost tolerance. *J. Exp. Bot.* 64, 1849–1862. doi: 10.1093/jxb/ert050

Sugiyama, S., and Shimazaki, T. (2007). Increased cell-wall mass and resistance to freezing and snow mold during cold acclimation of winter wheat under field conditions. *Plant Prod. Sci.* 10, 383–390. doi: 10.1626/pps.10.383

Su, C. F., Wang, Y. C., Hsieh, T. H., Lu, C. A., and Yu, T. (2010). A novel MYBS3-dependent pathway confers cold tolerance in rice. *Plant Physiol.* 153, 145–158. doi: 10.1104/pp.110.153015

Takahashi, D., Gorka, M., Erban, A., Graf, A., Kopka, J., Zuther, E., et al. (2019). Both cold and sub-zero acclimation induce cell wall modification and changes in the extracellular proteome in arabidopsis thaliana. *Sci. Rep.* 9, 1–15. doi: 10.1038/s41598-019-38688-3

Takahashi, J. K., Hao, P., Tuong, T., Erban, A, Sampathkumar, A, Bacic, A, et al. (2021). Cell wall modification by the xyloglucan endotransglucosylase/hydrolase XTH19 influences freezing tolerance after cold and sub-zero acclimation. *Plant Cell Environ.* 44, 915–930. doi: 10.1111/pce.13953

Tranel, D., Knapp, A., and Perdomo, A. (2009). Chilling effects during maize tassel development and the lack of compensational plasticity. *Crop Sci.* 49, 1852–1858. doi: 10.1111/pce.13953

Vigani, G., Bohic, S., Faoro, F., Vekemans, B., Vincze, L., and Terzano, R. (2018). Cellular fractionation and nanoscopic X-ray fluorescence imaging analyses reveal changes of zinc distribution in leaf cells of iron-deficient plants. *Front. Plant Sci.* 9, 1112. doi: 10.3389/fpls.2018.01112

Wang, J., Liu, Y., Yao, D., Zou, J., Xiao, S., and Sun, G. (2022). Identification on sensitivity of wheat to low temperature at reproductive stages. *Crop J.* 48, 1721–1729. doi: 10.3724/SP.J.1006.2022.11045.

Wang, B., Liu, C., Zhang, D., He, C., and Li, Z. (2019). Effects of maize organ-specific drought stress response on yields from transcriptome analysis. *BMC Plant Biol.* 19, 335. doi: 10.1186/s12870-019-1941-5

Wang, X., Wu, D., Yang, Q., Zeng, J., Jin, G., Chen, Z.-H., et al. (2016). Identification of mild freezing shock response pathways in barley based on transcriptome profiling. *Front. Plant Sci.* 7. doi: 10.3389/fpls.2016.00106

Willick, I. R., Takahashi, D., Fowler, D. B., Uemura, M., and Tanino, K. K. (2017). Tissue-specific changes in apoplastic proteins and cell wall structure during cold acclimation of winter wheat crowns. *J. Exp. Bot.* 10, 1221–1234. doi: 10.1093/jxb/erx450

Wood, A., Tan, D., Mamun, E., and Sutton, B. (2006). Sorghum can compensate for chilling-induced grain loss. *J. Agron. Crop Sci.* 192, 445–451. doi: 10.1111/j.1439-037X.2006.00233.x

Yang, L., Gao, C., and Jiang, L. (2022). Leucine-rich repeat receptor-like protein kinase AtORPK1 promotes oxidative stress resistance in an AtORPK1-AtKAPP mediated module in arabidopsis. *Plant Sci.* 315, 111147. doi: 10.1016/j.plantsci.2021.111147

Yang, L., Smyth, G. K., and Wei, S. (2014). featureCounts: an efficient general purpose program for assigning sequence reads to genomic features. *Bioinformatics* 30, 923–930. doi: 10.1093/bioinformatics/btt656

Yang, Y., Yao, N., Jia, Z., Duan, J., Chen, F., Sang, Z., et al. (2016). Effect of exogenous abscisic acid on cold acclimation in two magnolia species. *Biol. Plant* 60, 555–562. doi: 10.1007/s10535-016-0623-5

Yu, J., Cang, J., Lu, Q., Fan, B., Xu, Q., Li, W., et al. (2020). ABA enhanced cold tolerance of wheat 'dn1'via increasing ROS scavenging system. *Plant Signal Behav.* 15, 1780403. doi: 10.1080/15592324.2020.1780403

Yu, G., Wang, L. G., Han, Y., and He, Q. Y. (2012). clusterProfiler: An r package for comparing biological themes among gene clusters. *Omics* 16, 284–287. doi: 10.1089/omi.2011.0118

Zadoks, J. C., Chang, T. T., and Konzak, C. F. (1974). A decimal code for the growth stages of cereals. *Weed Res.* 14, 415–421. doi: 10.1111/j.1365-3180.1974.tb01084.x

Zhang, Z., and Huang, R. (2010). Enhanced tolerance to freezing in tobacco and tomato overexpressing transcription factor TERF2/LeERF2 is modulated by ethylene biosynthesis. *Plant Mol. Biol.* 73, 241–249. doi: 10.1007/s11103-010-9609-4

Zhang, H., Sun, Z., Feng, S., Zhang, J., Zhang, F., Wang, W., et al. (2022). The C2H2-type zinc finger protein PhZFP1 regulates cold stress tolerance by modulating galactinol synthesis in petunia hybrida. *J. Exp. Bot.* 73, 6434–6448. doi: 10.1093/jxb/erac274

Zhang, W., Wang, J., Huang, Z., Mi, L., Xu, K., Wu, J., et al. (2019). Effects of low temperature at booting stage on sucrose metabolism and endogenous hormone contents in winter wheat spikelet. *Front. Plant Sci.* 10. doi: 10.3389/fpls.2019.00498

Zhang, L., Zhang, L., Xia, C., Zhao, G., Jia, J. , and Kong, X. (2016). The novel wheat transcription factor TaNAC47 enhances multiple abiotic stress tolerances in transgenic plants. *Front. Plant Sci.* 6 1174. doi: 10.3389/fpls.2015.01174

Zhang, W., Zhao, Y., Li, L., Xu, X., Yang, L., Luo, Z., et al. (2021). The effects of short-term exposure to low temperatures during the booting stage on starch synthesis and yields in wheat grain. *Front. Plant Sci.* 12. doi: 10.3389/fpls.2021.684784

Zhao, Y., Zhou, M., Xu, K., Li, J., Li, S., Zhang, S., et al. (2019). Integrated transcriptomics and metabolomics analyses provide insights into cold stress response in wheat. *Crop J.* 7, 857–866. doi: 10.1016/j.cj.2019.09.002

frontiers | Frontiers in Plant Science

TYPE Original Research
PUBLISHED 20 June 2023
DOI 10.3389/fpls.2023.1218962

OPEN ACCESS

EDITED BY
Zemin Wang,
Gansu Agricultural University, China

REVIEWED BY
Xin Jin,
Gansu Agricultural University, China
Xinna Liu,
Chinese Academy of Sciences (CAS), China

*CORRESPONDENCE
Xi Zhu
zhuxi@catas.cn
Yu Zhang
zhangyu@catas.cn

RECEIVED 08 May 2023
ACCEPTED 06 June 2023
PUBLISHED 20 June 2023

CITATION
Zhu X, Duan H, Zhang G, Jin H, Xu C, Chen S, Zhou C, Chen Z, Tang J and Zhang Y (2023) *StMAPK1* functions as a thermos-tolerant gene in regulating heat stress tolerance in potato (*Solanum tuberosum*). *Front. Plant Sci.* 14:1218962. doi: 10.3389/fpls.2023.1218962

StMAPK1 functions as a thermos-tolerant gene in regulating heat stress tolerance in potato (*Solanum tuberosum*)

Xi Zhu[1,2*], Huimin Duan[1], Guodong Zhang[3], Hui Jin[1], Chao Xu[4], Shu Chen[1], Chuanmeng Zhou[5], Zhuo Chen[1], Jinghua Tang[1] and Yu Zhang[1*]

[1]Key Laboratory of Tropical Fruit Biology, Ministry of Agriculture and Rural Affairs of China/Key Laboratory of Hainan Province for Postharvest Physiology and Technology of Tropical Horticultural Products, South Subtropical Crops Research Institute, Chinese Academy of Tropical Agricultural Sciences, Zhanjiang, China, [2]National Key Laboratory for Tropical Crop Breeding, Sanya Research Institute, Chinese Academy of Tropical Agricultural Sciences, Sanya, China, [3]Department of Biology, Xinzhou Normal University, Xinzhou, China, [4]Institute of Horticultural Sciences, Jiangxi Academy of Agricultural Sciences, Nanchang, China, [5]Grain Crop Research Institute, Yulin Academy of Agricultural Sciences, Yulin, China

Background and aims: Mitogen-activated protein kinases (MAPKs) have been reported to respond to various stimuli including heat stress. This research aimed to investigate whether *StMAPK1* is implicated in the transduction of the heat stress signal to adapt heat stress as a thermos-tolerant gene.

Materials and methods: Potato plants were cultivated under mild (30°C) and acute (35°C) heat stress conditions to analyze mRNA expression of *StMAPKs* and physiological indicators. *StMAPK1* was up-regulated and down-regulated by transfection. Subcellular localization of StMAPK1 protein was observed by fluorescence microscope. The transgenic potato plants were assayed for physiological indexes, photosynthesis, cellular membrane integrity, and heat stress response gene expression.

Results: Heat stress altered the expression prolife of *StMAPKs*. *StMAPK1* overexpression changed the physiological characteristics and phenotypes of potato plants under heat stresses. *StMAPK1* mediates photosynthesis and maintains membrane integrity of potato plants in response to heat stress. Stress response genes (*StP5CS*, *StCAT*, *StSOD*, and *StPOD*) in potato plants were altered by *StMAPK1* dysregulation. mRNA expression of heat stress genes (*StHSP90*, *StHSP70*, *StHSP20*, and *StHSFA3*) was affected by *StMAPK1*.

Conclusions: *StMAPK1* overexpression increases the heat-tolerant capacity of potato plants at the morphological, physiological, molecular, and genetic levels.

KEYWORDS

heat stress, potato, mitogen-activated protein kinase 1, phenotypes, photosynthesis

Highlights

1. *StMAPK1* is increasingly expressed in potato plants in response to heat stress;
2. Elevated *StMAPK1* overexpression maintains physiological characteristics and growth phenotypes of potato plants;
3. *StMAPK1* is involved in protecting photosynthesis and membrane integrity against heat stresses.

Introduction

Climate change and global warming confer adverse effects on the crop growth and sustainable food development worldwide (Chen et al., 2020; Zandalinas et al., 2021). High temperature is one of the most predominant uncontrollable factors affecting potato yield (Handayani et al., 2019; Lee et al., 2020). Of particular, extreme heat negatively affects plant growth and crop yields, posing a significant threat to sustainable crop production. Continued greenhouse gas emissions will lead to further temperature increases, which lead to increased evaporation. This negative impact on crop yields may be aggravated in future. As consequence, the development of heat-stressed potato plants via genetic transformation is necessary to counter the negative impact of high temperature. In this scenario, identification of thermos-tolerant genes and understanding of functional mechanisms may facilitate the breeding of thermos-tolerant cultivars.

Potato (*Solanum tuberosum* L.) is the critical agricultural crop, being the third most significant crop after rice (*Oryza sativa*) and wheat (*Triticum* spp.). Additionally, high temperature negatively affects carbon synthesis (Wolf et al., 1991), photosynthesis (Wolf et al., 1990), biomass accumulation (Yubi et al., 2019), and sucrose translocation to tubers (Arreguin-Lozano and Bonner, 1949). High temperature delays the process of tuber formation and bulking (Menzel, 1983), contributes to tuber deformities and necrosis of the cultivated potato crop (Rykaczewska, 2015), and ultimately increases the risk in yield losses or quality decrease (Kim et al., 2017). In response to heat stress, plants have evolved to exhibit different strategies at the molecular, physiological, and morphological levels. Heat stress predisposes potato to oxidative stress, however, heat-tolerant potato plants display elevated antioxidant enzyme activity and altered secondary metabolism in response to heat stress (Almeselmani et al., 2006; Fogelman et al., 2019). It is still not fully understood about the mechanism by which potato plants perceive the initial heat stress and promptly respond to the high temperature at the molecular levels. The elucidation of such molecular mechanism may provide novel insights into the recognition of specific traits of potato plants responding to extreme hot climates.

Eukaryotic mitogen-activated protein kinase (MAPK or MPK) cascades play roles in relaying environmental and developmental signals into intracellular responses. Mitogen-activated protein kinases (MAPKs or MPKs) included in MAPK cascades are active in developmental processes and act in response to biotic and abiotic stresses. MAPKs are of major importance for transducing the heat stress signal to adapt to elevated temperatures (Link et al., 2002; Suri and Dhindsa, 2008). Genome sequence has identified 22 genes possibly encoding MAPKs in potato plants (Zaynab et al., 2021; Majeed et al., 2023). However, we have previously identified 15 *MAPK* genes in potato plant after aligning sequences from NCBI (Zhu et al., 2021a). The multiple sequence alignment of the conserved amino acid motif TxY divided *MAPKs* into 5 groups (Zaynab et al., 2021; Majeed et al., 2023). It has been confirmed that *MAPK1* belonging to Group B plays a positive role in response to heat stress in *Arabidopsis thaliana* (Wu et al., 2015). However, there is little knowledge of information about the molecular biological function of *MAPK1* in potato plants in response to heat stress.

Up to now, limited knowledge of heat tolerance mechanism hampered the efforts of enhancing heat stress tolerance of potatoes either by conventional or new approaches. Better understanding of key genes and overall network of genes with a role in potato thermotolerance is needed. Mitogen-activated protein kinases have been reported to respond to various stimuli including heat stress (Lin et al., 2021; Majeed et al., 2022). In this study, we aimed to investigate whether *StMAPK1* is implicated in the transduction of the heat stress signal to adapt heat stress as a thermos-tolerant gene.

Materials and methods

Plant growth and heat stress treatment

To analyze whether the expression profile of *StMAPKs* genes was affected by heat stress, Potato (*Solanum tuberosum* L.) cultivar "Atlantic" was cultivated under mild (30°C) and acute (35°C) heat stress conditions. Potato plants were *in vitro* planted in Murashige and Skoog (MS) medium (pH ranging among 5.8-6.0) in supplement with 3% sucrose for seedling growth or 8% sucrose for tuber generation. Potato plants were cultivated in a biotron at 22°C/15°C (day/night) with a 16-h photoperiod (2,800 Lux) and an air humidity of 50% (Zhanjiang, Guangzhou, China). Potato tubers with a sprouted bud of 1 mm in height were transferred into soil and vermiculite (1:1, v/v) pots measuring 26 cm × 27 cm × 18 cm and cultured for 5 weeks. The soil moisture remained at 70%-75%.

Heat stress is often defined as the rise in temperature beyond a threshold level for a period of time sufficient to cause irreversible damage to plant growth and development. In general, a transient elevation in temperature, usually 10-15°C above ambient, is considered heat stress. Hence, we chose 30°C and 35°C to study the response of potato plants to heat stress. The plants were cultivated under mild (30°C) and acute (35°C) heat stress conditions for 0 h, 1 h, 3 h, 6 h, 12 h, 24 h and 48 h, and the leaves were collected for detecting mRNA expression and physiological indicators. Plant height, fresh weight, dry weight, root fresh weight, and root dry weight were recorded 5 weeks after heat stress treatment.

For the quantitation of *StMAPKs* expression, there were 126 seedlings (1 line × 2 heat treatments × 7 different time periods × 3 replications × 3 pots); For the quantitation of heat-responsive genes, there were 630 seedlings (7 lines × 2 heat treatments × 5 different time periods × 3 replications × 3 pots); For the examination of physiological and photosynthetic indexes, there were 630 seedlings (7 lines × 2 heat treatments × 5 different time periods × 3 replications × 3 pots);

Plasmid construction and transformation

To develop *StMAPK1*-transgenic potato plants (OE for short), StMAPK1 protein-encoding region (GeneBank ID: XM_015312004.1) was amplified and ligated into pBI121-EGFP plasmid using the following primers: forward, 5'-CTCGAGATGGAGGCAAGTTTAGGTGATC-3' and reverse 5'-GTCGACGTGAGTTGGATCTGGATTAAAG-3', provided by Bioeditas (Shaanxi, China) according to a previous method (Li et al., 2020). The constructed plasmid was introduced into *Agrobacterium tumefaciens* strains LBA4404, followed by infecting the potato tuber according to Si's method (Si et al., 2003). In short, 12-20 week-old micro-tubers were cut into 1-2 mm discs, and submerged in 20 mL of bacterial solution for 10 min. Then the discs were transferred into shoot regeneration medium, sealed with parafilm and incubated for 2 days in dark at 26°C. *StMAPK1*-transgenic potato plants were selected using 75 mg/L of kanamycin. The transgenic potato plants were identified by sequencing PCR amplified products.

Potato plants with *StMAPK1* knocked down (RNAi for short) were constructed with a previous method (Lu et al., 2019). The sense cDNA sequence was amplified using forward primer (Kpn I) and reverse primer (EcoR I) and inserted as an Kpn I-EcoR I fragment into pHANNIBAL (pHAN-*StMAPK1*-F); The anti-sense cDNA sequence was amplified using forward primer (Hind III) and reverse primer (BamH I) and inserted as a Hind III-BamH I fragment into pHANNIBAL (pHAN-*StMAPK1*-RF). The pHAN-*StMAPK1*-RF were subcloned at Sac I and Spe I sites into pART vector (pART-*StMAPK1*-RNAi). pART-*StMAPK1*-RNAi was introduced into LBA4404 and incubated for 48 h at 28°C, followed by PCR confirmation using the specific primers for RNAi (forward: 5'-AATTCGTTCCAACCAACAATTG-3' and reverse: 5'-AGTTGCAACCAACTGACCAGATAT-3') and NPT II (forward: 5'-ATGACTGGGCACAACAGACAATCG-3' and reverse: 5'-TCAGAAGAACTCGTCAAGAAGGCG-3'). The stably transgenic plants were stored in MS medium.

Subcellular localization of StMAPK1

Protein-coding sequence of *StMAPK1* was amplified and ligated to the expression vector pCAM35s-GFP, using the following primers: forward, 5'-ATGGAGGCAAGTTTAGGTGATC-3' and reverse, 5'-GTGAGTTGGATCTGGATTAAAG-3'. The constructed plasmid was transformed into Agrobacterium tumefaciens Gv31. The transformed strain infiltrated tobacco epidermal cells in accordance with a previous method reported by Sparkes et al. (Sparkes et al., 2006). The green fluorescence was detected 48 h after infiltration under a Leica TCA confocal scanning laser microscopy (Leica, Weztlar, Germany).

Gene expression assay

Total RNA was extracted using TRIzol RNA Extraction Kit (Invitrogen, Carlsbad, CA, USA), following the manufacturer's description. The first-strand cDNA was generated using the First-Strand cDNA Synthesis Kit according to the instructions from the TransGen Biotech (Beijing, China). qPCR was carried out in a reaction system consisting of 100 ng of cDNA, 10 μL of SYBR Premix Ex Taq (2 ×) (Takara, Tokyo, Japan) and 0.8 μL of specific primers (0.5 μM) on ABI3000 system (Applied Biosystems, Foster City, CA, USA). The reaction procedures were as follows, one cycle at 94°C for 2 min and 40 cycles of amplification at 94°C for 30 s, 60°C for 34 s, and 72°C for 30s. The specific primers were listed in Table 1. The relative mRNA expression was calculated using the formula $2^{-\triangle\triangle Ct}$. Solanum tuberosum translation elongation factor 1α gene (StEf1α) served as an internal control.

H_2O_2, proline, and MDA contents assay

H_2O_2 content, proline content, and MDA content was determined according to our previous methods (Zhu et al., 2021b).

Chlorophyll content assay

Chlorophyll content in potato leaves was examined using the commercial chlorophyll assay kit according to the manuscript's instruction (Item No. Cat#BC0990; Solarbio, Beijing, China). Fresh potato leaves were collected and washed in distilled water. After draining the surface of the leaves, the midrib of the leaves was removed and cut into pieces. Approximately 0.1 g of leaves were weighted and ground thoroughly in 1 mL water in the dark, which were then entirely transferred into a 10-mL volumetric flsk, diluted with water to volume, and mixed. The volumetric flsk was maintained in the dark for 3 h. The absorbance of the supernatant was measured at a wavelength of 663 nm and 645 nm using a spectrophotometer model 552 (Perkin Elmer, Shelton, CT, USA).

Ion leakage assay

The top third functional leaves fully expanded were taken from the transgenic or non-transgenic potato plants at the same position. The leaves were washed with distilled water twice to remove any

10.3389/fpls.2023.1218962

TABLE 1 List of specific primers for qRT-PCR.

Genbank accession	Gene	Forward (5′-3′)	Reverse (5′-3′)	Product length (bp)	Tm
XM_006347752.2	StEf1α	GGTTGTATCTCTTCCGATAAAGGC	GGTTGTATCTCTTCCGATAAAGGC	132	60
HS106768.1	StHSP90	CAGTGGTATCAACGCAGAGTAA	TCCTTCACAGACTTGTCATTCTT	107	62
Z11982.1	StHSP70	GGCATTGATCTTGGTACAACTTAT	GGAGTTGTTCTGTTGCCTTG	95	61
JX576239	StsHSP20	GGAGAGAGGAATGTGGAGAAAG	CGCATTCTCCGGAAGTCTAAA	102	62
XM_006341106.1	StHSFA3	CAGCTTTGTTCGACAGCTTAATAC	CAAATGCCTCTTCCCTCTCAA	100	62
XM_015308529.1	StP5CS	TGCAATGCAATGGAAACGCT	ACAATTTCCACGGTGCAAGC	194	60
AY442179	StCAT	CCATGCTGAGGTGTATCCTATTC	CCTTTCTCCTGGTTGCTTGA	100	62
AF354748	StSOD	CATTGGAAGAGCTGTTGTTGTT	ATCCTTCCGCCAGCATTT	96	62
XM_006362636.2	StPOD	AGATGTTGTGGCCATGTCTGG	GCTTGTGTTGAAGGATGGAGC	118	60
XM_015312004.1	StMAPK1	CTTATGGCATCGTTTGTGCCG	TGTCATGACCCATGTGACGAA	144	60
NM_001288519.1	StMAPK3	TGGTCTGTGGGTTGCATCTT	GGAGTGCCAAGAAGCTCAGT	107	60
NM_001288256.1	StMAPK4	TACGGAATCGTCTGCTGTGC	TCCTCTCTGTCTGGTGGTCTT	188	60
NM_001318567.1	StMAPK6	ACAACCCCTTTTTCCTGGCA	GTTGCCTTGGGTACCTTGGA	149	60
NM_001287969.1	StMAPK7	TACGGCCTTGTATGTGCTGC	GTTTTCGTGGTCCAAGTGCC	144	61
XM_006340601.2	StMAPK8	TGCGGCATATAAGGCATGAGA	AGCCACGAAGGAGCTGAAAA	189	60
XM_006341910.2	StMAPK9	AAGCTCCTTCGCCACCTAAG	CAGACCTCGAAGCAACTGGA	198	60
XM_006359965.2	StMAPK10	TGCATTTTCGCGGAGGTACT	GCCTTCTCATTACGAACCCCA	134	60
XM_006348278.2	StMAPK11	CGTCTCTCTCCCGCGATCTA	GCCAGCAGTTGCCTTTTCTG	106	60
XM_006348888.2	StMAPK12	CCACTGCTGAAGAGGCACTA	CCTTCGTCACTCTTCGCCTC	123	59
XM_006339355.2	StMAPK13	ATCATCCCTGCCTAGGGCTT	CTTGCAGCACCACCTTGAAC	189	60
XM_006360347.2	StMAPK14-1	CCTCATTGCCCAGAGAACGA	GGTGTACTATGGCCAGCCTC	190	60
XM_006344181.2	StMAPK14-2	GTCATTAAGGCCAACGGCAG	TGGAACACGTTTGCTGTGTG	101	59
XM_006365344.2	StMAPK16-1	TGGGTTTATGTACCCAAGTGGT	CATGCTGCCTCTGAAGTGGA	107	59
XM_006367486.2	StMAPK16-2	CGTGAACCATGTAGACCACCA	ACCGATCAACACCACTTGGG	187	60

electrolytes adhering to the leaves or in the cut ends of the tissues. The water on the surface of the leaves were absorbed using filter paper. The leaf discs were punched with a 10 mm-punch from the potato leaves avoiding the central veins. The leaves were placed in 0.1 mol/L of mannitol aqueous solution and shaken at 100 times/min for 2 hours. The relative electrolyte leakage was examined using a conductometer (DDS-11A, Shanghai Scientific Instruments, Shanghai, China). The initial conductivity of the solution was recorded as L1. The solution was next boiled for 10 min and then cooled to 20°C before the determination of the final conductivity L2. The ion leakage was indicated as the ratio of L1 to L2.

Activity assay of CAT, SOD, and POD

The activity of catalase (CAT), superoxide dismutase (SOD), and peroxidase (POD) was determined according to our previous methods (Zhu et al., 2021b).

Net photosynthetic rate, transpiration rate and stomatal conductance assay

The third leaf from the plant top was collected when it fully expands during 9:30-11:30. Net photosynthetic rate, transpiration rate and stomatal conductance were examined using a portable photosynthetic LI-6400XT system (Li-COR, Lincoln, NE, USA). The photon flux density was set as 1,500 μmol·m^{-2}·s^{-1}. The relative humidity in leaf chamber was 50%-70%. CO_2 concentration was 400 μmol/mol.

Statistical analysis

All examinations were performed with three biological replicates and three technological replicates. Data are expressed as the mean ± standard deviation. Statistical analysis was performed with IBM SPSS 19.0 Statistical

10.3389/fpls.2023.1218962

Software (IBM, Chicago, IL, USA) and GraphPad Prism Software (GraphPad, San Diego, CA, USA). Heatmap was prepared with R-software. Multiple comparison was analyzed by one-way ANOVA with Tukey test, Dunnett's T3 or Sidak's test for *post-hoc* analysis.

Results

Expression profile of StMAPKs in potato plants under heat stresses

Potato plants were cultivated under mild (30°C) and acute (35°C) heat stresses, followed by examination of mRNA expression of *StMAPKs* (*StMAPK1*, *StMAPK3*, *StMAPK4*, *StMAPK6*, *StMAPK7*, *StMAPK8*, *StMAPK9*, *StMAPK10*, *StMAPK11*, *StMAPK12*, *StMAPK13*, *StMAPK14-1*, *StMAPK14-2*, *StMAPK16-1* and *StMAPK16-2*) (Figure 1). Transcript levels of *StMAPK* genes were found to be altered in response to mild (Figure 1A) and acute heat stresses (Figure 1B). Under heat stress conditions, *StMAPK1* and *StMAPK3* were induced to be expressed 1-48 h after heat stress (30°C and 35°C) treatment and peaked at 48 h and 6 h, respectively, with a 4.3-fold and 2.5-fold increase in expression, respectively (Figure 1). Notably, *StMAPK1* transcript levels were maintained at higher levels (expression increased more than 3-fold) at 6 h, 12 h, 24 h and 48 h of heat stress treatment ($P < 0.05$). The results indicated that heat stress at 30°C and 35°C induced a sustained and stable high expression of *StMAPK1*. Therefore, we focused on *StMAPK1* and studied its molecular function in the downstream experiment.

StMAPK1 affected the physiological characteristics and phenotypes of potato plants under heat stresses

MAPK cascade transduces the heat signals from the extracellular space to the nucleus, and MAPK is involved in plant signal transduction. The subcellular localization of MAPK1 protein was predicted using the online tool WoLFPSORT (https://wolfpsort.hgc.jp/). The results showed that MAPK1 protein locates in the nucleus. To ascertain the subcellular localization of *StMAPK1*, GFP-tagged StMAPK1 protein was imaged by confocal fluorescent microscopy. It was observed that GFP-StMAPK1 can localize to the nucleus (Figure 2). *StMAPK1* expression in the transgenic plants (OE and RNAi groups) was shown in Additional Figure 1. *StMAPK1* overexpression decreased the generation of H_2O_2 under mild and acute heat stresses compared to the NT group ($P < 0.05$, $P < 0.01$, $P < 0.001$) (Figure 3A). In contrast, *StMAPK1* knockdown induced the accumulation of H_2O_2 compared to the NT group ($P < 0.05$, $P < 0.01$, $P < 0.001$). *StMAPK1* overexpression elevated the contents of proline and chlorophyll compared to the NT group ($P < 0.05$, $P < 0.01$, $P < 0.001$) (Figure 3B and Figure 3C). However, *StMAPK1* knockdown leads to the decreased content of proline and chlorophyll when compared to the NT group ($P < 0.05$, $P < 0.01$, $P < 0.001$). The activity of CAT, SOD and POD was significantly enhanced in *StMAPK1*-transgenic plants compared to the NT group ($P < 0.05$, $P < 0.01$, $P < 0.001$) (Figures 3D-F). By comparison, potato plants with *StMAPK1* knockdown were observed with decreased activities of CAT, SOD, and POD ($P < 0.05$, $P < 0.01$, $P < 0.001$). Additionally, we observed that *StMAPK1* knockdown retarded the growth of potato plants in terms of plant height, fresh weight, dry weight, root fresh weight

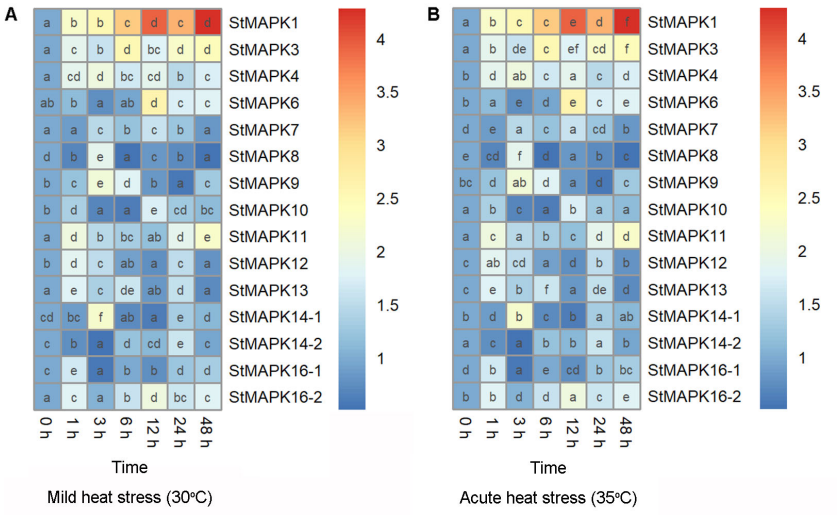

FIGURE 1
Heatmap showing mRNA expression of *StMAPK* gene family. Potato leaves were collected 0, 1, 3, 6, 12, 24, and 48 hours after cultivation under mild heat stress (30°C) **(A)** or wild heat stress (35°C) **(B)**. Data are mean ± standard deviation (n = 9). Different letters indicate significant difference ($P < 0.05$) among different samples by one-way ANOVA with Tukey test or Dunnett's T3 for *post-hoc* analysis.

10.3389/fpls.2023.1218962

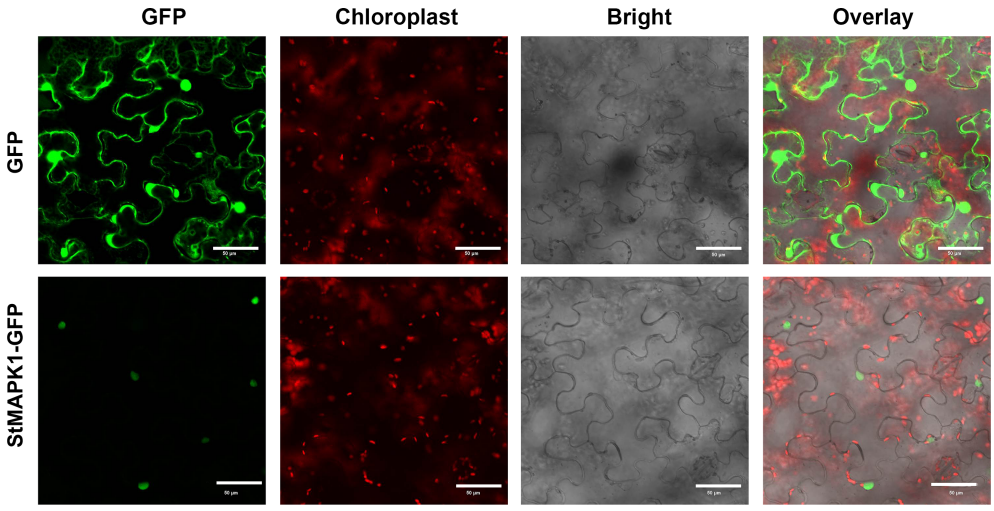

FIGURE 2
Subcellular localization of StMAPK1-GFP fusion protein. Confocal microscopy pictures showing the subcellular localization of StMAPK1-GFP in *Nicotiana tabacum* cells. StMAPK1-GFP construct was introduced into *Nicotiana tabacum* cells through agroinfiltration. The pictures were captured 48 h after infiltration. GFP served as a control. Scale bars = 50 μm.

and root dry weight (Additional Figure 2 and Additional Table 1). However, the potato plants were cultured at 35°C for 48 h and then transferred to 20°C for 72 h. The growth state of *StMAPK1* overexpressed plants was maintained, while the growth of *StMAPK1* low-expressed plants was delayed. Additionally, compared to the NT plants, both OE and Ri plants were observed with yellow leaves.

StMAPK1 modulates photosynthesis and membrane integrity under heat stresses

To identity the molecular mechanisms mediated by *StMAPK1* gene, we examined the photosynthesis and membrane integrity of potato plants under mild and acute heat stresses. It was noted that *StMAPK1* retained the net photosynthetic rate (Figure 4A), transpiration rate (Figure 4B) and stomatal conductance (Figure 4C) under mild and acute heat stresses ($P < 0.05$, $P < 0.01$, $P < 0.001$). *StMAPK1* knockdown conversely decreased the net photosynthesis, transpiration rate and stomatal conductance compared to the NT group ($P < 0.05$, $P < 0.01$, $P < 0.001$). We next quantitatively evaluated the thermo-tolerance of potato plants. The membrane integrity was assessed by measuring ion leakage and MDA content. Heat stresses increased MDA content and facilitated ion leakage, while *StMAPK1* overexpression significantly prevented the outcome ($P < 0.05$, $P < 0.01$, $P < 0.001$) (Figures 5A, B). On the contrary, *StMAPK1* knockdown had the opposite effects on the membrane integrity compared to the NT group ($P < 0.05$, $P < 0.01$, $P < 0.001$).

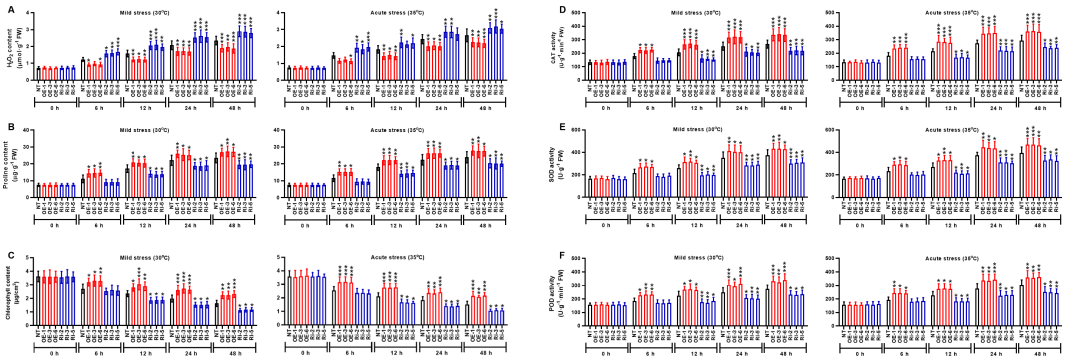

FIGURE 3
StMAPK1 gene overexpression increased the contents of proline and chlorophyll and activities of CAT, SOD, and POD while decreased H_2O_2 content in response to heat stresses, **(A)** H_2O_2 content, **(B)** proline content, **(C)** chlorophyll content, **(D)** CAT activity, **(E)** SOD activity and **(F)** POD activity in potato leaves were examined 0, 6, 12, 24, and 48 hours after exposure to mild heat stress (30°C) and wild heat stress (35°C). Data are mean ± standard deviation (n = 9). *P < 0.05, **P < 0.01, ***P < 0.001 (OE or Ri groups compared to NT group, two-way ANOVA corrected by Sidak's multiple comparisons test). Potato plants transfected with OE-1, OE-3 and OE-6 highly expressed *StMAPK1* mRNA; Potato plants in Ri-2, Ri-3 and Ri-5 lowly expressed *StMAPK1* mRNA.

10.3389/fpls.2023.1218962

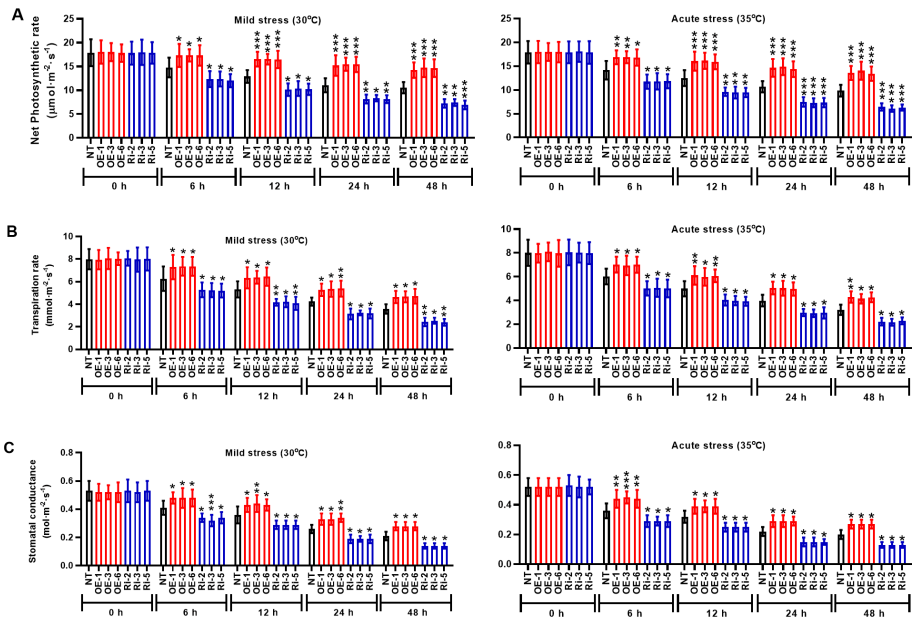

FIGURE 4
StMAPK1 gene overexpression elevated the photosynthesis of potato leaves in response to heat stresses. **(A)** Net photosynthetic rate, **(B)** transpiration rate, and **(C)** stomatal conductance of potato leaves were examined 0, 6, 12, 24, and 48 hours after exposure to mild heat stress (30°C) and wild heat stress (35°C). Data are mean ± standard deviation (n = 9). *P < 0.05, **P < 0.01, ***P < 0.001 (OE or Ri groups compared to NT group, two-way ANOVA corrected by Sidak's multiple comparisons test). Potato plants transfected with OE-1, OE-3 and OE-6 highly expressed *StMAPK1* mRNA; Potato plants in Ri-2, Ri-3 and Ri-5 lowly expressed *StMAPK1* mRNA.

StMAPK1 regulates the expression of stress response genes (StP5CS, StCAT, StSOD, and StPOD) in potato plants

Under mild and acute heat stresses, *StMAPK1* gene was involved in the regulation of the transcription of stress response genes such as *StP5CS*, *StCAT*, *StSOD*, and *StPOD*. Mild and acute heat stress induced the transcription of stress response genes *StP5CS* (Figure 6A), *StCAT* (Figure 6B), *StSOD* (Figure 6C), and *StPOD* (Figure 6D) with the extension of incubation time ($P < 0.05$, $P < 0.01$, $P < 0.001$). In *StMAPK1*-transgenic potato plants, mRNA expression of the examined stress response genes was significantly increased compared to the NT group ($P < 0.05$). By contrast, the transcript levels of *StP5CS*, *StCAT*, *StSOD*, and *StPOD* genes were significantly lower in the *StMAPK1* gene knockdown plants than those of the NT plants ($P < 0.05$). Hence, we hypothesized that *StMAPK1* gene may affect the heat response of potato plants by increasing the transcription of *StP5CS*, *StCAT*, *StSOD*, and *StPOD* genes.

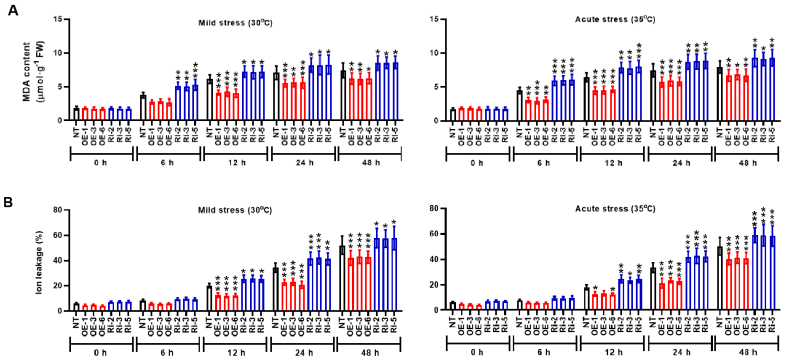

FIGURE 5
StMAPK1 gene overexpression retains the cell membrane integrity under heat stress. **(A)** MDA content and **(B)** ion leakage of potato leaves were examined 0, 6, 12, 24, and 48 hours after exposure to mild heat stress (30°C) and wild heat stress (35°C). Data are mean ± standard deviation (n = 9). *P < 0.05, **P < 0.01, ***P < 0.001 (OE or Ri groups compared to NT group, two-way ANOVA corrected by Sidak's multiple comparisons test). Potato plants transfected with OE-1, OE-3 and OE-6 highly expressed *StMAPK1* mRNA; Potato plants in Ri-2, Ri-3 and Ri-5 lowly expressed *StMAPK1* mRNA.

10.3389/fpls.2023.1218962

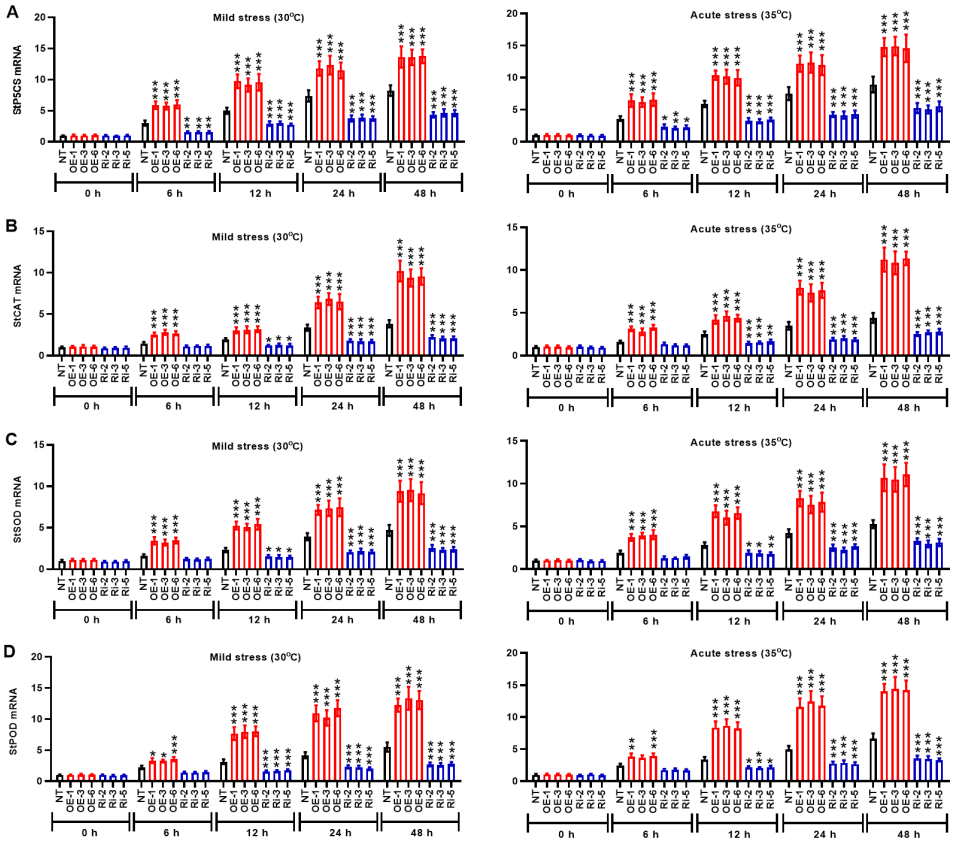

FIGURE 6
StMAPK1 gene overexpression elevated mRNA expression of stress response genes (*StP5CS*, *StCAT*, *StSOD*, and *StPOD*) in potato plants in response to heat stress. Transcription levels of **(A)** *StP5CS*, **(B)** *StCAT*, **(C)** *StSOD*, and **(D)** *StPOD* in potato leaves were examined 0, 6, 12, 24, and 48 hours after exposure to mild heat stress (30°C) and wild heat stress (35°C). Data are mean ± standard deviation (n = 9). *P < 0.05, **P < 0.01, ***P < 0.001 (OE or Ri groups compared to NT group, two-way ANOVA corrected by Sidak's multiple comparisons test). Potato plants transfected with OE-1, OE-3 and OE-6 highly expressed *StMAPK1* mRNA; Potato plants in Ri-2, Ri-3 and Ri-5 lowly expressed *StMAPK1* mRNA.

StMAPK1 induces the expression of heat stress genes (StHSP90, StHSP70, StHSP20, and StHSFA3) in potato leaves in response to heat stress

The kinetics of heat stress response were evaluated in potato plants of the OE group and Ri group in terms of the mRNA expression of *StHSP90*, *StHSP70*, *StHSP20*, and *StHSFA3* genes). During the entire period (0 h to 48 h) of heat stress, the mRNA levels of *StHSP90* (Figure 7A), *StHSP70* (Figure 7B), *StHSP20* (Figure 7C), and *StHSFA3* (Figure 7D) genes were prominently increased in the NT plants compared to the initial time (0 h) ($P < 0.05$). The mRNA expression of heat stress genes in the OE plants was significantly higher than that in the NT group at the same time after heat stress induction ($P < 0.05$). However, potato plants in the Ri group conversely exhibited low expression of heat stress genes *StHSP90*, *StHSP70*, *StHSP20*, and *StHSFA3* ($P < 0.05$) compared to the NT plants. Thus, *StMPAK1* may mediate the heat stress response of potato plants by increasing the transcription of heat stress genes *StHSP90*, *StHSP70*, *StHSP20*, and *StHSFA3*.

Discussion

Potato plants exposed to high temperatures (above 30°C) have been reported to produce and maintain relatively large canopies, but fail to generate tubers (Ewing, 1981; Singh et al., 2020). Zhanjiang (110°22′6″E, 21°15′55″N) is located to the south of the Tropic of Cancer, in the area of influence of the southern subtropical monsoon. In Zhanjiang, potato is grown in December (15-21°C) and harvested in March (19-24°C). However, as global warming continues to increase, Zhanjiang has recorded temperatures in excess of 30°C in March. Therefore, it is of significance to determine plant morphology, growth status, physiological indexes, and molecular responses of potato plants when exposed to temperature above 30°C.

In this study, we examined the mRNA level of potential candidate *MAPKs* family in potato plants exposed to mild heat stress (30°C) and acute heat stress (35°C). Among these genes, *MAPK1* gene exhibited a steady increase in transcript level in potato leaves under heat stress conditions, indicating that *MAPK1* gene may be in relevance with the sensitivity to high temperature and

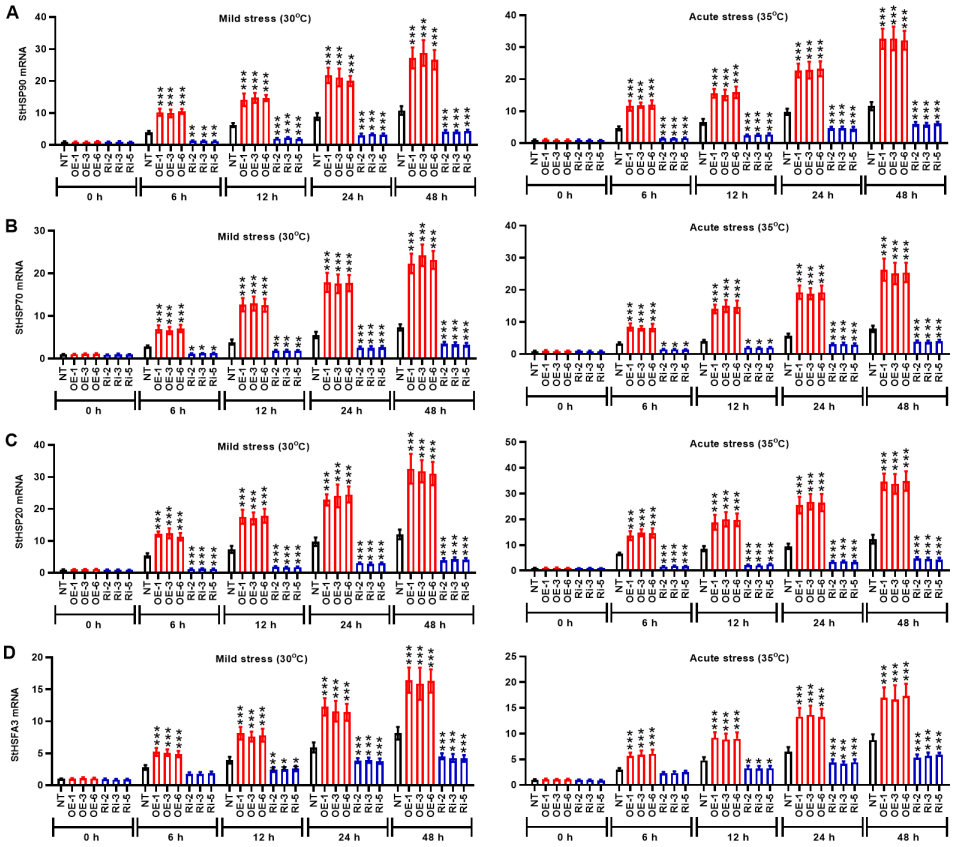

FIGURE 7
StMAPK1 gene overexpression enhances mRNA expression of heat response genes (*StHSP90*, *StHSP70*, *StHSP20*, and *StHSFA3*) in potato plants. Transcription levels of **(A)** *StHSP90*, **(B)** *StHSP70*, **(C)** *StHSP20*, and **(D)** *StHSFA3* in potato leaves were examined 0, 6, 12, 24, and 48 hours after exposure to mild heat stress (30°C) and wild heat stress (35°C). Data are mean ± standard deviation (n = 9). *P < 0.05, **P < 0.01, ***P < 0.001 (OE or Ri groups compared to NT group, two-way ANOVA corrected by Sidak's multiple comparisons test). Potato plants transfected with OE-1, OE-3 and OE-6 highly expressed *StMAPK1* mRNA; Potato plants in Ri-2, Ri-3 and Ri-5 lowly expressed *StMAPK1* mRNA.

modulate the acquired thermo-tolerance of potato plants. The serine/threonine protein kinase family of mitogen-activated protein kinases are highly conserved signaling transduction modules in signaling transduction processes through MAPK cascades (Bharti et al., 2021; Zhang and Zhang, 2022). As the temperature elevates from the optimal threshold to the limit temperature, MAPK protein activates downstream kinases, enzymes, transcription factors and other response factors, which accomplishes the transmission of extracellular environmental signals into cells (Bharti et al., 2021; Lin et al., 2021; Mo et al., 2021). Here, we found that StMAPK1 protein located to the cell nucleus, which may phosphorylate other specific transcription factors for functioning in further signal transmission.

At the biochemical level, plants alter the generation of compatible solutes such as H_2O_2 and proline to maintain redox balance and turgor pressure (Sarker and Oba, 2018; Forlani et al., 2019). Our results demonstrated that genetic manipulation of the expression of *MAPK1* gene predominantly enhances the tolerance to heat stresses in potato plant by altering several physiological indexes including H_2O_2 content, proline content, and chlorophyll content. $H_2O_2$is a well-recognized product produced in photosynthetic tissues under oxidative stress (Hirt, 2000). *AtMAPKKKs* regulate H_2O_2 signal transduction through activating *MAPKs* such as *AtMAPK3* and *AtMAPK6* (Hirt, 2000). Maize *MAPK1* plays a positive role in Arabidopsis, response to heat stress (Wu et al., 2015). Chlorophyll plays a major role in the process of photosynthesis, which is affected by high temperature (Singh et al., 2020). Our results suggested that heat stress decreased total chlorophyll content, however, upregulation of *StMAPK1* ameliorated the loss of chlorophyll. *StMAPK1* gene played an important role in plant growth in response to mild and acute heat stress, which was evidenced by the increased activities of CAT, SOD, and POD. In response to heat stress, MAPK pathway triggers the activation of its downstream redox-sensitive transcription factors that are involved in the generation of multitudinous antioxidant enzymes such as CAT, SOD and POD (Delaunay et al., 2002) (Gill and Tuteja, 2010) (Delaunay et al., 2002; Dąbrowska et al., 2007; Dąbrowska et al., 2007; Gill and Tuteja, 2010).

The prolonged increase in temperature or extreme high temperature moderates the photosynthetic efficiency, which may be ascribed to the denaturation of the active enzymes or lipid peroxidation of chlorophyll (Killi et al., 2020; Xu et al., 2021). Here, we observed that *StMAPK1* gene is a positive regulator of

photosynthesis in potato plants. Transgenic plants overexpressing *StMAPK1* exhibited increased net photosynthetic rate, transpiration rate and stomatal conductance. To maintain cellular homeostasis, plants have evolved mechanisms to maintain membrane stability (Conde et al., 2011). In this study, the available results indicated that *StMAPK1* decreased MDA content and reduced ion leakage, suggesting that *StMAPK1* maintained cell membrane integrity and inhibit cell injuries in response to extreme high temperature. The severely affected photosynthesis and heat stress-related injuries ultimately lead to growth inhibition and a decrease in crop yield.

In our study, *StMAPK1* gene was considered to affect mRNA expression of stress response genes (*StP5CS*, *StCAT*, *StSOD*, and *StPOD*) in potato plants. P5CS gene is confirmed to increase resistance of transgenic plants in response to heat, drought, salinity, which is accomplished via enhancing proline content (Amini et al., 2015). In particular, *StMAPK1* gene was involved in the regulation of heat response gene expression, such as *StHSP90*, *StHSP70*, *StHSP20*, and *StHSFA3* genes in potato plants. HSP90 and HSP70 belong to chaperone family involved in cellular homeostasis, which participate in the control of heat stress response by modulating heat stress transcription factors in plants (Hahn et al., 2011). Genome-wide analysis revealed that *StHSP20* gene is expressed in various tissues and organs, and its expression responds to heat, drought and salt stresses (Zhao et al., 2018). *HSFA3* encoding heat stress transcription factor HSFA3 is essential for plants to resist rapidly changing heat stresses and to enhance thermos-tolerance (Schramm et al., 2008). These results suggested that *StMAPK1* may be the upstream regulator of heat stress genes, which enlaces potato plants to adapt to or resist to high temperature stress.

Conclusions

In this study, we described that *StMAPK* gene family is involved in responses to heat stresses. Several lines of evidence suggested that *MAPK1* gene is included in signaling heat stress in potato plants, resulting in the induction of physiological cellular responses. Genetic studies of *MAPK1* gene knockdown revealed its importance in the regulation of the expression of defense genes and heat stress response genes. Summarily, the study elucidates a molecular mechanism enabling potato plants rapidly respond to heat stress conditions.

Data availability statement

The original contributions presented in the study are included in the article/supplementary material. Further inquiries can be directed to the corresponding authors.

Author contributions

XZ, HD, GZ, and YZ planned and designed the research. XZ, HD, GZ, CX, SC, and CZ collected the data. XZ, HD, HJ, ZC, and JT analyzed the data. XZ, HD, CX, and YZ drafted the manuscript. All authors have read and agreed to the published version of the manuscript. All authors contributed to the article.

Funding

This Research Program was financially supported by the Hainan Provincial Natural Science Foundation of China (No. 322MS116, 323MS095), and Central Public-interest Scientific Institution Basal Research Fund for Chinese Academy of Tropical Agricultural Sciences (No. 1630062023001, 1630062023002).

Acknowledgments

We thank Rongkai Wang (Bioediates, Shaanxi, China) for providing the plasmids pBI121-EGFP, pHANNIBAL, and pART.

Conflict of interest

The authors declare that the research was conducted in the absence of any commercial or financial relationships that could be construed as a potential conflict of interest.

Publisher's note

Supplementary material

The Supplementary Material for this article can be found online at: https://www.frontiersin.org/articles/10.3389/fpls.2023.1218962/full#supplementary-material

SUPPLEMENTARY FIGURE 1
mRNA expression of *StMAPK1* in potato plants transfected with pBI121-EGFP plasmid carrying StMAPK1 protein-coding gene **(A)** and pART plasmid carrying anti-sense cDNA sequence of *StMAPK1* gene **(B)**. Data are mean ± standard deviation (n = 9). ***P < 0.001 (OE or RNAi compared to NC, two-way ANOVA corrected by Sidak's multiple comparisons test).

SUPPLEMENTARY FIGURE 2
Effects of *StMAPK1* on potato phenotypes in response to heat stress. Phenotypic changes of potato plants cultivated 0 h, 12 h, 24 h, and 48 h after exposure to wild heat stress (35°C). The bottom group of potato pants was incubated at 35°C for 48 h, and then transferred to 20°C and cultivated for 72 h. Potato plants transfected with OE-1, OE-3 and OE-6 highly expressed *StMAPK1* mRNA; Potato plants in Ri-2, Ri-3 and Ri-5 lowly expressed *StMAPK1* mRNA.

References

Almeselmani, M., Deshmukh, P. S., Sairam, R. K, Kushwaha, S. R., and Singh, T. P. (2006). Protective role of antioxidant enzymes under high temperature stress. *Plant Sci.* 171 (3), 382–388. doi: 10.1016/j.plantsci.2006.04.009

Amini, S., Ghobadi, C., and Yamchi, A. (2015). Proline accumulation and osmotic stress: an overview of P5CS gene in plants. *J. Plant Mol. Breed.* 3 (2), 44–55.

Arreguin-Lozano, B., and Bonner, J. (1949). Experiments on sucrose formation by potato tubers as influenced by temperature. *Plant Physiol.* 24 (4), 720. doi: 10.1104/pp.24.4.720

Bharti, J., Sahil Mehta, S., Ahmad, S., Singh, B., Padhy, A. K., et al. (2021). Mitogen-activated protein kinase, plants, and heat stress. *Harsh Environ. Plant Resilience: Mol. Funct. Aspects* p, 323–354. doi: 10.1007/978-3-030-65912-7_13

Chen, C., Jiang, Y., van Groenigen, K. J., Hungate, B. A., Zhang, J., Liu, J., et al. (2020). Global warming and shifts in cropping systems together reduce china's rice production. *Global Food Secur.* 24, 100359. doi: 10.1016/j.gfs.2020.100359

Conde, A., Chaves, M. M., and Gerós, H. (2011). Membrane transport, sensing and signaling in plant adaptation to environmental stress. *Plant Cell Physiol.* 52 (9), 1583–1602. doi: 10.1093/pcp/pcr107

Dąbrowska, G., Kata, A., Goc, A., Szechyńska-Hebda, M., and Skrzypek, E. (2007). Characteristics of the plant ascorbate peroxidase family. *Acta Biologica Cracoviensia Ser. Botanica* 49 (1), 7–17.

Delaunay, A., Pflieger, D., Barrault, M.-B., Vinh, J., and Toledano, M. (2002). A thiol peroxidase is an H2O2 receptor and redox-transducer in gene activation. *Cell* 111 (4), 471–481. doi: 10.1016/S0092-8674(02)01048-6

Ewing, E. (1981). Heat stress and the tuberization stimulus. *Am. Potato J.* 58, 31–49. doi: 10.1007/BF02855378

Fogelman, E., Oren-Shamir, M., Hirschberg, J., Mandolino, G., Parisi, B., Ovadia, R., et al. (2019). Nutritional value of potato (Solanum tuberosum) in hot climates: anthocyanins, carotenoids, and steroidal glycoalkaloids. *Planta* 249, 1143–1155. doi: 10.1007/s00425-018-03078-y

Forlani, G., Trovato, M., Funck, D., and Signorelli, S. (2019). Regulation of proline accumulation and its molecular and physiological functions in stress defence. *Osmoprotectant-mediated abiotic Stress tolerance plants: Recent Adv. Future Perspect.* p, 73–97. doi: 10.1007/978-3-030-27423-8_3

Gill, S. S., and Tuteja, N. (2010). Reactive oxygen species and antioxidant machinery in abiotic stress tolerance in crop plants. *Plant Physiol. Biochem.* 48 (12), 909–930. doi: 10.1016/j.plaphy.2010.08.016

Hahn, A., Bublak, D., Schleiff, E., and Scharf, K.-D. (2011). Crosstalk between Hsp90 and Hsp70 chaperones and heat stress transcription factors in tomato. *Plant Cell* 23 (2), 741–755. doi: 10.1105/tpc.110.076018

Handayani, T., Gilani, S. A., and Watanabe, K. N. (2019). Climatic changes and potatoes: how can we cope with the abiotic stresses? *Breed. Sci.* 69 (4), 545–563. doi: 10.1270/jsbbs.19070

Hirt, H. (2000). Connecting oxidative stress, auxin, and cell cycle regulation through a plant mitogen-activated protein kinase pathway. *Proc. Natl. Acad. Sci.* 97 (6), 2405–2407. doi: 10.1073/pnas.97.6.2405

Killi, D., Raschi, A., and Bussotti, F. (2020). Lipid peroxidation and chlorophyll fluorescence of photosystem II performance during drought and heat stress is associated with the antioxidant capacities of C3 sunflower and C4 maize varieties. *Int. J. Mol. Sci.* 21 (14), 4846. doi: 10.3390/ijms21144846

Kim, Y.-U., Seo, B.-S., Choi, D.-H., Ban, H.-Y., and Lee, B.-W. (2017). Impact of high temperatures on the marketable tuber yield and related traits of potato. *Eur. J. Agron.* 89, 46–52. doi: 10.1016/j.eja.2017.06.005

Lee, Y.-H., Sang, W.-G., Baek, J.-K., Kim, J.-H., Shin, P, Seo, M.-C., et al. (2020). The effect of concurrent elevation in CO2 and temperature on the growth, photosynthesis, and yield of potato crops. *PloS One* 15 (10), e0241081. doi: 10.1371/journal.pone.0241081

Li, G., Cao, C., Yang, H., Wang, J., Wei, W., Zhu, D., et al. (2020). Molecular cloning and potential role of DiSOC1s in flowering regulation in davidia involucrata baill. *Plant Physiol. Biochem.* 157, 453–459. doi: 10.1016/j.plaphy.2020.11.003

Lin, L., Wu, J., Jiang, M., and Wang, Y. (2021). Plant mitogen-activated protein kinase cascades in environmental stresses. *Int. J. Mol. Sci.* 22 (4), 1543. doi: 10.3390/ijms22041543

Link, V., Sinha, A. K., Vashista, P., Hofmann, M. G., Proels, R. K., Ehness, R., et al. (2002). A heat-activated MAP kinase in tomato: a possible regulator of the heat stress response. *FEBS Lett.* 531 (2), 179–183. doi: 10.1016/S0014-5793(02)03498-1

Lu, H., Klocko, A. L., Brunner, A. M., Ma, C., Magnuson, A. C., Howe, G. T., et al. (2019). RNA Interference suppression of AGAMOUS and SEEDSTICK alters floral organ identity and impairs floral organ determinacy, ovule differentiation, and seed-hair development in populus. *New Phytol.* 222 (2), 923–937. doi: 10.1111/nph.15648

Majeed, Y., Zhu, X., Zhang, N., Rasheed, A., Tahir, M. M., and Si, H. (2022). Functional analysis of mitogen-activated protein kinases (MAPKs) in potato under biotic and abiotic stress. *Mol. Breed.* 42 (6), 31. doi: 10.1007/s11032-022-01302-y

Majeed, Y., Zhu, X., Zhang, N., ul-Ain, N., Raza, A., Haider, F. U., et al. (2023). Harnessing the role of mitogen-activated protein kinases against abiotic stresses in plants. *Front. Plant Sci.* 14, 932923. doi: 10.3389/fpls.2023.932923

Menzel, C. (1983). Tuberization in potato at high temperatures: interaction between shoot and root temperatures. *Ann. Bot.* 52 (1), 65–69. doi: 10.1093/oxfordjournals.aob.a086553

Mo, S., Qian, Y., Zhang, W., Qian, L., Wang, Y., Cailin, G., et al. (2021). Mitogen-activated protein kinase action in plant response to high-temperature stress: a mini review. *Protoplasma* 258, 477–482. doi: 10.1007/s00709-020-01603-z

Rykaczewska, K. (2015). The effect of high temperature occurring in subsequent stages of plant development on potato yield and tuber physiological defects. *Am. J. Potato Res.* 92, 339–349. doi: 10.1007/s12230-015-9436-x

Sarker, U., and Oba, S. (2018). Drought stress effects on growth, ROS markers, compatible solutes, phenolics, flavonoids, and antioxidant activity in amaranthus tricolor. *Appl. Biochem. Biotechnol.* 186, 999–1016. doi: 10.1007/s12010-018-2784-5

Schramm, F., Larkindale, J., Kiehlmann, E., Ganguli, A., Englich, G., Vierling, E., et al. (2008). A cascade of transcription factor DREB2A and heat stress transcription factor HsfA3 regulates the heat stress response of arabidopsis. *Plant J.* 53 (2), 264–274. doi: 10.1111/j.1365-313X.2007.03334.x

Si, H.-J., Xie, C.-H., and Liu, J. (2003). An efficient protocol for agrobacterium-mediated transformation with microtuber and the introduction of an antisense class I patatin gene into potato. *Acta Agronomica Sin.* 29 (6), 801–805.

Singh, B., Kukreja, S., and Goutam, U. (2020). Impact of heat stress on potato (Solanum tuberosum l.): present scenario and future opportunities. *J. Hortic. Sci. Biotechnol.* 95 (4), 407–424.

Suri, S. S., and Dhindsa, R. S. (2008). A heat-activated MAP kinase (HAMK) as a mediator of heat shock response in tobacco cells. *Plant Cell Environ.* 31 (2), 218–226. doi: 10.1111/j.1365-3040.2007.01754.x

Wolf, S., Olesinski, A. A., Rudich, J., and Marani, A. (1990). Effect of high temperature on photosynthesis in potatoes. *Ann. Bot.* 65 (2), 179–185. doi: 10.1093/oxfordjournals.aob.a087922

Wolf, S., Marani, A., and Rudich, J. (1991). Effect of temperature on carbohydrate metabolism in potato plants. *J. Exp. Bot.* 42 (5), 619–625. doi: 10.1093/jxb/42.5.619

Wu, L., Zu, X., Zhang, H., Wu, L., Xi, Z., and Chen, Y. (2015). Overexpression of ZmMAPK1 enhances drought and heat stress in transgenic arabidopsis thaliana. *Plant Mol. Biol.* 88 (4), 429–443. doi: 10.1007/s11103-015-0333-y

Xu, C., Wang, M. T., Yang, Z. Q., Han, W, and Zheng, S. H. (2021). Effects of high temperature on photosynthetic physiological characteristics of strawberry seedlings in greenhouse and construction of stress level. *Ying Yong Sheng tai xue bao= J. Appl. Ecol.* 32 (1), 231–240.

Yubi, Y., Jun, L., Haiyang, N., and Xiuyun, Z. (2019). Collaborative influence of elevated CO2 concentration and high temperature on potato biomass accumulation and characteristics. *Open Chem.* 17 (1), 728–737. doi: 10.1515/chem-2019-0085

Zandalinas, S. I., Fritschi, F. B., and Mittler, R. (2021). Global warming, climate change, and environmental pollution: recipe for a multifactorial stress combination disaster. *Trends Plant Sci.* 26 (6), 588–599. doi: 10.1016/j.tplants.2021.02.011

Zaynab, M., Hussain, A., Sharif, Y., Fatima, M., Sajid, M., Rehman, N., et al. (2021). Mitogen-activated protein kinase expression profiling revealed its role in regulating stress responses in potato (Solanum tuberosum). *Plants (Basel)* 10 (7), 1371. doi: 10.3390/plants10071371

Zhang, M., and Zhang, S. (2022). Mitogen-activated protein kinase cascades in plant signaling. *J. Integr. Plant Biol.* 64 (2), 301–341. doi: 10.1111/jipb.13215

Zhao, P., Wang, D., Wang, R., Kong, N., Zhang, C., Yang, C., et al. (2018). Genome-wide analysis of the potato Hsp20 gene family: identification, genomic organization and expression profiles in response to heat stress. *BMC Genomics* 19 (1), 61. doi: 10.1186/s12864-018-4443-1

Zhu, X., Zhang, N., Liu, X, Li, S., Yang, J., Hong, X., et al. (2021a). Mitogen-activated protein kinase 11 (MAPK11) maintains growth and photosynthesis of potato plant under drought condition. *Plant Cell Rep.* 40, 491–506. doi: 10.1007/s00299-020-02645-6

Zhu, X., Hong, X., Liu, X., Li, S., Yang, J., Wang, F., et al. (2021b). Calcium-dependent protein kinase 32 gene maintains photosynthesis and tolerance of potato in response to salt stress. *Scientia Hortic.* 285, 110179. doi: 10.1016/j.scienta.2021.110179

frontiers | Frontiers in Plant Science

TYPE Original Research
PUBLISHED 11 July 2023
DOI 10.3389/fpls.2023.1227526

OPEN ACCESS

EDITED BY
Zemin Wang,
Gansu Agricultural University, China

REVIEWED BY
Changbin Gao,
Wuhan Academy of Agricultural Sciences, China
Lei Kang,
Hunan Agricultural University, China

*CORRESPONDENCE
Xi Zhu
zhuxi@catas.cn
Yu Zhang
zhangyu@catas.cn

RECEIVED 23 May 2023
ACCEPTED 22 June 2023
PUBLISHED 11 July 2023

CITATION
Zhu X, Duan H, Jin H, Chen S, Chen Z, Shao S, Tang J and Zhang Y (2023) Heat responsive gene *StGATA2* functions in plant growth, photosynthesis and antioxidant defense under heat stress conditions.
Front. Plant Sci. 14:1227526.
doi: 10.3389/fpls.2023.1227526

Heat responsive gene *StGATA2* functions in plant growth, photosynthesis and antioxidant defense under heat stress conditions

Xi Zhu[1,2,3]*, Huimin Duan[1,2], Hui Jin[1,2], Shu Chen[1,2], Zhuo Chen[1,2], Shunwei Shao[4], Jinghua Tang[1,2] and Yu Zhang[1,2]*

[1]Key Laboratory of Tropical Fruit Biology, Ministry of Agriculture and Rural Affairs of China, Zhanjiang, China, [2]Key Laboratory of Hainan Province for Postharvest Physiology and Technology of Tropical Horticultural Products, South Subtropical Crops Research Institute, Chinese Academy of Tropical Agricultural Sciences, Zhanjiang, China, [3]National Key Laboratory for Tropical Crop Breeding, Sanya Research Institute, Chinese Academy of Tropical Agricultural Sciences, Sanya, China, [4]College of Horticulture and Forestry Science, Huazhong Agricultural University, Wuhan, China

Backgrounds: Potato is sensitive to heat stress particularly during plant seedling growth. However, limited studies have characterized the expression pattern of the *StGATA* family genes under heat stress and lacked validation of its function in potato plants.

Methods: Potato plants were cultivated at 30°C and 35°C to induce heat stress responses. qRT-PCR was carried out to characterize the expression pattern of *StGATA* family genes in potato plants subjected to heat stress. *StGATA2* loss-of-function and gain-of-function plants were established. Morphological phenotypes and growth were indicated by plant height and mass. Photosynthesis and transpiration were suggested by stomatal aperture, net photosynthetic rate, transpiration rate, and stomatal conductance. Biochemical and genetic responses were indicated by enzyme activity and mRNA expression of genes encoding CAT, SOD, and POD, and contents of H_2O_2, MDA, and proline.

Results: The expression patterns of *StGATA* family genes were altered in response to heat stress. StGATA2 protein located in the nucleus. *StGATA2* is implicated in regulating plant height and weight of potato plants in response to heat stresses, especially acute heat stress. *StGATA2* over-expression promoted photosynthesis while inhibited transpiration under heat stress. *StGATA2* overexpression induced biochemical responses of potato plant against heat stress by regulating the contents of H_2O_2, MDA and proline and the activity of CAT, SOD and POD. *StGATA2* overexpression caused genetic responses (CAT, SOD and POD) of potato plant against heat stress.

Conclusion: Our data indicated that *StGATA2* could enhance the ability of potato plants to resist heat stress-induced damages, which may provide an effective strategy to engineer potato plants for better adaptability to adverse heat stress conditions.

KEYWORDS

potato, heat stress, StGATA2, morphological phenotypes, photosynthesis, transpiration

Highlights

1. Expression patterns of *StGATAs* are altered in response to heat stresses;
2. *StGATA2* affects plant morphological phenotypes and growth under heat stress conditions;
3. The photosynthesis and transpiration are regulated by *StGATA2* in response to heat stress;
4. *StGATA2* induces biochemical and genetic responses of potato plants to heat stress.

Introduction

The GATA-binding transcription factors comprise a protein family whose members contain either one or two highly conserved zinc finger DNA-binding domains (Teakle et al., 2002).GATA factors normally recognize the consensus sequence W-GATA-R (W, thymidine (T) or an adenosine (A); R, guanidine (G) or adenosine (A)) (Behringer and Schwechheimer, 2015). The DNA binding domain of GATA factors is constituted by a type IV zinc finger in the form $CX_2CX_{17\text{-}20}CX_2C$ followed by a highly basic region (Gronenborn, 2005). GATA proteins present two of zinc fingers, where only the C-terminal finger (C-finger) is involved in DNA binding, and the N-terminal zinc finger (N-finger) can modulate the binding of the C-finger to specific GATA sites, bind DNA with different specificity, or mediate the interaction with transcription cofactors of the friend of GATA family (Bates et al., 2008). The majority of the plant GATA factors contain a single zinc finger domain and mostly fall into two different categories: those with 17-residue loops ($CX_2CX_{17}CX_2C$; also called zinger finger type IVa) and those with 18-residue loops ($CX_2CX_{18}CX_2C$; also called zinger finger type IVb) (Scazzocchio, 2000).

Members of GATA family have been identified in plant organisms. Reyes et al. documented the existence of 29 different loci encoding putative GATA factors in Arabidopsis and 28 in rice (Reyes et al., 2004). In rapeseed, 96 *GATAs* have been identified and classified into 4 subfamilies based on the phylogenetic relationships, DNA binding domains and intron-exon structures (Zhu et al., 2020). Unevenly distributing on 21 chromosomes, 79 *GATAs* have been characterized in wheat (Feng et al., 2022a). In *Ophiorrhiza pumila* (Rubiaceae), genome-wide survey identified a total of 18 *GATA* genes classified into 4 subfamilies (Shi et al., 2022). In *Brachypodium distachyon*, Peng et al. systematically identified 28 GATA transcription factors distributing on 5 chromosomes (Peng et al., 2021). As for *Solanum* (Family: *Solanaceae*) plants, 30 *GATAs* were recognized in tomato (*Solanum lycopersicum*) by genome-wide analysis (Yuan et al., 2018). Recently, Yu et al. confirmed 49 *GATAs* randomly distributing on 12 chromosomes in potato (*Solanum tuberosum*) (Yu et al., 2022).

Generally speaking, there appears to be evolutionary conservation with regard to function of GATA factors, which has been validated to play roles In the control of normal physiological processes, such as chloroplast development, plant architecture (Hudson et al., 2013), chlorophyll synthesis, glucose metabolism (Bi et al., 2005), apical meristem and flower development (Zhao et al., 2004). Additionally, *GATAs* are light-regulated genes and respond to signals from the circadian clock (Manfield et al., 2007). Studies have revealed the transcript abundance of several *GATAs* is responsive to salinity, drought, exogenous ABA, and gibberellins (Gupta et al., 2017; Guo et al., 2021). However, there is limited studies on the responses of *GATAs* to heat stresses in potato plants. Herein, the current study described the expression patterns of *StGATAs* under heat stress conditions. Further, we analyzed the functional aspects of *StGATA2* and stress responses-related genes. The biological functions of *GATA2* gene have been reported in biological processes, such as photomorphogenesis (Luo et al., 2010). However, its responses to abiotic or biotic stresses are rarely reported.

Materials and methods

Plant material and heat stress

Potato (*Solanum tuberosum* L.) cultivar "Atlantic" was used in this study, which is mainly due to its high yields of tubers and its resistance to common scab, latent and mild mosaics. Potato plants were *in vitro* planted in Murashige and Skoog (MS) medium with pH adjusted among 5.8-6.0. The medium was supplemented with 3% sucrose for seedling growth. To induce tuber generation, 8% sucrose was utilized. The cultivation was conducted in a controlled biotron, with the following conditions: 22°C/15°C (day/night), 16-h/8-h light/dark photoperiod (2,800 Lux), and 50% air humidity.

Potato tubers with a sprouted bud of 1 mm in height were transferred into soil and vermiculite (1:1, v/v) pots measuring 18 cm × 26 cm × 27 cm and maintained for 5 weeks. To induce heat stress, the plants were next fostered under mild (30°C) and acute (35°C) conditions. Potato leaves were collected for detecting transcriptional patterns of *StGATA* family genes, 0 h, 1 h, 2 h, 4 h, 8 h, 12 h, 24 h, and 48 h after heat treatment. For the quantitation of *StGATAs* genes expression, there were 144 seedlings (1 line × 2 heat treatments × 8 different time periods × 3 replications × 3 pots); For the quantitation of heat-responsive genes, there were 630 seedlings (7 lines × 2 heat treatments × 5 different time periods × 3 replications × 3 pots); For the examination of physiological and photosynthetic indexes, there were 630 seedlings (7 lines × 2 heat treatments × 5 different time periods × 3 replications × 3 pots).

Construction of transgenic plants

To generate potato plants highly expressing *StGATA2* gene (OE for short), StGATA2 protein-encoding gene (GenBank Accession No. XM_006347854.2) was amplified using the specific primers (forward, 5'-CTCGAGATGGATGTCTACGGCGTGCACTCT-3' and reverse 5'-GTCGACGCAGACCCGAAAGTGATGTCCGTACATTC-3') (Bioeditas, Shaanxi, China). The PCR products were cloned into pBI121-EGFP plasmid according to a previous method (Li et al., 2020). The constructed plasmid was introduced into *Agrobacterium tumefaciens* strains LBA4404, followed by infecting the potato tuber slide (2 mm) according to Si's method (Si et al., 2003). Potato plants with *StGATA2* knocked down (Ri for short) were constructed with a previous method (Lu et al., 2019). The sense cDNA sequence was amplified using forward primer (Kpn I) and reverse primer (EcoR I) and inserted as an Kpn I-EcoR I fragment into pHANNIBAL (pHAN-StMAPK1-F); The anti-sense cDNA sequence was amplified using forward primer (Hind III) and reverse primer (BamH I), and inserted as a Hind III-BamH I fragment into pHANNIBAL (pHAN-StGATA2-R). The pHAN-StGATA2-RF were subcloned at Sac I and Spe I sites into pART vector (pART-StGATA2-RNAi). pART-StGATA2-RNAi was introduced into LBA4404, which was used to infect potato tuber slides.

After agrobacterium-mediated transformation, the tuber slides were cultivated on a solid medium in the dark at 28°C for 48 h. Then plants were continually cultivated on differentiation media in the dark at 22°C with 16-h/8-h light/dark photoperiod (2,400 Lux). The medium was changed every 12 days and the plants were cultured for about 3 to 4 weeks for shoot differentiation. Plant shoots were cut after growing to 1.5 cm and the shoots were transferred to the rooting medium for screening with 75% mg/mL of kanamycin. After 3 weeks of cultivation on MS medium, the leaves were collected for detecting *StGATA2* by PCR using the specific primers for RNAi (forward: 5'-ATGGATGTCTACGG CGTGCACTCT-3' and reverse: 5'- ATTAGCCGGAAA ATTACTAAATGAAT-3') and NPT II (forward: 5'-CTCA CCTTGCTCCTGCCGAGA-3' and reverse: 5'-CGCCTT GAGCCTGG CGAACAG-3').

qRT-PCR

mRNA expression of *StGATA* family genes was examined 0 h, 1 h, 2 h, 4 h, 8 h, 12 h, 24 h, and 48 h after heat stress that has been described as abovementioned. For *StGATA2* mRNA expression in transgenic plants, the leaves were collected 3 weeks after cultivation on MS medium. To examine the expression of heat stress genes (*StSOD*, *StCAT*, *StPOD* and *StP5CS*), plants leaves were collected 0 h, 8 h, 12 h, 24 h and 48 h after heat treatments. TRIzol RNA Extraction Kit (Invitrogen, Carlsbad, CA, USA). The first-strand cDNA was synthesized using the First-Strand cDNA Synthesis Kit (TransGen Biotech, Beijing, China). qPCR was performed using 100 ng of cDNA, 10 µL of SYBR Premix Ex Taq (2 ×) (Takara, Tokyo, Japan), and 0.8 µL of specific primers (0.5 µM) on ABI3000 System (Applied Biosystems, Foster City, CA, USA). The reaction procedures were: one cycle at 94°C for 3 min and 36 cycles of amplification at 94°C for 45 s, 59°C for 34 s, and 72°C for 1 min. The relative mRNA expression was calculated using the formula $2^{-\triangle\triangle Ct}$. Solanum tuberosum translation elongation factor 1α gene (*StEF1α*) served as an internal control. The specific primers were listed in Table 1.

TABLE 1 Specific primers used in this study.

Gene ID	Gene	Forward (5'-3')	Reverse (5'-3')	Product length (bp)
XM_006347752.2	*StEf1α*	GGTTGTATCTCTTCCGATAAAGGC	GGTTGTATCTCTTCCGATAAAGGC	132
XM_015308529.1	*StP5CS*	TGCAATGCAATGGAAACGCT	ACAATTTCCACGGTGCAAGC	194
AY442179	*StCAT*	CCATGCTGAGGTGTATCCTATTC	CCTTTCTCCTGGTTGCTTGA	100
AF354748	*StSOD*	CATTGGAAGAGCTGTTGTTGTT	ATCCTTCCGCCAGCATTT	96
XM_006362636.2	*StPOD*	AGATGTTGTGGCCATGTCTGG	GCTTGTGTTGAAGGATGGAGC	118
PGSC0003DMT400006011	*StGATA1*	TGGAGATCGCAACTCCAGAAG	GCATTGCACAGCGACTTAGG	196
PGSC0003DMT400066953	*StGATA2*	CTCTGCGTTCCCAGTGATGA	TTCCGTGAAACGACGCAGTA	136
PGSC0003DMT400063771	*StGATA3*	TCCGACCCAAAAGGAGGAATC	TCCCACAAGCATTGCACAGT	137

(Continued)

10.3389/fpls.2023.1227526

TABLE 1 Continued

Gene ID	Gene	Forward (5′-3′)	Reverse (5′-3′)	Product length (bp)
PGSC0003DMT400061125	*StGATA4*	ATTGTGGCATCAAGCAAACCG	CTGTTTGCATGTCGGGGAAC	130
PGSC0003DMT400083773	*StGATA5*	CACCAAGATAGACACCAGCAAAC	TAGCGAATGTGAGGAGTAGGGTT	136
PGSC0003DMT400083774	*StGATA6*	GTGGAAGTGGAGGAGGAATAGAG	CCACACCATTCATCTCCATAGAAC	131
PGSC0003DMT400027729	*StGATA7*	CCCTGTAGATAGCGGCAGAGTTA	CCTCACACCCTCCTAATAATAGCA	142
PGSC0003DMT400027731	*StGATA8*	TGTGGGCTTATGTGGGCAAA	AGCTTCTTGCATATCCTCTTGAT	165
PGSC0003DMT400027733	*StGATA9*	CAGTTAACATTGATGAAGAGCAGGA	GCAGGCCAGTGAACACTCAT	130
PGSC0003DMT400027730	*StGATA10*	ACCACTGCTGAGCTGGATATG	TCCTGCTCTTCATCAATGTTAACTG	101
PGSC0003DMT400027728	*StGATA11*	ATGTGGGCAAACAAGGGTAT	CAGAAAGGAGAACTATCAGCAAAGT	187
PGSC0003DMT400008112	*StGATA12*	CTTCTTCTCCAACCTCTTCGTC	GGTCTCTGCTGATGGATTCTTT	142
PGSC0003DMT400008111	*StGATA13*	ACTCCCTATTCCGGTTGATGA	CGGTTCAGACCGGAACTCTG	145
PGSC0003DMT400031356	*StGATA14*	GAACTCAGTCTTCCTGGGGC	TCGTTCGGCACTAAACGGAA	192
PGSC0003DMT400040074	*StGATA15*	TTCTTCTTCGTCTTCCGTTGAT	ATGTAAGAAGAAGAAGAGCGACG	119
PGSC0003DMT400009117	*StGATA16*	AGTGAAATCAGTGTTCCGACTG	CCGGCAGGATAAGCAAGTGA	101
PGSC0003DMT400009118	*StGATA17*	CTTGTGGTGTTCGGTTCAAATC	TTTCTTCTGATTCCTTCTTCCG	137
PGSC0003DMT400009031	*StGATA18*	CATCGTTGTAGTGGGAGTATGGT	TGATAAGGCGAGTAGAAGGAGTTC	189
PGSC0003DMT400089018	*StGATA19*	CAAATTTCACCGTCTCTCTCACA	GAAGCTGTCCATCCCCTGC	100
PGSC0003DMT400006491	*StGATA20*	CGAACTCTGCGTTCCGTTTG	TGAACTGTCGGTGGTGATGG	148
PGSC0003DMT400070134	*StGATA21*	ATTCCTGACCTCAAGTCCTGTTT	AGAAACAGGACTTGAGGTCAGGA	124
PGSC0003DMT400070133	*StGATA22*	TTGGAACGATCCGTTGCCTG	AACGATATCCTCGTACGGAACT	106
PGSC0003DMT400070135	*StGATA23*	TCGGATTTCGTGGATGAGATAG	TCCTTACAATCAACAGCGTCAA	112
PGSC0003DMT400024208	*StGATA24*	TTGTGCTGATCTGGAAAAGAATC	TGCAGGAATGACGACCTCAG	154
PGSC0003DMT400024207	*StGATA25*	ATAGTGTCAGGAAAGAGGTTGCT	ACAGTTACAGAATGTTGTGTGCC	141
PGSC0003DMT400024206	*StGATA26*	GATGGAGGAGAAGAGACTATGGAT	TAGAAACTTCCACAACTCCACCT	123
PGSC0003DMT400024205	*StGATA27*	GGGAACTCCTGACAATCCCG	ACAGGCAGTCAACCTCAGTT	203
PGSC0003DMT400069864	*StGATA28*	AGCCCTTCATTTCCTGATTATGT	ACTGAATTTGGGCTGTGGTGA	137
PGSC0003DMT400069865	*StGATA29*	GCCCTTCATTTCCTGATTATGT	GTTGTTGTTGTTGTTGTTGCTG	172
PGSC0003DMT400060240	*StGATA30*	CAGCAGCAACAGTGAAGATAGTAA	AATGCTGCTTGTTCTACTTCTCC	167
PGSC0003DMT400060241	*StGATA31*	GGTGGATCTAAGTGATAAACAGGGT	GCAGGTCCACCTCTCCAAAG	141
PGSC0003DMT400060242	*StGATA32*	GCAGCAGCAACAGTGAAGATAGTA	ATGCTGCTTGTTCTACTTCTCCAA	167
PGSC0003DMT400059990	*StGATA33*	AGCTCTCAGTTCCGTATGAGG	GCCTTGGGATAACGGCTCTT	134
PGSC0003DMT400068348	*StGATA34*	ACAGCCTTCTCAAGGACACA	GCTTTCTTTGCACCTGCATACT	148
PGSC0003DMT400068347	*StGATA35*	GACATCCGAACTCAATAGGTAGAG	GTAGACAATCGTGAATAAGCCTCA	102
PGSC0003DMT400068346	*StGATA36*	AGTGACAAGCCTATGGTCTCTGTT	GGTAGACAATCGTGAATAAGCCTC	155
PGSC0003DMT400068349	*StGATA37*	GAAGTTACAGGAGGGCCCAA	CTGAAGCGAAATGGTCTGCAT	103
PGSC0003DMT400062488	*StGATA38*	CGAGGAAGATTGGGATGCGA	GGGACTCCAGAAATTCGTTAGGA	146
PGSC0003DMT400011449	*StGATA39*	TGGGAGATCAAAAGCAACAACC	CCACATGCGTTACACAATGACTTA	145
PGSC0003DMT400052800	*StGATA40*	TCCGAAGTGTTCAGGTGCAA	AGGCAAACGAGCTTCTTGGA	128
PGSC0003DMT400052799	*StGATA41*	AGAACCTTGTGACTTTGAGGAACA	GAGCCAGAACTTGACCTATTGCTA	188
PGSC0003DMT400052801	*StGATA42*	TCCGAAGTGTTCAGGTGCAAA	TTGGACTGAAGCAAGAGCCAT	113

(Continued)

TABLE 1 Continued

Gene ID	Gene	Forward (5′-3′)	Reverse (5′-3′)	Product length (bp)
PGSC0003DMT400074935	*StGATA43*	TTGTCCGGAAGCAATCACCC	CAGCCATATCTTCATATGGAACGG	100
PGSC0003DMT400067506	*StGATA44*	GTCGGTTGACAACAAGCACC	GGTGGTCCCTGCTCCTTTTA	170
PGSC0003DMT400067505	*StGATA45*	ACAACAATGCTCATACTTCTCTGG	GGCTTCTGATTCTTCTTCTCTACC	144
PGSC0003DMT400081417	*StGATA46*	CATCAGGTCCCAAGTCGTTG	GCCATCAATAATATCGCCGCT	187
PGSC0003DMT400030274	*StGATA47*	CAACTGCATGTTTCATGGTGGA	TTCTTCCTCTACACACTCAGGG	179
PGSC0003DMT400030276	*StGATA48*	GTGGATGATGACCTTCTCAACTTC	GAAGAAGGCTAACAAGAGGGTTTG	135
PGSC0003DMT400030708	*StGATA49*	ACCAACCACCTCCTACCGAT	TGCTACATCATCACTCGGAACA	110
PGSC0003DMT400020876	*StGATA50*	CATCCACACCCTCCGATCAA	CGAGGACGTACGGGAATGAC	152
PGSC0003DMT400020875	*StGATA51*	ACATCCACACCCTCCGATCA	ACTCTTTCCACCAGAGCAGG	112
PGSC0003DMT400000761	*StGATA52*	AGCAACAGCTCTTCCAACAAC	CATGCGTTACAAAGAGACTTAGGG	119
PGSC0003DMT400000760	*StGATA53*	CTCAAACTCTCACAGGAAAGTCGT	TACTCATAGGAACAAACTCTGGCG	172
PGSC0003DMT400000762	*StGATA54*	CTGATTACAGCAGCAACAGCTC	CCACATGCGTTACAAAGAGACTTA	133
PGSC0003DMT400011779	*StGATA55*	GACCTGCTGGACCTAAGTCAT	TTTCTCCGCTGCTGCTTGTA	186
PGSC0003DMT400011778	*StGATA56*	ATGTGGAATAAGGAGCAGGAAGA	GCTACTCTGGTTCTGAGGATGATG	120
PGSC0003DMT400011780	*StGATA57*	ACCTGCTGGACCTAAGTCATTGT	TGCTACTGCTATTGCTACTCTGGTT	164

The gene sequences described in this article are available at the National Center for Biotechnology Information (https://www.ncbi.nlm.nih.gov/) and Potato Genomics Resource (http://solanaceae.plantbiology.msu.edu/index.shtml) Heard the following login number.

Subcellular localization

Protein-coding sequence of *StGATA2* was amplified and ligated to the expression vector pPBI121-EGFP, using the following primers: forward, 5'-CTCGAGATGGATGTCTACGGC GTGCACTCT-3' and reverse, 5'-GTCGACGCAGACCCG AAAGTGATGTCCGTACATTC-3'. The constructed plasmid was transformed into *Agrobacterium tumefaciens* GV3101. The transformed strain infiltrated tobacco epidermal cells in accordance with a previous method reported by Sparkes et al. (2006). The green fluorescence was detected 48 h after infiltration under a Leica TCA confocal scanning laser microscopy (Leica, Weztlar, Germany).

Phylogenetic analysis and amino acid alignment

Phylogenetic tress for GATA domain-containing homologs with highly similarity was constructed using MEGA 5.05 Software. Multiple-sequence alignment of GATA domain-containing amino acid sequence was analyzed using DNAman tool (Lynnon Biosoft, San Ramon, CA, USA)

Measurements of plant growth

Potato plants were imaged 2 days after heat stress. Potato plants cultivated at 35°C were transferred to 22°C conditions and maintained for 7 days. CK plants were cultivated at 22°C for 2 days. The plants were measured for plant height, plant fresh weight (FW), plant dry weight (DW), root FW and root DW.

Stomatal apertures

Stomatal apertures were examined according to a previous method reported by Tricker et al. (2005). After 35 days of cultivation, transgenic or non-transgenic plants were subjected to heat stress treatment for 24 h or 48 h. The comparable fully-expanded leaves of transgenic or non-transgenic plants were selected between 9:30-11:00 am for measuring stomatal aperture. Clear nail polish was applied to the third fully expanded fully functional leaf located at the top of the plant, followed by covering with scotch tape. The leaves were mounted on glass slides and imaged using a Zeiss-Axiolmager M2 microscope (Zeiss, Germany). Three biological replicates were performed for each condition separately.

Net photosynthetic rate, transpiration rate, and stomatal conductance

The third leaf from the plant top was collected when it fully expands during 9:30-11:30. Net photosynthetic rate, transpiration rate and stomatal conductance were examined using a portable photosynthetic LI-6400XT system (Li-COR, Lincoln, NE, USA). The photon flux density was set as 1,500 $\mu mol \cdot m^{-2} \cdot s^{-1}$. The relative humidity in leaf chamber was 50%-70%. CO_2 concentration was 400 μmol/mol.

Contents of H_2O_2, proline, and MDA, and activities of CAT, SOD, and POD

To assess physiological and biochemical changes in plants under heat stress, 5-week-old *StGATA2* transgenic plants and non-transgenic control plants grown under greenhouse conditions were subjected to heat stress treatments at 30°C and 35°C. Contents of H_2O_2, proline, and malondialdehyde (MDA) and activities of catalase (CAT), superoxide dismutase (SOD), and peroxidase (POD) were determined according to our previous methods (Zhu et al., 2021).

Statistical analysis

All experiments were carried out with three biological replicates and three technological replicates. Data are shown as the mean ± standard deviation. Statistical analysis was done with IBM SPSS 19.0 Statistical Software (IBM, Chicago, IL, USA) and GraphPad Prism Software (GraphPad, San Diego, CA, USA). Multiple comparisons were analyzed by one-way ANOVA with Tukey test or Dunnett's T3 for *post-hoc* analysis or two-way ANOVA corrected by Sidak's multiple comparisons test. Histograms were computed with GraphPad Prism software, heatmap by the pheatmap function in R version 4.2.3.

Results

Expression signatures of *GATA* family genes in potato plants in response to heat stress

To provide an overview of expression patterns of *GATA* family genes, we cultivated potato plants under heat stresses. qRT-PCR results showed that mRNA expression of the 57 members from *GATA* family genes were distinctly altered during mild (30°C) or acute (35°C) heat stresses (0-48 h), which was presented in heatmaps (Figures 1A, B). Importantly, under heat stress conditions, *StGATA2* expression was induced 1-48 h after heat stress (30°C and 35°C) treatment and peaked at 48 h with 7.5-fold and 8.4-fold increases in mRNA expression, respectively (Figure 1). Notably, *StGATA2* transcript levels were maintained at higher levels (expression increased more than 7 folds) at 8 h, 12 h, 24 h and 48 h after heat stress treatment ($P < 0.05$). The results indicated that heat stress at 30°C and 35°C induced a sustained and stable high expression of *StGATA2*. Consequently, we speculated that *StGATA2* gene may play molecular functions in response to heat stresses.

Potato plants encoding GATA2 gene with CTHC-X18-CNAC motif

Phylogenetic tree of GATA factors was generated, including *Solanum tuberosum* GATA2 (StGATA2), *Solanum lycopersicum* GATA2 (SlGATA2), *Nicotiana tabacum* GATA4 (NtGATA4), *Capsicum annuum* GATA4 (CaGATA4), *Capsicum baccatum* GATA2 (CbGATA2), *Arabidopsis thaliana* GATA2 (AtGATA2), *Oryza sativa* GATA12 (OsGATA12) (Figure 2A). *Solanum tuberosum* GATA2 contains CTHC-X18-CNAC motif (Figure 2B). To examine *StGATA2* function, we obtained *StGATA2* overexpression plants by expressing pBI121-EGFP-StGATA2 and generated a loss-of-function plants by introducing pART-StGATA2-RNAi. The relative mRNA expression of *StGATA2* in transgenic plants were shown in Figures 2C, D, which significantly increased or knocked down when compared to the wild type ($p<0.001$). Amongst the overexpression lines, OE-1, OE-2 and OE-5 were selected as the significant over-expressors, and Ri-1, Ri-4 and Ri-6 as the significant under-expressors used for the functional analysis in response to heat stresses. StGATA2 protein obviously located in the nucleus (Figure 3). The subcellular localization of GATA2 to the nucleus is the structural premise for DNA binding and transcription activation.

Effects of *StGATA2* on plant morphological phenotypes and growth in response to heat stresses

Next, we cultivated the 5-week-old transgenic or non-transgenic plants under heat stresses for 2 days, and investigated whether *StGATA2* gene is involved in regulating plant morphology or growth such as plant height, plant weight and root weight. The morphological features of the plants were imaged 2 days after cultivation at 22°C (CK), 30°C, or 35°C. Figure 4A showed that neither *StGATA2* over-expression nor under-expression affected plant morphological structure, compared to wild-type plants at 22°C. However, the height of OE plants in Figure 4B or Ri plants in Figure 4C was significantly different from the non-transgenic plants.

The statistical analysis results revealed that under mild heat stress (30°C), OE plants were characterized by increased plant height (Figure 4E), while plant fresh weight (Figure 4F), plant dry weight (Figure 4G), root fresh weight (Figure 4H) or root dry weight (Figure 4I) were unchanged ($p>0.05$) relative to NT plants ($p<0.05$). In contrast, the height of Ri plants was not significantly different from NT plants ($p>0.05$) (Figure 4E), while *StMAPK1* under-expression reduced plant fresh weight (Figure 4F), plant dry weight (Figure 4G), root fresh weight (Figure 4H) or root dry weight (Figure 4I) ($p<0.05$) 2 days after growth at 30°C. As for the acute heat stress (35°C), OE plants displayed significant increases in plant height, plant fresh weight, plant dry weight, root fresh weight, and root dry weight, which were significantly decreased in Ri plants compared to non-transgenic plants ($p<0.05$).

Further, we compared the morphological structures of transgenic plants to non-transgenic plants 7 days after the plants receiving heat stresses were cultivated at 22°C. Figure 4D showed that compared to the non-transgenic plants, OE plants showed an increased plant height and more apical branches. However, Ri plants grows slowly, with a shorter height compared to NT plants. These results indicated that *StGATA2* is implicated in the growth of potato plants in response to heat stresses, especially acute heat stress.

10.3389/fpls.2023.1227526

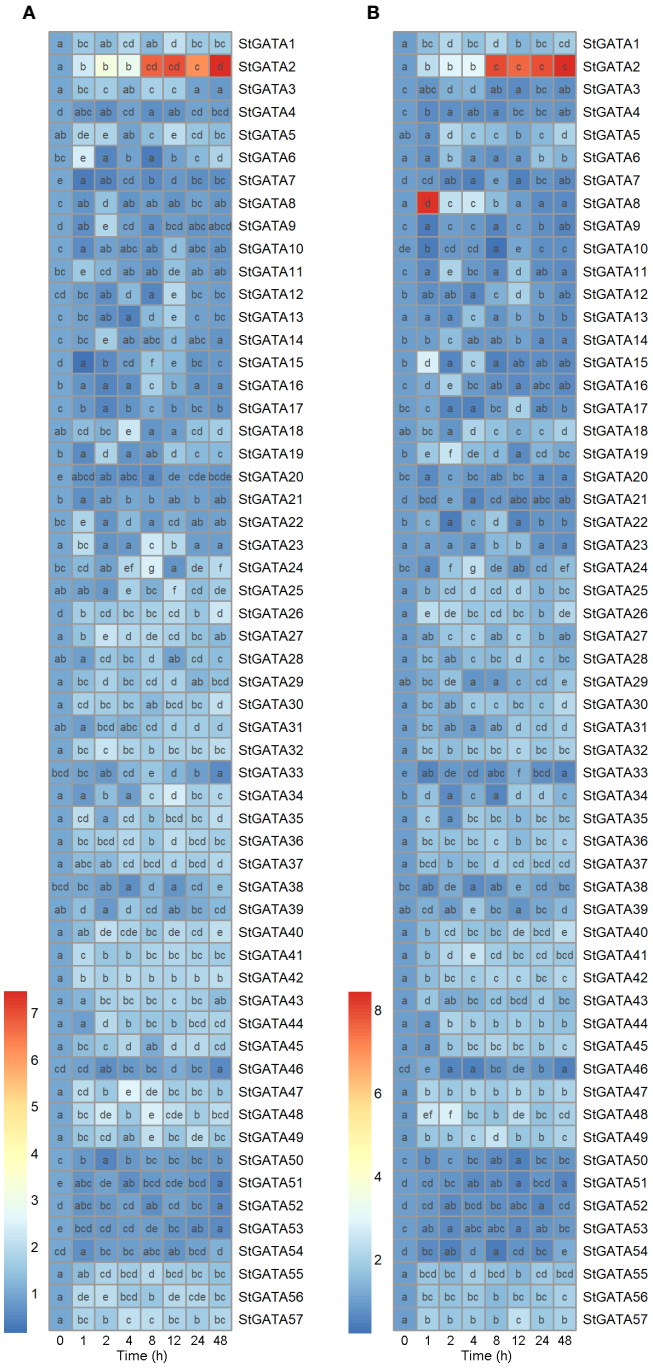

FIGURE 1
Heatmap suggesting mRNA expression of *StGATA* family genes in potato leaves in response to heat stress. Five-week-old normally grown plants were subjected to 0 h, 1 h, 2 h, 4 h, 8 h, 12 h, 24 h, or 48 h of **(A)** mild (30°C) or **(B)** acute (35 °C) heat stresses. Multiple comparisons were analyzed by one-way ANOVA with Tukey test or Dunnett's T3 for *post-hoc* analysis. Difference letters indicates the difference between the two groups ($p<0.05$).

StGATA2 over-expression enhanced photosynthetic rate and inhibited transpiration in response to heat stresses

Measurements revealed that average ratio of stomal width to length was significantly decreased in *StGATA2* overexpressing plants compared with NT plants, 24 or 48 h after mild heat stresses ($p<0.05$, $p<0.01$) (Figures 5A, B). *StGATA2* under-expression resulted in a significant increase in stomatal aperture ($p<0.05$), 24 h or 48 h after mild or acute heat stresses. Under heat stress conditions, the net photosynthetic rate was increasingly enhanced in OE plants, while decreased in Ri plants ($p<0.05$) (Figures 5C, D). Additionally, there were evidence of *StGATA2* overexpression inhibiting transpiration rate (Figures 5E, F) and decreasing stomatal conductance (Figures 5G, H) ($p<0.05$, $p<0.01$). Comparing to the NT plants, 30°C or 35°C heat stresses resulted in

10.3389/fpls.2023.1227526

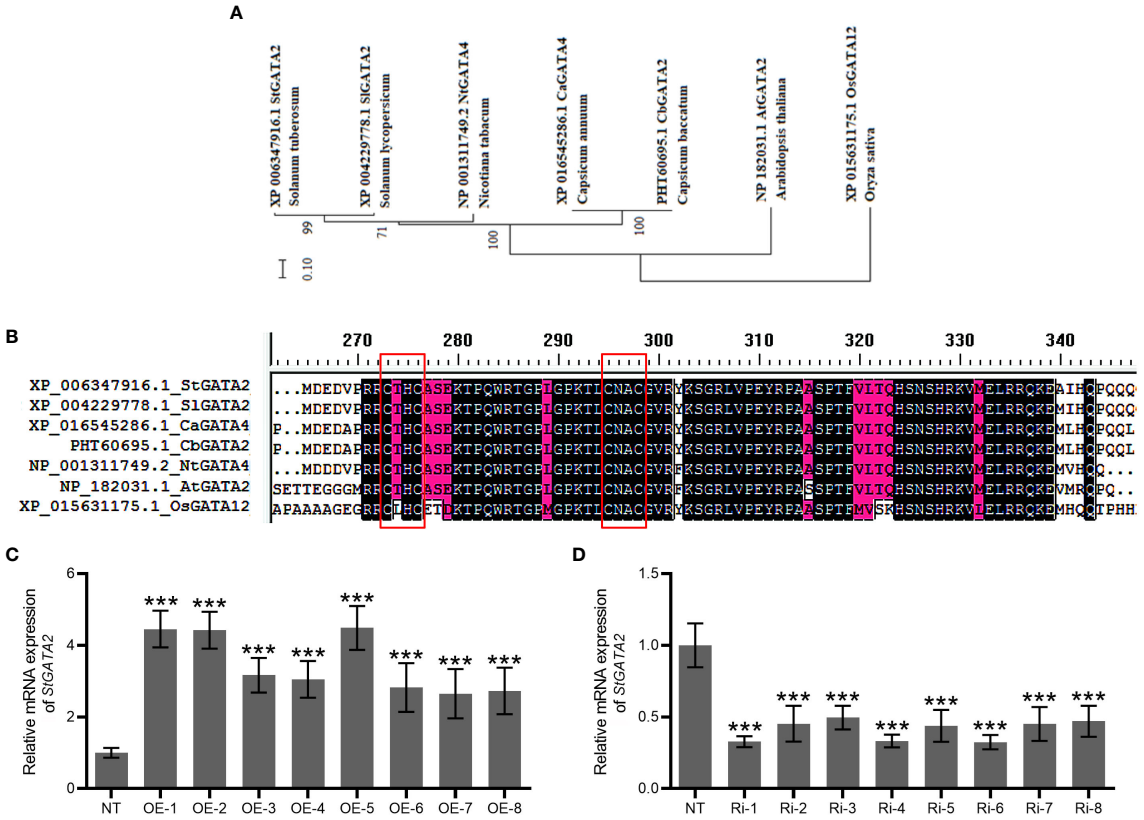

FIGURE 2
Bioinformatic analysis of StGATA2 protein and construction of *StGATA2* overexpression or under-expression plants. **(A)** Phylogenetic tree and schematic representation of GATA factors from *Solanum tuberosum* (St), *Solanum lycopersicum* (Sl), *Nicotiana tabacum* (Nt), *Capsicum annuum* (Ca), *Capsicum baccatum* (Cb), *Arabidopsis thaliana* (At), *Oryza sativa* (Os). The scale bar represents the difference degree of amino acid sequences. **(B)** Multiple-sequence alignment of conserved single CTHC-X18-CNAC motif highlighted in red boxes. **(C, D)** The quantification of *StGATA2* mRNA expression in potato plants; NT, non-transgenic plants; OE, pBI121-EGFP-StGATA2-transgenic lines; Ri, pART-StGATA2-RNAi-transgenic plants; Mean ± standard deviation; Student's t-test, ***p<0.001 (n = 9).

significant increases in transpiration rate and stomatal conductance of *StGATA2* under-expression plants (p<0.05, p<0.01, p<0.001). All of these results confirmed that *StGATA2* is closely correlated with heat stress-induced modifications in photosynthesis and transpiration rate.

Biochemical and genetic responses of *StGATA2*-transgenic potato plants to heat stress

Biochemical changes in potato plants were assayed to evaluate the capacity of *StGATA2* to trigger protective mechanisms against heat stress. There is a significantly increase in contents of H_2O_2, MDA, and proline, as well as the activity of CAT, SOD and POD, following mild and acute heat stress treatment (p<0.05, p<0.01) (Figure 6). Compared to the NT plants, *StGATA2* overexpression significantly restrained the accumulation of H_2O_2 and MDA, while further induced the generation of proline (Figures 6A–F). Under heat stress conditions, *StGATA2* overexpression enhanced the activity of CAT, SOD and POD compared to the non-transgenic plants (Figures 6G–L). However, there was an opposite trend toward the contents of H_2O_2, MDA and proline, as well as the activity of CAT, SOD, and POD in the Ri plants following heat stress, compared with OE plants. These data suggested that *StGATA2* overexpression induced biochemical responses of potato plant against heat stress.

Besides, under heat stress conditions, mRNA expression of heat stress responsive genes was increased in non-transgenic, including *StSOD* (Figures 7A, B), *StCAT* (Figures 7C, D), *StPOD* (Figures 7E, F), *StP5CS* (Figures 7G, H) (p<0.05, p<0.01, p<0.001). However, *StGATA2* over-expression further elevated the transcription of these 4 heat stress-responsive genes following heat stress treatment, compared to non-transgenic plants. In contrast, Ri plants showed the opposite results. This analysis indicated that *StGATA2* overexpression induced genetic responses of potato plant against heat stress.

Discussion

High temperature limited plant morphophysiological growth, photosynthesis, dark respiration, carbohydrate metabolism (Lafta and Lorenzen, 1995; Fahad et al., 2016), root system architecture

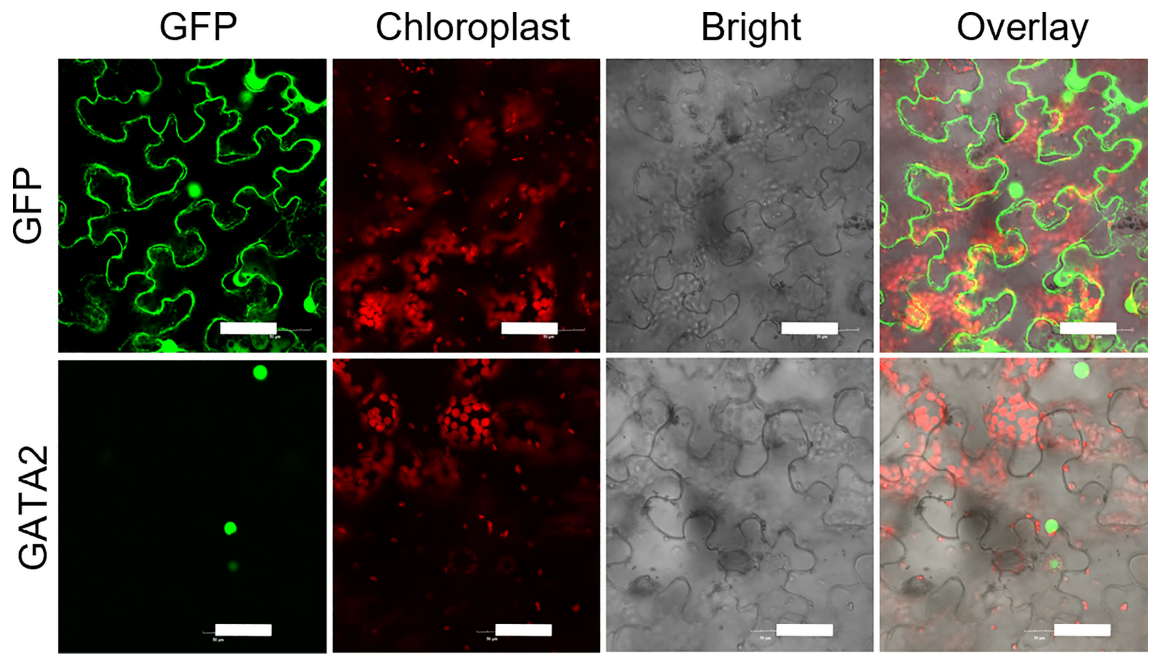

FIGURE 3
StGATA2 protein locates on the cellular nucleus of tobacco epidermal cells. GFP-StGATA2 fusion protein was transiently expressed in tobacco leaves and observed using a laser scanning confocal microscope. Bar = 50 μm.

(Luo et al., 2020), stomal regulation and water use (Körner, 2006). *GATA* family genes are heat-responsive genes, which has been identified in cucumber (Zhang et al., 2021), wheat (Feng et al., 2022b), and pepper (Yu et al., 2021). However, these studies only characterized the expression pattern of the *GATA* family genes under heat stress and lacked validation of its function. In the present study, we present the first evidence that *StGATA2* plays an important role in maintaining plant growth against heat stresses, through the regulation of heat-responsive gene expression in *Solanum tuberosum*.

Genome-wide analysis has identified the *GATA* family genes in wheat (Feng et al., 2022b), pepper (Yu et al., 2021), cucumber (Zhang et al., 2021), rice (Gupta et al., 2017), and foxtail millet (Lai et al., 2022). Based on the whole potato genome data, Yu et al. systematically identified 49 GATA proteins, of which mRNA expression is affected by *Ralstonia solanacearum*, abscisic acid and methyl jasmonate (Yu et al., 2022). Our previous study identified 57 GATA proteins randomly distributed on 12 chromosomes (unpublished data). The expression profile of *GATA* genes was significantly altered when plants are subjected to heat stress (Yu et al., 2021; Feng et al., 2022b), suggesting their potential roles involved in biological functions associated with heat tolerance. The expression pattern of *GATA* genes is still unexplored when potato plants are exposed to heat stresses. As a result, we cultivated potato plants under mild and acute heat stresses and determined mRNA expression of *GATA* genes. In mature potato plants, we noted an evident alteration in mRNA expression of *GATA* family genes under heat stress conditions during the observed intervals. We found a substantially and stably up-regulated gene *StGATA2* after heat stress treatment. This suggested that *StGATA2* is a positive heat stress-responsive gene in the wild-type potato plant. *StGATA2* gene was then selected for constructing transgenic plants to identify its roles in response to heat stress.

StGATA2 belongs to 18-residue loops (i.e. $CX_2CX_{18}CX_2C$; also called zinger finger type IVb). The zinc finger motifs are categorized into two groups: those with 17-residue loops ($CX_2CX_{17}CX_2C$ zinc finger type IVa) and those with 18-residue loops ($CX_2CX_{18}CX_2C$ zinc finger type IVb), which are based on the spacing between the cysteine pairs at the zinc finger loop (Park et al., 2006). GATA transcription factors play a crucial role in plant growth, biomass accumulation and plant height, of which *PdGNC* have been confirmed in poplar, for example (An et al., 2019). Studies have revealed the involvement of *GATAs* in responding to multiple stresses when the crops are exposed to salinity, drought, exogenous ABA, acid, alkali, dark, flooding, heat, and cold (Gupta et al., 2017; Yu et al., 2021; Zhang et al., 2021; Feng et al., 2022b; Lai et al., 2022). For instance, in tomato plants, *SlGATA17* expression was induced by heat stress (Wang et al., 2023). Transgenic Arabidopsis plants overexpressing GATA factors ZIM show enhanced petiole and hypocotyl cell elongation (Shikata et al., 2004). However, limited studies have been conducted to demonstrate the roles of *GATAs* in plant growth in response to heat stress. Potato is characterized by specific temperature requirements and develops best at about 20°C. Subsequently we constructed the loss-of-function and gain-of-function variants to examine the role of *StGATA2* in potato plant growth. Our results confirmed that potato plant growth was greatly reduced at 30 °C and 35°C higher than optimum, responding with decreases in plant height and weight. The

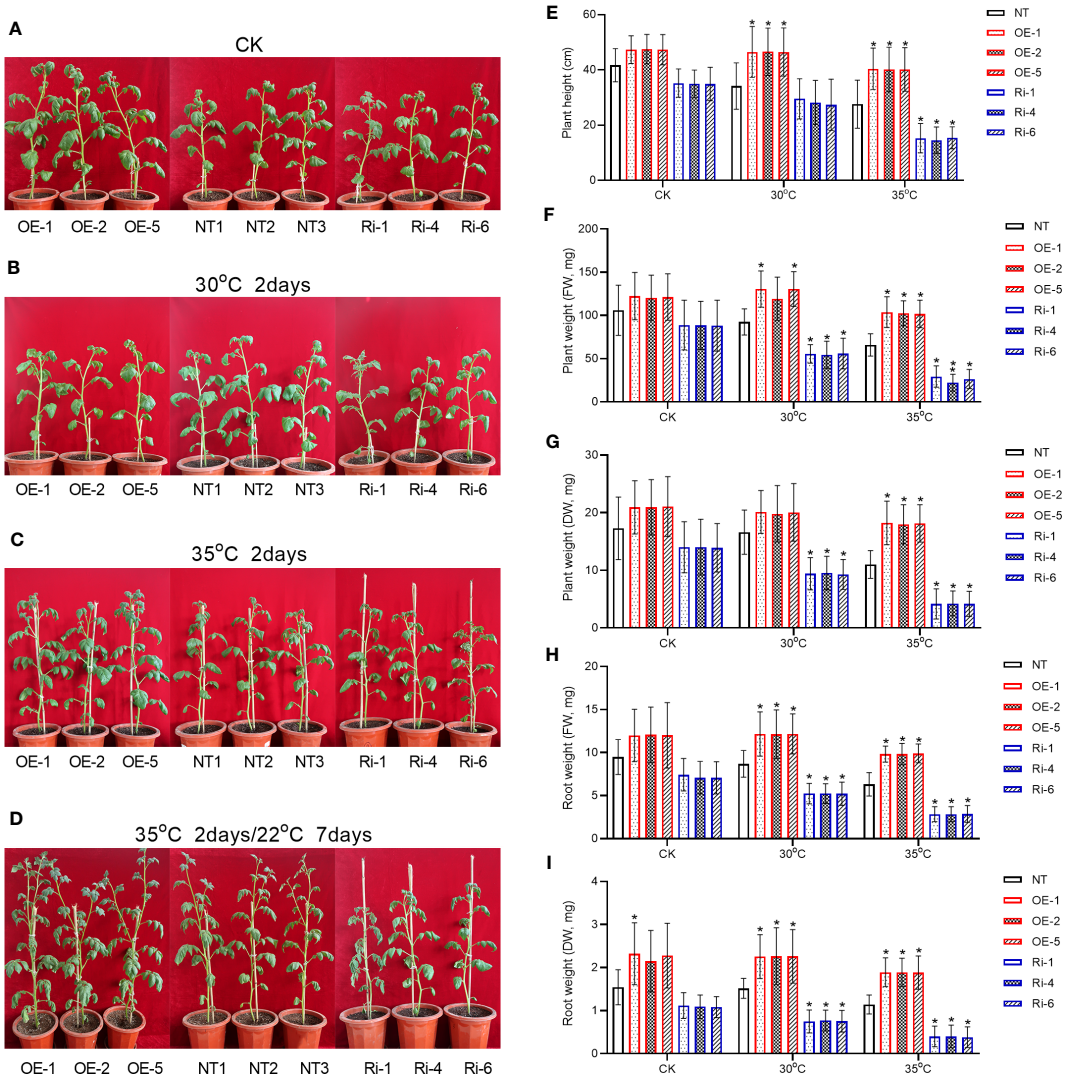

FIGURE 4
Growth characterizations of *StGATA2* over-expression or under-expression plants in response to heat stresses. **(A–D)** Representative photographs of potato plants with the specified genotypes (NT, OE, and Ri); Five-week-old plants were cultivated under **(A)** 22°C (CK), **(B)** 30°C (30°C), **(C)** 35°C, or **(D)** 35°C followed by moving to 22°C condition; Plants in A, B, and C were imaged 2 days after heat stress; After heat stress, plants in D were imaged 7 days after normal cultivation. **(E)** Plant height, **(F)** plant fresh weight (FW), **(G)** plant dry weight (DW), **(H)** root FW, and **(I)** root DW of transgenic or non-transgenic plants were measured 2 days after cultivation under the specified conditions (22°C, 30°C, and 35°C). NT, non-transgenic plants; OE, pBI121-EGFP-StGATA2-transgenic lines; Ri, pART-StGATA2-RNAi-transgenic plants; Mean ± standard deviation; Ordinary two-way ANOVA with Tukey's multiple comparisons test, *p<0.05 (n = 9).

transfer of plants from 35°C to 22°C had apparent effect on shoot growth. Besides, He et al. have validated that *GATA* is a crucial regulator of the flag leaf development in rice (He et al., 2018). These results suggested that *StGATA2*, a member of the *StGATA* family genes, is involved in the growth process of several organs such as root, shoot and leaf of the potato plants.

Stomata protects plants against immediate or long-term injuries caused by environmental alterations. It was recently shown that heat stress initiated a rapid local and systemic stomatal opening responses (Devireddy et al., 2020). In Arabidopsis, Klermund et al. reported that LLM-domain B-class *GATA* genes strongly promotes stomata formation, most strikingly in hypocotyls but also in cotyledons (Klermund et al., 2016). Whereas it is still unclear about how *GATA* genes affect the stomatal aperture. In our study, consistent heat stress decreases the stomatal aperture, and *StGATA2* expression significantly further inhibited the stomatal aperture, which may play roles in leaf temperature, CO_2 exchange rates and water vapor loss. In poplar, *PdGNC* affects chlorophyll content and photosynthetic rate (An et al., 2019). The conserved GATA transcription factor mediates plant architecture and chloroplast development by altering chlorophyll, chloroplast number, photosynthesis, and amnio acid and starch biosynthesis, which may be associate with a semidwarf phenotype of the transgenic rice (Hudson et al.,

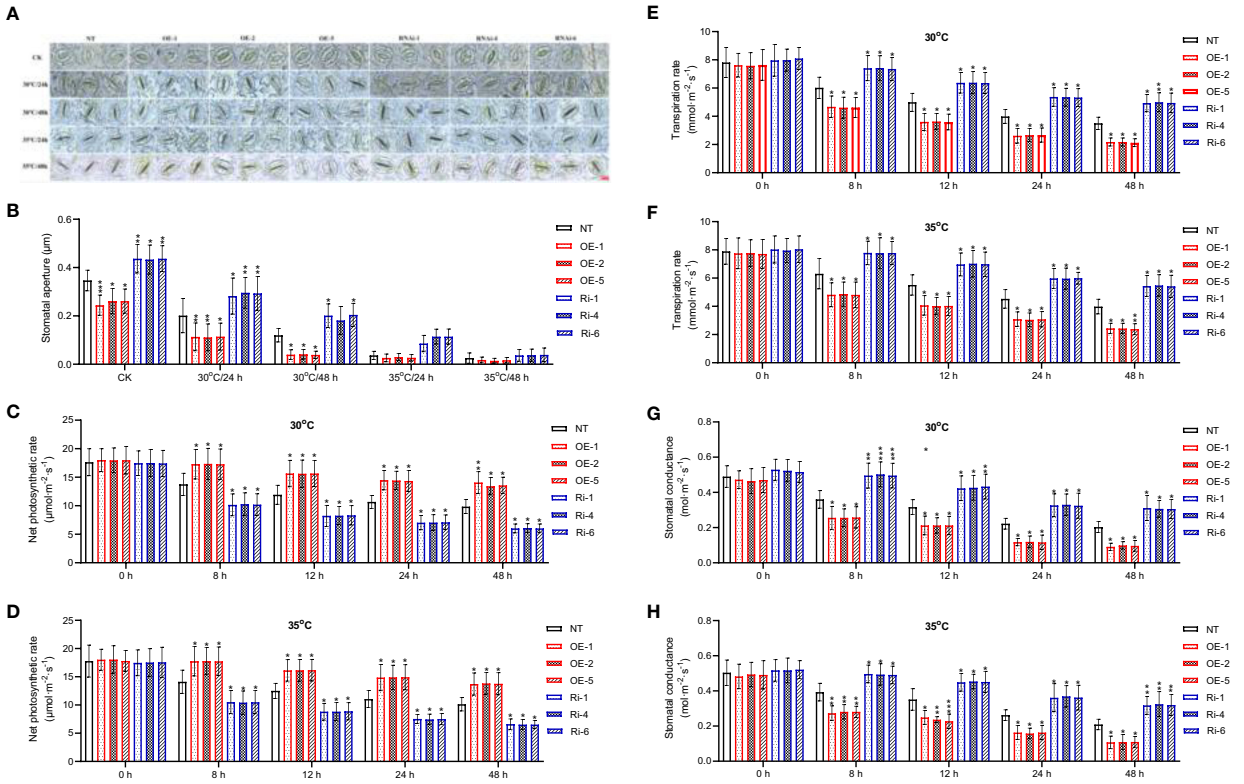

FIGURE 5
Stomatal apertures and photosynthesis of *StGATA2* over-expression or under-expression plants in response to heat stresses. **(A)** Representative images of *Solanum tuberosum* stomata; The scale bar equates to 10 μm. **(B)** Stomatal apertures depicted by the ratio of pore width to length. **(C, D)** Net photosynthetic rate, **(E, F)** transpiration rate and **(G, H)** stomatal conductance of potato leaves. The plants were measured 2 days after cultivation under the specified conditions (22°C, 30°C, and 35°C). NT, non-transgenic plants; OE, pBI121-EGFP-StGATA2-transgenic lines; Ri, pART-StGATA2-RNAi-transgenic plants. Mean ± standard deviation. Ordinary two-way ANOVA with Tukey's multiple comparisons test, *p<0.05, **p<0.01, ***p<0.001 (n = 9).

2013). Transcriptomic analysis found that *PdGNC* may potentially mediate nitrogen uptake in the root, cell division and carbohydrate utilization in the stem, and photosynthetic electron transfer and carbon assimilation in the leaf (An et al., 2019). However, the biological function of *GATAs* has not been studied under environmental stresses. Our data clearly demonstrated that *StGATA2* was involved in maintaining photosynthetic rate and mitigating respiratory rate.

Catalase functions as antioxidant enzyme, dissolving hydrogen peroxide into water and oxygen peroxisomes, of which encoding genes were found with cis-elements related to stress responses and plant hormones signaling in potato plants (Jbir Koubaa et al., 2023). Superoxide dismutase encoded by *StCuZnSODs*, *StFeSOD3* and *StMnSOD* play a significant role in catalyzing the conversion or dismutation of toxic superoxide anion radical into H_2O_2 and O_2, representing the first line of antioxidant defense against ROS induced by heat stress (Rudić et al., 2022). Peroxidase also serves as ROS-scavenging enzyme, catalyzing the conversion of H_2O_2 into H_2O with ascorbate as a specific electron donor (Caverzan et al., 2012). The expression of peroxidase-encoding gene is regulated in response to abiotic stresses such as heat stress during plant development (Caverzan et al., 2012). Our data suggested that the changes in enzyme activities of SOD, CAT, and POD at high temperature were coordinated with alterations in the transcription of the protein-encoding genes. The increases in activities of antioxidant enzymes at high temperature is more likely due to an increase in *StGATA2* expression. In the present experiments, increased proline content was observed at high temperature, which has been related to elevated transcripts of *StP5CS*. A study has confirmed the efficacy of proline in countering the damages in plant growth and enzymes of carbon and antioxidative metabolism (Kaushal et al., 2011). We found that *StGATA2* gene was associated with the maintained expression of *StP5CS* and proline level.

Plant GATAs containing GATA-type zinc fingers with two CX_2C motifs interspaced by a 17-20 amino acid long loop recognize the DNA sequence W-G-A-T-A-R through a single type IV zinc finger (Patient and McGhee, 2002; Reyes et al., 2004). Sugimoto et al. reported that the GATA-type zinc finger region is required for binding activity and activate expression from

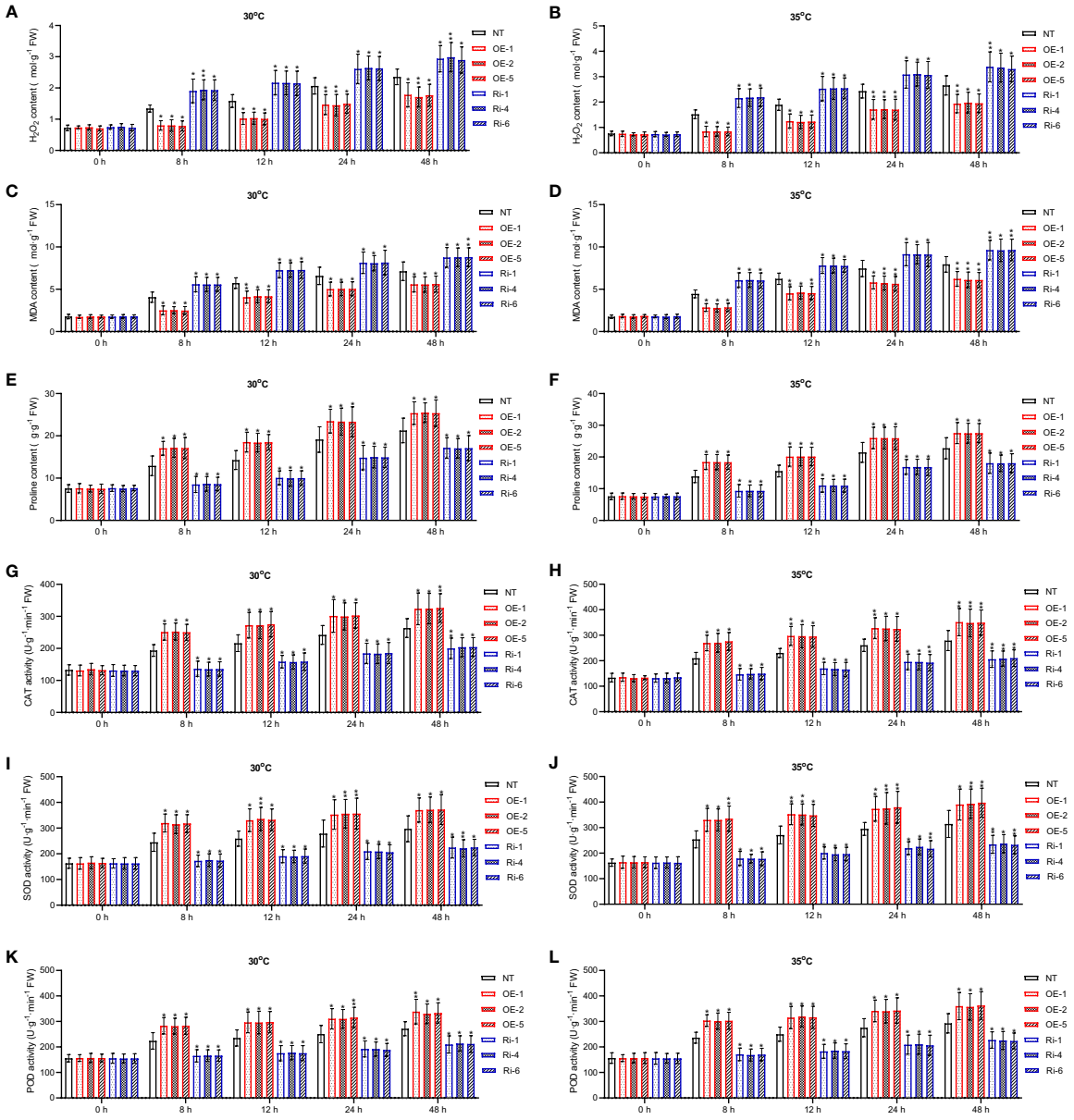

FIGURE 6
Effects of *StGATA2* expression on biochemical indexes of potato plants in response to heat stresses. **(A, B)** H_2O_2 content, **(C, D)** MDA content, **(E, F)** proline content, **(G, H)** CAT activity, **(I, J)** SOD activity, and **(K, L)** POD activity in potato leaves were estimated 2 days after cultivation under the specified conditions (22°C, 30°C, and 35°C). NT, non-transgenic plants; OE, pBI121-EGFP-StGATA2-transgenic lines; Ri, pART-StGATA2-RNAi-transgenic plants. Mean ± standard deviation. Ordinary two-way ANOVA with Tukey's multiple comparisons test, *p<0.05, **p<0.01, ***p<0.001 (n = 9).

NtMyb2 promoter (Sugimoto et al., 2003). In reverse, Gupta et al. presented that the alternative splice variant of *OsGATA23* (*OsGATA23b*) was unable to respond to abiotic tresses, which throws a novel light on the tight regulation of the spliced variants of *OsGATA* genes in response to salinity, drought and exogenous ABA (Gupta et al., 2017). Wang et al. performed yeast one assay and dual-luc assay and confirmed that the GATA-box of *SlGATA17* promoter was bound by SlHY5 and its expression was then regulated, which causes the hypersensitivity of Arabidopsis to NaCl at the post-germination stage (Wang et al., 2023). However, it is not yet possible to explain how the StGATA2 gene regulates the expression of heat responsive genes based on the available results of this study. *GATA*-encoded proteins contain higher conserved DNA binding domain that consist of two zinc finger motifs and two adjacent stretches of basic amino acids (Molkentin, 2000). The N-terminal finger can interact with adjacent GATA DNA sequence elements or with protein cofactors (Trainor et al., 1996; Weiss et al., 1997). The nuclear localization and transcriptional activation

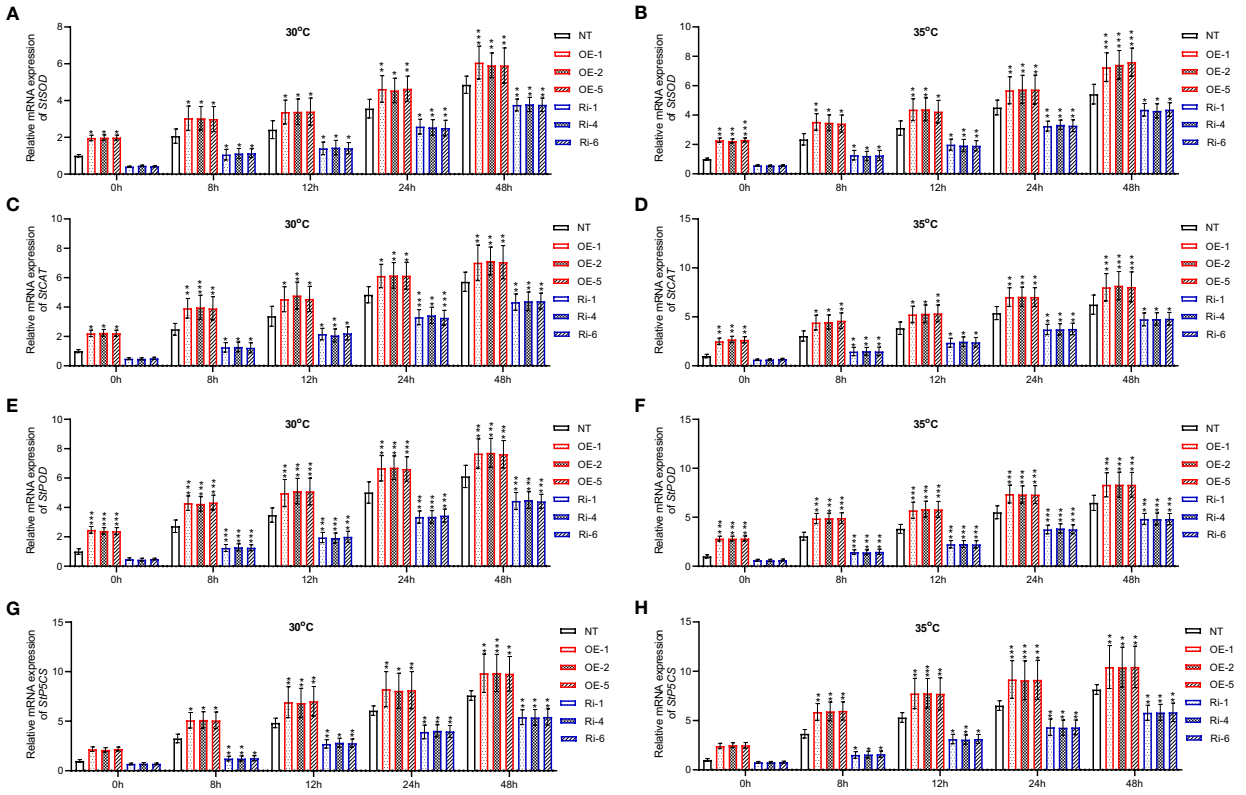

FIGURE 7
Changes in relative mRNA expression of heat-stress responsive genes in *StGATA2* over-expression or under-expression plants in response to heat stresses. **(A, B)** mRNA expression of *StSOD*, **(C, D)** *StCAT*, **(E, F)** *StPOD*, and **(G, H)** *StP5CS* in potato leaves were estimated 2 days after cultivation under the specified conditions (22°C, 30°C, and 35°C). NT, non-transgenic plants; OE, pBI121-EGFP-StGATA2-transgenic lines; Ri, pART-StGATA2-RNAi-transgenic plants. Mean ± standard deviation. Ordinary two-way ANOVA with Tukey's multiple comparisons test, *p<0.05, **p<0.01, ***p<0.001 (n = 9).

domains of *GATA2*-encoding protein may promote or inhibit the transcriptional activation of *StSOD*, *StCAT*, *StPOD*, and *StP5CS*. However, the identification of the protein domain needs protein domain deletion analysis.

Data availability statement

The original contributions presented in the study are included in the article/supplementary material. Further inquiries can be directed to the corresponding authors. The GATA protein sequences described in this article are available at the National Center for Biotechnology Information (https://www.ncbi.nlm.nih.gov/) with the following number: SlGATA2 (XP_004229778.1), StGATA2 (XP_006347916.1), CaGATA4 (XP 016545286.1), CbGATA2 (PHT60695.1), NtGATA4 (NP_001311749.2), AtGATA2 (NP_182031.1), OsGATA12 (XP_015631175.1).

Author contributions

XZ, HD, and YZ planned and designed the research. XZ, HD, HJ, SC, ZC, SS, JT, and YZ collected the data. XZ, HD, HJ, SC, ZC, SS, JT, and YZ analyzed the data. XZ, HD, and YZ drafted the manuscript. All authors contributed to the article and approved the submitted version.

Funding

This Research Program was financially supported by the Hainan Provincial Natural Science Foundation of China (No. 322MS116, 323MS095), and Central Public-interest Scientific Institution Basal Research Fund for Chinese Academy of Tropical Agricultural Sciences (No. 1630062023001, 1630062023002).

Acknowledgments

We thank Rongkai Wang (Bioediates, Shaanxi, China) for providing the plasmids pBI121-EGFP, pHANNIBAL, and pART.

Conflict of interest

The authors declare that the research was conducted in the absence of any commercial or financial relationships that could be construed as a potential conflict of interest.

Publisher's note

References

An, Y., Zhou, Y., Han, Y., Shen, C., Wang, S., Liu, C., et al. (2019). The GATA transcription factor GNC plays an important role in photosynthesis and growth in poplar. *J. Exp. Bot.* 71 (6), 1969–1984. doi: 10.1093/jxb/erz564

Bates, D. L., Chen, Y., Kim, G., Guo, L., and Chen, L. (2008). Crystal structures of multiple GATA zinc fingers bound to DNA reveal new insights into DNA recognition and self-association by GATA. *J. Mol. Biol.* 381 (5), 1292–1306. doi: 10.1016/j.jmb.2008.06.072

Behringer, C., and Schwechheimer, C. (2015). B-GATA transcription factors – insights into their structure, regulation, and role in plant development. *Front. Plant Sci.* 6. doi: 10.3389/fpls.2015.00090

Bi, Y-M., Zhang, Y., Signorelli, T., Zhao, R., Zhu, T., and Rothstein, S.. (2005). Genetic analysis of arabidopsis GATA transcription factor gene family reveals a nitrate-inducible member important for chlorophyll synthesis and glucose sensitivity. *Plant J.* 44 (4), 680–692. doi: 10.1111/j.1365-313X.2005.02568.x

Caverzan, A., Passaia, G., Rosa, S. B., Ribeiro, C. W., Lazzarotto, F., Margis-Pinheiro, M., et al. (2012). Plant responses to stresses: role of ascorbate peroxidase in the antioxidant protection. *Genet. Mol. Biol.* 35, 1011–1019. doi: 10.1590/S1415-47572012000600016

Devireddy, A. R., Arbogast, J., and Mittler, R. (2020). Coordinated and rapid whole-plant systemic stomatal responses. *New Phytol.* 225 (1), 21–25. doi: 10.1111/nph.16143

Fahad, S., Hussain, S., Saud, S., Hassan, S., Ihsan, Z., Shah, A. N., et al. (2016). Exogenously applied plant growth regulators enhance the morpho-physiological growth and yield of rice under high temperature. *Front. Plant Sci.* 7, 1250. doi: 10.3389/fpls.2016.01250

Feng, X., Yu, Q., Zeng, J., He, X., and Liu, W. (2022a). Genome-wide identification and characterization of GATA family genes in wheat. *BMC Plant Biol.* 22 (1), 372. doi: 10.1186/s12870-022-03733-3

Feng, X., Yu, Q., Zeng, J., He, X., and Liu, W. (2022b). Genome-wide identification and characterization of GATA family genes in wheat. *BMC Plant Biol.* 22 (1), 1–15. doi: 10.1186/s12870-022-03733-3

Gronenborn, A. M. (2005). *The DNA-binding domain of GATA transcription factors–a prototypical type IV Cys2-Cys2 zinc finger* (Springer Boston, MA: Molecular Biology Intelligence Unit).

Guo, J., Bai, X., Dai, K., Yuan, X., Guo, P., Zhou, M., et al. (2021). Identification of GATA transcription factors in brachypodium distachyon and functional characterization of BdGATA13 in drought tolerance and response to gibberellins. *Front. Plant Sci.* p, 2386. doi: 10.3389/fpls.2021.763665

Gupta, P., Nutan, K. K., Singla-Pareek, S. L., and Pareek, A. (2017). Abiotic stresses cause differential regulation of alternative splice forms of GATA transcription factor in rice. *Front. Plant Sci.* 8. doi: 10.3389/fpls.2017.01944

He, P., Wang, X., Zhang, X., Jiang, Y., Tian, W., Zhang, X., et al. (2018). Short and narrow flag leaf1, a GATA zinc finger domain-containing protein, regulates flag leaf size in rice (*Oryza sativa*). *BMC Plant Biol.* 18 (1), 273. doi: 10.1186/s12870-018-1452-9

Hudson, P., Guevara, D. R., Hand, A. J., Xu, Z., and Hao, L. (2013). Rice cytokinin GATA transcription Factor1 regulates chloroplast development and plant architecture. *Plant Physiol.* 162 (1), 132–144. doi: 10.1104/pp.113.217265

Jbir Koubaa, R., Ayadi, M., Saidi, M N., Charfeddine, S., Bouzid, R. G, and Nouri-Ellouz, O. (2023). Comprehensive genome-wide analysis of the catalase enzyme toolbox in potato (*Solanum tuberosum* l.). *Potato Res.* 66 (1), 23–49. doi: 10.1007/s11540-022-09554-z

Kaushal, N., Gupta, K., Bhandhari, K., Kumar, S., Thakur, P., and Nayyar, H. (2011). Proline induces heat tolerance in chickpea (Cicer arietinum l.) plants by protecting vital enzymes of carbon and antioxidative metabolism. *Physiol. Mol. Biol. Plants* 17, 203–213. doi: 10.1007/s12298-011-0078-2

Klermund, C., Ranftl, Q. L., Diener, J., Bastakis, E., Richter, R., and Schwechheimer, C. (2016). LLM-domain b-GATA transcription factors promote stomatal development downstream of light signaling pathways in arabidopsis thaliana hypocotyls. *Plant Cell* 28 (3), 646–660. doi: 10.1105/tpc.15.00783

Körner, C. (2006). Significance of temperature in plant life. *Plant Growth Climate Change* 100, 48–66. doi: 10.1002/9780470988695.ch3

Lafta, A. M., and Lorenzen, J. H. (1995). Effect of high temperature on plant growth and carbohydrate metabolism in potato. *Plant Physiol.* 109 (2), 637–643. doi: 10.1104/pp.109.2.637

Lai, D., Yao, X., Yan, J., Gao, A., Yang, H., Xiang, D., et al. (2022). Genome–wide identification, phylogenetic and expression pattern analysis of GATA family genes in foxtail millet (Setaria italica). *BMC Genomics* 23 (1), 549. doi: 10.1186/s12864-022-08786-0

Li, G., Cao, C., Yang, H., Wang, J., Wei, W., Zhu, D., et al. (2020). Molecular cloning and potential role of DiSOC1s in flowering regulation in davidia involucrata baill. *Plant Physiol. Biochem.* 157, 453–459. doi: 10.1016/j.plaphy.2020.11.003

Lu, H., Klocko, A. L., Brunner, A. M., Ma, C., Magnuson, A. C., Howe, G. T., et al. (2019). RNA Interference suppression of AGAMOUS and SEEDSTICK alters floral organ identity and impairs floral organ determinacy, ovule differentiation, and seed-hair development in populus. *New Phytol.* 222 (2), 923–937. doi: 10.1111/nph.15648

Luo, X.-M., Lin, W.-H., Zhu, S., Zhu, J.-Y., Sun, Y., Fan, X.-F., et al. (2010). Integration of light-and brassinosteroid-signaling pathways by a GATA transcription factor in arabidopsis. *Dev. Cell* 19 (6), 872–883. doi: 10.1016/j.devcel.2010.10.023

Luo, H., Xu, H., Chu, C., He, F., and Fang, S. (2020). High temperature can change root system architecture and intensify root interactions of plant seedlings. *Front. Plant Sci.* 11, 160. doi: 10.3389/fpls.2020.00160

Manfield, I. W., Devlin, P. F., Jen, C.-H., Westhead, D. R., and Gilmartin, P. M. (2007). Conservation, convergence, and divergence of light-responsive, circadian-regulated, and tissue-specific expression patterns during evolution of the arabidopsis GATA gene family. *Plant Physiol.* 143 (2), 941–958. doi: 10.1104/pp.106.090761

Molkentin, J. D. (2000). The zinc finger-containing transcription factors GATA-4,-5, and-6: ubiquitously expressed regulators of tissue-specific gene expression. *J. Biol. Chem.* 275 (50), 38949–38952. doi: 10.1074/jbc.R000029200

Park, J., Kim, H., Kim, S., Kong, S., Park, J., Kim, S., et al. (2006). A comparative genome-wide analysis of GATA transcription factors in fungi. *Genomics Inf.* 4 (4), 147–160.

Patient, R. K., and McGhee, J. D. (2002). The GATA family (vertebrates and invertebrates). *Curr. Opin. Genet. Dev.* 12 (4), 416–422. doi: 10.1016/S0959-437X(02)00319-2

Peng, W., Li, W., Song, N., Tang, Z., Liu, J., Wang, Y., et al. (2021). Genome-wide characterization, evolution, and expression profile analysis of GATA transcription factors in brachypodium distachyon. *Int. J. Mol. Sci.* 22 (4), 2026. doi: 10.3390/ijms22042026

Reyes, J. C., Muro-Pastor, M. I., and Florencio, F. J. (2004). The GATA family of transcription factors in arabidopsis and rice. *Plant Physiol.* 134 (4), 1718–1732. doi: 10.1104/pp.103.037788

Rudić, J., Dragićević, M. B., Momčilović, I., Simonović, A. D., and Pantelić, D. (2022). In silico study of superoxide dismutase gene family in potato and effects of elevated temperature and salicylic acid on gene expression. *Antioxidants* 11 (3), 488. doi: 10.3390/antiox11030488

Scazzocchio, C. (2000). The fungal GATA factors. *Curr. Opin. Microbiol.* 3 (2), 126–131. doi: 10.1016/S1369-5274(00)00063-1

Shi, M., Huang, Q., Wang, Y., Wang, C., Zhu, R., Zhang, S., et al. (2022). Genome-wide survey of the GATA gene family in camptothecin-producing plant ophiorrhiza pumila. *BMC Genomics* 23 (1), 256. doi: 10.1186/s12864-022-08484-x

Shikata, M., Matsuda, Y., Ando, K., Nishii, A., Takemura, M., Yokota, A., et al. (2004). Characterization of arabidopsis ZIM, a member of a novel plant-specific GATA factor gene family. *J. Exp. Bot.* 55 (397), 631–639. doi: 10.1093/jxb/erh078

Si, H.-J., Xie, C.-H., and Liu, J. (2003). An efficient protocol for agrobacterium-mediated transformation with microtuber and the introduction of an antisense class I patatin gene into potato. *Acta Agronomica Sin.* 29 (6), 801–805.

Sparkes, I. A., Runions, J., Kearns, A., and Hawes, C. (2006). Rapid, transient expression of fluorescent fusion proteins in tobacco plants and generation of stably transformed plants. *Nat. Protoc.* 1 (4), 2019–2025. doi: 10.1038/nprot.2006.286

Sugimoto, K., Takeda, S., and Hirochika, H. (2003). Transcriptional activation mediated by binding of a plant GATA-type zinc finger protein AGP1 to the AG-motif (AGATCCAA) of the wound-inducible myb gene NtMyb2. *Plant J.* 36 (4), 550–564. doi: 10.1046/j.1365-313X.2003.01899.x

Teakle, G. R., Manfield, I. W., Graham, J. F., and Gilmartin, P. M. (2002). Arabidopsis thaliana GATA factors: organisation, expression and DNA-binding characteristics. *Plant Mol. Biol.* 50, 43–56. doi: 10.1023/A:1016062325584

Trainor, C. D., Omichinski, J. G., Vandergon, T. L., Gronenborn, A. M., Clore, G. M., and Felsenfeld, G. (1996). A palindromic regulatory site within vertebrate GATA-1 promoters requires both zinc fingers of the GATA-1 DNA-binding domain for high-affinity interaction. *Mol. Cell Biol.* 16 (5), 2238–2247. doi: 10.1128/MCB.16.5.2238

Tricker, P. J., Trewin, H., Kull, O., Clarkson, G. J. J., Eensalu, E., Tallis, M. J., et al. (2005). Stomatal conductance and not stomatal density determines the long-term reduction in leaf transpiration of poplar in elevated CO 2. *Oecologia* 143, 652–660. doi: 10.1007/s00442-005-0025-4

Wang, Y., Cao, X., Zhang, D., Li, Y., Wang, Q., and Ma, F., et al. (2023). SlGATA17, a tomato GATA protein, interacts with SlHY5 to modulate salinity tolerance and germination. *Environ. Exp. Bot.* 206, 105191. doi: 10.1016/j.envexpbot.2022.105191

Weiss, M. J., Yu, C., and Orkin, S. H. (1997). Erythroid-cell-specific properties of transcription factor GATA-1 revealed by phenotypic rescue of a gene-targeted cell line. *Mol. Cell Biol.* 17 (3), 1642–1651. doi: 10.1128/MCB.17.3.1642

Yu, C., Li, N., Yin, Y., Wang, F., Gao, S., Jiao, C., et al. (2021). Genome-wide identification and function characterization of GATA transcription factors during development and in response to abiotic stresses and hormone treatments in pepper. *J. Appl. Genet.* 62, 265–280. doi: 10.1007/s13353-021-00618-3

Yu, R., Chang, Y., Chen, H., Feng, J., Wang, H., Tian, T., et al. (2022). Genome-wide identification of the GATA gene family in potato (*Solanum tuberosum* l.) and expression analysis. *J. Plant Biochem. Biotechnol.* 31 (1), 37–48. doi: 10.1007/s13562-021-00652-6

Yuan, Q., Zhang, C., Zhao, T., Meini Yao, M., and Xu, X. (2018). A genome-wide analysis of GATA transcription factor family in tomato and analysis of expression patterns. *Int. J. Agric. Biol.* 20 (6), 1274–1282.

Zhang, K., Jia, L., Yang, D., Hu, Y., Njogu, M. K., Wang, P., et al. (2021). Genome-wide identification, phylogenetic and expression pattern analysis of GATA family genes in cucumber (Cucumis sativus l.). *Plants* 10 (8), 1626. doi: 10.3390/plants10081626

Zhao, Y., Medrano, L., Ohashi, K., Fletcher, J. C., Yu, H., Sakai, H., et al. (2004). HANABA TARANU is a GATA transcription factor that regulates shoot apical meristem and flower development in arabidopsis. *Plant Cell* 16 (10), 2586–2600. doi: 10.1105/tpc.104.024869

Zhu, W., Guo, Y., Chen, Y., Wu, D., and Jiang, L. (2020). Genome-wide identification, phylogenetic and expression pattern analysis of GATA family genes in brassica napus. *BMC Plant Biol.* 20 (1), 543. doi: 10.1186/s12870-020-02752-2

Zhu, X., Hong, X., Liu, X., Li, S., Yang, J., Wang, F., et al. (2021). Calcium-dependent protein kinase 32 gene maintains photosynthesis and tolerance of potato in response to salt stress. *Scientia Hortic.* 285, 110179. doi: 10.1016/j.scienta.2021.110179

frontiers | Frontiers in Plant Science

TYPE Original Research
PUBLISHED 22 November 2023
DOI 10.3389/fpls.2023.1308721

OPEN ACCESS

EDITED BY
Zemin Wang,
Gansu Agricultural University, China

REVIEWED BY
Wang Aimin,
Jiangsu Normal University, China
Linchuan Fang,
Wuhan Academy of Agricultural Sciences, China

*CORRESPONDENCE
Fei Wang
20966954@qq.com
Minghua Yao
yaomh_2008@126.com

†These authors have contributed equally to this work

RECEIVED 07 October 2023
ACCEPTED 06 November 2023
PUBLISHED 22 November 2023

CITATION
Wang X, Li N, Zan T, Xu K, Gao S, Yin Y, Yao M and Wang F (2023) Genome-wide analysis of the TIFY family and function of *CaTIFY7* and *CaTIFY10b* under cold stress in pepper (*Capsicum annuum* L.). *Front. Plant Sci.* 14:1308721. doi: 10.3389/fpls.2023.1308721

Genome-wide analysis of the TIFY family and function of *CaTIFY7* and *CaTIFY10b* under cold stress in pepper (*Capsicum annuum* L.)

Xiaodi Wang[1†], Ning Li[1†], Tianxiang Zan[1,2], Kai Xu[1], Shenghua Gao[1], Yanxu Yin[1], Minghua Yao[1,3*] and Fei Wang[1,3*]

[1]Hubei Key Laboratory of Vegetable Germplasm Innovation and Genetic Improvement, Cash Crops Research Institute, Hubei Academy of Agricultural Sciences, Wuhan, China, [2]College of Horticulture and Gardening, Yangtze University, Jingzhou, China, [3]Hubei Hongshan Laboratory, Wuhan, Hubei, China

TIFY [TIF(F/Y)XG] proteins are a plant particular transcription factor family that regulates plant stress responses. Therefore, to fill this gap, we investigated *CaTIFY* genes in pepper. Gene structure and conserved motifs of the pepper TIFY gene family were systematically analyzed using sequence alignment analysis, *Cis*-acting element analysis, transcriptomic data, and RT-qPCR analysis, and their expression patterns were further analyzed using Virus-Induced Gene Silencing (VIGS) and cold stress reactive oxygen species (ROS) response. We identified 16 *CaTIFY* genes in pepper, which were dispersed among seven subgroups (JAZI, JAZII, JAZIII, PPD, TIFY, and ZIM/ZML). Several *CaTIFY* members had stress-related harmonic-responsive elements, and four (*CaTIFY7*, *CaTIFY10b*, *CaTIFY1b*, and *CaTIFY6b*) had low-temperature-responsive elements. Transcriptomic data and RT-qPCR analysis revealed that the TIFY genes in pepper displayed different expression patterns in the roots, stems, leaves, flower fruits, and seeds. In particular, *CaTIFY7* was highly expressed in young leaves, and *CaTIFY10b* was highly expressed in roots. *CaTIFY*s participated in the regulation of several different abiotic stresses and *CaTIFY7* and *CaTIFY10b* were significantly induced by cold stress. Additionally, Virus-Induced Gene Silencing (targeting *CaTIFY7* and *CaTIFY10b*) resulted in plants that were sensitive to cold stress. Conversely, overexpression of *CaTIFY7* and *CaTIFY10b* enhanced plant cold tolerance by promoting the expression of genes related to cold stress and the ROS response. CaTIFY7 and CaTIFY10b interacted with themselves and CaTIFY7 also interacted with CaTIFY10b in the yeast two-hybrid (Y2H) system. Our data provide a basis for further analysis of the role of pepper TIFY genes in cold-stress responses in the future.

KEYWORDS

pepper (*Capsicum annuum* L.), CaTIFY, genome-wide analysis, cold stress, gene expression

Introduction

The *TIFY* gene family encodes a transcription factor unique to plants characterized by a highly conserved TIFY domain, which plays an important regulatory role in plant growth, development, and stress tolerance. The TIFY domain is composed of 36 amino acids and a TIF[F/Y] XG core region (Vanholme et al., 2007). Many studies have shown that the TIFY family of proteins can be divided into four subfamilies: TIFY, JAZ, PPD, and ZML (Bai et al., 2011). The first TIFY gene was identified in *Arabidopsis thaliana* (Nishii et al., 2000). Subsequently, the TIFY gene family was identified in rice (Ye et al., 2009), maize (Heidari et al., 2021), cassava (Zheng et al., 2022), tomato (Heidari et al., 2021), and other species (Huang et al., 2016; Sirhindi et al., 2016; Xia et al., 2017; He et al., 2020; Du et al., 2022).

The TIFY protein is a key regulator of the jasmonic acid signaling pathway, participates in defense and stress responses during plant development, and plays a major role in responses to biological and abiotic stresses (Thireault et al., 2015; Ebel et al., 2018). There are few reports on the response of the TIFY family to biotic stress, mainly focusing on the abiotic stress response of the TIFY family. Multiple TIFY genes have been shown to respond to drought and salt stress in arabidopsis, apples, grapes, rice, soybeans, and corn (Ye et al., 2009; Zhang et al., 2012; Li et al., 2015; Zhou et al., 2015; Meng et al., 2019; Zhao et al., 2020). In rice, the overexpression of *OsTIFY11a* significantly improves its tolerance to salt and dehydration stress (Ye et al., 2009). In addition, OsJAZ1 interacts with OsbHLH148, a transcription regulator in the jasmonic acid signaling pathway, resulting in enhanced drought tolerance in rice (Seo et al., 2011). Among solanaceous plants, only the TIFY genes of tomato have been identified, and transcriptome data show that most *SlJAZ* genes respond to salt, osmotic stress, or JA-ABA treatments (Chini et al., 2017).

With the rapid development of transcriptome sequencing, an increasing number of TIFY genes have been found to respond to low-temperature stress (Ye et al., 2009; Zhang et al., 2012; Zhang et al., 2015; Huang et al., 2016; He et al., 2020). Most *BdTIFY* genes are responsive to one or more abiotic stressors, including drought, salinity, low temperature, and heat (Zhang et al., 2015). In grapes, *VvJAZ4*, *5*, *9*, *11*, and *VvZML1* respond to cold stress and are regulated by drought or salinity (Zhang et al., 2012). In *Brassica napus*, recent research has found that *TIFY11b*, *TIFY10a*, *TIFY3*, *TIFY5a/b*, and *TIFY6* are induced by cold acclimation and overexpression of *BnaJAZ7-A3/BnaJAZ7-C3* enhances cold injury stress (He et al., 2020). In rice, some *OsTIFY* genes are induced by cold but not induced or even repressed by ABA, which suggests *OsTIFY* participated in the cold-stress response via ABA-independent signaling pathways (Ye et al., 2009). Studies on Arabidopsis have found that the interaction between JAZ1/JAZ4 and C-repeat binding factor (CBF) inducers inhibits the function of transcriptional ICE1, thereby weakening the expression of CBFs (Huang et al., 2012; Hu et al., 2013). Furthermore, the overexpression of *JAZ1* or *JAZ4* inhibits the response of Arabidopsis to freezing stress (Hu et al., 2013). However, few studies have revealed the function of the TIFY protein in plant low-temperature responses.

Pepper (*Capsicum annum* L.) is a versatile vegetable belonging to the Solanaceae family and is an economically important crop worldwide. The average yield loss caused by low temperatures is enormous (Chinnusamy et al., 2007; Legris et al., 2017). Although there have been many advances in understanding the cold resistance mechanisms of crops, there are still few reports on the low-temperature tolerance of pepper. Transcription factors also play an important role in the response of pepper to low-temperature stress; however, only a small number of transcription factor families, including MADS, NAC, and bHLH, have been shown to participate in the low-temperature regulation process in pepper (Guo et al., 2015; Chen et al., 2019; Hou et al., 2020; Zhang et al., 2020; Wang et al., 2022; Zhang et al., 2023). So far, the TIFY protein in pepper has not been identified, and its role in the cold-stress response has not been studied. Therefore, to fill this gap, we investigated *CaTIFY* genes in pepper.

In this study, we identified 16 genes encoding TIFY proteins in the pepper genome. Chromosomal position, phylogenetics, gene structure, conserved domains, and promoter cis-element analyses were carried out to provide genome-wide identification and investigation of CaTIFY genes. Furthermore, the expression of all CaTIFY genes was investigated in various tissues and organs at different developmental stages and under various abiotic stresses, using published transcriptome data. We also examined their expression profiles after cold treatments and in different tissues by RT-qPCR assays and found *CaTIFY7* and *CaTIFY10b* were induced by cold stress in leaves significantly. Gene function analysis of *CaTIFY7* and *CaTIFY10b* showed that they positively regulated cold-stress tolerance in pepper plants. Further analysis demonstrated that the downregulation or overexpression of *CaTIFY7* and *CaTIFY10b* influenced the expression levels of cold-stress and reactive oxygen species (ROS)-related genes. Further, the Y2H assay proved CaTIFY7 and CaTIFY10b interacted with themselves and CaTIFY7 also interacted with CaTIFY10b. By performing this study, we have laid a foundation for further research on the function and molecular mechanism of the TIFY gene family in the pepper stress response and provide a basis for improving plant stress resistance in the future.

Materials and methods

Identification of CaTIFY gene family

TIFY domain (PF06200) hidden Markov file was downloaded from Pfam database (http://pfam.xfam.org/). HMMER software was used to screen for possible TIFY proteins in the pepper genome and candidate members were submitted to Pfam and SMART (https://smart.embl.de/) online programs to verify the composition of conservative structural domains for further screening.

Gene structure analysis

The CDS and genome sequence of the pepper TIFY gene family were submitted to the GSDS (http://gsds.gao-lab.org/) online website for visual analysis of the intron–exon substructure of the TIFY gene family.

Functional structural domain analysis

TBtools was used to extract the TIFY protein sequence of pepper and MEGA software was used to perform multiple sequence alignments on the TIFY protein sequence of pepper. The functional domain of the TIFY protein in chili pepper was analyzed based on conserved domain sequence characteristics.

Phylogenetic tree analysis

First, we used MEGA5 software to conduct multiple sequence alignments of Arabidopsis, rice, tomato, and identified pepper TIFY protein sequences. Alignment results were used to build a phylogenetic tree based on the maximum parsimony method, and the bootstrap value was set to 1000. Next, the online program Itol (https://itol.embl.de/) was used to further refine the evolutionary tree.

Chromosome localization analysis

We obtained the genome sequences and GFF files of peppers from the PepperHub database (http://122.205.95.132/index.php) (Liu et al., 2017). TBtools software was used to extract the chromosome length and location information of TIFY genes in the pepper genome from the GFF files and to perform visual analysis.

Conserved motifs analysis of CaTIFY proteins by MEME

Conserved motifs in CaTIFYs were predicted using MEME-Suite (https://meme-suite.org/meme/tools/meme) and visualized using TBtools. Specific parameters were set as follows: 'Any number of repetitions' was selected as the site distribution, and up to ten motifs were retrieved.

Promoter *cis*-acting elements analysis

First, 2000 bp upstream DNA sequences of the pepper TIFY gene CDS were extracted from the pepper genome sequence using the TBtools software. We then uploaded these sequences to the PlantCARE database (http://bioinformatics.psb.ugent.be/webtools/plantcare/html/) to obtain *cis*-acting element information on the promoter of CaTIFY genes in pepper. Subsequently, the *cis*-acting elements related to stress and hormones were classified. TB tools software was used to visualize the analysis of CaTIFY gene promoters in pepper.

Protein interaction network prediction

The identified BvTIFY protein sequence was uploaded to the STRING database (https://cn.string-db.org/) for prediction of the biological functions of homologous CaTIFY and other proteins and their potential interactions.

Expression patterns of GmTIFY genes under abiotic stresses

RNA-seq data of CaTIFY family members in different tissues and organs (roots, shoots, young leaves, mature leaves, old leaves, flowers, fruits, and seeds) under several abiotic stresses (salt, drought, H_2O_2, heat, and cold) were obtained from the PepperHub Database. HEMI software was used to visualize the expression levels of CaTIFYs.

Plant materials and cold-stress treatment

Peppers (*Capsicum annuum* L.) were cultivated under a 25°C temperature and 16/8-h day/night photoperiod. Pepper plants of uniform size were selected and exposed to cold stress (4°C) at the 6-8 true leaf stage in growth chambers. Leaves and roots were sampled at 1, 3, 6, 12, and 24 h after cold treatment.

Real-Time Fluorescence Quantitative PCR (RT-qPCR)

TRIzol and chloroform reagents were used to extract total RNA from pepper leaves and roots. A HiScript II 1st Strand cDNA Synthesis Kit (+ gDNA wiper) (Vazyme, Nanjing, China) was used for reverse transcription. ChamQ Universal SYBR® qPCR Master Mix (Vazyme) and CFX384 Real-Time PCR Detection System (Bio-Rad, Hercules, CA, USA) were used to perform RT-qPCR. The quantitative results were analyzed by the $2^{-\Delta\Delta Ct}$ method and the CaUBI3 gene (Wan et al., 2011) was used as the internal control for normalizing gene expression. Each experiment was performed in triplicate. The primers used in the qPCR analysis are listed in Supplementary Table 1.

Virus-Induced Gene Silencing (VIGS) assay in pepper

The silence-specific 312 bp fragment of *CaTIFY7* was selected and inserted into the pTRV2 vector between the KpnI and XhoI

sites to form the pTRV2:*CaTIFY7* recombinant plasmid. The pTRV2:*CaTIFY7*, pTRV2, and pTRV1 were individually transformed into Agrobacterium GV3101 cells. Suspensions of pTRV2:*CaTIFY7* and pTRV2 were individually mixed with equal volumes of pTRV1 and injected into the cotyledons of two true-leaf-stage pepper seedlings as described previously (Wang et al., 2013). The same experimental method was used for *CaTIFY10b* and specific 331 bp fragments of *CaTIFY10b* were used to build a carrier.

Transient expression of *CaTIFY7* and *CaTIFY10b* in pepper leaves

The full-length *CaTIFY7* cDNA (Capana01g003720) and *CaTIFY10b* cDNA (Capana07g000750) were obtained from the Pepper Genome Database. PCR-amplified products of *CaTIFY7* and *CaTIFY10b* were cloned into empty vectors to generate 35S:*CaTIFY7* and 35S:*CaTIFY10b*. The empty vectors 35S:*CaTIFY7* and 35S:*CaTIFY10b* were individually transformed into Agrobacterium GV3101. The suspensions were infiltrated into the leaves of pepper plants at the eight-leaf stage as described previously (Cai et al., 2021). After 48 h, half of the infiltrated plants were moved to 4 °C treatment. All infiltrated leaves were collected for further use 24 h after cold stress.

Cold tolerance indices in pepper

To assess cold-stress biochemical indices, 3,3'-diaminobenzidine (DAB) and nitro blue tetrazolium staining (Coolaber, Beijing, China) were used to stain the transformed leaves as per the manufacturer's instructions.

Yeast two-hybrid (Y2H) assay

To determine the relationship between CaTIFY7 and CaTIFY10b, we performed a Y2H assay using the MatchmakerTM Two-Hybrid System (Clontech, USA). The CDS of CaTIFY7 and CaTIFY10b were amplified with specific primers and cloned into the pGBKT7-BD vector between the *Eco*RI and *Pst*I sites and the pGADT7-AD vector between the *Eco*RI and *Bam*HI sites. The fusion pGBKT7-BD and pGADT7-AD constructs were co-transformed into the Y2H Gold strain and screened for SD/-Leu/-Trp. Then multiple monoclonal clones were mixed and spotted onto SD/-Leu/-Trp/-His/-Ade media at 30°C for 3-5 d. The fusion of pGBKT7-53 and pGADT7-T was used as a positive control.

Results

Identification of TIFY members in pepper

To identify TIFY members in pepper, the TIFY domain (PF06200) was used to screen for possible TIFY proteins in the pepper genome. 16 *TIFY* genes were identified in the pepper genome and named CaTIFYs, according to their homologous TIFY genes in Arabidopsis (Figure 1). The numbers of amino acids in CaTIFYs ranged from 135 to 411 and their molecular weights ranged from 14.61 to 45.7 KDa. The theoretical PIs of the CaTIFYs ranged from 4.65 to 10.68 (Table 1). In addition, the subcellular location prediction analysis showed that all CaTIFYs were located in the nucleus.

Conserved domain and motif analysis of CaTIFY proteins

Multiple sequence comparisons revealed that all members of the TIFY gene family contained TIFY and Jaz domains (Figure 2A). The TIFY domain of the CaTIFY proteins was more conserved than the Jaz domain. CaTIFY3, CaTIFY9, and CaTIFY10d contained almost no Jaz domains (Figure 2A). In addition, conserved motifs were also identified. As shown in Figure 2B, a total of 10 motifs were predicted in CaTIFY proteins using the MEME website and TBtools software. The numbers of CaTIFY motifs ranged from one (CaTIFY8) to five (CaTIFY10b/c). There were four motifs in the seven CaTIFY (CaTIFY1b, CaTIFY1c, CaTIFY2, CaTIFY4a, CaTIFY4b, CaTIFY10a, and CaTIFY10d) proteins and their proportions exceeded 30% of the total proteins. Almost all proteins had motif1 and motif2, except for CaTIFY8, which only

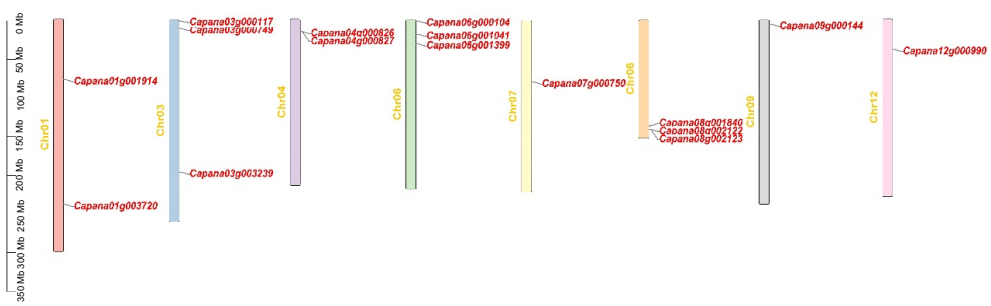

FIGURE 1
Distribution of the TIFY genes on chromosomes of pepper. The scale on the right is in million bases (Mb).

10.3389/fpls.2023.1308721

TABLE 1 CaTIFY gene feature information in pepper.

Gene name	Locus ID	Chromosome	Starting site	Ending site	ORF (aa)	CDS (bp)	MW (kDa)	pI	Subcellular location
CaTIFY9	Capana01g001914	Chr01	78262060	78263252	153	459	17.11	6.69	Nucleus.
CaTIFY7	Capana01g003720	Chr01	239982070	239985708	346	1038	36.56	8.9	Nucleus.
CaTIFY10a	Capana03g000117	Chr03	1604329	1606207	299	897	32.47	9.17	Nucleus.
CaTIFY6a	Capana03g000749	Chr03	10975774	10979194	329	987	33.89	9.52	Nucleus.
CaTIFY4a	Capana03g003239	Chr03	196914896	196921253	411	1233	45.7	8.71	Nucleus.
CaTIFY2	Capana04g000826	Chr04	16098710	16101334	269	807	29.78	7.33	Nucleus.
CaTIFY1a	Capana04g000827	Chr04	16106805	16109264	168	504	18.79	4.65	Nucleus.
CaTIF Y4b	Capana06g000104	Ch06	1376792	1379848	378	1134	42.06	8.84	Nucleus.
CaTIFY6b	Capana06g001041	Chr06	18388538	18393631	300	900	33.56	10.68	Nucleus.
CaTIFY8	Capana06g001399	Chr06	30846359	30852144	383	1149	40.09	9.87	Nucleus.
CaTIFY10b	Capana07g000750	Chr07	79075974	79076928	229	687	25.15	9.58	Nucleus.
CaTIFY1b	Capana08g002122	Chr08	141545179	141560486	340	1020	35.71	6.74	Nucleus.
CaTIFY1c	Capana08g002123	Chr08	141562343	141568832	374	1122	41.07	4.92	Nucleus.
CaTIFY3	Capana08g001840	Chr08	137205501	137206502	135	405	14.61	7.51	Nucleus.
CaTIFY10c	Capana09g000144	Chr09	5548125	5549825	251	753	27.93	10.09	Nucleus.
CaTIFY10d	Capana12g000990	Chr12	39269034	39274278	209	627	23.04	10.36	Nucleus.

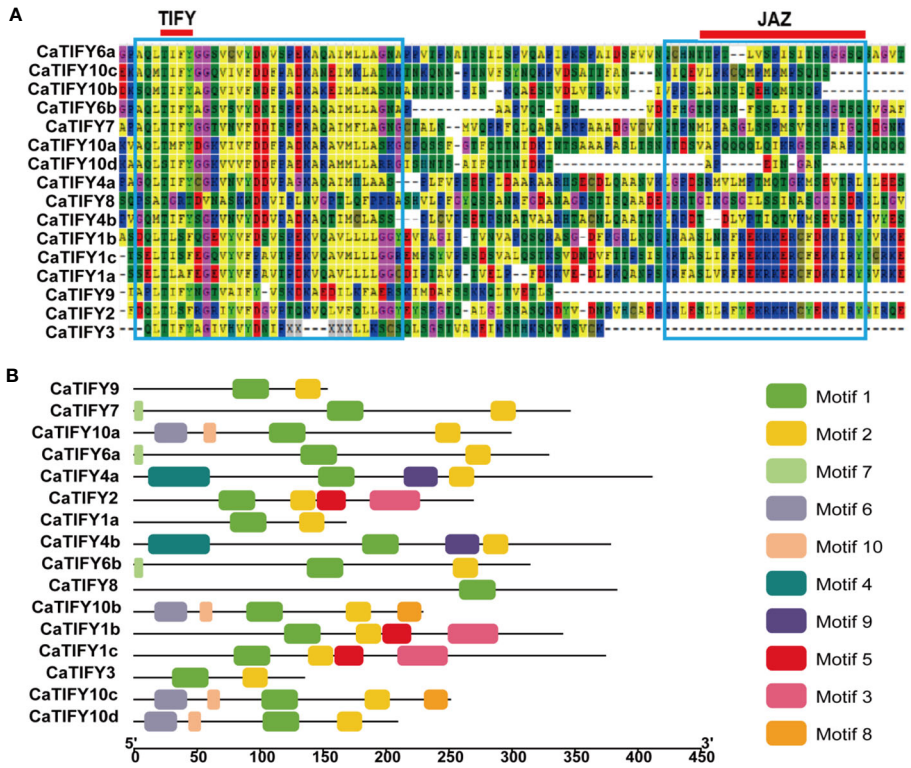

FIGURE 2
Multiple sequences alignment of CaTIFYs and conserved motif distributions of CaTIFYs proteins in pepper. **(A)** The blue boxes indicate conserved amino acids. The red line indicate the core amino acids of TIFY and Jas domain. **(B)** Distribution of the conserved motifs in pepper TIFY proteins. Ten conserved motifs are marked with different colored boxes. The scale bar indicates 50 aa.

had motif1. Proteins in the same clade (for example CaTIFY10a, CaTIFY10b, CaTIFY10c, and CaTIFY10d) contained similar conserved motifs. However, CaTIFY1a had only two motifs, unlike CaTIFY1b and CaTIFY1c which had four motifs.

Phylogenetic relationships and gene structures of *TIFY* genes in pepper

To investigate the phylogenetic relationships among the CaTIFYs, Pepper CaTIFY, rice OsTIFY, Arabidopsis AtTIFY, and tomato SlTIFY sequences were used to construct a phylogenetic tree (Figure 3). Phylogenetic analysis showed that CaTIFY proteins could be divided into 11 groups belonging to the JAZ, PPD, TIFY, and ZIM/ZML groups. In pepper, no TIFY gene belonged to JAZ7/8 (the AtTIFY5 homologous gene). Among the CaTIFYs, TIFY10 had the highest number of homologous genes. Rice has 11 homologous genes of TIFY10/11 and there were four homologous genes in pepper. Notably, although tomatoes and peppers are Solanaceae plants, there are only four TIFY homologous genes in tomatoes.

To understand the structural diversity of TIFY genes, we further analyzed the structure of the *CaTIFY* gene family. The intron–exon substructures of *CaTIFY* genes are visualized in Supplementary Figure 1. According to the evolutionary relationships of the CaTIFY protein, there were significant differences in sequence length and structure among genes, indicating that large sequence differences existed among the different *CaTIFY* genes (Supplementary Figure 1). The number of CaTIFY introns ranged between 1 and 9, of which CaTIFY1c contained nine introns and CaTIFY9 had only one. All other CaTIFY intron numbers ranged from 2 to 8. There were no strong correlations between phylogeny and exons/introns. Genes with high homology did not have similar gene structures and the length of introns varied greatly, indicating significant gene differentiation in the TIFY family in pepper.

Cis-acting element analysis of pepper *TIFY* gene family

Cis-acting elements can affect and predict gene expression in response to stress or hormones. The 2000 bp region upstream of the start codon of each pepper *TIFY* gene was extracted from the Pepper Genome Database. PlantCARE software was used to analyze the cis-acting elements related to stress or hormones. As shown in Figure 4, 81.2% of the members of the TIFY gene family in peppers had anaerobic induction elements. Of the five hormones, 25% of the *CaTIFY* members had auxin-responsive elements and 56.2% of the *CaTIFY* members had ABA-, MeJA-, and gibberellin-responsive elements. Fifty percent of *CaTIFY* members had a salicylic acid-responsive element. In addition, four *CaTIFY* members (*CaTIFY7*, *CaTIFY10b*, *CaTIFY1b* and *CaTIFY6b*) had a low-temperature-

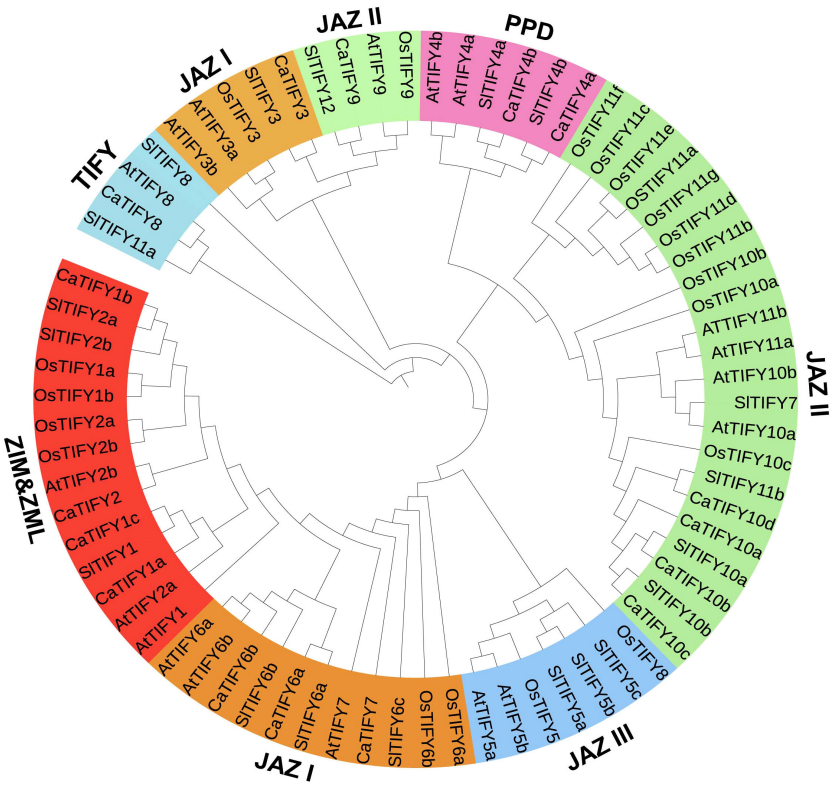

FIGURE 3
Evolutionary relationship of the TIFY proteins across different plant species. 58 TIFY proteins come from Arabidopsis (18), rice (20), tomato(19), and pepper(16).The resulting 9 groups are classified in four subfamilies, which belong to JAZ, PPD, TIFY and ZIM/ZML.

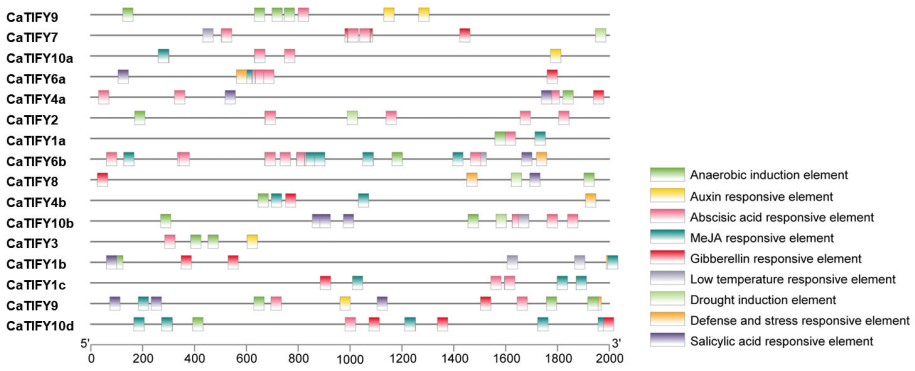

FIGURE 4
Promoter *cis*-element analysis of *CaTIFY* genes. Nine *cis*-acting elements related to abiotic stress are detected in each species, in which they are represented by distinct colored boxes.

responsive element, four *CaTIFY* members (*CaTIFY7*, *CaTIFY2*, *CaTIFY8* and *CaTIFY10b*) had drought induction elements, and four *CaTIFY* members had defense- and stress-responsive elements (Figure 4).

Expression patterns of *CaTIFY* genes in different tissues and under abiotic stresses

To understand the expression patterns of *CaTIFY* genes in different pepper tissues, the relative expression levels of *CaTIFY* family genes in eight tissues (roots, shoots, young leaves, mature leaves, old leaves, flowers, fruits, and seeds) were determined based on published RNA-seq data. As is shown in Supplementary Figure 3A, a heat map was generated to illustrate the expression profiles. The relative expression levels of the 16 *CaTIFY* genes differed among the eight tissues (roots, shoots, young leaves, mature leaves, old leaves, flowers, fruits, and seeds). The expression levels of *CaTIFY1c*, *CaTIFY2*, *CaTIFY3*, and *CaTIFY6b* were very low in all tissues. *CaTIFY7* was highly expressed in young leaves, mature leaves, old leaves, flowers, and fruits but had very low transcription levels in roots, shoots, and seeds (Supplementary Figure 3A). Significantly, the expression level of *CaTIFY10b* in the roots was the highest among all *CaTIFY* genes, but its expression level in other tissues was relatively low, especially in the leaves and seeds. Additionally, CaTIFY10c showed a tissue-specific expression pattern similar to that of *CaTIFY10b*. However, its overall expression level was lower than that of *CaTIFY10b* (Supplementary Figure 3A). Interestingly, although *CaTIFY10d* is homologous to *CaTIFY10a/b/c*, its tissue-specific expression patterns were completely different. *CaTIFY10d* was hardly expressed in roots and seeds but had relatively high expression levels in flowers. Subsequently, we validated the tissue expression patterns of these CaTIFY genes in pepper leaves using RT-qPCR (Supplementary Figures 2A–P). Consistent with the transcriptome data, *CaTIFY7* was highly expressed in young leaves and flowers and *CaTIFY10b* was highly expressed in roots (Supplementary Figures 2J, N). Overall, most *CaTIFY* genes had the highest expression levels in leaves. The exceptions were *CaTIFY1b* and *CaTIFY6a*, which showed the highest expression levels in roots, and *CaTIFY6b*, which showed the highest expression level in flowers (Supplementary Figure 2).

To characterize the abiotic-responsive *CaTIFY* genes, the Fragments Per Kilobase of exon model per million mapped fragments (FPKM) values of each gene in leaves and roots treated with NaCl, mannitol, H_2O_2, heat, or cold were determined (Supplementary Figures 3B–F). Under salt stress, the transcript levels of *TIFY4a*, *TIFY6b*, and *TIFY8* in leaves were significantly repressed, whereas the expression levels of TIFY6b and TIFY8 in the roots were induced by NaCl treatment. *TIFY10b* and *TIFY10c* were strongly induced by salt stress, especially in roots (Supplementary Figure 3B). Mannitol treatment induces drought stress responses in plants. As shown in Supplementary Figure 3C, *TIFY7*, *TIFY10b*, and *TIFY10c* were induced by drought stress in the leaves and roots of pepper. *TIFY6a* and *TIFY6b* were strongly induced by drought stress in roots, whereas *TIFY6b* was strongly repressed by drought stress in leaves. H_2O_2 is one of the most abundant reactive oxygen species (ROS) in cells, and its accumulation causes oxidative damage to cells. It is a key signaling molecule involved in plant growth, development, and stress resistance. In the leaves, *TIFY6a*, *TIFY7*, *TIFY10a*, *TIFY10b*, and *TIFY10c* were induced by H_2O_2 whereas *TIFY6b* was reduced by H_2O_2. *TIFY6a*, *TIFY6b*, *TIFY7*, *TIFY8*, *TIFY10a*, *TIFY10b* and *TIFY10c* were induced by H_2O_2 in roots while the expression level of *TIFY1a* was reduced by H_2O_2 in roots (Supplementary Figure 3D).

Temperature is an important factor that restricts plant growth, and either too high or too low a temperature can cause stress on plant growth. Under high-temperature stress, *TIFY6a* and *TIFY7* were strongly repressed, whereas *TIFY1a* and *TIFY10b* were induced by heat stress (Supplementary Figure 3E). Additionally, *TIFY6a*, *TIFY6b*, *TIFY10b*, and *TIFY10c* were induced by heat stress (Supplementary Figure 3E). As expected, cold stress also affected the expression of some *TIFY* genes in pepper plants. As shown in Supplementary Figure 3F, *TIFY10a*, *TIFY10b*, and *TIFY10c* were strongly induced by cold stress, whereas they were not induced by chilling in either roots or leaves. Surprisingly, *TIFY6a* and *TIFY6b* were strongly induced by cold stress in the roots but were repressed by cold stress in the leaves. The expression levels of *TIFY1a* in the

10.3389/fpls.2023.1308721

roots and leaves reduced under cold treatment. The responses of the other genes to cold stress were not significant.

RT-qPCR analysis of expression patterns of *CaTIFY* genes under cold stress

To examine the changes in *CaTIFY* gene expression of pepper in response to cold stress, the pepper seedlings were subjected to 4 °C treatment. We determined the abundance of transcripts of sixteen *CaTIFY* genes under cold stress using RT-qPCR to confirm the results of the RNA-seq data. As shown in Figure 5, *CaTIFY7* and *CaTIFY10b* were significantly induced by cold stress in leaves, whereas *CaTIFY1b*, *CaTIFY1c*, *CaTIFY2*, and *CaTIFY4b* were significantly reduced by cold treatment (Figures 5B–D, G, J, N). Additionally, the expression of *CaTIFY3*, *CaTIFY6a* and *CaTIFY10d* tended to be induced after cold stress treatment (Figures 5E, H, P). However, the constitutive expression levels of *CaTIFY3*, *CaTIFY6a* and *CaTIFY10d* were much lower than *CaTIFY7* and *CaTIFY10b* in leaf and under low-temperature

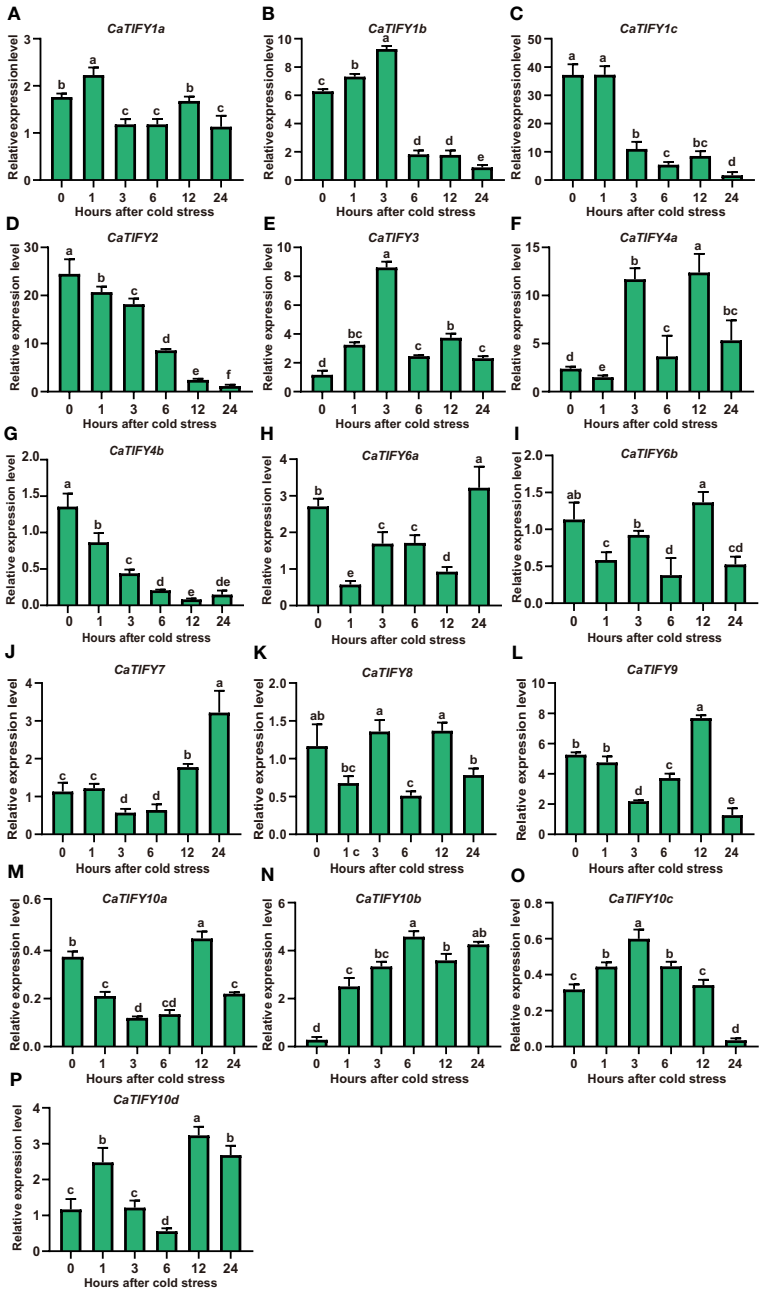

FIGURE 5
RT-qPCR analysis of expression patterns of *CaTIFY* genes in pepper leaf under cold stress. **(A–P)** Expression levels of sixteen *CaTIFY* genes were measured using RT-qPCR at different times under 4 °C cold stress. RT-qPCR data were normalized using *CaUBI3* as the reference gene and were displayed relative to 0 h. Different letters indicate significant differences between samples according to the Student-Newman-Keuls test (P <0.05).

10.3389/fpls.2023.1308721

treatment as shown in published transcriptome data (Supplementary Figures 3A, F). In summary, all of the results identified *CaTIFY7* and *CaTIFY10b* as candidates for further studies on the potential important roles of *CaTIFY* genes in enhancing low-temperature stress tolerance in pepper leaves.

CaTIFY7 enhanced the cold-stress tolerance in pepper

To confirm the role of *CaTIFY7* in pepper under cold stress, Virus-Induced Gene Silencing (VIGS) was used to knock down the gene. Silencing *CaTIFY7* significantly increased the sensitivity of pepper to cold stress. As shown in Figure 6A, pepper plants transformed with TRV2:00 and TRV2:*CaTIFY7*-silenced both showed normal, undifferentiated growth under normal conditions. However, the growth of pepper plants transformed with an empty vector was significantly better than those with *CaTIFY7* under 4 °C cold stress treatment. RT-qPCR analysis revealed that the *CaTIFY7* silencing efficiency was high and showed a 68.6% or 80.6% reduction compared to the control group under normal or cold stress, respectively (Figure 6B). *CaTIFY7* knockdown led to significant downregulation of cold-induced genes (*CaERD15*, *CaCBF1a*, *CaCBF1b*, *CaCOR47-like*, and *CaKIN*) and ROS-related genes (*CaPOD*, *CaSOD*, *CaCAT2*, and *CaAPX1*) under cold stress (Figures 6C–K). *CaTIFY7* overexpression markedly increased the reactive oxygen species content and expression levels of cold-induced genes and ROS-related genes under cold stress (Figures 7A–L). Preliminary results indicated that *CaTIFY7* plays a positive role in regulating pepper tolerance to cold stress.

CaTIFY10b also promoted pepper tolerance to cold stress

To further confirm the function of *CaTIFY10b* in cold-stress response, transgenic pepper leaves containing the 35S:*CaTIFY10b*

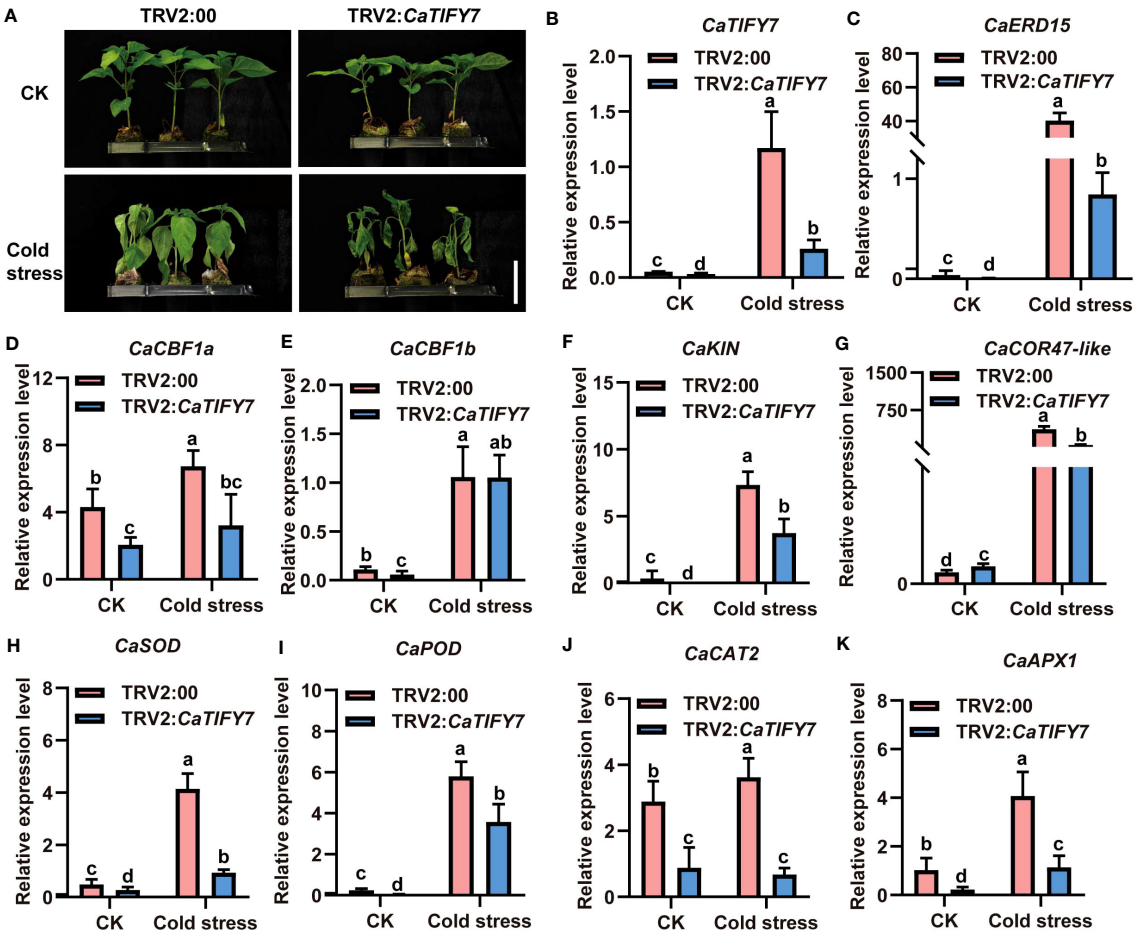

FIGURE 6
Knock down of *CaTIFY7* in pepper weaken plant tolerance significantly under cold stress. **(A)** The phenotype of pepper plants with reduced expression *CaTIFY7* under 4 °C cold stress for 48 (h) Bar=4 cm. **(B)** The silencing efficiency of *CaTIFY7* under normal or cold stress. **(C-K)** The expression level of *CaERD15*, *CaCBF1a*, *CaCBF1b*, *CaKIN*, *CaCOR47-like*, *CaSOD*, *CaPOD*, *CaCAT2* and *CaAPX1* were analyzed in transgenic pepper plants with TRV2:*CaTIFY7* under normal or cold stress. *CaUBI3* were used as the reference gene. All the values are the averages ± SD from three independent experiments. Different letters indicate significant differences between samples according to the Student-Newman-Keuls test (P <0.05).

10.3389/fpls.2023.1308721

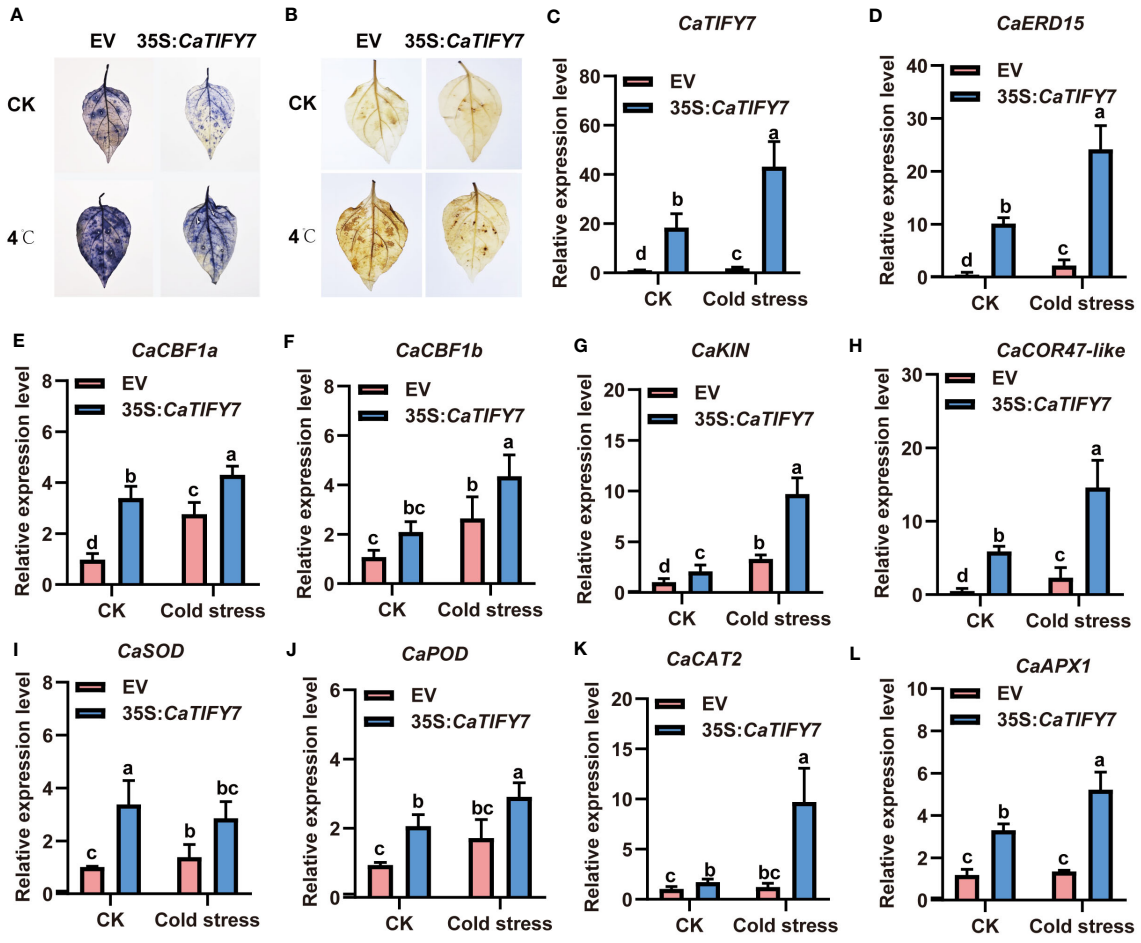

FIGURE 7
Overexpression of *CaTIFY7* enhances cold stress tolerant in pepper. **(A)** O_2^- detecting with NBT after cold stress. **(B)** H_2O_2 staining with DAB under normal or cold stress. **(C)** The expression level of *CaTIFY7* were analyzed in transgenic pepper plants having 35S:*CaTIFY7* under normal or cold stress. **(D-L)** The transcription level of *CaERD15*, *CaCBF1a*, *CaCBF1b*, *CaKIN*, *CaCOR47-like*, *CaSOD*, *CaPOD*, *CaCAT2* and *CaAPX1* were detected in transgenic pepper plants with 35S:*CaTIFY7* after cold stress treatment. The gene expression levels were normalized to those of *CaUBI3*. The relative transcript level was determined and normalized using the reference level and averaged over the three technical replicates. All the values are the averages ± SD from three independent experiments. Different letters indicate significant differences between samples according to the Student-Newman-Keuls test (P <0.05).

vector were generated to explore the role of *CaTIFY10b* in cold tolerance. After 24 h, the *CaTIFY10b*-silenced plants showed a more severe degree of withering than the control plants (Figure 8A). The RT-qPCR results showed that *CaTIFY10b* expression was successfully reduced in TRV2:*CaTIFY10b*-silenced plants (Figure 8B). Subsequently, the expression of cold-induced and ROS-related genes in *CaTIFY10b*-silenced pepper leaves was analyzed and the knockdown of *CaTIFY10b* significantly suppressed the expression of cold-induced and ROS-related genes under cold stress (Figures 8C–K). As expected, overexpression of *CaTIFY10b* also increased the reactive oxygen content in plant leaves and significantly increased the expression of these genes under cold stress in pepper (Figures 9A–L). These results showed that *CaTIFY10b* positively regulated cold tolerance in pepper by promoting the expression of stress-related genes.

CaTIFY7 interacted with CaTIFY10b in yeast

Because CaTIFY7 and CaTIFY10b are both involved in cold-stress reactions, it would be interesting to explore whether they can form heterodimers in response to cold-stress signals. The interaction network of the 16 CaTIFY proteins was predicted using the STRING database, and the results are shown in Supplementary Figure 4. Surprisingly, the results indicated that CaTIFY7 and CaTIFY10b may have a conserved interaction relationship in the model plant. To confirm this relationship, we performed a yeast two-hybrid analysis to verify their interaction. As shown in Figure 10, CaTIFY7 interacted with CaTIFY10b in the Y2H assay (Figure 10). In addition, CaTIFY7 and CaTIFY10b interacted with each other (Figure 10). These results showed that CaTIFY7 and CaTIFY10b may form heterodimers or homodimers to regulate the cold-stress response in pepper.

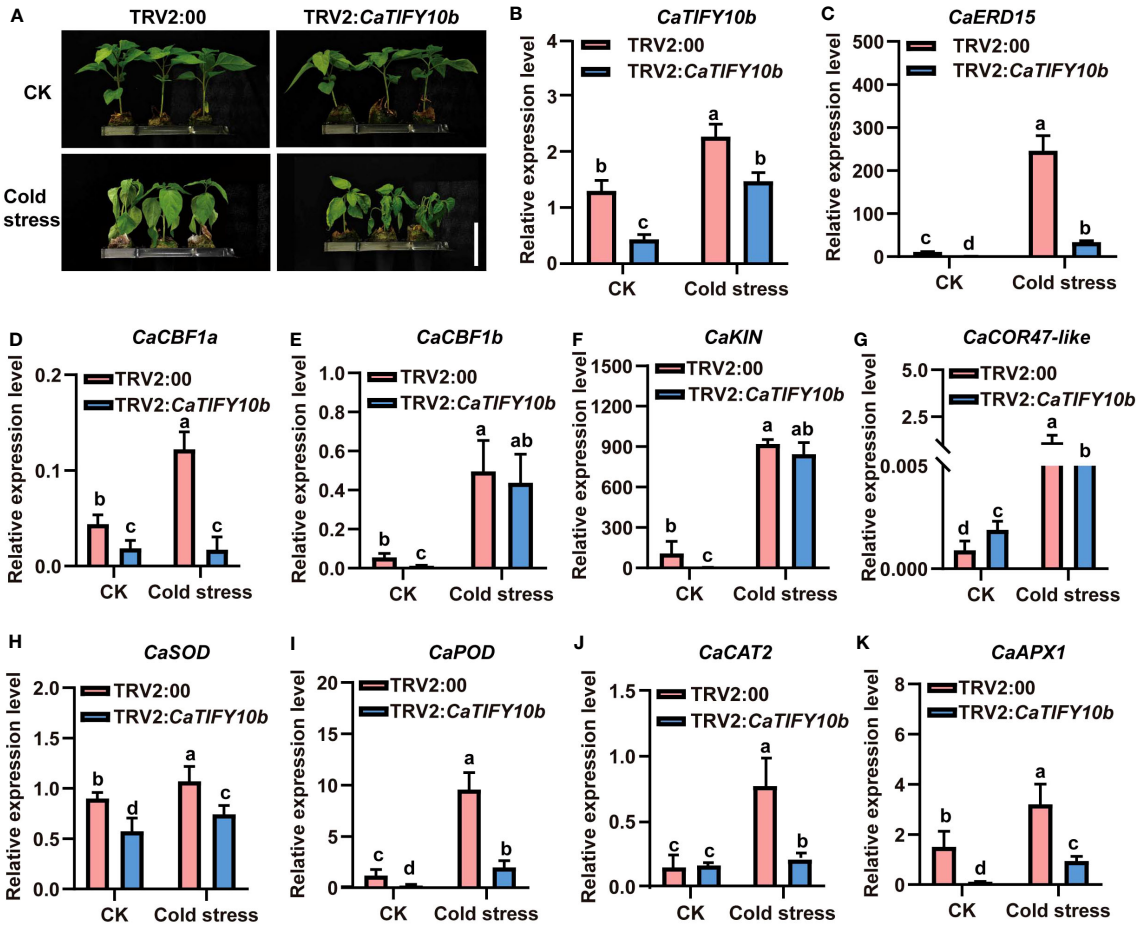

FIGURE 8
Knock down of *CaTIFY10b* in pepper seedlings improves sensitiveness under cold stress. **(A)** The phenotype of pepper plants with suppression of *CaTIFY10b* under cold stress for 48 **(h)** Bar=4 cm. **(B)** The expression level of *CaTIFY10b* were analyzed in transgenic pepper plants under normal or cold stress. **(C-K)** The transcription level of *CaERD15*, *CaCBF1a*, *CaCBF1b*, *CaKIN*, *CaCOR47-like*, *CaSOD*, *CaPOD*, *CaCAT2* and *CaAPX1* were detected in transgenic pepper plants with TRV2:*CaTIFY7* under normal or cold stress. The gene expression levels were normalized to those of *CaUBI3*. All the values are the averages ± SD from three independent experiments. Different letters indicate significant differences between samples according to the Student-Newman-Keuls test (P <0.05).

Discussion

TIFY proteins are defined as TIFY transcription factors because of their specific binding to consensus sequences. TIFY proteins are important regulators of abiotic and biotic stress responses in plants. Several TIFY proteins have been identified in various plant species. However, the *TIFY* gene family in Solanaceae crops, including pepper, has not previously been identified or characterized. We identified sixteen *TIFY* genes in pepper and the *TIFY* gene family members all contained the conservative TIFY▪motif and JAZ domains (Figures 1; 2). The lack of a homologous gene for Arabidopsis *AtTIFY5* among the TIFY members in pepper suggests that this homologous gene may have undergone selective loss in pepper. All *CaTIFY* genes were distributed on chromosomes 1, 3, 4, 6, 7, 8, 9, and 12 and only *CaTIFY1b/c* formed a homologous gene cluster on chromosome 8 (Figure 3).

Many elements were related to hormones and stress in the *CaTIFYs* promoter of peppers, but there were significant differences among the different *CaTIFY* genes (Figure 4). Most members of the TIFY gene family in pepper had anaerobic induction elements, and more than half of the *TIFY* genes responded to ABA, MeJA, salicylic acid, and gibberellin. In addition, some genes contained different stress response elements, suggesting that *CaTIFYs* may be involved in the regulation of different hormone signal transduction pathways, thereby responding to environmental stress.

The TIFY family is widely distributed in plants and its members play important roles in regulating the development of stems, leaves, and flowers in plants (Zhu et al., 2011; Hakata et al., 2012; He et al., 2015; Baekelandt et al., 2018). To better understand the differential expression of *CaTIFYs* genes in peppers, we analyzed the gene expression of *CaTIFYs* in different tissues. RNA-seq data showed that the expression levels of the majority of pepper *TIFY* did not show tissue-specific expression patterns (Supplementary Figures 2, 3). The expression levels of *CaTIFY7* were high in most tissues, suggesting that they have an important role in pepper development. Notably, *CaTIFY10* was most highly expressed in the roots, suggesting that it has a key role in the root development and growth of pepper.

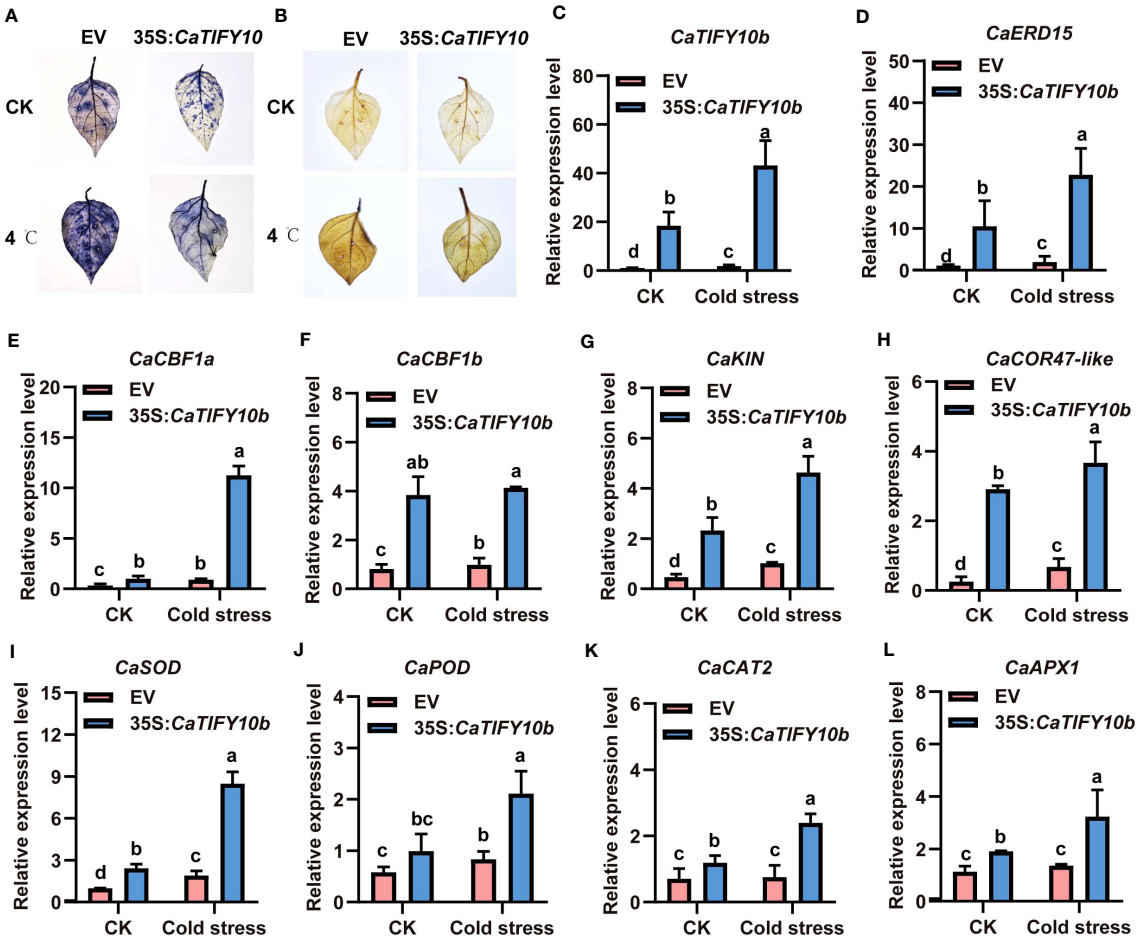

FIGURE 9
Overexpression of *CaTIFY10b* positively regulated cold stress response in pepper. **(A)** O_2^- detecting with NBT under normal or cold stress. **(B)** H_2O_2 staining with DAB after cold stress. **(C)** The transcription level of *CaTIFY10b* were analyzed in transgenic pepper plants having 35S:*CaTIFY10b* under normal or cold stress. **(D-L)** The expression of cold stress and ROS-related genes were detected in transgenic pepper plants with 35S:*CaTIFY10b* after cold stress treatment. *CaUBI3* were used as the reference gene. All the values are the averages ± SD from three independent experiments. Different letters indicate significant differences between samples according to the Student-Newman-Keuls test (P <0.05).

Next, we analyzed the gene expression patterns of this family under different stress conditions (Supplementary Figure 3). Salt stress induced expression of *TIFY6b*, *TIFY8*, *TIFY10b*, and *TIFY10c* in roots, but repressed the transcription levels of *TIFY6b* and *TIFY4a* in leaves, suggesting that *TIFY6b* expression is regulated by different mechanisms in different tissues. The significant induction of *TIFY10b* and *TIFY10c* expression suggests that they are likely to participate in salt stress responses, which is consistent with the function of their homologous genes (*GmTIFY10e* and *GmTIFY10g*) in the positive regulation of salt tolerance in soybeans (Liu et al., 2022). Under drought stress, the induced expression of *TIFY10a*, *TIFY10b*, and *TIFY10c* in leaves and roots indicates that *TIFY10* might play an important role in the drought response of pepper. Based on the discovery that multiple members of the TIFY family enhance the drought resistance of different plants (Ye et al., 2009; Zhao et al., 2016; Zhang et al., 2023), it can be predicted that CaTIFY10a/b/c may also regulate drought resistance in pepper.

Among all *TIFY* genes, the responses of *TIFY6a*, *TIFY6b*, *TIFY7* and *TIFY10b* to high temperatures were the most significant (Supplementary Figure 3). The induced expression of *TIFY6a*, *TIFY6b*, and *TIFY10b*, and the inhibited expression of *TIFY7*, suggest that *TIFY6a*, *TIFY6b*, and *TIFY10b* might play a role in enhancing high-temperature resistance in pepper while the function of *TIFY10b* might be the opposite. However, there are almost no reports on the function of *TIFY* in responses of plants to high temperatures and this is a direction worth studying further. Similarly, the function of TIFY during the low-temperature response is unclear. In pepper, we found that several TIFY (*TIFY1a*, *TIFY4a*, *TIFY6a*, *TIFY6b*, *TIFY10a*, *TIFY10b*, and *TIFY10c)* genes responded to cold stress, suggesting that they may be important candidate genes for the cold response in pepper.

To cope with low-temperature stress, plants have evolved a "cold adaptation" mechanism. Many transcription factors play an important role in the regulation of cold-stress adaptation in plants (Chinnusamy et al., 2010; Ding et al., 2019). It has long been known that the *TIFY* gene responds to cold stress in rice, rape, tomato, bamboo, and grain sorghum (Ye et al., 2009; Huang et al., 2016; Chini et al., 2017; He et al., 2020; Du et al., 2022). However, there

10.3389/fpls.2023.1308721

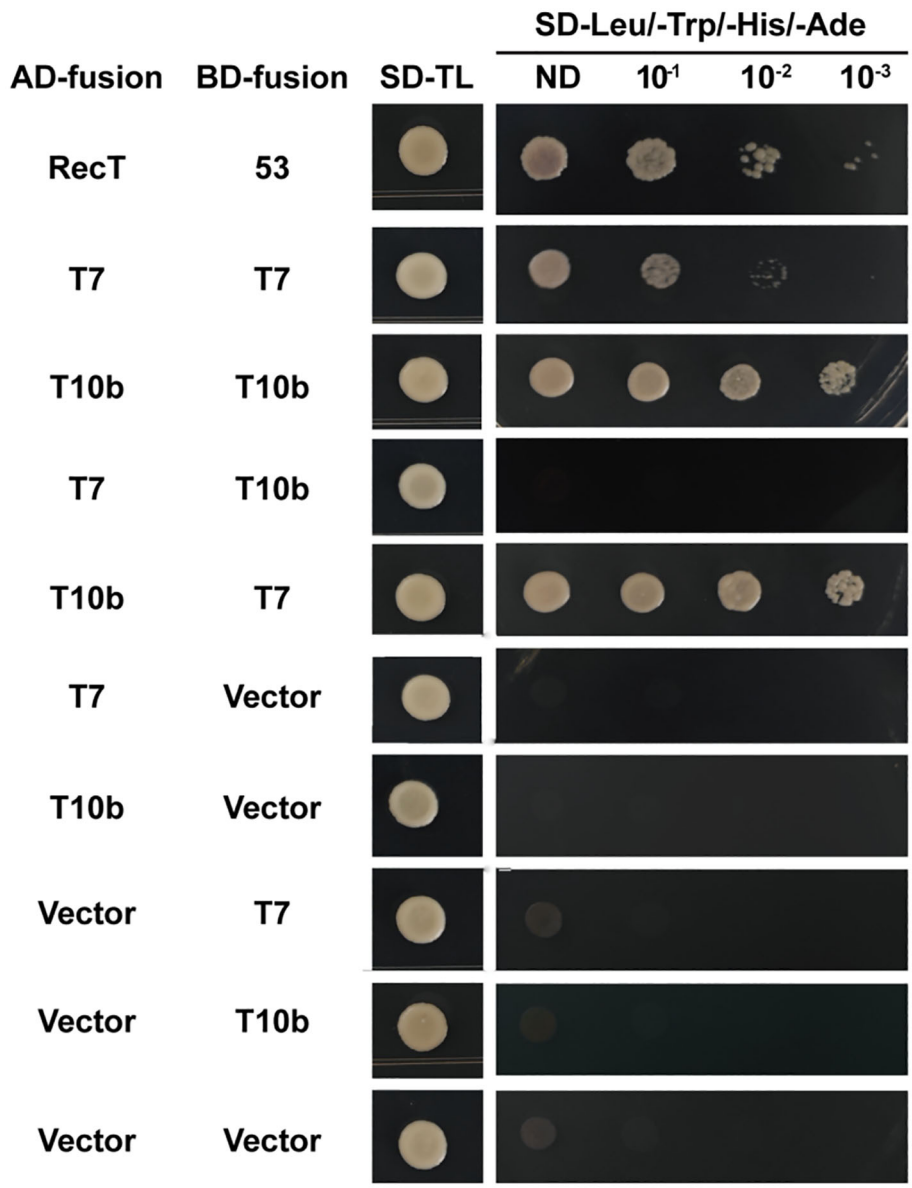

FIGURE 10
Y2H assay between CaTIFY7 and CaTIFY10b. CaTIFY7 interacts with itself or CaTIFY10b and CaTIFY10b interacts with itself or CaTIFY7 in the Y2H assay. Protein interactions were analyzed by the growth of yeast in the medium without leucine, tryptophan, histidine and adenine medium.

have been few reports on the function of *TIFY* in plant responses to low temperatures. Our results confirmed that pepper *CaTIFY7* and *CaTIFY10b* were positive regulators of plant responses under cold stress, where they regulated the expression levels of cold-induced and ROS-related genes (Figures 6–9). We also demonstrated that *CaTIFY7* and *CaTIFY10b* play important roles in pepper plants under salt stress.

To further analyze the regulatory mechanism of *CaTIFY7* and *CaTIFY10b* in terms of protein interactions, we analyzed the CaTIFY protein interaction network using the STRING database (Supplementary Figure 4). Many CaTIFYs, except for CaTIFY1b, CaTIFY1c, CaTIFY1a, and CaTIFY2, interacted with each other to form complexes, indicating that most CaTIFYs formed heterodimers that may affect protein function. Some members of the CaTIFY family formed a complex regulatory network with COI1 protein, MYC2 transcription factor, and Ninja and bHLH13 proteins. It's known that COI1/JAZs/MYC2 acts as the core jasmonic acid-signaling module in the plant jasmonic acid signaling pathway (Chini et al., 2009; Chung and Howe, 2009), which means that these CaTIFYs have a conserved function in sensing JA signals and regulating JA levels in pepper. However, CaTIFY1a/b/c and CaTIFY2 are independent of this signaling pathway, suggesting that these genes may exert regulatory functions through unique mechanisms. Interestingly, CaTIFY7 interacted with CaTIFY10b, as demonstrated by the Y2H assay (Figure 10), suggesting that CaTIFY7 and CaTIFY10b act as heterodimers or homodimers to regulate the cold-stress response in pepper.

Conclusions

We identified 16 *CaTIFY* genes in pepper, of which *CaTIFY7* and *CaTIFY10b* were significantly upregulated by cold stress. Silencing *CaTIFY7* and *CaTIFY10b* significantly repressed the cold tolerance of transgenic pepper plants and the expression of cold-induced and ROS-related genes. Conversely, overexpression of *CaTIFY7* and *CaTIFY10b* enhanced cold tolerance by promoting the expression of cold-induced and ROS-related genes. Further, we showed that CaTIFY7 and CaTIFY10b interacted with each other and that CaTIFY7 interacted with CaTIFY10b. This study provides a basis for further research on how TIFY family members regulate cold tolerance in plants.

Data availability statement

The original contributions presented in the study are included in the article/Supplementary Material. Further inquiries can be directed to the corresponding authors.

Author contributions

XW: Data curation, Formal Analysis, Investigation, Methodology, Software, Writing – original draft, Writing – review & editing. NL: Writing – original draft, Conceptualization, Data curation, Formal Analysis, Writing – review & editing. TZ: Writing – original draft, Investigation, Project administration. KX: Conceptualization, Data curation, Writing – original draft, Formal Analysis. SG: Conceptualization, Data curation, Project administration, Writing – original draft. YY: Conceptualization, Project administration, Resources, Writing – original draft. MY: Funding acquisition, Supervision, Validation, Writing – review & editing. FW: Funding acquisition, Supervision, Validation, Writing – review & editing.

Funding

The author(s) declare financial support was received for the research, authorship, and/or publication of this article. This research was funded by National High Technology Research and Development Program of China (2021YFD1600300-4-2), Key Research and Development Program of Hubei Province (2022BBA0066, 2022BBA0060), Key Research and Development Program of Hubei Province (2023BBB044), Major Project of Hubei Hongshan Laboratory (2022hszd009), Postdoctoral Innovation Practice Positions of Hubei Province, Youth Fund of Hubei Academy of Agricultural Sciences (2024NKYJJ06), High-quality Seed Industry Development Program of Hubei Province and China Agriculture Research System (CARS-23-G28).

Acknowledgments

We thank Professor Feng Li (Huazhong Agricultural University) for his gift of pTRV1-C2b and pTRV2-C2b vectors. We would like to thank Editage (www.editage.cn) for English language editing.

Conflict of interest

The authors declare that the research was conducted in the absence of any commercial or financial relationships that could be construed as a potential conflict of interest.

Publisher's note

Supplementary material

The Supplementary Material for this article can be found online at: https://www.frontiersin.org/articles/10.3389/fpls.2023.1308721/full#supplementary-material

References

Baekelandt, A., Pauwels, L., Wang, Z., Li, N., De Milde, L., Natran, A., et al. (2018). Arabidopsis leaf flatness is regulated by PPD2 and NINJA through repression of CYCLIN D3 genes. *Plant Physiol.* 178 (1), 217–232. doi: 10.1104/pp.18.00327

Bai, Y., Meng, Y., Huang, D., Qi, Y., and Chen, M. (2011). Origin and evolutionary analysis of the plant-specific TIFY transcription factor family. *Genomics.* 98, 128–136. doi: 10.1016/j.ygeno.2011.05.002

Cai, W., Yang, S., Wu, R., Cao, J., Shen, L., Guan, D., et al. (2021). Pepper NAC-type transcription factor NAC2c balances the trade-off between growth and defense responses. *Plant Physiol.* 186 (4), 2169–2189. doi: 10.1093/plphys/kiab190

Chen, R., Ma, J., Luo, D., Hou, X., Ma, F., Zhang, Y., et al. (2019). CaMADS, a MADS-box transcription factor from pepper, plays an important role in the response to cold, salt, and osmotic stress. *Plant Sci.* 280, 164–174. doi: 10.1016/j.plantsci.2018.11.020

Chini, A., Ben-Romdhane, W., Hassairi, A., and Aboul-Soud, M. A. M. (2017). Identification of TIFY/JAZ family genes in Solanum lycopersicum and their regulation in response to abiotic stresses. *PloS One* 12 (6), e0177381. doi: 10.1371/journal.pone.0177381

Chini, A., Boter, M., and Solano, R. (2009). Plant oxylipins: COI1/JAZs/MYC2 as the core jasmonic acid-signalling module. *FEBS J.* 276 (17), 4682–4692. doi: 10.1111/j.1742-4658.2009.07194.x

Chinnusamy, V., Zhu, J. K., and Sunkar, R. (2010). Gene regulation during cold stress acclimation in plants. *Methods Mol. Biol.* 639, 39–55. doi: 10.1007/978-1-60761-702-0_3

Chinnusamy, V., Zhu, J., and Zhu, J. K. (2007). Cold stress regulation of gene expression in plants. *Trends Plant Sci.* 12, 444–451. doi: 10.1016/j.tplants.2007.07.002

Chung, H. S., and Howe, G. A. (2009). A critical role for the TIFY motif in repression of jasmonate signaling by a stabilized splice variant of the JASMONATE ZIM-domain protein JAZ10 in Arabidopsis. *Plant Cell.* 21 (1), 131–145. doi: 10.1105/tpc.108.064097

Ding, Y., Shi, Y., and Yang, S. (2019). Advances and challenges in uncovering cold tolerance regulatory mechanisms in plants. *New Phytol.* 222, 1690–1704. doi: 10.1111/nph.15696

Du, Q., Fang, Y., Jiang, J., Chen, M., Li, X., and Xie, X. (2022). Genome-wide identification and characterization of the JAZ gene family and its expression patterns under various abiotic stresses in Sorghum bicolor. *J. Integr. Agric.* 21 (12), 3540–3555. doi: 10.1016/j.jia.2022.08.104

Ebel, C., BenFeki, A., Hanin, M., Solano, R., and Chini, A. (2018). Characterization of wheat (*Triticum aestivum*) TIFY family and role of Triticum durum TdTIFY11a in salt stress tolerance. *PloS One* 13 (7), e0200566. doi: 10.1371/journal.pone.0200566

Guo, W. L., Wang, S. B., Chen, R. G., Chen, B. H., Du, X. H., Yin, Y. X., et al. (2015). Characterization and expression profile of CaNAC2 pepper gene. *Front. Plant Sci.* 6. doi: 10.3389/fpls.2015.00755

Hakata, M., Kuroda, M., Ohsumi, A., Hirose, T., Nakamura, H., Muramatsu, M., et al. (2012). Overexpression of a rice TIFY gene increases grain size through enhanced accumulation of carbohydrates in the stem. *Biosci. Biotechnol. Biochem.* 76 (11), 2129–2134. doi: 10.1271/bbb.120545

He, X., Kang, Y., Li, W., Liu, W., Xie, P., Liao, L., et al. (2020). Genome-wide identification and functional analysis of the TIFY gene family in the response to multiple stresses in *Brassica napus* L. *BMC Genomics* 21, 736. doi: 10.1186/s12864-020-07128-2

He, D. H., Lei, Z. P., Tang, B. S., Xing, H. Y., Zhao, J. X., and Jing, Y. L. (2015). Identification and analysis of the TIFY gene family in *Gossypium raimondii*. *Genet. Mol. Res.* 14 (3), 10119–10138. doi: 10.4238/2015

Heidari, P., Faraji, S., Ahmadizadeh, M., Ahmar, S., and Mora-Poblete, F. (2021). New insights into structure and function of TIFY genes in *Zea mays* and *Solanum lycopersicum*: A Genome-Wide Comprehensive Analysis. *Front. Genet.* 12. doi: 10.3389/fgene.2021.657970

Hou, X. M., Zhang, H. F., Liu, S. Y., Wang, X. K., Zhang, Y. M., Meng, Y. C., et al. (2020). The NAC transcription factor CaNAC064 is a regulator of cold stress tolerance in peppers. *Plant Sci.* 291, 110346. doi: 10.1016/j.plantsci.2019.110346

Hu, Y., Jiang, L., Wang, F., and Yu, D. (2013). Jasmonate regulates the inducer of CBF expression-C-repeat binding factor/DRE binding factor1 cascade and freezing tolerance in Arabidopsis. *Plant Cell.* 25 (8), 2907–2924. doi: 10.1105/tpc.113.112631

Huang, Z., Jin, S. H., Guo, H. D., Zhong, X. J., He, J., Li, X., et al. (2016). Genome-wide identification and characterization of TIFY family genes in Moso Bamboo (*Phyllostachys edulis*) and expression profiling analysis under dehydration and cold stresses. *PeerJ.* 4, e2620. doi: 10.7717/peerj.2620

Huang, G. T., Ma, S. L., Bai, L. P., Zhang, L., Ma, H., Jia, P., et al. (2012). Signal transduction during cold, salt, and drought stresses in plants. *Mol. Biol. Rep.* 39 (2), 969–987. doi: 10.1007/s11033-011-0823-1

Legris, M., Nieto, C., Sellaro, R., Prat, S., and Casal, J. J. (2017). Perception and signalling of light and temperature cues in plants. *Plant J.* 90 (4), 683–697. doi: 10.1111/tpj.13467

Li, X., Yin, X., Wang, H., Li, J., Guo, C., Gao, H., et al. (2015). Genome-wide identification and analysis of the apple (*Malus×domestica* Borkh.) *TIFY* gene family. *Tree Genet. Genomes.* 11 (1), 808. doi: 10.1007/s11295-014-0808-z

Liu, F., Yu, H., Deng, Y., Zheng, J., Liu, M., Ou, L., et al. (2017). PepperHub, an informatics hub for the chili pepper research community. *Mol. Plant* 10, 1129–1132. doi: 10.1016/j.molp.2017.03.005

Liu, Y. L., Zheng, L., Jin, L. G., Liu, Y. X., Kong, Y. N., Wang, Y. X., et al. (2022). Genome-wide analysis of the soybean TIFY family and identification of GmTIFY10e and GmTIFY10g response to salt stress. *Front. Plant Sci.* 13. doi: 10.3389/fpls.2022.845314

Meng, L., Zhang, T., Geng, S., Scott, P. B., Li, H., and Chen, S. (2019). Comparative proteomics and metabolomics of JAZ7-mediated drought tolerance in Arabidopsis. *J. Proteomics.* 196, 81–91. doi: 10.1016/j.jprot.2019.02.001

Nishii, A., Takemura, M., Fujita, H., Shikata, M., Yokota, A., and Kohchi, T. (2000). Characterization of a novel gene encoding a putative single zinc-finger protein, ZIM, expressed during the reproductive phase in Arabidopsis thaliana. *Biosci. Biotechnol. Biochem.* 64, 1402–1409. doi: 10.1271/bbb.64.1402

Seo, J. S., Joo, J., Kim, M. J., Kim, Y. K., Nahm, B. H., Song, S. I., et al. (2011). OsbHLH148, a basic helix-loop-helix protein, interacts with OsJAZ proteins in a jasmonate signaling pathway leading to drought tolerance in rice. *Plant J.* 65 (6), 907–992. doi: 10.1111/j.1365-313X.2010.04477.x

Sirhindi, G., Sharma, P., Arya, P., Goel, P., Kumar, G., Acharya, V., et al. (2016). Genome-wide characterization and expression profiling of TIFY gene family in pigeonpea (*Cajanus cajan* (L.) Millsp.) under copper stress. *J. Plant Biochem. Biotechnol.* 25, 301–310. doi: 10.1007/s13562-015-0342-6

Thireault, C., Shyu, C., Yoshida, Y., St Aubin, B., Campos, M. L., and Howe, G. A. (2015). Repression of jasmonate signaling by a non-TIFY JAZ protein in Arabidopsis. *Plant J.* 82 (4), 669–667. doi: 10.1111/tpj.12841

Vanholme, B., Grunewald, W., Bateman, A., Kohchi, T., and Gheysen, G. (2007). The TIFY family previously known as ZIM. *Trends Plant Sci.* 12, 239–244. doi: 10.1016/j.tplants.2007.04.004

Wan, H., Yuan, W., Ruan, M., Ye, Q., Wang, R., Li, Z., et al. (2011). Identification of reference genes for reverse transcription quantitative real-time PCR normalization in pepper (*Capsicum annuum* L.). *Biochem. Biophys. Res. Commun.* 416 (1-2), 24–30. doi: 10.1016/j.bbrc.2011.10.105

Wang, J. E., Liu, K. K., Li, D. W., Zhang, Y. L., Zhao, Q., He, Y. M., et al. (2013). A novel peroxidase CanPOD gene of pepper is involved in defense responses to phytophtora capsici infection as well as abiotic stress tolerance. *Int. J. Mol. Sci.* 14 (2), 3158–3177. doi: 10.3390/ijms14023158

Wang, Z., Zhang, Y., Hu, H., Chen, L., Zhang, H., and Chen, R. (2022). CabHLH79 acts upstream of CaNAC035 to regulate cold stress in pepper. *Int. J. Mol. Sci.* 23 (5), 2537. doi: 10.3390/ijms2305253

Xia, W., Yu, H., Cao, P., Luo, J., and Wang, N. (2017). Identification of TIFY family genes and analysis of their expression profiles in response to phytohormone treatments and *Melampsora larici-populina* infection in poplar. *Front. Plant Sci.* 8. doi: 10.3389/fpls.2017.00493

Ye, H., Du, H., Tang, N., Li, X., and Xiong, L. (2009). Identification and expression profiling analysis of TIFY family genes involved in stress and phytohormone responses in rice. *Plant Mol. Biol.* 71 (3), 291–305. doi: 10.1007/s11103-009-9524-8

Zhang, Y., Gao, M., Singer, S. D., Fei, Z., Wang, H., and Wang, X. (2012). Genome-wide identification and analysis of the TIFY gene family in grape. *PloS One* 7 (9), e44465. doi: 10.1371/journal.pone.0044465

Zhang, H., Guo, J. Z., Chen, X., Zhou, Y., Pei, Y., Chen, L., et al. (2023). Transcription factor CabHLH035 promotes cold resistance and homeostasis of reactive oxygen species in pepper. *Hortic. Plant J.* doi: 10.1016/j.hpj.2023.03.007

Zhang, H., Ma, F., Wang, X., Liu, S., Saeed, U. H., Hou, X., et al. (2020). Molecular and functional characterization of CaNAC035, an NAC transcription factor from pepper (*Capsicum annuum* L.). *Front. Plant Sci.* 11. doi: 10.3389/fpls.2020.00014

Zhang, L., You, J., and Chan, Z. (2015). Identification and characterization of TIFY family genes in Brachypodium distachyon. *J. Plant Res.* 128 (6), 995–1005. doi: 10.1007/s10265-015-0755-2

Zhao, C., Pan, X., Yu, Y., Zhu, Y., Kong, F., Sun, X., et al. (2020). Overexpression of a TIFY family gene, GsJAZ2, exhibits enhanced tolerance to alkaline stress in soybean. *Mol. Breeding.* 40 (3), 255–265. doi: 10.1007/s11032-020-01113-z

Zhao, G., Song, Y., Wang, C., Butt, H. I., Wang, Q., Zhang, C., et al. (2016). Genome-wide identification and functional analysis of the TIFY gene family in response to drought in cotton. *Mol. Genet. Genom.* 291 (6), 2173–2187. doi: 10.1007/s00438-016-1248-2

Zheng, L., Wan, Q., Wang, H., Guo, C., Niu, X., Zhang, X., et al. (2022). Genome-wide identification and expression of TIFY family in cassava (*Manihot esculenta Crantz*). *Front. Plant Sci.* 13. doi: 10.3389/fpls.2022.1017840

Zhou, X., Yan, S., Sun, C., Li, S., Li, J., Xu, M., et al. (2015). A Maize Jasmonate Zim-Domainprotein, ZmJAZ14, associates with the JA, ABA, and GA signalingpathways in transgenic Arabidopsis. *PloS One* 10 (3), e0121824. doi: 10.1371/journal.pone.0121824

Zhu, D., Bai, X., Chen, C., Chen, Q., Cai, H., Li, Y., et al. (2011). GsTIFY10, a novel positive regulator of plant tolerance to bicarbonate stress and a repressor of jasmonate signaling. *Plant Mol. Biol.* 77, 285–297. doi: 10.1007/s11103-011-9810-0

frontiers | Frontiers in Plant Science

TYPE Original Research
PUBLISHED 08 January 2024
DOI 10.3389/fpls.2023.1314021

OPEN ACCESS

EDITED BY
Darren Wong,
Australian National University, Australia

REVIEWED BY
Monika Tuleja,
Jagiellonian University, Poland
Pablo Bolaños-Villegas,
University of Costa Rica, Costa Rica
Ljiljana Kuzmanovic,
University of Tuscia, Italy

*CORRESPONDENCE
Attila Fábián
fabian.attila@atk.hun-ren.hu

RECEIVED 10 October 2023
ACCEPTED 13 December 2023
PUBLISHED 08 January 2024

CITATION
Fábián A, Péntek BK, Soós V and Ságі L (2024) Heat stress during male meiosis impairs cytoskeletal organization, spindle assembly and tapetum degeneration in wheat. *Front. Plant Sci.* 14:1314021. doi: 10.3389/fpls.2023.1314021

Heat stress during male meiosis impairs cytoskeletal organization, spindle assembly and tapetum degeneration in wheat

Attila Fábián[1,2,3]*, Barbara Krárné Péntek[1], Vilmos Soós[1] and László Ságі[1,4]

[1]Centre for Agricultural Research, Hungarian Research Network, Martonvásár, Hungary, [2]Department of Applied Biotechnology and Food Science, Budapest University of Technology and Economics, Budapest, Hungary, [3]Institute of Genetics and Biotechnology, Hungarian University of Agriculture and Life Sciences, Gödöllő, Hungary, [4]Agribiotechnology and Precision Breeding for Food Security National Laboratory, Plant Biotechnology Section, Centre for Agricultural Research, Hungarian Research Network, Martonvásár, Hungary

The significance of heat stress in agriculture is ever-increasing with the progress of global climate changes. Due to a negative effect on the yield of staple crops, including wheat, the impairment of plant reproductive development triggered by high ambient temperature became a restraint in food production. Although the heat sensitivity of male meiosis and the following gamete development in wheat has long been recognized, a detailed structural characterization combined with a comprehensive gene expression analysis has not been done about this phenomenon. We demonstrate here that heat stress severely alters the cytoskeletal configuration, triggers the failure of meiotic division in wheat. Moreover, it changes the expression of genes related to gamete development in male meiocytes and the tapetum layer in a genotype-dependent manner. 'Ellvis', a heat-tolerant winter wheat cultivar, showed high spikelet fertility rate and only scarce structural aberrations upon exposure to high temperature. In addition, heat shock genes and genes involved in scavenging reactive oxygen species were significantly upregulated in 'Ellvis', and the expression of meiosis-specific and major developmental genes showed high stability in this cultivar. In the heat-sensitive 'Mv 17-09', however, genes participating in cytoskeletal fiber nucleation, the spindle assembly checkpoint genes, and tapetum-specific developmental regulators were downregulated. These alterations may be related to the decreased cytoskeleton content, frequent micronuclei formation, and the erroneous persistence of the tapetum layer observed in the sensitive genotype. Our results suggest that understanding the heat-sensitive regulation of these gene functions would be an essential contribution to the development of new, heat-tolerant cultivars.

KEYWORDS

cytoskeleton, gene expression, heat stress, meiosis, RNA-seq, spindle apparatus, tapetum, *Triticum aestivum*

Introduction

The ongoing global warming exerts an increasingly negative impact on agriculture, decreasing the realized yield of crop plants, including wheat, worldwide (Pachauri et al., 2014; Lesk et al., 2016). The reproductive development of plants is especially vulnerable to extreme temperature stress (Farooq et al., 2011; Ullah et al., 2022), also supported by current models that predict a serious decrease in the global yield of wheat due to waves of high ambient temperatures during the vegetation period (Sun et al., 2019). Disturbances during early reproductive development can frequently lead to a decreased seed number, with evident yield penalties (Dolferus et al., 2011). Since winter wheat (*Triticum aestivum* L.) is one of the most important staple crops, characterization of its heat stress response and the improvement of tolerance will be a priority task for plant biologists and breeders for the next decades (Stratonovitch and Semenov, 2015). Literature data indicate that the male gametophyte exhibits higher sensitivity to high temperatures when compared to the female counterpart (Hedhly, 2011; Giorno et al., 2013). However, our previous results showed that pre-anthesis heat stress combined with drought severely impairs the function of wheat stigma papilla cells, decreasing spikelet fertility and, subsequently, the grain yield (Fábián et al., 2019).

Plants, being sessile organisms, are obliged to adapt to various environmental factors, such as heat stress. Negative impacts of high temperature are alleviated by the heat stress response (HSR) (Chaturvedi et al., 2021). HSR includes the activation of heat shock transcription factors (HSF), which induce the expression of heat shock proteins (HSP) (Haider et al., 2022). These proteins contribute to the alleviation of damage induced by high temperature stress and various other abiotic and biotic stress factors (ul Haq et al., 2019). Antioxidant molecules and enzymes are also substantial part of the HSR, lowering the amount of reactive oxygen species triggered by the high temperature (Medina et al., 2021). In the case of wheat, several studies were published on the possible heat tolerance mechanisms (Sharma et al., 2019; Poudel and Poudel, 2020; Sarkar et al., 2021; Ullah et al., 2022). These papers emphasize the role of heat shock proteins (HSP40-100 and smallHSPs), as well as the involvement of enzymatic (superoxide dismutase, ascorbate peroxidase, catalase, glutathione peroxidase, glutathione reductase) and non-enzymatic antioxidants (ascorbic acid, glutathione, tocopherols, carotenoids and phenolic compounds). Other elements of tolerance include the osmolyte adjustment, protein refolding, inhibition of apoptosis and protection of cytoskeleton (Sarkar et al., 2021).

Meiosis is the cornerstone of reproductive processes in eukaryotes (Lenormand et al., 2016). This specialized division of diploid mega- and microspore mother cells yields haploid daughter cells, enabling the start of gametogenesis (Bennett et al., 1973). Since meiosis has a high impact on plant yield it is desirable to reveal the exact mechanisms responsible for its sensitivity to heat stress in cultivated plants besides model species like *Arabidopsis* (Wang et al., 2021). Thus, future tackling of the meiotic process may contribute to crop improvement (Lambing and Heckmann, 2018; Kuo et al., 2021; Fayos et al., 2022).

The plant cytoskeleton is a dynamic filamentous network consisting of microtubules (MTs), actin filaments (AFs), and intermediate filaments (He et al., 2020). This complex system has diverse roles in the life of a cell: it participates in the formation of cell shape, sets up and maintains cell polarity, transports organelles, and coordinates cell division (Kost and Chua, 2002). Correct organization of mitosis and meiosis requires a complex regulatory system that consists of microtubule- and actin filament-associated proteins (Krtková et al., 2016; Paez-Garcia et al., 2018). These proteins are responsible for the controlled polymerization, depolymerization, nucleation, severing, and crosslinking of MTs and AFs. Microtubule organization and spindle dynamics play a crucial role in the correct segregation and movement of chromosomes and the accomplishment of cytokinesis during meiosis (Zamariola et al., 2014; Li et al., 2015). Recent studies revealed the involvement of plant cytoskeleton in abiotic stress response (Kumar et al., 2023). Consequently, the possible detrimental effects on cytoskeletal integrity triggered by high temperature may severely impair the structure and function of daughter cells and, subsequently, the gametes. Depolymerization of microtubules (Smertenko et al., 1997) and actin filaments (Malerba et al., 2010) were observed following *in vitro* heat treatments in tobacco somatic cell suspensions. However, a detailed analysis of heat-triggered effects on the cytoskeleton and the general structure of germline cells is still missing in plants.

The execution of meiosis and the following gametogenesis depends on completing numerous milestones. Chromosome pairing, synapsis- and crossing-over formation occur during the meiotic prophase I, enabling the flawless accomplishment of genetic recombination (Ur and Corbett, 2021). Spindle construction, supervised by the spindle assembly checkpoint (SAC), happens during metaphase. This intricate mechanism ensures the proper segregation of chromosomes, preventing aneuploidy in daughter cells (Motta and Schnittger, 2021).

A plethora of different factors influences the development of pollen grains. Microsporogenesis and microgametogenesis are controlled by several tightly regulated transcription factors (for a review, see Gómez et al., 2015). Another factor for appropriate microspore development is the adequate callose wall formation of tetrads. While exact function of this wall is yet to be revealed, it is generally accepted that normal callose deposition is required for successful microgametogenesis (Dong et al., 2005). Improper building or incorrect dissolution of this callose wall lead to sterility (Zhang et al., 2007; Zhu et al., 2008; Lu et al., 2014). In the male gametophyte, the successful development of gametes from microspore mother cells (MMCs) largely depends on the proper function of the tapetum, which is the innermost cell layer of the anther. This specialized tissue provides nutrients and developmental factors for the microspores and undergoes programmed cell death (PCD) before the completion of gametogenesis (Lei and Liu, 2020). In addition to the nourishing role of tapetum, recent studies indicate that this layer also provides essential regulatory elements, such as small RNAs to complete the male meiotic cycle (Lei and Liu, 2020). Construction of the sporopollenin pollen wall and the pollen coat, important factor of

pollen viability is also carried out mainly by the tapetum (Jiang et al., 2013). The undisturbed accomplishment of male meiosis and the following gametogenesis requires a well-regulated network of numerous gene sets, from the meiotic prophase I to the PCD of tapetum cells (Chen et al., 2010; Yamada and Goshima, 2017; Yao et al., 2022). Despite the agronomic significance of wheat, the differential expression of these relevant genes triggered by heat stress has not been described in wheat anthers.

The molecular mechanisms and the signaling of the heat sensitivity observed during gametogenesis are long-standing questions in plant reproduction biology. Despite the crucial role of the cytoskeleton in meiosis, there is no detailed analysis available about heat-driven cytoskeletal changes in meiocytes. Only cytological (Omidi et al., 2014) and histological (Saini et al., 1984; Browne et al., 2021) studies have been made on wheat meiocytes. Transcriptomic investigations on meiosis- and cytoskeleton-specific genes and of genes taking part in tapetal functions are still missing.

Our objectives during the present study were (1) to identify the possible origins of heat-triggered spikelet fertility loss through the structural comparison of meiocytes from heat-sensitive and -tolerant wheat genotypes and (2) to reveal corresponding differential gene expression patterns in these genotypes. Via a combined analysis of morphological and transcriptomic data, our goal was to shed light on the background of meiotic heat sensitivity in the wheat male gametophyte.

Materials and methods

Plant material and cultivation

Two winter wheat genotypes were selected for the experiments based on their significantly different spikelet fertility (seed-set) after a meiosis-staged heat-stress treatment, as confirmed in several studies (Végh et al., 2018; Balla et al., 2019; Janda et al., 2019; Marček et al., 2019). The Hungarian 'Mv 17-09' genotype was considered sensitive to heat, and 'Ellvis', a German cultivar, was taken as heat tolerant. For each experiment, seeds (n=50 per genotype and treatment) were sown in Jiffy peat pellets. Seedlings were subjected to 7 weeks of vernalization at 4°C, then planted in plastic pots containing 2 kg of a soil-sand-peat mixture (3:1:1 parts, by volume). Plants were transferred to growth chambers (Conviron, Winnipeg, Canada) and grown using the T1 spring climatic program (Tischner et al., 1997).

Developmental staging of meiocytes

Determination of anther developmental stage for treatment and sample collection was based on measurement of flag leaf emergence from the leaf sheath and spike length of main tillers. First, we determined the above mentioned parameters each morning from the beginning of flag leaf emergence on a separate population of plants. Each day, developmental stage of the meiocytes from the measured plants were identified by staining the anthers using 2% acetocarmine according to Shunmugam et al. (2018). Onset of meiosis was considered when meiocytes at the middle region of spikes were at prophase (flag leaf emergence 6 cm, spike length 5 cm). Leaf emergence and spike length characteristic for the day before the onset was determined as well (5 cm and 4.5 cm, respectively) The above mentioned parameters were measured for each plant at each morning, and when the parameters reached the value characteristic for the day before the onset of meiosis, plants were assigned as control or treated (50-50% of the plants). For treated plants, heat stress was immediately started by transferring these plants in a stress chamber. For control plants, cultivation continued as before.

Stress treatment, sample collection

Heat stress was delivered by exposing the plants to 35 °C for 24 h at a stress chamber. For sample collection, main spikes from treated plants and control plants at the same developmental stage were harvested. Anther collections for cytoskeleton staining and RNA extraction were carried out from the main spikes at the end of the treatments. Anther collections for histology, as well as anther and pistil collections for morphology were carried out from control and treated plants before anthesis when anthers at the middle region of the spike are fully developed and start to turn yellow (on the day before anthesis started). For pollen grain morphology, sample collections were carried out at anthesis (pollen shed). Anthers collected for RNA extraction were immediately placed in RNA*later* stabilization solution (Thermo Fisher Scientific, Waltham, United States) to stabilize and protect RNA. We provide a summary table on sample collection (Supplementary Table 1).

Determination of spikelet fertility rate and yield

Ten plants per genotype and treatment were grown to full maturity, and then the floret number, grain number, and grain yield of the main spikes were determined. The spikelet fertility rate (or seed-set, Prasad et al., 2006) was calculated as follows:

$$\textit{Spikelet fertility rate (seed set)} = \frac{(\textit{number of filled grains})}{(\textit{total number of florets})} * 100$$

Histology

For histological studies, anthers were isolated from five plants per genotype and treatment on the day before anthesis, fixed in 50 mM Na-cacodylate buffer (pH 7.2) containing 4% (w/v) formaldehyde at room temperature (RT) for 4 h, washed, dehydrated in an ethanol series, and gradually infiltrated with LR white resin (Ted Pella, Redding, CA, United States). The resin was polymerized at 55°C for 48 h. Semi-thin sections (1 µm) were cut using an Ultracut-E microtome (Reichert-Jung, Heidelberg,

Germany) and stained with periodic acid-Schiff (PAS) for polysaccharides and with 1% (w/v) Amido Black for proteins. Stained sections were mounted in DPX (Sigma-Aldrich, 100579) and examined under a DMI-6000 microscope (Leica Microsystems GmbH, Wetzlar, Germany).

Cytoskeleton labeling and confocal microscopy

To study the cytoskeleton elements, anthers from 20 control and 20 treated plants per genotype were collected at the end of treatment, and the developmental stage was determined by acetocarmine staining of one another per floret. The remaining anthers containing meiocytes at interphase, prophase, metaphase, anaphase and telophase, as well as uninucleate microspores were fixed for 60 min at room temperature (RT) in a microtubule-stabilizing buffer [100 mM 1,4-piperazinediethanesulfonic acid (PIPES), 1 mM $MgCl_2$, 2 mM ethylene glycol-bis(β-aminoethyl)-N,N,N′,N′-tetraacetic acid (EGTA), 10% (v/v) dimethyl sulfoxide, 4% formaldehyde, 400 µM 3-maleimidobenzoic acid N-hydroxysuccinimide ester (MBS), 1% (v/v) Triton X-100, and 1.55% (w/v) sucrose, pH 7.0). At the beginning of fixation, anthers were vacuum infiltrated for 2 × 5 min, then washed three times for 10 min in the same buffer with formaldehyde and MBS omitted. Sporogenous archesporial columns containing MMCs were isolated by the MeioCapture method (Shunmugam et al., 2018), and MMCs were settled on adhesive slides for staining. F-actin was stained with Alexa Fluor™ 488-labeled phalloidin (Thermo Fisher Scientific, A12379) at 1:100 dilution for 30 min at RT, mounted in 4',6-diamidino-2-phenylindole (DAPI)-containing Vectashield Plus medium (Vector Labs, H-2000) and imaged after 15 min.

For microtubule labeling, MMCs were permeabilized in 1% Triton X-100-containing phosphate-buffered saline (PBS), then blocked (1% bovine serum albumin, 0.1 M glycine in PBS) for 30 min. Cells were incubated with a rabbit primary anti-alpha tubulin polyclonal antibody (Agrisera, AS10 680) in 1:500 dilution at RT for 60 min, then at 4°C overnight. MMCs were washed three times in PBS for 30 min, then incubated with an Alexa Fluor 633-labeled anti-rabbit secondary antibody (Thermo Fisher Scientific, A21071) for 60 min at 1:500 dilution. After washing three times, cells were mounted as mentioned before and imaged after 15 min.

The cytoskeleton structure was visualized using a Leica SP8 laser scanning confocal microscope (Leica Microsystems). In the case of F-actin, samples were excited at 488 nm and the emitted fluorescence was detected at 490–550 nm. The microtubule-specific signal was excited at 633 nm, and the signal detected at 640–700 nm. In both cases, DNA was stained with DAPI that was excited at 405 nm and detected at 410-480 nm. *Z*-stack series of MMCs were made at the voxel size of 54 and 200 nm, along the *X*/*Y* and *Z* axes, respectively. Confocal images were deconvoluted using the Huygens v18.04 program and imported in the Imaris v9.8.2 program for 3D reconstruction and cytoskeleton model generation in the case of the following developmental phases: interphase, all phases of meiosis I, and post-meiotic uninucleate microspores (UMs). Three dimensional models of actin filaments and microtubules were generated using the Filaments tool in Imaris (with the following settings: threshold mode, connective baseline=10, minimal ratio of branch length to trunk radius=5. Cumulative lengths of microtubules and actin fibers were automatically measured on the 3D models by the program and were obtained by using the Statistics tab (n=10-16 cells per genotype, treatment, studied phase, and filament type) and expressed as the quantity of cytoskeleton. Since cytoskeletal structures show highly dynamic behavior during the meiotic process (e.g., spindle formation, phragmoplast formation, and expansion), only the MMCs characteristic for each phase were measured to avoid high variation in the data.

RNA extraction and transcriptome sequencing

For molecular work, all surfaces and equipment were made RNase-free using the RNase AWAY decontamination reagent (Thermo Fisher Scientific, 7002). Anther tissue was ground using a mortar and pestle in liquid nitrogen. Total RNA was extracted using Direct-zol™ RNA MiniPrep Kit, following the manufacturer's protocol (Zymo Research, Irvine, CA, USA). The RNA concentration and quality were determined by a Qubit 3.0 fluorometer (Thermo Fisher Scientific). Samples having RNA integrity number (RIN) values of at least 7 were used for sequencing. The libraries for RNA-seq were prepared with the NEBNext Ultra II Directional RNA Library Prep Kit for Illumina (NEB, Ipswitch, MA, USA). Briefly, ribosomal RNA was depleted from 400 ng of total RNA using the QIAseq FastSelect rRNA Plant Kit (Qiagen, Hilden, Germany). The depleted RNA was fragmented, end-prepped, adapter-ligated, and the libraries were amplified according to the manufacturer's instructions. The quality of the libraries was checked on the 4200 TapeStation System using D1000 Screen Tape (Agilent Technologies, Palo Alto, CA, USA), and the quantity was measured on Qubit 3.0. Sequencing was performed on the NovaSeq 6000 system (Illumina, San Diego, CA, USA) with a 2 × 150 bp paired-end run configuration. Every sample had three biological replicates that were sequenced independently.

RNA-seq analysis

Sequencing results were analyzed by FASTQC v0.11.8 (Babraham Bioinformatics, https://www.bioinformatics.babraham.ac.uk/projects/fastqc/) to assess the read quality. Trimming and adapter removal were performed using CLC Genomics Workbench v23.3 (Qiagen). The trimmed short reads were mapped to the IWGSC RefSeq v2.1 reference genome assembly (Zhu et al., 2021, https://wheat-urgi.versailles.inra.fr/Seq-Repository/Assemblies) by CLC Genomics Workbench v23.3. Expression values were normalized by the TMM method (Robinson and Oshlack, 2010). In order to control the number of potential false positive genes, both Wald test and the likelihood ratio test were applied for the statistical analysis of differential gene expressions, using CLC Genomics Workbench v23.3. *P*-values of both gene lists were adjusted by the FDR *p*-value correction method

(Benjamini and Hochberg, 1995). The coding sequences were considered as differentially expressed genes (DEGs) when the FDR *p*-value was lower than 1.0E-6 according to both statistical methods and the normalized fold-change was at least two-fold in absolute value at the same time. Functional annotation of the IWGSC RefSeq v2.1 genome assembly was done by a local BLAST search in the Blast2GO v6.0.3 program (Conesa and Götz, 2008) against the refseq_rna database available at the NCBI website (https://blast.ncbi.nlm.nih.gov/doc/blast-help/downloadblastdata.html#databases) with the following parameter settings: blastn program (-task megablast), E-value cutoff = 1.0E-5. For gene ontology (GO) enrichment analysis, GO terms of DEGs were retrieved by NCBI BLAST search in Blast2GO v6.0.3 using the blastx program against the refseq_protein database at the BLAST expectation value of 1.0E-5, followed by GO mapping and annotation. Overrepresented GO terms of up- and downregulated DEGs were identified in the BiNGO v3.0.5 plugin (Maere et al., 2005) of Cytoscape v3.9.1 program (Shannon et al., 2003), using the hypergeometric statistical test. The whole annotation was used as a reference set, and the *p*-values were adjusted by FDR correction.

Validation of RNA-seq data was done by quantitative PCR

RNA extraction, DNase treatment, and cDNA synthesis were carried out as described previously (Soós et al., 2012). qPCR was performed on an ABI 7500 Fast real-time PCR System with ABI Fast SYBR Green Master Mix (Thermo Fisher Scientific) according to Soós et al. (2012). Oligonucleotides are listed in Supplementary Table 2.

Identification of wheat ortholog genes

Wheat orthologs of known meiosis-specific genes (Chen et al., 2010) and genes participating in spindle assembly (Yamada and Goshima, 2017) or tapetal functions (Yao et al., 2022) were identified mainly by using the Ensembl Plants database. The conversion between IWGSC RefSeq v1.2 orthologous gene IDs retrieved from Ensembl Plants and the IWGSC RefSeq v2.1 IDs used during mapping and gene expression analysis was done by the ID correspondence table, which can be found in the annotation resources of the IWGSC RefSeq v2.1 genome assembly. The functions of the collected orthologs were verified using our functional annotation carried out by the Blast2GO program. Additional orthologs were identified using the same annotation solely.

Data handling: statistical analysis and figures

For the assessment of heat stress effects, data were collected for three independent biological replicates. Statistical comparison of spikelet fertility rates, yields, and cytoskeleton measurements of control and treated plants were made by two-way ANOVA and Tukey's *post-hoc* test (α=0.05) in GraphPad Prism v 10.1.0 program (GraphPad Software Inc., San Diego, CA), with the two main factors tested as genotype and heat stress treatment.

Venn diagrams, horizontal bar plots for enriched GO terms, and bar plots for the fold change expression of the studied gene sets were plotted by SRplot, an online platform for data analysis and visualization (Tang et al., 2023). Box plots were generated using the BoxPlotR web tool (Spitzer et al., 2014).

Results

Spikelet fertility showed genotype-dependent reduction after heat stress

The spikelet fertility rate in the main spikes of heat-sensitive 'Mv 17-09' plants dropped by 40.73%, which was statistically more significant when compared to the 13.91% decrease in the tolerant 'Ellvis' (Figure 1A). Two-way ANOVA revealed that the effect of genotype and heat treatment were both significant on spikelet fertility, with a significant interaction between these factors (Table 1). This indicates that Ellvis showed higher tolerance against heat stress at the time of meiosis. The grain yield of 'Mv 17-09' main spikes significantly decreased by 36.96%, while 'Ellvis' did not show statistically significant yield loss (Figure 1B). According to the results of ANOVA, only the treatment had significant effect on grain yield (Table 1).

Anther and microspore development of the sensitive genotype are negatively influenced by heat stress

Morphological study of florets revealed that pistil and stigma morphology remained normal in both genotypes after the treatment, and heat stress triggered the appearance of retarded and abortive anthers in 'Mv 17-09' by the time of anthesis (Figure 2). Similar anther wall structure was observed in the control anthers of both varieties, including the degenerated tapetum layer (Figures 3A, B, E, F). Although the epidermis and endothecium layers showed normal structure in treated anthers of both genotypes, the development of the tapetum was seriously changed in 'Mv 17-09' after heat stress (Figures 3C, D). In contrast to the control, tapetal cells remained largely intact, and most of them were cytoplasm-rich, possessing a normally structured nucleus, which suggests that PCD of this layer was delayed significantly (Figures 3C, D). A large proportion of microspores was aborted, consisting of only the collapsed wall without cytoplasm (Figures 3C, D). Cytoplasm-containing pollen grains exhibited fewer starch grains and larger vacuoles when compared to the control (Figures 3C, D; Supplementary Figure 1). Treated pollen grains of 'Ellvis' did not show serious structural deviations (Figures 3G, H). The percentage of structurally abnormal pollen grains (weaker staining, scorched walls, only one nucleus) was determined after pollen shedding, showing a much higher rate

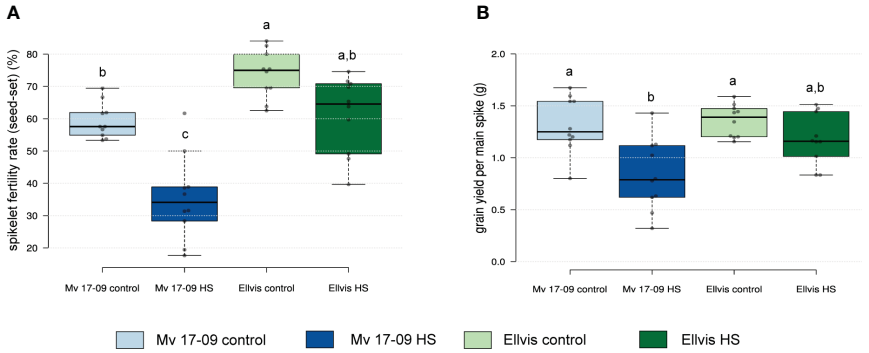

FIGURE 1
Effect of heat stress on spikelet fertility rate (seed-set) **(A)** and grain yield **(B)** of main spikes in a heat-sensitive ('Mv 17-09') and -tolerant wheat ('Ellvis') (n=10 per treatment). Different letters above boxes indicate significant differences at least at the P ≤ 0.05 level of probability, according to Tukey's post-hoc test (α=0.05). Stripes within boxes of the plots indicate median values. Grey dots represent data points.

of aborted (20.74 ± 5.42 for 'Mv 17-09' and 0% for Ellvis) and structurally abnormal (36.62 ± 7.79% for 'Mv 17-09' and 6.54 ± 3.62% for Ellvis) pollen grains in the sensitive genotype (Supplementary Figures 1, 2).

Heat stress severely impaired cytoskeleton integrity and chromosome movement during male meiosis

Both genotypes showed altered cytoskeleton morphology, although the impact was more severe in the sensitive 'Mv 17-09' during all studied meiotic phases and in daughter cells. In the case of interphase and prophase I MMCs, majority of the microtubules disappeared in the central region of cytoplasm, while, most cortical filaments near the plasma membrane remained intact (Figure 4). Depolymerization of actin filaments was observed after heat stress during these phases. Actin bundles located near the nuclei were the most resistant to this effect. Spindle assembly at metaphase I was seriously affected by the treatment, especially in 'Mv 17-09'. Indirect immunofluorescence assay of the 'Mv 17-09' metaphase meiocytes revealed that the formation of kinetochore fibers was severely impaired, causing a narrower, deficient spindle with fewer and/or fragmented fibers (Figure 4). Metaphase plate defects occurred frequently, such as improper chromosome disposition outside the plate and asymmetric location of the whole plate. Spindle-associated actin structure was less pronounced, and actin rings were visible throughout the cytoplasm in heat-treated MMCs (Figure 4). Chromosome movement was frequently asynchronous during anaphase I of treated meiocytes, leading to multiple lagging chromosomes and later the exclusion of these chromosomes from the forming daughter nuclei at telophase I. The phragmoplast structure showed irregularities during telophase. Micronuclei formed from lagging chromosomes were frequently observed in UMs (Figure 4). Perturbed cytoskeleton organization led to various structural defects in meiocytes and daughter cells, such as the formation of tripolar spindle and the resultant trilateral symmetry of the phragmoplast (Figures 5A, B), and diverse forms of nonseparated or unevenly divided daughter cells after meiosis I (Figures 5C–F). The ratio of structurally damaged meiocytes and UMs counted after heat stress was significantly higher in the case of 'Mv 17-09' plants when compared to 'Ellvis' (60.76%, n=130 and 32.74%, n=113, respectively, in three independent experiments, p=0.039).

TABLE 1 Results of the two-way ANOVA analysis carried out on the outcome of spikelet fertility and grain yield per spike studies.

	Two-way ANOVA (P-values)		
Studied parameters	Genotype	Heat Stress	Interaction
Spikelet fertility (seed-set)	<0.0001 ***	<0.0001 ***	0,0418 *
Grain yield per spike	0,1191 ns	0,0004 ***	0,2412 ns

Statistical differences were determined using a two-way ANOVA to examine the effects of genotype, treatment (heat stress) and/or the interaction of these factors. Asterisks denote statistically significant differences (*p<0.05; **p<0.01; ***p<0.001; ns, not significant).

The microtubule cytoskeleton of 'Ellvis' showed higher stability after heat stress

Quantification of microtubules (Figure 6A) and actin cytoskeleton (Figure 6B) revealed differential stress responses of 'Mv 17-09' and 'Ellvis'. The cumulative length of microtubules was decreased significantly in all studied phases of meiosis and in the UMs of the sensitive 'Mv 17-09' (44.82% at interphase, by 41.70% at prophase, by 58.61% at metaphase, by 31.85% at anaphase, by 48.91% at telophase and by 47.15% at the uninuclear microspore stage). In contrast, this parameter differed significantly in 'Ellvis' from the control only at interphase and metaphase I (by 68.15% and 35.11%, respectively; Figure 6A). Our results of two-way ANOVA showed that the effect of genotype on microtubule amount was significant only at the prometa- and anaphase, while heat treatment affected the parameter significantly at all studied phases. In addition, the interaction of the studied factors (genotype and heat treatment) significantly influenced the amount of microtubules at all phases, which implies the higher stability of microtubules in Ellvis (Table 2). The amount of filamentous actin dropped significantly at interphase and during all phases of meiosis I (by 47.42% at interphase, by 22.68%

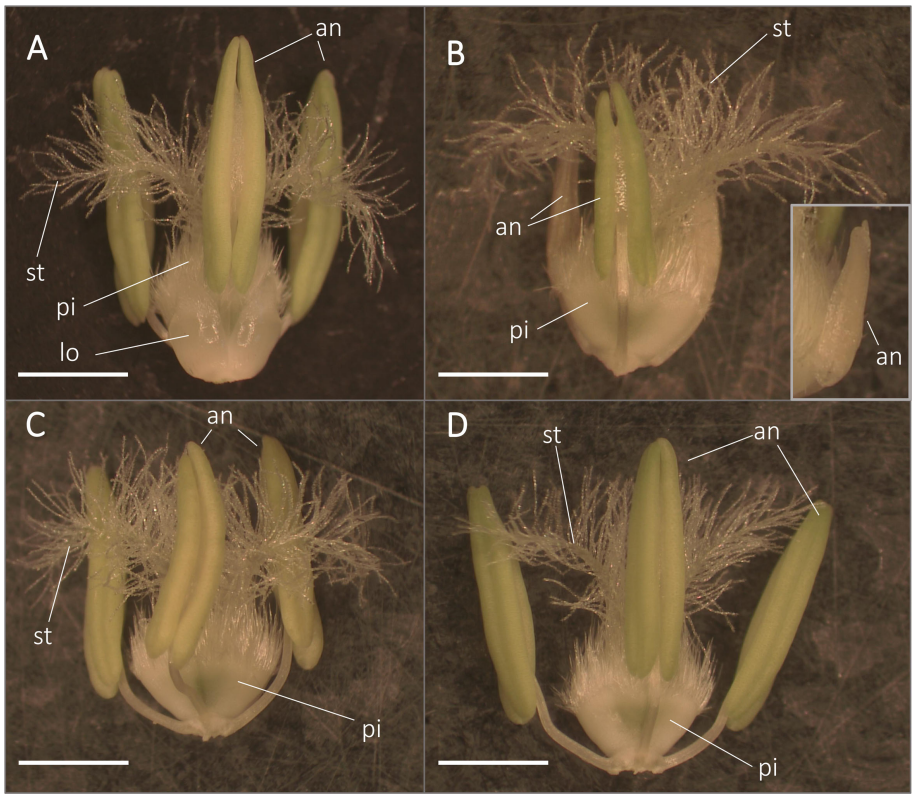

FIGURE 2
Morphology of anthers and pistils from control **(A, C)** and heat-stressed **(B, D)** 'Mv 17-09' **(A, B)** and 'Ellvis' **(C, D)** main spikes sampled on the day before anthesis. Note that heat-stressed florets of 'Mv 17-09' frequently contained retarded **(B)** and aborted sterile (inset of **B**) anthers. an, anther; lo, lodicule; pi, pistil; st, stigma. Bars represent 2 mm.

at prophase, by 38.11% at metaphase, by 51.23% at anaphase and by 46.29% at telophase), while remained constant in UMs in the treated cells of 'Mv 17-09' (Figure 6B). In the case of 'Ellvis', the cumulative length of AFs decreased significantly only at interphase and prophase I (by 60.17 and 38.86%, respectively). Two-way ANOVA revealed that effect of genotype was significant only during interphase and prophase on actin filament amount, while heat treatment influenced this parameter at all phases significantly, with the only exception of metaphase (Table 2). Interaction between genotype and treatment factors was significant only at metaphase, which indicates that reaction of actin cytoskeleton to high temperature was basically similar in 'Mv 17-09' and Ellvis (Table 2).

Transcriptome analysis and validation

RNA-seq yielded an average of 73 million 150-bp paired-end reads per sample (Supplementary Table 3). The GC content of samples ranged from 49% to 52%, and the Phred Q scores in all the samples were higher than 30. Clean reads were aligned to the reference genome assembly at 84.74% to 90.52% efficiency (Supplementary Table 3). A total of 4,434 DEGs (1,390 up- and 3,044 downregulated) were identified in 'Mv 17-09' and 2,030 DEGs in 'Ellvis' (1,115 up- and 915 downregulated), indicating that the rate of downregulated genes was significantly higher after heat stress in the sensitive genotype (Figure 7). To validate our RNA-seq dataset, we performed a qPCR study of 10 DEGs on three independent RNA samples (not the same ones used for the RNA-seq). Overall, the fold changes of a panel of DEGs reported by RNA-seq correlated well (r = 0.9099) with the fold changes reported by qPCR (Figure 8), indicating that the RNA-seq data are robust.

Gene ontology enrichment analysis

To shed light on the genome-wide picture of the transcriptomic stress response, gene ontology enrichment analysis was performed on DEGs. We provide a summary of all significantly enriched GO terms at Supplementary Table 4. The study revealed that the most highly enriched GO terms among upregulated genes were directly related to stress response in both genotypes, such as response to reactive oxygen species (GO:0000302), unfolded protein binding (GO:0051082), protein folding (GO:0006457), response to oxidative stress (GO:0006979) and response to heat (GO:0009408). All these GO terms showed much higher significance in 'Ellvis', confirming the more robust heat-stress response of this cultivar (Figure 9A). Other metabolism-related GO terms were enriched in both genotypes, with higher significance in 'Mv 17-09', like iron ion binding (GO:0005506); lipid biosynthetic process (GO: 0008610); lipid transport (GO: 0006869) and metal ion transmembrane

10.3389/fpls.2023.1314021

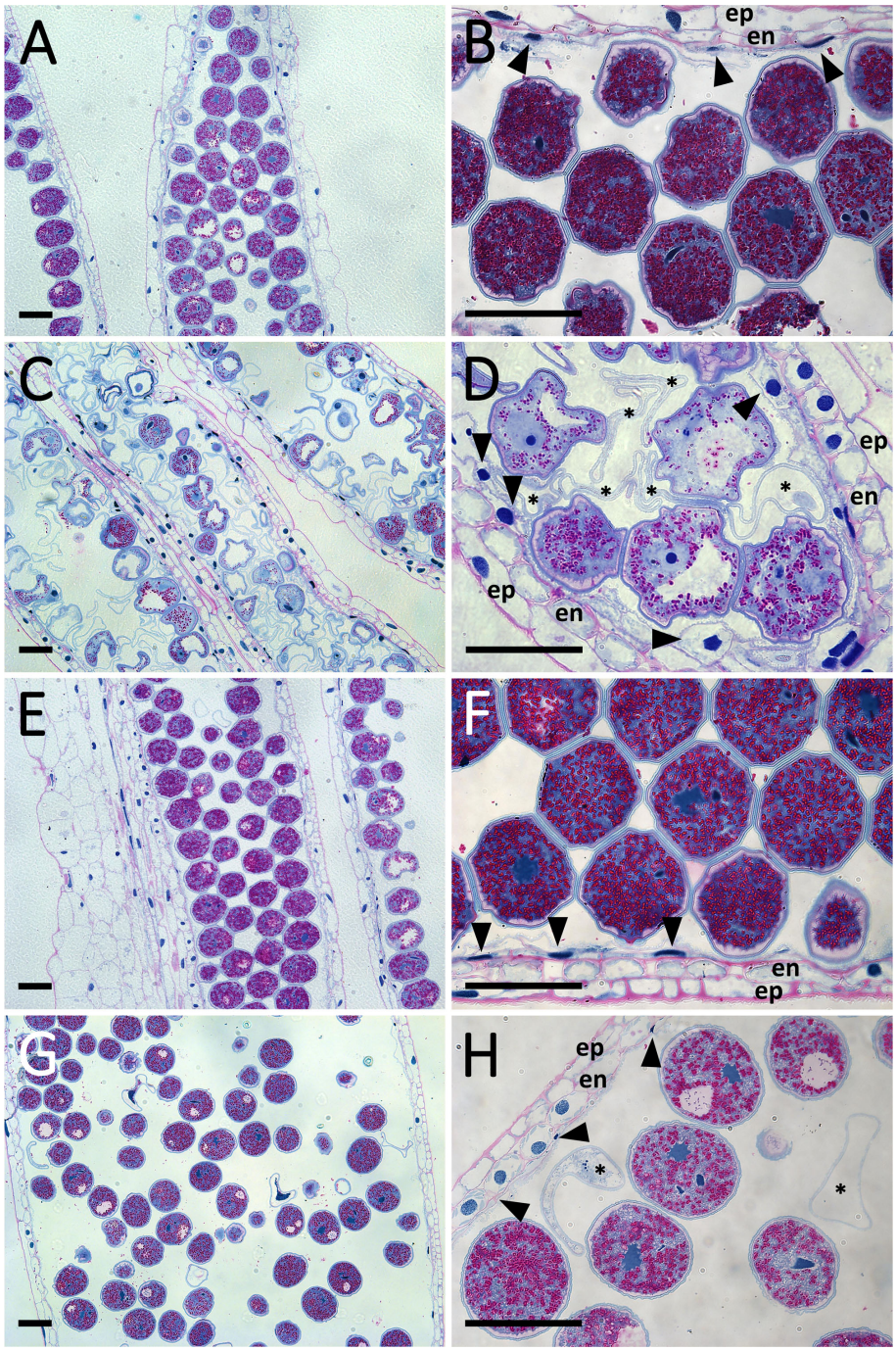

FIGURE 3
PAS and Amido Black-stained sections of control **(A, B)** and heat-stress treated **(C, D)** 'Mv 17-09' as well as control **(E, F)** and heat-stressed **(G, H)** 'Ellvis' anthers sampled on the day before anthesis (n= 5 per genotype and treatment). Note the persistent tapetal cells of treated 'Mv 17-09' **(D)**. Arrowhead, tapetal cell; asterisk, abortive microspore; en, endothecium; ep, epidermis. Bars represent 50 µm.

transporter activity (GO: 0046873) (Figure 9A). GO terms associated with pollen development were enriched in greater number in 'Ellvis' (3) compared to 'Mv 17-09' (1) (Figure 9A). Enriched GO terms of downregulated DEGs depicted a radically different stress response between the two genotypes (Figure 9B). GO terms associated with the cytoskeleton, meiosis/cell cycle, and microspore/anther development were represented by great numbers and at high significance values in the sensitive 'Mv 17-09'. In the light of our results regarding MMC and anther structure as well as cytoskeletal organization, the following downregulated terms were the most interesting: spindle organization (GO:0007051), spindle assembly (GO:0051225), anaphase-promoting complex (GO:0005680), pollen grain wall assembly (GO:0010208), tapetal layer development (GO:0048658) sporopollenin biosynthetic process (GO:0080110) and pollen exine formation (GO:0010584). While some of these GO terms

10.3389/fpls.2023.1314021

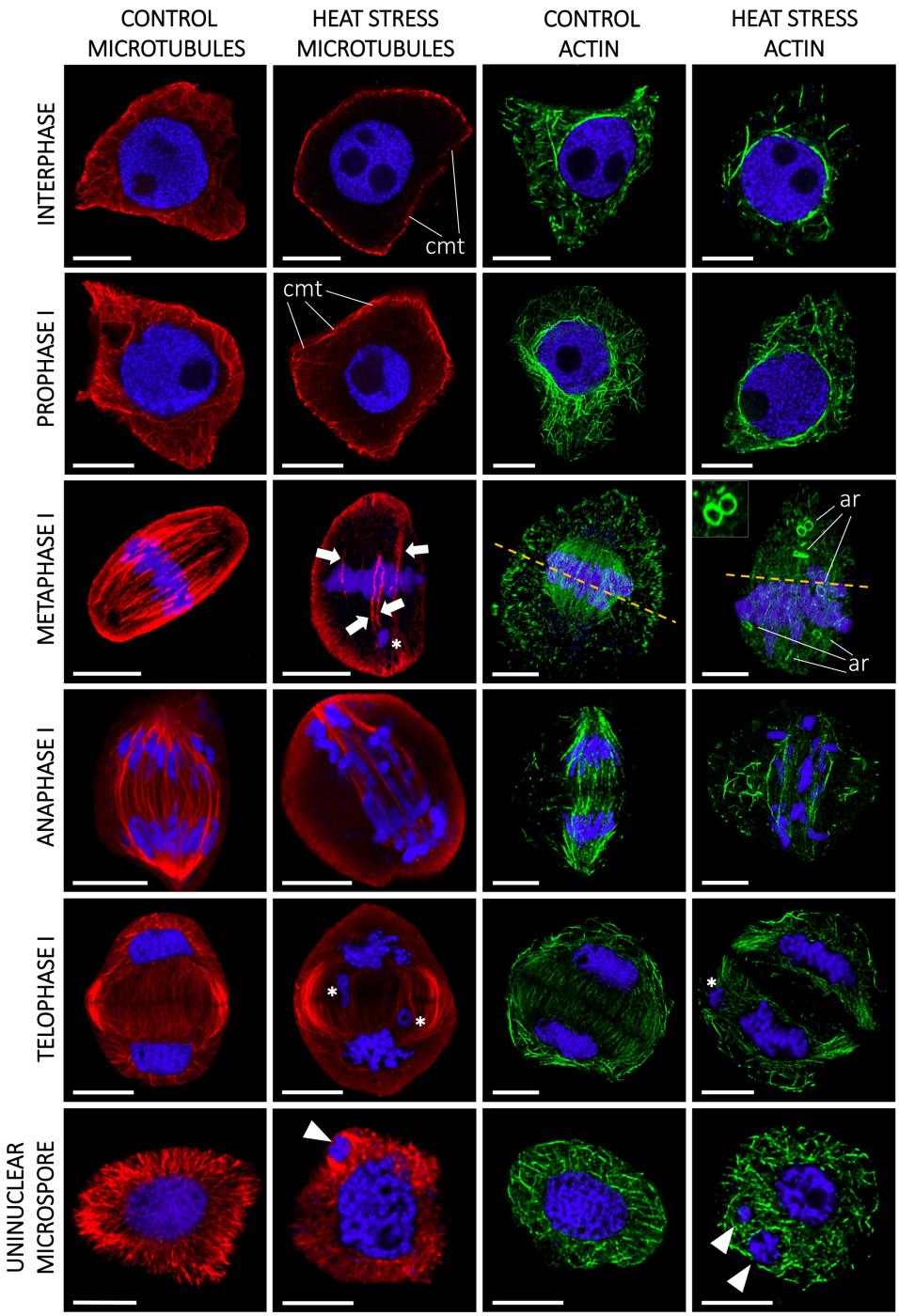

FIGURE 4
Heat stress significantly altered the microtubule (red) and actin cytoskeleton (green) structure of microspore mother cells (MMCs) during consecutive phases of meiosis and in the uninucleate microspore stage of 'Mv 17-09' (n=130). The chromatin is counterstained with DAPI (blue). Note the asynchronous chromosome movement in heat-treated MMCs during anaphase I, which triggered the formation of micronuclei. Arrow, defective spindle filament, arrowhead, micronucleus; asterisk, lagging chromosome; dashed line, symmetry plane; ar, actin ring (see inset, metaphase I); cmt, cortical microtubules. Bars represent 10 µm.

were also enriched in 'Ellvis', their FDR *p*-values were much lower when compared to 'Mv 17-09' (Figure 9B). Response to unfolded protein (GO:0006986) and protein refolding (GO:0042026) were enriched among up- and downregulated DEGs in both genotypes, which implies the existence of different gene sets in wheat to cope with protein denaturation under normal and stress conditions. However, 'Ellvis' exhibited higher FDR *p*-values regarding these GOs in the case of up- and downregulated DEGs as well (Figure 9B).

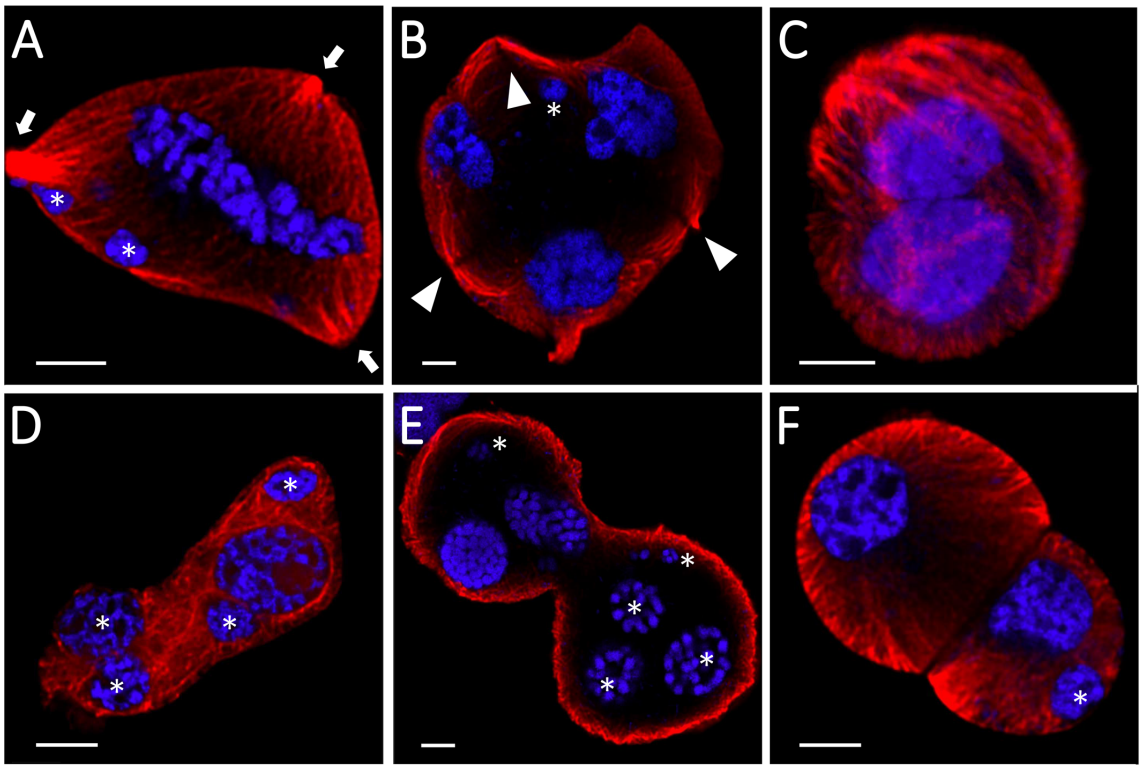

FIGURE 5
Structural defects of heat-stressed meiocytes and daughter cells of Mv17-09 (n=130). Trilateral symmetry **(A, B)**, nonseparated **(C–E)**, and unevenly divided **(F)** daughter cells. The chromatin is counterstained with DAPI (blue). Arrow, spindle pole; arrowhead, phragmoplast; asterisk, micronucleus. Bars represent 5 µm.

Analysis of genes taking part in male meiosis, spindle assembly, and tapetal functions

The results of the morphological and GO analyses prompted us to study changes in the expression of meiosis-, spindle assembly-, cytoskeleton-, and tapetum-specific gene sets at single-gene resolution. Our search for the wheat orthologs of 67 *Arabidopsis thaliana* genes with known meiosis-related functions (Chen et al., 2010) yielded 209 genes (Supplementary Table 5), from which eight were downregulated in 'Mv 17-09', while two were up- and also two were downregulated in 'Ellvis', respectively (Figure 10). The expression of two synapsis-related genes, *Arabidopsis-mei2-like* (*AML*) and *ZIP* decreased only in 'Mv 17-09'. Two serpin-coding genes showed elevated expression exclusively in 'Ellvis' (Figure 10).

Yamada and Goshima (2017) provided a list of 92 *Arabidopsis* genes crucial for forming a functional microtubule spindle. We found 240 wheat orthologs of these genes and also added 43 tubulin monomer genes and 26 microtubule severase (*catanin p60* and *p80*, *spastin* and *fidgetin*) genes identified using our BLAST functional annotation (Supplementary Table 6). The number of downregulated genes was more than two-fold in 'Mv 17-09' (26) when compared to 'Ellvis' (only 11), belonging to three categories of functions, namely microtubule-associated proteins, microtubule nucleation and spindle assembly checkpoint proteins (Figure 10) No significantly upregulated genes were identified in this gene set. We also studied the expression of 108 actin- and actin-associated proteins (Supplementary Table 7) and found that formin genes were the most affected by heat stress, suggesting that actin nucleation was decreased in 'Mv 17-09', in contrast to 'Ellvis' (Figure 10).

The fourth studied gene set was a group of tapetum-specific genes orchestrating the PCD of the tapetum layer and microspore development. We found 202 wheat orthologs of the 36 genes listed by Yao et al. (2022) (Supplementary Table 8). The expression of these orthologs was fundamentally different in the genotypes tested here, as these genes were predominantly downregulated in 'Mv 17-09' (with 17 up- and 57 downregulated DEGs), while we found only a handful of genes with decreased expression in 'Ellvis' (13 up-, and three downregulated orthologs; Figure 11). Transcription factors positively regulating the PCD of tapetal cells and genes required for pectin dissolution and sporopollenin synthesis declined in the heat-sensitive genotype while remaining constant in the tolerant 'Ellvis'. On the contrary, the expression of genes taking part in callose dissolution and pollen coat synthesis was found to be upregulated in both genotypes (Figure 11).

10.3389/fpls.2023.1314021

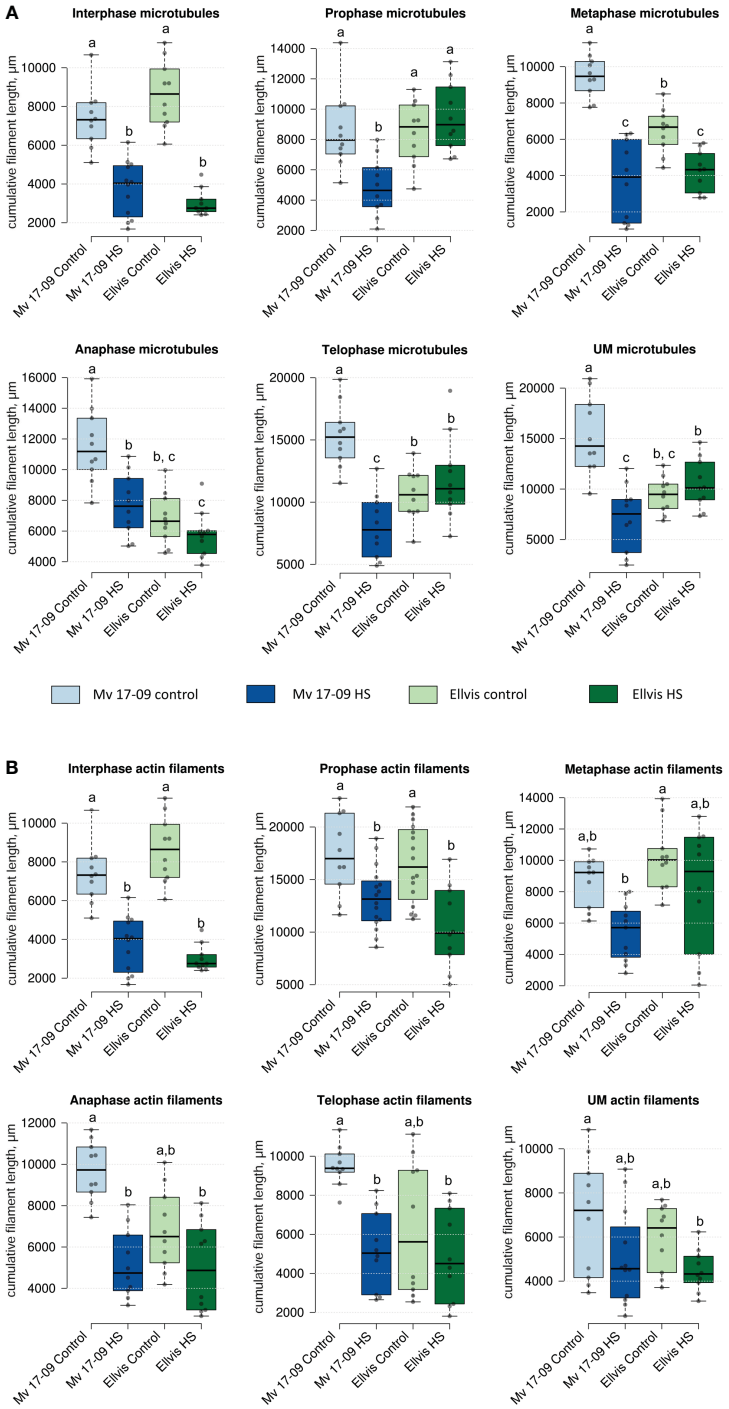

FIGURE 6
Effect of heat stress on the cumulative length of microtubules **(A)** and actin filaments **(B)** of meiocytes and uninucleate microspores of 'Mv 17-09' and 'Ellvis' (n=10 to 16 per genotype, treatment and developmental phase). Different letters above boxes indicate significant differences at least at the $P \leq 0.05$ level of probability, according to Tukey's post-hoc test (α=0.05). Stripes within boxes of the plots indicate median values. Grey dots represent data points. ns, not significant; UM, uninucleate microspore.

10.3389/fpls.2023.1314021

TABLE 2 Results of the two-way ANOVA analysis carried out on the outcome of microtubule and actin filament cumulative length studies.

Studied parameters	Two-way ANOVA (P-values)		
	Genotype	Heat Stress	Interaction
Interphase MT cumulative length (μm)	0.4514 ns	<0.0001 ***	0.006 **
Prophase MT cumulative length (μm)	0.0003 ***	0.0196 *	0.0001 ***
Metaphase MT cumulative length (μm)	0.0033 **	<0.0001 ***	<0.0001 ***
Anaphase MT cumulative length (μm)	<0.0001 ***	<0.0001 ***	0.0059 **
Telophase MT cumulative length (μm)	0.5198 ns	<0.0001 ***	<0.0001 ***
UM MT cumulative length (μm)	0.0931 ns	<0.0001 ***	<0.0001 ***
Interphase AF cumulative length (μm)	0.0469 *	<0.0001 ***	0.052 ns
Prophase AF cumulative length (μm)	0.0266 *	<0.0001 ***	0.2634 ns
Metaphase AF cumulative length (μm)	0.1862 ns	0.0949 ns	0.0054 **
Anaphase AF cumulative length (μm)	0.5979 ns	0.0005 ***	0.8266 ns
Telophase AF cumulative length (μm)	0.4687 ns	0.017 *	0.7366 ns
UM AF cumulative length (μm)	0.1297 ns	0.0012 **	0.7509 ns

Statistical differences were determined using a two-way ANOVA to examine the effects of genotype, treatment (heat stress) and/or the interaction of these factors. MT, microtubule; AF, actin filament; UM, uninucleate microspore. Asterisks denote statistically significant differences (*p<0.05; **p<0.01; ***p<0.001; ns, not significant).

Discussion

Global transcriptome analysis implicates the key role of cytoskeleton, spindle assembly, and tapetal functions in heat sensitivity

Spikelet fertility and yield data from our experiments confirmed the superior stress-alleviating potential of 'Ellvis' over 'Mv 17-09'. The results of GO enrichment analysis implied various stress reactions behind the differential heat response of the two genotypes. A higher enrichment of upregulated heat- and oxidative stress-related genes, as well as genes related to protein folding and refolding, supported the general stress tolerance of 'Ellvis'. In addition, we found that the number of downregulated genes was significantly higher after heat stress in the anthers of sensitive 'Mv 17-09'. This led us to hypothesize that these downregulated gene functions may act behind this differential heat-stress sensitivity. Our GO enrichment analysis revealed that cytoskeleton organization, spindle assembly and tapetum development were the most important downregulated functions which were enriched exclusively, or significantly higher in the sensitive genotype. To draw a detailed picture of the heat-driven impairment during male meiosis and gametogenesis, we investigated the structural deviations, in parallel to expression changes at single-gene resolution.

First, we studied wheat orthologs identified based on meiosis-specific *Arabidopsis* genes (Chen et al., 2010). Although a few synapsis-related genes, such as *Arabidopsis-mei2-like* (*AML*) and *ZIP* (Kaur et al., 2006; De Muyt et al., 2018), were exclusively downregulated in 'Mv 17-09', we did not observe structural problems related to this phenomenon. However, serpin genes showed selective upregulation in 'Ellvis' anthers. The serpin protease inhibitors are thought to regulate different cell-cycle checkpoints in response to DNA damage (Ahn et al., 2009). Consequently, the upregulation of these genes may improve the stability of the cell cycle at stress. Increased expression of serpins was also observed in heat-stressed durum wheat grains (Laino et al., 2010). *Disruption of meiotic control 1* (*Dmc1*), a meiosis-specific recombinase (Kagawa and Kurumizaka, 2010), was suspected earlier as a meiotic temperature-tolerance gene in wheat, as deletion of its 5D chromosome-specific ortholog was linked to the temperature sensitivity of male meiosis (Draeger et al., 2020). In our experiments, this gene (TraesCS5D02G141200/TraesCS5D03G0353500) did not show significant expression change in either genotype, confirming that meiotic heat sensitivity is a phenomenon with multiple, independent factors involved.

The frequent formation of impaired spindles and the asynchronous movement of chromosomes prompted us to investigate the regulation of cytoskeleton organization and the process of spindle assembly. It was shown previously that the cell division-specific cytoskeletal microtubule structures, such as the spindle and the phragmoplast, exhibit elevated sensitivity to heat stress when compared to cortical microtubules (Smertenko et al., 1997). Our question was whether these structural problems are triggered at least partly by gene expression changes or are induced solely by heat-driven protein denaturation and oxidative stress. Quantitation of MT and AF pools in meiocytes revealed that the cumulative length of both arrays decreased in all phases of meiosis I in 'Mv 17-09'. However, the mRNA amount of tubulin and actin genes remained the same as in the controls. The dynamics of both networks are orchestrated by a plethora of specific regulatory proteins (Krtková et al., 2016; Paez-Garcia et al., 2018). Decline of cumulative filament length can be caused by depolymerization or decreased nucleation. We found that the expression of neither the MT-severing proteins (severases, like katanin, spastin, and fidgetin, reviewed by Kuo and Howard, 2021) nor the AF-depolymerizing proteins (like actin capping proteins, actin depolymerizing factors (ADFs) or villins (reviewed by de Ruijter and Emons, 1999) showed elevation. In contrast, genes taking part in MT nucleation, such as *mitotic-spindle organizing protein 1* (*Mozart-1*) and several orthologs of the AF-nucleating and -elongation promoting formin genes (Nakamura et al., 2012; Lee and Liu, 2019), were downregulated exclusively in the sensitive genotype. Taken together, silencing of MT and AF nucleation probably contributed to the defective cytoskeletal organization in 'Mv 17-09', in contrast to the higher chaperone activity in 'Ellvis'.

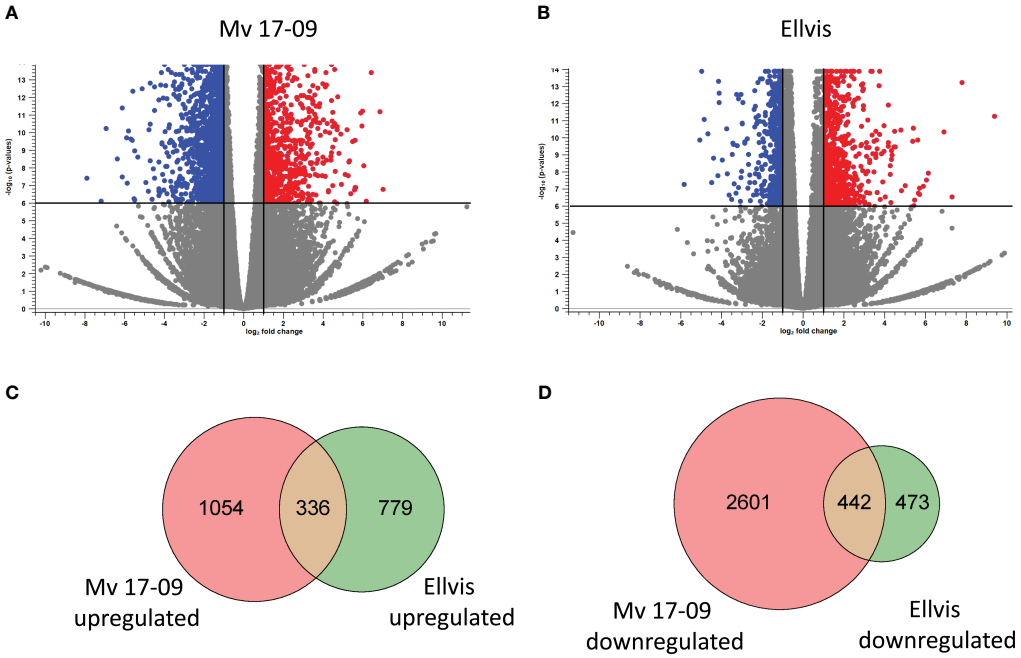

FIGURE 7
Distribution of significantly (FDR p<0.000005, |fold change|≥2) upregulated (red) and downregulated (blue) genes in 'Mv 17-09' **(A)** and 'Ellvis' **(B)** anthers sampled at the end of treatment. Grey dots represent genes with unchanged expression when compared to the control. Venn diagrams presenting the number of upregulated **(C)** and downregulated **(D)** DEGs in the two wheat genotypes.

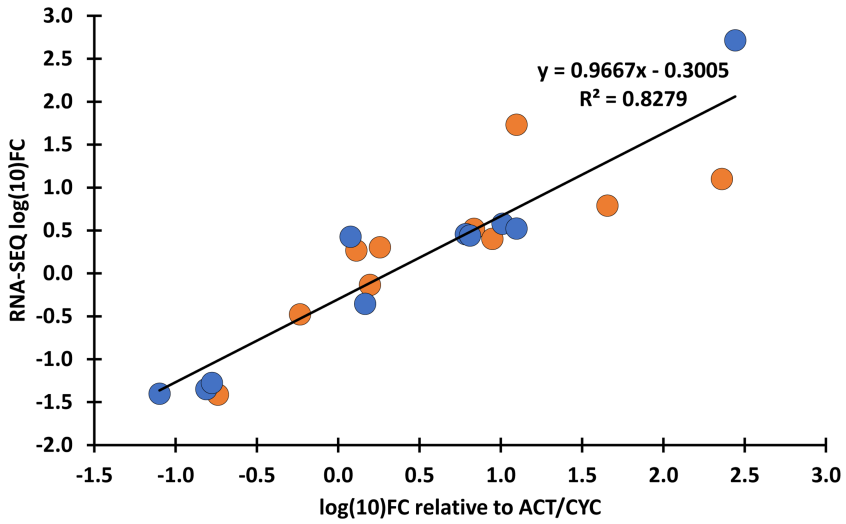

FIGURE 8
Verification of transcriptome expression data with qPCR. Fold changes (FC) values of the RNA-seq data were compared with the FC calculated as relative expression values of the selected genes to *Ta*ACT3 and *Ta*CYC reference genes as internal controls. Blue: 'Mv 17-09'; orange: Ellvis. An adjusted coefficient of determination (R^2) of 0.8279 is observed between the RNA-seq and qPCR data of 10 genes (Pearson's r = 0.9099). qPCR analysis was performed using three independent RNA samples (not the same ones used for RNA-seq). The selected genes, FC values and corresponding primer sequences are listed in Supplementary Table 2.

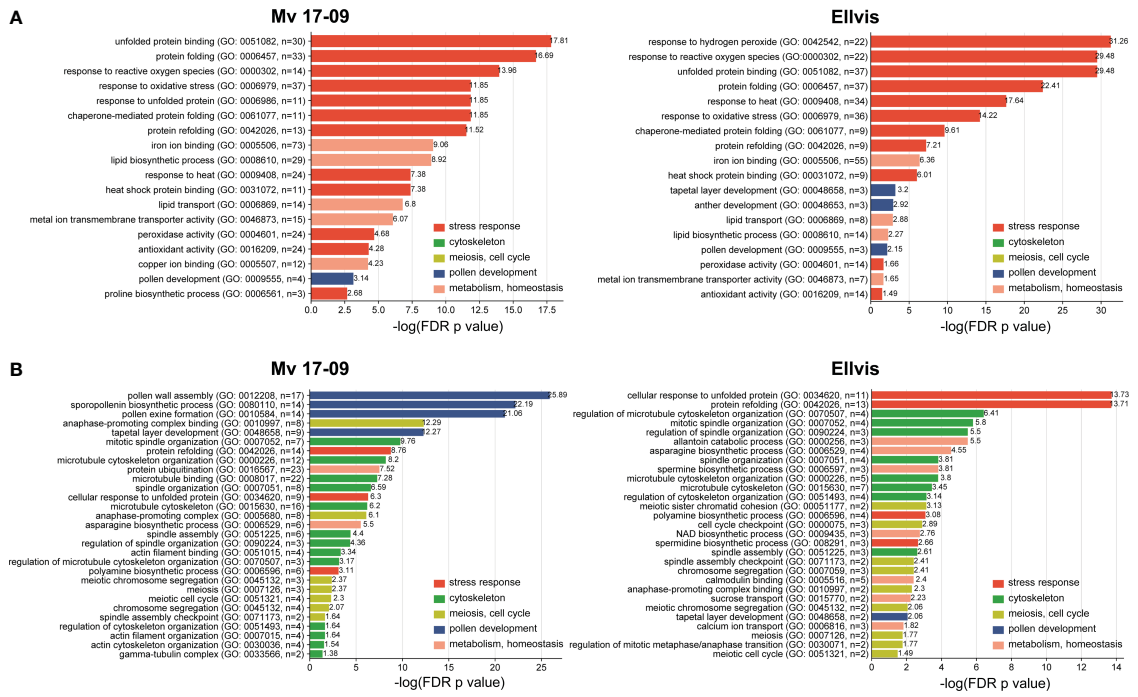

FIGURE 9
Gene ontology (GO) terms enriched significantly ($p<0.05$) following heat stress among the upregulated **(A)** and downregulated **(B)** DEGs. GO terms are classified based on their functionality.

Downregulation of spindle assembly checkpoint genes may lead to genetically unbalanced pollen grains

Precise execution of male meiosis is ensured through a series of checkpoints. However, these checkpoints are less stringent in plants when compared to other eukaryotes, allowing the generation of genetically unbalanced gametes (Wijnker and Schnittger, 2013). Our structural studies indicated that impairment of the spindle assembly checkpoint (SAC) might be a key event triggering the more frequent formation of micronuclei-containing, functionally damaged microspores in the sensitive genotype. SAC prevents aneuploidy of daughter cells by blocking the onset of anaphase and sister chromatid segregation until all kinetochores are attached properly to the spindle fibers (McAinsh and Kops, 2023). In addition, SAC ensures the correct formation of the metaphase plate, supporting the implementation of equal cell division (Tan et al., 2015). Erroneous operation of SAC leads to asynchronous chromosome movement and lagging chromosomes during anaphase and eventually to the formation of micronuclei. Several genes are known to play a role in this intricate mechanism in model plants (Yamada and Goshima, 2017). Our gene expression study confirmed that numerous orthologs of these genes, such as *Aurora* kinases, *targeting protein for XKLP2* (*TPX2*), *mitotic arrest deficient 1* (*Mad1*), and *Bub1-Related* (*BubR1*), were downregulated in both genotypes after heat stress. *Aurora* kinases are conserved regulators of SAC functions, with three genes in *Arabidopsis*: *Aurora1* and *2* (subgroup A), and *Aurora3* (subgroup B) (Demidov et al., 2005). Though their localizations differ, all of them are suspected to manage the function of other SAC proteins by phosphorylating the H3 histone protein. Reduced expression of these kinases resulted in meiotic defects, aneuploidy, and unreduced pollen grain formation in *Arabidopsis* (Kawabe et al., 2005; Demidov et al., 2014). TPX2 is an important conserved microtubule-associated regulator, acting through the activation of Aurora kinases (Vos et al., 2008; Dvořák Tomaštíková et al., 2020). There are two main protein complexes involved in the SAC mechanism: the anaphase-promoting complex/cyclosome (APC/C) and the mitotic checkpoint complex (MCC) (Hein and Nilsson, 2014). APC/C, a multi-subunit E3 ubiquitin ligase complex, is the effector of SAC, degrading securin and cyclin B, thus promoting the transition to anaphase (Schrock et al., 2020). MCC is another complex of mitotic arrest deficient 2 (Mad2), cell division cycle 20 (Cdc20), BubR1, and *budding uninhibited* by *benzimidazole* (*Bub3*) proteins, which inhibits the activity of the APC/C complex until all chromosomes are properly attached to spindle fibers (Lara-Gonzalez et al., 2021). Although the expression of APC/C subunits did not change after the treatment, several genes of MCC proteins were downregulated. While expression of *BubR1* transcripts decreased in both genotypes, we found that the orthologs of *Cdc20* genes downregulated primarily in the sensitive 'Mv 17-09'. The role of Cdc20 protein is intriguing in SAC regulation, as it has dual functions in *Arabidopsis* (Lara-Gonzalez et al., 2021). One molecule is needed as an activator of APC/C, taking part in substrate recognition of the complex (Peters, 2006), while another serves as part of the inhibitory MCC complex (Izawa and Pines, 2015). Not surprisingly, a decreased amount of Cdc20 proteins results in abnormal spindle formation, as Niu et al. (2015) found in *Arabidopsis*. According to the Ensembl Plants database, the five existing *Arabidopsis* Cdc20 genes (Cdc 20.1-

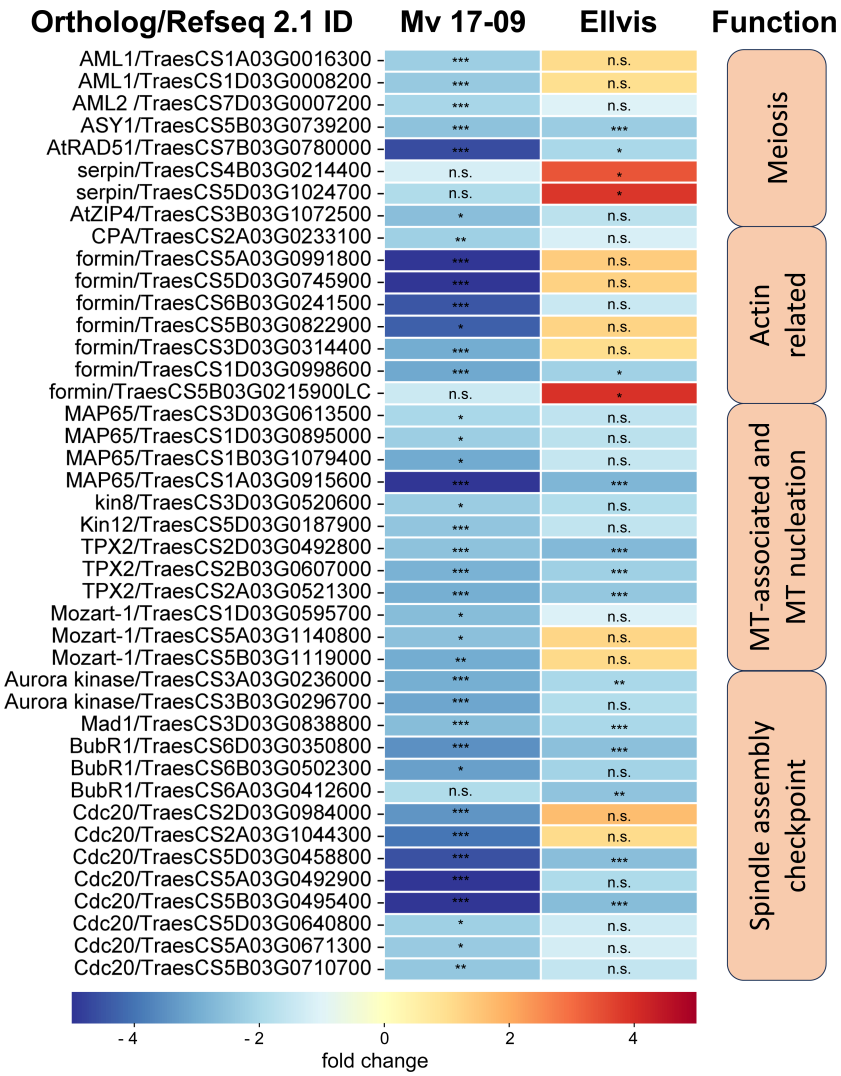

FIGURE 10
Expression of significant(FDR p<1.0E-6, |fold change|≥2) DEGs involved in meiosis, actin nucleation/reorganization and spindle assembly in 'Mv 17-09' and 'Ellvis'anthers sampled at the end of treatment. Asterisks denote statistically significant differences (*p<1.0E-7; **p<1.0E-10; ***p<1.0E-13) between the control and heat stress treated plants of the genotypes. ns, not significant.

20.5, Kevei et al., 2011) have 13 orthologues in bread wheat. Expression of these orthologs showed significantly higher stability in the case of 'Ellvis', with only two downregulated genes as opposed to eight in 'Mv 17-09'. Till today, there aren't any public data on *Cdc20* expression values following heat stress in plant generative cells from any species. However, in *Festuca* leaves, *Cdc20* expression was elevated after 12 h and 36 h of heat stress (Hu et al., 2014), suggesting that the regulation of SAC genes is different between vegetative and generative cells.

Phragmoplast formation is affected by heat stress

We observed frequent unequal divisions and the failure of cytokinesis in daughter cells. These symptoms implied the perturbance of phragmoplast formation. The phragmoplast is a bipolar array of MTs and AFs responsible for constructing the cell plate in *Arabidopsis* and tobacco (Smertenko et al., 2018) and, subsequently, the new cell wall. We found that two phragmoplast-related proteins, *phragmoplast orienting kinesin 2*, (*POK2*, *kinesin12*) and *microtubule-associated* protein 65-3 (*MAP65-3*), were downregulated because of high temperature, predominantly in the sensitive 'Mv 17-09'. *POK2* (AT3G19050 in *Arabidopsis*) is a member of the kinesin 12 family and serves as a signal for the correct phragmoplast orientation at the cell cortex (Müller et al., 2006; Lipka et al., 2014). MAP65-3, a 65-kDa MT-associated protein, promotes the recruitment of POK2 to the phragmoplast (Herrmann et al., 2018), thus the appropriate formation of new cell walls. Mutation of *MAP65-3* and the closely related *MAP65-4* genes triggered lethal alterations in gametophytic cell lines of *Arabidopsis* (Li et al., 2017). In a previous study, cold stress was also reported to

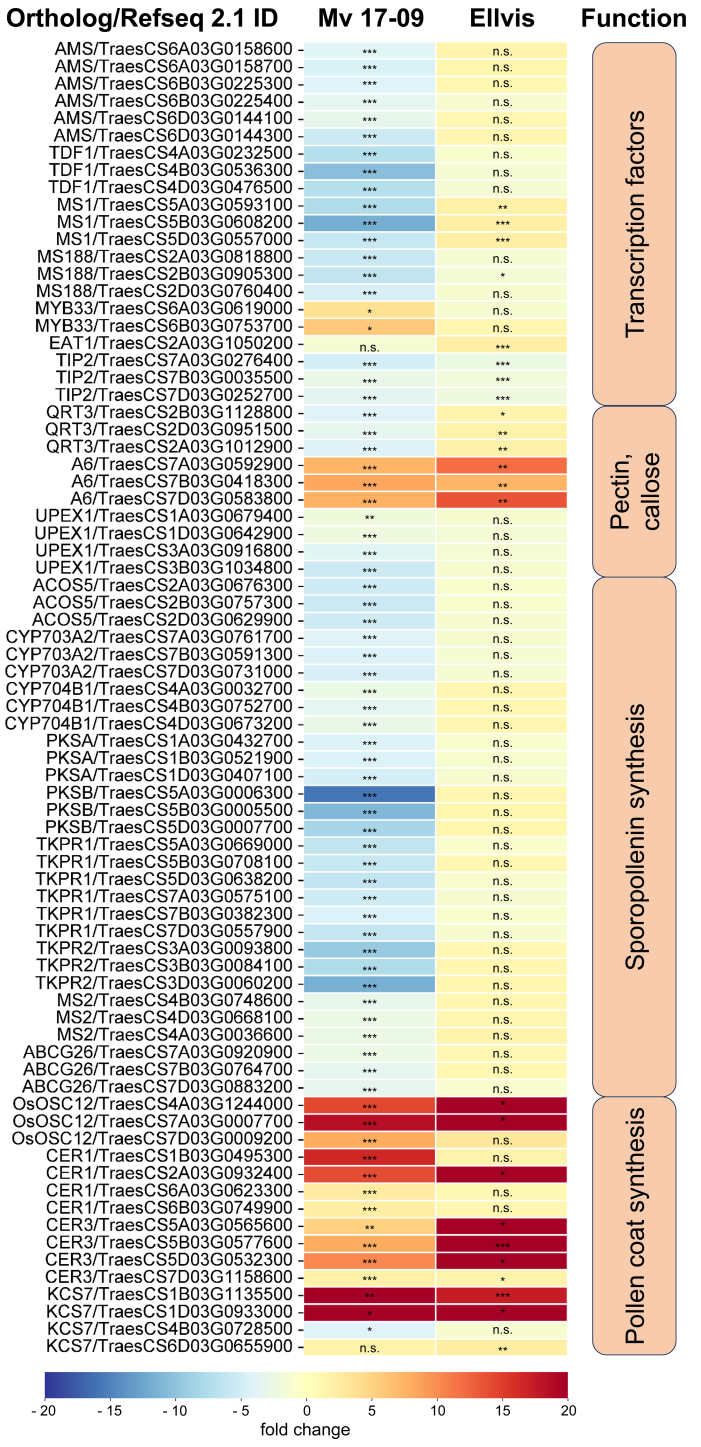

FIGURE 11
Expression of significant (FDR p<1.0E-6, |fold change|≥2) tapetum specific DEGs in 'Mv 17-09' and 'Ellvis'anthers sampled at the end of treatment. Asterisks denote statistically significant differences (*p<1.0E-7; **p<1.0E-10; ***p<1.0E-13) between the control and heat stress treated plants of the genotypes. MT, microtubule. ns, not significant.

alter significantly the organization of phragmoplast and cell plate formation in a thermosensitive genic male sterile wheat line (Tang et al., 2011). However, chromosome segregation and tapetal development were unaffected by cold stress.

Although we frequently observed serious structural deviations in the sensitive genotype at the end of heat treatment, pollen grain samples at the time of anthesis contained either dead pollen grains with empty pollen walls or living cells with minor structural alterations.

While we did not study occurrence of PCD in developing microspores, it is likely that the microspores containing serious structural defects will undergo PCD and degenerate. It was shown previously that micronuclei degenerate and are eliminated in wheat (Gernand et al., 2005), causing the loss of genetic material. Thus, a fraction of apparently normal mature pollen grains can be functionally defective and contribute to sterility.

Failure of tapetum degeneration and sporopollenin synthesis contributes to decreased spikelet fertility

It is generally accepted that tapetal dysfunction and/or early tapetal degeneration is a major factor responsible for the low pollen grain viability of heat-treated anthers (Saini et al., 1984; Oshino et al., 2007). As much of the ROS is generated in the mitochondrial respiratory chain, the tapetum, a mitochondria-rich tissue, is highly vulnerable to oxidative stress (Navrot et al., 2007; De Storme and Geelen, 2014). Besides direct damage caused by ROS, such as peroxidation of proteins, nucleic acids, and lipids, these substances may promote premature PCD of the tapetum, triggering the starvation and death of the developing pollen grains in rice (Li et al., 2012; Luo et al., 2013). Other studies, however, point out that failure of tapetum PCD also leads to microspore death and drastically decreased spikelet fertility in *Arabidopsis* and crop plants (reviewed by Lei and Liu, 2020). Li et al. (2011) found that *persistent tapetal cell 1* (*PTC1*), the rice ortholog of the *Arabidopsis male sterility 1* (*MS1*) gene, promotes tapetal PCD and is required for normal microspore development.

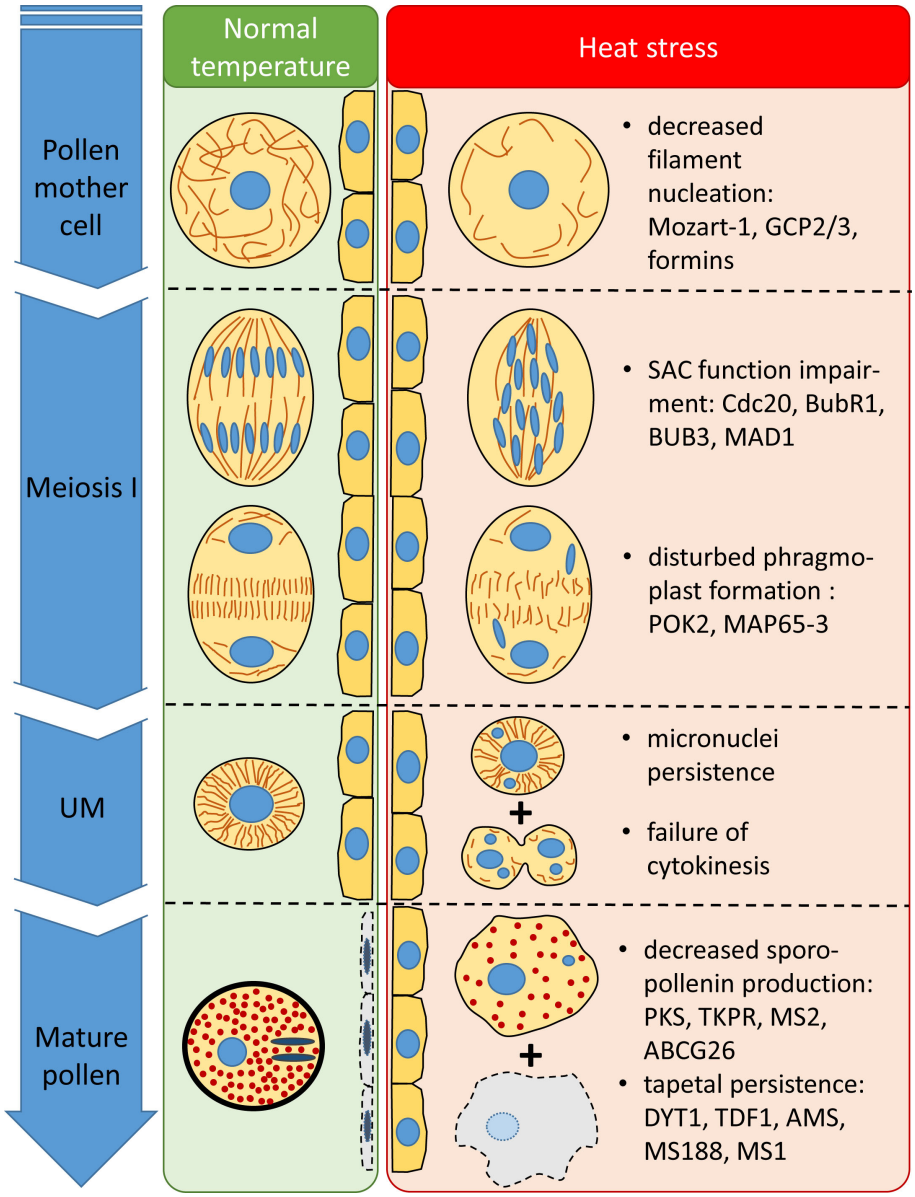

FIGURE 12
Structural and temporal alterations of wheat male meiocytes and tapetal cells and their supposed transcriptional background triggered by meiosis-timed heat stress.

MS1 is the final member of a tapetum-specific regulation cascade (consisting of *dysfunctional tapetum* 1 (*DYT1*), *defective in tapetal development and function 1* (*TDF1*), *aborted microspores* (*AMS*), *male sterile 188* (*MS188*), and *MS1* genes), each promoting the expression of the subsequent element. Mutants of these genes showed delayed PCD of tapetum, seriously affecting male spikelet fertility in *Arabidopsis* and rice (Yao et al., 2022). In our study, the expression of these regulators was repressed after heat stress in the sensitive 'Mv 17-09', but did not change in 'Ellvis'. These findings agree with the delayed tapetum degeneration of 'Mv 17-09', also revealed by light microscopy (Figures 3C, D). The *eternal tapetum1* (*EAT1*) and *TDR interacting protein2* (*TIP2*) transcription factors promote tapetum PCD in rice (Fu et al., 2014; Ko et al., 2014) by upregulating the expression of two aspartic protease genes (Ji et al., 2013; Niu et al., 2013). One *EAT1* ortholog was upregulated in 'Ellvis', while *TIP2* orthologs were downregulated in both genotypes. In contrast to our study, it was previously reported that heat stress treatments timed at or right after meiosis resulted in premature tapetal degeneration instead of its persistence in wheat (Saini et al., 1984; Browne et al., 2021). While the applied temperatures were different in these studies (30°C and 35°C, respectively), both groups used a longer, three-day stress treatment. We assume that the longer stress may have triggered the production of higher ROS levels in these experiments, accelerating the degeneration of tapetal cells. In contrast to our results, Browne et al. (2021) did not observe the downregulation of PCD-promoting *AMS* and *myb domain protein8* (*MYB8*) transcription factors in wheat, though they found similar changes to our findings in the case of EAT1 and TIP2 gene expression levels in sensitive genotypes. While our results confirm the previous findings regarding the crucial role of the tapetum in heat-induced sterility, we also clearly showed that failure of tapetal functions can be induced in different ways even by the same kind of stress.

Besides the nourishing function of the tapetum, production of glucanases for callose degradation and tetrade separation is another important task. An important contributor to tetrad separation is the *A6* glucanase gene in *Arabidopsis* (Xu et al., 2016). Wheat orthologs of this gene were found to be upregulated in both genotypes after heat stress. While we did not study the deposition or the correct degradation of callose in tetrad walls by direct methods (such as aniline blue staining), we found that tetrad separation occurred normally after heat treatment. Thus, it can be assumed that elevated expression of *A6* genes did not affect spikelet fertility.

Tapetum-specific sporopollenin synthesis genes were downregulated exclusively in 'Mv 17-09', which can be another factor contributing to elevated sterility. It was reported previously that a heat-driven block of sporopollenin synthesis can lead to lethal defects in a temperature-sensitive male sterile wheat line (Yang et al., 2020). In contrast to sporopollenin, pollen coat synthesis genes were upregulated in both genotypes in our experiments. These data suggest that the regulation of tapetal PCD, sporopollenin synthesis, and pollen coat formation are controlled separately, in a genotype-dependent manner.

In our study, heat stress triggered various structural and developmental changes, impairing male fertility. These alterations and their supposed transcriptional background were summarized in Figure 12.

Conclusion

We investigated the factors involved in meiotic heat sensitivity during male gametogenesis of wheat. We demonstrated that even a short exposition to high ambient temperature at the time of meiosis triggers multiple defects in the structure and function of meiocytes. Our results implicate that the failure of the spindle assembly checkpoint and subsequent erroneous chromosome segregation might be the major contributors to spikelet fertility loss via the generation of genetically unbalanced male gametes. In addition, we revealed that heat stress can induce the repression of tapetal degeneration, which is another important factor in pollen grain abortion. Our comparative RNA-seq analysis between heat-sensitive and -tolerant genotypes revealed the transcriptomic basis of these injuries, possibly providing an inventory and baseline of tolerance mechanisms for future breeding efforts. However, further research should be done to reveal the regulatory mechanisms of heat-sensitive gene expression patterns during male gametogenesis.

Data availability statement

The datasets presented in this study can be found in online repositories. The names of the repository/repositories and accession number(s) can be found below: https://www.ncbi.nlm.nih.gov/geo/, GSE244819.

Author contributions

AF: Conceptualization, Data curation, Formal analysis, Funding acquisition, Investigation, Methodology, Visualization, Writing – original draft, Writing – review & editing. BP: Investigation, Methodology, Writing – review & editing. VS: Methodology, Validation, Visualization, Writing – review & editing. LS: Formal analysis, Funding acquisition, Visualization, Writing – review & editing, Writing – original draft.

Funding

The author(s) declare financial support was received for the research, authorship, and/or publication of this article. This work was supported by the Hungarian National Research, Development, and Innovation Fund – NKFIH (grant FK134992), the Hungarian National Laboratories Program (grant number RRF-2.3.1-21-2022-00007), the Bolyai Janos Research Scholarship from the Hungarian Academy of Sciences (grant BO/00837/21), and the ÚNKP-21-5 and ÚNKP-22-5 New National Excellence Programs of the Ministry for

Innovation and Technology from the source of the National Research, Development and Innovation Fund (grants ÚNKP-21-5-BME-383 and ÚNKP-22-5-MATE/13).

Acknowledgments

We thank Adél Sepsi for her constructive advice on this project and Erika Gondos for her help in growing plants.

Conflict of interest

The authors declare that the research was conducted in the absence of any commercial or financial relationships that could be construed as a potential conflict of interest.

Publisher's note

Supplementary material

The Supplementary Material for this article can be found online at: https://www.frontiersin.org/articles/10.3389/fpls.2023.1314021/full#supplementary-material

References

Ahn, J.-W., Atwell, B. J., and Roberts, T. H. (2009). Serpin genes *AtSRP2* and *AtSRP3* are required for normal growth sensitivity to a DNA alkylating agent in *Arabidopsis*. *BMC Plant Biol.* 9, 52. doi: 10.1186/1471-2229-9-52

Balla, K., Karsai, I., Bónis, P., Kiss, T., Berki, Z., Horváth, Á., et al. (2019). Heat stress responses in a large set of winter wheat cultivars (*Triticum aestivum* L.) depend on the timing and duration of stress. *PloS One* 14, e0222639. doi: 10.1371/journal.pone.0222639

Benjamini, Y., and Hochberg, Y. (1995). Controlling the false discovery rate: A practical and powerful approach to multiple testing. *J. R. Stat. Soc Ser. B Methodol.* 57, 289–300. doi: 10.1111/j.2517-6161.1995.tb02031.x

Bennett, M. D., Rao, M. K., Smith, J. B., and Bayliss, M. W. (1973). Cell development in the anther, the ovule, and the young seed of *Triticum aestivum* L. var. Chinese Spring. *Philos. Trans. R. Soc Lond. B Biol. Sci.* 266, 39–81. doi: 10.1098/rstb.1973.0036

Browne, R. G., Li, S. F., Iacuone, S., Dolferus, R., and Parish, R. W. (2021). Differential responses of anthers of stress tolerant and sensitive wheat cultivars to high temperature stress. *Planta* 254, 4. doi: 10.1007/s00425-021-03656-7

Chaturvedi, P., Wiese, A. J., Ghatak, A., Záveská Drábková, L., Weckwerth, W., and Honys, D. (2021). Heat stress response mechanisms in pollen development. *New Phytol.* 231, 571–585. doi: 10.1111/nph.17380

Chen, C., Farmer, A. D., Langley, R. J., Mudge, J., Crow, J. A., May, G. D., et al. (2010). Meiosis-specific gene discovery in plants: RNA-Seq applied to isolated *Arabidopsis* male meiocytes. *BMC Plant Biol.* 10, 280. doi: 10.1186/1471-2229-10-280

Conesa, A., and Götz, S. (2008). Blast2GO: A comprehensive suite for functional analysis in plant genomics. *Int. J. Plant Genomics* 2008, 619832. doi: 10.1155/2008/619832

Demidov, D., Lermontova, I., Weiss, O., Fuchs, J., Rutten, T., Kumke, K., et al. (2014). Altered expression of Aurora kinases in *Arabidopsis* results in aneu- and polyploidization. *Plant J.* 80, 449–461. doi: 10.1111/tpj.12647

Demidov, D., Van Damme, D., Geelen, D., Blattner, F. R., and Houben, A. (2005). Identification and dynamics of two classes of Aurora-like kinases in *Arabidopsis* and other plants. *Plant Cell* 17, 836–848. doi: 10.1105/tpc.104.029710

De Muyt, A., Pyatnitskaya, A., Andréani, J., Ranjha, L., Ramus, C., Laureau, R., et al. (2018). A meiotic XPF–ERCC1-like complex recognizes joint molecule recombination intermediates to promote crossover formation. *Genes Dev.* 32, 283–296. doi: 10.1101/gad.308510.117

de Ruijter, N. C. A., and Emons, A. M. C. (1999). Actin-binding proteins in plant cells. *Plant Biol.* 1, 26–35. doi: 10.1111/j.1438-8677.1999.tb00705.x

De Storme, N., and Geelen, D. (2014). The impact of environmental stress on male reproductive development in plants: biological processes and molecular mechanisms. *Plant Cell Environ.* 37, 1–18. doi: 10.1111/pce.12142

Dolferus, R., Ji, X., and Richards, R. A. (2011). Abiotic stress and control of grain number in cereals. *Plant Sci.* 181, 331–341. doi: 10.1016/j.plantsci.2011.05.015

Dong, X., Hong, Z., Sivaramakrishnan, M., Mahfouz, M., and Verma, D. P. S. (2005). Callose synthase (CalS5) is required for exine formation during microgametogenesis and for pollen viability in *Arabidopsis*. *Plant J.* 42, 315–328. doi: 10.1111/j.1365-313X.2005.02379.x

Draeger, T., Martin, C., Alabdullah, A. K., Pendle, A., Rey, M.-D., Shaw, P., et al. (2020). *Dmc1* is a candidate for temperature tolerance during wheat meiosis. *Theor. Appl. Genet.* 133, 809–828. doi: 10.1007/s00122-019-03508-9

Dvořák Tomaštíková, E., Rutten, T., Dvořák, P., Tugai, A., Ptošková, K., Petrovská, B., et al. (2020). Functional divergence of microtubule-associated TPX2 family members in *Arabidopsis thaliana*. *Int. J. Mol. Sci.* 21, 2183. doi: 10.3390/ijms21062183

Fábián, A., Sáfrán, E., Szabó-Eitel, G., Barnabás, B., and Jäger, K. (2019). Stigma functionality and fertility are reduced by heat and drought co-stress in wheat. *Front. Plant Sci.* 10. doi: 10.3389/fpls.2019.00244

Farooq, M., Bramley, H., Palta, J. A., and Siddique, K. H. M. (2011). Heat stress in wheat during reproductive and grain-filling phases. *Crit. Rev. Plant Sci.* 30, 491–507. doi: 10.1080/07352689.2011.615687

Fayos, I., Frouin, J., Meynard, D., Vernet, A., Herbert, L., and Guiderdoni, E. (2022). Manipulation of meiotic recombination to hasten crop improvement. *Biology* 11, 369. doi: 10.3390/biology11030369

Fu, Z., Yu, J., Cheng, X., Zong, X., Xu, J., Chen, M., et al. (2014). The rice basic helix-loop-helix transcription factor TDR INTERACTING PROTEIN2 is a central switch in early anther development. *Plant Cell* 26, 1512–1524. doi: 10.1105/tpc.114.123745

Gernand, D., Rutten, T., Varshney, A., Rubtsova, M., Prodanovic, S., Brüß, C., et al. (2005). Uniparental chromosome elimination at mitosis and interphase in wheat and pearl millet crosses involves micronucleus formation, progressive heterochromatinization, and DNA fragmentation. *Plant Cell* 17, 2431–2438. doi: 10.1105/tpc.105.034249

Giorno, F., Wolters-Arts, M., Mariani, C., and Rieu, I. (2013). Ensuring reproduction at high temperatures: the heat stress response during anther and pollen development. *Plants* 2, 489–506. doi: 10.3390/plants2030489

Gómez, J. F., Talle, B., and Wilson, Z. A. (2015). Anther and pollen development: A conserved developmental pathway. Journal of Integrative. *Plant Biol.* 57, 876–891. doi: 10.1111/jipb.12425

Haider, S., Raza, A., Iqbal, J., Shaukat, M., and Mahmood, T. (2022). Analyzing the regulatory role of heat shock transcription factors in plant heat stress tolerance: a brief appraisal. *Mol. Biol. Rep.* 49, 5771–5785. doi: 10.1007/s11033-022-07190-x

He, F., Chen, H., and Han, R. (2020). The plant cytoskeleton and crosslinking factors. *CellBio* 9, 85. doi: 10.4236/cellbio.2020.92004

Hedhly, A. (2011). Sensitivity of flowering plant gametophytes to temperature fluctuations. *Environ. Exp. Bot.* 74, 9–16. doi: 10.1016/j.envexpbot.2011.03.016

Hein, J. B., and Nilsson, J. (2014). Stable MCC binding to the APC/C is required for a functional spindle assembly checkpoint. *EMBO Rep.* 15, 264–272. doi: 10.1002/embr.201337496

Herrmann, A., Livanos, P., Lipka, E., Gadeyne, A., Hauser, M.-T., Van Damme, D., et al. (2018). Dual localized kinesin-12 POK2 plays multiple roles during cell division and interacts with MAP65-3. *EMBO Rep.* 19, e46085. doi: 10.15252/embr.201846085

Hu, T., Sun, X., Zhang, X., Nevo, E., and Fu, J. (2014). An RNA sequencing transcriptome analysis of the high-temperature stressed tall fescue reveals novel insights into plant thermotolerance. *BMC Genomics* 15, 1147. doi: 10.1186/1471-2164-15-1147

Izawa, D., and Pines, J. (2015). The mitotic checkpoint complex binds a second CDC20 to inhibit active APC/C. *Nature* 517, 631–634. doi: 10.1038/nature13911

Janda, T., Khalil, R., Tajti, J., Pál, M., and Darkó, É. (2019). Responses of young wheat plants to moderate heat stress. *Acta Physiol. Plant* 41, 137. doi: 10.1007/s11738-019-2930-x

Ji, C., Li, H., Chen, L., Xie, M., Wang, F., Chen, Y., et al. (2013). A novel rice bHLH transcription factor, DTD, acts coordinately with TDR in controlling tapetum function and pollen development. *Mol. Plant* 6, 1715–1718. doi: 10.1093/mp/sst046

Jiang, J., Zhang, Z., and Cao, J. (2013). Pollen wall development: the associated enzymes and metabolic pathways. *Plant Biol.* 15, 249–263. doi: 10.1111/j.1438-8677.2012.00706.x

Kagawa, W., and Kurumizaka, H. (2010). From meiosis to postmeiotic events: Uncovering the molecular roles of the meiosis-specific recombinase Dmc1. *FEBS J.* 277, 590–598. doi: 10.1111/j.1742-4658.2009.07503.x

Kaur, J., Sebastian, J., and Siddiqi, I. (2006). The *Arabidopsis-mei2-like* genes play a role in meiosis and vegetative growth in *Arabidopsis*. *Plant Cell* 18, 545–559. doi: 10.1105/tpc.105.039156

Kawabe, A., Matsunaga, S., Nakagawa, K., Kurihara, D., Yoneda, A., Hasezawa, S., et al. (2005). Characterization of plant Aurora kinases during mitosis. *Plant Mol. Biol.* 58, 1–13. doi: 10.1007/s11103-005-3454-x

Kevei, Z., Baloban, M., Ines, O. D., Tiricz, H., Kroll, A., Regulski, K., et al. (2011). Conserved CDC20 cell cycle functions are carried out by two of the five isoforms in *Arabidopsis thaliana*. *PloS One* 6, e20618. doi: 10.1371/journal.pone.0020618

Ko, S.-S., Li, M.-J., Sun-Ben Ku, M., Ho, Y.-C., Lin, Y.-J., Chuang, M.-H., et al. (2014). The bHLH142 transcription factor coordinates with TDR1 to modulate the expression of EAT1 and regulate pollen development in rice. *Plant Cell* 26, 2486–2504. doi: 10.1105/tpc.114.126292

Kost, B., and Chua, N.-H. (2002). The plant cytoskeleton: vacuoles and cell walls make the difference. *Cell* 108, 9–12. doi: 10.1016/S0092-8674(01)00634-1

Krtková, J., Benáková, M., and Schwarzerová, K. (2016). Multifunctional microtubule-associated proteins in plants. *Front. Plant Sci.* 7. doi: 10.3389/fpls.2016.00474

Kumar, S., Jeevaraj, T., Yunus, M. H., Chakraborty, S., and Chakraborty, N. (2023). The plant cytoskeleton takes center stage in abiotic stress responses and resilience. *Plant Cell Environ.* 46, 5–22. doi: 10.1111/pce.14450

Kuo, P., Da Ines, O., and Lambing, C. (2021). Rewiring meiosis for crop improvement. *Front. Plant Sci.* 12. doi: 10.3389/fpls.2021.708948

Kuo, Y.-W., and Howard, J. (2021). Cutting, amplifying, and aligning microtubules with severing enzymes. *Trends Cell Biol.* 31, 50–61. doi: 10.1016/j.tcb.2020.10.004

Laino, P., Shelton, D., Finnie, C., De Leonardis, A. M., Mastrangelo, A. M., Svensson, B., et al. (2010). Comparative proteome analysis of metabolic proteins from seeds of durum wheat (cv. Svevo) subjected to heat stress. *Proteomics* 10, 2359–2368. doi: 10.1002/pmic.200900803

Lambing, C., and Heckmann, S. (2018). Tackling plant meiosis: from model research to crop improvement. *Front. Plant Sci.* 9. doi: 10.3389/fpls.2018.00829

Lara-Gonzalez, P., Pines, J., and Desai, A. (2021). Spindle assembly checkpoint activation and silencing at kinetochores. *Semin. Cell Dev. Biol.* 117, 86–98. doi: 10.1016/j.semcdb.2021.06.009

Lee, Y.-R. J., and Liu, B. (2019). Microtubule nucleation for the assembly of acentrosomal microtubule arrays in plant cells. *New Phytol.* 222, 1705–1718. doi: 10.1111/nph.15705

Lei, X., and Liu, B. (2020). Tapetum-dependent male meiosis progression in plants: increasing evidence emerges. *Front. Plant Sci.* 10. doi: 10.3389/fpls.2019.01667

Lenormand, T., Engelstädter, J., Johnston, S. E., Wijnker, E., and Haag, C. R. (2016). Evolutionary mysteries in meiosis. *Philos. Trans. R. Soc B Biol. Sci.* 371, 20160001. doi: 10.1098/rstb.2016.0001

Lesk, C., Rowhani, P., and Ramankutty, N. (2016). Influence of extreme weather disasters on global crop production. *Nature* 529, 84–87. doi: 10.1038/nature16467

Li, S., Sun, T., and Ren, H. (2015). The functions of the cytoskeleton and associated proteins during mitosis and cytokinesis in plant cells. *Front. Plant Sci.* 6. doi: 10.3389/fpls.2015.00282

Li, H., Sun, B., Sasabe, M., Deng, X., Machida, Y., Lin, H., et al. (2017). *Arabidopsis* MAP65-4 plays a role in phragmoplast microtubule organization and marks the cortical cell division site. *New Phytol.* 215, 187–201. doi: 10.1111/nph.14532

Li, S., Wan, C., Hu, C., Gao, F., Huang, Q., Wang, K., et al. (2012). Mitochondrial mutation impairs cytoplasmic male sterility rice in response to H2O2 stress. *Plant Sci.* 195, 143–150. doi: 10.1016/j.plantsci.2012.05.014

Li, H., Yuan, Z., Vizcay-Barrena, G., Yang, C., Liang, W., Zong, J., et al. (2011). PERSISTENT TAPETAL CELL1 encodes a PHD-finger protein that is required for tapetal cell death and pollen development in rice. *Plant Physiol.* 156, 615–630. doi: 10.1104/pp.111.175760

Lipka, E., Gadeyne, A., Stöckle, D., Zimmermann, S., De Jaeger, G., Ehrhardt, D. W., et al. (2014). The phragmoplast-orienting kinesin-12 class proteins translate the positional information of the preprophase band to establish the cortical division zone in *Arabidopsis* thaliana. *Plant Cell* 26, 2617–2632. doi: 10.1105/tpc.114.124933

Lu, P., Chai, M., Yang, J., Ning, G., Wang, G., and Ma, H. (2014). The *Arabidopsis* CALLOSE DEFECTIVE MICROSPORE1 gene is required for male fertility through regulating callose metabolism during microsporogenesis. *Plant Physiol.* 164, 1893–1904. doi: 10.1104/pp.113.233387

Luo, D., Xu, H., Liu, Z., Guo, J., Li, H., Chen, L., et al. (2013). A detrimental mitochondrial-nuclear interaction causes cytoplasmic male sterility in rice. *Nat. Genet.* 45, 573–577. doi: 10.1038/ng.2570

Maere, S., Heymans, K., and Kuiper, M. (2005). BiNGO: a Cytoscape plugin to assess overrepresentation of gene ontology categories in biological networks. *Bioinformatics* 21, 3448–3449. doi: 10.1093/bioinformatics/bti551

Malerba, M., Crosti, P., and Cerana, R. (2010). Effect of heat stress on actin cytoskeleton and endoplasmic reticulum of tobacco BY-2 cultured cells and its inhibition by Co^{2+}. *Protoplasma* 239, 23–30. doi: 10.1007/s00709-009-0078-z

Marček, T., Hamow, K.Á., Végh, B., Janda, T., and Darko, E. (2019). Metabolic response to drought in six winter wheat genotypes. *PloS One* 14, e0212411. doi: 10.1371/journal.pone.0212411

McAinsh, A. D., and Kops, G. J. P. L. (2023). Principles and dynamics of spindle assembly checkpoint signaling. *Nat. Rev. Mol. Cell Biol.* 24, 543–559. doi: 10.1038/s41580-023-00593-z

Medina, E., Kim, S.-H., Yun, M., and Choi, W.-G. (2021). Recapitulation of the function and role of ROS generated in response to heat stress in plants. *Plants* 10, 371. doi: 10.3390/plants10020371

Motta, M. R., and Schnittger, A. (2021). A microtubule perspective on plant cell division. *Curr. Biol.* 31, R547–R552. doi: 10.1016/j.cub.2021.03.087

Müller, S., Han, S., and Smith, L. G. (2006). Two kinesins are involved in the spatial control of cytokinesis in *Arabidopsis thaliana*. *Curr. Biol.* 16, 888–894. doi: 10.1016/j.cub.2006.03.034

Nakamura, M., Yagi, N., Kato, T., Fujita, S., Kawashima, N., Ehrhardt, D. W., et al. (2012). *Arabidopsis* GCP3-interacting protein 1/MOZART 1 is an integral component of the γ-tubulin-containing microtubule nucleating complex. *Plant J. Cell Mol. Biol.* 71, 216–225. doi: 10.1111/j.1365-313X.2012.04988.x

Navrot, N., Rouhier, N., Gelhaye, E., and Jacquot, J.-P. (2007). Reactive oxygen species generation and antioxidant systems in plant mitochondria. *Physiol. Plant* 129, 185–195. doi: 10.1111/j.1399-3054.2006.00777.x

Niu, B., Wang, L., Zhang, L., Ren, D., Ren, R., Copenhaver, G. P., et al. (2015). *Arabidopsis* cell division cycle 20.1 is required for normal meiotic spindle assembly and chromosome segregation. *Plant Cell* 27, 3367–3382. doi: 10.1105/tpc.15.00834

Niu, N., Liang, W., Yang, X., Jin, W., Wilson, Z. A., Hu, J., et al. (2013). EAT1 promotes tapetal cell death by regulating aspartic proteases during male reproductive development in rice. *Nat. Commun.* 4, 1445. doi: 10.1038/ncomms2396

Omidi, M., Siahpoosh, M. R., Mamghani, R., and Modarresi, M. (2014). The influence of terminal heat stress on meiosis abnormalities in pollen mother cells of wheat. *Cytologia (Tokyo)* 79, 49–58. doi: 10.1508/cytologia.79.49

Oshino, T., Abiko, M., Saito, R., Ichiishi, E., Endo, M., Kawagishi-Kobayashi, M., et al. (2007). Premature progression of anther early developmental programs accompanied by comprehensive alterations in transcription during high-temperature injury in barley plants. *Mol. Genet. Genomics* 278, 31–42. doi: 10.1007/s00438-007-0229-x

Pachauri, R. K., Allen, M. R., Barros, V. R., Broome, J., Cramer, W., Christ, R., et al. (2014). *Climate change 2014: synthesis report. Contribution of working groups I, II and III to the fifth assessment report of the intergovernmental panel on climate change*. Eds. R. K. Pachauri and L.M. Geneva (Switzerland: IPCC). Available at: http://epic.awi.de/37530/.

Paez-Garcia, A., Sparks, J. A., de Bang, L., and Blancaflor, E. B. (2018). "Plant actin cytoskeleton: new functions from old scaffold," in *Concepts in cell biology - history and evolution plant cell monographs*. Eds. V. P. Sahi and F. Baluška (Cham: Springer International Publishing), 103–137. doi: 10.1007/978-3-319-69944-8_6

Peters, J.-M. (2006). The anaphase promoting complex/cyclosome: a machine designed to destroy. *Nat. Rev. Mol. Cell Biol.* 7, 644–656. doi: 10.1038/nrm1988

Poudel, P. B., and Poudel, M. R. (2020). Heat stress effects and tolerance in wheat: A review. *J. Biol. Today's World* 9, 1–6.

Prasad, P. V. V., Boote, K. J., Allen, L. H., Sheehy, J. E., and Thomas, J. M. G. (2006). Species, ecotype and cultivar differences in spikelet fertility and harvest index of rice in response to high temperature stress. *Field Crops Res.* 95, 398–411. doi: 10.1016/j.fcr.2005.04.008

Robinson, M. D., and Oshlack, A. (2010). A scaling normalization method for differential expression analysis of RNA-seq data. *Genome Biol.* 11, R25. doi: 10.1186/gb-2010-11-3-r25

Saini, H., Sedgley, M., and Aspinall, D. (1984). Development anatomy in wheat of male sterility induced by heat stress, water deficit or abscisic acid. *Funct. Plant Biol.* 11, 243–253. doi: 10.1071/PP9840243

Sarkar, S., Islam, A. K. M. A., Barma, N. C. D., and Ahmed, J. U. (2021). Tolerance mechanisms for breeding wheat against heat stress: A review. *S. Afr. J. Bot.* 138, 262–277. doi: 10.1016/j.sajb.2021.01.003

Schrock, M. S., Stromberg, B. R., Scarberry, L., and Summers, M. K. (2020). APC/C ubiquitin ligase: functions and mechanisms in tumorigenesis. *Semin. Cancer Biol.* 67, 80–91. doi: 10.1016/j.semcancer.2020.03.001

Shannon, P., Markiel, A., Ozier, O., Baliga, N. S., Wang, J. T., Ramage, D., et al. (2003). Cytoscape: a software environment for integrated models of biomolecular interaction networks. *Genome Res.* 13, 2498–2504. doi: 10.1101/gr.1239303

Sharma, D., Singh, R., Tiwari, R., Kumar, R., and Gupta, V. K. (2019). "Wheat responses and tolerance to terminal heat stress: A review," in *Wheat production in changing environments: responses, adaptation and tolerance*. Eds. M. Hasanuzzaman, K. Nahar and M. Hossain (Singapore: Springer), 149–173. doi: 10.1007/978-981-13-6883-7_7

Shunmugam, A. S. K., Bollina, V., Dukowic-Schulze, S., Bhowmik, P. K., Ambrose, C., Higgins, J. D., et al. (2018). MeioCapture: an efficient method for staging and isolation of meiocytes in the prophase I sub-stages of meiosis in wheat. *BMC Plant Biol.* 18, 293. doi: 10.1186/s12870-018-1514-z

Smertenko, A., Dráber, P., Viklický, V., and Opatrný, Z. (1997). Heat stress affects the organization of microtubules and cell division in *Nicotiana tabacum* cells. *Plant Cell Environ.* 20, 1534–1542. doi: 10.1046/j.1365-3040.1997.d01-44.x

Smertenko, A., Hewitt, S. L., Jacques, C. N., Kacprzyk, R., Liu, Y., Marcec, M. J., et al. (2018). Phragmoplast microtubule dynamics – a game of zones. *J. Cell Sci.* 131, jcs203331. doi: 10.1242/jcs.203331

Soós, V., Sebestyén, E., Posta, M., Kohout, L., Light, M. E., Van Staden, J., et al. (2012). Molecular aspects of the antagonistic interaction of smoke-derived butenolides on the germination process of Grand Rapids lettuce (*Lactuca sativa*) achenes. *New Phytol.* 196, 1060–1073. doi: 10.1111/j.1469-8137.2012.04358.x

Spitzer, M., Wildenhain, J., Rappsilber, J., and Tyers, M. (2014). BoxPlotR: a web tool for generation of box plots. *Nat. Methods* 11, 121–122. doi: 10.1038/nmeth.2811

Stratonovitch, P., and Semenov, M. A. (2015). Heat tolerance around flowering in wheat identified as a key trait for increased yield potential in Europe under climate change. *J. Exp. Bot.* 66, 3599–3609. doi: 10.1093/jxb/erv070

Sun, Q., Miao, C., Hanel, M., Borthwick, A. G. L., Duan, Q., Ji, D., et al. (2019). Global heat stress on health, wildfires, and agricultural crops under different levels of climate warming. *Environ. Int.* 128, 125–136. doi: 10.1016/j.envint.2019.04.025

Tan, C. H., Gasic, I., Huber-Reggi, S. P., Dudka, D., Barisic, M., Maiato, H., et al. (2015). The equatorial position of the metaphase plate ensures symmetric cell divisions. *eLife* 4, e05124. doi: 10.7554/eLife.05124

Tang, D., Chen, M., Huang, X., Zhang, G., Zeng, L., Zhang, G., et al. (2023). SRplot: A free online platform for data visualization and graphing. *PloS One* 18, e0294236. doi: 10.1371/journal.pone.0294236

Tang, Z., Zhang, L., Yang, D., Zhao, C., and Zheng, Y. (2011). Cold stress contributes to aberrant cytokinesis during male meiosis I in a wheat thermosensitive genic male sterile line. *Plant Cell Environ.* 34, 389–405. doi: 10.1111/j.1365-3040.2010.02250.x

Tischner, T., Kőszegi, B., and Veisz, O. (1997). Climatic programs used in the Martonvásár phytotron most frequently in recent years. *Acta Agron. Hung.* 45, 85–104.

ul Haq, S., Khan, A., Ali, M., Khattak, A. M., Gai, W.-X., Zhang, H.-X., et al. (2019). Heat shock proteins: dynamic biomolecules to counter plant biotic and abiotic stresses. *Int. J.of Mol. Sci.* 20, 5321. doi: 10.3390/ijms20215321

Ullah, A., Nadeem, F., Nawaz, A., Siddique, K. H. M., and Farooq, M. (2022). Heat stress effects on the reproductive physiology and yield of wheat. *J. Agron. Crop Sci.* 208, 1–17. doi: 10.1111/jac.12572

Ur, S. N., and Corbett, K. D. (2021). Architecture and dynamics of meiotic chromosomes. *Annu. Rev. Genet.* 55, 497–526. doi: 10.1146/annurev-genet-071719-020235

Végh, B., Marček, T., Karsai, I., Janda, T., and Darkó, É. (2018). Heat acclimation of photosynthesis in wheat genotypes of different origin. *S. Afr. Bot.* 117, 184–192. doi: 10.1016/j.sajb.2018.05.020

Vos, J. W., Pieuchot, L., Evrard, J.-L., Janski, N., Bergdoll, M., de Ronde, D., et al. (2008). The plant TPX2 protein regulates prospindle assembly before nuclear envelope breakdown. *Plant Cell* 20, 2783–2797. doi: 10.1105/tpc.107.056796

Wang, Y., van Rengs, W. M. J., Zaidan, M. W. A. M., and Underwood, C. J. (2021). Meiosis in crops: from genes to genomes. *J. Exp. Bot.* 72, 6091–6109. doi: 10.1093/jxb/erab217

Wijnker, E., and Schnittger, A. (2013). Control of the meiotic cell division program in plants. *Plant Reprod.* 26, 143–158. doi: 10.1007/s00497-013-0223-x

Xu, T., Zhang, C., Zhou, Q., and Yang, Z.-N. (2016). Pollen wall pattern in *Arabidopsis*. *Sci. Bull.* 61, 832–837. doi: 10.1007/s11434-016-1062-6

Yamada, M., and Goshima, G. (2017). Mitotic spindle assembly in land plants: molecules and mechanisms. *Biology* 6, 6. doi: 10.3390/biology6010006

Yang, X., Ye, J., Zhang, L., and Song, X. (2020). Blocked synthesis of sporopollenin and jasmonic acid leads to pollen wall defects and anther indehiscence in genic male sterile wheat line 4110S at high temperatures. *Funct. Integr. Genomics* 20, 383–396. doi: 10.1007/s10142-019-00722-y

Yao, X., Hu, W., Yang, Z.-N., Yao, X., Hu, W., and Yang, Z.-N. (2022). The contributions of sporophytic tapetum to pollen formation. *Seed Biol.* 1, 1–13. doi: 10.48130/SeedBio-2022-0005

Zamariola, L., Tiang, C. L., De Storme, N., Pawlowski, W., and Geelen, D. (2014). Chromosome segregation in plant meiosis. *Front. Plant Sci.* 5. doi: 10.3389/fpls.2014.00279

Zhang, Z.-B., Zhu, J., Gao, J.-F., Wang, C., Li, H., Li, H., et al. (2007). Transcription factor AtMYB103 is required for anther development by regulating tapetum development, callose dissolution and exine formation in *Arabidopsis*. *Plant J.* 52, 528–538. doi: 10.1111/j.1365-313X.2007.03254.x

Zhu, J., Chen, H., Li, H., Gao, J.-F., Jiang, H., Wang, C., et al. (2008). *Defective in Tapetal Development and Function 1* is essential for anther development and tapetal function for microspore maturation in *Arabidopsis*. *Plant J.* 55, 266–277. doi: 10.1111/j.1365-313X.2008.03500.x

Zhu, T., Wang, L., Rimbert, H., Rodriguez, J. C., Deal, K. R., De Oliveira, R., et al. (2021). Optical maps refine the bread wheat *Triticum aestivum* cv. Chinese Spring genome assembly. *Plant J.* 107, 303–314. doi: 10.1111/tpj.15289

frontiers | Frontiers in Plant Science

TYPE Original Research
PUBLISHED 06 February 2024
DOI 10.3389/fpls.2023.1332414

OPEN ACCESS

EDITED BY
Darren Wong,
Australian National University, Australia

REVIEWED BY
Farah Deeba,
Council of Scientific and Industrial Research (CSIR), India
Attila Fábián,
Hungarian Research Network, Hungary

*CORRESPONDENCE
Zahid Hussain Shah
zahid.uaar578@hotmail.com
Seung Hwan Yang
ymichigan@jnu.ac.kr

RECEIVED 02 November 2023
ACCEPTED 29 December 2023
PUBLISHED 06 February 2024

CITATION
Ding C, Alghabari F, Rauf M, Zhao T, Javed MM, Alshamrani R, Ghazy A-H, Al-Doss AA, Khalid T, Yang SH and Shah ZH (2024) Optimization of soybean physiochemical, agronomic, and genetic responses under varying regimes of day and night temperatures.
Front. Plant Sci. 14:1332414.
doi: 10.3389/fpls.2023.1332414

Optimization of soybean physiochemical, agronomic, and genetic responses under varying regimes of day and night temperatures

Chuanbo Ding[1], Fahad Alghabari[2], Muhammad Rauf[2], Ting Zhao[1], Muhammad Matloob Javed[3], Rahma Alshamrani[1], Abdel-Halim Ghazy[3], Abdullah A. Al-Doss[3], Taimoor Khalid[2], Seung Hwan Yang[4]* and Zahid Hussain Shah[2]*

[1]College of Traditional Chinese Medicine, Jilin Agriculture Science and Technology College, Jilin, China, [2]Department of Plant Breeding and Genetics, Pir Mehr Ali Shah, Arid Agriculture University, Rawalpindi, Pakistan, [3]Department of Plant Production, College of Food and Agriculture Science, King Saud University, Riyadh, Saudi Arabia, [4]Department of Biotechnology, Chonnam National University, Yeosu, Republic of Korea

Soybean is an important oilseed crop worldwide; however, it has a high sensitivity to temperature variation, particularly at the vegetative stage to the pod-filling stage. Temperature change affects physiochemical and genetic traits regulating the soybean agronomic yield. In this regard, the current study aimed to comparatively evaluate the effects of varying regimes of day and night temperatures (T1 = 20°C/12°C, T2 = 25°C/17°C, T3 = 30°C/22°C, T4 = 35°C/27°C, and T5 = 40°C/32°C) on physiological (chlorophyll, photosynthesis, stomatal conductance, transpiration, and membrane damage) biochemical (proline and antioxidant enzymes), genetic (*GmDNJ1*, *GmDREB1G;1*, *GmHSF-34*, *GmPYL21*, *GmPIF4b*, *GmPIP1;6*, *GmGBP1*, *GmHsp90A2*, *GmTIP2;6*, and *GmEF8*), and agronomic traits (pods per plant, seeds per plant, pod weight per plant, and seed yield per plant) of soybean cultivars (Swat-84 and NARC-1). The experiment was performed in soil plant atmosphere research (SPAR) units using two factorial arrangements with cultivars as one factor and temperature treatments as another factor. A significant increase in physiological, biochemical, and agronomic traits with increased gene expression was observed in both soybean cultivars at T4 (35°C/27°C) as compared to below and above regimes of temperatures. Additionally, it was established by correlation, principal component analysis (PCA), and heatmap analysis that the nature of soybean cultivars and the type of temperature treatments have a significant impact on the paired association of agronomic and biochemical traits, which in turn affects agronomic productivity. Furthermore, at corresponding temperature regimes, the expression of the genes matched the expression of physiochemical traits.

The current study has demonstrated through extensive physiochemical, genetic, and biochemical analyses that the ideal day and night temperature for soybeans is T4 (35°C/27°C), with a small variation having a significant impact on productivity from the vegetative stage to the grain-filling stage.

KEYWORDS

antioxidant, correlogram, gene expression, heat stress, principal component analysis, soybean

1 Introduction

Soybean (*Glycine max* L.) is an important legume crop providing approximately 29% of the oil and 71% of protein for humans and livestock in the world (Alsajri et al., 2022). With the sudden rise of the world population, there is a need to keep the pace of soybean production compatible with human demand under changing climatic conditions (Raza et al., 2019). Among projected climatic changes, the temperature is reported to have more adverse effects on main crops, such as soybeans (Osei et al., 2023). The average annual temperatures of regions producing wheat, rice, corn, and soybean have increased by 1°C during the past century (Zhao et al., 2017). Climate modeling experts forecast that the 21st century will witness a rise of temperatures by 1°C–4°C depending upon the region (Fahad et al., 2017). The coincidence of high temperature with flowering and grain-filling stages causes a severe reduction in yield due to the impairment of physiological processes (Alsajri et al., 2019). Furthermore, high temperatures trigger oxidative stress due to the generation of reactive oxygen species (ROS) (Sachdev et al., 2021). Plants like other living systems tend to retain their homeostatic balance (Awasthi et al., 2015). Therefore, plants activate ROS scavenging mechanisms by enhancing the activities of antioxidant enzymes such as peroxidase (POD), catalase (CAT), and superoxide dismutase (SOD) (Rajput et al., 2021). Additionally, a high concentration of ROS impairs the structural integrity of the cell membrane, resulting in membrane damage and less water retentively due to more electrolyte leakage (Jianing et al., 2022). With every 0.8°C rise above the mean temperature, soybean yield is projected to decrease by 2.4% (Djanaguiraman et al., 2019). Hence, it is mandatory to understand the responses of soybeans to temperature variations for devising mitigation strategies. Although a rise in temperature impacts adversely the soybean reproductive phase and seed formation, the effect of temperature changes varies with extent, the period, and cultivars (Djanaguiraman et al., 2019). It has been projected that soybean production decreased by 17% with every 1°C rise in temperature above optimum in soybean-growing regions (Yang et al., 2023). In addition, the rise of temperature above optimum significantly decreases agronomic yield such as pods per plant, seed size, seed number, and seed yield in soybeans (Choi et al., 2016). Likewise, reproductive and grain-filling stages, biochemical, and physiological activities are also highly susceptible to high temperatures. Photosynthesis is among the primary cell events that are highly prone to high-temperature stress and are impaired on priority before the inhibition of other events (Mathur et al., 2014). The foremost target site of high temperature is photosystem II (PSII), which is an integral part of chlorophyll (Sasi et al., 2018). Therefore, reduction in chlorophyll content and disruption of chloroplast function lead to decreased photosynthesis and crop productivity. With every 4°C rise in temperature up to optimum, soybean shows a 59% increase in net photosynthesis (Alsajri et al., 2022). Additionally, there is a 17% drop in net photosynthesis when the temperature is raised by the same percentage above the optimal level (Ortiz et al., 2022). Plant responses to environmental stresses are genetically regulated; therefore, it is important to elucidate the relative expression of temperature stress-associated genes under varying regimes of temperatures. Heat shock proteins (HSPs) play an essential role in providing tolerance against biotic and abiotic stresses. In addition, HSPs increase the scavenging of ROS by positively regulating the antioxidant enzymes and enhancing membrane stability (Ul-Haq et al., 2019). For instance, Huang et al. (2019) noticed that the overexpression of soybean gene *GmHsp90A2* under high temperatures is associated with a decrease in oxidative stress and high chlorophyll content. Similarly, *GmDNJ1*, a type of HSP-40, also regulates the antioxidant enzymes and chlorophyll under heat stress as reported by Li et al. (2021). The dehydration-responsive element-binding protein (DREB) regulates the expression of the pyrabactin resistance 1-like (PYL) gene that enables plants to retain normal physiological and biochemical activities under the increasing regime of temperatures (Kidokoro et al., 2015). Moreover, Di et al. (2018) identified 14 PYL genes in *Brassica napus* that play vital roles in ABA signaling during different regimes of heat stress. In fact, heat stress raises endogenous ABA content that keeps water balanced and increases heat tolerance by regulating stomatal conductance (Hsieh et al., 2013). Additionally, the phytochrome interacting factor 4 (PIF4) mediates physiological and molecular processes in soybean by regulating the HSPs and transcripts of heat shock factors (HSP) (Arya et al., 2023). The HSF proteins increase plants' endurance to heat stress and enable plants to retain their essential metabolic activities under heat stress (Li et al., 2014). The overexpression of soybean plasma membrane intrinsic protein 1;6 (*GmPIP1;6*) during heat stress optimizes the physiological processes and agronomic yield (Zhou et al., 2014). Moreover,

tonoplast intrinsic proteins (TIPs) are also responsible for regulating the movement of water and the molecules of physiological significance; hence, they facilitate plants to sustain essential physio-chemical processes during abiotic stress (Kapilan et al., 2018). Likewise, in another study, Feng et al. (2019) reported that gene *GmTIP2;6* enhances plant growth under heat stress by modulating the activities of some essential proteins. Correspondingly, the gibberellic acid myeloblastosis (GAMYB)-binding protein (GBP) is an important gene of the GA pathway and encodes a gibberellin-induced regulatory protein that is involved in plant reproductive development (Bienias et al., 2020). Moreover, GBP plays a vital role in plant growth, cell differentiation, physiological processes, secondary metabolism, and tolerance to abiotic stress (Zhang et al., 2020). For instance, the gene *GmGBP1* depicts positive upregulation with the increasing regime of heat stress, enables tolerance to heat stress, and sustains soybean normal growth activities (Zhao et al., 2013). The elongation factor (EF) gene *GmEF8* enhances protein levels when soybean faces temperature stress and has a protective role *via* osmotic adjustments (Zhang et al., 2022). Soybean plants with high tolerance to temperature stress show a high transcript level of *GmEF8* with high proline content as compared to plants grown under control conditions (Jianing et al., 2022). The understanding of genetic responses under varying levels of temperature provides a foundation to further understand the temperature response pathway (Jianing et al., 2022). Tariq et al. (2022) performed transcriptome analysis of soybean genotypes NARC-1 and Swat-84 under the same conditions within a glass house; however, the detailed genetic analysis in association with physiological, biochemical, and morphological traits is lacking. Additionally, soybean is a temperature-sensitive crop; therefore, we comprehensively evaluated soybean genotypes at varying regimes of day and night temperatures by focusing on physiological, biochemical, agronomic, and genetic indices. Temperature directly affects the genetic, physiological, and biochemical traits of soybeans, which are ultimate determinants of agronomic productivity. In this context, the current study aimed to investigate the impacts of varying regimes of temperature on the genetic, physiological, biochemical, and agronomic traits of soybean cultivars (NARC-1 and Swat-84). Furthermore, the current study aimed to know how physiological, biochemical, and genetic traits are interconnected to determine the agronomic productivity of soybean cultivars.

2 Materials and methods

The present study was performed in soil plant atmosphere research (SPAR) units located at the experimental area of Jilin Agricultural Science and Technology Center, Jilin, China. Two soybean cultivars, the thermosensitive Swat-84, released in 1984 by the Agricultural Research Institute, Swat Pakistan (Asad et al., 2020), and the thermotolerant NARC-1, released in 1991 by National Agricultural Research Center, Islamabad, Pakistan (Asad et al., 2020), were evaluated at five different regimes of day/night temperatures (T1 = 20°C/12°C, T2 = 25°C/17°C, T3 = 30°C/22°C, T4 = 35°C/27°C, and T5 = 40°C/32°C), which were obtained *via* thermo-static adjustments of the five SPAR units (Alsajri et al., 2020). The tri-replicate experiment was conducted in a two-factorial design, with cultivars as one factor and temperature as the other factor.

2.1 Plant growth and temperature treatment

The temperature during the day was applied at sunrise, while the temperature during the night was applied after sunset. Seeds were sown at 2-cm depth in a plastic container having a diameter of 30 cm and a height of 50 cm. The pots were supplemented with gravel at the bottom and filled with a 3:1 mixture of topsoil and sand. Additionally, plants were fertilized with Hoagland nutrient solution using an automated drip irrigation system every day at 7:00 a.m., 12:00 a.m., and 5 p.m. Furthermore, solar radiations were recorded regularly using a pyranometer. Moreover, temperature treatments were applied starting at the vegetative stage V3-Vn (Purcell et al., 2014) and continued till the seed-setting stage R5 (Purcell et al., 2014). For each treatment in a replicate, five pots each containing three plants were used.

2.2 Physiological quantification

The chlorophyll (Chl) content was determined using the SPAD-502Plus (Konica Minolta, Langenhagen, Germany) from three different leaves of each plant, and data were recorded as average. Furthermore, the IRGA apparatus (ADC Bioscientific, Hoddesdon, UK) was used to record stomatal conductance (Gs), photosynthesis rate (Pn), and transpiration rate (Tr) from soybean leaves between 8:00 a.m. and 10:00 a.m. Moreover, the cell membrane damage (MD) was measured following the procedure used by Sairam et al. (1997). To measure MD, two test tubes each with 20 mL of deionized water were used, and 100 mg of soybean leaf pieces was placed in each tube. One tube was put in the water bath at 40°C for 30 min to record conductivity A, and a second tube was put in a water bath at 100°C for 10 min to record conductivity B. Afterward, the MD was calculated using relation $[1 - (A/B)] \times 100$. For physiological assessments, the data for each treatment were collected from randomly selected five plants on a weekly basis from the start to the end of treatment. The data for each treatment were averaged for statistical analysis. Additionally, the results showing the significant variation at the R5 stage were only included for analysis.

2.3 Biochemical quantification

For the assay of antioxidant enzymes, 1 g of frozen leaves was homogenously mixed in 1 mL of ice-cold 0.1 M Tris-HCl buffer with pH 7.4. Afterward, the mixture was centrifuged at 20,000 *g* and 4°C for 15 min, and the supernatant was extracted to record the enzymatic activity following the procedure opted by Djanaguiraman et al. (2018). The SOD activity was estimated using the SOD assay kit (Cell Biolabs, San Diego, CA, USA) following the

instructions provided by the manufacturer. Correspondingly, the CAT activity was estimated using the CAT assay kit (Cell Biolabs, USA) according to the manufacturer's instructions. Likewise, the POD assay kit (Cell Biolabs, USA) was used for the estimation of POD activity following the manufacturer's protocol. Meanwhile, proline content was measured using a UV-Vis spectrophotometer (Konica Minolta, Langenhagen, Germany) based on ninhydrin reactivity. For the measurement of biochemical traits, the data for each treatment in a replicate were taken from randomly selected five plants on a weekly basis from the start till the end of temperature treatments. Afterward, the data for each treatment were averaged for analysis. Additionally, the results illustrating significant variation at the R5 stage were only included in the analysis.

2.4 Measurement of agronomic characters

The agronomic characters, pods per plant (PPP), and seeds per plant (SPP) from randomly selected five plants of each treatment were counted and averaged for statistical analysis. Correspondingly, pod weight per plant (PWPP) and seed yield per plant (SYPP) from randomly selected plants of each treatment were measured using weighing balance and averaged afterward for statistical analysis.

2.5 Gene relative expression analysis

The genes *GmDNJ1*, *GmDREB1*, *GmHSF-34*, *GmPYL21*, *GmPIF4b*, *GmPIP1;6*, *GmGBP1*, *GmHsp90A2*, *GmTIP2;6*, and *GmEF8* were relatively analyzed at R5 stage for their expression. For relative gene expression, RNA was extracted from selected leaf samples of soybean genotypes (Swat-84 and NARC-1) exposed to varying regimes of day and night temperatures (T1 = 20°C/12°C, T2 = 25°C/17°C, T3 = 30°C/22°C, T4 = 35°C/27°C, and T5 = 40°C/32°C) by using an RNA extraction kit (Cell Biolabs, USA). Afterward, the cDNA library was established according to Ding et al. (2020). For this purpose, 2 µg of RNA sample was used, and qRT-PCR was performed according to the cited procedure. In addition, the relative gene expression was normalized by the *GmActin* gene. The sequences of primers are indicated in Table 1.

2.6 Data analysis

Analysis of variance (ANOVA) at a 5% probability level was applied to analyze the data statistically. For this purpose, Statistix ver. 8.1 (McGraw-Hill, 2008) was used. Furthermore, correlation, principal component analysis (PCA), and heatmap cluster analysis were carried out using RStudio version 1.1.456 (RStudio Team, 2020). For PCA, "factoextra" and "FactoMineR" R packages were used. Pearson's correlation was performed using R packages "GGally" and "ggplot2", and heatmap cluster analysis was performed using "pheatmap" and complex Heatmap R packages.

3 Results

3.1 Physiological traits

All physiological traits including chlorophyll (Chl), stomatal conductance (Gs), photosynthesis rate (Pn), transpiration rate (Tr), and MD varied significantly ($p \leq 0.05$) with varying regimes of day

TABLE 1 List of primers used for relative expression of genes under changing regimes of temperatures.

Gene	Accession no.	Primer sequence
GmDNJ1	Glyma.12G095700	TAAGACATCTTGGCCCATCC (F) CACAACCTTCTCTCCCTTGC (R)
GmDREB1G;1	Glyma.14G084700	CAACTCCAAAGGGAGGGTTCC (F) CAAAAGAACCTTTCAGAACCTCCTTC (R)
GmPYL21	Glyma.13g29380	TGAGGTGGTTTCAAGCTGTCA (F) GCCTACAAAGGAATCGAATCAATC (R)
GmHSF-34	Glyma.17g34540	ACTTACAGAAGGCACAGAGGA (F) ACACTTGTTTCAGTTCAGGGA (R)
GmPIF4b	Glyma.14G032200.1	CTGTGGCAGCAGTCATATCC (F) TCTGATTTTCCTTTGTCACTCC (R)
GmPIP1;6	Glyma.08G015300	AACTATGAGTTGTTCAAAGGA (F) AGAAAACGGTGTAGACAAGAAC (R)
GmHsp90A2	Glyma.14g40320	CTGTTTTGTGTTCTAACAATGGCT (F) GATTTGTAACTTATTCTATGAGGGCA (R)
GmGBP1	Glyma.01G008600v4	TGAGAAATAAAAGTGGATAGGAAAAG (F) TGGAAGATATAATATATGAGGGAGGA (R)
GmTIP2;6	Glyma.15G018100	CACTGGCTATGACACTCCTATTC (F) ACACCGTGTACACTAATCCAAA (R)
GmEF8	Glyma.19G052400	GGCTGATTGTGCTGTCCTT (F) GGTAGTGGCATCCATCTTGTTA (R)

10.3389/fpls.2023.1332414

and night temperatures (Figure 1). The chlorophyll (Chl), photosynthesis rate (Pn), and stomatal conductance (Gs) illustrated a steady increase from temperature regimes T1 (20°C/12°C) to T4 (35°C/27°C) with a sudden decrease at regime T5 in both soybean cultivars Swat-84 and NARC-1 (Figure 1). However, at the same regimes of day and night temperatures, NARC-1 recorded higher Chl, Pn, and Gs values as compared to Swat-84 (Figure 1). Moreover, at T1 (20°C/12°C), these traits showed minimum mean values in Swat-84 (Chl = 16 g/kg, Gs = 700 mmol m^{-2} s^{-1}, and Pn = 20 µmol m^{-2} s^{-1}) and NARC-1 (Chl = 20 g/kg, Gs = 750 mmol m^{-2} s^{-1}, and Pn = 25 µmol m^{-2} s^{-1}) and maximum mean values at T4 (35°C/27°C) in both Swat-84 (Chl = 30 g/kg, Gs = 800 mmol m^{-2} s^{-1}, and Pn = 30 µmol m^{-2} s^{-1}) and NARC-1 (Chl = 35 g/kg, Gs = 850 mmol m^{-2} s^{-1}, and Pn = 38 µmol m^{-2} s^{-1}). In contrast, Tr and MD depicted consistently dramatic increases in both cultivars with increasing day and night temperature regimes T1 (20°C/12°C) to T5 (40°C/32°C) (Figure 1). Additionally, MD and Tr depicted minimum values at

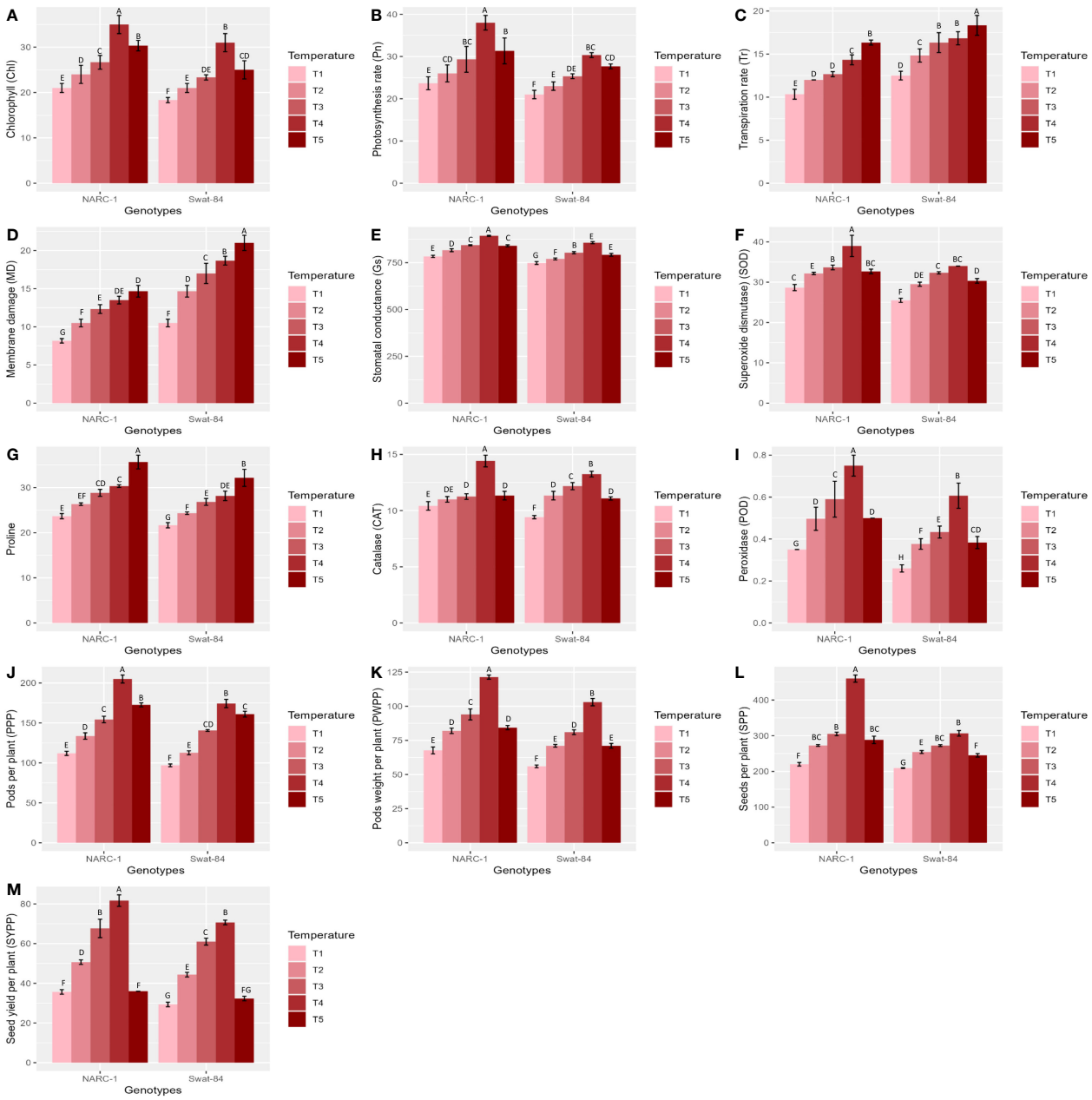

FIGURE 1
(A–M) Effect of varying regimes of day and night temperatures on physiological, biochemical, and agronomic traits of soybean cultivars. Chl, chlorophyll; CAT, catalase; Gs, stomatal conductance; MD, membrane damage; Pn, photosynthesis; POD, peroxidase; PPP, pods per plant; PWPP, pods weight per plant; SOD, superoxide dismutase; SPP, seeds per plant; SYPP, seed yield per plant; Tr, transpiration rate. T1 = 20°C/12°C, T2 = 25°C/17°C, T3 = 30°C/22°C, T4 = 35°C/27°C, and T5 = 40°C/32°C. Values in figures are mean estimates averaged at R5 stage of soybean development, bars show standard deviation (± SD), and letters represent significant differences at $p \leq 0.05$. Units: Gs (mmol m^{-2} s^{-1}); Pn (µmol m^{-2} s^{-1}); Tr (mmol m^{-2} s^{-1}); Chl (g/kg); POD, CAT, and CAT activities (enzyme units); proline (µg/g FW); MD (%); PWPP (g); SYPP (g).

10.3389/fpls.2023.1332414

T1 (20°C/12°C) in Swat-84 (MD = 10% and Tr = 13 mmol m^{-2} s^{-1}) and NARC-1 (MD = 8% and Tr = 10 mmol m^{-2} s^{-1}) and maximum mean values in both Swat-84 (MD = 20%, Tr = 19 mmol m^{-2} s^{-1}) and NARC-1 (MD = 15% and Tr = 17 mmol m^{-2} s^{-1}) at T5 (40°C/32°C). Contrary to Chl, Pn, and Gs, the Tr and MD recorded higher values in Swat-84 as compared to NARC-1 at corresponding regimes of day and night temperatures (Figure 1).

3.2 Biochemical traits

The activity of all biochemical traits including antioxidant enzymes (SOD, CAT, and POD) and proline varied significantly ($p \leq 0.05$) under varying regimes of day and night temperatures (Figure 1). The activity of antioxidant enzymes in terms of enzyme unit increased consistently from T1 (20°C/12°C) to T4 (35°C/27°C) and decreased afterward at T5 (40°C/32°C) in both cultivars (Figure 1). However, as compared to Swat-84, the cultivar NARC-1 revealed the maximum activities of antioxidant enzymes at the same regimes of temperatures (Figure 1). Furthermore, at T1 (20°C/12°C), the enzymes SOD, CAT, and POD illustrated the minimum activities in both genotypes Swat-84 (SOD = 28, CAT = 8, and POD = 0.2) and NARC-1 (SOD = 28, CAT = 8, and POD = 0.4) and the maximum mean values at T4 (35°C/27°C) in both Swat-84 (SOD = 35, CAT = 12, and POD = 0.6) and NARC-1 (SOD = 39, CAT = 14, and POD = 0.7). However, the concentration of proline depicted a significant ($p \leq 0.05$) consistent increase in both cultivars with increasing regimes of temperatures from T1 (20°C/12°C) to T5 (40°C/32°C) (Figure 1). Moreover, at corresponding regimes of temperature, the soybean cultivar NARC-1 showed higher proline content as compared to Swat-84 (Figure 1). Additionally, proline showed the minimum value at T1 (20°C/12°C) in Swat-84 (proline = 20 µg/g FW) and NARC-1 (proline = 25 µg/g FW) and the maximum mean value in both Swat-84 (proline = 30 µg/g FW) and NARC-1 (proline = 35 µg/g FW) at T5 (40°C/32°C).

3.3 Agronomic traits

All agronomic traits such as PPP, PWPP, SPP, and SYPP varied significantly ($p \leq 0.05$) due to varying regimes of day and night temperatures (Figure 1). All agronomic traits manifested a consistent increase in both soybean cultivars from temperature regimes T1 (20°C/12°C) to T4 (35°C/27°C) with a sudden decline at T5 (40°C/32°C) (Figure 1). However, under corresponding regimes of temperatures, NARC-1 showed comparatively high values of PPP, PWPP, SPP, and SYPP as compared to Swat-84 (Figure 1). Additionally, at T1 (20°C/12°C), the agronomic traits recorded minimum values in soybean genotypes, Swat-84 (PPP = 90, PWPP = 50 g, SPP = 200, and SYPP = 30 g) and NARC-1 (PPP = 110, PWPP = 70 g, SPP = 210, and SYPP = 38 g) and maximum mean values at T4 (35°C/27°C) in Swat-84 (PPP = 180, PWPP = 105 g, SPP = 310, and SYPP = 60 g) and NARC-1 (PPP = 210, PWPP = 125 g, SPP = 450, and SYPP = 85 g).

3.4 Correlation, principal component analysis, and heatmap analysis

All traits showed a significant degree of paired association in a positive direction according to correlation analysis, with correlation coefficients ranging from 0.196 to 0.978 (Figure 2). Among physiological traits, Chl illustrated significantly high paired association with Pn, Gs, SOD, CAT, POD, PPP, PWPP, SPP, and SYPP excluding Tr, MD, and pro-line. In contrast, Tr, MD, and proline showed weak and non-significant associations with all biochemical, physiological, and agronomic traits (Figure 2). Additionally, except for Tr, MD, and proline, the activities of antioxidant enzymes (SOD, POD, and CAT) demonstrated a significant paired association with Chl, Pn, Gs, PWPP, SPP, and SYPP (Figure 2). Furthermore, all agronomic traits such as PPP, PWPP, SPP, and SYPP depicted strong correlations among themselves. Additionally, PCA showed varying dispersion of physiochemical and agronomic traits from biplot origin due to changing regimes of temperature that explicated changing expression and association pattern of traits due to variation of temperature (Figure 3). Furthermore, both genotypes showed a comparative difference in the orientation of trait clusters in the PCA graph under corresponding regimes of temperature that indicated the differential physiochemical responses of each genotype (Figure 4). Different cultivars of soybeans responded differently to applied temperature regimes, as demonstrated by PCA. In terms of the paired association of traits at T1, T2, T3, and T5, the genotype Swat-84 of the thermosensitive soybean showed a negative deviation (Figures 3, 4). At the temperature T4, Swat-84 demonstrated a greater positive influence on the paired association of trait variables. The high dispersion of Swat-84 from the biplot origin further supports its high-rated sensitivity against varying temperature regimes (Figures 3, 4). Conversely, at T1, the thermotolerant cultivar NARC-1 solely displayed a negative deviation concerning its origin, whereas, in the remaining temperature regimes, it demonstrated a positive influence on the trait-variable association (Figures 3, 4). Additionally, at T4, NARC-1 had a significant effect on paired association. Overall, the close distribution of NARC-1 to the biplot origin at varying temperature regimes confirmed its tolerance against varying temperature regimes (Figures 3, 4). Additionally, heatmap analysis further validated the results from PCA by grouping the traits into various clusters because of variations in the strength of their association with genotypes as well as with different day and night temperature regimes (Figure 5).

3.5 Relative expression analysis

The relative expression of genes *GmDNJ1*, *GmDREB1G;1*, *GmHSF-34*, *GmPLY21*, *GmPIF4b*, *GmPIP1;6*, *GmGBP1*, *GmHsp90A2*, *GmTIP2;6*, and *GmEF8* showed significant ($p \leq 0.05$) change with changing regimes of day and night temperatures (Figure 6). The transcript levels of *GmDNJ1*, *GmDREB1G;1GmPLY21*, and *GmPIF4b*

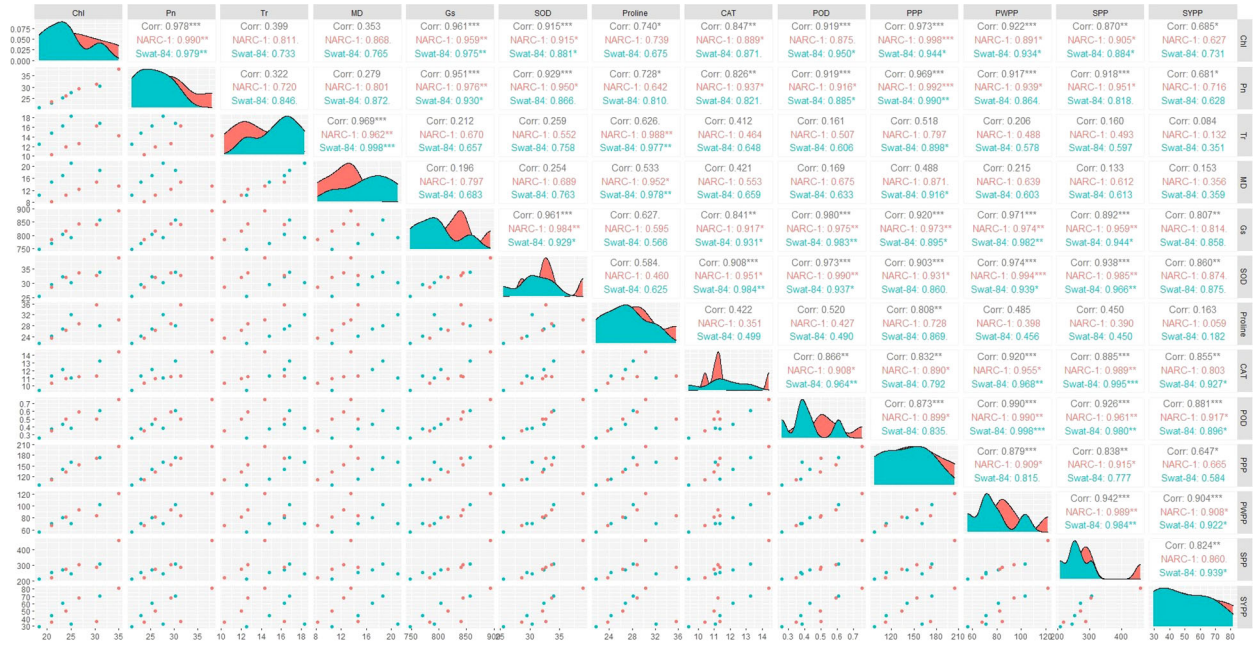

FIGURE 2
Correlogram showing the extent of overall paired association between physiological, biochemical, and agronomic traits in soybean cultivars due to varying regimes of temperature. Chl, chlorophyll; CAT, catalase; Gs, stomatal conductance; MD, membrane damage; Pn, photosynthesis; POD, peroxidase; PPP, pods per plant; PWPP, pods weight per plant; SOD, superoxide dismutase; SPP, seeds per plant; SYPP, seed yield per plant; Tr, transpiration rate. ***, Significant at $p \leq 0.001$; **, Significant at $p \leq 0.01$; *, Significant at $p \leq 0.05$.

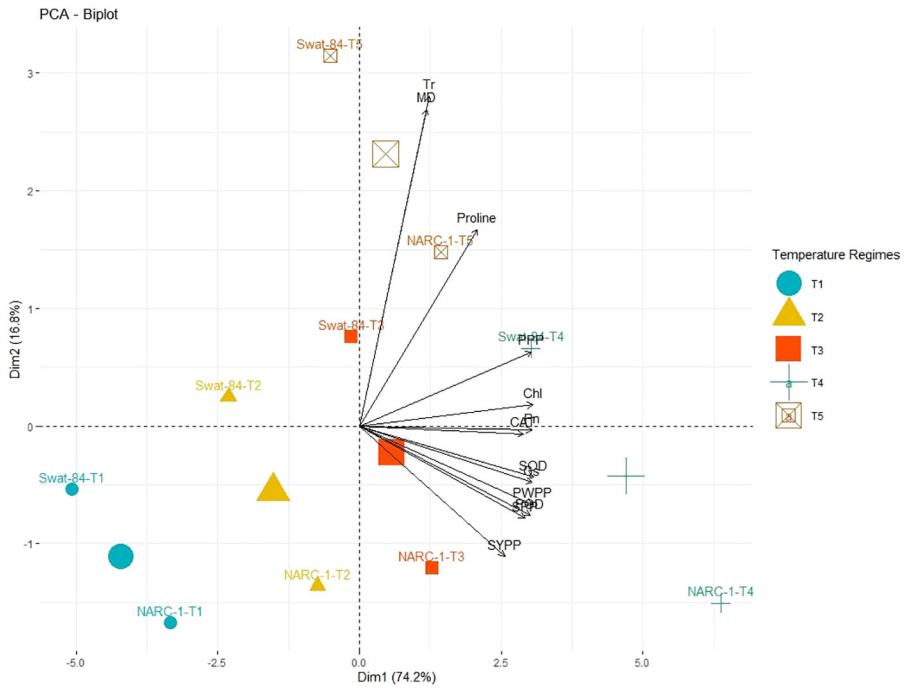

FIGURE 3
Principal component analysis (PCA) biplot of physiological, biochemical, and agronomic parameters grouped concerning their similarity and dissimilarity at varying regimes of day and night temperature. The varying lengths of vectors for origin indicate differential association with treatments, while the closeness of vectors indicates their strong association. The varying orientations of temperature regimes on biplots indicate that each treatment exhibits a different impact on trait association and expression. Chl, chlorophyll; CAT, catalase; Gs, stomatal conductance; MD, membrane damage; Pn, photosynthesis; POD, peroxidase; PPP, pods per plant; PWPP, pods weight per plant; SOD, superoxide dismutase; SPP, seeds per plant; SYPP, seed yield per plant; Tr, transpiration rate. T1 = 20°C/12°C, T2 = 25°C/17°C, T3 = 30°C/22°C, T4 = 35°C/27°C, and T5 = 40°C/32°C.

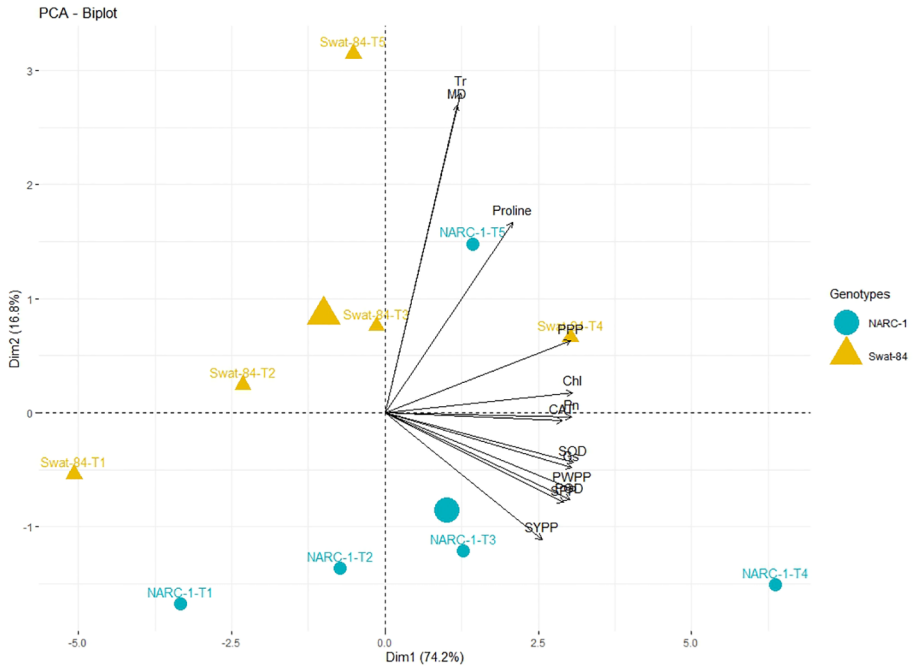

FIGURE 4
Principal component analysis (PCA) biplot of physiological, biochemical, and agronomic parameters grouped with respect to soybean cultivars based upon their similarity and dissimilarity. The varying lengths of vectors for origin indicate differential association with treatments, while the closeness of vectors indicates their strong association. The varying orientations of the cultivars on biplots indicate that each genotype exhibits a different impact on trait association and expression. Chl, chlorophyll; CAT, catalase; Gs, stomatal conductance; MD, membrane damage; Pn, photosynthesis; POD, peroxidase; PPP, pods per plant; PWPP, pods weight per plant; SOD, superoxide dismutase; SPP, seeds per plant; SYPP, seed yield per plant; Tr, transpiration rate.

significantly increased from T1 (20°C/12°C) to T4 (35°C/27°C) and dropped dramatically at T5 (40°C/32°C) in both soybean cultivars (Figure 6). The relative expression of growth-mediating gene *GmGBP1* increased significantly ($p \leq 0.05$) from T1 (20°C/12°C) to T4 (35°C/27°C) and declined suddenly at T5 (40°C/32°C) in both soybean cultivars Swat-84 and NARC-1 (Figure 6). Correspondingly, *GmHsp90A2* recorded significantly ($p \leq 0.05$) increasing relative expression from T1 (20°C/12°C) to T4 (35°C/27°C), which decreased dramatically at T5 (40°C/32°C) in both soybean cultivars (Figure 6). The gene *GmTIP2;6* illustrated significantly ($p \leq 0.05$) high upregulation at T2 (25°C/17°C) and T4 (35°C/27°C) and low expression at T1 (20°C/12°C), T3 (30°C/22°C), and T5 (40°C/32°C) in both soybean cultivars (Figure 6). Conversely, the relative expression of genes *GmHSF-34*, *GmPIP1;6*, and *GmEF8* increased significantly ($p \leq 0.05$) with increasing regimes of day and night temperatures from T1 (20°C/12°C) to T5 (40°C/32°C) in both soybean cultivars (Figure 6). Overall, the relative expression of all genes was higher in NARC-1 as compared to Swat-84 at all corresponding regimes of temperatures (Figure 6). Overall, the overexpression of all genes was consistent with increased activities of antioxidant enzymes (SOD, POD, and CAT), proline content, and physiological traits (Chl, Gs, and Pn) as shown in Figure 7.

4 Discussion

The current study was performed to assess the impact of varying regimes of day and night temperatures on the physiochemical, genetic, and agronomic traits of soybean cultivars. Like any other living organism, plants are equipped with the tendency to respond to their metrological environment (Raza et al., 2019). In this context, temperature is an eminent environmental factor regulating plant physiochemical processes both directly and indirectly (Osei et al., 2023). The optimum temperature is a prerequisite to regulate the plant's essential physiological processes including chlorophyll biosynthesis, Pn, Gs, and Tr (Muhammad et al., 2021). Photosynthetic machinery in leaves is a tentatively logical place to begin particularly when speculating the effects of temperature on crop photosynthesis, as various steps of photosynthesis are highly temperature-dependent (Moore et al., 2021). From a biochemical perspective, CO_2 assimilation is determined by the activation and efficiency of the enzyme Rubisco at ambient temperature (Muhammad et al., 2021). Additionally, enhanced enzymatic activity till optimum temperature triggers the function of the photosystem due to an increase in chlorophyll biosynthesis (Moore et al., 2021). However, temperatures beyond the optimum impede the function of the photosystem and hamper the Rubisco activation in addition to the decrease in chlorophyll content, which collectively result in a substantial reduction in Pn and CO_2 assimilation in soybean as reviewed by Herritt and Fritschi (2020). Consistent with these findings, the current study reported a significant decline in chlorophyll content and Pn below and beyond the ambient regime of the temperature T4 (35°C/27°C) (Figure 1). In contrast, stomatal behavior is significantly important to control the gaseous exchange between plant interior and atmosphere (Driesen et al., 2020).

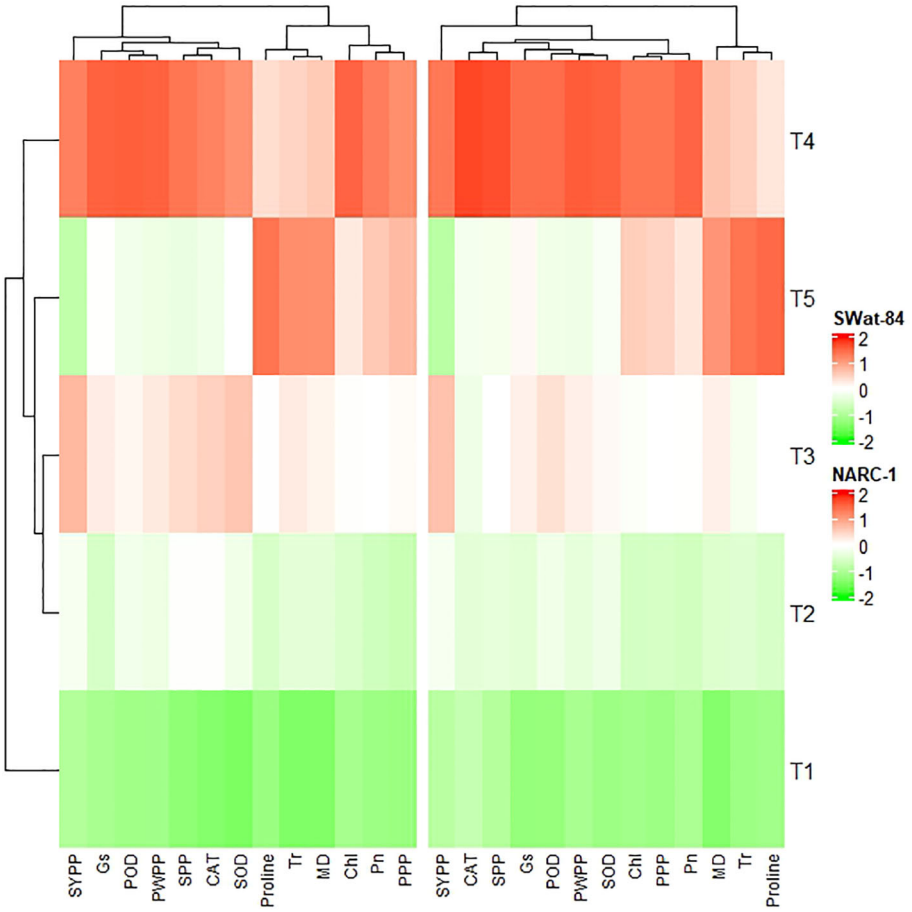

FIGURE 5
Heatmap cluster analysis depicting the differential impacts of varying regimes of day and night temperatures on the extent of expression of physiological, biochemical, and agronomic traits in two different soybean cultivars, Swat-84 (left) and NARC-1 (right). Chl, chlorophyll; CAT, catalase; Gs, stomatal conductance; MD, membrane damage; Pn, photosynthesis; POD, peroxidase; PPP, pods per plant; PWPP, pods weight per plant; SOD, superoxide dismutase; SPP, seeds per plant; SYPP, seed yield per plant; Tr, transpiration rate. T1 = 20°C/12°C, T2 = 25°C/17°C, T3 = 30°C/22°C, T4 = 35°C/27°C, and T5 = 40°C/32°C.

Moreover, Gs is imperative for CO_2 uptake and leaf water Tr in addition to an indicator of increased Pn (Xu et al., 2016). The tendency of plants to sustain Gs, Tr, and Pn under wide ranges of temperature is directly correlated with their potential to tolerate wide regimes of temperatures (Driesen et al., 2020). The decline in chlorophyll pigment below or beyond the ambient temperature is respectively a consequence of the decline in Chl synthase activity and peroxidation of chloroplast and thylakoid membrane (Hasanuzzaman et al., 2013). Furthermore, Alsajri et al. (2019) and Djanaguiraman et al. (2019) respectively evaluated the effect of specific and varying regimes of day and night temperatures on physiological and agronomic traits of soybean and found a strong relation between chlorophyll, Gs, Pn, and yield-related traits. The Gs is a measure of stomata opening, which determines the uptake of CO_2 and release of water vapors (Farquhar and Sharkey, 1982). Interestingly the stomatal Gs was maximum at T4 (35°C/27°C), while Tr was maximum at T5 (40°C/32°C) (Figure 1). This was probably due to the robust CO_2 fixation at T4 (35°C/27°C) as confirmed by the maximum rate of Pn at this temperature. Furthermore, at T4 (35°C/27°C), the CO_2 fixation contributed maximally to Gs as compared to Tr. Moreover, temperature above optimum results in decreased membrane stability and enhanced Tr (Jianing et al., 2022). This reflects that all these processes strongly adhere to and are affected by the temperature as a unit as indicated in Figures 2, 3. In contrast, a consistent increase in temperature enhances the level of ROS in plant cellular systems, inducing lipid peroxidation in cell membranes that disrupts the structural integrity of the membranes (Awasthi et al., 2015). An increase in membrane damage leads to the inhibition of plant vital physiological processes including Pn. However, plants are not passive entities; instead, they respond actively to metrological factors intended to perturb plant homeostasis. In this way, the increasing regimes of temperature trigger the activities of antioxidant enzymes that are actively involved in cellular homeostasis and ROS scavenging (Rajput et al., 2021). Siebers et al. (2015) noticed that the activities of CAT, SOD, and POX increase in soybean due to oxidative stress caused by high temperatures. Consistent with these findings, the current study reported a dynamic increase in the activities of antioxidant enzymes with increasing regimes of temperatures from T1 (20°C/12°C) to T4 (35°C/27°C) to mask the effect of ROS through

FIGURE 6
Relative expression analysis of heat stress-associated genes in soybean cultivars Swat-84 and NARC-1 under varying regimes of day and night temperatures. T1 = 20°C/12°C, T2 = 25°C/17°C, T3 = 30°C/22°C, T4 = 35°C/27°C, and T5 = 40°C/32°C. Bars show standard deviation (± SD). * indicates significant difference at $p \leq 0.01$ and ns indicates non-significant difference.

scavenging (Figure 1). Correspondingly, proline acts as an excellent osmolyte in plants subjected to various types of stresses by playing its role as an antioxidative defense and signaling molecule (Hayat et al., 2012). Consistently increasing variations of temperature facilitate the speedy production of proline, which not only balances cellular water and osmotic potential but also activates the physiological and biochemical processes monitoring plant yield directly and indirectly as confirmed by the present study (Figure 1). Temporal and specific variations in temperature over soybean growing areas affect soybean yield (Alsajri et al., 2022). Plants continuously struggle for survival under varying regimes of temperature. Plant endures, to some extent, the dynamically changing temperature in various ways, specifically by producing osmo-protectants with a tendency to modify the antioxidant system for reestablishing the cell redox ionic homeostasis (Ghosh et al., 2021). In this perspective, it is important to consider the impact of temperature while optimizing the

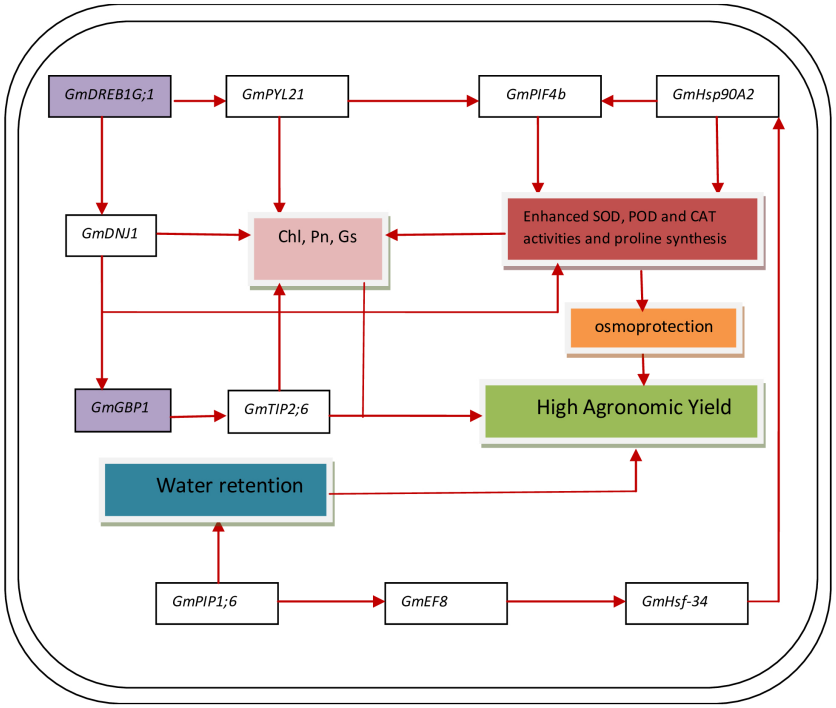

FIGURE 7
A general model representing how genes (*GmDNJ1, GmHSF-34, GmPYL21, GmPIF4b, GmPIP1;6, GmHsp90A2, GmTIP2;6,* and *GmEF8*) and TFs (*GmDREB1G;1* and *GmGBP1)* interact in both soybean genotypes for enhancing the physiochemical processes and increasing the agronomic yield when temperature regime is optimum. Chl, chlorophyll; CAT, catalase; Gs, stomatal conductance; Pn, photosynthesis; POD, peroxidase; SOD, superoxide dismutase. The red arrows indicate the activation of gene expression or process.

metrological conditions for the cultivation of soybeans (Yang et al., 2023). The temperature has a direct relationship with physiological and biochemical processes determining agronomic productivity (Vogel et al., 2021). Additionally, the variation of temperature exhibits multifarious, and often detrimental, changes in plant physiological processes, development, metabolism, and agronomic yield (Vogel et al., 2021; Yang et al., 2023). This strong connection was further confirmed through correlation and PCA (Figures 2–4). The optimal regime for soybeans is essentially important from seedling to grain filling for efficient physiological processes to maximize the agronomic yield in terms of PPP, PWPP, SPP, and SYPP (Alsajri et al., 2022; Jianing et al., 2022). The agronomic yield varies corresponding to physiological yield at changing regimes of day and night temperatures. Consistent with these studies, the current study reported a complete parallelism between the variation in physiological and biochemical traits below and beyond the optimum temperature T4 (35°C/27°C) (Figures 1–3), which was in accordance with the results of Alsajri et al. (2019); Yang et al. (2023), and Choi et al. (2016). Additionally, the paired association of physiological, biochemical, and agronomic traits varies not only with changing regimes of temperatures but also with the nature of the cultivar used. This speculation was further confirmed by PCA and heatmap studies (Figures 4, 5). To unravel the complex response of soybean genotypes to changing regimes of temperature, both cultivars Swat-84 and NARC-1 were further evaluated for their genetic response. In the present study, the expression of temperature-related genes varied significantly in both soybean cultivars due to varying regimes of day and night temperatures (Figure 6). The *GmDNJ1*, a type 1 HSP-40 protein, has a tendency to sustain overall soybean growth under heat stress by modulating the activities of various enzymes involved in ROS scavenging and chlorophyll synthesis in addition to inhibition of protein catabolism (Li et al., 2021). Correspondingly, the current study recorded the maximum expression of *GmDNJ1* at T4 (35°C/27°C), the temperature at which the activity of antioxidant enzymes and amount of chlorophyll, Pn, and Gs were maximum (Figures 1, 6). Furthermore, the upregulation of DREB1 target genes such as *GmDREB1B;1*, *GmDREB1C;1*, and *GmDREB1F;1* play an essential role in triggering the expression of various genes under heat stress (Kidokoro et al., 2015). The enhanced expression of *GmDREB1G;1* activates the expression of other heat-responsive genes such as *GmPYL21* that ensure plant normal physiological and molecular processes (Kidokoro et al., 2015). This was the most probable reason for the maximum transcript level of *GmDREB1G;1* and *GmPYL21* at T4 (35°C/27°C) in both soybean cultivars in proportion to enhanced physiochemical activities (Figures 1, 6). Heat shock transcription factors (HSFs) play a significant role in responses against heat stress. Additionally, HSFs in association with heat stress elements activate HSPs in plants to strengthen their thermotolerance (Li et al., 2014). Moreover, Guo et al. (2016) found that overexpression of *GmHSF1A* strengthens the thermotolerance of transgenic soybeans due to activation of *GmHSP70*, *GmHSP22*, and *GmHSP90A2* under heat stress. Correspondingly, the activity of *GmHSF-34* increased consistently till T5 (40°C/32°C) in both soybean cultivars, and

plants retained their activities essential for survival (Figure 6). Furthermore, Arya et al. (2023) confirmed through qRT-PCR analysis that the soybean cultivars with upregulating *GmPIF4b* had higher heat shock proteins *GmHSP90A2* and transcripts of heat shock factor. Hence, the gene *GmPIF4b* regulates multiple morphological (plant height, number of branches, and leaf surface area) and physiological traits (chlorophyll and proline) for better crop yield under high temperatures. Accordingly, the present study recorded a complementary increase in the expression of the aforementioned genes at T4 (35°C/27°C) in addition to high proline and chlorophyll contents (Figures 1, 6). The overexpressing soybean plasma membrane intrinsic protein 1;6 (*GmPIP1;6*) is an aquaporin with multiple functions that regulate plant normal water uptake, photosynthesis, and grain filling under saline stress as confirmed by Zhou et al. (2014). The current study reported similar results under temperature regime T4 (35°C/27°C) in addition to enhanced Pn, Gs, and chlorophyll (Figures 1, 6). The overexpression of soybean gene *GmHsp90A2* under high temperatures is associated with countering oxidative stress and maximizing chlorophyll production as reported by Huang et al. (2019). Correspondingly, the current study recorded the maximum expression of *GmHsp90A2* at T4 (35°C/27°C), the temperature at which chlorophyll production and antioxidant activities were also maximum (Figures 1, 6). Similarly, Zhao et al. (2013) and Feng et al. (2019) respectively found that high expression of *GmGBP1* and *GmTIP2;6* produces specific proteins that modulate agronomic growth under specific temperatures. In agreement with these findings, the current study recorded high expressions of *GmGBP1* and *GmTIP2;6* in both soybean cultivars at temperature regime T4 (35°C/27°C), where the highest agronomic yield was recorded (Figures 1, 6). Unlike *GmDNJ1*, *GmDREB1G;1*, *GmPYL21*, *GmPIF4b*, *GmHsp90A2*, *GmGBP1*, and *GmTIP2;6*, the genes *GmHSF-34*, *GmPIP1;6*, and *GmEF8* showed the highest level of transcript at T5 (40°C/32°C) in both soybean cultivars, which was consistent with the rise in proline content (Figures 1, 6). In fact, *GmEF8*, *GmHSF-34*, and *GmPIP1;6* respectively enhance proline, HSP, and water uptake when soybean faces temperature stress, and they have a protective role *via* osmolyte adjustments (Zhou et al., 2014; Zhang et al., 2022; Arya et al., 2023). High-temperature regimes accelerate the loss of water from plant surfaces due to transpiration and create a water-deficit environment within plants (Fahad et al., 2017). Plants, being active entities, respond to water-deficit conditions through osmotic adjustments. In response to high temperatures, plants alter their metabolism in different ways, particularly by enhancing the production of solutes that re-establish cellular homeostasis and redox balance by organizing proteins, modifying the antioxidant system, and maintaining cell turgor owing to osmotic adjustments (Hasanuzzaman et al., 2013). The plant copes with heat stress through the synthesis of compatible solutes known as osmoprotectants that regulate the water contents. Among extensively studied osmolytes, proline is one of the most effective compatible solutes and is ranked as the top osmoprotectant in plants (Siddique et al., 2018). Despite proline being an important signaling molecule, the most important functions of accumulated proline are osmoregulation, cell membrane maintenance, and protein stability under water-deficit conditions (Liang et al., 2013). The present study confirmed these essential roles of proline under increasing temperature regimes that were consistent with the expression of proline-regulating genes (Figures 1, 6). Additionally, the regulation of aquaporins (AQPs) is vital for maintaining water balance during heat stress, as excessive transpiration can lead to water loss and dehydration (Afzal et al., 2016). Aquaporins are channel proteins facilitating the across-membrane transport of water, which plays an important role in biological processes (Li et al., 2019). In this perspective, the overexpression *GmPIP1;6* retains the water conductance to enhance the thermotolerance during heat stress, which is not an astonishing phenomenon. Moreover, *GmEF8* has tendency to regulate the production of proline through interaction with other genes involved in the proline synthesis pathway (Kishor et al., 2005). Although high temperature increases the level of HSP in plants, to some extent, it is correlated with the expression of antioxidant enzymes as reported by Wang et al. (2021) in rice. Perhaps, the decreased activities of antioxidant enzymes at T5 (40°C/32°C) were the cause of the reduced expression of *GmHsp90A2*. Like all other organisms, plant processes including physiological and biochemical are genetically regulated. The change in the transcript level of genes with different temperature regimes was complementary to the variation of physiological and biochemical traits that determine the crop agronomic productivity (Figure 7). In general, the soybean cultivar NARC-1 showed significantly high values of physiological, biochemical, agronomic, and genetic traits as compared to Swat-84 at corresponding regimes of temperatures, which confirms that NARC-1 is more tolerant against temperature variations as compared to Swat-84. Overall, the current study proved that physiological, biochemical, agronomic, and genetic traits are deeply linked and susceptible to varying regimes of temperature. Different regimes impact the physiological and agronomic productivity differently; however, thorough investigation through genetic study proved that the optimum day and night temperature for soybean from the vegetative stage to the grain-filling stage was T4 (35°C/27°C), whose slight variation impacts its productivity significantly. Soybean is a highly temperature-sensitive crop; therefore, breeding against temperature stress should be an integral part of soybean future breeding programs. To devise an efficient breeding program to breed soybeans with tolerance against temperature stress, there is a need to consolidate the screening techniques of genotypes. Temperature stress is a major problem in arid regions where farmers face substantial losses in soybean production due to inappropriate selection of genotypes that are not adaptable to the metrological conditions of that particular area. Therefore, soybean germplasm requires comprehensive screening at molecular, biochemical, physiological, and morphological levels to optimize their adaptability in regions where temperature variation is a potential constraint at the terminal stages of soybean.

Data availability statement

The original contributions presented in the study are included in the article/supplementary material. Further inquiries can be directed to the corresponding author.

Author contributions

CD: Methodology, Data Curation, Writing – original draft. FA: Methodology, Data Curation, Writing – review & editing. MR: Formal analysis, Writing – original draft. TZ: Methodology, Data Curation, Writing – original draft. MMJ: Formal analysis, writing – original draft. RA: Formal analysis, Writing – original draft. A-HG: Writing – review & editing. AA-D: Methodology, Supervision, Writing – review & editing. TK: Methodology, Data Curation, Writing – review & editing. SHY: Supervision, Writing – review & editing. ZS: Supervision, Writing – review & editing.

Funding

The author(s) declare financial support was received for the research, authorship, and/or publication of this article. This work was supported by National Research Foundation of Korea (NRF) grant funded by the Korean Government (MSIT) (NRF-2021R1F1A1055482).

Acknowledgments

The authors extend their appreciation to the researchers supporting the project (number RSPD-2024R954), King Saud University, Riyadh, Saudi Arabia.

Conflict of interest

The authors declare that the research was conducted in the absence of any commercial or financial relationships that could be construed as a potential conflict of interest.

Publisher's note

References

Afzal, Z., Howton, T. C., Sun, Y., and Mukhtar, M. S. (2016). The roles of aquaporins in plant stress responses. *J. Dev. Biol.* 4 (1), 9. doi: 10.3390/jdb4010009

Alsajri, F. A., Singh, B., Wijewardana, C., Irby, J. T., Gao, W., and Reddy, K. R. (2019). Evaluating soybean cultivars for low- and high-temperature tolerance during the seedling growth stage. *Agronomy* 9 (1), 13. doi: 10.3390/agronomy9010013

Alsajri, F. A., Wijewardana, C., Bheemanahalli, R., Irby, J. T., Krutz, J., Golden, B., et al. (2022). Morpho-physiological, yield, and transgenerational seed germination responses of soybean to temperature. *Front. Plant Sci.* 13, 839270. doi: 10.3389/fpls.2022.839270

Alsajri, F. A., Wijewardana, C., Rosselot, R., Singh, B., Krutz, L. J., Gao, W., et al. (2020). Temperature effects on soybean seedling shoot and root growth and developmental dynamics. *J. Miss. Acad. Sci.* 65 (3).

Arya, H., Singh, M. B., and Bhalla, P. L. (2023). Overexpression of GmPIF4b affects morpho-physiological traits to reduce heat-induced grain loss in soybean. *Plant Physiol. Biochem.* 206, 108233.

Asad, S. A., Wahid, M. A., Farina, S., Ali, R., and Muhammad, F. (2020). Soybean production in Pakistan: experiences, challenges and prospects. *IJAB* 24 (4), 995–1005.

Awasthi, R., Bhandari, K., and Nayyar, H. (2015). Temperature stress and redox homeostasis in agricultural crops. *Front. Environ. Sci.* 3, 11. doi: 10.3389/fenvs.2015.00011

Bienias, A., Góralska, M., Masojć, P., Milczarski, P., and Myśków, B. (2020). The GAMYB gene in rye: sequence, polymorphisms, map location, allele-specific markers, and relationship with α-amylase activity. *BMC Genomics* 21, 1-15. doi: 10.1186/s12864-020-06991-3

Choi, D. H., Ban, H. Y., Seo, B. S., Lee, K. J., and Lee, B. W. (2016). Phenology and seed yield performance of determinate soybean cultivars grown at elevated temperatures in a temperate region. *PloS One* 11 (11), e0165977. doi: 10.1371/journal.pone.0165977

Di, F., Jian, H., Wang, T., Chen, X., Ding, Y., Du, H., et al. (2018). Genome-wide analysis of the PYL gene family and identification of PYL genes that respond to abiotic stress in Brassica napus. *Genes* 9 (3), 156. doi: 10.3390/genes9030156

Ding, X., Guo, Q., Li, Q., Gai, J., and Yang, S. (2020). Comparative transcriptomics analysis and functional study reveal important role of high-temperature stress response gene GmHSFA2 during flower bud development of CMS-based F1 in soybean. *Front. Plant Sci.* 11, 600217. doi: 10.3389/fpls.2020.600217

Djanaguiraman, M., Boyle, D. L., Welti, R., Jagadish, S. V. K., and Prasad, P. V. V. (2018). Decreased photosynthetic rate under high temperature in wheat is due to lipid desaturation, oxidation, acylation, and damage of organelles. *BMC Plant Biol.* 8 (1), 55. doi: 10.1186/s12870-018-1263-z

Djanaguiraman, M., Schapaugh, W., Fritschi, F., Nguyen, H., and Prasad, P. V. (2019). Reproductive success of soybean (*Glycine max* L. Merril) cultivars and exotic lines under high daytime temperature. *Plant Cell Environ.* 42 (1), 321–336.

Driesen, E., Van den Ende, W., De Proft, M., and Saeys, W. (2020). Influence of environmental factors light, CO_2, temperature, and relative humidity on stomatal opening and development: a review. *Agronomy* 10, 1975. doi: 10.3390/agronomy10121975

Fahad, S., Bajwa, A. A., Nazir, U., Anjum, S. A., Farooq, A., Zohaib, A., et al. (2017). Crop production under drought and heat stress: plant responses and management options. *Front. Plant Sci.*, 1147. doi: 10.3389/fpls.2017.01147

Farquhar, G. D., and Sharkey, T. D. (1982). Stomatal conductance and photosynthesis. *Ann. Rev. Plant Physiol.* 33 (1), 317–345. doi: 10.1146/annurev.pp.33.060182.001533

Feng, Z. J., Liu, N., Zhang, G. W., Niu, F. G., Xu, S. C., and Gong, Y. M. (2019). Investigation of the AQP family in soybean and the promoter activity of TIP2; 6 in heat stress and hormone responses. *Int. J. Mol. Sci.* 20, 262. doi: 10.3390/ijms20020262

Ghosh, U. K., Islam, M. N., Siddiqui, M. N., and Khan, M. A. R. (2021). Understanding the roles of osmolytes for acclimatizing plants to changing environment: a review of potential mechanism. *PlantSignal. Behav.* 16 (8), 1913306. doi: 10.1080/15592324.2021.1913306

Guo, M., Liu, J. H., Ma, X., Luo, D. X., Gong, Z. H., and Lu, M. H. (2016). The plant heat stress transcription factors (HSFs): structure, regulation, and function in response to abiotic stresses. *Front. Plant Sci.* 7, 114. doi: 10.3389/fpls.2016.00114

Hasanuzzaman, M., Nahar, K., Alam, M. M., Roychowdhury, R., and Fujita, M. (2013). Physiological, biochemical, and molecular mechanisms of heat stress tolerance in plants. *Int. J. Mol. Sci.* 14, 9643–9684. doi: 10.3390/ijms14059643

Hayat, S., Hayat, Q., AlYemeni, M. N., Wani, A. S., Pichtel, J., and Ahmad, A. (2012). Role of proline under changing environments: a review. *Plant Signal. Behav.* 7 (11), 1456–1466. doi: 10.4161/psb.21949

Herritt, M. T., and Fritschi, F. B. (2020). Characterization of photosynthetic phenotypes and chloroplast ultrastructural changes of soybean (*Glycine max*) in response to elevated air temperatures. *Front. Plant Sci.* 11, 153. doi: 10.3389/fpls.2020.00153

Hsieh, E. J., Cheng, M. C., and Lin, T. P. (2013). Functional characterization of an abiotic stress-inducible transcription factor AtERF53 in Arabidopsis thaliana. *Plant Mol. Biol.* 82, 223–237. doi: 10.1007/s11103-013-0054-z

Huang, Y., Xuan, H., Yang, C., Guo, N., Wang, H., Zhao, J., et al. (2019). *GmHsp90A2* is involved in soybean heat stress as a positive regulator. *Plant Sci.* 285, 26–33. doi: 10.1016/j.plantsci.2019.04.016

Jianing, G., Yuhong, G., Yijun, G., Rasheed, A., Qian, Z., Zhiming, X., et al. (2022). Improvement of heat stress tolerance in soybean (*Glycine max* L), by using conventional and molecular tools. *Front. Plant Sci. 13* 993189. doi: 10.3389/fpls.2022.993189

Kapilan, R., Vaziri, M., and Zwiazek, J. J. (2018). Regulation of aquaporins in plants under stress. *Biol. Res.* 51 (1), 4. doi: 10.1186/s40659-018-0152-0

Kidokoro, S., Watanabe, K., Ohori, T., Moriwaki, T., Maruyama, K., Mizoi, J., et al. (2015). Soybean DREB1/CBF-type transcription factors function in heat and drought

as well as cold stress-responsive gene expression. *Plant J.* 81 (3), 505–518. doi: 10.1111/tpj.12746

Kishor, P. K., Sangam, S., Amrutha, R. N., Laxmi, P. S., Naidu, K. R., Rao, K. S., et al. (2005). Regulation of proline biosynthesis, degradation, uptake and transport in higher plants: its implications in plant growth and abiotic stress tolerance. *Curr. Sci.* 10, 424–438.

Li, K. P., Wong, C. H., Cheng, C. C., Cheng, S. S., Li, M. W., Mansveld, S., et al. (2021). GmDNJ1, a type-I heat shock protein 40 (HSP40), is responsible for both Growth and heat tolerance in soybean. *Plant Direct* 5 (1), e00298. doi: 10.1002/pld3.298

Li, P. S., Yu, T. F., He, G. H., Chen, M., Zhou, Y. B., Chai, S. C., et al. (2014). Genome-wide analysis of the Hsf family in soybean and functional identification of GmHsf-34 involvement in drought and heat stresses. *BMC Genomics* 15 (1), 1009. doi: 10.1186/1471-2164-15-1009

Li, S., Liu, J., An, Y., Cao, Y., Liu, Y., Zhang, J., et al. (2019). MsPIP2; 2, a novel aquaporin gene from Medicago sativa, confers salt tolerance in transgenic Arabidopsis. *Environ.Exp. Bot.* 165, 39–52. doi: 10.1016/j.envexpbot.2019.05.020

Liang, X., Zhang, L., Natarajan, S. K., and Becker, D. F. (2013). Proline mechanisms of stress survival. *Antioxidants Redox Signaling* 19 (9), 998–1011. doi: 10.1089/ars.2012.5074

Mathur, S., Agrawal, D., and Jajoo, A. (2014). Photosynthesis: response to high temperature stress. *J. Photochem. Photobiol. B.* 137, 116–126. doi: 10.1016/j.jphotobiol.2014.01.010

McGraw-Hill, C. (2008). *Statistix 8.1 (Analytical software, Tallahassee, Florida)* (Florida, USA: Maurice/Thomas text).

Moore, C. E., Meacham-Hensold, K., Lemonnier, P., Slattery, R. A., Benjamin, C., Bernacchi, C. J., et al. (2021). The effect of increasing temperature on crop photosynthesis: from enzymes to ecosystems. *J. Exp. Bot.* 72 (8), 2822–2844. doi: 10.1093/jxb/erab090

Muhammad, I., Shalmani, A., Ali, M., Yang, Q. H., Ahmad, H., and Li, F. B. (2021). Mechanisms regulating the dynamics of photosynthesis under abiotic stresses. *Front. Plant Sci.* 11, 615942. doi: 10.3389/fpls.2020.615942

Ortiz, A. C., De Smet, I., Sozzani, R., and Locke, A. M. (2022). Field-grown soybean shows genotypic variation in physiological and seed composition responses to heat stress during seed development. *Environ. Exp. Bot.* 195, 104768. doi: 10.1016/j.envexpbot.2021.104768

Osei, E., Jafri, S. H., Saleh, A., Gassman, P. W., and Gallego, O. (2023). Simulated climate change impacts on corn and soybean yields in Buchanan County, Iowa. *Agriculture* 13, 268. doi: 10.3390/agriculture13020268

Purcell, L. C., Salmeron, M., and Ashlock, L. (2014). Soybean growth and development. *Arkans. Soyb. Product. Handbook MP.* 197, 1–8.

Rajput, V. D., Harish,, Singh, R. K., Verma, K. K., Sharma, L., Quiroz-Figueroa, F. R., et al. (2021). Recent developments in enzymatic antioxidant defence mechanism in plants with special reference to abiotic stress. *Biology* 10, 267. doi: 10.3390/biology10040267

Raza, A., Razzaq, A., Mehmood, S. S., Zou, X., Zhang, X., Lv, Y., et al. (2019). Impact of climate change on crops adaptation and strategies to tackle its outcome: a review. *Plants* 8, 34. doi: 10.3390/plants8020034

RStudio Team. (2020). *RStudio: integrated development for R* (PBC, Boston, MA: RStudio). Available at: http://www.rstudio.com/.

Sachdev, S., Ansari, S. A., Ansari, M. I., Fujita, M., and Hasanuzzaman, M. (2021). Abiotic stress and reactive oxygen species: generation, signaling, and defense mechanisms. *Antioxidants* 10, 277. doi: 10.3390/antiox10020277

Sairam, R. K., Deshmukh, P. S., and Shukla, D. S. (1997). Tolerance to drought and temperature stress in relation to increased antioxidant enzyme activity in wheat. *J. Agron. Crop Sci.* 178, 171–177. doi: 10.1111/j.1439-037X.1997.tb00486.x

Sasi, S., Venkatesh, J., Daneshi, R. F., and Gururani, M. A. (2018). Photosystem II extrinsic proteins and their putative role in abiotic stress tolerance in higher plants. . *Plants* 7, 100. doi: 10.3390/plants7040100

Siddique, A., Kandpal, G., and Kumar, P. (2018). Proline accumulation and its defensive role under diverse stress condition in plants: an overview. *J. Pure Appl. Microbiol.* 12 (3), 1655–1659. doi: 10.22207/JPAM.12.3.73

Siebers, M. H., Yendrek, C. R., Drag, D., Locke, A. M., Rios,, Acosta, L., et al. (2015). Heat waves imposed during early pod development in soybean (*Glycine max*) cause significant yield loss despite a rapid recovery from oxidative stress. *Glob. Change Biol.* 21 (8), 3114–3125. doi: 10.1111/gcb.12935

Tariq, A., Jabeen, Z., Farrakh, S., Noreen, K., Arshad, W., Ahmed, H., et al. (2022). Exploring the genetic potential of Pakistani soybean cultivars through RNA-seq based transcriptome analysis. *Mol. Biol. Rep.* 49, 2889–2897. doi: 10.1007/s11033-021-07104-3

Ul-Haq, S., Khan, A., Ali, M., Khattak, A. M., Gai, W. X., Zhang, H. X., et al. (2019). Heat shock proteins: dynamic biomolecules to counter plant biotic and abiotic stresses. *Int. J. Mol. Sci.* 20, 5321. doi: 10.3390/ijms20215321

Vogel, J. T., Liu, W., Olhoft, P., Crafts-Brandner, S. J., Pennycooke, J. C., and Christiansen, N. (2021). Soybean yield formation physiology–a foundation for precision breedingbased improvement. *Front. Plant Sci.* 12, 719706. doi: 10.3389/fpls.2021.719706

Wang, Y., Huang, M., Gao, P., Chen, H., Zheng, Y., Yang, C., et al. (2021). Expression of heat shock protein ('HSP') genes and antioxidant enzyme genes in hybrid rice II YOU 838 during heat stress. *Aust. J. Crop Sci.* 15 (9), 37–42. doi: 10.21475/ajcs.21.15.09.sp-4

Xu, Z., Jiang, Y., Jia, B., and Zhou, G. (2016). Elevated-CO2 response of stomata and its dependence on environmental factors. *Front. Plant Sci.* 7, 657. doi: 10.3389/fpls.2016.00657

Yang, L., Song, W., Xu, C., Sapey, E., Jiang, D., and Wu, C. (2023). Effects of high night temperature on soybean yield and compositions. *Front. Plant Sci.* 14, 1065604. doi: 10.3389/fpls.2023.1065604

Zhang, H. Y., Hou, Z. H., Zhang, Y., Li, Z. Y., Chen, J., Zhou, Y. B., et al. (2022). A soybean EF-Tu family protein GmEF8, an interactor of GmCBL1, enhances drought and heat tolerance in transgenic Arabidopsis and soybean. *Int. J. Biol. Macromol.* 205, 462–472. doi: 10.1016/j.ijbiomac.2022.01.165

Zhang, Y., Zhang, B., Yang, T., Zhang, J., Liu, B., Zhan, X., et al. (2020). The GAMYB-like gene SlMYB33 mediates flowering and pollen development in tomato. *Hortic. Res.* 7, 133. doi: 10.1038/s41438-020-00366-1

Zhao, C., Liu, B., Piao, S., Wang, X., Lobell, D. B., Huang, Y., et al. (2017). Temperature increase reduces global yields of major crops in four independent estimates. *PNAS* 114 (35), 9326–9331. doi: 10.1073/pnas.1701762114

Zhao, L., Wang, Z., Lu, Q., Wang, P., Li, Y., Lv, Q., et al. (2013). Overexpression of a GmGBP1 ortholog of soybean enhances the responses to flowering, stem elongation and heat tolerance in transgenic tobaccos. *Plant Mol. Biol.* 82 (3), 279–299. doi: 10.1007/s11103-013-0062-z

Zhou, L., Wang, C., Liu, R., Han, Q., Vandeleur, R. K., Du, J., et al. (2014). Constitutive overexpression of soybean plasma membrane intrinsic protein GmPIP1; 6 confers salt tolerance. *BMC Plant Biol.* 14 (1), 1–13.

frontiers | Frontiers in Plant Science

TYPE Original Research
PUBLISHED 09 February 2024
DOI 10.3389/fpls.2024.1353365

OPEN ACCESS

EDITED BY
Yi Wang,
Chinese Academy of Sciences (CAS), China

REVIEWED BY
Qian Tong,
Changzhi Medical College, China
Yongzan Wei,
Chinese Academy of Tropical Agricultural Sciences, China

*CORRESPONDENCE
Junji Su
sujj@gsau.edu.cn
Xianliang Zhang
zhangxianliang@caas.cn
Caixiang Wang
wangcaix@gsau.edu.cn

RECEIVED 10 December 2023
ACCEPTED 23 January 2024
PUBLISHED 09 February 2024

CITATION
Wei W, Ju J, Zhang X, Ling P, Luo J, Li Y, Xu W, Su J, Zhang X and Wang C (2024) *GhBRX.1*, *GhBRX.2*, and *GhBRX4.3* improve resistance to salt and cold stress in upland cotton. *Front. Plant Sci.* 15:1353365. doi: 10.3389/fpls.2024.1353365

GhBRX.1, *GhBRX.2*, and *GhBRX4.3* improve resistance to salt and cold stress in upland cotton

Wei Wei[1], Jisheng Ju[1], Xueli Zhang[1], Pingjie Ling[1], Jin Luo[1], Ying Li[1], Wenjuan Xu[1], Junji Su[1,2]*, Xianliang Zhang[2,3]* and Caixiang Wang[1]*

[1]State Key Laboratory of Aridland Crop Science, College of Life Science and Technology, Gansu Agricultural University, Lanzhou, China, [2]Center for Western Agricultural Research, Chinese Academy of Agricultural Sciences (CAAS), Changji, China, [3]Institute of Cotton Research, State Key Laboratory of Cotton Biology, Chinese Academy of Agricultural Sciences (CAAS), Anyang, China

Introduction: Abiotic stress during growth readily reduces cotton crop yield. The different survival tactics of plants include the activation of numerous stress response genes, such as *BREVIS RADIX* (*BRX*).

Methods: In this study, the *BRX* gene family of upland cotton was identified and analyzed by bioinformatics method, three salt-tolerant and cold-resistant *GhBRX* genes were screened. The expression of *GhBRX.1*, *GhBRX.2* and *GhBRXL4.3* in upland cotton was silenced by virus-induced gene silencing (VIGS) technique. The physiological and biochemical indexes of plants and the expression of related stress-response genes were detected before and after gene silencing. The effects of *GhBRX.1*, *GhBRX.2* and *GhBRXL4.3* on salt and cold resistance of upland cotton were further verified.

Results and discussion: We discovered 12, 6, and 6 *BRX* genes in *Gossypium hirsutum*, *Gossypium raimondii* and *Gossypium arboreum*, respectively. Chromosomal localization indicated that the retention and loss of *GhBRX* genes on homologous chromosomes did not have a clear preference for the subgenomes. Collinearity analysis suggested that segmental duplications were the main force for *BRX* gene amplification. The upland cotton genes *GhBRX.1*, *GhBRX.2* and *GhBRXL4.3* are highly expressed in roots, and *GhBRXL4.3* is also strongly expressed in the pistil. Transcriptome data and qRT–PCR validation showed that abiotic stress strongly induced *GhBRX.1*, *GhBRX.2* and *GhBRXL4.3*. Under salt stress and low-temperature stress conditions, the activities of superoxide dismutase (SOD), peroxidase (POD) and catalase (CAT) and the content of soluble sugar and chlorophyll decreased in *GhBRX.1*-, *GhBRX.2*- and *GhBRXL4.3*-silenced cotton plants compared with those in the control (TRV: 00). Moreover, *GhBRX.1*-, *GhBRX.2*- and *GhBRXL4.3*-silenced cotton plants exhibited greater malondialdehyde (MDA) levels than did the control plants. Moreover, the expression of stress marker genes (*GhSOS1*, *GhSOS2*, *GhNHX1*, *GhCIPK6*, *GhBIN2*, *GhSnRK2.6*, *GhHDT4D*, *GhCBF1* and *GhPP2C*)

decreased significantly in the three target genes of silenced plants following exposure to stress. These results imply that the *GhBRX.1*, *GhBRX.2* and *GhBRXL4.3* genes may be regulators of salt stress and low-temperature stress responses in upland cotton.

KEYWORDS

BREVIS RADIX, salt stress, cold stress, virus-induced gene silencing (VIGS), upland cotton

1 Introduction

Cotton is an annual herbaceous plant of the Malvaceae family that is not only used to produce natural textile fibers but is also one of the major cash crops and a significant source of protein and seed oil worldwide (John and Crow, 1992). Despite the economic importance of cotton, various environmental factors, including both biotic and abiotic stresses, pose a great threat to cotton production (Potters et al., 2007). Due to global climate change, drought, salinity, extreme temperature, waterlogging, heavy metals, hypoxia and other major abiotic stresses will impede the development and growth of plants and affect crop yield and quality and sustainable agricultural development (Hasanuzzaman et al., 2020). To increase their chances of survival, plants have developed numerous defense strategies and mechanisms to handle a range of challenging circumstances (Westerheide et al., 2012; Van Zelm et al., 2020; Nian et al., 2021). In plant defense mechanisms, many stress-response genes help plants tolerate the adverse effects of various stressors by regulating their transcriptome levels.

The highly conserved *BREVIS RADIX* (*BRX*) family of plant-specific genes is found in all higher plants for which data are known but not in animals or single-celled organisms (Mouchel et al., 2004). For the first time, *BRX* was isolated from *Arabidopsis thaliana* UK-1 plants with a short root phenotype using map-based cloning (Mouchel et al., 2004). There are five *BRX* genes in *Arabidopsis*: *BRX*, *BRXL1* to *BRXL4*. Although the sequences of *BRX* are highly conserved, the functions of the five genes in the *Arabidopsis BRX* family are largely nonredundant (Briggs et al., 2006). BRX proteins have four highly conserved domains, two of which are short N-terminal domains and two of which are BRX domains (Briggs et al., 2006; Beuchat et al., 2010a; Liu et al., 2010). These include a 9–10 amino acid region at the N-terminus that is thought to contain palmitoylation signals and is crucial for the membrane localization of *BRX* (Rowe et al., 2019). The adjacent domains are a 25-amino acid N-terminal domain with a KDMA motif and two BRX domains with 55 amino acid extensions consisting of tandem repeats (Koh et al., 2021). The BRX domain may represent a new protein–protein interaction domain, which is the first indication of the biological function of the BRXL protein (Briggs et al., 2006). Adding one BRX domain to the corresponding BRX^{N140} fragment partially restored functionality (Briggs et al., 2006). However, the addition of two BRX domains to the corresponding BRX^{N140} fragment, as with full-length *BRX*, significantly alleviated the *brx* root growth phenotype and elicited hypocotyl function to acquire the phenotype (Briggs et al., 2006; Scacchi et al., 2009). The conserved N-terminal domain of BRX family proteins may play only secondary functional roles (Briggs et al., 2006). However, according to *Ka*/*Ks* analysis, the diversity of *BRX* family genes may be caused by the variable N-terminal region, which could be the cause of the nonredundant functions of most *AtBRX* family genes (Briggs et al., 2006; Beuchat et al., 2010a).

BRX is a growth regulator needed for root growth that regulates cell proliferation and elongation in root growth areas (Mouchel et al., 2006). Auxin substantially stimulates *BRX* expression, while brassinosteroid (BR) marginally inhibits expression (Mouchel et al., 2006). This finding suggests that *BRX* forms a feedback loop between BR and auxin, which maintains brassinosteroid thresholds and controls the root response to auxin, while auxin completes the cycle by controlling *BRX* expression (Mouchel et al., 2006). The *BRX* functional allele (*brx-2*) is highly sensitive to ABA-mediated root growth inhibition, and it has also been shown to be insensitive to cytokinin-induced lateral root initiation inhibition, indicating crosstalk between BR and cytokinin (Bari and Jones, 2009; Scacchi et al., 2009). Therefore, *BRX* could be a key node in the interconnection of auxin, BR, ABA, and cytokinin signaling during root development. (John and Crow, 1992; Scacchi et al., 2009). The BRX protein is associated with the plasma membrane but is translocated to the nucleus after auxin treatment to regulate gene expression (Scacchi et al., 2009). The *BRX* gene family has been studied and identified in a variety of plant species (Li et al., 2009; Liu et al., 2010; Zhang Y. et al., 2021; Tiwari et al., 2023). *BRX* is involved in the longitudinal and radial expansion of hypocotyls and roots, the development of embryos and leaves, and the asymmetric division of stomatal lineage cells in *Arabidopsis*, and unlike their partial or nonredundant roles in roots, *BRX* genes play redundant roles in stomatal development (Rowe et al., 2019). The *brx* mutants also exhibited significant reductions in cotyledon and leaf growth, and deletion of the *BRX* functional allele (*brx-2*) resulted in a decrease in rosette area in comparison to that of Col-0, but the quantity of leaves remained the same (Rodrigues et al., 2009). In contrast, plants with functionally acquired *BRX* exhibit elongated hypocotyls and epicotyl leaves (Scacchi et al., 2009; Gill and Tuteja,

2010). In rice, compared with those of WT plants, *OsBRXL4*-overexpressing transgenic plants had significantly longer roots and greater sensitivity to auxin under normal growth conditions (Liu et al., 2010). These results suggest that *OsBRXL4* may regulate primary root growth via auxin signaling (Liu et al., 2010). The optimal tillering angle is essential for an ideal plant structure, and the molecular mechanism controlling the tillering angle in rice will improve our ability to rationally change the structure of rice plants, thereby increasing grain yield. *OsBRX* regulates auxin transport to control the tiller angle of rice plants. (Scacchi et al., 2009; Liu et al., 2010). Overexpression of three different *BrBRX* genes in *Brassica rapa* significantly increased the number of rosette leaves, decreased the rosette area and increased the petiole length in transgenic plants (Zhang Y. et al., 2021). *TaBRXL1* is generally expressed in all analyzed tissues except flag leaves, and the expression levels of *TaBRXL2*, *TaBRXL3* and *TaBRXL4* are significantly increased under auxin treatment, indicating that *TaBRX* family genes may contribute to functional diversity (Tiwari et al., 2023).

Studies have shown that the expression of *BRX*s is differentially induced by different types of abiotic stress (Liu et al., 2010; Tiwari et al., 2023). In rice, *OsBRXL1* and *OsBRXL4* respond to drought, salt and cold stress; *OsBRXL3* responds to drought and salt stress; *OsBRXL2* and *OsBRXL5* respond only to cold stress; and the expression of these five *OsBRXL* genes is upregulated under drought and salt stress and downregulated under low-temperature stress (Liu et al., 2010). *TaBRXL1* was found to be involved primarily in developmental processes, whereas *TaBRXL2* was highly regulated by development, hormones, and other abiotic stimuli (Tiwari et al., 2023). In addition to *TaBRXL2*, the other *TaBRX* genes were significantly downregulated under drought conditions in common wheat. Under osmotic stress (200 mM mannitol), *TaBRXL2*, *TaBRXL3* and *TaBRXL4* were upregulated (Tiwari et al., 2023). In summary, the *BRX* gene family plays an important role in enhancing plant tolerance to abiotic stress.

Cotton is a valuable economic crop that provides "oil, fiber, feed, and medicine." Yield losses readily occur due to abiotic stress during the growth development process of cotton. Thus, it is important to screen and apply key genes in cotton that respond well to abiotic stress and improve cotton stress resistance through biological breeding. To date, the relationship between the *GhBRX* gene and abiotic stress has not been studied. The whole genomes of 12 *GhBRX* genes were discovered in this work. Its evolutionary model, physical and chemical properties, chromosomal location, gene structure, *cis*-acting elements and expression pattern were comprehensively analyzed. Using the virus-induced gene silencing (VIGS) approach, we further elucidated the biological function of the *GhBRX.1*, *GhBRX.2* and *GhBRXL4.3* genes in response to salt and cold stress.

2 Materials and methods

2.1 Identification of *BRX* genes

To identify cotton *BRX* gene families, we used CottonFGD (http://www.cottonfgd.org/) and *Arabidopsis thaliana* genome sequence data from TAIR (http://www.arabidopsis.org) for five AtBRX protein sequences from Pfam (https://pfam.xfam.org/), which was subsequently used to download the PF08381 hidden Markov model (HMM) version 3.0 (El-Gebali et al., 2019). Then, we used HMMER 3.0 software with default parameter settings (http://www.HMMER.org/) to obtain the *BRX* gene, for which the E value was $<1e^{-5}$ (Zhu et al., 2017). We used Pfam (https://www.ebi.ac.uk/Tools/pfa/pfamscan/) and SMART (https://smart.embl.de/) to further evaluate the results of our genes for confirmation. Finally, we manually confirmed the identified *BRX* genes. The BRX protein sequence was predicted through ExPASy (https://us.expasy.org/tools/protparam.html) to predict the molecular weight (MW), theoretical isoelectric point (pI), etc. In addition, Wolfpsort (https://www.wolfpsort.hgc.jp/) was used to predict the subcellular localization of the cotton BRX protein.

2.2 Sequence alignment and phylogenetic analysis

The ClustalW program (version 2.0) was used to align the full-length amino acid sequences of the *BRX*-encoded *Gossypium hirsutum* (*Gh*), *Gossypium arboreum* (*Ga*), *Gossypium raimondii* (*Gr*), *Arabidopsis thaliana* (*At*), *Brassica rapa* (*Br*), *Oryza sativa* (*Os*), and *Triticum aestivum* (*Ta*). The alignment was then manually modified in MEGA 7.0. Subsequently, we constructed a neighbor joining (NJ) tree with 1000 bootstrap repetitions using MEGA 7.0's Poisson substitution model with default parameters (Kumar et al., 2016). The Interactive Tree of Life (iTOL) tool was utilized to enhance the visualization of the phylogenetic tree (http://itol.embl.de/).

2.3 Analysis of conserved gene structures and protein motifs

To find conserved protein motifs, we utilized the motif elicitation (multiple EM for motif elicitation) website (http://meme-suite.org/) (Bailey et al., 2009). A conservative motif map was generated using TBtools software (Chen et al., 2018). The upland cotton CDS and genome sequence and NWK file from phylogenetic tree analysis were used to map gene structure through the Server (Gene Structure Display Server, GSDS) program (http://gsds.cbi.pku.edu.cn/).

2.4 Analysis of chromosomal positions and gene collinearity

GFF3 files extracted from the CottonFGD database were used to determine chromosome locations. The *GhBRX* gene was located on the chromosome using TBtools software (Chen et al., 2020). During collinear analysis, to compare the GhBRX protein sequences, the Basic Local Alignment Search Tool (BLAST) was utilized, and the cutoff E value was $< 10^{-5}$. The MCScanX tool of the TBtools software was subsequently used to evaluate the above BLASTP

results, extract collinear pairs of GhBRX family proteins, and construct a collinearity map of the *GhBRX* family using TBtools (Chen et al., 2020). *Ka*/*Ks* values of the *GhBRX* gene were determined by using TBtools (Chen et al., 2020). TBtools was subsequently used to construct interspecific collinearity maps of *G. hirsutum*, *G. raimondii* and *G. arboretum* (Chen et al., 2020).

2.5 *Cis*-regulatory element analysis

We obtained an upstream sequence of our genes spanning 2 kb from the translation start site from CottonFGD (https://cottonfgd.net/) to identify *cis*-regulatory regions in *BRX* genes. Then, we predicted the *cis*-regulatory elements in the promoter region of the *GhBRX* genes using the PlantCARE website (http://bioinformatics.psb.ugent.be/beg).

2.6 Expression pattern analysis

To verify the *GhBRX* gene expression profile in upland cotton organizations, RNA-seq data from Zhejiang University (ZJU) (http://cotton.zju.edu.cn/) were downloaded to determine the *GhBRX* gene organization and response to salt, drought, cold and heat stresses(Zhang et al., 2015). Heatmaps of 12 *GhBRX* genes were generated using TBtools.

2.7 Plant material, RNA extraction, and fluorescence quantitative PCR

Healthy plants of the new upland cotton variety XinshiK25 were selected and treated with 15% PEG (PEG-6000), 250 mmol/L NaCl, 12°C and 42°C, respectively. The leaves were removed every 3 h and treated for 24 h. RNA and reverse transcription cDNA were extracted using a kit produced by Tiangen Biochemical Technology (Beijing) Co., Ltd. *GhBRX* gene primers were constructed using NCBI Prime-BLAST (primer design tool, https://www.ncbi.nlm.nih.gov/tools/primer-blast/index.cgi?LINK_LOC=BlastHome). Supplementary Table S1 shows the primers used. Real-time fluorescence quantitative PCR was performed (SYBR Green, FP209, Tiangen, China) according to the instructions for the thermal cycling process. AY305733 is an internal control gene that employs the $2^{-\Delta\Delta C}{}_{T}$ technique (Livak and Schmittgen, 2001). The comparative expression values of *GhActin* and *GhBRX*s were calculated, and the relative expression levels of three independent biological replicates and technical replicates were averaged.

2.8 Cotton vector creation and the VIGS technique

The coding sequences of the *GhBRX.1*, *GhBRX.2* and *GhBRXL4.3* genes were downloaded from CottonFGD, and specific primers (Supplementary Table S2) were designed. Using the online tool NCBI Prime-BLAST, specific primers for gene silencing and related stress response gene fluorescence were designed (Supplementary Table S3). Specific cDNA sequences of *GhBRX.1*, *GhBRX.2* and *GhBRXL4.3* were amplified, constructed into Figure vectors, and subsequently introduced into Agrobacterium strain GV3101. Then, the cotyledons of two 8-day-old XinshiK25 plants were grown at 25°C for 24 h in the dark and injected with the vector (Gao et al., 2013). RNA was collected from cotton leaves that had been silenced at the four-leaf stage, and RT–qPCR was used to assess the silencing efficacy. RT–qPCR was used to test the expression of nine stress-responsive genes, *GhSOS1*, *GhSOS2*, *GhNHX1*, *GhCIPK6*, *GhBIN2*, *GhSnRK2.6*, *GhHDT4D*, *GhCBF1* and *GhPP2C*, associated with salt stress and cold stress in control and silenced plants.

2.9 Physiological and biochemical parameters of the silenced and control plants under salt and cold stress conditions

The activities of peroxidase (POD), catalase (CAT), and superoxide dismutase (SOD), three antioxidant enzymes that are important to plants under abiotic stress conditions, were evaluated. SOD activity was determined by tracking the suppression of the photochemical reduction of nitroblue tetrazole (Giannopolitis and Ries, 1977). POD activity was evaluated using ortho-methoxyphenol (guaiacol) as a substrate (Castro et al., 2017). POD can oxidize guaiacol to o-4-methoxyphenol, which can be detected via spectrophotometry at 470 nm. CAT activity is determined by UV absorption (Beers and Sizer, 1952), and the malondialdehyde (MDA) content is a marker of lipid peroxidation (Liu et al., 2018). Chlorophyll was extracted with 95% ethanol and measured spectrophotometrically at 665 nm and 649 nm (Lichtenthaler and Wellburn, 1983).

3 Results

3.1 Identification of *BRX*s in cotton

The amino acid sequences of the BRX proteins found in *Arabidopsis* and rice were used as query sequences. As shown in Supplementary Table S4, the presence of 12, 6, and 6 *BRX* genes was confirmed in *G. hirsutum*, *G. raimondii* and *G. arboreum*. The number of *BRX* genes in allotetraploid cotton was twice as high as that in the two diploid cotton lines, suggesting that the *BRX* gene family experienced expansion during evolution in *Gossypium* spp. while maintaining their unique genetic makeup. The predicted protein sequences were used to calculate the number of amino acids, MW, and pI. The 24 BRX proteins that were found had amino acid ranges of 342–405, protein pIs that varied from 5.73 to 8.59, and MWs that varied from 38.58 to 45.59 kDa. Bioinformatics analysis revealed that 24 BRX proteins were predicted to locate in the nucleus. All features and chromosomal locations of the identified *BRX*s are shown in Additional file Supplementary Table S4.

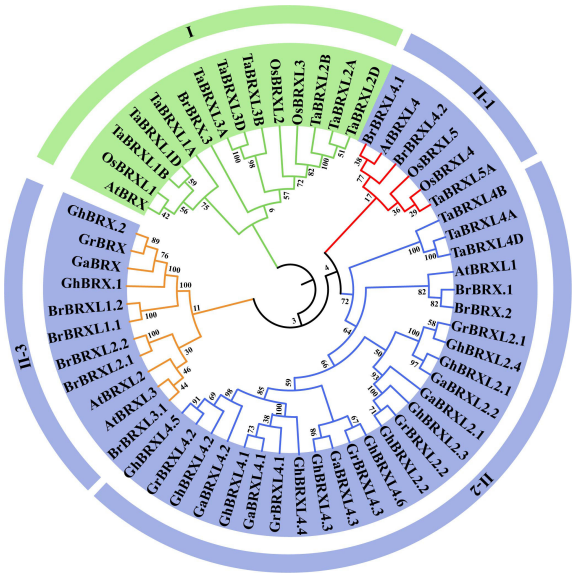

FIGURE 1
Phylogenetic relationships of BRX proteins in seven plant species. *Gossypium hirsutum (Gh), Gossypium raimondii (Gr), Gossypium arboreum (Ga), Brassica rapa (Br), Arabidopsis thaliana (At), Tariticum aestivum (Ta)*, and *Oryza sativa (Os)*. At each node, the bootstrap values were displayed.

3.2 Phylogenetic analysis of the *BRX* genes

Using 57 BRX protein sequences obtained from *G. hirsutum, G. raimondii, G. arboreum*, *B. rapa*, *A. thaliana*, *T. aestivum*, and *O. sativa*, we constructed a phylogenetic tree based on multiple alignment analyses using the neighbor–joining (NJ) method to examine the phylogenetic relationships among the *BRX* family genes (Figure 1). Based on bootstrap values (=1,000), the 57 BRX proteins were found to precluster into two main groups (Group I and Group II). Group I was defined by *AtBRX* (*At1G31880*) and had no *BRX* members from the three cotton species. Group II was divided into three subgroups: II-1, II-2 and II-3. All the *OsBRX* genes clustered in group I and subgroup II-1, and all three *Gossypium* spp. species *BRX* genes clustered in subgroups II-2 and II-3. As shown in Figure 1, mutually homologous *BRX* family genes clustered together, with one copy in diploid cotton species and two copies in heterotetraploid cotton species in almost every direct homologous group. The results of the clustering analysis provide additional evidence that the upland cotton species heterotetraploid is the product of an ancestral cross between *G. raimondii* and *G. arboreum*, two diploid cotton species, and doubles in number.

3.3 Structure and conserved motif analysis of *GhBRX* genes

We analyzed the structural features of *GhBRX* using the GSDS program and the exon and intron structures and conserved structural domains using the MEME tool. The *GhBRX* genes exhibited a comparatively high level of structural similarity according to the exon/intron structure analysis (Supplementary Figure S1A). All the *GhBRX* genes contained five exons. Most of the homologous genes had similar gene lengths, with *GhBRXL4.3* being the longest. The results suggest that exon structure is associated with phylogenetic relationships, further supporting the structural classification of the *GhBRX* gene family. Using MEME software, the functional regions of the GhBRX proteins were divided into five different motifs (Supplementary Figure S1B). Motifs 1, 2, 3 and 5 (BRX motifs) were widely distributed among all *GhBRX* family members, with only *GhBRX.1* and *GhBRX.2* without motif 4; these two genes also had the shortest lengths. The motif compositions of GhBRX proteins in a given branch were strikingly similar, indicating that these proteins may early every play comparable role.

3.4 Genetic replication and collinearity analysis of *GhBRX*

Gene duplication events in *G. hirsutum* were explored with TBtools to elucidate the amplification patterns and determine the homologous locus linkages of the *GhBRX* gene family members between the At and Dt subgenomes (Figure 2). One tandem duplicate gene was identified on chromosome A05. In addition, the *GhBRX* gene family contained 20 segmentally duplicated genes (Figure 3). These data suggest that segmental duplications are important in the evolution of *GhBRX* gene families, indicating the dominance of segmental repeats over tandem repeats in the evolution of the *GhBRX* gene family (Supplementary Table S5). Furthermore, to gain a deeper understanding of the homologous gene functions and evolutionary relationships of the *BRX* genes, the outcomes of the genome symbiosis study between upland cotton and two other species of cotton were examined (Supplementary Figure S2). In conclusion, the current findings suggest that *BRX* genes may undergo certain genomic rearrangements during polyploidy. The nonsynonymous substitution (*Ka*), synonymous substitution (*Ks*), and *Ka*/*Ks* ratio were estimated to better

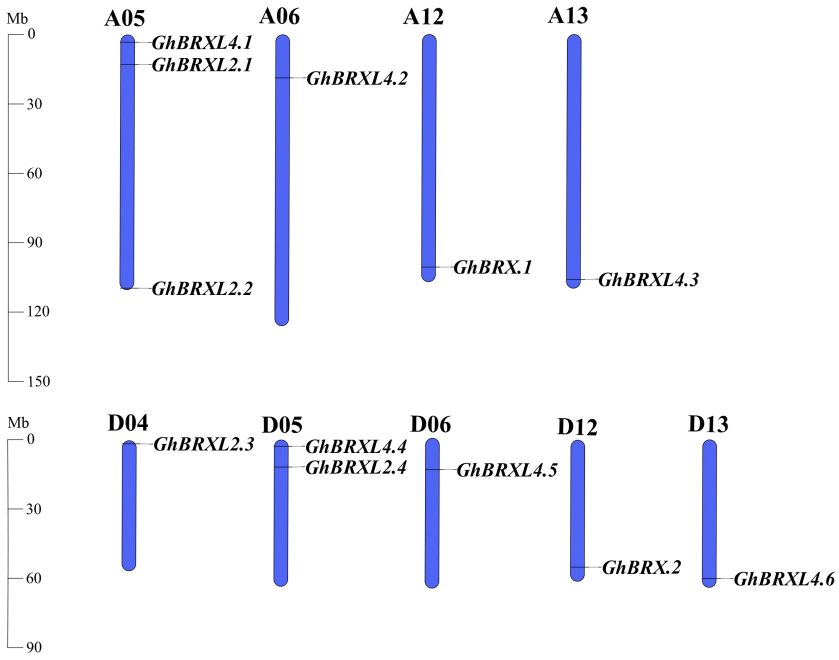

FIGURE 2
GhBRX locations on *Gossypium hirsutum* chromosomes. The blue bars represent the At and Dt subgenomes of *G. hirsutum*. The subgenomes' matching gene names were showned on the right side of each chromosome.

understand the evolutionary constraints regulating the functional divergence of the *GhBRX* gene family (Supplementary Table S6). The *Ka*/*Ks* ratio of all duplicate *GhBRX* gene pairs was less than 1, indicating that selective pressure may have been applied to the *GhBRX* family genes throughout their evolutionary history.

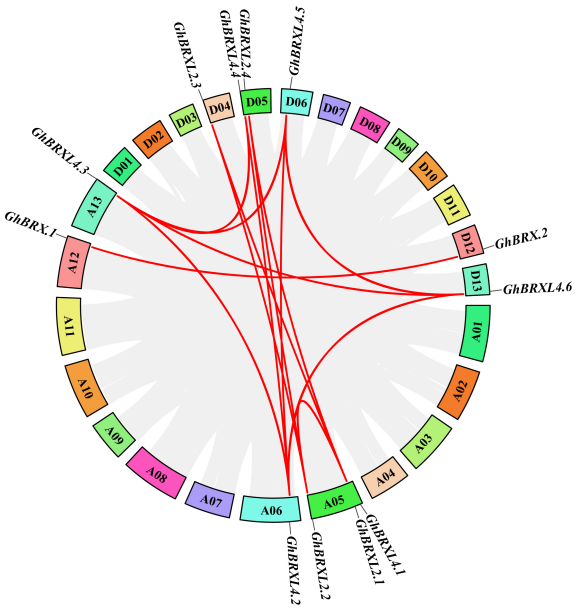

FIGURE 3
Duplication of *GhBRX* genes. Duplications of *GhBRX* genes on the chromosome of *G. hirsutum*; the red lines represented gene pairs of *GhBRX*. The rectangles represented chromosomes.

3.5 Analysis of *cis*-elements in the promoters of *GhBRX*s

We examined and characterized the *cis*-acting region in the 2 kb promoter sequence of *GhBRX*s to further investigate the putative regulatory roles of the *BRX* gene in response to abiotic stressors. We discovered 38 different types of *cis*-regulatory elements that are involved in tissue-specific expression, stress responses, phytohormone responses, and light responses (Figure 4). Five elements associated with tissue-specific expression were identified, namely, the RY element, O2 site, CAT box, GCN4 motif and HD-Zip 1. The *cis*-regulatory element associated with meristematic tissue expression (CAT-box) was only present in the promoter regions of the homologs *GhBRXL2.1* and *GhBRXL2.4*, and the seed-specific regulatory element (RY-element) is specific to *GhBRXL2.4*. Six elements associated with stress responsiveness were identified, and these *cis*-acting elements are involved in defense and stress responsiveness, drought, low temperature, anaerobic and wounding responses. Abiotic stress response elements, such as the drought response element (MBS) and low temperature response element (LTR), were present in variable amounts in the homologous genes *GhBRX.1*, *GhBRX.2*, *GhBRXL4.2* and *GhBRXL4.5*. The *cis*-acting regulatory elements necessary for anaerobic induction (ARE) were more abundant in most *GhBRX* genes. In addition, four hormone-related elements were identified, namely, the gibberellin response element (GARE motif-containing element, P-box and TATC motif-containing element), the abscisic acid response element (ABRE), the salicylic acid response element (TCA-element) and the methyl jasmonate (MeJA) response element (CGTCA motif-containing element and TGACG motif-containing element). Among them, ABRE and MeJA response elements were

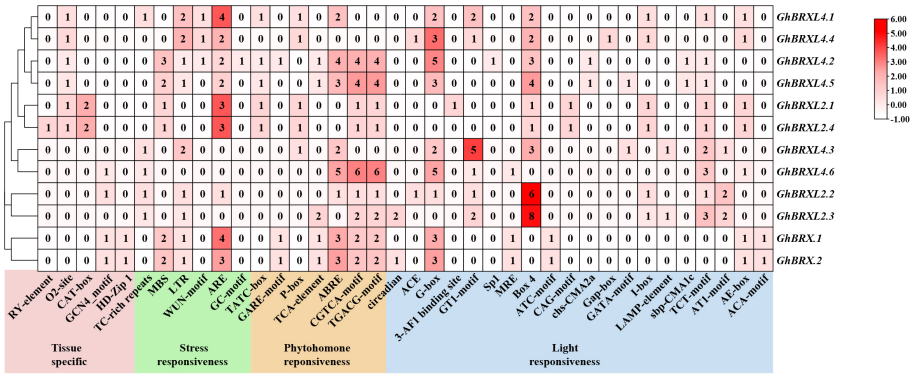

FIGURE 4
Cis-regulatory element prediction outcomes in the promoter regions of *GhBRX* gene family members. Shades and digits in the boxes denoted the number of *cis*-elements.

relatively abundant in most *GhBRX* genes. Light-responsive *cis*-elements, including Box 4, G-box, and TCT-motif, were present in all the *GhBRX* promoters. Among the light-responsive *cis*-acting regulatory elements, Box 4 and G-box were relatively more common. Taken together, these findings imply that *GhBRX* genes might be crucial for defense-related signaling, phytohormone responses, and abiotic stress responses.

3.6 Expression analysis of *BRX* genes in upland cotton

To determine the purpose of the *GhBRX* gene, we analyzed the expression profile data in the cotton functional database. Tissue-specific expression analysis indicated that the *GhBRX.1*, *GhBRX.2*, *GhBRXL2.3*, *GhBRXL4.1* and *GhBRXL4.4* genes were expressed mainly in roots; *GhBRXL2.2*, *GhBRXL4.2*, and *GhBRXL4.5* were expressed mainly in ovules; and *GhBRXL2.4*, *GhBRXL4.3* and *GhBRXL4.6* were expressed highly in fibers, pistils, and flowers, respectively (Figure 5A). According to the expression analysis, the response of five genes, namely, *GhBRX.1*, *GhBRXL2.1*, *GhBRXL2.4*, *GhBRXL4.3* and *GhBRXL4.6*, to abiotic stress significantly increased under salt treatment (Figure 5B). Under PEG stress, *GhBRX.2*, *GhBRXL4.2*, *GhBRXL4.3*, *GhBRXL4.5* and *GhBRXL4.6* were also significantly upregulated (Figure 5B). Under heat stress treatment, four genes were upregulated, namely, *GhBRXL4.1*, *GhBRXL4.2*, *GhBRXL4.3* and *GhBRXL4.6* (Figure 5C). Under cold stress treatment, *GhBRX.1* and *GhBRXL4.6* were upregulated, while *GhBRXL2.1* and *GhBRXL2.4* were downregulated (Figure 5C).

3.7 Expression of *GhBRX* genes in response to abiotic stresses

To further determine whether the level of *GhBRX* gene family expression was related to abiotic stress, we investigated the

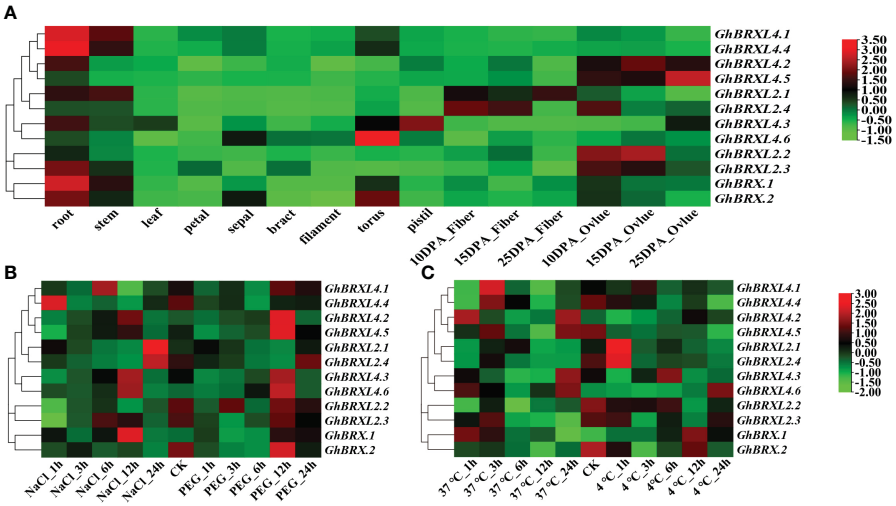

FIGURE 5
GhBRX gene expression patterns in distinct tissues and under four abiotic stimuli in upland cotton. **(A)** Expression patterns of 12 *GhBRX*s in various tissues. **(B)** Salt and PEG stress expression patterns of 12 *GhBRX*s. **(C)** Expression patterns of 12 *GhBRX*s under heat and cold stress.

10.3389/fpls.2024.1353365

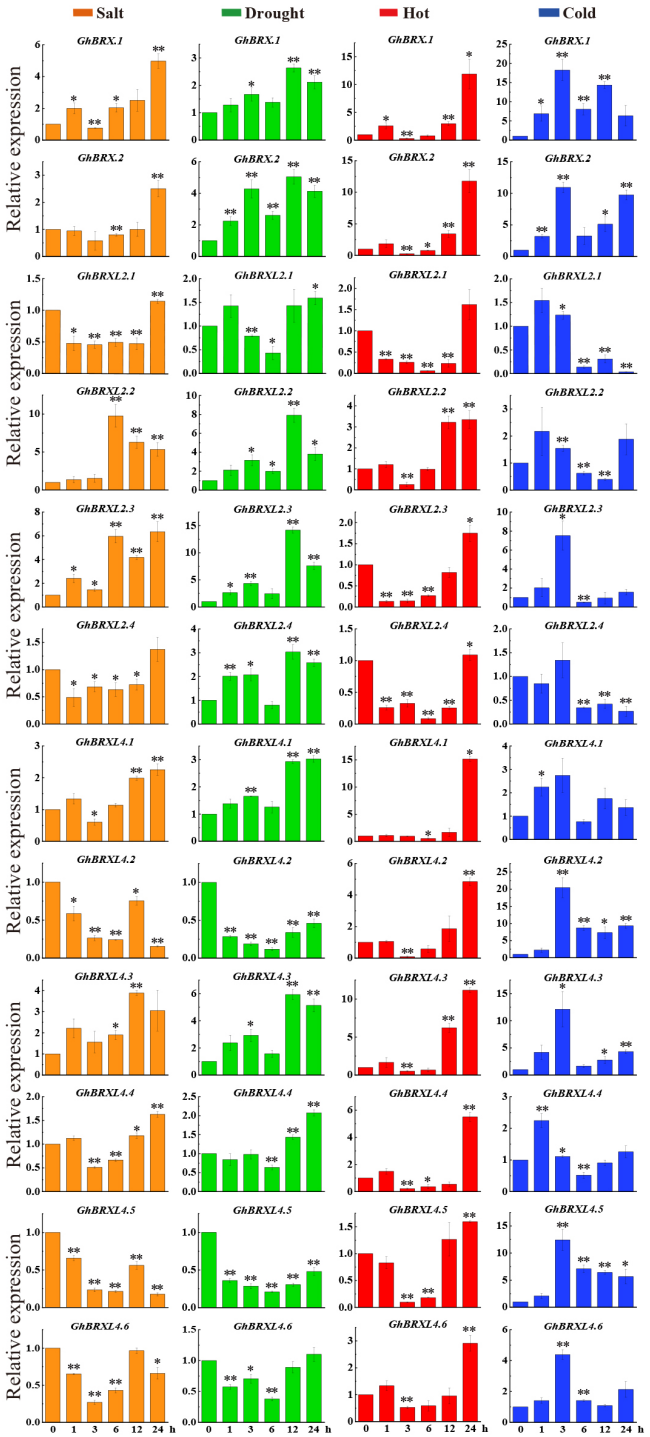

FIGURE 6
Relative *GhBRX*s expression levels in response to heat, cold, drought, and salt treatments. The standard deviations of the three biological replicates were represented by error bars. Orange denoted salt stress, green denoted drought stress, red denoted heat stress, and blue denoted cold stress. Asterisks were used to indicate a significant difference in expression compared to the control value (* P <0.05; * * P <0.01).

expression levels of 12 *GhBRX* genes via qRT–PCR. Seedlings leaves were sampled at five different stress periods (0, 1, 3, 6, 12 and 24 h) to analyze the expression of *GhBRX* genes under different abiotic stress conditions, including salt, drought, cold and heat stress (250 mM NaCl, 15% PEG, 12°C and 42°C). Under four different stresses (PEG, NaCl, cold, and heat), all the tested genes responded to at least one stress (Figure 6). Following a three-hour salt stress treatment, the expression levels of *GhBRX.1*, *GhBRX.2*, *GhBRXL2.4*, *GhBRXL4.1*, and *GhBRXL4.4* increased when the stress duration was extended. *GhBRXL4.5* and *GhBRXL4.6* exhibited increasing and then decreasing trends, respectively. After 3 h of drought stress treatment, the expression of *GhBRX.1*,

10.3389/fpls.2024.1353365

GhBRX.2, *GhBRXL2.2*, *GhBRXL2.3*, *GhBRXL2.4* and *GhBRXL4.3* first increased and then decreased, and that of *GhBRXL2.1*, *GhBRXL4.1*, *GhBRXL4.2*, *GhBRXL4.4*, *GhBRXL4.5* and *GhBRXL4.6* first decreased and then increased. *GhBRX.1*, *GhBRX.2*, *GhBRXL2.2*, *GhBRXL2.3*, *GhBRXL4.1*, *GhBRXL4.2*, *GhBRXL4.3*, *GhBRXL4.4*, *GhBRXL4.5* and *GhBRXL4.6* were subjected to high-temperature stress for 3 h, after which the expression levels increased with increasing duration of stress. Similarly, the expression of *GhBRX.1*, *GhBRX.2*, *GhBRXL4.2*, *GhBRXL4.3* and *GhBRXL4.5* significantly increased after 24 h of low-temperature stress treatment compared with that at 0 h. In summary, *GhBRX.1*, *GhBRX.2* and *GhBRXL4.3*, which are highly responsive to all four kinds of stress, were selected as stress candidate genes.

3.8 Knockdown of the *GhBRX.1*, *GhBRX.2*, and *GhBRXL4.3* genes reduces cotton resistance to salt and cold stress

We selected the *GhBRX.1*, *GhBRX.2*, and *GhBRXL4.3* genes for further investigation based on the transcriptome and qRT–PCR results. It is assumed that the *GhBRX.1*, *GhBRX.2* and *GhBRXL4.3* genes are potentially important in the regulation of the stress response. To test our hypothesis, we used the VIGS method to knock down the *GhBRX.1*, *GhBRX.2* and *GhBRXL4.3* genes by constructing the vectors TRV: *GhBRX.1*, TRV: *GhBRX.2* and TRV: *GhBRXL4.3*, respectively. TRV: *CLA* served as a positive control (Figures 7A, B). Ten days after VIGS, when albino plants were observed in the positive control group, the expression levels in the

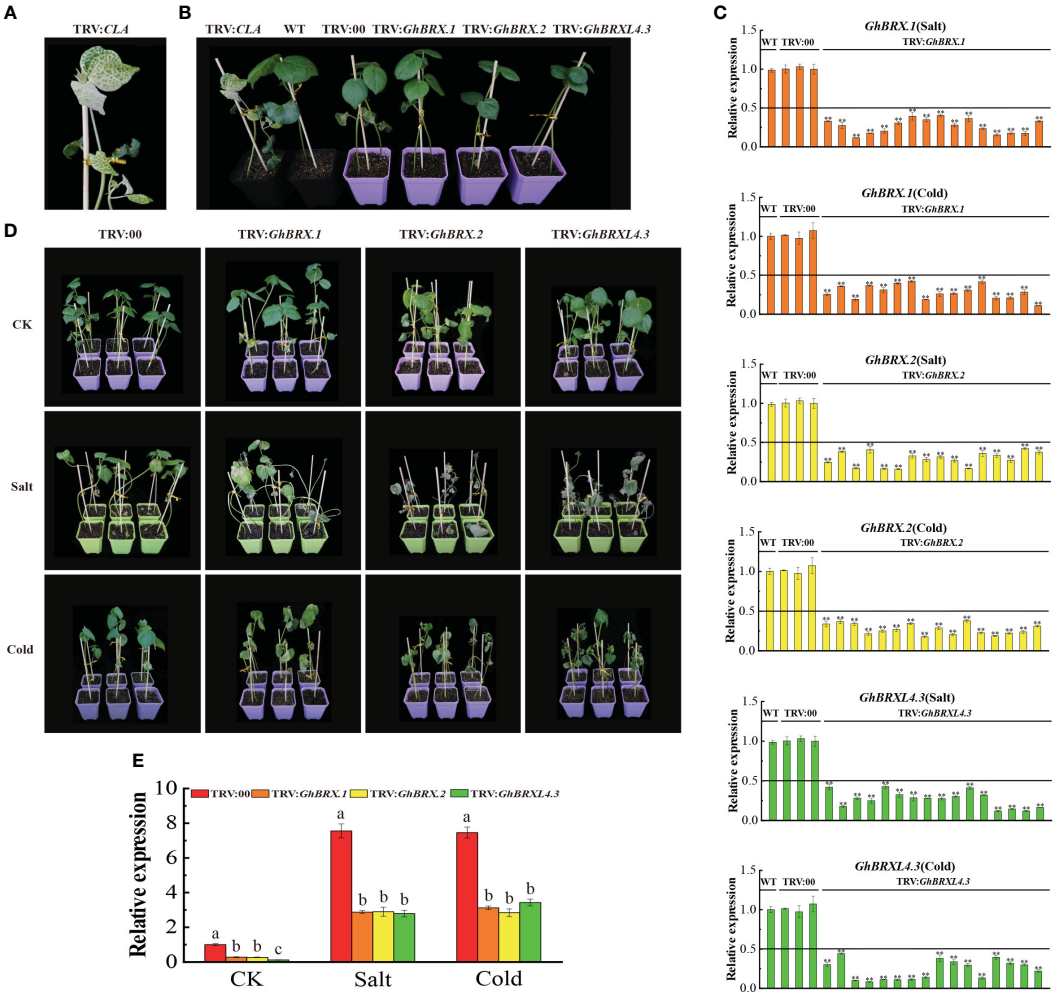

FIGURE 7
Silencing of *GhBRX.1*, *GhBRX.2* and *GhBRXL4.3* affects tolerance to salt and cold stress in upland cotton plants. **(A)** Positive control. **(B)** Representative VIGS images (TRV: *CLA*, WT, TRV: 00, TRV: *GhBRX.1*, TRV: *GhBRX.2*, and TRV: *GhBRXL4.3*). **(C)** The silencing efficiency of the WT, TRV: 00, TRV: *GhBRX.1*, TRV: *GhBRX.2* and TRV: *GhBRXL4.3* plants were tested for salt and cold stress, and the standard deviation determined from three separate experiments were represented by the error lines. **(D)** Phenotypes of the target gene-silenced plants in comparison to those of the control plants growing under normal growth conditions **(CK)** and under stress conditions (250 mmol/L NaCl, 12°C). **(E)** RT–qPCR analysis of changes in the expression levels of the *GhBRX.1*, *GhBRX.2* and *GhBRXL4.3* genes in target gene-silenced plants before and after stress treatment. "TRV: 00" represented plants carrying the empty vector control; "TRV: *GhBRX.1*, TRV: *GhBRX.2*, and TRV: *GhBRXL4.3*" represented plants with *GhBRX.1*, *GhBRX.2* and *GhBRXL4.3* silenced, respectively. The error line represented the standard deviation calculated from three independent experiments. Asterisks indicated a t test for statistically significant differences (* * P <0.01). Significant changes between control and gene-silenced plants were indicated by different letters (ANOVAs; P<0.05).

leaves of the VIGS-silenced and control plants were determined via qRT–PCR. The qRT–PCR results showed that *GhBRX.1*, *GhBRX.2* and *GhBRXL4.3* were effectively repressed (Figure 7C). Silenced plants (TRV: *GhBRX.1*, TRV: *GhBRX.2*, TRV: *GhBRXL4.3*) and control plants (TRV: 00) were treated under different abiotic stress conditions, and the silenced plants showed more severe wilting after two weeks of salt and cold stress treatment (Figure 7D). Compared with those in control plants (TRV: 00), the expression levels of *GhBRX.1*, *GhBRX.2* and *GhBRXL4.3* were significantly lower after 0 days (CK) and 8 days (salt and low temperature) in the silenced plants (TRV: *GhBRX.1*, TRV: *GhBRX.2*, TRV: *GhBRXL4.3*) (Figure 7E). Taken together, these findings showed that cotton tolerance to cold and salt stress was decreased by silencing *GhBRX.1*, *GhBRX.2*, and *GhBRXL4.3*.

3.9 Physiological and biochemical indices of *GhBRX.1*-, *GhBRX.2*-, and *GhBRXL4.3*-silenced plants under salt and cold stress

Plants with silenced target genes were less resistant to salt and cold stress. To investigate the impact of salt and cold stress on the silenced plants, we determined the activities of the reactive oxygen species (ROS) scavenger enzymes SOD, POD, and CAT and the MDA, soluble sugar and chlorophyll contents in the leaves before and 8 days after salt or cold stress. Under normal growth conditions, there was no significant difference in physiological parameters between the silenced plants (TRV: *GhBRX.1*, TRV: *GhBRX.2*, TRV: *GhBRXL4.3*) and the control plants (TRV:00). After 8 days of salt and cold stress, the SOD, POD and CAT activities of the silenced plants (TRV: *GhBRX.1*, TRV: *GhBRX.2*, and TRV: *GhBRXL4.3*) were significantly lower than those of the control plants (TRV: 00) (Figures 8A–C), indicating that the VIGS-silenced plants suffered extensive oxidative damage. The contents of soluble sugars and chlorophyll in the silenced plants were significantly lower than those in the control plants, while the content of MDA in the silenced plants was significantly greater than that in the control plants (Figures 8D–F), indicating that the resistance of the silenced plants decreased under adverse conditions and that the degree of adverse damage increased. The results showed that the silenced plants were very sensitive to salt stress and cold stress and that silencing the *GhBRX.1*, *GhBRX.2* and *GhBRXL4.3* genes significantly reduced their ability to tolerate salt stress and cold stress.

3.10 Expression analysis of stress-responsive genes in control and targeted gene-silenced plants under salt and cold conditions

The nine genes associated with tolerance to salt stress or low-temperature stress were selected for analysis of the response characteristics of the control and targeted gene-silenced plants under salt and cold conditions. The nine genes included *GhSOS1* (Na^+/H^+ antiporter salt overly sensitive 1), *GhSOS2* (salt overly sensitive 2), *GhNHX1* (Na^+/H^+ antiporter), *GhCIPK6* (Ser/Thr protein kinase 6), *GhBIN2* (glycogen synthase kinase 3 (GSK3)-like kinase), *GhSnRK2.6* (SnRK2 protein kinase), *GhHDT4D* (a member of the HD2 subfamily of histone deacetylases), *GhCBF1* (C-repeat binding factor) and *GhPP2C* (protein phosphatase 2C). The expression levels of these nine genes were high in the leaves of the control plants but were significantly lower in the targeted gene-silenced plants under salt or cold stress (Figure 9). The downregulated expression of these genes indicated that the plants were very sensitive to salt and cold stress and had a significantly reduced ability to tolerate various abiotic stress factors, resulting in greater oxidative damage.

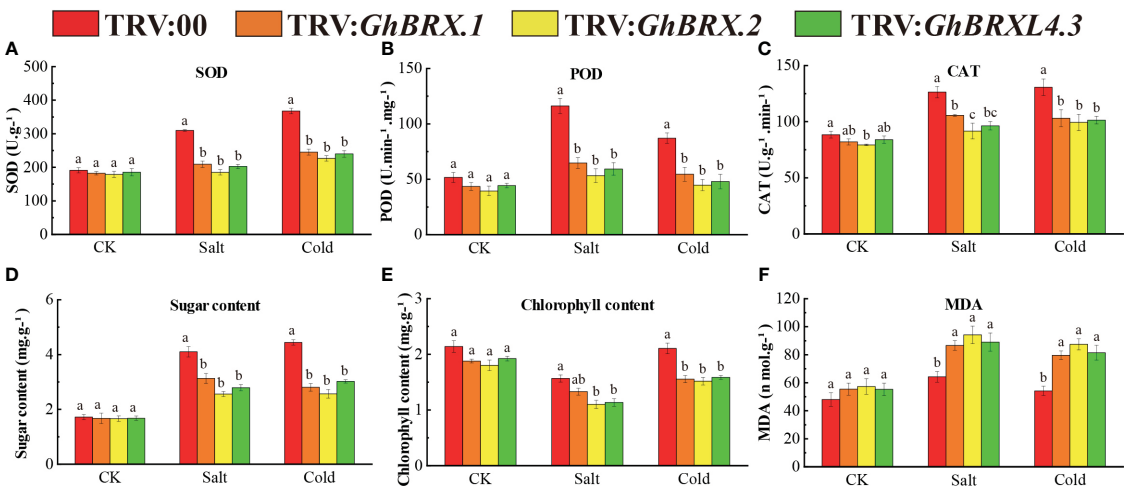

FIGURE 8
Determination of antioxidant enzyme activities and soluble sugar, chlorophyll and MDA concentrations in *GhBRX.1*-, *GhBRX.2*- and *GhBRXL4.3*-silenced plants and control plants under abiotic stress: **(A)** SOD activity; **(B)** POD activity; **(C)** CAT activity; **(D)** soluble sugar content; **(E)** chlorophyll activity; **(F)** MDA concentration. The standard deviation of three biological replicates were shown by error bars. Significant changes between control and gene-silenced plants were indicated by different letters (ANOVA; $P < 0.05$).

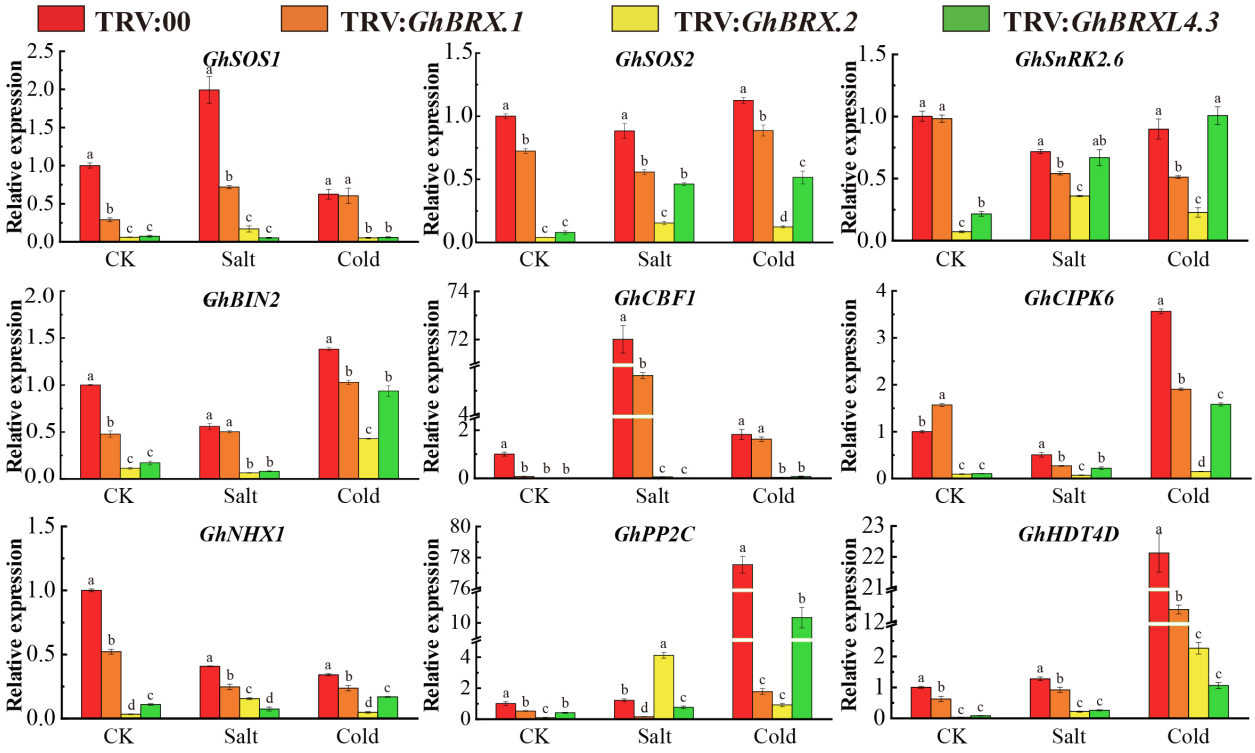

FIGURE 9
Expression of stress-responsive genes associated with salt stress tolerance or cold stress tolerance in control and silenced plants before and after stress. The error line represents the standard deviation calculated from three independent experiments. Significant changes between control and gene-silenced plants were indicated by different letters (ANOVA; $P < 0.05$).

4 Discussion

Drought, high temperature, salinity, and cold are all environmental stressors that harm plant growth and output (Suzuki et al., 2014), change the internal balance within plants, and affect all biological and physiological activities within plants (Aasamaa and Sõber, 2011). Therefore, it is crucial to develop new varieties with enhanced performance and maintain and improve cotton production (Kuppu et al., 2013; Kirungu et al., 2019; Hajihashemi et al., 2020; Li et al., 2021). *BRX* is involved in the control of plant embryonic development, root and bud growth, tiller angle and stomatal development (Scacchi et al., 2009; Beuchat et al., 2010b; Liu et al., 2010; Li et al., 2019; Rowe et al., 2019; Zhang Y. et al., 2021; Tiwari et al., 2023). Further studies have shown that *BRX* regulates crosstalk between signaling pathways of various phytohormones, including BRs, auxin, ABA and cytokinin (Mouchel et al., 2006; Li et al., 2009; Rodrigues et al., 2009). The *BRX* gene family in rice may be implicated in BR and auxin signaling, and *BRX* genes respond differently to abiotic stress and may play a role in the abiotic stress response (Liu et al., 2010). *TaBRXL1* is involved primarily in developmental processes, whereas *TaBRXL2* is extensively regulated by hormones, development, and other abiotic stressors (Tiwari et al., 2023).

Although *BRX* genes have been found throughout the genomes of many plant species, only rice (Liu et al., 2010) and wheat (Tiwari et al., 2023) have been found to contain evidence of their possible roles in stress adaptation. The *BRX* gene has not been identified in cotton, and its function in cotton has rarely been studied. By using the AtBRX protein as a query, we identified 12, 6 and 6 *BRX* gene family members in *G. hirsutum*, *G. raimondii* and *G. arboreum*, respectively. There are 5 *BRX* genes in *Arabidopsis* and rice, 10 *in B. rapa*, and 13 in *T. aestivum* (Briggs et al., 2006; Liu et al., 2010; Zhang Y. et al., 2021; Tiwari et al., 2023). The monocots wheat and rice clustered together with stronger homology. Among the dicotyledonous plants, the three cotton species exhibited greater similarity and formed a cluster. The allotetraploid cotton species *G. hirsutum* is the product of the doubling of the ancestral cross between two diploid cotton species, *G. raimondii* and *G. arboreum*, according to a phylogenetic tree study. Research has demonstrated that sequence similarities across genes belonging to the same taxonomic category can result in similar activities (Nan et al., 2021). The gene structure of the *GhBRX* genes is largely conserved between orthologous genes. Homologs of *GhBRX*, *GhBRX2* and *GhBRXL4* are predicted to have exons similar to those reported for *AtBRX*, *AtBRXL2* and *AtBRXL4*. The GhBRX proteins have similar MEME motifs. A few motifs have varying copy numbers in different proteins, and some motifs share two or more proteins, which could account for the functional discrepancies described among BRX family proteins.

The primary mechanism of gene family expansion is gene duplication. Segment and tandem repeats are thought to be the primary drivers of gene family expansion in plants (Cannon et al., 2004; Flagel and Wendel, 2009). Twenty segmentally duplicated genes and one tandemly duplicated gene were identified in the *GhBRX* gene family. Therefore, our study points to segmental duplication as the primary cause of the increase in *GhBRX*s. One

technique for researching gene evolution and relationships is to analyze the collinearity of various species (Yu et al., 2020). The results of intergenomic symbiosis analysis between upland cotton and the other two cotton species were compared to acquire better knowledge of the homologous gene functions and evolutionary linkages of the genes. The results indicate that *BRX* gene duplication events and chromosomal rearrangements may be conserved in cotton given the numbers of *G. raimondii* and *G. arboreum*. Analysis revealed the same number of direct homologous gene pairs between *G. hirsutum* and *G. raimondii* and *G. arboreum*, indicating high conservation of *BRX* genes in cotton. To study the differences after gene duplication, the *Ka* and *Ks* values of the replicated *GhBRX* genes in upland cotton were calculated. The results showed that the *Ka/Ks* ratio of all the duplicate *GhBRX* gene pairs was <1, indicating that the *GhBRX* gene family experienced selection pressure during evolution.

Identification and characterization of *cis*-regulatory DNA sequences in response to coordinated developmental and environmental cues are critical for plant biology (Schmitz et al., 2022). We isolated the upstream promoter segments of the candidate genes and examined the distribution of *cis*-acting elements in the promoter region of *GhBRX* to gain additional insight into the potential role of *GhBRX* in upland cotton under various environmental conditions. In the present study, 38 *cis*-acting elements (those involved in stress responsiveness, tissue specificity, plant hormone responsiveness, and photoresponsiveness) were confirmed within the promoters of the *GhBRX*s. Photoresponsive elements are widely found in plants; for example, AT-rich G-boxes, GT1, Box 4, and I-boxes are commonly present in photoinducible promoters (Lam and Chua, 1989; Gilmartin et al., 1992; Foster et al., 1994). The upland cotton genes *GhBRX.1*, *GhBRX.2*, and *GhBRXL4.3* were highly expressed in roots, and *GhBRXL4.3* was also strongly expressed in pistils. These findings were based on the prediction of *cis*-elements in *GhBRX* genes and RNAseq expression data. The *GhBRX* gene promoter contains *cis*-acting regions linked to the abiotic stress response, including MBS (drought-induced MYB junction) and LTR (*cis*-acting element of cold responsiveness), suggesting that the regulation of drought and cold stress in cotton may be mediated by *GhBRX* genes. The presence of *cis*-elements in the promoter regions of genes provides clues to the spatiotemporal and hormonal regulation of genes and their response to different environmental stresses. We studied the expression of *GhBRX*s in various cotton leaves under normal and abiotic stress conditions to better understand the use of *GhBRX*s in cotton growth and abiotic stress resistance. The transcriptomic data of *GhBRX* genes in leaves under abiotic stress were obtained from the RNA-seq data of Zhejiang University, and most of the *GhBRX* genes responded to at least one stressor. In addition, to confirm the prior transcriptome findings, *GhBRX* transcript levels under abiotic stress were evaluated using quantitative RT–PCR. Quantitative RT–PCR analysis revealed that the expression of the *GhBRX.1*, *GhBRX.2* and *GhBRXL4.3* genes was significantly upregulated 24 h after the four stress treatments. *GhBRXL2.2*, *GhBRXL2.3* and *GhBRXL4.1* were significantly elevated under salt and drought stress, while *GhBRXL4.2* was significantly elevated under both heat and cold stress. These findings suggested that these genes may play a significant biological role in enhancing upland cotton tolerance to abiotic stress.

Since genes were significantly upregulated under all four stress treatments, to further explore the role of the *GhBRX.1*, *GhBRX.2* and *GhBRXL4.3* genes in abiotic stress regulation in upland cotton, we constructed a VIGS vector for further functional analysis. We treated the silenced plants with abiotic stress (salt, drought, high temperature and low temperature) and found that the silenced plants were more sensitive to salt stress and low-temperature stress, and the silenced plants exhibited a more obvious phenotype and water loss phenotype. These findings may indicate that the *GhBRX.1*, *GhBRX.2* and *GhBRXL4.3* genes may play significant biological roles in enhancing tolerance to salt and cold stress in cotton plants. To investigate the stress-related mechanisms of these three genes, we analyzed the physiological and biochemical indicators, including ROS scavenger enzyme (SOD, POD, CAT) activities and MDA, soluble sugar and chlorophyll contents, of silenced plants and control plants before and after stress. The induction of salt stress and cold stress leads to the overproduction of ROS and other oxygen radicals, leading to oxidative destruction of plant cell structure and their components and eventually plant death; antioxidant defense systems work together to control uncontrolled oxidative cascades and protect plant cells from oxidative damage by removing ROS (Gill and Tuteja, 2010; Malhan et al., 2015). Therefore, the removal of excess ROS is a key process for plant protection against salt stress and cold stress (Zhang et al., 2011; Ullah et al., 2018). Essential ROS scavenging enzymes include SOD, POD, and CAT, whose activities increase in plants exposed to cold and salt stress (Salih et al. 2024). The results showed that SOD, POD, and CAT enzyme activities increased significantly after stress due to the overproduction of plant ROS in upland cotton, and the ability to eliminate ROS was significantly reduced after the silencing of *GhBRX.1*, *GhBRX.2* and *GhBRXL4.3*. Therefore, after stress, the SOD, POD and CAT activities of the *GhBRX.1*-, *GhBRX.2*- and *GhBRXL4.3*-silenced plants significantly decreased compared with those of the control plants. The MDA concentration is a crucial indicator of the body's ability to respond to antioxidants and can also be used to infer the extent of cell damage (Yu et al., 2016). The soluble sugar content can reflect not only the growth status of crops but also their quality (Jiang et al., 2020). After stress, the degree of oxidative damage to the cotton plants increased, the MDA content of the silenced plants increased, and the soluble sugar and chlorophyll contents decreased, indicating that the VIGS-mediated silencing of these plants increased cell damage and decreased quality. This further revealed the important role of the proteins encoded by the *GhBRX.1*, *GhBRX.2* and *GhBRXL4.3* genes in enhancing salt tolerance and low-temperature tolerance in cotton.

Finally, we examined the expression levels of nine known stress response genes, *GhSOS1*, *GhSOS2*, *GhNHX1*, *GhCIPK6*, *GhBIN2*, *GhSnRK2.6*, *GhHDT4D*, *GhCBF1* and *GhPP2C*, in the leaf tissue of VIGS and control plants (TRV:00) under salt and cold stress conditions. Under salt and cold stress conditions, most stress-related genes exhibited considerable downregulation. The *SOS1* and *SOS2* genes can improve the salt tolerance of transgenic plants (Liu et al., 2000; Yue et al., 2012). Before and after salt stress, the expression of both *GhSOS1* and *GhSOS2*, including *GhBRX.2* and *GhBRXL4.3*, was downregulated, and the two gene-silenced plants were the most significantly downregulated. The *SnRK2.6* and *CBF1* genes play important roles in improving salt and cold tolerance in plants under stress (Novillo et al., 2007; Song

et al., 2016; Wang et al., 2018; Yan et al., 2023). *PCaP2* can activate the *CBF* and *SnRK2* transcriptional networks and play an important role in cold stress tolerance (Wang et al., 2018). When subjected to salt and cold stress, although *GhSnRK2.6* was not significantly expressed in the *GhBRXL4.3* gene-silenced plants, both *GhSnRK2.6* and *GhCBF1* were downregulated in the VIGS-treated plants. *BIN2* interacts with and phosphorylates the *CBF EXPRESSION1* inducer (*ICE1*) to inhibit *SOS2* kinase activity and further inhibit the salt stress response, thus negatively regulating salt stress and low-temperature stress (Ye et al., 2019). Similarly, compared with that in the absence of stress, *GhBIN2* expression in silenced plants was broadly upregulated. The *CIPK6*, *NHX1*, *PP2C* and *HDT4D* genes play important roles in salt stress tolerance and cold stress and can be used to regulate growth and development and improve crop tolerance to salt and low-temperature stress (Teakle et al., 2010; Chen et al., 2013; Dubrovina et al., 2015; Imran et al., 2020; Zhang Y. et al., 2021; Zhu et al., 2022; Wu et al., 2023). Compared with those in control plants, except for in *GhBRX.2* gene-silenced plants, the expression of the *CIPK6*, *NHX1*, *PP2C* and *HDT4D* genes was significantly lower in VIGS-treated plants. The expression of stress-related genes in VIGS–generated cotton leaves revealed that silencing *GhBRX.1*, *GhBRX.2*, and *GhBRXL4.3* affected the expression of genes involved in the cotton stress response under salt and cold stress conditions, suggesting that *BRX* genes play an important role in upland cotton tolerance to salt and cold stress.

5 Conclusion

In summary, the cotton genome encodes 24 highly conserved *BRX* genes. The *BRX* genes in upland cotton have similar gene structures. Multiple *cis*-acting regions linked with hormonal or abiotic stress responses can be found in the *GhBRX* promoter sequence. qRT–PCR data also showed that different abiotic stresses could induce *GhBRX* expression. Further functional characterization of *GhBRX.1*, *GhBRX.2* and *GhBRXL4.3* by VIGS indicated that silencing of the *GhBRX.1*, *GhBRX.2* and *GhBRXL4.3* genes may weaken the response of cotton to salt and low-temperature stress. This work could lead to additional research on the function of *GhBRX*s in the cotton response and resistance to abiotic stress.

Data availability statement

The datasets presented in this study can be found in online repositories. The names of the repository/repositories and accession number(s) can be found in the article/Supplementary Material.

Author contributions

WW: Writing – original draft, Writing – review & editing, Data curation, Formal Analysis, Investigation, Validation, Visualization, Conceptualization, Methodology, Project administration, Software, Supervision. JJ: Validation, Writing – review & editing, Software. XuZ: Writing – review & editing. PL: Writing – review & editing, Validation. JL: Writing – review & editing, Validation. YL: Writing – review & editing, Validation. WX: Writing – review & editing, Validation. JS: Writing – review & editing, Funding acquisition, Resources, Supervision. XiZ: Writing – review & editing, Funding acquisition, Resources, Supervision. CW: Writing – review & editing, Formal Analysis, Funding acquisition, Resources, Supervision.

Funding

The author(s) declare financial support was received for the research, authorship, and/or publication of this article. This research was funded by the State Key Laboratory of Aridland Crop Science, Gansu Agricultural University (GSCS-2019-10); the Natural Science Foundation of Xinjiang Uygur Autonomous Region (Project Nos. 2022D01E103 and 2023D01A015); and the Project for Postdoctoral and High-level Flexible Talents of Xinjiang Uygur Autonomous Region (Grant. No: RSSQ00066509); Changji Prefecture "Two Districts" Science and Technology Development Plan Project: (No: 2023LQG04); Major Science and Technology Program of Changji Hui Autonomous Prefecture (Grant. No: 2021Z01-01); Central Leading Local Science and Technology Development Fund Project of Xinjiang Uygur Autonomous Region (No: ZYYD2023C06).

Acknowledgments

The author is especially special thanks to Qifeng Ma, Institute of Cotton Research of CAAS, for the TRV vectors and Yonglin Yang, Shihezi Academy of Agricultural Sciences, for the cotton seeds of XinshiK25.

Conflict of interest

The authors declare that the research was conducted in the absence of any commercial or financial relationships that could be construed as potential conflicts of interest.

Publisher's note

Supplementary material

The Supplementary Material for this article can be found online at: https://www.frontiersin.org/articles/10.3389/fpls.2024.1353365/full#supplementary-material

References

Aasamaa, K., and Sõber, A. (2011). Stomatal sensitivities to changes in leaf water potential, air humidity, CO_2 concentration and light intensity, and the effect of abscisic acid on the sensitivities in six temperate deciduous tree species. *Environ. Exp. Bot.* 71 (1), 72–78. doi: 10.1016/j.envexpbot.2010.10.013

Bailey, T. L., Boden, M., Buske, F. A., Frith, M., Grant, C. E., Clementi, L., et al. (2009). MEME SUITE: tools for motif discovery and searching. *Nucleic Acids Res.* 37 (suppl_2), W202–W208. doi: 10.1093/nar/gkp335

Bari, R., and Jones, J. D. (2009). Role of plant hormones in plant defence responses. *Plant Mol. Biol.* 69, 473–488. doi: 10.1007/s11103-008-9435-0

Beers, R. F., and Sizer, I. W. (1952). A spectrophotometric method for measuring the breakdown of hydrogen peroxide by catalase. *J. Biol. Chem.* 195 (1), 133–140. doi: 10.1016/S0021-9258(19)50881-X

Beuchat, J., Li, S., Ragni, L., Shindo, C., Kohn, M. H., and Hardtke, C. S. (2010a). A hyperactive quantitative trait locus allele of *Arabidopsis BRX* contributes to natural variation in root growth vigor. *Proc. Natl. Acad. Sci. U.S.A.* 107 (18), 8475–8480. doi: 10.1073/pnas.0913207107

Beuchat, J., Scacchi, E., Tarkowska, D., Ragni, L., Strnad, M., and Hardtke, C. S. (2010b). *BRX* promotes *Arabidopsis* shoot growth. *New Phytol.* 188 (1), 23–29. doi: 10.1111/j.1469-8137.2010.03387.x

Briggs, G. C., Mouchel, C. F., and Hardtke, C. S. (2006). Characterization of the plant-specific *BREVIS RADIX* gene family reveals limited genetic redundancy despite high sequence conservation. *Plant Physiol.* 140 (4), 1306–1316. doi: 10.1104/pp.105.075382

Cannon, S. B., Mitra, A., Baumgarten, A., Young, N. D., and May, G. (2004). The roles of segmental and tandem gene duplication in the evolution of large gene families in. *Arabidopsis thaliana. BMC Plant Biol.* 4 (1), 1–21. doi: 10.1186/1471-2229-4-10

Castro, D., Contreras, L. M., Kurz, L., and Wilkesman, J. (2017). "Detection of guaiacol peroxidase on electrophoretic gels," in *Zymography: methods mol. Biol.*, vol. 1626. (New York, NY: Humana Press). doi: 10.1007/978-1-4939-7111-4_18

Chen, C., Chen, H., He, Y., and Xia, R. (2018). TBtools, a toolkit for biologists integrating various biological data handling tools with a user-friendly interface. *BioRxiv* 289660 (10.1101), 289660. doi: 10.1101/289660

Chen, C., Chen, H., Zhang, Y., Thomas, H. R., Frank, M. H., He, Y., et al. (2020). TBtools: an integrative toolkit developed for interactive analyses of big biological data. *Plant Mol.* 13 (8), 1194–1202. doi: 10.1016/j.molp.2020.06.009

Chen, L., Wang, Q. Q., Zhou, L., Ren, F., Li, D. D., and Li, X. B. (2013). *Arabidopsis* CBL-interacting protein kinase (CIPK6) is involved in plant response to salt/osmotic stress and ABA. *Mol. Biol. Rep.* 40, 4759–4767. doi: 10.1007/s11033-013-2572-9

Dubrovina, A. S., Kiselev, K. V., Khristenko, V. S., and Aleynova, O. A. (2015). *VaCPK20*, a calcium-dependent protein kinase gene of wild grapevine *Vitis amurensis* Rupr., mediates cold and drought stress tolerance. *J. Plant Physiol.* 185, 1–12. doi: 10.1016/j.jplph.2015.05.020

El-Gebali, S., Mistry, J., Bateman, A., Eddy, S. R., Luciani, A., Potter, S. C., et al. (2019). The Pfam protein families database in 2019. *Nucleic Acids Res.* 47 (D1), D427–D432. doi: 10.1093/nar/gky995

Flagel, L. E., and Wendel, J. F. (2009). Gene duplication and evolutionary novelty in plants. *New Phytol.* 183 (3), 557–564. doi: 10.1111/j.1469-8137.2009.02923.x

Foster, R., Izawa, T., and Chua, N. H. (1994). Plant bZIP proteins gather at ACGT elements. *FASEB J.* 8 (2), 192–200. doi: 10.1096/fasebj.8.2.8119490

Gao, W., Long, L., Zhu, L. F., Xu, L., Gao, W. H., Sun, L. Q., et al. (2013). Proteomic and virus-induced gene silencing (VIGS) analyses reveal that gossypol, brassinosteroids, and jasmonic acid contribute to the resistance of cotton to. *Verticillium dahliae. Mol. Cell Proteomics* 12 (12), 3690–3703. doi: 10.1074/mcp.M113.031013

Giannopolitis, C. N., and Ries, S. K. (1977). Superoxide dismutases: II. Purification and quantitative relationship with water-soluble protein in seedlings. *Plant Physiol.* 59 (2), 315–318. doi: 10.1104/pp.59.2.315

Gill, S. S., and Tuteja, N. (2010). Reactive oxygen species and antioxidant machinery in abiotic stress tolerance in crop plants. *Plant Physiol. Biochem.* 48 (12), 909–930. doi: 10.1073/pnas.95.12.6705

Gilmartin, P. M., Memelink, J., Hiratsuka, K., Kay, S. A., and Chua, N. H. (1992). Characterization of a gene encoding a DNA binding protein with specificity for a light-responsive element. *Plant Cell* 4 (7), 839–849. doi: 10.1105/tpc.4.7.839

Hajihashemi, S., Brestic, M., Landi, M., and Skalicky, M. (2020). Resistance of *Fritillaria imperialis* to freezing stress through gene expression, osmotic adjustment and antioxidants. *Sci. Rep.* 10 (1), 10427. doi: 10.1038/s41598-020-63006-7

Hasanuzzaman, M., Bhuyan, M. B., Zulfiqar, F., Raza, A., Mohsin, S. M., Mahmud, J. A., et al. (2020). Reactive oxygen species and antioxidant defense in plants under abiotic stress: Revisiting the crucial role of a universal defense regulator. *Antioxidants* 9 (8), 681. doi: 10.3390/antiox9080681

Imran, M., Shafiq, S., Naeem, M. K., Widemann, E., Munir, M. Z., Jensen, K. B., et al. (2020). *Histone deacetylase* (*HDAC*) gene family in allotetraploid cotton and its diploid progenitors: In silico identification, molecular characterization, and gene expression analysis under multiple abiotic stresses, DNA damage and phytohormone treatments. *Int. J. Mol. Sci.* 21 (1), 321. doi: 10.3390/ijms21010321

Jiang, W., Li, N., Zhang, D., Meinhardt, L., Cao, B., Li, Y., et al. (2020). Elevated temperature and drought stress significantly affect fruit quality and activity of anthocyanin-related enzymes in jujube (*Ziziphus jujuba* Mill. cv. 'Lingwuchangzao'). *PloS One* 15 (11), e0241491. doi: 10.1371/journal.pone.0241491

John, M. E., and Crow, L. J. (1992). Gene expression in cotton (*Gossypium hirsutum* L.) fiber: cloning of the mRNAs. *Proc. Natl. Acad. Sci. U.S.A.* 89 (13), 5769–5773. doi: 10.1073/pnas.89.13.5769

Kirungu, J. N., Magwanga, R. O., Lu, P., Cai, X., Zhou, Z., Wang, X., et al. (2019). Functional characterization of *Gh_A08G1120* (*GH3.5*) gene reveal their significant role in enhancing drought and salt stress tolerance in cotton. *BMC Genom.* 20, 1–17. doi: 10.1186/s12863-019-0756-6

Koh, S. W., Marhava, P., Rana, S., Graf, A., Moret, B., Bassukas, A. E., et al. (2021). Mapping and engineering of auxin-induced plasma membrane dissociation in BRX family proteins. *Plant Cell* 33 (6), 1945–1960. doi: 10.1093/plcell/koab076

Kumar, S., Stecher, G., and Tamura, K. (2016). MEGA7: molecular evolutionary genetics analysis version 7.0 for bigger datasets. *Mol. Biol. Evol.* 33 (7), 1870–1874. doi: 10.1093/molbev/msw054

Kuppu, S., Mishra, N., Hu, R., Sun, L., Zhu, X., Shen, G., et al. (2013). Water-deficit inducible expression of a cytokinin biosynthetic gene *IPT* improves drought tolerance in cotton. *PloS One* 8 (5), e64190. doi: 10.1371/journal.pone.0064190

Lam, E., and Chua, N. H. (1989). ASF-2: a factor that binds to the cauliflower mosaic virus 35S promoter and a conserved GATA motif in *Cab* promoters. *Plant Cell* 1 (12), 1147–1156. doi: 10.1105/tpc.1.12.1147

Li, J., Mo, X., Wang, J., Chen, N., Fan, H., Dai, C., et al. (2009). *BREVIS RADIX* is involved in cytokinin-mediated inhibition of lateral root initiation in *Arabidopsis*. *Planta* 229, 593–603. doi: 10.1007/s00425-008-0854-6

Li, X. T., Feng, X. Y., Zeng, Z., Liu, Y., and Shao, Z. Q. (2021). Comparative analysis of *HSF* genes from *Secale cereale* and its Triticeae relatives reveal ancient and recent gene expansions. *Front. Genet.* 12. doi: 10.3389/fgene.2021.801218

Li, Z., Liang, Y., Yuan, Y., Wang, L., Meng, X., Xiong, G., et al. (2019). *OsBRXL4* regulates shoot gravitropism and rice tiller angle through affecting LAZY1 nuclear localization. *Plant Mol.* 12 (8), 1143–1156. doi: 10.1016/j.molp.2019.05.014

Lichtenthaler, H. K., and Wellburn, A. R. (1983). Determinations of total carotenoids and chlorophylls a and b of leaf extracts in different solvents. *Biochem. Soc Trans.* 11, 591–592. doi: 10.1042/BST0110591

Liu, H., Jiang, W., Cao, J., and Ma, L. (2018). A combination of 1-methylcyclopropene treatment and intermittent warming alleviates chilling injury and affects phenolics and antioxidant activity of peach fruit during storage. *Sci. Hortic.* 229, 175–181. doi: 10.1016/j.scienta.2017.11.010

Liu, J., Ishitani, M., Halfter, U., Kim, C. S., and Zhu, J. K. (2000). The *Arabidopsis thaliana SOS2* gene encodes a protein kinase that is required for salt tolerance. *Proc. Natl. Acad. Sci. U.S.A.* 97 (7), 3730–3734. doi: 10.1073/pnas.97.7.3730

Liu, J., Liang, D., Song, Y., and Xiong, L. (2010). Systematic identification and expression analysis of *BREVIS RADIX*-like homologous genes in rice. *Plant Sci.* 178 (2), 183–191. doi: 10.1016/j.plantsci.2009.11.009

Livak, K. J., and Schmittgen, T. D. (2001). Analysis of relative gene expression data using real-time quantitative PCR and the $2^{-\Delta\Delta C_T}$ method. *Methods* 25 (4), 402–408. doi: 10.1006/meth.2001.1262

Malhan, D., Bhatia, S., and Yadav, R. K. (2015). Genome wide gene expression analyses of *Arabidopsis* shoot stem cell niche cell populations. *Plant Signal. Behav.* 10 (4), e1011937. doi: 10.1080/15592324.2015.1011937

Mouchel, C. F., Briggs, G. C., and Hardtke, C. S. (2004). Natural genetic variation in *Arabidopsis* identifies *BREVIS RADIX*, a novel regulator of cell proliferation and elongation in the root. *Genes Dev.* 18 (6), 700–714. doi: 10.1101/gad.1187704

Mouchel, C. F., Osmont, K. S., and Hardtke, C. S. (2006). *BRX* mediates feedback between brassinosteroid levels and auxin signalling in root growth. *Nature* 443 (7110), 458–461. doi: 10.1038/nature05130

Nan, H., Lin, Y., Wang, X., and Gao, L. (2021). Comprehensive genomic analysis and expression profiling of cysteine-rich polycomb-like transcription factor gene family in tea tree. *Hortic. Plant J.* 7 (5), 469–478. doi: 10.1016/j.hpj.2021.03.001

Nian, L., Zhang, X., Yi, X., Liu, X., Nu, A., Yang, Y., et al. (2021). Genome-wide identification of ABA receptor *PYL*/*RCAR* gene family and their response to cold stress in *Medicago sativa* L. *Physiol. Mol. Biol. Plants* 27, 1979–1995. doi: 10.1007/s12298-021-01066-3

Novillo, F., Medina, J., and Salinas, J. (2007). *Arabidopsis CBF1* and *CBF3* have a different function than *CBF2* in cold acclimation and define different gene classes in the *CBF* regulon. *Proc. Natl. Acad. Sci. U.S.A.* 104 (52), 21002–21007. doi: 10.1073/pnas.0705639105

Potters, G., Pasternak, T. P., Guisez, Y., Palme, K. J., and Jansen, M. A. (2007). Stress-induced morphogenic responses: growing out of trouble? *Trends Plant Sci.* 12 (3), 98–105. doi: 10.1016/j.tplants.2007.01.004

Rodrigues, A., Santiago, J., Rubio, S., Saez, A., Osmont, K. S., Gadea, J., et al. (2009). The short-rooted phenotype of the *brevis radix* mutant partly reflects root abscisic acid hypersensitivity. *Plant Physiol.* 149 (4), 1917–1928. doi: 10.1104/pp.108.133819

Rowe, M. H., Dong, J., Weimer, A. K., and Bergmann, D. C. (2019). A plant-specific polarity module establishes cell fate asymmetry in the *Arabidopsis* stomatal lineage. *BioRxiv*, 614636. doi: 10.1101/614636

Salih, H., Bai, W., Liang, W., Yang, R., Zhao, M., and Muhammd, S. M. (2024). ROS scavenging enzyme-encoding genes play important roles in the desert moss *Syntrichia caninervis* response to extreme cold and desiccation stresses. *Int. J. Biol. Macromol.* 254, 127778. doi: 10.1016/j.ijbiomac.2023.127778

Scacchi, E., Osmont, K. S., Beuchat, J., Salinas, P., Navarrete-Gómez, M., Trigueros, M., et al. (2009). Dynamic, auxin-responsive plasma membrane-to-nucleus movement of *Arabidopsis BRX*. *Development* 136 (12), 2059–2067. doi: 10.1242/dev.035444

Schmitz, R. J., Grotewold, E., and Stam, M. (2022). *Cis*-regulatory sequences in plants: Their importance, discovery, and future challenges. *Plant Cell* 34 (2), 718–741. doi: 10.1093/plcell/koab281

Song, X., Yu, X., Hori, C., Demura, T., Ohtani, M., and Zhuge, Q. (2016). Heterologous overexpression of poplar *SnRK2* genes enhanced salt stress tolerance in *Arabidopsis thaliana.* Front. *Plant Sci.* 7. doi: 10.3389/fpls.2016.00612

Suzuki, N., Rivero, R. M., Shulaev, V., Blumwald, E., and Mittler, R. (2014). Abiotic and biotic stress combinations. *New Phytol.* 203 (1), 32–43. doi: 10.1111/nph.12797

Teakle, N. L., Amtmann, A., Real, D., and Colmer, T. D. (2010). *Lotus tenuis* tolerates combined salinity and waterlogging: maintaining O^2 transport to roots and expression of an *NHX1*-like gene contribute to regulation of Na^+ transport. *Physiol. Plant* 139 (4), 358–374. doi: 10.1111/j.1399-3054.2010.01373.x

Tiwari, S., Muthusamy, S. K., Roy, P., and Dalal, M. (2023). Genome wide analysis of *BREVIS RADIX* gene family from wheat (*Triticum aestivum*): A conserved gene family differentially regulated by hormones and abiotic stresses. *Int. J. Biol. Macromol.* 232, 123081. doi: 10.1016/j.ijbiomac.2022.12.300

Ullah, A., Sun, H., Yang, X., and Zhang, X. (2018). A novel cotton *WRKY* gene, *GhWRKY6*-like, improves salt tolerance by activating the ABA signaling pathway and scavenging of reactive oxygen species. *Physiol. Plant* 162 (4), 439–454. doi: 10.1111/ppl.12651

Van Zelm, E., Zhang, Y., and Testerink, C. (2020). Salt tolerance mechanisms of plants. *Annu. Rev. Plant Biol.* 71, 403–433. doi: 10.1146/annurev-arplant-050718-100005

Wang, X., Wang, L., Wang, Y., Liu, H., Hu, D., Zhang, N., et al. (2018). *Arabidopsis PCaP2* plays an important role in chilling tolerance and ABA response by activating *CBF*-and *SnRK2*-mediated transcriptional regulatory network. *Front. Plant Sci.* 9. doi: 10.3389/fpls.2018.00215

Westerheide, S. D., Raynes, R., Powell, C., Xue, B., and N Uversky, V. (2012). *HSF* transcription factor family, heat shock response, and protein intrinsic disorder. *Curr. Protein Pept. Sci.* 13 (1), 86–103. doi: 10.2174/138920312799277956

Wu, Z., Luo, L., Wan, Y., and Liu, F. (2023). Genome-wide characterization of the *PP2C* gene family in peanut (*Arachis hypogaea* L.) and the identification of candidate genes involved in salinity-stress response. *Front. Plant Sci.* 14. doi: 10.3389/fpls.2023.1093913

Yan, J., Liu, Y., Yan, J., Liu, Z., Lou, H., and Wu, J. (2023). The salt-activated CBF1/CBF2/CBF3-GALS1 module fine-tunes galactan-induced salt hypersensitivity in *Arabidopsis*. *J. Integr. Plant Biol.* 65 (8), 1904–1917. doi: 10.1111/jipb.13501

Ye, K., Li, H., Ding, Y., Shi, Y., Song, C., Gong, Z., et al. (2019). *BRASSINOSTEROID-INSENSITIVE2* negatively regulates the stability of transcription factor *ICE1* in response to cold stress in *Arabidopsis*. *Plant Cell* 31 (11), 2682–2696. doi: 10.1105/tpc.19.00058

Yu, J., Xie, Q., Li, C., Dong, Y., Zhu, S., and Chen, J. (2020). Comprehensive characterization and gene expression patterns of *LBD* gene family in *Gossypium*. *Planta* 251 (4), 1–16. doi: 10.1007/s00425-020-03364-8

Yu, X., Liu, Y., Wang, S., Tao, Y., Wang, Z., Shu, Y., et al. (2016). *CarNAC4*, a NAC-type chickpea transcription factor conferring enhanced drought and salt stress tolerances in *Arabidopsis*. *Plant Cell Rep.* 35, 613–627. doi: 10.1007/s00299-015-1907-5

Yue, Y., Zhang, M., Zhang, J., Duan, L., and Li, Z. (2012). *SOS1* gene overexpression increased salt tolerance in transgenic tobacco by maintaining a higher K^+/Na^+ ratio. *J. Plant Physiol.* 169 (3), 255–261. doi: 10.1016/j.jplph.2011.10.007

Zhang, B., Chen, N., Peng, X., and Shen, S. (2021). Identification of the *PP2C* gene family in paper mulberry (*Broussonetia papyrifera*) and its roles in the regulation mechanism of the response to cold stress. *Biotechnol. Lett.* 43, 1089–1102. doi: 10.1007/s10529-021-03110-4

Zhang, T., Hu, Y., Jiang, W., Fang, L., Guan, X., Chen, J., et al. (2015). Sequencing of allotetraploid cotton (*Gossypium hirsutum* L. acc. TM-1) provides a resource for fiber improvement. *Nat. Biotechnol.* 33 (5), 531–537. doi: 10.1038/nbt.3207

Zhang, Y., Liang, J., Cai, X., Chen, H., Wu, J., Lin, R., et al. (2021). Divergence of three *BRX* homoeologs in *Brassica rapa* and its effect on leaf morphology. *Hortic. Res.* 8, 68. doi: 10.1038/s41438-021-00504-3

Zhang, Y. J., Yang, J. S., Guo, S. J., Meng, J. J., Zhang, Y. L., Wan, S. B., et al. (2011). Over-expression of the *Arabidopsis CBF1* gene improves resistance of tomato leaves to low temperature under low irradiance. *Plant Biol. (Stuttg)* 13 (2), 362–367. doi: 10.1111/j.1438-8677.2010.00365.x

Zhu, L., Fang, H., Lian, Z., Zhang, J., Li, X., Shi, J., et al. (2022). Genome-wide investigation and expression analysis of the *Nitraria sibirica* Pall. *CIPK* gene family. *Int. J. Mol. Sci.* 23 (19), 11599. doi: 10.3390/ijms231911599

Zhu, T., Liang, C., Meng, Z., Sun, G., Meng, Z., Guo, S., et al. (2017). CottonFGD: an integrated functional genomics database for cotton. *BMC Plant Biol.* 17 (1), 1–9. doi: 10.1186/s12870-017-1039-x

frontiers | Frontiers in Plant Science

TYPE Original Research
PUBLISHED 16 May 2024
DOI 10.3389/fpls.2024.1392425

OPEN ACCESS

EDITED BY
Yi Wang,
Chinese Academy of Sciences (CAS), China

REVIEWED BY
Jing Li,
Hainan University, China
Tong Si,
Qingdao Agricultural University, China
Dechang Cao,
Chinese Academy of Sciences (CAS), China

*CORRESPONDENCE
Jiannan Zhou
zhoujiannan@aliyun.com
Yu Zhang
zhangyu@catas.cn
Huaijun Si
hjsi@gsau.edu.cn

†These authors have contributed equally to this work

RECEIVED 27 February 2024
ACCEPTED 29 April 2024
PUBLISHED 16 May 2024

CITATION
Zhu X, Li W, Zhang N, Jin H, Duan H, Chen Z, Chen S, Wang Q, Tang J, Zhou J, Zhang Y and Si H (2024) *StMAPKK5* responds to heat stress by regulating potato growth, photosynthesis, and antioxidant defenses. *Front. Plant Sci.* 15:1392425. doi: 10.3389/fpls.2024.1392425

StMAPKK5 responds to heat stress by regulating potato growth, photosynthesis, and antioxidant defenses

Xi Zhu[1,2,3†], Wei Li[1,2†], Ning Zhang[4,5], Hui Jin[1,2], Huimin Duan[1,2], Zhuo Chen[1,2], Shu Chen[1,2], Qihua Wang[1,2], Jinghua Tang[1,2], Jiannan Zhou[1,2*], Yu Zhang[1,2*] and Huaijun Si[4,5*]

[1]Key Laboratory of Tropical Fruit Biology, Ministry of Agriculture and Rural Affairs, Zhanjiang, Guangdong, China, [2]Key Laboratory of Hainan Province for Postharvest Physiology and Technology of Tropical Horticultural Products, Zhanjiang, Guangdong, China, [3]National Key Laboratory for Tropical Crop Breeding, Sanya Research Institute, Chinese Academy of Tropical Agricultural Sciences, Sanya, China, [4]State Key Laboratory of Aridland Crop Science, Gansu Agricultural University, Lanzhou, China, [5]College of Life Science and Technology, Gansu Agricultural University, Lanzhou, China

Backgrounds: As a conserved signaling pathway, mitogen-activated protein kinase (MAPK) cascade regulates cellular signaling in response to abiotic stress. High temperature may contribute to a significant decrease in economic yield. However, research into the expression patterns of *StMAPKK* family genes under high temperature is limited and lacks experimental validation regarding their role in supporting potato plant growth.

Methods: To trigger heat stress responses, potato plants were grown at 35°C. qRT-PCR was conducted to analyze the expression pattern of *StMAPKK* family genes in potato plants. Plant with *StMAPKK5* loss-of-function and gain-of-function were developed. Potato growth and morphological features were assessed through measures of plant height, dry weight, and fresh weight. The antioxidant ability of *StMAPKK5* was indicated by antioxidant enzyme activity and H_2O_2 content. Cell membrane integrity and permeability were suggested by relative electrical conductivity (REC), and contents of MDA and proline. Photosynthetic capacity was next determined. Further, mRNA expression of heat stress-responsive genes and antioxidant enzyme genes was examined.

Results: In reaction to heat stress, the expression profiles of *StMAPKK* family genes were changed. The StMAPKK5 protein is located to the nucleus, cytoplasm and cytomembrane, playing a role in controlling the height and weight of potato plants under heat stress conditions. *StMAPKK5* over-expression promoted photosynthesis and maintained cell membrane integrity, while inhibited transpiration and stomatal conductance under heat stress. Overexpression of *StMAPKK5* triggered biochemical defenses in potato plant against heat stress, modulating the levels of H_2O_2, MDA and proline, as well as the antioxidant activities of CAT, SOD and POD. Overexpression of *StMAPKK5* elicited genetic responses in potato plants to heat stress, affecting heat stress-responsive genes and genes encoding antioxidant enzymes.

10.3389/fpls.2024.1392425

Conclusion: *StMAPKK5* can improve the resilience of potato plants to heat stress-induced damage, offering a promising approach for engineering potatoes with enhanced adaptability to challenging heat stress conditions.

KEYWORDS

potato, heat stress, StMAPKK5, transpiration, photosynthesis

Highlights

- In response to heat stresses, expression patterns of *StMAPKKs* are altered in different potato tissues;
- *StMAPKK5* influences potato morphological characteristics, including plant weight and height under heat stress conditions;
- *StMAPKK5* regulates the physiological index of potato plants responding to heat stress.
- *StMAPKK5* regulates photosynthesis and transpiration in response to heat stress;
- *StMAPKK5* leads to altered expression of heat stress-responsive genes and antioxidant enzyme genes in potato plants under heat stress conditions.

Introduction

Over the past century, the Earth's average surface temperature has been rising (Hansen et al., 2022; Katlane et al., 2023). Evidence indicates that extreme weather events, including heat waves, are increasing in both frequency and intensity (Walsh et al., 2020). Extreme temperatures confer negative roles in photosynthesis, flower pollination, and fruit setting, which leads to lower crop yields and affects food availability (Beillouin et al., 2020; Dalhaus et al., 2020; Nicholson and Egan, 2020; Wi et al., 2020). As the fourth most important crop in agricultural production, potatoes (*Solanum tuberosum* L.) are susceptible to high temperature or adverse water supply (Singh et al., 2020). Due to climate change, tuber growth is inhibited above 33°C and high temperature above 25°C induces leaf senescence (Rykaczewska, 2015). We need to better understand how heat stress affects plant growth and development as global temperatures rise in the future. This could offer valuable insights into breeding programs to improve plant heat-stress tolerance.

Protein kinases (PK) constitute a vast and crucial superfamily of enzymes involved in cellular signaling, regulating a wide array of biological processes (Chen et al., 2021a). The mitogen-activated protein kinases (MAPKs) are important and evolutionarily conserved subfamily of protein kinases that play a central role in transducing signals from the cell surface to the nucleus responding to a variety of stimuli, for instance, heat stress (He et al., 2020; Kumar et al., 2020). The hierarchical organization of MAPK signaling cascades, encompassing the MAPKs, MAPK kinases (MAPKKs or MEKs), and MAPKKs kinases (MAPKKKs or MEKKs), forms a crucial framework for transmitting external signals, amplifying stress signaling, and ultimately facilitating communication between the cellular environment and transcriptional responses (Zwerger and Hirt, 2001; Taj et al., 2010; Zhang and Zhang, 2022). Heat stress can indeed trigger various signaling mechanisms within biological systems in three pathways, including Ca^{2+}-dependent salt overlay sensitive signaling and osmotic/oxidative stress signaling (Rodriguez et al., 2010). The role of oxidative stress signaling in promoting osmolyte accumulation through the MAPK cascade, involving G-protein receptors, histidine kinases, and protein tyrosine kinases, aligns with known cellular responses to stress (Ara and Sinha, 2014; Röhm et al., 2021).

Genome-wide analyses have progressively identified multiple *MAPKKs* genes in various plant species. Yin et al. identified 23 *MAPKKs* in the *Gossypiumhirsutum* genome and divided into 4 groups. Most of these genes feature the active site motif-D(I/L)K-, which includes two conserved residues, K (lysine) and D (aspartic acid) (Yin et al., 2021). The cucumber genome contains 6 *MAPKK* genes classified into 4 groups (A-D) (Wang et al., 2015). Ten *MAPKK* genes have been reported in *Arabidopsis* genome, which are also classified into 4 groups (A-D) (Danquah et al., 2014; Choi et al., 2017). Bioinformatic analysis of maize genome revealed 9 *MAPKK* genes and identified 11 subdomains of protein kinases showing serine/threonine specificity (Kong et al., 2013). From the available genome, 5 *MAPKK* genes were identified in tomato (Wu et al., 2014) and 7 in rice (Kumar et al., 2008), respectively. However, systematic studies of the *MAPKK* gene family are still required for potato plant.

The MAPKK factors, as the components of the MAPK signaling pathway, exhibit evolutionary conservation across various organisms and regulate a wide array of functions, such as stomatal development (Bergmann et al., 2004), plant architecture (Yu et al., 2014), chlorophyll synthesis (Li et al., 2022), glucose metabolism (Chardin et al., 2017a), apical meristem (Lee et al., 2019), and flower development (Lafleur et al., 2015). However, studies on how *StMAPKKs* respond to heat stress in potato plants are scarce. This study aimed to describe the expression features of *StMAPKKs* under

heat stress situations. Then, our study analyzed the functional aspects of *StMAPKK5*, including its roles in potato plant growth, antioxidation, cell membrane integrity, photosynthesis capacity, and mRNA expression of heat stress-responsive genes and antioxidant enzyme genes. The potato cultivar "Atlantic" is a cultivar introduced and popularised in Guangdong Province. As a high-quality and high-yield potato variety, "Atlantic" has been studied rarely under heat stress. Meanwhile, this study aimed to screen heat tolerance genes, which may provide an effective basis for its molecular breeding for heat stress tolerance.

Materials and methods

Plant materials and cultivation

The potato (*Solanum tuberosum* L.) cultivar "Atlantic" was cultivated *in vitro* using Murashige and Skoog (MS) medium with a pH of 5.8–6.0. The medium was supplemented with 8% sucrose and the plants were cultivated for 4 weeks. Next, four-week seedlings were cultured in the dark for 30 days to induce tuber generation. Approximately 1 g of potato tubers with 1 mm germinated buds were transferred into containers (19 cm ×25 cm ×26 cm) filled with soil-vermiculite mixture (1:1, v/v) and cultivated for 5 weeks in Zhanjiang located at latitude 21°11'43"N and longitude 110°34'56"E. Soil water holding capacity ranged from 75% to 80%, supplemented with 100 mL of nutrient solution (pH: 5.8; 0.20 mmol/L $FeSO_4$, 2.57 mmol/L KH_2PO_4, 2.08 mmol/L $MgSO_4$, 1.29 mmol/L $(NH_4)_2SO_4$, and 9.89 mmol/L KNO_3) every 7 days. Potato plants in each group exhibiting uniform growth appearance were next cultivated under 35°C. Physiological and photosynthetic indexes were assayed at 0 h, 8 h, 12 h, 24 h, and 48 h after cultivation under heat stress conditions. The control plants were cultivated at 22°C. Each group was prepared with three biological replicates and three technical replicates.

To examine the mRNA expression of *MAPKK* family genes in various plant tissues, the potted plants were continually cultured. Flower, root, stem, leaf, petiole, stolon, and shoot were collected at the developmental stage, and tuber was collected at the maturity stage. Next, the plants were cultivated under 35°C, and *StMAPKKs* expression in leaf, stem, and root were examined at 0 h, 1 h, 2 h, 4 h, 8 h, 12 h, 24 h, and 48 h after cultivation under heat stress conditions.

Construction of transgenic plants

The gene encoding the StMAPKK5 protein was cloned into the pBI121-EGFP plasmid using a previously described method (Li et al., 2020), to develop *StMAPKK5*-overexpressing plants (OE for short). *Agrobacterium tumefaciens* strains LBA4404 was used for transformation experiments. Potato plants low expressing *StMAPKK5* (RNAi or Ri for short) were established with a previously described method (Lu et al., 2019). The primers utilized for plasmid construction are listed in Table 1.

Agrobacterium containing plasmids were cultured for about 48 h in LB medium in addition with 50 mg/L gentamicin and 50 mg/L spectinomycin at 28°C, next harvested by centrifugation (5,000 rpm, 10 min), and re-suspended in MS medium (OD600 = 0.3). The sterile seedling stems (2 cm) were incubated in Agrobacterium suspension for 10 min, and then grown in MS medium (pH: 5.8) containing 7.4 g/L agar, 30 g/L sucrose, 0.5 mg/L 6-BA, 2.0 mg/L ZT, 0.2 mg/L GA3, and 1.0 mg/L IAA and maintained in the dark for 48–72 h. Next, the plants were transferred into differentiation media (MS, 7.4 g/L agar, 30 g/L sucrose, 300 mg/L Timentin, 100 mg/L kan, 0.5 mg/L 6-BA, 2.0 mg/L ZT, 0.2 mg/L GA3, and 1.0 mg/L IAA; PH: 5.8), with media changed every 2 weeks. After induction of adventitious bud, the resistant adventitious buds were transferred to formulated root medium (MS + 7.4 g/L agar+ 30 g/L sucrose + 300 mg/L Timentin + 100 mg/L kan, pH=5.8) until adventitious roots were induced.

qRT-PCR

TRIzol RNA Extraction kit (Invitrogen, Carlsbad, CA, USA) was used to extract total RNA from the collected samples. The first-strand cDNA of the target genes were synthesized using the First-Strand cDNA Synthesis Kit (TransGen Biotech, Beijing, China). qPCR was conducted using a LightCycler 480 II real-time PCR system (Roche, Rotkreuz, Switzerland) with the reaction mixture comprising 0.8 µL of specific primers (0.5 µM), 100 ng of cDNA (Table 1), and 10 µL of SYBR Premix Ex Taq (2 ×) (Takara, Tokyo, Japan). The reactions underwent an initial incubation at 94°C for 3 min, followed by the procedures: 36 cycles of 94°C for 45 s, 59°C for 34 s, and 72°C for 1 min. The relative transcription levels were determined using the $2^{-\triangle\triangle Ct}$ method.

Subcellular localization

The expression vector pPBI121-EGFP carrying protein-coding sequence of *StMAPKK5* gene was transformed into *Agrobacterium tumefaciens* GV3101. The primers utilized for plasmid construction are detailed in Table 1. Following the method described by Sparkes et al. (2006), tobacco epidermal cells were infiltrated with the transformed strain. A confocal laser scanning microscope (Olympus, Tokyo, Japan) was used to observe the sample. For the autofluorescence of chlorophyll in chloroplasts, the excitation wavelength and transmission range for emission were set at 640 nm and 675 nm, and 488 nm and 510 nm for the GFP-tagged *StMAPKK5* protein. The software Olympus Fluovie was used for imaging processing.

Phylogenetic analysis and amino acid alignment

MEGA 5.05 software was utilized to construct a phylogenetic tree with a neighbor-joining algorithm. DNAman tool (Lynnon

10.3389/fpls.2024.1392425

TABLE 1 List of specific primers for qRT-PCR and plasmid construction.

Genbank accession	Gene	Forward (5′-3′)	Reverse (5′-3′)	Product length (bp)	Tm
XM_006347752.2	*StEf1α*	GGTTGTATCTCTTCCGATAAAGGC	GGTTGTATCTCTTCCGATAAAGGC	132	60
XM_006363922.2	*StMAPKK1*	TTCCCACGTGCTTTCTCCTC	TCGGCGATCACGAACTAAGG	148	60
NM_001288477.1	*StMAPKK2*	CGATCACAACGGCGAAATCC	CCTCACGCCTGGAGTTGATT	197	60
NM_001318629.1	*StMAPKK3*	TCCAGCTTCTTGACTGCGAG	TGAACAACACCCCCACTTCC	188	60
XM_006353485.2	*StMAPKK4*	CTCGAGTGTGCAACAGGTCA	TGCACAAGGTTCTGGTTGGT	111	60
XM_006351467.2	*StMAPKK5*	GTCAATCTCAAGGGGGAGCC	TTCGTTCCGGCGACATGTAA	118	60
XM_006358116.2	*StFeSOD2*	GCAGCCAAATTCAGCACACT	GGACCAGCTTTCCTCGCTAA	164	60
XM_006350307.2	*StFeSOD3*	TGCTGCCCAGGTATGGAATC	CCTCTCTGCTCAAGACGAGC	194	60
XM_006358693.2	*StMnSOD*	TAGACGTTTGGGAACACGCA	CTCTTCAGGGGCACTCGTTT	129	60
XM_049521383.1	*StCuZnSOD1*	CCTCCAACAGGTCACTGCTC	TCAGGTCACCCTTGAATGGC	141	60
AF354748	*StCuZnSOD2*	TGTGGCACCATCCTCTTCAC	TCCTGTTGACATGCAGCCAT	138	60
XM_006358985.2	*StPOD12*	CGGCCTTCTTCGTCTTCACT	AAACGACTCTACCGCAGTCC	188	60
XM_006350750.2	*StPOD47*	AGTCTGAGCAGGCCTTTGAC	GCCCATTTTACGCATGGCTT	197	60
XM_006362636.2	*StPOD66*	GCTTTGCCAACAGGGGATTG	TTCAAGCTCGGGTCAGTGTC	139	60
AY442179	*StCAT1*	GCACAGGGATGAGGAGATCG	CTTCTCACGTTTGCCACTGC	106	60
XM_006340770.2	*StCAT2*	GCACAGGGATGAGGAGATCG	CTTCTCACGTTTGCCACTGC	106	60
XM_006341106.1	*StHSFA3*	AGTGCTGGCACCGAGTTATG	GCTGCCTGCAAGGGATCTAT	104	60
XM_006350742.2	*StHSP20-20*	TTTCGGTGATCGACGAAGCA	TTAAGCCCTGGAAGATCGGC	183	60
XM_006360759.2	*StHSP20-33*	TCCAAGCTTCTTCGGTGGTC	CGAGCAGAGGATGGAGCATT	102	60
XM_006345188.2	*StHSP20-44*	GGAGCAATATCGTCGACCCA	AACATGAGCTTCCGGGGTTT	146	60
Z11982.1	*StHSP70*	GTGTTGGTGTATGGCAAAACGA	AGCAACTTGATTCTTGGCTGC	131	60
XM_006362602.2	*StHSP90.2*	AACTCTCCGTTCTTGGAGCG	TTCAATCCCTCCTTGGTGGC	140	60
XM_006352486.1	*StHSP90.4*	TATAGCAGCCGGTGCAGATG	GCTCTCACCAGAAGTGTCCC	178	60
XM_015308529.1	*StP5CS*	CTCAGTCCGTGTGCTTGCTA	AAGAGGCCATTCCCACTTCG	189	60
Subcellular localization		ATGGCTGGACTGGAGGAATTG	TTGAGTAATGAAAAGTTCATGCT		
Overexpression		CTCGAGATGGCTGGACTGGAGGAATTG	GTCGACTTGAGTAATGAAAAGTTCATGCT		
RNA interference		ATGGCTGGACTGGAGGAATTG	AATATGAATTGCTCTCTGAACAAC		

Biosoft, San Ramon, CA, USA) was applied to multiple-sequence alignment of the conserved subdomains.

Measurements of plant growth

Non-transgenic (NT) and transgenic plantlets, uniformly measuring 2 cm in height, were planted in MS medium under controlled conditions in an incubator with an 8 h-dark cycle and 16 h-photoperiod at 22°C and 3,000 Lx. To induce heat stress, plants were cultivated under 35°C. Four weeks after heat stress treatment, we measured root fresh/dry weight, plant fresh/dry weight, and plant height.

Measurements of stomatal conductance, transpiration rate, and net photosynthetic rate

Four-week-old potted plants were cultivated under 35°C. After 0 h, 8 h, 16 h, 24 h, and 48 h, we examined stomatal conductance, transpiration rate, and net photosynthetic rate. Stomatal conductance, transpiration rate, and net photosynthetic rate were assessed using a portable LI-6400XT system (Li-COR, Lincoln, NE, USA) between 9:30–11:30. The fourth fully expanded functional leaf was collected from the plant top. The parameters were configured as follows, 50%-70% of relative humidity in leaf chamber, 1,500 $\mu mol \cdot m^{-2} \cdot s^{-1}$ of the photon flux density, and 400 μmol/mol of CO_2.

10.3389/fpls.2024.1392425

Assays for levels of proline, MDA, and H_2O_2, and activities of POD, SOD, and CAT

Four-week-old potted plants were cultivated under 35°C. Following exposure to heat stress for durations of 0 h, 8 h, 16 h, 24 h, and 48 h, the potted plants were assayed for the levels of proline, malondialdehyde (MDA), and hydrogen peroxide (H_2O_2), and activities of peroxidase (POD), superoxide dismutase (SOD), and catalase (CAT), superoxide dismutase (SOD), and peroxidase (POD) activities with methodologies previously established in our research (Zhu et al., 2021). Description of detailed experimental procedures are provided in Supplementary Methods.

Assays for relative electrical conductivity and chlorophyll content

Relative electrical conductivity (REC) and chlorophyll content were assayed according to our previous methods (Zhu et al., 2023). Description of detailed experimental procedures are provided in Supplementary Methods.

Statistical analysis

Statistical analysis was performed using GraphPad Prism Software (GraphPad, San Diego, CA, USA) and IBM SPSS 19.0 Statistical Software (IBM, Chicago, IL, USA). Results are presented as mean ± standard deviation. Histograms and line charts were generated using GraphPad Prism software. For multiple comparisons, one-way ANOVA with Tukey test or Dunnett's T3 for *post-hoc* analysis or two-way ANOVA corrected by Sidak's multiple comparisons test were employed.

Results

Phylogenetic analysis and sequence comparison of StMAPKK proteins

After phylogenetic analysis of the amino acid sequences of the reported plant MAPKK homologs, we found StMAPKK5 was homologous with SlMAPKK5, AtMAPKK3 and OsMAPKK3 (Figure 1A). There was a high degree of homology between StMAPKK4 and SlMAPKK4, StMAPKK2 and SlMAPKK2,

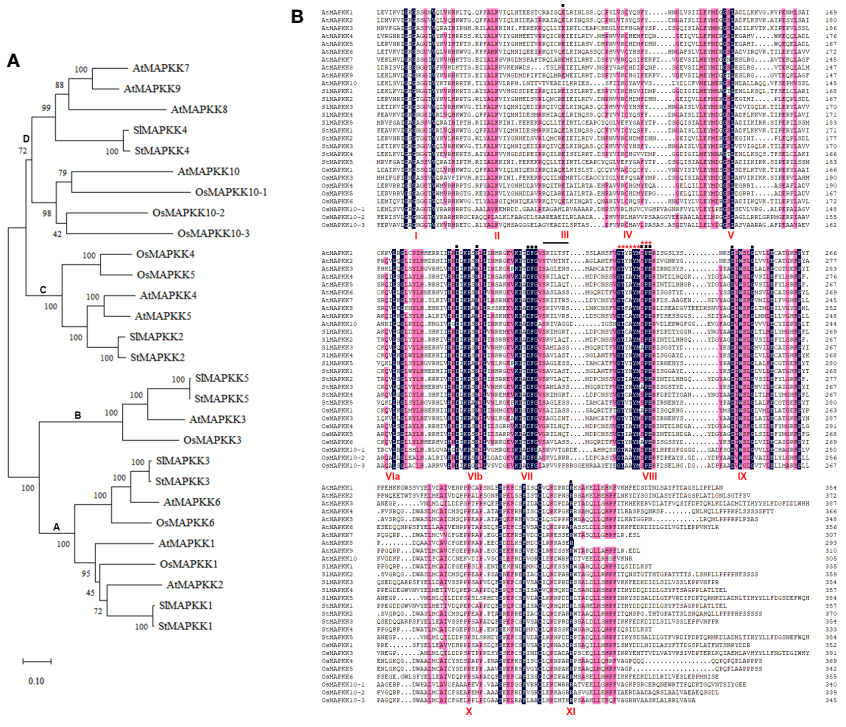

FIGURE 1
The phylogenetic relationship and protein sequence alignment of MAPKK proteins with MAPKK proteins. **(A)** Dendrogram of MAPKK proteins from *Solanum tuberosum* (St) (StMAPKK1–5), *Arabidopsis thaliana* (At) (AtMAPKK1–10), *Solanum lycopersicum* (Sl) (SlMAPKK1–5), and *Oryza sativa* (Os) (1,3,4,5,6,10–1 and 10–2); Bootstrap values were calculated from 500 resampled datasets with a 50% cut-off; MEGA-X software was used to establish the neighbor-joining phylogenetic tree. **(B)** Protein sequence of MAPKK proteins were aligned using DNAman software; Identical and similar amnio acids were marked in the same colors. The conserved subdomains were indicated on the bottom, using the Roman numbers (I-XI). The dark line marks the active site motif. Red asterisks indicate substrate specificity, and the black dots above the sequences represent activating sites. The conserved consensus motif GXGXXG is marked as I.

StMAPKK3 and SlMAPKK3, as well as StMAPKK1 and SlMAPKK1. A comparison of the MAPKK proteins from *Solanum tuberosum* (St) (StMAPKK1–5), *Arabidopsis thaliana* (At) (AtMAPKK1–10), *Solanum lycopersicum* (Sl) (SlMAPKK1–5), and *Oryza sativa* (Os) (1, 3, 4, 5, 6, 10–1 and 10–2) showed the presence of the highly conserved domains (Figure 1B). StMAPKK5 contains 11 conserved catalytic subdomains typical of MAPKKs and the conserved consensus motif GXGXXG.

Characterization of *StMAPKK* family genes expression of the various organs of potato

A variety of plant tissues (flower, root, stem, leaf, petiole, stolon, tuber, and shoot) were collected to analyze the expression features of *StMAPKK* family genes. *StMAPKK1* showed the highest level of expression in root (Figure 2A). *StMAPKK2* displayed the maximum expression in leaf (Figure 2B), *StMAPKK3* in stem and shoot (Figure 2C), *StMAPKK4* in root (Figure 2D), stem and leaf, and *StMAKK5* in leaf (Figure 2E). These results represented the tissue-specific expression profiles of *StMAPKK* family genes. We speculated genes within the *StMAPKKs* family may play a crucial role in regulating the growth and development of different tissues and organs in potato.

Heat stress resulted in differential expression of *StMAPKK* family genes

Potato leaves, stems and roots were chosen for quantification because the relative expression of *StMAPKK5* gene was found to be higher than in other tissues. At 0 h, 1 h, 2 h, 4 h, 8 h, 16 h, 24 h, or 48 h after exposure to heat stress (35°C), potato leaves, stem and roots were obtained. qRT-PCR was then performed to assay the expression features of *StMAPKK* family genes. The expression of *StMAPKK1* increased steadily with the duration of heat stress ($p < 0.05$) (Figure 3A). However, we observed that the expression of *StMAPKK2* (Figure 3B), *StMAPKK3* (Figure 3C), and *StMAPKK4* (Figure 3D) in leaves, stems and roots changed in a disordered manner in response to heat stress ($p < 0.05$). Likewise, we noted that heat stress conditions resulted in a consistent increase in the transcript levels of *StMAPK5* in potato leaves, stems, and roots ($p < 0.05$) (Figure 3E). Considering that after treatment, *StMAPKK5* transcript levels were up-regulated at a higher rate than *StMAPKK1–4* ($p < 0.05$). Therefore, we speculated that in response to heat stress, *StMAPKK5* gene may perform crucial molecular functions.

Impacts of *StMAPKK5* on plant morphological phenotypes under heat stress conditions

We generated *StMAPKK5* overexpression plants by introducing pBI121-EGFP-StMAPKK5 and create loss-of-function plants through the induction of pART-StMAPKK5-RNAi. In transgenic plants, *StMAPKK5* mRNA expression was significantly elevated or decreased relative to the wild-type plant ($p < 0.001$) (Figures 4A, B). Within the under-expression lines, Ri-2, Ri-3, and Ri-5 were chosen as notable under-expressors, while OE-2, OE-3 and OE-6 were identified as significant over-expressors for subsequent functional analysis under heat stress conditions. In order to better assess the location of *StMAPKK5* protein, we examined by tagging *StMAPKK5* protein with GFP and dissecting the green fluorescence, with the red autofluorescence of chlorophyll as a location reference. The green fluorescence is evenly distributed in the nucleus, cytoplasm and

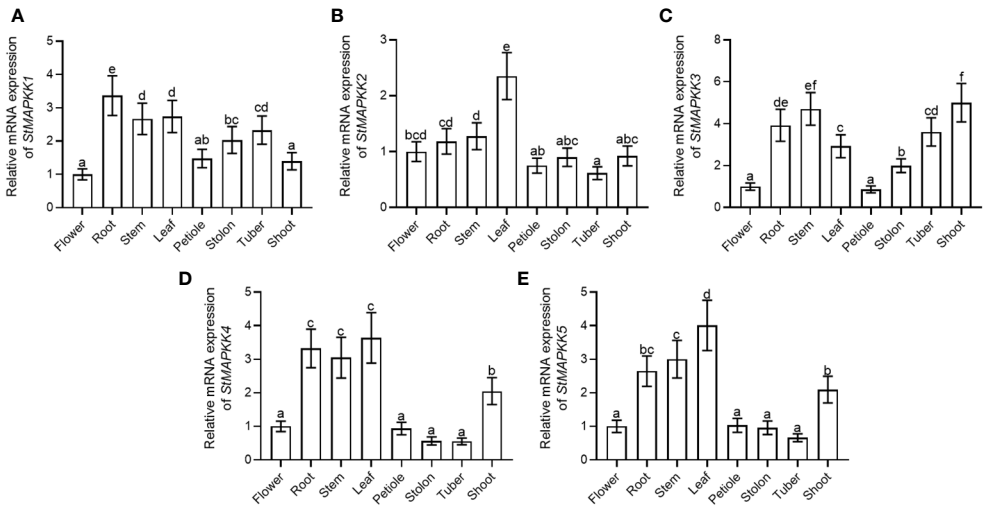

FIGURE 2
mRNA expression of *StMAPKK* family genes of the various tissues of potato. Relative expression of **(A)** *StMAPKK1*, **(B)** *StMAPKK2*, **(C)** *StMAPKK3*, **(D)** *StMAPKK4*, and **(E)** *StMAPKK5* at mRNA levels, in flower, root, stem, leaf, petiole, stolon, tuber, and shoot. Data were the means ± standard deviation. Different letters indicated significant difference between two groups (p-value less than 0.05, calculated by one-way ANOVA, followed by LSD and Duncan or Dunnett's T3).

10.3389/fpls.2024.1392425

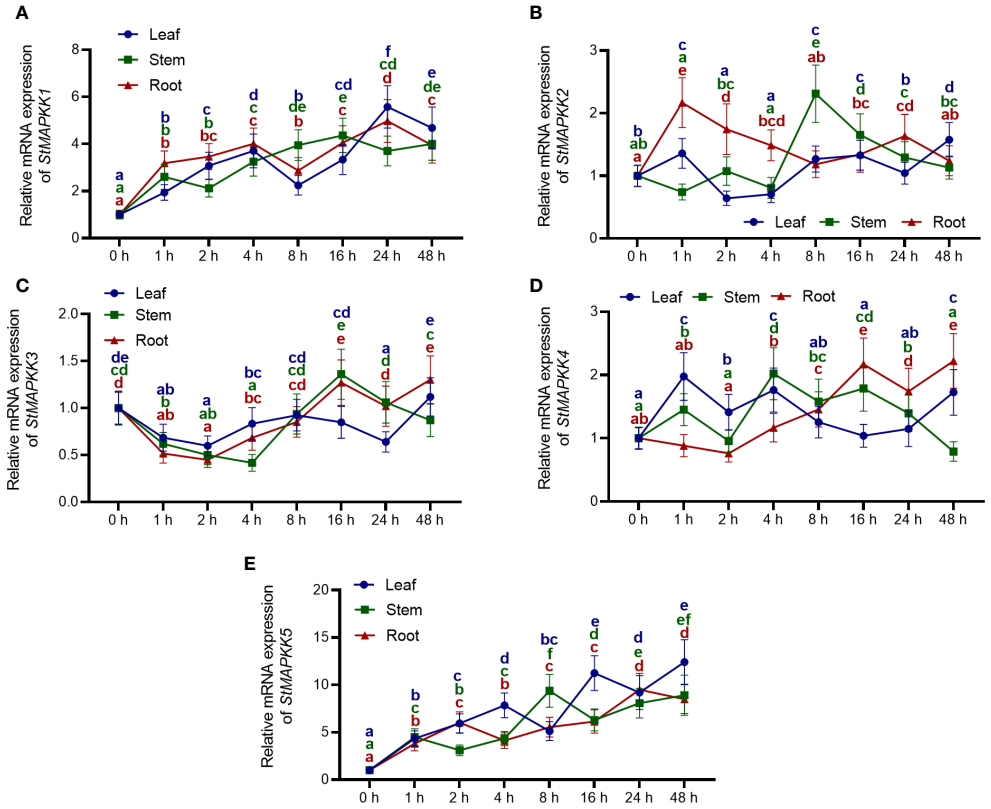

FIGURE 3
Expression profiles of *StMAPKK* family genes at mRNA level in potato leaves, stem and roots in response to heat stress. Relative mRNA levels of **(A)** *StMAPK1*, **(B)** *StMAPKK2*, **(C)** *StMAPKK3*, **(D)** *StMAPKK4*, and **(E)** *StMAPKK5* in leaves, stem, and roots. Four-week-old normally grown plants were exposed to heat stress (35°C) for 0 h, 1 h, 2 h, 4 h, 8 h, 16 h, 24 h, or 48 h. Data were the means ± standard deviation. Different letters indicated significant difference between two groups (p-value less than 0.05, calculated by one-way ANOVA, followed by LSD and Duncan or Dunnett's T3).

cytomembrane (Figure 4C), which was consistent with our previous result (Luo et al., 2024). In comparison with the NT plants, *StMAPKK5* overexpression significantly enhanced the thermotolerance of potato plants as evidenced by the increases in plant height, dry weight, dry root weight, fresh weight, and root fresh weight, under normal and heat stress conditions after 4 weeks of cultivation ($p < 0.001$) (Figures 4D, E). In contrast, under normal or heat stress conditions, RNAi-mediated silencing of *StMAPKK5* apparently resulted in the inhibition of plant growth, compared to non-transgenic plants ($p < 0.001$).

StMAPKK5 overexpression elevated the ability of ROS scavenging under heat stress condition

Heat stresses led to a significant increase in H_2O_2 in non-transgenic plants, and it continually increased with prolonged duration of heat stress ($p < 0.001$) (Figure 5A). *StMAPKK5* transgenic lines showed significantly reduced H_2O_2 production at 8 h, 16 h, 24 h, and 48 h following cultivation under heat stress conditions, compared to non-transgenic plants, while RNAi-mediated silencing of *StMAPKK5* reversely increased the accumulation of H_2O_2 ($p < 0.001$). MAD generated in non-transgenic plant was found significantly increased as the extension of heat stress ($p < 0.001$) (Figure 5B). Compared to non-transgenic plants, MAD content was decreased in *StMAPKK5* transgenic lines (OE-2, OE-3, and OE-6 after heat stress. In contrast, as compared to non-transgenic plants, knockdown of *StMAPKK5* resulted in the accumulation of MDA under heat stress. The level of proline, as a consequence of heat stress, was increased in non-transgenic plants in a time-dependent manner (Figure 5C). The transgenic lines (OE-2, OE-3, and OE-6) accumulated more proline compared to non-transgenic plants under heat stress condition, while *StMAPKK5*-silencing plants were detected with decreased proline content. Under heat stress conditions, the specific activities of CAT, SOD, and POD were consistently higher in non-transgenic plants ($p < 0.001$) (Figures 5D–F). After 48 h of heat stress, the activity of CAT, SOD, and POD was found higher in *StMAPKK5*-transgenic lines compared to non-transgenic plants, respectively. However, compared to non-transgenic plants, *StMAPKK5*-silencing plants displayed decreased activities of CAT, SOD, and POD, 48 h after heat stress.

In general, chlorophyll synthesis is sensitive to heat stress, serving as an indicator of the extent of heat stress injury. It was observed that heat stress had an adverse effect on chlorophyll in potato plants (Figure 5G). Overexpression of *StMAPKK5* may

10.3389/fpls.2024.1392425

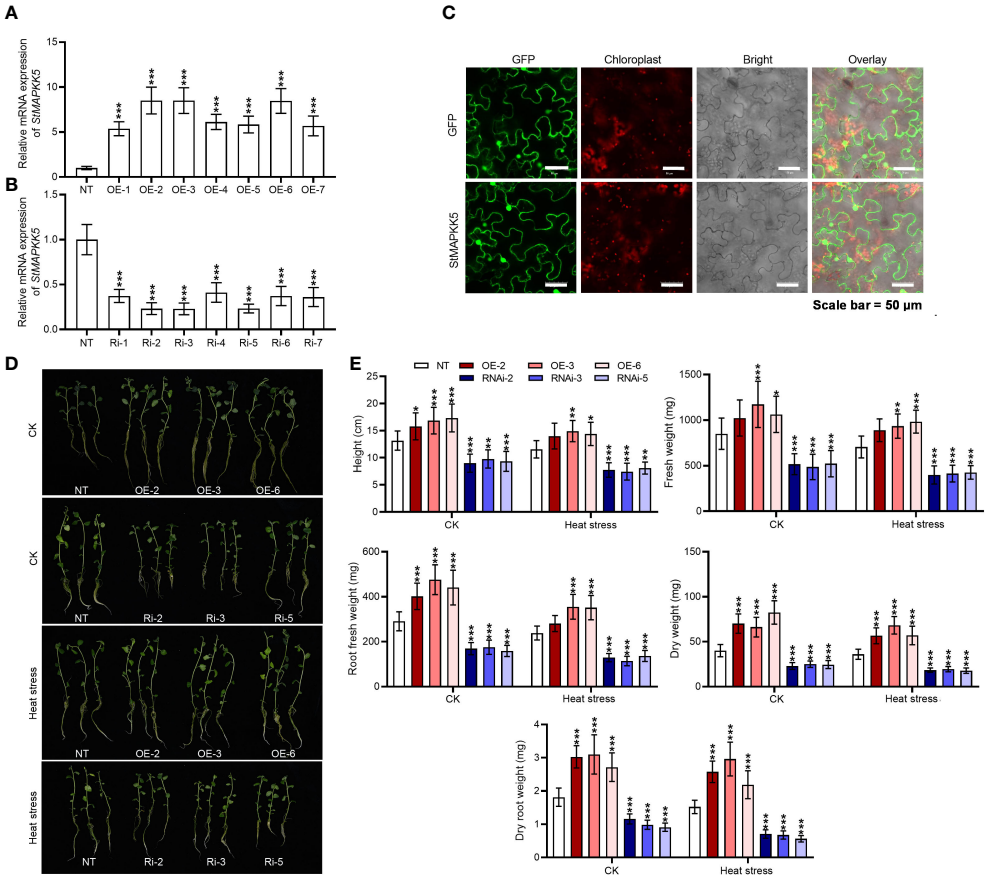

FIGURE 4
StMAPKK5 overexpression and under-expression altered the growth of potato plant under heat stress condition. *StMAPKK5* transcription levels in **(A)** *StMAPKK5* overexpression plants and **(B)** *StMAPKK5* under-expression plants. **(C)** Fluorescence images showed *StMAPKK5*-encoding protein located in the nucleus, cytoplasm and cytomembrane; bars = 50 μm; *StMAPKK5* protein was tagged with EGFP (enhanced green fluorescent protein); red fluorescence derives from the chlorophyll. **(D)** Growth morphology of potato plant cultivated under normal and heat stress conditions. **(E)** Plant growth indexes were assayed, including plant height, dry root weight, dry weight, fresh root weight, and fresh weight. Transgenic or non-transgenic plants were measured 0 h, 8 h, 16 h, 24 h, and 48 h after cultivation under normal or heat stress conditions. NT, non-transgenic plants; Ri, pART-StMAPKK5-RNAi-transgenic plants (RNAi-2, RNAi-3, and RNAi-5); OE, pBI121-EGFP-StMAPKK5-transgenic lines (OE-2, OE-3, and OE-6); Data were the means ± standard deviation; p-values (*$p < 0.05$, **$p < 0.01$, ***$p < 0.001$) were calculated by ordinary two-way ANOVA, followed by Tukey's multiple comparisons test (n = 9).

increase the heat stress tolerance of potato plants by maintaining the total chlorophyll content, compared to non-transgenic plants ($p < 0.001$). *StMAPKK5*-silencing lines appeared to be more susceptible to heat stress, evidenced by a higher reduction in total chlorophyll content than non-transgenic plants ($p < 0.001$). REC have commonly been examined to reflect stress-induced injury of cell membrane. Heat stress significantly exacerbated REC with the extension of time (Figure 5H). *StMAPKK5* overexpression profoundly inhibited REC while *StMAPKK5* silence significantly increased REC, compared to the NT plants ($p < 0.001$).

Overexpression of *StMAPKK5* improved the photosynthetic rate and reduced transpiration responding to heat stresses

Comparisons of measured rates of net photosynthesis suggested that direct suppression of photosynthesis happens at temperatures higher than about 35°C. Cultivation under heat stress contributed to the inhibition of net photosynthetic rate for the NT plants ($p < 0.05$) (Figure 6A). However, compared to the NT plants, *StMAPKK5*-overexpressing plants showed increased net photosynthetic rates in response to heat stress ($p < 0.001$). Potato plants lowly expressing *StMAPKK5* failed to maintain net photosynthetic rate in comparison with the NT plants ($p < 0.001$). Transpiration is an essential physiological process, during which course water and mineral nutrients are transferred from soils to plants to dissipate heat. In this study, the transpiration rate of the plants decreased as the duration of thermal incubation increased (Figure 6B). *StMAPKK5* overexpression further inhibited transpiration in potato plants, whereas *StMAPKK5* low expression promoted transpiration in instead ($p < 0.001$). Leaf stomata manages plant CO_2 absorption through transpiration and photosynthesis. It was shown that stomatal conductance was decreased responding to increased temperatures (Figure 6C). In transgenic plants, compared to the NT plants, stomatal conductance of *StMAPKK5* overexpression plants decreased

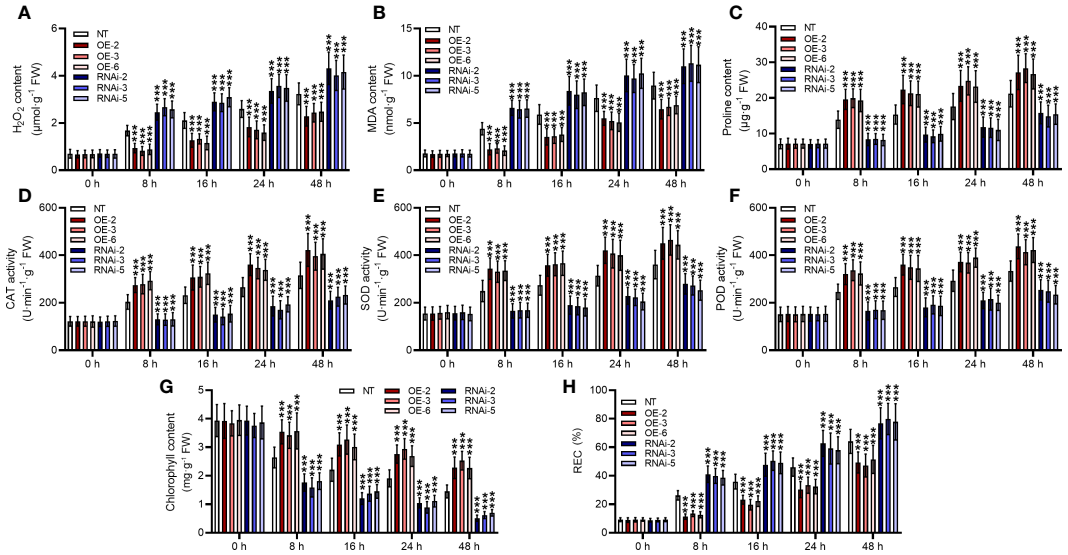

FIGURE 5
Elevated performance of *StMAPKK5* transgenic plants in scavenging ROS in response to heat stress. **(A)** H_2O_2 accumulation, **(B)** MDA content, **(C)** proline content, antioxidant enzyme activity of **(D)** CAT, **(E)** SOD, and **(F)** POD, **(G)** chlorophyll content, and **(H)** REC of potato plant cultivated under normal and heat stress conditions. Transgenic or non-transgenic plants were measured 0 h, 8 h, 16 h, 24 h, and 48 h after cultivated under heat stress conditions. NT, non-transgenic plants; Ri, pART-StMAPKK5-RNAi-transgenic plants (RNAi-2, RNAi-3, and RNAi-5); OE, pBI121-EGFP-StMAPKK5-transgenic lines (OE-2, OE-3, and OE-6); Data were the means ± standard deviation; p-values (***$p < 0.001$) were calculated by ordinary two-way ANOVA, followed by Tukey's multiple comparisons test (n = 9).

markedly ($p < 0.001$). Reversely, *StMAPKK5* silence maintained the stomatal conductance relative to the NT plants ($p < 0.001$). These results indicated that in response to heat stresses, overexpression of *StMAPKK5* increased photosynthetic rate and decreased transpiration and stomatal conductance.

StMAPKK5 participated in regulating heat-responsive gene expression

To protect the structure and operation of plant cells from the damaging effects of oxidative stress caused by heat stress, the antioxidant defense system is generated, consisting of antioxidant enzymes, like FeSOD, MnSOD, and CuZnSOD, in chloroplasts, mitochondria, and peroxisomes. Under heat stress conditions, NT plants showed a significant increase in mRNA expression of *StFeSOD2*, *StFeSOD*, *StMnSOD*, *StCuZnSOD1*, and *StCuZnSOD2* (Figures 7A–E). *StMAPKK5*-transgenic plants (OE-2, OE-3, and OE-6 lines) exhibited increased sensitivity to heat stress, suggesting a higher mRNA expression of *StFeSOD2*, *StFeSOD3*, *StMnSOD*, *StCuZnSOD1* and *StCuZnSOD2*, while Ri-2, Ri-3, and Ri-5 plants exhibited a decreased expressed compared to the NT plants, after 48 h of cultivation under heat stress condition ($p < 0.001$). However, *StMAPKK5*-low expressing plants showed decreased gene expression ($p < 0.001$). Peroxidases, encoded by *StPOD66*, *StPOD47*, and *StPOD12* are enzymes involved in scavenging ROS, in response to heat stress. The *CAT* genes encode for catalase, such as *StCAT1* and *StCAT2*, playing a vital role in the antioxidant defense system by scavenging ROS generated under heat stress situations. In the NT plants, *StPOD66* (Figure 7F), *StPOD47* (Figure 7G), *StPOD1* (Figure 7H), *StCAT1* (Figure 7I), and *StCAT2* (Figure 7J) was highly expressed in response to heat stress ($p < 0.001$). Compared to the NT plants, the transgenic potato lines (OE-2, OE-3, and OE-6) increased the gene expression, while the RNAi plants profoundly decreased the mRNA expression of peroxidases, in response to heat stress ($p < 0.001$). The *StHSFA3*-encoded protein belongs to the plant heat shock transcription factor family, orchestrating the transcription of genes that encode heat shock proteins (HSP) assisting the plant in coping with heat-induced damage (Friedrich et al., 2021). After 48 h of cultivation under heat stress condition, the NT plants displayed increased mRNA expression of *StHSFA3* (Figure 7K), *StHsp20–20* (Figure 7L), *StHsp20–33* (Figure 7M), *StHsp20–44* (Figure 7N), *StHsp70* (Figure 7O), *StHsp90.2* (Figure 7P), and *StHsp90.4* (Figure 7Q). In contrast to the NT plants, the OE lines showed enhanced transcriptional levels, while the Ri plants exhibited decreased expression of the genes, under heat stress conditions ($p < 0.001$). The *StP5CS* gene, which encodes △1-pyrroline-5-carboxylate synthetase, plays a critical role in proline biosynthesis, and proline is an important amino acid involved in maintaining cellular osmotic balance and scavenging ROS. Consistently, the NT plants increased the mRNA expression of *StP5CS*, 48 h after cultivation under heat stress conditions ($p < 0.001$) (Figure 7R). In comparison with the NT plants, the mRNA expression of *StP5CS* was evidently enhanced in the OE lines, while reduced in the Ri plants, in response to heat stress. Our results suggested that overexpression of *StMAPKK5* triggered genetic responses of potato plant to combat heat stress.

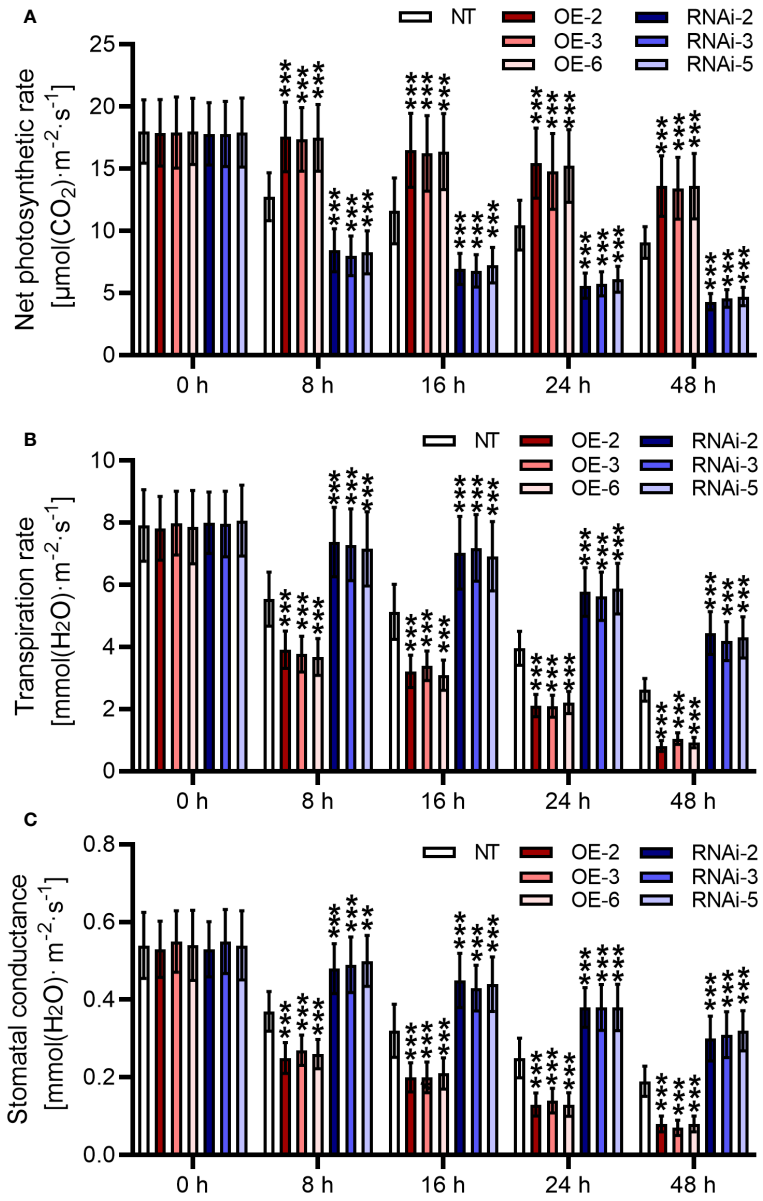

FIGURE 6
Stomatal apertures and photosynthesis in plants with overexpression or under-expression of *StMAPKK5* responding to heat stresses. **(A)** Net photosynthetic rate, **(B)** transpiration rate and **(C)** stomatal conductance of potato leaves. Transgenic or non-transgenic plants were measured 0 h, 8 h, 16 h, 24 h, and 48 h after cultivated under heat stress conditions. NT, non-transgenic plants; Ri, pART-StMAPKK5-RNAi-transgenic plants (RNAi-2, RNAi-3, and RNAi-5); OE, pBI121-EGFP-StMAPKK5-transgenic lines (OE-2, OE-3, and OE-6). Mean ± standard deviation. p-values (***$p < 0.001$) were calculated by ordinary two-way ANOVA, followed by Tukey's multiple comparisons test (n = 9).

Discussion

The effects of high temperatures are now evident in the reduced yield, nutrient depletion, and diminished quality of potatoes in an aberrant environment (Lee et al., 2020; Singh et al., 2020). The MAPK cascade is a crucial signaling pathway that plays a key module in transducing signals from environmental factors such as heat. The cascade has been extensively investigated and detailed in model plants like Arabidopsis, and crops such as rice owing to their relatively well-established research resources (Kumar et al., 2020; Chen et al., 2021). However, understanding the MAPK cascade in response to heat stress has been more challenging due to the complexity of its genome. Here, transgenic potato plants overexpressing *StMAPKK5* displayed an improved heat stress tolerance in comparison to the non-transformed controls. Overexpression of *StMAPKK5* triggered antioxidant enzyme genes, such as *StFeSOD2*, which was then implicated in regulating potato growth and physiology. As a result, *StMAPKK5* can be used to create varieties that are more resistant to heat stress.

Numerous MAPKKs have been detected in a variety of plant species, including *Arabidopsisthaliana* (MAPK group, 2002), *Populus trichocarpa* (Nicole et al., 2006), *Capsicum annuum*

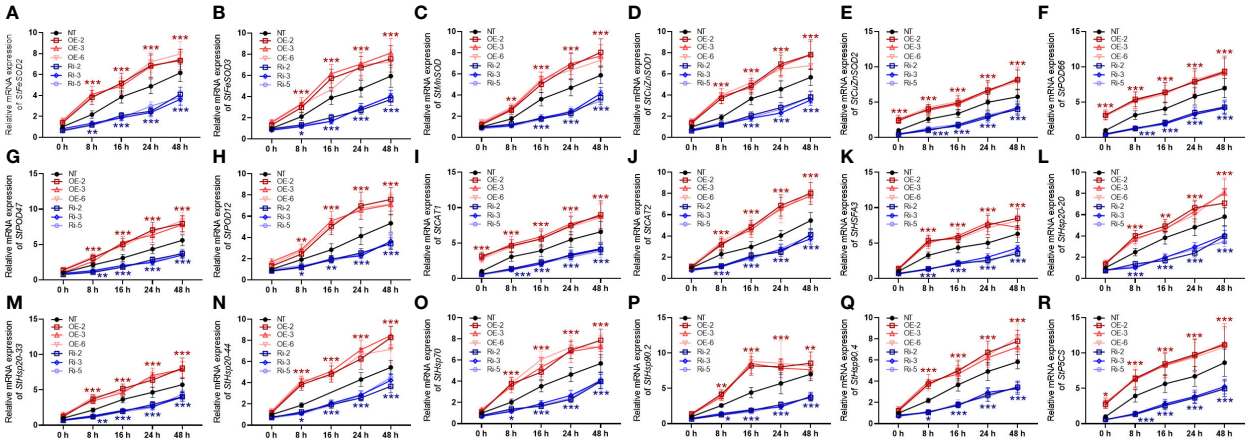

FIGURE 7
Alterations in mRNA expression of antioxidant enzyme genes and heat-stress responsive genes in plants with overexpression or under-expression of *StMAPKK5* under heat stress conditions. mRNA expression of **(A)** *StFeSOD2*, **(B)** *StFeSOD2*, **(C)** *StPOD*, **(D)** *StCuZnSOD1*, **(E)** *StCuZnSOD2*, **(F)** *StPOD66*, **(G)** *StPOD47*, **(H)** *StPOD12*, **(I)** *StCAT1*, **(J)** *StCAT2*, **(K)** *StHSFA3*, **(L)** *StHsp20–20*, **(M)** *StHsp20–33*, **(N)** *StHsp20–44*, **(O)** *StHsp70*, **(P)** *StHsp90.2*, **(Q)** *StHsp90.4*, and **(R)** *StP5CS* in potato leaves were estimated 0 h, 8 h, 16 h, 24 h, and 48 h after cultivation under 35°C. NT, non-transgenic plants; Ri, pART-StMAPKK5-RNAi-transgenic plants (RNAi-2, RNAi-3, and RNAi-5); OE, pBI121-EGFP-StMAPKK5-transgenic lines (OE-2, OE-3, and OE-6). Mean ± standard deviation. p-values (*$p < 0.05$, **$p < 0.01$, ***$p < 0.001$) were calculated by ordinary two-way ANOVA, followed by Tukey's multiple comparisons test (n = 9).

(Liu et al., 2015), *Zea mays* (Kong et al., 2013), and *Oryza sativa* (Kumar et al., 2008). We analyzed the phylogenetic relationship of MAPKK proteins from *Solanum tuberosum*, *Arabidopsis thaliana*, *Solanum lycopersicum*, and *Oryza sativa*, and performed multiple alignment, to provide a systematic phylogenetic analysis of MAPKK proteins. Plant MAPKKs feature the phosphorylation site motif S/T-X_5-S/T and a presumptive MAPK-docking domain characterized by the sequence K/R-K/R-K/R-X_{1-6}-LX-L/V/I (Chae et al., 2010). In StMAPKK1, StMAPKK2, StMAPKK3, StMAPKK4, and StMAPKK5, we found S/G-X5-S/T/G/R motif, while K/R-K/R-K/R-X1–6-LX-L/V/I was not noted. Sequence alignment placed the potato MAPKKs into four groups, A (StMAPKK1 and StMAPKK3), B (StMAPKK5), C (StMAPKK2), and D (StMAPKK4).

The modification of MAPKK protein expression under abiotic and biotic stress conditions appear to be a plant strategy for adapting and defending against challenging survival environments. Yang et al. revealed that in response to heat stress, the transcription level of *OsMKK1* in *Xanthomonas oryzae* was apparently up-regulated (Yang et al., 2024). As for the abiotic stress, Kumar et al. *OsMAPKK1*, *OsMAPKK3*, *OsMAPKK4*, *OsMAPKK6*, and *OsMAPKK10–2* expression levels are differentially regulated by heat, cold, drought, and salinity stresses (Kumar et al., 2008). In *Prunus mume* under exposure to cold, the expression of 4 *PmMKK* genes (*PmMKK5*, *PmMKK6*, *PmMKK20*, and *PmMKK3*) is reduced with prolonged treatment (Wen et al., 2023). The expression patterns of *MKK* genes were determined in different tissues of poplar by Wang et al., and the expression of *MKK2a* was altered after cultivation under salt tress (Wang et al., 2022). However, limited studies have explored the expression patterns of *StMAPKKs* under heat stress conditions. Considering that plant MAPKKs have crucial functions responding to abiotic stresses, and their expressions are regulated by heat stress (Kumar et al., 2008; Kumar and Sinha, 2013), we firstly investigated *StMAPKKs* expression distribution in different organs of potato plant and expression profile under heat stress conditions. The expression of *StMAPKK1*, *StMAPKK2*, *StMAPKK3*, *StMAPKK4*, and *StMAPKK5* was distinctly distributed in flower, root, stem, leaf, petiole, stolon, tuber, and shoot. Furthermore, mRNA expression of the five genes in leaf, stem and root were affected to different extent. It is noteworthy that the increase in *StMAPKK5* expression was relatively high and stable. Subsequently, we further constructed *StMAPKK5* overexpression and low-expression plants to analyze its biological functions.

It's concerning to see the visible impact of aberrant environmental conditions on potato production, nutrient levels, and quality. Transgenic technology has been explored in creating varieties with traits like resistance to tolerance to environmental stressors like high temperature. Chen et al. concluded that the interaction between SaMKK2 and SaMAPK4/7 positively induces the expression of the downstream genes (*SLD2*, *OPR2*, and *CBFs*), thereby endowing potatoes with innate cold resistance (Chen et al., 2022). *StMKK1* is involved in potato defense against the potato late-blight pathogen *Phytophthora infestans*, the gray-mold fungal pathogen *Botrytis cinerea*, and the bacterial wilt pathogen *Ralstonia solanacearum* (Chen et al., 2021b). However, it is still unknown whether *StMAPKK5* mediates the growth of potato plant under heat stress. Our results showed that in response to heat stress, *StMAPKK5* overexpression maintained or even fostered the plant growth, while *StMAPKK5* down-regulation even decreased the growth compared to the non-transgenic plants. Duan et al. suggested a potential relationship between *OsMKK4* and grain size or growth (Duan et al., 2014). *GhMKK3* overexpression facilitates root growth in transgenic *N. benthamiana* (Wang et al., 2016). These findings are consistent with our results, providing a rationale for the involvement of *MAPKK* genes in plant growth.

Plants activate various defense mechanisms to alleviate the harmful impacts of oxidative stress or consequential injury to cells or tissues in

response to abiotic stresses (drought, cold, heat, and salinity stresses) (Sachdev et al., 2021). These defense mechanisms include various non-enzymatic antioxidants and antioxidant enzymes (SOD, CAT, and POD) to neutralize ROS and maintain cellular homeostasis (Ahmad et al., 2009; Caverzan et al., 2016). High temperature affects multiple cellular processes, including photosynthesis, respiration and protein stability, and the disruption of these normal physiological activities leads to an overproduction of ROS and causes oxidative stress (Kumar, 2012; Posch et al., 2019; Zahra et al., 2023). Previous work has reported that in response to heat stress, MAPK cascade is involved in signal transduction, which affects plant physiological processes, such as photosynthesis, respiration, transpiration, nutrient uptake, tropisms, and senescence (Lee et al., 2016; Chardin et al., 2017b; Gouda et al., 2020; Liu et al., 2020). In this study, there was a reduction in contents of H_2O_2 and MDA, and an increase in antioxidant activities, induced by *StMAPKK5* overexpression under heat stress conditions. Chlorophyll content and REC are regarded as the physiological parameters mostly affected by heat and drought stress (Rehman et al., 2016). From our findings, it can be concluded that *StMAPKK5* overexpression can alleviate the adverse effects on photosynthetic efficiency and cell membrane integrity.

SOD functions in the primary defense against oxidative damage in cells, and participates in the detoxification, neutralization, scavenging, and converting of superoxide radicals (Alscher et al., 2002; Mishra and Sharma, 2019). There are three main types of SOD, each containing a different metal cofactor, including FeSOD, MnSOD, and CuZnSOD (Mishra and Sharma, 2019). Catalase detoxifies hydrogen peroxide and maintains redox homeostasis responding to heat stress (Dat et al., 1998). Peroxidase prevents the accumulation of hydrogen peroxide and reduce oxidative stress, working in coordination with other antioxidants like SOD and catalase (Veal and Day, 2011). *StMAPKK5* overexpression significantly enhances the mRNA expression of SOD, catalase and peroxidase responding to heat stress. HSFA protein activate HSP expression, which are molecular chaperones that assist in protein refolding and prevent protein denaturation under heat stress conditions (Bourgine and Guihur, 2021; Khan et al., 2021). From our results, the increase in *StHSFA3* mRNA expression and the induction of *StHsp20–20*, *StHsp20–33*, *StHsp20–44*, *StHsp70*, *StHsp90.2*, and *StHsp90.4* seems to be related to *StMAPKK5* overexpression. P5CS gene is involved in the biosynthesis of proline that serves as an osmoprotectant, maintaining osmotic balance during heat stress (Liu and Wang, 2020). *StMAPKK5* overexpression-induced heat stress resistance may be through the regulation of StP5CS gene. Thus, *StMAPKK5* overexpression modulated relative expression of heat-stress responsive genes in response to heat stress.

Conclusions

Extreme high temperature leads to lower crop yields and confers negative roles in food availability. Here, we found the constructed *StMAPKK5*-transgenic potato plants exhibited an intensified heat stress tolerance compared to the non-transgenic plants. However, *StMAPKK5* deficiency showed relatively poor thermal stress resistance. The adverse effects of heat stress on antioxidant activities POD, CAT, and SOD, photosynthetic efficiency and cell membrane integrity were alleviated by *StMAPKK5* overexpression. The enhanced heat stress resistance in plants due to *StMAPKK5* overexpression may be attributed to alterations in the relative expression of antioxidant enzyme genes and heat-stress responsive genes.

Data availability statement

The original contributions presented in the study are included in the article/Supplementary Material, further inquiries can be directed to the corresponding author/s. The MAPKK protein sequences discussed in this article can be accessed at the National Center for Biotechnology Information (NCBI) website (https://www.ncbi.nlm.nih.gov/) under the specified accession number: AtMKK1 (NP_194337.1), AtMKK2 (NP_001031751.1), AtMKK3 (NP_001318713.1), AtMKK4 (NP_175577.1), AtMKK5 (NP_001319606.1), AtMKK6 (NP_200469.1), AtMKK7 (NP_173271.1), AtMKK8 (NP_187274.1), AtMKK9 (NP_177492.1), AtMKK10 (NP_174510.1), SlMAPKK1 (NP_001304158.1), SlMAPKK2 (NP_001234588.1), SlMAPKK3 (NP_001234591.1), SlMAPKK4 (NP_001234595.1), SlMAPKK5 (XP_010317547.1), StMAPKK1 (XP_006353547.1), StMAPKK2 (NP_001275406.1), StMAPKK3 (NP_001305558.1), StMAPKK4 (XP_006363984.1), StMAPKK5 (XP_006351529.1), OsMAPKK1 (XP_015644525.1), OsMAPKK3 (XP_015643944.1), OsMAPKK4 (XP_015627603.1), OsMAPKK5 (XP_015643444.1), OsMAPKK6 (XP_015621394.1), OsMAPKK10–1 (XP_015624529.2), OsMAPKK10–2 (XP_015628376. 1), OsMAPKK10–3 (XP_015629634.1).

Author contributions

XZ: Writing – original draft, Writing – review & editing. WL: Writing – original draft, Writing – review & editing. NZ: Writing – original draft, Writing – review & editing. HJ: Writing – original draft, Writing – review & editing. HD: Writing – original draft, Writing – review & editing. ZC: Writing – original draft, Writing – review & editing. SC: Writing – original draft, Writing – review & editing. QW: Writing – original draft, Writing – review & editing. JT: Writing – original draft, Writing – review & editing. JZ: Writing – original draft, Writing – review & editing. YZ: Writing – original draft, Writing – review & editing. HS: Writing – original draft, Writing – review & editing.

Funding

The author(s) declare financial support was received for the research, authorship, and/or publication of this article. This Research Program was financially supported by the National Natural Science Foundation of China (No. 32360459), the Hainan Provincial Natural Science Foundation of China (No. 322MS116, 323MS095, 324MS098, 324QN327), and Central Public-interest

Scientific Institution Basal Research Fund for Chinese Academy of Tropical Agricultural Sciences (No. 1630062024005).

Acknowledgments

We thank Rongkai Wang (Bioediates, Shaanxi, China) for providing the plasmids pBI121-EGFP, pHANNIBAL, and pART.

Conflict of interest

The authors declare that the research was conducted in the absence of any commercial or financial relationships that could be construed as a potential conflict of interest.

Publisher's note

Supplementary material

The Supplementary Material for this article can be found online at: https://www.frontiersin.org/articles/10.3389/fpls.2024.1392425/full#supplementary-material

References

Ahmad, P., Jaleel, C. A., Azooz, M. M., and Nabi, G. (2009). Generation of ROS and non-enzymatic antioxidants during abiotic stress in plants. *Bot. Res. Int.* 2, 11–20.

Alscher, R. G., Erturk, N., and Heath, L. S. (2002). Role of superoxide dismutases (SODs) in controlling oxidative stress in plants. *J. Exp. Bot.* 53, 1331–1341. doi: 10.1093/jexbot/53.372.1331

Ara, H., and Sinha, A. K. (2014). Conscientiousness of mitogen activated protein kinases in acquiring tolerance for abiotic stresses in plants. *Proc. Ind. Natl. Sci. Acad.* 80, 211–219. doi: 10.16943/ptinsa/2014/v80i2/1

Beillouin, D., Schauberger, B., Bastos, A., Ciais, P., and Makowski, D. (2020). Impact of extreme weather conditions on European crop production in 2018. *Philos. Trans. R Soc. Lond B Biol. Sci.* 375, 20190510. doi: 10.1098/rstb.2019.0510

Bergmann, D. C., Lukowitz, W., and Somerville, C. R. (2004). Stomatal development and pattern controlled by a MAPKK kinase. *Science* 304, 1494–1497. doi: 10.1126/science.1096014

Bourgine, B., and Guihur, A. (2021). Heat shock signaling in land plants: From plasma membrane sensing to the transcription of small heat shock proteins. *Front. Plant Sci.* 12, 710801. doi: 10.3389/fpls.2021.710801

Caverzan, A., Casassola, A., and Brammer, S. P. (2016). Reactive oxygen species and antioxidant enzymes involved in plant tolerance to stress. *Abiotic biotic Stress plants-recent Adv. Future Perspect.* 17, 463–480.

Chae, L., Pandey, G. P., Luan, S., and Cheong, Y. H. (2010). Protein kinases and phosphatases for stress signal transduction in plants. *Abiotic Stress adaptation plants: physiological Mol. genomic foundation* p, 123–163.

Chardin, C., Schenk, S. T., Hirt, H., Colcombet, J., and Krapp, A. (2017a). Review: Mitogen-Activated Protein Kinases in nutritional signaling in Arabidopsis. *Plant Sci.* 260, 101–108. doi: 10.1016/j.plantsci.2017.04.006

Chardin, C., Schenk, S. T., Hirt, H., Colcombet, J., and Krapp, A. (2017b). Mitogen-activated protein kinases in nutritional signaling in Arabidopsis. *Plant Sci.* 260, 101–108. doi: 10.1016/j.plantsci.2017.04.006

Chen, X., Ding, Y., Yang, Y., Song, C., Wang, B., Yang, S., et al. (2021a). Protein kinases in plant responses to drought, salt, and cold stress. *J. Integr. Plant Biol.* 63, 53–78. doi: 10.1111/jipb.13061

Chen, X., Wang, W., Cai, P., Wang, Z., Li, T., and Du, Y. (2021b). The role of the MAP kinase–kinase protein StMKK1 in potato immunity to different pathogens. *Horticulture Res.* 8, 117. doi: 10.1038/s41438-021-00556-5

Chen, Y., Chen, L., Sun, X., Kou, S., Liu, T., Dong, J., et al. (2022). The mitogen-activated protein kinase MKK2 positively regulates constitutive cold resistance in the potato. *Environ. Exp. Bot.* 194, 104702. doi: 10.1016/j.envexpbot.2021.104702

Chen, J., Wang, L., and Yuan, M. (2021). Update on the roles of rice MAPK cascades. *Int. J. Mol. Sci.* 22, 1679. doi: 10.3390/ijms22041679

Choi, S. W., Lee, S. B., Na, Y. J., Jeung, S. G., and Kim, S. Y. (2017). Arabidopsis MAP3K16 and other salt-inducible MAP3Ks regulate ABA response redundantly. *Mol. Cells* 40, 230–242. doi: 10.14348/molcells.2017.0002

Dalhaus, T., Schlenker, W., Blanke, M. M., Bravin, E., and Finger, R. (2020). The effects of extreme weather on apple quality. *Sci. Rep.* 10, 7919. doi: 10.1038/s41598-020-64806-7

Danquah, A., Zelicourt, A. D., Colcombet, J., and Hirt, H. (2014). The role of ABA and MAPK signaling pathways in plant abiotic stress responses. *Biotechnol. Adv.* 32, 40–52. doi: 10.1016/j.biotechadv.2013.09.006

Dat, J. F., Lopez-Delgado, H., Foyer, C. H., and Scott, I. M. (1998). Parallel changes in H2O2 and catalase during thermotolerance induced by salicylic acid or heat acclimation in mustard seedlings. *Plant Physiol.* 116, 1351–1357. doi: 10.1104/pp.116.4.1351

Duan, P., Rao, Y., Zeng, D., Yang, Y., Xu, R., Zhang, B., et al. (2014). *SMALL GRAIN 1, which encodes a mitogen-activated protein kinase 4, influences grain size in rice*. *Plant J.* 77, 547–557. doi: 10.1111/tpj.12405

Friedrich, T., Oberkofler, V., Trindade, I., Altmann, S., Brzezinka, K., Lamke, J., et al. (2021). Heteromeric HSFA2/HSFA3 complexes drive transcriptional memory after heat stress in Arabidopsis. *Nat. Commun.* 12, 3426. doi: 10.1038/s41467-021-23786-6

Gouda, M. B., Zhang, C., Wang, J., and Peng, S. (2020). ROS and MAPK cascades in the post-harvest senescence of horticultural products. *J. Proteomics Bioinform.* 13, 1–7.

Hansen, J., Sato, M., and Ruedy, R. (2022). *Global temperature in 2021* Vol. 1 (Diponível em, Washington D.C). Available at: http://www.columbia.edu/~jeh1/mailings/2022/Temperature2021.13January2022.pdf.

He, X., Wang, C., Wang, H., Li, L., and Wang, C. (2020). The function of MAPK cascades in response to various stresses in horticultural plants. *Front. Plant Sci.* 11, 952. doi: 10.3389/fpls.2020.00952

Katlane, R., Kilani, B. E., Dhaoui, O., Kateb, F., and Chehata, N. (2023). Monitoring of sea surface temperature, chlorophyll, and turbidity in Tunisian waters from 2005 to 2020 using MODIS imagery and the Google Earth Engine. *Regional Stud. Mar. Sci.* 66, 103143. doi: 10.1016/j.rsma.2023.103143

Khan, S., Jabeen, R., Deeba, F., and Waheed, U. (2021). Heat shock proteins: classification, functions and expressions in plants during environmental stresses. *J. Bioresource Manage.* 8, 85–97. doi: 10.35691/JBM.1202.0183

Kong, X., Pan, J., Zhang, D., Jiang, S., Cai, G., Wang, L., et al. (2013). Identification of mitogen-activated protein kinase gene family and MKK-MAPK interaction network in maize. *Biochem. Biophys. Res. Commun.* 441, 964–969. doi: 10.1016/j.bbrc.2013.11.008

Kumar, K., Rao, K. P., Sharma, P., and Sinha, A. K. (2008). Differential regulation of rice mitogen activated protein kinase (MKK) by abiotic stress. *Plant Physiol. Biochem.* 46, 891–897. doi: 10.1016/j.plaphy.2008.05.014

Kumar, R. R. (2012). Protection against heat stress in wheat involves change in cell membrane stability, antioxidant enzymes, osmolyte, H2O2 and transcript of heat shock protein. *Int. J. Plant Physiol. Biochem.* 4, 83–91.

Kumar, R. R., Arora, K., Goswami, S., Sakhare, A., Singh, B., Chinnusamy, V., et al. (2020). *MAPK enzymes: a ROS activated signaling sensors involved in modulating heat stress response, tolerance and grain stability of wheat under heat stress*. *3 Biotech.* 10, 380. doi: 10.1007/s13205-020-02377-0

Kumar, K., Raina, S. K., and Sultan, S. M. (2020). Arabidopsis MAPK signaling pathways and their cross talks in abiotic stress response. *J. Plant Biochem. Biotechnol.* 29, 700–714. doi: 10.1007/s13562-020-00596-3

Kumar, K., and Sinha, A. K. (2013). Overexpression of constitutively active mitogen activated protein kinase 6 enhances tolerance to salt stress in rice. *Rice (N Y)* 6, 25. doi: 10.1186/1939-8433-6-25

Lafleur, E., Kapfer, C., Joly, V., Liu, Y., Tebbji, F., Daigle, C., et al. (2015). The FRK1 mitogen-activated protein kinase (MAPKKK) from Solanum chacoense is involved in embryo sac and pollen development. *J. Exp. Bot.* 66, 1833–1843. doi: 10.1093/jxb/eru524

Lee, Y., Kim, Y. J., Kim, M. H., and Kwak, J. M. (2016). MAPK cascades in guard cell signal transduction. *Front. Plant Sci.* 7, 80. doi: 10.3389/fpls.2016.00080

Lee, H., Lee, H., Jun, Y. S., Cha, O. K., and Sheen, J. (2019). Mitogen-activated protein kinases MPK3 and MPK6 are required for stem cell maintenance in the Arabidopsis shoot apical meristem. *Plant Cell Rep.* 38, 311–319. doi: 10.1007/s00299-018-2367-5

Lee, Y.-H., Sang, W. G., Baek, J. K., Kim, J. H., Shin, P., Seo, M. C., et al. (2020). The effect of concurrent elevation in CO2 and temperature on the growth, photosynthesis, and yield of potato crops. *PloS One* 15, e0241081. doi: 10.1371/journal.pone.0241081

Li, G., Cao, C., Yang, H., Wang, J., Wei, W., Zhu, D., et al. (2020). Molecular cloning and potential role of DiSOC1s in flowering regulation in Davidia involucrata Baill. *Plant Physiol. Biochem.* 157, 453–459. doi: 10.1016/j.plaphy.2020.11.003

Li, C., Zhu, J., Cheng, Y., Hou, J., Sun, L., and Ge, Y. (2022). Acibenzolar-S-methyl activates mitogen-activated protein kinase cascade to mediate chlorophyll and carotenoid metabolisms in the exocarp of Docteur Jules Guyot pears. *J. Sci. Food Agric.* 102, 4435–4445. doi: 10.1002/jsfa.11797

Liu, Z., Shi, L., Liu, Y., Tang, Q., Shen, L., Yang, S., et al. (2015). Genome-wide identification and transcriptional expression analysis of mitogen-activated protein kinase and mitogen-activated protein kinase genes in Capsicum annuum. *Front. Plant Sci.* 6, 780. doi: 10.3389/fpls.2015.00780

Liu, J., Wang, X., Yang, L., Nan, W., Ruan, M., and Bi, Y. (2020). Involvement of active MKK9-MAPK3/MAPK6 in increasing respiration in salt-treated Arabidopsis callus. *Protoplasma* 257, 965–977. doi: 10.1007/s00709-020-01483-3

Liu, J., and Wang, Y.-S. (2020). Proline metabolism and molecular cloning of AmP5CS in the mangrove Avicennia marina under heat stress. *Ecotoxicology* 29, 698–706. doi: 10.1007/s10646-020-02198-0

Lu, H., Klocko, A. M., Brunner, A. M., Ma, C., Magnuson, A. C., Howe, G. T., et al. (2019). RNA interference suppression of AGAMOUS and SEEDSTICK alters floral organ identity and impairs floral organ determinacy, ovule differentiation, and seed-hair development in Populus. *New Phytol.* 222, 923–937. doi: 10.1111/nph.15648

Luo, Y., et al. (2024). StMAPKK5 positively regulates response to drought and salt stress in potato. *Int. J. Mol. Sci.* 25, 3662. doi: 10.3390/ijms25073662

MAPK group. (2002). Mitogen-activated protein kinase cascades in plants: a new nomenclature. *Trends Plant Sci.* 7, 301–308. doi: 10.1016/S1360-1385(02)02302-6

Mishra, P., and Sharma, P. (2019). Superoxide Dismutases (SODs) and their role in regulating abiotic stress induced oxidative stress in plants. *Reactive oxygen nitrogen sulfur species plants: production metabolism Signaling defense Mech.* p, 53–88. doi: 10.1002/9781119468677.ch3

Nicholson, C. C., and Egan, P. A. (2020). Natural hazard threats to pollinators and pollination. *Glob Chang Biol.* 26, 380–391. doi: 10.1111/gcb.14840

Nicole, M.-C., Hamel, L. P., Morency, M. J., Beaudoin, N., Ellis, B. E., and Seguin, A. (2006). MAP-ping genomic organization and organ-specific expression profiles of poplar MAP kinases and MAP kinase kinases. *BMC Genomics* 7, 223. doi: 10.1186/1471-2164-7-223

Posch, B. C., Kariyawasam, B. C., Bramley, H., Coast, O., Richards, R. A., Reynolds, M. P., et al. (2019). Exploring high temperature responses of photosynthesis and respiration to improve heat tolerance in wheat. *J. Exp. Bot.* 70, 5051–5069. doi: 10.1093/jxb/erz257

Rehman, S. U., Bilal, M., Rana, R. M., Tahir, M. N., Shah, M. K., Ayalew, H., et al. (2016). Cell membrane stability and chlorophyll content variation in wheat (Triticum aestivum) genotypes under conditions of heat and drought. *Crop Pasture Sci.* 67, 712–718. doi: 10.1071/CP15385

Rodriguez, M. C., Petersen, M., and Mundy, J. (2010). Mitogen-activated protein kinase signaling in plants. *Annu. Rev. Plant Biol.* 61, 621–649. doi: 10.1146/annurev-arplant-042809-112252

Röhm, S., Krämer, A., and Knapp, S. (2021). *Function, structure and topology of protein kinases* (Springer, Cham).

Rykaczewska, K. (2015). The effect of high temperature occurring in subsequent stages of plant development on potato yield and tuber physiological defects. *Am. J. Potato Res.* 92, 339–349. doi: 10.1007/s12230-015-9436-x

Sachdev, S., Ansari, S. A., Ansari, M. I., Fujita, M., and Hasanuzzaman, M. (2021). Abiotic stress and reactive oxygen species: Generation, signaling, and defense mechanisms. *Antioxidants* 10, 277. doi: 10.3390/antiox10020277

Singh, B., Kukreja, S., and Goutam, U. (2020). Impact of heat stress on potato (Solanum tuberosum L.): Present scenario and future opportunities. *J. Hortic. Sci. Biotechnol.* 95, 407–424. doi: 10.1080/14620316.2019.1700173

Sparkes, I. A., Runions, J., Kearns, A., and Hawes, C. (2006). Rapid, transient expression of fluorescent fusion proteins in tobacco plants and generation of stably transformed plants. *Nat. Protoc.* 1, 2019–2025. doi: 10.1038/nprot.2006.286

Taj, G., Agarwal, P., Grant, M., and Kumar, A. (2010). MAPK machinery in plants: recognition and response to different stresses through multiple signal transduction pathways. *Plant Signal Behav.* 5, 1370–1378. doi: 10.4161/psb.5.11.13020

Veal, E., and Day, A. (2011). Hydrogen peroxide as a signaling molecule. *Antioxidants Redox Signaling* 15, 147–151. doi: 10.1089/ars.2011.3968

Walsh, J. E., Ballinger, T. H., Euskirchen, E. S., and Hanna, E. (2020). Extreme weather and climate events in northern areas: A review. *Earth-Science Rev.* 209, 103324. doi: 10.1016/j.earscirev.2020.103324

Wang, J., Pan, C., Wang, Y., Ye, L., Wu, J., Chen, L., et al. (2015). Genome-wide identification of MAPK, MAPKK, and MAPKKK gene families and transcriptional profiling analysis during development and stress response in cucumber. *BMC Genomics* 16, 386. doi: 10.1186/s12864-015-1621-2

Wang, C., Lu, W., He, X., Wang, F., Zhou, Y., Guo, X., et al. (2016). The cotton mitogen-activated protein kinase 3 functions in drought tolerance by regulating stomatal responses and root growth. *Plant Cell Physiol.* 57, 1629–1642. doi: 10.1093/pcp/pcw090

Wang, J., Sun, Z., Chen, C., and Xu, M. (2022). The MKK2a gene involved in the MAPK signaling cascades enhances populus salt tolerance. *Int. J. Mol. Sci.* 23, 10185. doi: 10.3390/ijms231710185

Wen, Z., Li, M., Meng, J., Miao, R., Liu, X, Fan, D., et al. (2023). Genome-wide identification of the MAPK and MAPKK gene families in response to cold stress in prunus mume. *Int. J. Mol. Sci.* 24, 8829. doi: 10.3390/ijms24108829

Wi, S. H., Lee, H. J., An, S., and Kim, S. K. (2020). Evaluating growth and photosynthesis of Kimchi cabbage according to extreme weather conditions. *Agronomy* 10, 1846. doi: 10.3390/agronomy10121846

Wu, J., Wang, J., Pan, C., Guan, X., Wang, Y., Liu, S., et al. (2014). Genome-wide identification of MAPKK and MAPKKK gene families in tomato and transcriptional profiling analysis during development and stress response. *PloS One* 9, e103032. doi: 10.1371/journal.pone.0103032

Yang, Z., Zhu, Z., Guo, Y., Lan, J., Zhang, J., Chen, S., et al. (2024). OsMKK1 is a novel element that positively regulates the Xa21-mediated resistance response to Xanthomonas oryzae pv. oryzae in rice. *Plant Cell Rep.* 43, 31. doi: 10.1007/s00299-023-03085-8

Yin, Z., Zhu, W., Zhang, X., Chen, X., Wang, W., Lin, H., et al. (2021). Molecular characterization, expression and interaction of MAPK, MAPKK and MAPKKK genes in upland cotton. *Genomics* 113, 1071–1086. doi: 10.1016/j.ygeno.2020.11.004

Yu, S., Zhang, L., Chen, C., Li, J., Ye, S., Liu, G., et al. (2014). Isolation and characterization of BnMKK1 responsive to multiple stresses and affecting plant architecture in tobacco. *Acta physiologiae plantarum* 36, 1313–1324. doi: 10.1007/s11738-014-1510-3

Zahra, N., Hafeez, M. B., Ghaffar, A., Kausar, A., Zeidi, M. A., Siddiaue, K. H., et al. (2023). Plant photosynthesis under heat stress: Effects and management. *Environ. Exp. Bot.* 206, 105178. doi: 10.1016/j.envexpbot.2022.105178

Zhang, M., and Zhang, S. (2022). Mitogen-activated protein kinase cascades in plant signaling. *J. Integr. Plant Biol.* 64, 301–341. doi: 10.1111/jipb.13215

Zhu, X., Hong, X., Liu, X., Li, S., Yang, J., Wang, F., et al. (2021). Calcium-dependent protein kinase 32 gene maintains photosynthesis and tolerance of potato in response to salt stress. *Scientia Hortic.* 285, 110179. doi: 10.1016/j.scienta.2021.110179

Zhu, X., Duan, H., Zhang, G., Jin, H., Xu, C., Chen, S., et al. (2023). StMAPK1 functions as a thermos-tolerant gene in regulating heat stress tolerance in potato (Solanum tuberosum). *Front. Plant Sci.* 14, 1218962. doi: 10.3389/fpls.2023.1218962

Zwerger, K., and Hirt, H. (2001). Recent advances in plant MAP kinase signalling. *Biol. Chem.* 382, 1123–1131. doi: 10.1515/BC.2001.142

frontiers | Frontiers in Plant Science

TYPE Original Research
PUBLISHED 24 June 2024
DOI 10.3389/fpls.2024.1417204

OPEN ACCESS

EDITED BY
Yi Wang,
Chinese Academy of Sciences (CAS), China

REVIEWED BY
Tengfei Liu,
Huazhong Agricultural University, China
Wen Huang,
The Sainsbury Laboratory, United Kingdom

*CORRESPONDENCE
Bailin Liu
liubl@nwafu.edu.cn

†These authors have contributed equally to this work

RECEIVED 14 April 2024
ACCEPTED 03 June 2024
PUBLISHED 24 June 2024

CITATION
Cui D, Song Y, Jiang W, Ye H, Wang S, Yuan L and Liu B (2024) Genome-wide characterization of the GRF transcription factors in potato (*Solanum tuberosum* L.) and expression analysis of *StGRF* genes during potato tuber dormancy and sprouting. *Front. Plant Sci.* 15:1417204. doi: 10.3389/fpls.2024.1417204

Genome-wide characterization of the GRF transcription factors in potato (*Solanum tuberosum* L.) and expression analysis of *StGRF* genes during potato tuber dormancy and sprouting

Danni Cui[1,2†], Yin Song[1,2†], Weihao Jiang[1,2], Han Ye[1,2], Shipeng Wang[1,2], Li Yuan[1] and Bailin Liu[1,2*]

[1]Shenzhen Research Institute, Northwest A&F University, Shenzhen, China, [2]State Key Laboratory for Crop Stress Resistance and High-Efficiency Production, College of Agronomy, Northwest A&F University, Yangling, China

Growth-regulating factors (GRFs) are transcription factors that play a pivotal role in plant growth and development. This study identifies 12 *Solanum tuberosum* GRF transcription factors (StGRFs) and analyzes their physicochemical properties, phylogenetic relationships, gene structures and gene expression patterns using bioinformatics. The StGRFs exhibit a length range of 266 to 599 amino acids, with a molecular weight of 26.02 to 64.52 kDa. The majority of *StGRFs* possess three introns. The promoter regions contain a plethora of *cis*-acting elements related to plant growth and development, as well as environmental stress and hormone response. All the members of the StGRF family contain conserved WRC and QLQ domains, with the sequences of these two conserved domain modules exhibiting high levels of conservation. Transcriptomic data indicates that *StGRFs* play a significant role in the growth and development of stamens, roots, young tubers, and other tissues or organs in potatoes. Furthermore, a few *StGRFs* exhibit differential expression patterns in response to *Phytophthora infestans*, chemical elicitors, heat, salt, and drought stresses, as well as multiple hormone treatments. The results of the expression analysis indicate that *StGRF1*, *StGRF2*, *StGRF5*, *StGRF7*, *StGRF10* and *StGRF12* are involved in the process of tuber sprouting, while *StGRF4* and *StGRF9* may play a role in tuber dormancy. These findings offer valuable insights that can be used to investigate the roles of *StGRFs* during potato tuber dormancy and sprouting.

KEYWORDS

GRF transcription factors, gene expression, regulatory network, tuber dormancy, sprouting, potato

Introduction

Transcription factors (TFs), also referred to as *trans*-acting elements, can bind to specific sequences (*cis*-acting elements) in the gene promoter region to regulate the expression of a target gene. TFs exhibit a wide range of functions and play crucial roles in numerous biological processes and regulatory pathways in plants. To date, 320,370 transcription factors have been identified and classified into 58 families across 165 species (Jin et al., 2017). Among these families, growth-regulating factors (GRFs) are a plant-specific type of TF that were originally identified for their roles in stem and leaf development in rice (van der Knaap et al., 2000). To date, members of the GRF family have been identified in a number of plant species, including thale cress (*Arabidopsis thaliana*), maize (*Zea mays*), rice (*Oryza sativa*), oilseed rape (*Brassica napus*), soybean (*Glycine max*), tomato (*Solanum lycopersicum*), and moss (*Physcomitrella patens*) (Kim et al., 2003; Choi et al., 2004; Zhang et al., 2008; Khatun et al., 2017; Ma et al., 2017; Chen et al., 2019). The GRF proteins share common features, including the QLQ (Gln, Leu, Gln) and WRC (Trp, Arg, Cys) domains at the N-terminus, and the relatively variable regions at the C-terminus. They form complexes with their co-activators, known as GRF-interacting factors (GIFs), which can bind to the *cis*-acting region of downstream target genes and regulate their expression, inferring a role in transcriptional regulation.

GRF family genes are involved in the growth, development, and regeneration of plants. In *Arabidopsis*, *AtGRF1*, *AtGRF2*, and *AtGRF3* are predominantly expressed in shoots, roots, and stems (Kim et al., 2003). *AtGRF4* and *AtGRF6* are expressed in the midvein of leaves, while *AtGRF5* is expressed in leaf primordia (Horiguchi et al., 2005). *AtGRF7* is expressed in the blades and petioles of true leaves, while *AtGRF7* and *AtGRF8* are predominantly expressed in the shoot tips (Kim et al., 2003). Additionally, *AtGRF1*, *AtGRF2*, *AtGRF4*, *AtGRF5*, *AtGRF6*, *AtGRF7*, and *AtGRF9* are expressed in the flower (http://bar.utoronto.ca/eplant/). *AtGRF1*, *AtGRF2*, *AtGRF3*, *AtGRF4*, *AtGRF5*, and *AtGRF7* are strongly expressed in the meristematic zone (Kim et al., 2003; Rodriguez et al., 2010; Kim et al., 2012; Bao et al., 2014; **Pajoro et al., 2014**). GRFs have been reported to alter leaf cell numbers, thereby affecting the leaf size and longevity (Debernardi et al., 2014; **Wu et al., 2014**; Nelissen et al., 2015; Vercruyssen et al., 2015), stem elongation (van der Knaap et al., 2000; Kuijt et al., 2014), root development (Hewezi et al., 2012; Bao et al., 2014), floral organ development and regulation of flowering time (Pajoro et al., 2014), and seed oil content (Liu et al., 2012). GIFs act as transcriptional co-regulators of GRFs. GIF1 interacts with AtGRF1, AtGRF2, AtGRF4, AtGRF5 and AtGRF9 through its conserved QLQ domain (Kim and Kende, 2004; Horiguchi et al., 2005). The overexpression of *GIF1*/*AN3* leads to an increase in leaf area due to an increase in cell number (Horiguchi et al., 2005). Conversely, a moderate reduction in *GIF1* expression results in smaller leaves due to a reduction in cell number. Moreover, a number of *GRF* genes contain the miRNA396 target site, and it is known that miRNA396 plays a role in regulating *GRF* genes during plant development (Rodriguez et al., 2010; Debernardi et al., 2012). In *Arabidopsis*, miR396a and miR396b regulate leaf growth and development by post-transcriptional repression of *GRF* genes (Rodriguez et al., 2010; Wang et al., 2011). OsmiR396d targets *OsGRF6* and *OsGRF10*, and overexpression of OsmiR396 results in an abnormal number of stigmas and stamens (Liu et al., 2014). Furthermore, evidences indicate that GRFs play a role in the plant adaptation to stress (Kim et al., 2012; Casadevall et al., 2013; Liu et al., 2014), and are closely associated with plant hormones (Choi et al., 2004; Bazin et al., 2013).

Potato (*Solanum tuberosum* L.) is the third most important food crop worldwide, after rice and wheat. It plays a vital role in ensuring global food security, particularly in light of the growing population and the concomitant increase in hunger. It is estimated that over one billion people worldwide consume potatoes, with global production exceeding 300 million metric tons. The release of the potato's complete genome sequence has enabled a comprehensive analysis of the *GRF* genes (Xu et al., 2011). GRFs are involved in regulating the growth of different plant tissues and organs. The potato tuber is a swollen underground stem formed by shortened internodes and nodes that develop into tuber eyes. Meristematic activity in the tuber eyes is completely suppressed during the development of the tuber. Even when placed in optimal conditions for sprouting, such as warm temperature, darkness, and high humidity, the tuber buds are generally dormant and will not sprout or grow. Subsequently, the tuber enters a period of dormancy, during which the eye exhibits visible growth of a bud. As tuber dormancy is an important agronomic trait, a short dormancy period renders potato tubers challenging to store for an extended period, whereas a long dormancy period makes them difficult to plant in a timely manner. Tuber sprouting typically originates from the tuber apical meristem (TAM), although GRFs are among the most crucial regulators of meristem development and cell differentiation restriction in the shoot apical meristem (SAM). Nevertheless, the role of GRF genes in potato tuber dormancy and sprouting remains elusive. In order to gain a better understanding of the role of GRF transcription factors in potato, a genome-wide identification and analysis of the potato (*S. tuberosum*) *GRF* family members (*StGRFs*) was conducted. In the present study, a total of 12 *GRF* genes in the potato genome were identified. The expression patterns of *StGRFs* in different tissues were analyzed. Furthermore, the expression profiles of *StGRFs* under multiple external stimuli and hormones, as well as during tuber dormancy were examined. The results demonstrated that *StGRF* genes exhibited distinct expression patterns in different tissues, and that their transcription was induced by diverse biotic and abiotic stresses. Further analysis of the expression patterns of these *StGRFs* revealed that they may play a significant role in regulating the release of tuber dormancy.

Materials and methods

Plant materials

A diploid potato line EB063 derived from a cross between parent E (ED25) and B (CW2–1) (Xiao et al., 2018) was utilized in the present study. The sprouted seed tubers were planted at the Yulin potato breeding station, located in the Shaanxi Province of China. Local cultural practices were employed to ensure optimal

plant growth. The tubers were harvested at the appropriate stage of maturity and stored in the dark at room temperature for a period of two weeks, during which time they underwent wound healing. Subsequently, tubers of a similar size were then placed in light-proof boxes at a temperature of 22 ± 2°C in order to facilitate the release of dormancy. The tubers were designated as dormant tubers (DT) at the point at which they were fully mature (0 day at dormancy release array), while any sprouts that were ≥2 mm in length were considered to be sprouting tubers (ST). For the purpose of sample collection, the apical bud meristems (also known as the dormancy eye) were excised at day 0 of the dormancy release array. The sprouting sprouts and sprouting sprout bases were collected at five weeks of the dormancy release array, respectively, from three to five tubers using a 6 mm size cork borer. The samples were immediately frozen in liquid nitrogen and stored at −80°C, after which they were subjected to RNA isolation.

Identification and physicochemical properties analysis of the GRF family members in potato

The potato genome files (version number DM v6.1) were downloaded from the Spud DB database (http://spuddb.uga.edu/). Amino acid sequences of *Arabidopsis* (TAIR, http://www.arabidopsis.org/) and rice (RGAP, http://rice.uga.edu/) GRF proteins were employed as queries in a BlastP homology search to identify candidate GRF proteins against the potato genome DM v6.1. All retrieved amino acid sequences of potato were subjected to verification for the presence of both the QLQ and WRC (PF08880, PF08879, respectively; http://pfam.xfam.org/) domains through the CDD (Conserved Domains Database; https://www.ncbi.nlm.nih.gov/cdd/) and SMART (http://smart.embl-heidelberg.de/) programs. The physiochemical properties of StGRF proteins including the amino acid number, molecular weight (MW), isoelectric point (pI), and grand average of hydropathicity (GRAVY), were analyzed by the ExPASy ProtParam tool (http://www.expasy.org/protparam/). The subcellular localization of StGRF proteins was determined by web-server predictors in the Cell-PLoc package (http://www.csbio.sjtu.edu.cn/bioinf/plant-multi/).

Phylogenetic analysis, gene structure, and conserved motifs of StGRFs

To visualize the evolutionary relationship of GRF family members, full-length amino acid sequences of StGRFs, AtGRFs, OsGRFs and PtGRFs were then aligned using ClustalW. A phylogenetic tree was constructed using the neighbor-joining method in MEGA11 software (https://www.megasoftware.net/) and the bootstrap test was carried out with 1000 replicates. A homology analysis of potato GRF proteins was conducted by aligning of the amino acid sequences using ClustalW (https://www.genome.jp/tools-bin/clustalw), and the resulting alignment was visualized using the SnapGene tool. The map of exon-intron structures of the *StGRF* genes were visualized using GSDS2.0 (Gene Structure Display Server 2.0, http://gsds.cbi.pku.edu.cn/index.php). Furthermore, the MEME tool (https://meme-suite.org/meme/tools/meme) was employed to predict conserved motifs of the potato GRF family member. The number of motifs was set to 8 and zero or one occurrence per sequence.

Cis-acting element analysis of the *StGRF* promoters

The 2000 bp upstream sequences of *StGRF* genes were extracted using TBtools software (Chen et al., 2020) based on the full-length DNA sequence of the potato genome. The *cis*-acting elements in the potential promoter regions were identified using the PlantCARE database (http://bioinformatics.psb.ugent.be/webtools/plantcare/html/). The potential interactions of transcription factors in the 2000 bp upstream regions of *StGRF* genes were predicted using the Plant Transcriptional Regulatory Map (http://plantregmap.gao-lab.org/) with the following parameters: the P-value was set to 1e-6, and *Arabidopsis thaliana* as set to as the reference species. The results of the prediction were visualized using Cytoscape software (v3.9.1). The occurrence frequencies of transcription factors were employed to generate a wordcloud using the wordcloud package in the R project.

Expression profiles of *StGRF* genes

The expression profiles of *StGRF* genes were determined using RNA-Seq data available at the SpudDB (http://spuddb.uga.edu/). The tissue specificity of different tissues (tuber cortex, tuber pith, tuber peel and shoot apex) and organs (leaf, stem, flower, root, stamen, petiole, stolon, mature tuber and young tuber) and potato plants subjected to diverse stresses (microbial pathogen infection, salt, heat, BAP, IAA, ABA and GA3) was analyzed. Gene expression levels of *StGRF*s were represented by reads per kb per million reads (RFKM). The heatmap of the expression patterns was constructed using TBtools (https://github.com/CJ-Chen/TBtools/).

RNA isolation and RT-qPCR

Total RNA was extracted using the RNA simple Total RNA Kit (Cat. No. DP419, TIANGEN) in accordance with the manufacturer's instructions. RNA quality was analyzed using a NanoDrop One spectrophotometer and agarose gel electrophoresis. One microgram of total RNA was employed to synthesize the first strand of cDNA using the HiFiScript gDNA Removal cDNA Synthesis Kit (Cat. No. CW2020M, CWBIO) according to the manufacturer's instructions. The polymerase chain reaction (PCR) was conducted in a total volume of 10 μL, comprising 5 μL of 2×qPCR Smart Mix (SYBR Green) (Cat. No. DY20302, DEEYEE), 0.5 μL (10 μM) of each gene-specific primer, 3.5 μL of ddH_2O, and 1 μL of cDNA. The target gene was detected using the QuantStudioTM7 Flex System (Applied Biosystems, Thermo Fisher Scientific, USA). *StUBI3* was employed as an internal control, and the primers used for the qPCR are listed in Supplementary Table S1. The $2^{-\Delta\Delta CT}$ method was used to calculate

the relative gene expression, and all RT-qPCR experiments were performed in triplicate.

Results

Identification of *StGRF* genes in the potato genome

A total of 12 *GRF* family members in potato were identified and named *StGRF1* to *StGRF12* according to their physical locations on the chromosomes (Table 1) through the use of bi-directional BLAST and conserved domain analysis. Amino acid length analysis revealed a considerable range in the amino acid lengths of the *StGRF* proteins, with *StGRF8* having the shortest length of 226 amino acids and *StGRF2* having the longest length of 599 amino acids (Table 1). The molecular weight of the StGRFs exhibited a similarly wide range, from 26.02 kDa (*StGRF8*) to 64.52 kDa (*StGRF2*), while the isoelectric point of *StGRFs* displayed a similar range, from 6.31 (StGRF3) to 9.20 (StGRF1 and StGRF8) (Table 1). The 12 *StGRF* genes were unevenly distributed across nine chromosomes (Table 1). Among the 12 *StGRF* genes, the chromosome 8 contains four *StGRF* genes, namely *StGRF6*, *StGRF7*, *StGRF8* and *StGRF9*. In contrast, the remaining chromosomes each contain only one *StGRF* gene (Table 1). Subcellular localization prediction indicated that all the StGRF proteins were localized in the nucleus (Table 1).

Phylogenetic, conserved motif and gene structure analysis

To explore the evolutionary relationships and sequence homology among GRF proteins from potato, *Arabidopsis* (Kim et al., 2003), rice (Choi et al., 2004) and poplar (Wang et al., 2020), a neighbor-joining phylogenetic tree was constructed using MEGA11 software (Figure 1). The evolutionary relationships of the GRFs were analyzed and a total of 52 GRFs from four plant species were clustered into five subgroups with supported bootstrap values. These were designated as Group I, Group II, Group III, Group IV and Group V (Figure 1). A total of three, one, two, two, and four StGRF members were assigned to subgroups I, II, III, IV and V, respectively (Figure 1). The phylogenetic tree indicates that the StGRFs are more closely related to PtGRFs and AtGRFs than with to OsGRFs (Figure 1). This could be attributed to the fact that potato, poplar and *Arabidopsis* are dicotyledonous plants. In order to ascertain the structural diversity and functional prediction of StGRFs, multiple alignments of the amino acid sequences of StGRF family members were performed (Figure 2A). A total of eight conserved motifs were identified, with the length of these motifs ranging from 9 to 41 amino acids (Supplementary Table S2). Among these, motifs 1 and 2 were respectively annotated as the WRC and QLQ domain, which were included in all StGRF family members (Figures 2A, B), indicating that two domains are highly conserved. All family members, with the exception of *StGRF1*, *StGRF8* and *StGRF9*, contained a TQL (Thr, Gln, Leu) domain at the C-terminus (Figures 2A, B). In contrast, the C-termini of all StGRF members, with the exception of *StGRF1*, *StGRF3*, *StGRF8* and *StGRF9*, were found to contain an FFD (Phe, Phe, Asp) domain (Figures 2A, B). *StGRF2*, *StGRF3, StGRF4, StGRF9, StGRF10*, and *StGRF11* possess a GGPL (Gly, Gly, Pro, Leu) domain at the C-terminus (Figures 2A, B). A multiple sequence alignment of the core QLQ and WRC domain of StGRFs is presented in Supplementary Figure S1. It is notable that the characteristics of these motifs were consistent within the same cluster (Figures 2A, B). For example, *StGRF6*, *StGRF7* and *StGRF12* exhibited seven common conserved motifs (motifs 1, 2, 3, 4, 5, 6 and 7) (Figures 2A, B). The gene structure of the *StGRF* gene family was further analyzed using the GSDS online tool. The *StGRFs* exhibited a length range of 1000 bp to 6000 bp, with the number of introns was found to be 2 to 3

TABLE 1 Members of the *GRF* gene family in the potato genome.

Name	Gene ID	Gene length (bp)	Protein length (aa)	Chromosome location	Molecular weight (kDa)	pI	Prediction of the subcellular localization
StGRF1	Soltu.DM.01G032200	3805	420	1	46.61	9.20	Nucleus
StGRF2	Soltu.DM.02G027350	4632	599	2	64.52	7.28	Nucleus
StGRF3	Soltu.DM.03G021710	2573	469	3	51.53	6.31	Nucleus
StGRF4	Soltu.DM.04G032220	3375	597	4	64.33	8.48	Nucleus
StGRF5	Soltu.DM.07G012510	1818	340	7	39.08	8.88	Nucleus
StGRF6	Soltu.DM.08G003530	5386	352	8	38.59	8.84	Nucleus
StGRF7	Soltu.DM.08G021510	3887	341	8	38.08	8.14	Nucleus
StGRF8	Soltu.DM.08G026330	1644	226	8	26.02	9.20	Nucleus
StGRF9	Soltu.DM.08G030120	1969	422	8	45.99	7.59	Nucleus
StGRF10	Soltu.DM.09G004090	4404	377	9	41.79	8.82	Nucleus
StGRF11	Soltu.DM.10G024900	4273	391	10	42.65	8.59	Nucleus
StGRF12	Soltu.DM.12G004310	4164	352	12	39.31	8.11	Nucleus

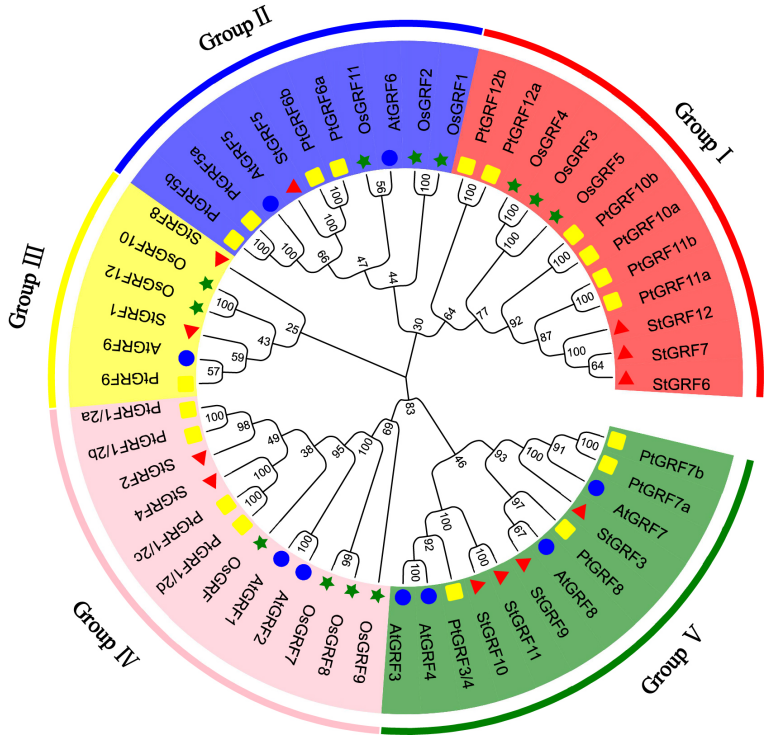

FIGURE 1
Phylogenetic tree of *GRF* proteins from *Arabidopsis thaliana* (At), *Oryza sativa* (Os), *Solanum tuberosum* (St), and *Populus trichocarpa* (Pt). Blue circle: *Arabidopsis thaliana* (At), green pentagram: *Oryza sativa* (Os), red triangle: *Solanum tuberosum* (St), yellow square: *Populus trichocarpa* (Pt).

(Figure 2C). *StGRFs* from the same clusters exhibited similar exon/intron structure patterns (Figure 2), suggesting that phylogenetic relationships among gene family members are highly correlated with gene structure. Furthermore, *StGRF7* has only a 3' untranslated region (UTR), whereas the other 11 *StGRF* genes possess 5'- and 3'-UTRs at both ends.

Cis-acting elements in the promoter regions of *StGRF* genes

Cis-acting elements within the gene promoters are specific binding sites for proteins involved in the initiation and regulation of gene transcription. To gain further insights into the functions of

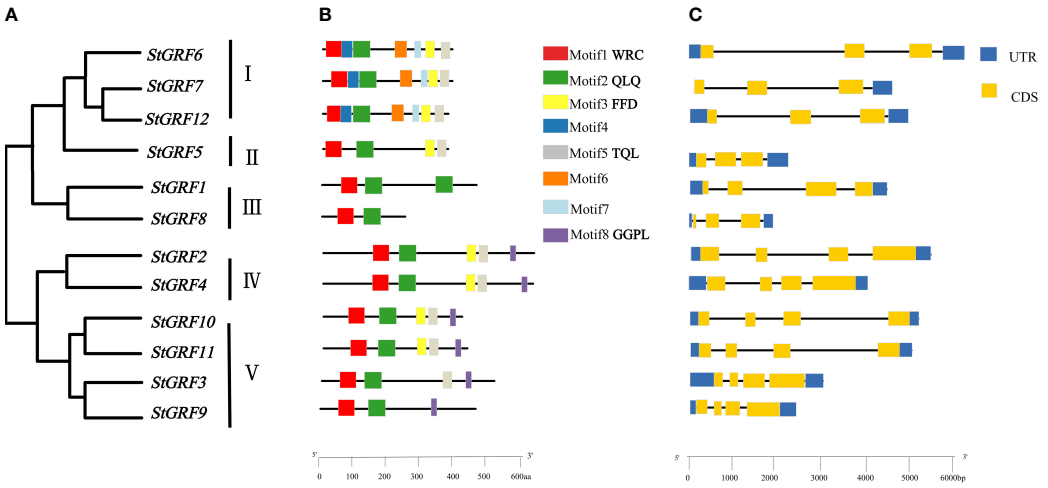

FIGURE 2
Phylogenetic tree, gene structure and motif of the *GRF* gene family in potato (*Solanum tuberosum*). **(A)** Phylogenetic relationship of *StGRF* proteins. **(B)**The distribution of eight conserved motifs in *StGRF* proteins, identified by the MEME program, as indicated by different colored blocks. **(C)** Exon/intron structures of *StGRFs*. The exons and introns were represented by yellow boxes and black lines, respectively. The dark blue boxes indicate the upstream and downstream untranslated regions, respectively.

cis-acting elements within the promoter region of *StGRFs*, the promoter sequences for *StGRFs* were submitted to PlantCARE for prediction (Figure 3). The *cis*-acting elements within the *StGRFs* promoters are primarily responsible for plant growth and development, as well as responses to hormones and abiotic or biotic stresses (Figure 3). *StGRF2*, *StGRF9* and *StGRF12* were found to contain several *cis*-acting elements closely associated with hormone responses, including ABRE (related to the abscisic acid responsiveness), AuxRR-core (auxin responsiveness), TCA-element (involved in salicylic acid responsiveness), CGTCA- and TGACG-motif (involved in MeJA-responsiveness), TATC-box and P-box (gibberellin-responsive element) (Figure 3). The majority of *StGRF* genes contained MeJA-responsive elements, CGTCA and TGACG motifs, which were observed 22 times, representing 42% of the hormone-related *cis*-acting elements. ABRE, the abscisic acid responsiveness elements, were observed 13 times, which represented 25% of the hormone-responsive elements of *StGRFs* (Figure 3). The promoter regions of nine *StGRFs* contain *cis*-acting elements related to environmental stresses (Figure 3). For example, LTR, a low-temperature responsiveness *cis*-acting element identified in *StGRF5* and *StGRF12*. MBS, a drought-inducibility *cis*-acting element identified in *StGRF2*, *StGRF3*, *StGRF11* and StGRF12. The TC-rich repeats and wound-responsive element 3 (WRE 3), which are known to be involved in wounding and pathogen response, have been identified in *StGRF1*, *StGRF2*, *StGRF4*, *StGRF5*, *StGRF11* and *StGRF12*. The ARE motif, which is essential for the anaerobic induction, has been identified on nine occasions, representing for 31% of the stress-related *cis*-acting elements (Figure 3). Furthermore, the promoters of 11 *StGRFs* carry *cis*-acting elements related to plant growth and development (Figure 3). The promoters of *StGRF5*, *StGRF7*, *StGRF8*, and *StGRF9* contain the CAT-box, which is associated with meristem development (Figure 3). Similarly, the promoters of *StGRF1*, *StGRF3*, *StGRF10*, and *StGRF11* contain the GCN4 motif, which is involved in plant endosperm development (Figure 3). The promoters of *StGRF6*, *StGRF8*, *StGRF9*, *StGRF10*, *StGRF11*, and *StGRF12* contain the O2-site, which is involved in the regulation of zein metabolism (Figure 3). The O2-site and GCN4 motifs were identified on 8 and 7 occasions, respectively, and accounted for 50% of the plant growth and development-related motifs (Figure 3). Additionally, *cis*-acting elements related to circadian control (circadian) and light response elements (G-box and Sp1) were also identified in the promoters of the *StGRFs* (Figure 3).

Bioinformatic analysis of StGRFs-mediated regulatory network

To predict the potential roles of *StGRFs* in potato, a StGRFs-mediated regulatory network was further constructed. Data indicated that a total of 52 transcription factors belonging to 15 different TF families, including Dof, MYB, C2H2, BBR-BPC, MIKC_MADS, AP2, etc., were identified as the potential regulators of *StGRFs* (Figure 4A, Supplementary Table S3). The predicted TFs were found to be most abundant in the Dof family (54), followed by the MIKC_MADS family (33), the BBR-BPC family (32) and the C2H2 family (20) (Figure 4B, Supplementary Table S3). In contrast, the least abundant TF families contain only a few members, including the Trihelix family (1), the TCP family (1), the C3H family (1) and the GATA family (2), the CPP family (2) (Supplementary Table S3). The predictions indicate that *StGRF6* has the largest class of TFs among all *StGRFs* (10 TFs), followed by *StGRF7* (7 TFs), *StGRF1* (6 TFs) and *StGRF4* (5 TFs) (Supplementary Table S3). These enriched transcription factor

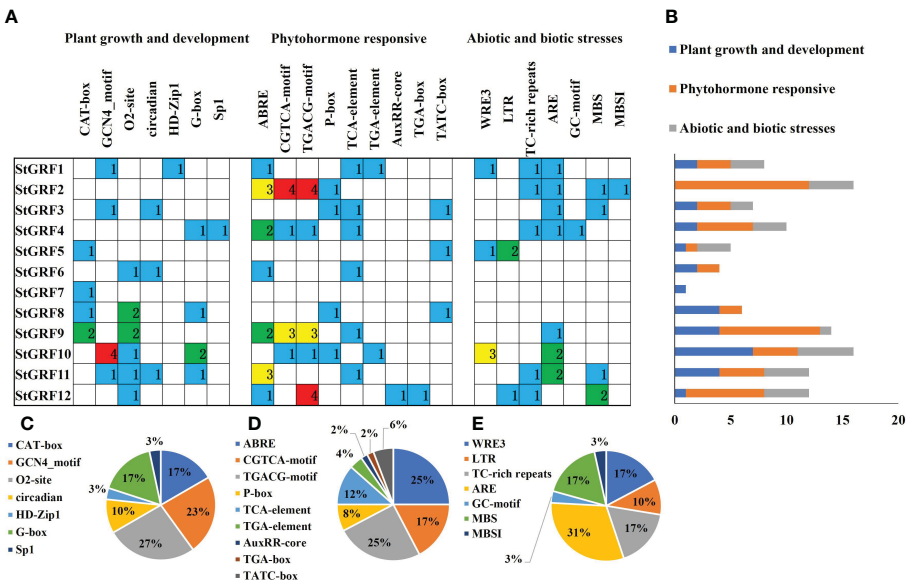

FIGURE 3
Cis-acting element analysis of the potato *GRF* family genes. The different colors represent different *cis*-acting elements. **(A)** Investigation of the number of *cis*-acting elements in the *StGRF* promoter regions. **(B)** Statistics for the number of the promoter elements in three major subfamilies. **(C–E)** The proportion of each promoter in the category.

10.3389/fpls.2024.1417204

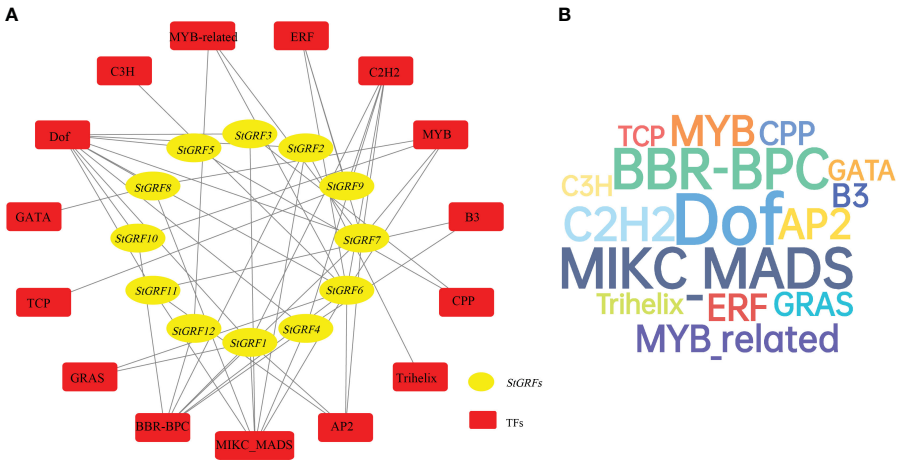

FIGURE 4
(A) The putative transcription factors (TFs) regulatory network analysis of *StGRFs*. Red rounded rectangle nodes represent TFs; yellow ellipse nodes represent *StGRFs*. **(B)** Wordcloud for TFs. The font size is positively correlated with the number of corresponding TFs.

families may play an essential role in regulating the expression of *StGRFs* in potato. Collectively, the predicted regulatory network of *StGRFs* indicates that they may be involved in a number of biological processes, including plant growth and development, biotic and abiotic stress responses, and network associations.

Tissue-specific expression of *StGRFs* in potato

A comparative analysis of the tissue-specific expression of the 12 *StGRFs* revealed differential expression in different potato tissues and developmental stages (Figure 5). The majority of *StGRFs* exhibited low expression in stamens, mature flowers, and mature fruits, whereas high expression was observed in immature tubers, including *StGRF2*, *StGRF4*, *StGRF6*, *StGRF10* and *StGRF12* (Figure 5). In heterozygous diploids, all *StGRFs* except for *StGRF1*, *StGRF5*, *StGRF8* and *StGRF11* were expressed in different organs, including roots, stolons, petioles, flowers and tubers, with varying levels of expression. The expression of different *StGRF* members exhibited tissue-specific characteristics. *StGRF4* exhibited high expression in stolons and young tubers, while lower expression was observed in stems and stamens (Figure 5). *StGRF12* was predominantly expressed in roots, stolons, tuber sprouts and young tubers (Figure 5). *StGRF9* exhibited high expression in flowers, stolons, and leaves, suggesting an essential role in flower

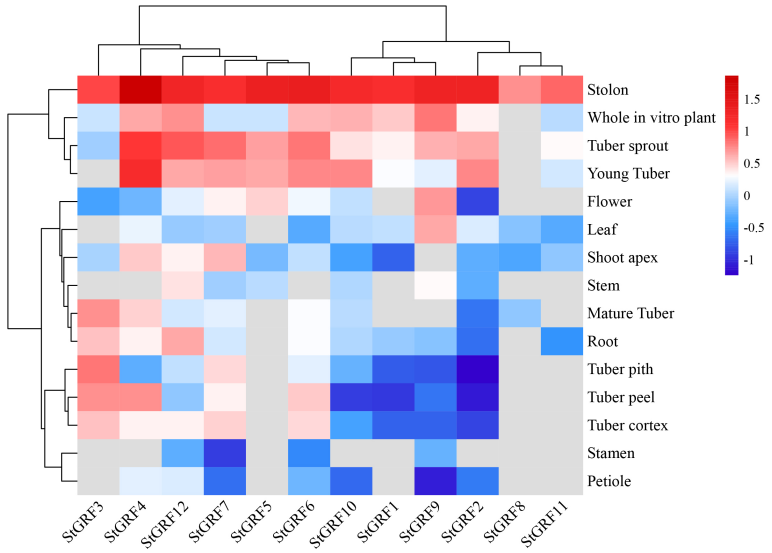

FIGURE 5
Expression profile analysis of *StGRF* genes in different potato tissues and organs. The color spectrum, ranging from red to blue, represents the expression levels of the genes, with red indicating high expression and blue indicating low expression. Grey indicates the value of zero in the original RNA-Seq data, which the software automatically recognizes this part of the data as 'missing'.

10.3389/fpls.2024.1417204

growth and development (Figure 5). Notably, *StGRF6* exhibited high expression in four tissues, yet displayed a lower transcript level in stamens, leaves and stems (Figure 5). *StGRF3* was highly specifically expressed in stolons, tuber piths and mature tubers, whereas *StGRF7* was highly expressed in stolons and tuber sprouts (Figure 5). *StGRF5* showed high expression in stolons, tuber sprouts and young tubers, with very weak expression in other tissues. *StGRF2* and *StGRF10* were highly expressed in young tubers, tuber sprouts, and stolons, with minimal expression in other tissues. *StGRF1*, *StGRF8*, and *StGRF11* showed weak expression in the majority of the examined tissues, with the exception of stolons (Figure 5). Collectively, all the 12 *StGRFs* exhibited distinct expression patterns according to the SpudDB database, indicating that they may have diverse biological functions in various tissues.

Expression analysis of *StGRF* genes under multiple external stimuli and hormones

The expression patterns of the *StGRF* genes in response to abiotic stresses (salt, heat, osmotic shock) were investigated. Salt stress induced up-regulation of *StGRF1*, *StGRF3*, *StGRF4*, *StGRF5*, *StGRF6*, *StGRF7*, *StGRF8* and *StGRF10*, *StGRF11* and *StGRF12*, and down-regulation of *StGRF9*, whereas *StGRF2* showed negligible changes under the NaCl treatment (Figure 6A). A rapid increase in the transcript levels of *StGRF1*, *StGRF3*, *StGRF4*, *StGRF5*, *StGRF6*, *StGRF7*, *StGRF9*, *StGRF10* and *StGRF11* was observed during osmotic shock induced by the mannitol treatment (Figure 6A). Upon exposure to heat stress, the mRNA abundance of *StGRF1*, *StGRF2*, *StGRF3*, *StGRF4*, *StGRF5*, *StGRF6*, *StGRF8*, *StGRF9*, *StGRF10* and *StGRF12* was found to be down-regulated, whereas *StGRF7* and *StGRF11* were up-regulated (Figure 6B). To ascertain whether *StGRFs* are involved in the hormone response, the expression patterns of *StGRF* genes in potato upon treatment with ABA (abscisic acid), GA_3 (gibberellic acid), IAA (indole-3-acetic acid) and BAP (6-benzylaminopurine) were investigated (Figure 6C). The expression levels of *StGRF6*, *StGRF7*, and *StGRF9* were significantly elevated in response to ABA stimulation, whereas the expression levels of *StGRF2*, *StGRF4*, *StGRF8*, *StGRF10*, *StGRF11* and *StGRF12* were significantly reduced, and *StGRF1* showed no significant changes (Figure 6C). Upon IAA treatment, the expression levels of *StGRF1*, *StGRF2*, *StGRF3*, *StGRF4*, *StGRF5*, *StGRF6*, *StGRF8* and *StGRF12* were down-regulated (Figure 6C). The application of GA_3 led to the up-regulation of *StGRF5* and *StGRF9*, while the expression levels of *StGRF1*, *StGRF2*, *StGRF4*, *StGRF6*, *StGRF7*, *StGRF8*, *StGRF10*, *StGRF11* and *StGRF12* were downregulated (Figure 6C). Treatment with BAP induced an increase in *StGRF5*, *StGRF8* and *StGRF9*, while the steady-state mRNA levels of other *StGRF* members exhibited a decrease (Figure 6C). Notably, the assays also revealed that the up-regulation of *StGRF1*, *StGRF3*, *StGRF4* and *StGRF9* was observed in leaves infected with the biotic factor *Phytophthora infestans*. Furthermore, except for *StGRF1*, the down-regulation of *StGRF2*, *StGRF4*, *StGRF6*, *StGRF7*, *StGRF9* was observed. The expression of *StGRF10* and *StGRF11* was observed in leaves treated with the chemical elicitor BABA (β-aminobutyric acid), whereas the expression of *StGRF1*, *StGRF6*, *StGRF9* and *StGRF12* was repressed in leaves treated with the chemical elicitor BTH (benzothiadiazole) (Figure 6D). This indicates that *StGRF1* and *StGRF9* play an essential role in potato

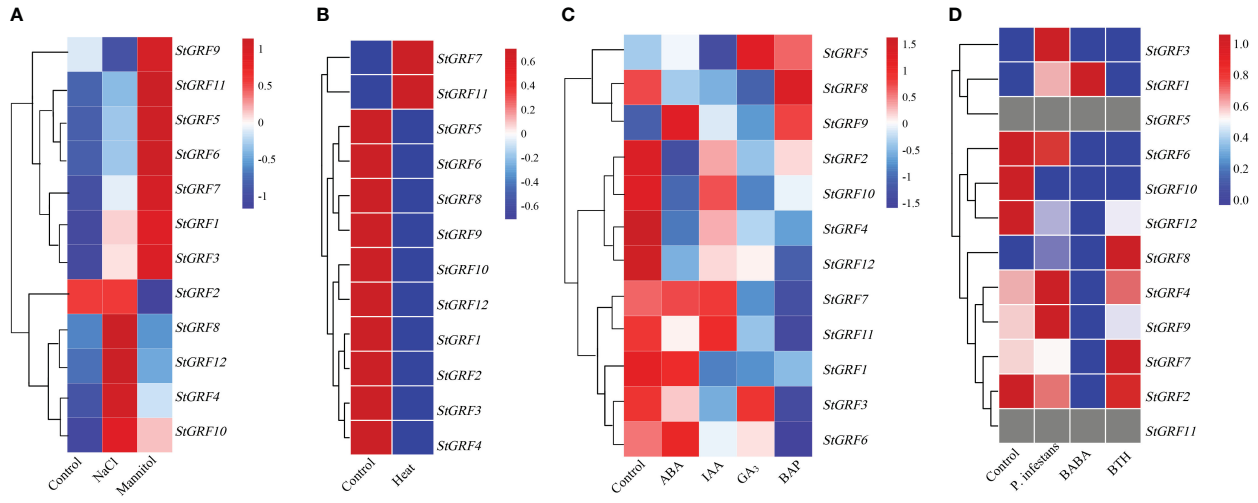

FIGURE 6
Heatmaps of the expression profiles of ten *StGRF* genes under ten different biotic or abiotic stresses. The transcripts were identified through the use of RNA-Seq technology. **(A)** Salt stresses include 150 mM NaCl for 24 h, and 260 μM mannitol for 24 h. **(B)** The heat stress treatment was 35°C for 24 h. **(C)** The phytohormone treatments included 50 μM ABA (abscisic acid) for 24 h, 10 μM IAA (indole-3-acetic acid) for 24 h, 50 μM GA_3 (gibberellic acid) for 24 h and 10 μM BAP (6-benzylaminopurine) for 24 h. **(D)** Biotic stresses include *Phytophthora infestans*, the stress elicitors BTH (benzothiadiazole), and BABA (β-aminobutyric acid), which are applied to leaves for 48 hours each. The color patterns, ranging from red (up-regulated expression level) to green (down-regulated expression level), provide an indication of the expression levels of the detected genes under the given conditions. The grey color indicates the value of zero in the original RNA-Seq data, and the software automatically recognizes this part of the data as 'missing'. The conditions (vertical) and genes (horizontal) with similar profiles were hierarchically clustered (Pearson correlation, average linkage).

defense against invading microbes. Taken together, the detailed expression analyses suggest that *StGRF* genes may be involved in the regulation of biotic and abiotic stresses in potato.

Expression profiles of *StGRFs* during the process of potato tuber dormancy release

The expression of *StGRF* genes was evaluated based on TPM (transcripts per kilobase of exon model per million mapped reads) values during the process of tuber dormancy release in publicly available RNA-Seq datasets from potato cultivars Longshu3 and Russet Burbank (Spud DB). In the case of the potato cultivar Longshu3, the transcript levels of the *StGRF1*, *StGRF2*, *StGRF5*, *StGRF6*, *StGRF7*, *StGRF10*, *StGRF11* and *StGRF12* increased in the dormancy-release tuber and sprouting tuber compared to the dormant tuber. In contrast, the transcript levels of *StGRF3* and *StGRF4* showed a decrease after tuber dormancy release, while the transcription of *StGRF8* was practically undetectable (Figure 7A). In the potato cultivar Russet Burbank, the expression profiles of *StGRF2*, *StGRF5*, *StGRF7*, *StGRF8*, *StGRF10* and *StGRF12* are up-regulated after tuber dormancy release or in nondormant tuber, whereas the expression profiles of *StGRF3*, *StGRF4*, *StGRF6*, *StGRF9* and *StGRF11* decrease after tuber dormancy release or in nondormant tuber (Figure 7B). A reduction in the expression of *StGRF3* and *StGRF4* was observed in potato cultivars Longshu3 and Russet Burbank following the release of tuber dormancy. This indicates that these genes may be involved in maintaining tuber dormancy. An up-regulation of *StGRF2*, *StGRF5*, *StGRF7*, *StGRF10* and *StGRF12* was observed in cultivars Longshu3 and Russet Burbank after tuber dormancy release, suggesting an association of these genes with the breaking of tuber dormancy and sprouting. To investigate whether *StGRF* genes were implicated in tuber dormancy, an RT-qPCR assay was conducted on all members of the *StGRF* family to ascertain their respective RNA accumulation profiles during the process of potato tuber dormancy release (Figure 8). The mRNA levels of *StGRF5*, *StGRF6*, *StGRF8*, and *StGRF12* were observed to increase after the tuber dormancy release in sprouts, and remained high in apical parts lacking sprouts compared to dormant apical parts. The mRNA levels of *StGRF1*, *StGRF7*, and *StGRF11* were observed to increase following the release of tuber dormancy in sprouts but decreased in apical parts without sprouts. This indicates that these *StGRFs* may be involved in promoting bud outgrowth. The expression of *StGRF4* and *StGRF9* decreased dramatically during tuber dormancy release, indicating that they play a role in of the regulation of tuber sprouting. No transcription was observed for *StGRF3* in sprouts and apical sections. The relative abundance levels of these *StGRFs* as

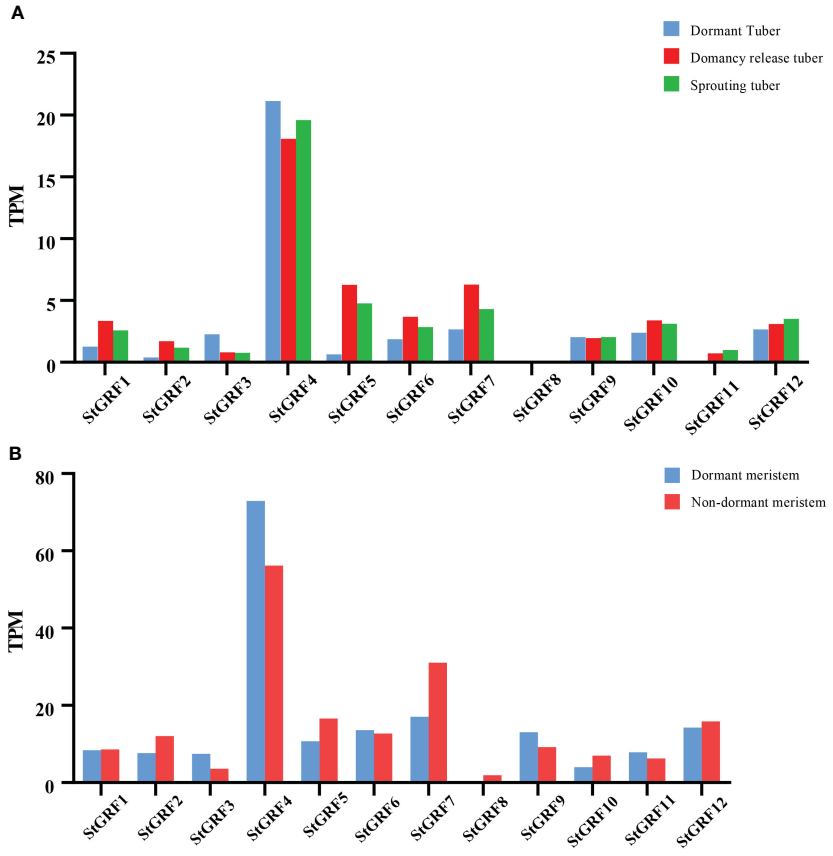

FIGURE 7
Expression profiles of *StGRFs* during dormancy release. Transcripts from the potato cultivars Longshu3 **(A)**, and Russet Burbank **(B)** were detected using RNA-Seq technology, as described by Liu et al. (Liu et al., 2015) and Campbell et al. (Campbell et al., 2008).

10.3389/fpls.2024.1417204

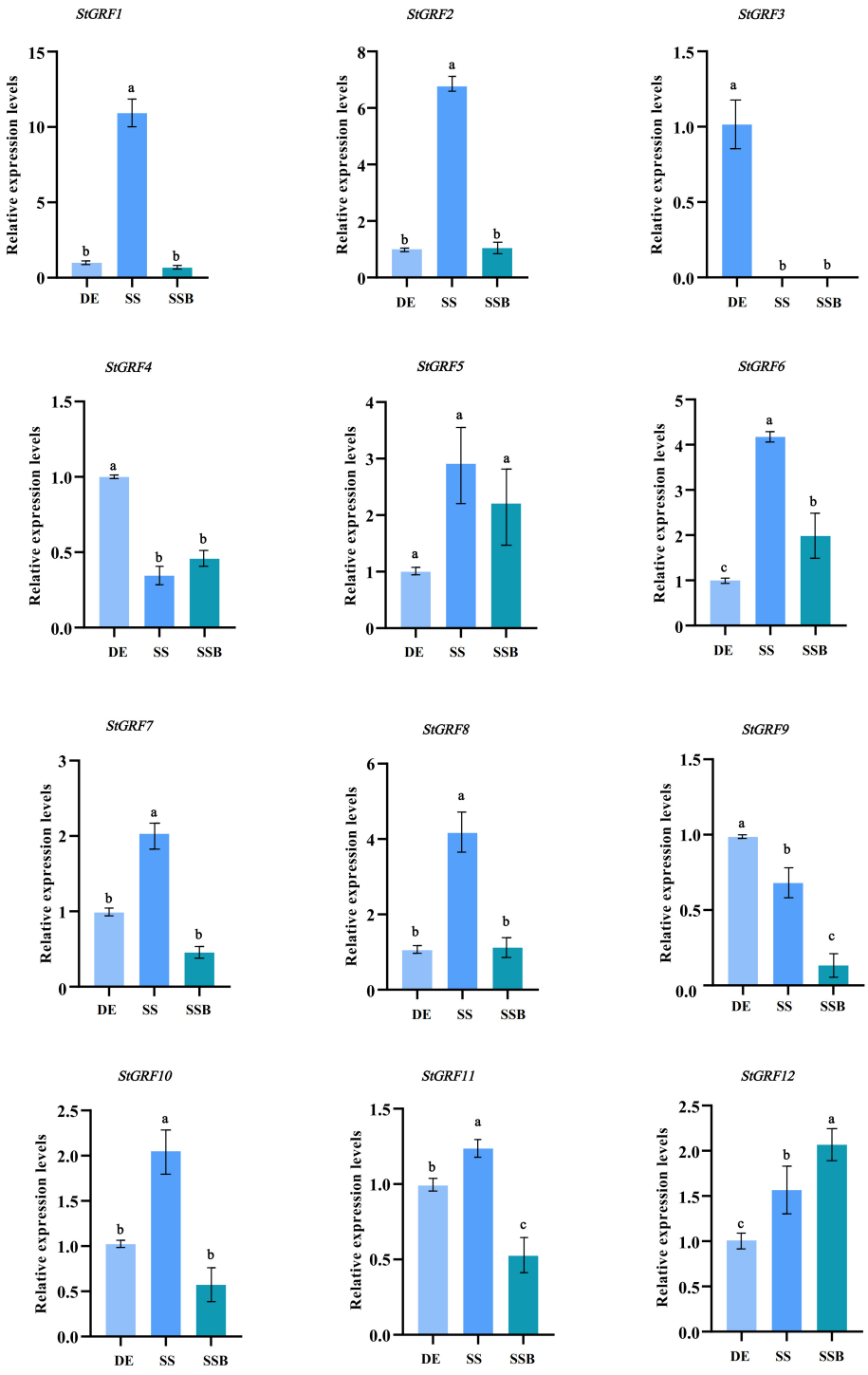

FIGURE 8
The expression levels of *StGRF* genes from the diploid potato line EB063 during dormancy release were determined by quantitative reverse transcription-polymerase chain reaction (RT-qPCR). Using the dormant eye as a control (DE), data represent the mean ± SEM (n=3). Analysis of variance and multiple comparisons (Tukey) were performed using the software GraphPad Prism9.0. The different letters indicate significant differences between samples ($p < 0.05$), and the same letter indicates that there is no significant difference between samples ($p \geq 0.05$).

determined by qPCR were found to be generally consistent with those generated from the RNA-Seq datasets (Figures 7, 8), suggesting that *StGRF1*, *StGRF2*, *StGRF5*, *StGRF7*, *StGRF10* and *StGRF12* may be sprout-related genes, while *StGRF4* and *StGRF9* may be dormancy-related genes.

Discussion

In this study, 12 potato *GRF* genes (*StGRFs*) were identified through database analysis (Figure 1), followed by an in-depth investigation of gene structure, protein motifs, phylogenetic

relationships, and gene expression patterns. StGRF proteins contain conserved WRC (Motif1) and QLQ (Motif2) domains (Figure 2; Supplementary Figure S1). The QLQ domain is responsible for protein-protein interactions, whereas the WRC domain is involved in DNA binding and nuclear targeting of the transcription factor (van der Knaap et al., 2000). Notably, StGRF1 contains a second WRC domain in its C-terminal region, similar to BrGRF12 from the Chinese cabbage *Brassica rapa* (Wang et al., 2014). In addition to the N-terminal conserved WRC and QLQ domains, the StGRF proteins carry additional C-terminal motifs, namely FFD, TQL, and GGPL, located in Motif 3, Motif 5, and Motif 8, respectively, in addition to the N-terminal conserved WRC and QLQ domains. The TQL motif, which has been described in AtGRF1 to AtGRF4, as well as in OsGRF1 to OsGRF5 (Omidbakhshfard et al., 2015), is present in StGRF2 to StGRF7, StGRF10 to StGRF12 (Figure 2). The FFD motif reported in the sweet orange (*Citrus sinensis*) GRF family members (Fu et al., 2024) is present in StGRF family members StGRF2, StGRF4, StGRF5, StGRF6, StGRF7, StGRF10, StGRF11 and StGRF12 (Figure 2). Similarly, the GGPL motif, which was reported in AtGRF1 to AtGRF4, AtGRF7, and AtGRF8 (van der Knaap et al., 2000; Kim et al., 2003; Choi et al., 2004), has been found to be located in StGRF2 to StGRF4, StGRF9 to StGRF11 (Figure 2). These TQL, FFD and GGPL motifs are also present in several GRFs from other plant species and are crucial for GRF function in plant tissues and organs (Omidbakhshfard et al., 2015). It is noteworthy that motifs 4, 6 and 7 are exclusive to the StGRF family members StGRF6, StGRF7 and StGRF12, which were categorized as subgroup I (Figures 1, 2). This suggests that these three motifs may be specific to subgroup I. The divergent C-terminal motifs of GRFs act as binding sites for transcriptional co-regulators and also have transcriptional transactivation activities (van der Knaap et al., 2000). Consequently, the conservation of both the N-terminal and C-terminal motifs is of significant importance for the evolutionary expansion and functional conservation of GRF family members in potato.

GRF genes are typically highly expressed in relatively active tissues such as germinating seeds and buds (Kim et al., 2003; Horiguchi et al., 2005; Kim et al., 2012; Zhang et al., 2018). RNA-Seq data show that *StGRF* genes are expressed at higher levels in the roots, shoot apices, flowers, and young tubers, where cell proliferation is strong in *Arabidopsis* (Kim et al., 2003; Rodriguez et al., 2010). The increased expression of *StGRF9* in the leaf, flower and stolon, in comparison to the root, suggests a role for this gene in these organs, analogous to its presumed orthologue *AtGRF8* (Kim et al., 2003). *StGRF5* is expressed in the flower (Figure 5), in a manner analogous to its putative orthologue *AtGRF5*, which is predominantly expressed in the floral meristem (Pajoro et al., 2014). The overexpression of *AtGRF5* in *Arabidopsis* results in an increase in cell proliferation in leaf primordia, leading to the formation of larger leaves than those observed in wild-type plants (Horiguchi et al., 2005). *StGRF3* is highly expressed in the root and clusters with *AtGRF3*, *AtGRF4* and *AtGRF7* (Figures 1, 5), suggesting that it may perform similar functions in the root. *AtGRF3* is expressed in the meristematic zone and elongation zone of primary and emerging lateral roots (Gorlova et al., 2014; Hepworth and Lenhard, 2014; Lee et al., 2018). *AtGRF4* has been identified in carpels and roots, with the highest levels of expression observed in the root tip and differential zone (Bao et al., 2014). *AtGRF4* is strongly expressed in the meristematic zone but weakly expressed in the elongation zone (Bao et al., 2014). *AtGRF7* is mainly expressed in flowers and shoot tips, with minimal expression in roots (Kim et al., 2003). Furthermore, *AtGRF7* is also expressed in developing tissues, including the vascular tissues, the inflorescence meristem, the bud pistil, the silique replum, the veins of leaf blades, and the petioles of true leaves (Kim et al., 2012). The same subfamily, *StGRF1* and *StGRF8*, demonstrated weak expression in all tissues examined (Figures 1, 5). However, *StGRF6*, *StGRF7* and *StGRF12*, which belong to the same subfamily as their homologs *OsGRF3*, *OsGRF4*, and *OsGRF5*, exhibited high expression in the young tubers, tuber sprouts and stolons (Figures 1, 5). This high expression may be involved in biological pathways that contribute to plant growth and development. The tissue-specific expression profiles of genes are typically associated with *cis*-regulatory elements (Saeed et al., 2006). It was observed that most of the *StGRF*s contain one or more than one *cis*-element related to plant growth and development in their promoter regions (Figure 3). The 12 *StGRF* genes containing these *cis*-elements may be involved in a variety of functions (Figure 3). The diversity of their functions and the distribution of *cis*-elements in the promoter regions of these genes suggest that *StGRFs* may differentially regulate the expression of genes involved in potato tuber development. Further functional characterization of the *StGRF* genes is essential to gain new insights into the molecular mechanism of tuber development in potato. Tuber initiation and development are of significant importance in potato production. The initiation and development of tubers are regulated by members of the FLOWERING LOCUS T (FT) clade and multiple environmental factors (Navarro et al., 2011). The high expression of the majority of *StGRF* genes in young tubers suggests their involvement in tuber formation and development (Figure 5), potentially through the association with other tuber-specific expression genes. For instance, *StGRF4* expression was significantly higher in young tubers than in mature tubers (Figure 5), which is consistent with previous findings indicating that *GRFs* are involved in the initial stages of growth and development in various tissues.

A number of studies have investigated the impact of abiotic stresses, including heat, drought, and salinity, on potato yield, tuber quality, and market value (Liu et al., 2009; Liang et al., 2014; Dahal et al., 2019; **Tiwari et al., 2022**). Moreover, it has been demonstrated that *GRFs* may play a role in response to drought and salt stress (Kim et al., 2012). In comparison to the wild-type and *AtGRF7*-overexpressor lines, the *atgrf7* mutant line exhibits increased tolerance to drought and salt stress. Conversely, *AtGRF7* suppresses the expression of osmotic stress-responsive genes, including *DREB2A*, even in the absence of stress treatment (Liu et al., 1998; Kim et al., 2012). This indicates that abiotic stress causes the repression of *AtGRF7* expression, which in turn induces the activation of osmotic stress-responsive genes. It was shown that salt stress resulted in the down-regulation of five *GhGRF* genes (*GhGRF3, GhGRF4, GhGRF5, GhGRF7*, and *GhGRF16*) in *Gossypium hirsutum* (Liu et al., 2022). However, the majority of *StGRF* genes were found to be up-regulated under NaCl stress, with the exception of *StGRF2* and *StGRF9* (Figure 6A). Furthermore, the expression levels of *StGRF1*, *StGRF3*, *StGRF5, StGRF6, StGRF7, StGRF9* and *StGRF11* genes showed a significant increase following

mannitol treatment (Figure 6A). This indicates that osmotic stress is responsible for the activation of *StGRF* gene expression. It was demonstrated that poplar *GRF15* was induced by heat stress. Compared to wild-type poplar plants, the transgenic lines overexpressing *PtGRF15* and lacking the miR396a target sites exhibited enhanced photosynthetic efficiency and heat tolerance (Zhao et al., 2021). The expression of most *StGRF* genes was suppressed under heat stress, while *StGRF7* and *StGRF11* genes exhibited a slight induction (Figure 6B). Nevertheless, further research is required to elucidate the underlying mechanisms of these phenomena.

Phytohormones exert a profound influence on the growth, differentiation, and development of plants. Previous reports have shown that GA_3 treatment increases the expression of several *GRF* genes in rice and cabbage (van der Knaap et al., 2000; Choi et al., 2004; Wang et al., 2014), whereas *AtGRFs* do not appear to be induced by GA_3 (Kim et al., 2003). KNOTTED1-like homeobox (KNOX) transcription factors are known to restrict cell differentiation and are important regulators of meristem development. GRFs have been demonstrated to act as upstream repressors of *KNOX* genes, which inhibit GA biosynthesis (Kuijt et al., 2014). The application of GA_3 induces the expression of *KNOX*, which subsequently leads to the up-regulation of *GRFs* at low levels of KNOX expression (Kuijt et al., 2014). The expression of several *NtabGRF* genes in *Nicotiana tabacum* is triggered by a number of different treatments, including GA_3, IAA, BR, ABA, and BAP (Zhang et al., 2018). Further analysis revealed that the *NtabGRF* promoters contain several hormone-related *cis*-elements, including the GARE-motif, TATC-box, and P-box (gibberellin responsiveness) elements in GA_3-inducible *NtabGRF* genes and ABRE (abscisic acid responsiveness) elements in ABA-inducible *NtabGRF* genes (Zhang et al., 2018). In *Camellia sinensis*, only one *GRF* gene was induced by GA_3 treatment, whereas most of *GRFs* were induced by SA or IAA (Wu et al., 2017). This study revealed that the expression levels of *StGRF2*, *StGRF4*, *StGRF8* and *StGRF12* were simultaneously downregulated, while *StGRF9* was induced by GA_3, IAA, and ABA (Figure 6C). The *StGRF12* gene was also differentially downregulated by BAP treatment (Figure 6C), suggesting that *StGRF12* may be a key negative regulator of potato in response to GA_3, IAA, ABA, and BAP treatments. It can be concluded that these *StGRFs* play a crucial role in regulating hormone feedback mechanisms in potato. A promoter analysis revealed that the potential functions of *StGRFs* are induced by different hormones (Figure 3). The promoter regions of *StGRF2*, *StGRF3*, *StGRF8* and *StGRF10* contain GA-responsive elements, specifically P-box motifs (Figure 3). Similarly, *StGRF12* contains auxin-responsive TGA-box motifs (Figure 3). Furthermore, the ABA-responsive ABRE motifs were identified in *StGRF1*, *StGRF2*, *StGRF4*, *StGRF6*, *StGRF9*, *StGRF11*, and *StGRF12* (Figure 3). It is therefore postulated that *StGRFs* may have a role in regulating physiological processes related to hormonal feedback mechanisms in potato.

Potato tubers are formed from shortened internodes, which subsequently undergo swelling and the formation of tuber eyes. Meristematic activity in the tuber eyes is completely ceased, resulting in the tuber entering a period of dormancy. Consequently, potato tuber dormancy is confined to the tuber eyes, where the meristem is located, while the remainder of the tuber continues to undergo physiological metabolic activity (Aksenova et al., 2013). It is postulated that changes in meristematic activity represent a pivotal factor in the process of dormancy release. It is hypothesized that the reactivation of meristematic function coincides with the breaking of dormancy. Meristematic activity typically resumes prior to tuber bud emergence, which is referred to as the breaking of dormancy or tuber dormancy release. Subsequently, an increase in cell division results in the visible growth of the bud, which is known as tuber sprouting. This often occurs with buds that are larger than 2 mm. *GRFs* are frequently highly expressed in actively growing tissues. The data indicate that *AtGRFs* are highly expressed in developing and growing tissues where cell proliferation occurs, in different parts of *Arabidopsis* roots and shoots (Kim et al., 2003). Gene expression profiles provide valuable insights into the potential functions of genes. In the present study, publicly available RNA-Seq data and RT-qPCR were used to elucidate the expression of *StGRFs* during potato tuber dormancy and sprouting (Figures 7, 8). The gene expression patterns of *StGRFs* in dormant and sprouting tubers were analyzed in order to identify the complex expression patterns exhibited by these genes (Figure 8). The *StGRF* genes displayed spatiotemporally specific patterns (Figures 7, 8). *StGRF2*, *StGRF5*, *StGRF7*, *StGRF10*, and *StGRF12* showed high expression levels following dormancy release, indicating their expression in growing tissues (Figures 7, 8). *AtGRF1*, *AtGRF2*, and *AtGRF3* have been shown to regulate cell proliferation, leaf, and cotyledon development (Kim et al., 2003). *AtGRF5* overexpression results in larger leaf areas due to increased cell number (Horiguchi et al., 2005). Conversely, *ZmGRF10* overexpression in maize leads to a decrease in plant height and leaf size, particularly leaf length, accompanied by impaired cell proliferation (Wu et al., 2014). This indicates that the reduction in leaf size observed in transgenic maize is likely due to a limitation in cell proliferation. Transcriptome data indicated a reduction in the expression level of the *StGRF3* gene following germination, while RT-qPCR results demonstrated that the expression level of the *StGRF3* gene was reduced to zero after germination (Figures 7, 8). This suggests that the *StGRF3* gene may act as a negative regulator in the process of tuber dormancy. The expression of the *StGRF8* gene was not detected during the germination of the potato cultivar Longshu 3. In contrast, in the diploid potato line EB063, *StGRF8* gene expression increased with the release of dormancy, which was consistent with the expression observed in the potato cultivar Russert Burbank (Figures 7, 8). These findings indicate that *StGRF8* exhibits distinct expression patterns during the germination process in different potato genotypes. Therefore, it is therefore necessary to further verify its specific role. Furthermore, *StGRF4* and *StGRF9* exhibited comparable reduced expression levels after the release of dormancy (Figure 8), indicating that these two *StGRF* genes may be involved in bud dormancy.

Conclusions

In this study, 12 members of the potato GRF family were identified and their conserved N-terminal WRC and QLQ domains, as well as C-terminal FFD, TQL, and GGPL motifs were characterized. The intron–exon organization was analyzed, and the

evolutionary relationships between the StGRFs and their homologs from two representative plant species were investigated. A total of 30 *cis*-acting elements related to plant growth and development, 30 *cis*-acting elements related to abiotic stress, and 40 *cis*-acting elements related to hormone response were identified in the promoter regions of *StGRFs*. A StGRFs-mediated regulatory network was constructed, comprising 52 transcription factors belonging to 15 different TF families, which were identified as the potential regulators of *StGRFs*. Furthermore, we examined tissue-specific gene expression patterns, as well as gene expression patterns induced by the heat, salt, drought stress, several phytohormones, *Phytophthora infestans*, and chemical elicitors. The involvement of seven *StGRF* genes, *StGRF1*, *StGRF2*, *StGRF5*, *StGRF6*, *StGRF7*, *StGRF10* and *StGRF12*, in tuber sprouting was confirmed. Furthermore, it was demonstrated that two *StGRF* genes, *StGRF4* and *StGRF9*, may be associated with tuber dormancy. The results of our analysis of gene structure, phylogenetic relationships, and transcript expression profiles suggest that *StGRF* genes may have specific roles in potato developmental processes and environmental stresses, particularly during potato tuber dormancy and sprouting.

Data availability statement

The original contributions presented in the study are included in the article/Supplementary Material. Further inquiries can be directed to the corresponding author.

Author contributions

DC: Writing – original draft. YS: Writing – review & editing. WJ: Writing – original draft. HY: Writing – original draft, Writing – review & editing. SW: Writing – original draft. LY: Supervision, Writing – review & editing. BL: Writing – original draft, Writing – review & editing.

Funding

The author(s) declare financial support was received for the research, authorship, and/or publication of this article. This work was supported by Key-Area R&D Program of Guangdong Province in China (grant number 2022B0202060001), Key R&D Program of Shaanxi Province in China (grant number 2018ZDCXL-NY-03-03, 2022NY-174).

Conflict of interest

The authors declare that the research was conducted in the absence of any commercial or financial relationships that could be construed as a potential conflict of interest.

Publisher's note

Supplementary material

The Supplementary Material for this article can be found online at: https://www.frontiersin.org/articles/10.3389/fpls.2024.1417204/full#supplementary-material

SUPPLEMENTARY FIGURE 1
Multiple sequence alignment **(A)** and composition **(B-C)** of conserved domains (QLQ and WRC domains) in *StGRF* proteins.

References

Aksenova, N. P., Sergeeva, L. I., Konstantinova, T. N., Golyanovskaya, S. A., Kolachevskaya, O. O., and Romanov, G. A. (2013). Regulation of potato tuber dormancy and sprouting. *Russ. J. Plant Physiol.* 60, 301–312. doi: 10.1134/s1021443713030023

Bao, M. L., Bian, H. W., Zha, Y. L., Li, F. Y., Sun, Y. Z., Bai, B., et al. (2014). miR396a-mediated basic helix-loop-helix transcription factor bHLH74 repression acts as a regulator for root growth in *Arabidopsis* seedlings. *Plant Cell Physiol.* 55, 1343–1353. doi: 10.1093/pcp/pcu058

Bazin, J., Khan, G. A., Combier, J. P., Bustos-Sanmamed, P., Debernardi, J. M., Rodriguez, R., et al. (2013). miR396 affects mycorrhization and root meristem activity in the legume *Medicago truncatula*. *Plant J.* 74, 920–934. doi: 10.1111/tpj.12178

Campbell, M., Segear, E., Beers, L., Knauber, D., and Suttle, J. (2008). Dormancy in potato tuber meristems: chemically induced cessation in dormancy matches the natural process based on transcript profiles. *Funct. Integr. Genomics* 8 (4), 317–328. doi: 10.1007/s10142-008-0079-6

Casadevall, R., Rodriguez, R. E., Debernardi, J. M., Palatnik, J. F., and Casati, P. (2013). Repression of growth regulating factors by the MicroRNA396 inhibits cell proliferation by uv-b radiation in *Arabidopsis* leaves. *Plant Cell* 25, 3570–3583. doi: 10.1105/tpc.113.117473

Chen, C., Chen, H., Zhang, Y., Thomas, H. R., Frank, M. H., He, Y., et al. (2020). TBtools: An integrative toolkit developed for interactive analyses of big biological data. *Mol. Plant* 13 (8), 1194–1202. doi: 10.1016/j.molp.2020.06.009

Chen, F., Yang, Y. Z., Luo, X. F., Zhou, W. G., Dai, Y. J., Zheng, C., et al. (2019). Genome-wide identification of GRF transcription factors in soybean and expression analysis of *GmGRF* family under shade stress. *BMC Plant Biol.* 19 (1), 269. doi: 10.1186/s12870–019-1861–4

Choi, D., Kim, J. H., and Kende, H. (2004). Whole genome analysis of the *OsGRF* gene family encoding plant-specific putative transcription activators in rice (*Oryza sativa* L.). *Plant Cell Physiol.* 45, 897–904. doi: 10.1093/pcp/pch098

Dahal, K., Li, X. Q., Tai, H., Creelman, A., and Bizimungu, B. (2019). Improving potato stress tolerance and tuber yield under a climate change scenario - A current overview. *Front. Plant Sci.* 10. doi: 10.3389/fpls.2019.00563

Debernardi, J. M., Mecchia, M. A., Vercruyssen, L., Smaczniak, C., Kaufmann, K., Inze, D., et al. (2014). Post-transcriptional control of *GRF* transcription factors by microRNA miR396 and *GIF* co-activator affects leaf size and longevity. *Plant J.* 79, 413–426. doi: 10.1111/tpj.12567

Debernardi, J. M., Rodriguez, R. E., Mecchia, M. A., and Palatnik, J. F. (2012). Functional specialization of the plant mir396 regulatory network through distinct microrna-target interactions. *PloS Genet.* 8 (1), e1002419. doi: 10.1371/journal.pgen.1002419

Fu, M. K., He, Y. N., Yang, X. Y., Tang, X., Wang, M., and Dai, W. S. (2024). Genome-wide identification of the *GRF* family in sweet orange (*Citrus sinensis*) and

functional analysis of the *CsGRF04* in response to multiple abiotic stresses. *BMC Genom.* 25 (1), 37. doi: 10.1186/s12864–023-09952–8

Gorlova, O., Fedorov, A., Logothetis, C., Amos, C., and Gorlov, I. (2014). Genes with a large intronic burden show greater evolutionary conservation on the protein level. *BMC Evol. Biol.* 14 (1), 50. doi: 10.1186/1471–2148-14–50

Hepworth, J., and Lenhard, M. (2014). Regulation of plant lateral-organ growth by modulating cell number and size. *Curr. Opin. Plant Biol.* 17, 36–42. doi: 10.1016/j.pbi.2013.11.005

Hewezi, T., Maier, T. R., Nettleton, D., and Baum, T. J. (2012). The Arabidopsis MicroRNA396-*GRF1/GRF3* regulatory module acts as a developmental regulator in the reprogramming of root cells during cyst nematode infection. *Plant Physiol.* 159, 321–335. doi: 10.1104/pp.112.193649

Horiguchi, G., Kim, G. T., and Tsukaya, H. (2005). The transcription factor AtGRF5 and the transcription coactivator AN3 regulate cell proliferation in leaf primordia of *Arabidopsis thaliana*. *Plant J.* 43, 68–78. doi: 10.1111/j.1365–313X.2005.02429.x

Jin, J. P., Tian, F., Yang, D. C., Meng, Y. Q., Kong, L., Luo, J. C., et al. (2017). PlantTFDB 4.0: toward a central hub for transcription factors and regulatory interactions in plants. *Nucleic Acids Res.* 45, D1040–D1045. doi: 10.1093/nar/gkw982

Khatun, K., Robin, A. H. K., Park, J. I., Nath, U. K., Kim, C. K., Lim, K. B., et al. (2017). Molecular characterization and expression profiling of tomato *GRF* transcription factor family genes in response to abiotic stresses and phytohormones. *Int. J. Mol. Sci.* 18 (5), 1056. doi: 10.3390/ijms18051056

Kim, J. H., Choi, D. S., and Kende, H. (2003). The AtGRF family of putative transcription factors is involved in leaf and cotyledon growth in *Arabidopsis*. *Plant J.* 36, 94–104. doi: 10.1046/j.1365–313X.2003.01862.x

Kim, J. H., and Kende, H. (2004). A transcriptional coactivator, AtGIF1, is involved in regulating leaf growth and morphology in *Arabidopsis*. *Proc.Natl. Acad. Sci. U.S.A.* 101, 13374–13379. doi: 10.1073/pnas.0405450101

Kim, J. S., Mizoi, J., Kidokoro, S., Maruyama, K., Nakajima, J., Nakashima, K., et al. (2012). *Arabidopsis* GROWTH-REGULATING FACTOR7 functions as a transcriptional repressor of abscisic acid- and osmotic stress-responsive genes, including *DREB2A*. *Plant Cell* 24, 3393–3405. doi: 10.1105/tpc.112.100933

Kuijt, S. J. H., Greco, R., Agalou, A., Shao, J. X., t Hoen, C. C. J., Övernäs, E., et al. (2014). Interaction between the *GROWTH-REGULATING FACTOR* and *KNOTTED1-LIKE HOMEOBOX* families of transcription factors. *Plant Physiol.* 164, 1952–1966. doi: 10.1104/pp.113.222836

Lee, S. J., Lee, B. H., Jung, J. H., Park, S. K., Song, J. T., and Kim, J. H. (2018). GROWTH-REGULATING FACTOR and GRF-INTERACTING FACTOR specify meristematic cells of gynoecia and anthers. *Plant Physiol.* 176, 717–729. doi: 10.1104/pp.17.00960

Liang, G., He, H., Li, Y., Wang, F., and Yu, D. Q. (2014). Molecular mechanism of microRNA396 mediating pistil development in *Arabidopsis*. *Plant Physiol.* 164, 249–258. doi: 10.1104/pp.113.225144

Liu, B., Zhang, N., Wen, Y., Jin, X., Yang, J., Si, H., et al. (2015). Transcriptomic changes during tuber dormancy release process revealed by RNA sequencing in potato. *J. Biotechnol.* 198, 17–30. doi: 10.1016/j.jbiotec.2015.01.019

Liu, D. M., Song, Y., Chen, Z. X., and Yu, D. Q. (2009). Ectopic expression of miR396 suppresses *GRF* target gene expression and alters leaf growth in *Arabidopsis*. *Physiol. Plantarum* 136, 223–236. doi: 10.1111/j.1399–3054.2009.01229.x

Liu, H. H., Guo, S. Y., Xu, Y. Y., Li, C. H., Zhang, Z. Y., Zhang, D. J., et al. (2014). OsmiR396d-regulated *OsGRFs* function in floral organogenesis in rice through binding to their targets *OsJMJ706* and *OsCR4*. *Plant Physiol.* 165, 160–174. doi: 10.1104/pp.114.235564

Liu, J., Hua, W., Yang, H. L., Zhan, G. M., Li, R. J., Deng, L. B., et al. (2012). The *BnGRF2* gene (*GRF2*-like gene from *Brassica napus*) enhances seed oil production through regulating cell number and plant photosynthesis. *J. Exp. Bot.* 63, 3727–3740. doi: 10.1093/jxb/ers066

Liu, K., Kabir, N., Wei, Z. Z., Sun, Z. J., Wang, J., Qi, J., et al. (2022). Genome-wide identification and expression profile of *GhGRF* gene family in *Gossypium hirsutum* L. *Peerj* 10, e13372. doi: 10.7717/peerj.13372

Liu, Q., Kasuga, M., Sakuma, Y., Abe, H., Miura, S., Yamaguchi-Shinozaki, K., et al. (1998). Two transcription factors, *DREB1* and *DREB2*, with an EREBP/AP2 DNA binding domain separate two cellular signal transduction pathways in drought- and low-temperature-responsive gene expression, respectively, in *Arabidopsis*. *Plant Cell* 10, 1391–1406. doi: 10.2307/3870648

Ma, J. Q., Jian, H. J., Yang, B., Lu, K., Zhang, A. X., Liu, P., et al. (2017). Genome-wide analysis and expression profiling of the *GRF* gene family in oilseed rape (*Brassica napus* L.). *Gene* 620, 36–45. doi: 10.1016/j.gene.2017.03.030

Navarro, C., Abelenda, J. A., Cruz-Oró, E., Cuéllar, C. A., Tamaki, S., Silva, J., et al. (2011). Control of flowering and storage organ formation in potato by FLOWERING LOCUS T. *Nature* 478, 119–U132. doi: 10.1038/nature10431

Nelissen, H., Eeckhout, D., Demuynck, K., Persiau, G., Walton, A., van Bel, M., et al. (2015). Dynamic changes in ANGUSTIFOLIA3 complex composition reveal a growth regulatory mechanism in the maize leaf. *Plant Cell* 27, 1605–1619. doi: 10.1105/tpc.15.00269

Omidbakhshfard, M. A., Proost, S., Fujikura, U., and Mueller-Roeber, B. (2015). Growth-regulating factors (GRFs): A small transcription factor family with important functions in plant biology. *Mol. Plant* 8 (7), 998–1010. doi: 10.1016/j.molp.2015.01.013

Pajoro, A., Madrigal, P., Muiño, J. M., Matus, J. T., Jin, J., Mecchia, M. A., et al. (2014). Dynamics of chromatin accessibility and gene regulation by MADS-domain transcription factors in flower development. *Genome Biol.* 15 (3), R41. doi: 10.1186/gb-2014–15-3-r41

Rodriguez, R. E., Mecchia, M. A., Debernardi, J. M., Schommer, C., Weigel, D., and Palatnik, J. F. (2010). Control of cell proliferation in *Arabidopsis thaliana* by microRNA miR396. *Development* 137, 103–112. doi: 10.1242/dev.043067

Saeed, A. I., Hagabati, N. K., Braisted, J. C., Liang, W., Sharov, V., Howe, E. A., et al. (2006). TM4 microarray software suite. *Methods Enzymol.* 411, 134–193. doi: 10.1016/S0076-6879(06)11009-5

Tiwari, J. K., Buckseth, T., Zinta, R., Bhatia, N., Dalamu, D., Naik, S., et al. (2022). Germplasm, breeding, and genomics in potato improvement of biotic and abiotic stresses tolerance. *Front. Plant Sci.* 13. doi: 10.3389/fpls.2022.805671

van der Knaap, E., Kim, J. H., and Kende, H. (2000). A novel gibberellin-induced gene from rice and its potential regulatory role in stem growth. *Plant Physiol.* 122, 695–704. doi: 10.1104/pp.122.3.695

Vercruyssen, L., Tognetti, V. B., Gonzalez, N., Van Dingenen, J., De Milde, L., Bielach, A., et al. (2015). GROWTH REGULATING FACTOR5 stimulates Arabidopsis chloroplast division, photosynthesis, and leaf longevity. *Plant Physiol.* 167, 817. doi: 10.1104/pp.114.256180

Wang, L., Gu, X. L., Xu, D. Y., Wang, W., Wang, H., Zeng, M. H., et al. (2011). miR396-targeted *AtGRF* transcription factors are required for coordination of cell division and differentiation during leaf development in *Arabidopsis*. *J. Exp.Bot.* 62, 761–773. doi: 10.1093/jxb/erq307

Wang, F. D., Qiu, N. W., Ding, Q., Li, J. J., Zhang, Y. H., Li, H. Y., et al. (2014). Genome-wide identification and analysis of the growth-regulating factor family in Chinese cabbage (*Brassica rapa* L. ssp. *pekinensis*). *BMC Genom.* 15 (1), 807. doi: 10.1186/1471–2164-15–807

Wang, J., Zhou, H., Zhao, Y., Sun, P., Tang, F., Song, X., et al. (2020). Characterization of poplar growth-regulating factors and analysis of their function in leaf size control. *BMC Plant Biol.* 20 (1), 509. doi: 10.1186/s12870–020-02699–4

Wu, Z. J., Wang, W. L., and Zhuang, J. (2017). Developmental processes and responses to hormonal stimuli in tea plant (*Camellia sinensis*) leaves are controlled by *GRF* and *GIF* gene families. *Funct. Integr. Genomic* 17, 503–512. doi: 10.1007/s10142–017-0553–0

Wu, L., Zhang, D. F., Xue, M., Qian, J. J., He, Y., and Wang, S. C. (2014). Overexpression of the maize *GRF10*, an endogenous truncated growth-regulating factor protein, leads to reduction in leaf size and plant height. *J. Integr. Plant Biol.* 56, 1053–1063. doi: 10.1111/jipb.12220

Xiao, G., Huang, W., Cao, H., Tu, W., Wang, H., Zheng, X., et al. (2018). Genetic loci conferring reducing sugar accumulation and conversion of cold-stored potato tubers revealed by QTL analysis in a diploid population. *Front. Plant Sci.* 9, 315. doi: 10.3389/fpls.2018.00315

Xu, X., Pan, S. K., Cheng, S. F., Zhang, B., Mu, D. S., Ni, P. X., et al. (2011). Genome sequence and analysis of the tuber crop potato. *Nature* 475, 189–U194. doi: 10.1038/nature10158

Zhang, D. F., Li, B., Jia, G. Q., Zhang, T. F., Dai, J. R., Li, J. S., et al. (2008). Isolation and characterization of genes encoding GRF transcription factors and GIF transcriptional coactivators in maize (*Zea mays* L.). *Plant Sci.* 175, 809–817. doi: 10.1016/j.plantsci.2008.08.002

Zhang, J. F., Li, Z. F., Jin, J. J., Xie, X. D., Zhang, H., Chen, Q. S., et al. (2018). Genome-wide identification and analysis of the growth-regulating factor family in tobacco (*Nicotiana tabacum*). *Gene* 639, 117–127. doi: 10.1016/j.gene.2017.09.070

Zhao, Y. Y., Xie, J. B., Wang, S., Xu, W. J., Chen, S. S., Song, X. Q., et al. (2021). Synonymous mutation in *Growth Regulating Factor 15* of miR396a target sites enhances photosynthetic efficiency and heat tolerance in poplar. *J. Exp. Bot.* 72, 4502–4519. doi: 10.1093/jxb/erab120

frontiers | Frontiers in Plant Science

TYPE Original Research
PUBLISHED 06 August 2024
DOI 10.3389/fpls.2024.1451403

OPEN ACCESS

EDITED BY
Zemin Wang,
Gansu Agricultural University, China

REVIEWED BY
Xi Zhu,
Chinese Academy of Tropical Agricultural Sciences, China
Wenwu Wu,
Zhejiang Agriculture and Forestry University, China

*CORRESPONDENCE
Ming Zhou
mingzhou@zju.edu.cn

RECEIVED 19 June 2024
ACCEPTED 17 July 2024
PUBLISHED 06 August 2024

CITATION
Zhang R, Xi X, Chen X, Wang Y and Zhou M (2024) Comparing time-series transcriptomes between chilling-resistant and -susceptible rice reveals potential transcription factors responding to chilling stress.
Front. Plant Sci. 15:1451403.
doi: 10.3389/fpls.2024.1451403

Comparing time-series transcriptomes between chilling-resistant and -susceptible rice reveals potential transcription factors responding to chilling stress

Rui Zhang[1], XiaoHui Xi[1], XinYi Chen[1], Yi Wang[1] and Ming Zhou[1,2]*

[1]State Key Laboratory of Plant Environmental Resilience, College of Life Sciences, Zhejiang University, Hangzhou, China, [2]Key Laboratory of Nuclear Agricultural Sciences of Ministry of Agriculture and Zhejiang Province, Zhejiang University, Hangzhou, China

Low temperature is one of the most important environmental factors that inhibits rice growth and grain yield. Transcription factors (TFs) play crucial roles in chilling acclimation by regulating gene expression. However, transcriptional dynamics and key regulators responding to low temperature remain largely unclear in rice. In this study, a transcriptome-based comparative analysis was performed to explore genome-wide gene expression profiles between a chilling-resistant cultivar DC90 and a chilling-susceptible cultivar 9311 at a series of time points under low temperature treatment and recovery condition. A total of 3,590 differentially expressed genes (DEGs) between two cultivars were determined and divided into 12 co-expression modules. Meanwhile, several biological processes participating in the chilling response such as abscisic acid (ABA) responses, water deprivation, protein metabolic processes, and transcription regulator activities were revealed. Through weighted gene co-expression network analysis (WGCNA), 15 hub TFs involved in chilling conditions were identified. Further, we used the gene regulatory network (GRN) to evaluate the top 50 TFs, which might have potential roles responding to chilling stress. Finally, five TFs, including a C-repeat binding factor (*OsCBF3*), a zinc finger-homeodomain protein (*OsZHD8*), a tandem zinc finger protein (*OsTZF1*), carbon starved anther (*CSA*), and indeterminate gametophyte1 (*OsIG1*) were identified as crucial candidates responsible for chilling resistance in rice. This study deepens our understanding in the gene regulation networks of chilling stress in rice and offers potential gene resources for breeding climate-resilient crops.

KEYWORDS

comparative transcriptome, gene regulatory network, transcription factors, chilling stress, rice

1 Introduction

Higher plants encounter a wide variety of environmental stresses in their growth and development (Nawaz et al., 2023). The chilling stress (0°C–15°C) is one of main abiotic stresses bringing serious negative impacts on plant development and causing huge economic losses in crops (Ding et al., 2019). Encountering with low temperatures, crops, especially in the tropical and subtropical climatic zones, show irreversible physiological and biochemical perturbations, including leaf falling, incomplete ripening, seedling wilting, and even death (Lukatkin, 2005; Xu et al., 2008; Lukatkin et al., 2012; Sun et al., 2017).

To gain deeper insights into gene networks responding to the chilling stress, plenty of differentially expressed genes (DEGs), especially for transcription factors (TFs), have been identified when treated with chilling stress (Seki et al., 2001). These TFs play key roles in responding to chilling in plants. For example, overexpression of the *C-repeat binding factor1* (*CBF1*) triggered the expression of cold-responsive (COR) genes and, subsequently, the identification of ICE (inducer of *CBF* expression) function led to the establishment of the ICE-CBF-COR pathway to enhance the chilling resistance in *Arabidopsis* (Thomashow, 1999; Chinnusamy et al., 2006; Nie et al., 2022). Overexpression each of *osmotic stress/abscisic acid (ABA)–activated protein kinase 6* (*OsSAPK6*), *ideal plant architecture 1* (*IPA1*), and *OsCBF3* forms a chilling-induced OsSAPK6-IPA1-OsCBF3 signal cascade, and enhances rice chilling tolerance (Jia et al., 2022). Other TFs, such as *MaNAC1*, *OsWRKY63*, and *ZmMYB31*, are also involved in chilling tolerance by regulating the expression of downstream genes as well (Li et al., 2019; Zhang et al., 2022; Yin et al., 2024). In addition, plant hormones usually show a close connection with chilling stresses. ABA regulates several biochemical functions including fruit ripening, leaf senescence, and stomatal closure (Kumar et al., 2022). Studies also show that chilling stress impacts the development and stress resistance of plants by influencing the accumulation of endogenous ABA or inducing key molecular hub genes in ABA synthesis and transduction pathways (Guan et al., 2023). In tomato, overexpression of *abscisic acid-insensitive 5* (*MaABI5-like*) increases fatty acid desaturation and enhances cold tolerance (Song et al., 2022). In melon seedlings, *abscisic acid-responsive element-binding factor 1* (*CmABF1*) and *CmCBF4* cooperatively regulate putrescine synthesis to help melon seedlings to response to chilling stress (Li et al., 2022).

Rice, which is cultivated across an expanse of 164 million hectares in over 100 countries, serves as a major staple food crop and provides dietary energy for half of the population in the world (Shafi et al., 2023). Since it is a tropical and subtropical crop, the growth of rice is sensitive to the chilling stress, which affects the seedling growth, heading, grain filling, and seed setting of rice. Therefore, understanding gene networks responsive to the chilling stress will provide crucial clues for breeding climate resilient rice breeding. DC90 is a chromosome segment substitution line that is introgressed with the chilling-tolerance locus CTS-12 from the wild rice, while 9311 is a chilling-sensitive cultivar. After 5 days chilling treatment, there was no significant difference between DC90 and 9311, and phenotypic differences were observed to develop gradually between DC90 and 9311 during the recovery period. After 7 days recovery, the seedlings of 9311 were completely wilted, and the seedlings of DC90 were survived after the chilling stress (Cen et al., 2018, Cen et al., 2020). In previous study, DEGs in DC90 and 9311 under 72h chilling treatment (time-course RNA-seq at 0h, 12h, 24h, and 72h) and 24h recovery (at 84h and 96h) have been characterized by Cen et al (Cen et al., 2020). Nevertheless, transcriptional dynamics and crucial TFs responding to low temperature between DC90 and 9311 at various time points remain unclear. Thus, we aimed to conduct weighted gene co-expression network analysis (WGCNA) and gene regulatory network (GRN) analyses and identified potential TFs responsible for chilling resistance in rice.

In this study, we re-analyzed time-course transcriptomes from DC90 and 9311. The expression data were compared at 0h, 12h, 24h, 72h, 84h, and 96h between two rice cultivars through co-expression and regulatory networks. We revealed key genes that had positive and negative regulatory effects on the low temperature and constructed a gene co-expression network for chilling stress in rice. Further, we discovered that crucial genes involved in the ABA synthesis and signal-transduction pathway that were induced by low temperature, suggesting ABA might plays a significant role in chilling signaling cascades. Importantly, several TFs potentially responsible for chilling resistance and their relationship with each other in the regulatory network were identified. Collectively, our findings identified a hub-TFs regulatory network of chilling stress in rice. These data might provide clues for breeding climate-resilient crops.

2 Materials and methods

2.1 Plant materials and data sources

DC90 and 9311 are two rice cultivars that are resistant and sensitive to the chilling stress, respectively (Cen et al., 2018, Cen et al., 2020). All rice seedlings (three-leaf stage) were grown in Guangxi University, China, and then exposed to low temperature at 10°C/8°C (day/night) (artificial light was supplemented with day-13h/night-11h circadian rhythm). The seedling leaves were collected at 12h, 24h, and 72h under chilling stress treatments, and at 84h and 96h for recovery stages; 0h was set as control. The collected samples were immediately ground with liquid nitrogen with three biological replicates. The paired-end reads were generated from Illumina 2500 platform and the RNA-seq datasets were deposited in NCBI under the accession number PRJNA601963.

2.2 Differential gene expression analysis

For RNA-seq data, we employed Fastqc v0.11.9 (https://www.bioinformatics.babraham.ac.uk/projects/fastqc/) to examine sequence quality and Trimmomatic v0.39 (Bolger et al., 2014) to remove low-quality reads. The clean reads were mapped to rice

msu7 genome (http://rice.uga.edu/downloads_gad.shtml) with Hisat2 v2.2.1 (Kim et al., 2019). Gene expression was uniform in fragments per kilobase of exon model per million (FPKM) mapped reads using feature Counts v2.0.1 (Liao et al., 2014). DEGs at 6 time points related to chilling stress between DC90 and 9311 were calculated using the R package DESeq2 (Love et al., 2014). The threshold of DEGs was set to $|\log_2 \text{Fold Change}| \geq 1$ and p.adjust ≤ 0.05. These DEGs were grouped as upregulated or downregulated genes based on positive or negative logarithmic changes in threshold value. Heatmaps and Venn diagrams were drawn with the R packages ggplot2 (Ginestet, 2011) and UpSetR (Conway et al., 2017).

2.3 Co-expression network recognition based on the expression level of DEGs

Co-expression network analysis was performed using the R package WGCNA (Langfelder and Horvath, 2008). Briefly, the FPKM matrix of all DEGs was used as input data and these datasets of all time points with three replicates were filtered to remove some genes at low-expression level (FPKM <1) of any sampling replicates. For these resulting genes, we firstly estimated the soft threshold power by the pickSoftThreshold function, which provided the best-weighted coefficient $\beta = 8$ for the scale-free network construction. Second, a correlation matrix was constructed and a topological overlap matrix was calculated based on this correlation matrix. Finally, these genes were classified into different modules according to the topological overlap dissimilarity by average hierarchical clustering algorithm. These modules with different colors were then calculated based on a dynamic tree with minimum group size of 30 genes and merging threshold function of 0.25. Hub genes can represent the maximum correlation points with each module and they are usually represented by the kME value. The threshold used to screen hub genes in each module was |kME| > 0.85. The intricate networks were achieved based on the kME value by employing Cytoscape v3.8.2 (Gnanaraj, 2008).

2.4 Gene ontology annotation and enrichment analysis

Gene Ontology (GO) annotation was conducted using the Ensembl (Hubbard et al., 2002). Functional enrichment analysis was exhibited by the R package clusterProfiler v4.6.2 (Wu et al., 2021) with p.adjust ≤ 0.05. All dotplots were visualized with the R package ggplot2 (Ginestet, 2011).

2.5 Construction of GRN

According to the PlantTFDB v5.0 (https://planttfdb.gao-lab.org/download.php) annotations, 261 of 3,590 genes encoded TFs were identified. These 261 genes were defined as potential regulators based on the machine learning. We used the R packages GENIE3 (Vân and Geurts, 2018) to measure the confidence levels ("weights" ≥ 0) and the top 10,000 inferred regulatory relationships were found from GRN as potential GRN. The top 50 TFs with the heaviest summed weights in the GRN were retained as the candidates. The networks were drawn by Cytoscape v3.8.2 software (Gnanaraj, 2008).

3 Results

3.1 Identification of DEGs under chilling stress between two rice cultivars

DC90 and 9311 are two rice cultivars that are resistant and sensitive to the chilling stress at seedling stage, respectively. To understand their distinguished responses to chilling stress at transcriptional level, samples were collected for time-course transcriptomes (Cen et al., 2020). For the chilling treatment (see Methods), samples were collected at 0h, 12h, 24h, and 72h, while samples were subsequently collected at 84h and 96h for recovery (Cen et al., 2020). To explore the transcriptome dynamics responding to chilling stress in DC90 and 9311, we analyzed the complete gene expression in seedlings at the 6 time points with three biological replicates. Based on principal component analysis, we found that all time points in two rice cultivars could be divided into two main components (Figure 1A). The first principal component (PC1) accounted for 61% of the variance and was explained by samples with chilling stress and samples without treatment or after recovery. The second principal component (PC2) accounts for 16% of the variation and was interpreted by the genetic differences between DC90 and 9311. This result indicates that transcriptomes of the chilling stress do not only reflect the chilling treatment versus the recovery condition but also present a unique transcriptome composition in different genetic backgrounds.

To identify DEGs responding to chilling stresses, pairwise comparisons among the same 6 points of DC90 relative to 9311 were performed using the DESeq2 program (Love et al., 2014). A total of 3,590 genes were obtained showing a clear distinction between different treatment points and the detailed information for those DEGs were listed in Supplementary Table S1. Among these 6 time points, the greatest number of DEGs was found after 72h chilling treatment (1,204 upregulated and 952 downregulated) (Figure 1B). Most of these DEGs were unique at 72h, including 897 unique upregulated genes and 764 unique downregulated genes (Figures 1C, D), indicating that a longer duration of exposure to the chilling stress led to profound changes of rice transcriptome profile. According to the multiple-point comparison, we detected 54 upregulated DEGs and 51 downregulated DEGs that commonly changed at 6 time points between DC90 and 9311 (Supplementary Tables S2, S3). Globally, the number of upregulated DEGs was more than the number of downregulated genes under chilling treatment (0h, 12h, 24h, and 72h), while the number of downregulated DEGs was more than the number of upregulated genes at each time point under the chilling recovery stages (84h and 96h). These results presented a huge difference of DEGs in response to chilling stress between these two rice cultivars.

10.3389/fpls.2024.1451403

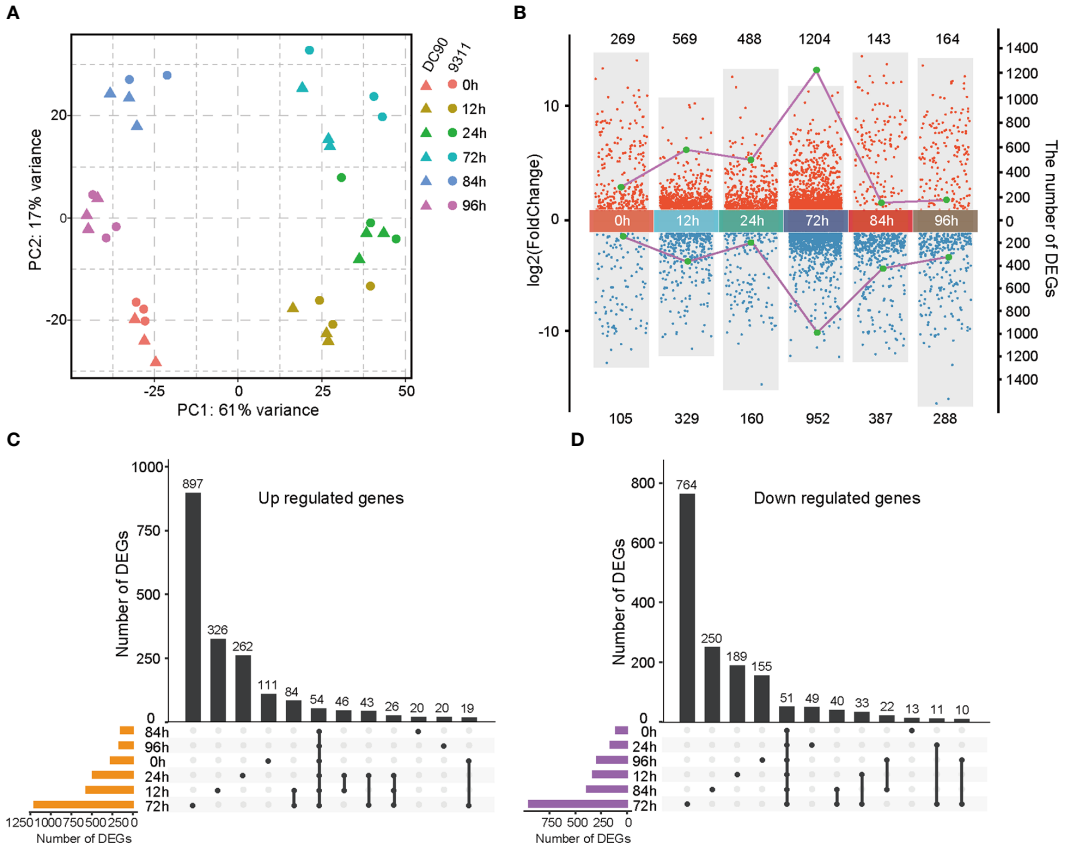

FIGURE 1
Transcriptomic analyses of DC90 and 9311 under 72h chilling treatment and 24h recovery. **(A)** Principal component analysis (PCA) of DC90 and 9311 samples at 6 time points (0h, 12h, 24h, 72h, 84h, and 96h). **(B)** Statistics of differentially expressed genes (DEGs) numbers in DC90 relative to 9311 at 6 time points. Each dot presents a DEG. Dots in blue show downregulated genes, and dots in red represent upregulated genes. The left coordinate (y-axis) represents the $\log_2$ fold change values of DEGs and the right coordinate (y-axis) represents the numbers of DEGs. **(C)** Upset plot shows unique and shared upregulated genes at each time point in DC90 relative to 9311. **(D)** Upset plot shows unique and shared downregulated genes in DC90 relative to 9311.

3.2 Co-expression analysis reveals co-regulated modules of chilling responsive genes

In order to investigate key regulators responsive to chilling stress in rice, lowly expressed gene (the FPKM value <1) were filtered, and remaining DEGs were further employed for WGCNA analysis (Langfelder and Horvath, 2008). We constructed the analysis of network topology for soft-thresholding powers from 1 to 40 and identified a relatively balanced scale independence and mean connectivity (Figure 2A). In the current research, β = 8 was selected with scale free (R^2 = 0.9030) to ensure the network topology. Then a gene tree based on hierarchical cluster were established, and a total of 12 co-expression modules with were obtained except the gray module which was contained the genes (n = 524) that were not effectively clustered (Figure 2B). All genes in the same module shared the similar expression patterns and the number of DEGs in these modules ranged from 35 DEGs (the dark orange module) to 1,291 (the magenta module) (Supplementary Table S4). We identified eigengenes (ME, defined as the first principal component of genes in module) as representative patterns of module and evaluated the similarity of each module by correlating their eigengenes (Figure 2C).

According to these eigengenes expression patterns, we found that at 3 time points after chilling stress, expression levels of eigengenes including salmon, green yellow, cyan, and light green modules were showed significantly higher in DC90 when compared to 9311. At the same time, expression levels of DEGs in these module eigengenes were higher under chilling stage (12h, 24h, and 72h) compared to unchilling stage (0h, 84h, and 96h), indicating that they were consistently stimulated in DC90 and might play crucial roles in response to chilling stress (Figures 2D–G). In addition, some modules also correlated with specific genotypes according to expression profiles of eigengenes (Figures 2H, I). The eigengenes of DC90 showed higher expression levels in tan modules but showed lower expression levels in light yellow modules when compared to 9311, suggesting that differences in gene expression between these two modules are mainly due to variety differences, rather than being significantly correlated with cold stress.

10.3389/fpls.2024.1451403

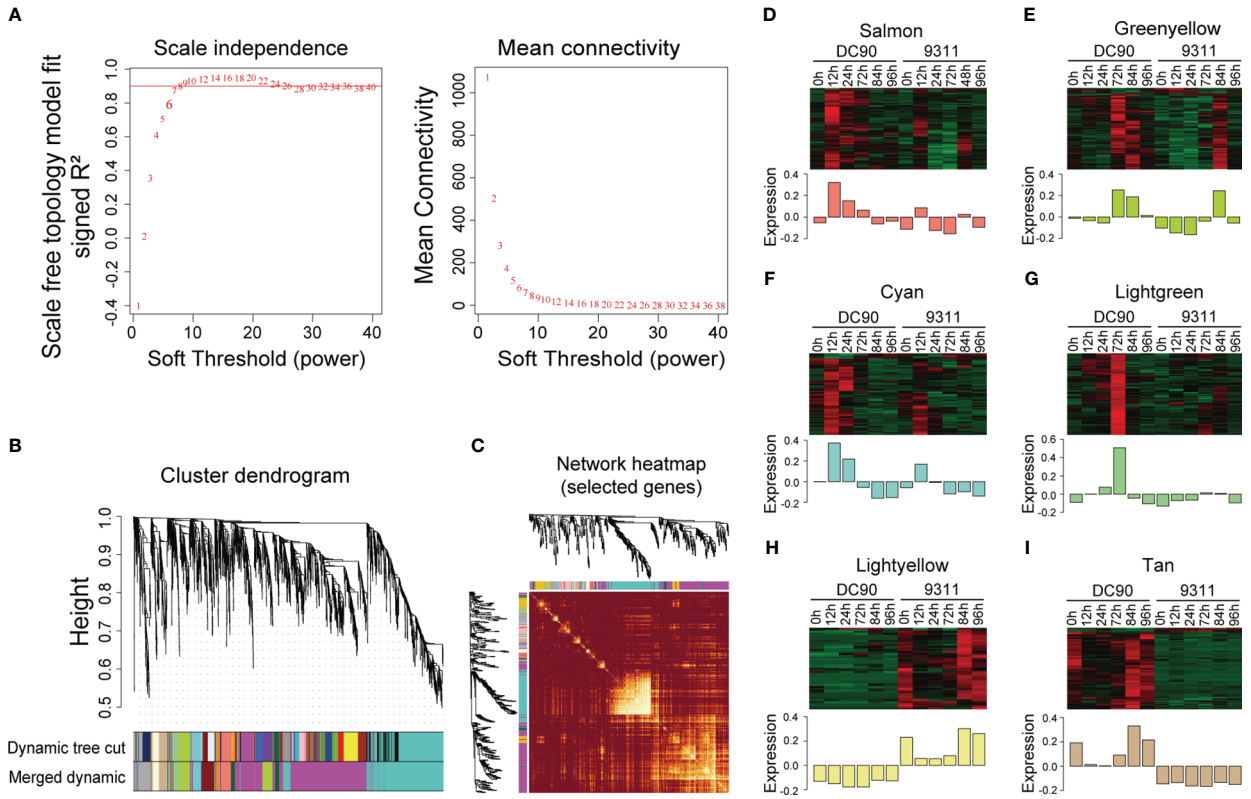

FIGURE 2
Weighted gene co-expression analysis (WGCNA) of DEGs between DC90 and 9311 under 72h chilling treatment and 24h recovery. **(A)** Scale independence and mean connectivity of the network for various soft-thresholding powers. **(B)** A hierarchical cluster tree of the DEGs distributed in different modules. The assigned modules are depicted by color bands and branches. Genes are represented by the tips of the branches. **(C)** The correlation between co-expression networks based on eigengenes. The intensity of color on the heatmap signifies the extent of overlap and the darker yellow denoting greater correlation. **(D–I)** Expression patterns of co-expressed genes in six modules, including **(D)** salmon, **(E)** green yellow, **(F)** cyan, **(G)** light green, **(H)** light yellow, and **(I)** tan modules. The expression quantity was processed with z-score normalization, and the relative expression levels are shown in colorful scale.

3.3 Gene ontology enrichment analysis of DEGs in different modules

To assess if these DEGs have any biological function in response to chilling stresses, we used gene ontology functional enrichment analyses for DEGs corresponding to each module and the top 15 GO terms in each module were given (Figure 3A; Supplementary Figure S1). For the six modules in Figures 2D–I, we have discovered many terms potentially involved in chilling stress response. In the salmon module, the most enriched significant processes contained transcription regulator activity, temperature stimulus, cold, hormones, hormone-mediated signaling pathways and cellular responses to hormone stimulus (Figure 3A). These results suggested that plant hormones might play key roles in response to chilling stress in rice. In the green yellow module, the most enriched significant processes were responsive to translation, peptide biosynthetic process, peptide metabolic process, and protein metabolic process, suggesting that genes in this module were likely involved in protein synthesis and metabolism (Figure 3B). In the cyan module, transcription regulator activity was the most significant function-enriched GO term, indicating that the TFs might play crucial roles in response to chilling stress (Figure 3C). In the light green module, the most significant processes were enriched for sequence-specific DNA binding, response to stress, and response to stimulus, while in the tan module, oxidoreductase activity, metal ion binding, and cation binding were enriched (Figures 3D, E). Although the genes in light yellow modules were not significantly enriched in any GO functions, we found that the GO annotations of many genes in this module were related to calmodulin-binding protein, oxidoreductase, and heavy metal-associated (Supplementary Table S4). Taken together, the analysis reveals that chilling stress influences the expression of genes that regulate plant hormone levels, protein contents, and TF activities, and these DEGs may be severed as a versatile resource for breeding chilling-resistant plants, thus we keep salmon, green yellow, cyan, and light green modules as the “rice chilling resistance response” modules for subsequent analyses.

3.4 ABA biosynthesis and signaling genes actively respond to the chilling stress

In the GO analysis, we found that ABA was a highly enriched term, which is consistent with previous study (Cen et al., 2020). To understand roles of ABA in rice chilling stresses, the intricate

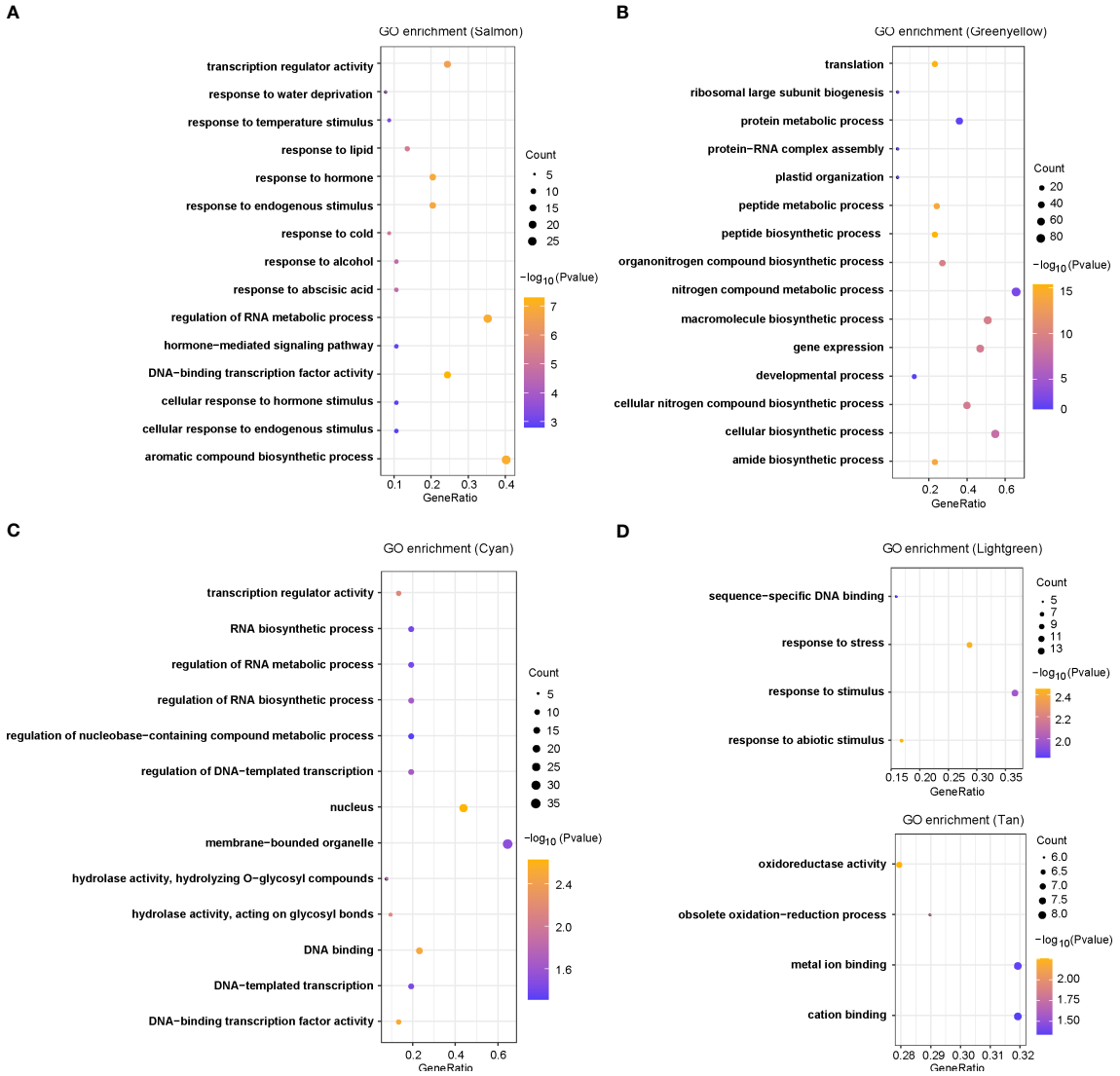

FIGURE 3
GO enrichments for co-expression genes in five selected modules, including **(A)** salmon, **(B)** green yellow, **(C)** cyan, **(D)** light green, and **(E)** tan modules.

synthesis and signal-transduction pathway of ABA responding to low temperature were further analyzed (Figure 4). In the ABA biosynthesis pathway, *9-cis-epoxycarotenoid dioxygenase* (*OsNCED3/5*) displayed a high expression level in DC90 than that in 9311 after 12h chilling treatment, whereas *aldehyde oxidase* (*OsAAO3;1*) showed a low expression level at all chilling hours in two rice cultivars (Figure 4A). Of particular significance, genes situated at the inception of the ABA signal-transduction cascade exhibited obvious induction in the wake of chilling signals. (Figure 4B). Among them, *OsPP2C11*, *OsPP2C27*, and *OsPP2C41* showed high expression profiles in 9311 at 72h than that in DC90 that might because of PP2Cs as a negative regulator of ABA signaling pathway. We also investigated expression levels of genes involved in other hormone pathways, such as brassinosteroids (BR), cytokinin (CTK), ethylene (ETH), gibberellin (GA), auxin (IAA), and jasmonic acid (JA), but no significant differences were found between these two varieties under chilling stress (Supplementary Figures S2–S7). These results indicate that under low temperature stress, ABA synthesis and signal transduction pathways play key roles in responding to chilling stress in DC90 versus 9311.

3.5 Identification of hub TFs responding to the chilling stress

TFs served as key regulators to regulate plant development and responses toward the chilling stress (Kaufmann et al., 2010). To investigate hub TFs and genes involved in chilling resistance response, we calculated the module membership values (kME) among the four “rice chilling resistance response modules” based on WGCNA packages. We chose candidate TFs with the |kME| >0.85 in these modules, and this analysis retained a lot of hub genes in each module (Supplementary Table S5). Based on WGCNA analysis, totally, we identified 15 hub TFs from four modules that

10.3389/fpls.2024.1451403

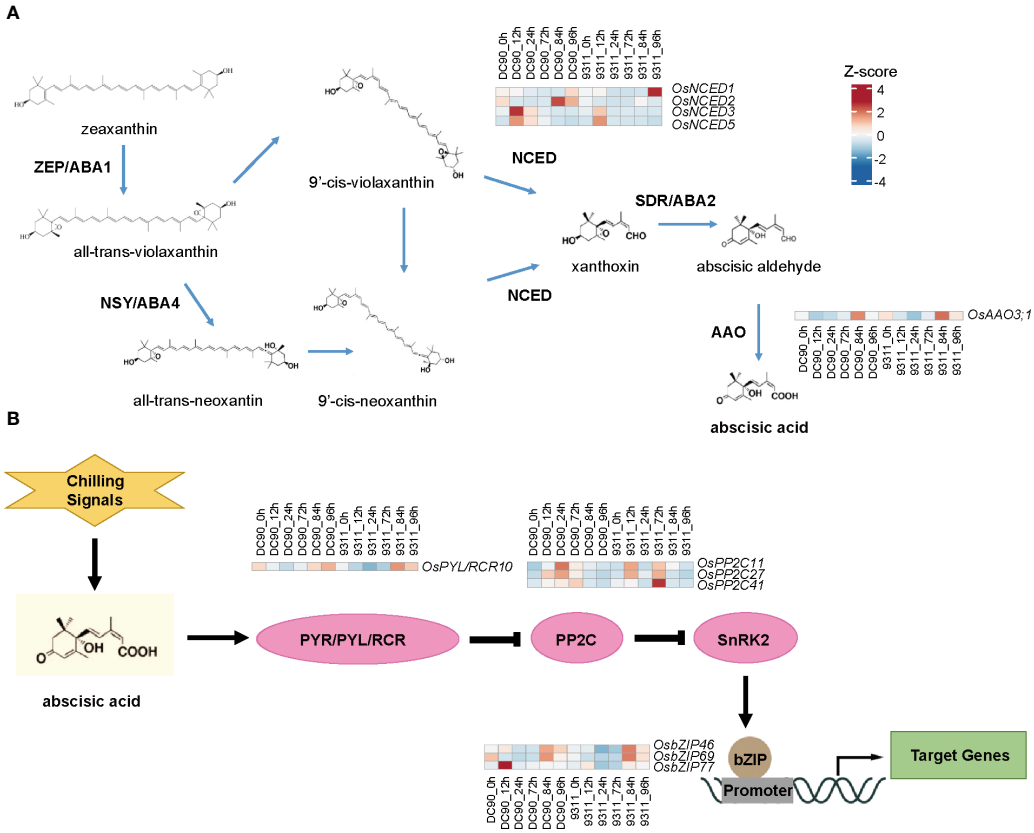

FIGURE 4
Heatmaps of related differentially expressed genes (DEGs) in abscisic acid (ABA) biosynthesis and signaling pathways. **(A)** Heatmaps of relevant genes involved in the pathway of ABA biosynthesis. **(B)** Heatmaps of relevant genes involved in the pathway of ABA signaling. The heatmap indicates z-score normalized expression levels of DEGs. The red color presents upregulation of genes and blue indicates downregulation of genes.

belong to MYB, ethylene-responsive element binding factor (ERF), zinc finger and INDETERMINATE DOMAIN protein (IDD), lateral organ boundaries domain (LBD), and other TF families (Figure 5A). These TFs formed a complex regulatory network, which may play crucial roles in chilling resistance in rice. We also investigated the expression profiles of these 15 TFs in DC90 and 9311 among six different points (Figure 5B). We found 13 of these 15 TFs were highly induced at 12h or 24h after chilling stress in

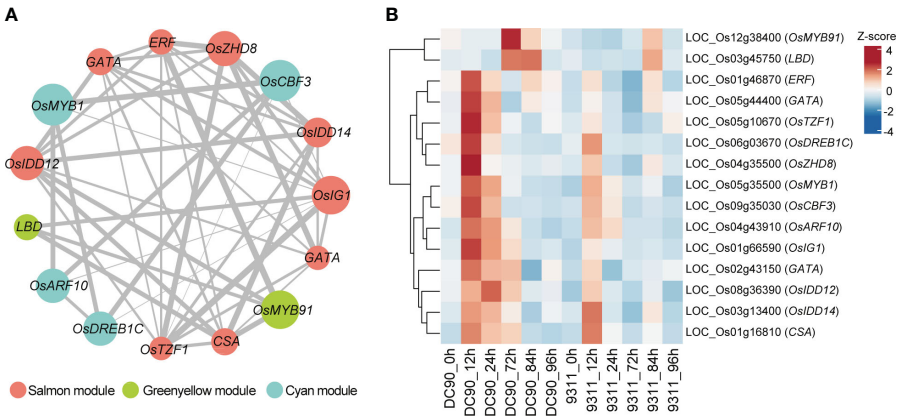

FIGURE 5
Identification of hub transcription factors (TFs) in three selected modules involved in chilling stress and their co-expression network. **(A)** Visualization of the 15 key TFs co-expression networks. Hub TFs of salmon, green yellow, and cyan modules are indicated with salmon, green yellow, and cyan color, respectively. Gray lines indicate the correlations between hub TFs. The size of the points represents the level of |KME|, and the width of the gray line represents the strength of co-expression intensity. **(B)** The heatmap of these 15 hub TFs in DC90 and 9311. The values in the heatmap represent the z-scores of FPKM at 6 time points in two cultivars. The red and blue colors indicate a high and low expression profiles, respectively.

DC90 compared with that in 9311, while the other two TFs were highly accumulated after 72h chilling stress in DC90. All these 15 TFs expressed higher under chilling stress (12h, 24h, and 72h) in DC90 than that of 9311, suggesting that these TF might serve as key TFs to regulate the chilling resistance.

3.6 Inferring the TFs regulatory network by machine learning

WGCNA is an effective method to explore the gene co-expression networks and hub genes; however, the regulatory relationships between different genes are not easy to evaluate through this method. An analytical pipeline (see Methods) suggested 15 TFs served as reliable candidates for the chilling response network (Figure 5), but the regulation direction between these TFs was not captured. Therefore, we employed the GENIE3 package (Vân and Geurts, 2018), which was used to predict the regulatory relationships of different genes and TFs based on a machine learning algorithm.

According to the random forest method, 50 TFs, which rapidly respond to the chilling stress, with the potential regulatory relationships were explored by GENIE3 (Supplementary Table S6). After associating these 50 TFs with 15 hub TFs presented in former modules (salmon, green yellow, cyan, and light green) related to chilling response, we finally retained five TFs, *OsCBF3* (LOC_Os09g35030, an ERF family member), *OsZHD8* (LOC_Os04g35500, a ZF-HD family member), *OsTZF1* (LOC_Os05g10670, a C3H family member), *OsCSA* (LOC_Os01g16810, an MYB family member), and *OsIG1* (LOC_Os01g66590, an LBD family member), as key regulators controlling gene expression networks responding to chilling stress in rice (Figure 6A; Supplementary Table S7). Among these TFs, OsCBF3 is a well-studied TF in rice chilling stress. In rice, OsSAPK6 interacts with IPA1 and phosphorylates IPA1 to stabilize it, allowing IPA1 to accumulate and activate the expression of OsCBF3 downstream to enhance rice chilling stress resistance (Jia et al., 2022). Thus, this analysis indicates our analysis is efficient and reliable.

Subsequently, we extracted the sub-regulatory network based on these five TFs of the entire gene regulator network (GRN). This subset of data contained 141 genes for salmon, greenyellow, cyan, and lightgreen modules accounting for approximately 59.75% of the total 236 genes of the entire sub-network (Figure 6A). A lot of genes were simultaneously regulated by multiple TFs (Figure 6B). For example, *OsCBF3* in cyan module was calculated to be regulated by *OsCSA*, and the other four TFs (*OsTZF1*, *OsZHD8*, *OsIG1*, and *OsCSA*) in the salmon module were also predicted to regulate each other, indicating a complex feedback regulation network among the crucial regulators (Figure 6C).

In our analysis, we uncovered that five TFs might play as key regulators that fitness the resistance of chilling stress in DC90 compared to 9311. To validate the accuracy of our results, we used transcriptomes derived from the chilling resistant (Volano) and chilling susceptible (Thaibonnet) varieties treated with chilling stresses (4°C for 0h, 2h, and 10h) conditions (Figure 6D). We found that *OsTZF1* and *OsCBF3* were highly expressed at 2h, while *OsCSA*, *OsIG1*, and *OsZHD8* were showed higher expression at 12h in the chilling resistant cultivar Volano than Thaibonnet. Similar result was also detected in the tolerance glutinous rice 89-1 and the susceptible indica rice R07 (Figure 6E). Taken together, we suppose that these five TFs serve as major and common TFs responding to the chilling stress and play crucial roles in rice chilling resistance.

4 Discussion

Chilling stress often leads to a severe decline for rice growth distribution. Therefore, exploring new rice chilling tolerance regulatory genes/TFs will provide key clues for breeding climate-resilient rice. To this end, understanding the transcriptome dynamics under chilling stress in rice is crucial. In our study, we investigated a set of time-course transcriptomes in rice of DC90 (a chilling-resistant cultivar) and 9311 (a chilling-susceptible cultivar) treated with a low-temperature stress. We revealed 12 modules based on the DEGs and a set of hub genes/TFs involved in chilling stress.

Chilling stress can induce alterations of the gene expression profiles in plants. We have found that a lot of DEGs showed rapidly changes at transcriptional levels in response to chilling stimuli in DC90 and 9311. However, it is difficult to explore crucial genes, which might involve in the chilling conditions because of numerous members of DEGs. WGCNA was confirmed as an effective method to help researchers find key hub genes related to specific traits among a large concentration of DEGs (Kuang et al., 2021; Chen et al., 2024; Hu et al., 2024; Xie et al., 2024). In this research, we have divided the DEGs involved in chilling stress into 12 co-expression modules using the WGCNA algorithm to find key genes. Performing functional enrichment annotation on these modules, we found some significant GO terms of "response to temperature stimulus," "response to hormone," "protein metabolic process," and "transcription regulator activity." These results revealed complicated networks in rice seedlings responsible for or adaptation to the chilling stress.

Based on WGCNA, our analysis revealed some "rice chilling resistance response" modules (salmon, green yellow, cyan, and light green modules), and 15 hub TFs from these modules involved in chilling conditions in rice. Among these 15 TFs, some of them have been validated and confirmed as key TFs related to the chilling stress and other abiotic stress, such as *OsDREB1C*, *OsIDD14*, *OsIDD12*, and *OsMYB91*. *OsDREB1C* serves as a DREB homolog encoding an SLK protein which has been proved to response to chilling acclimation (Mao and Chen, 2012). IDD14 protein interacts with IDD12 and IDD13 to form a transcriptional complex, activating MAPK expression (Cui et al., 2022). *OsMAPK3* and *OsMAPK6* positively regulate rice chilling tolerance and *OsMAPK3* can effectively respond to ABA stimulation, so we speculate that *IDD12/14* might response to low temperature through MAPK cascade signaling pathway (Liu et al., 2023). In addition, overexpression of *OsMYB91* enhances tolerance to abiotic stress and alters the sensitivity of seed germination to ABA (Zhu et al., 2015). Thus, our data support that these 15 TFs are potential

10.3389/fpls.2024.1451403

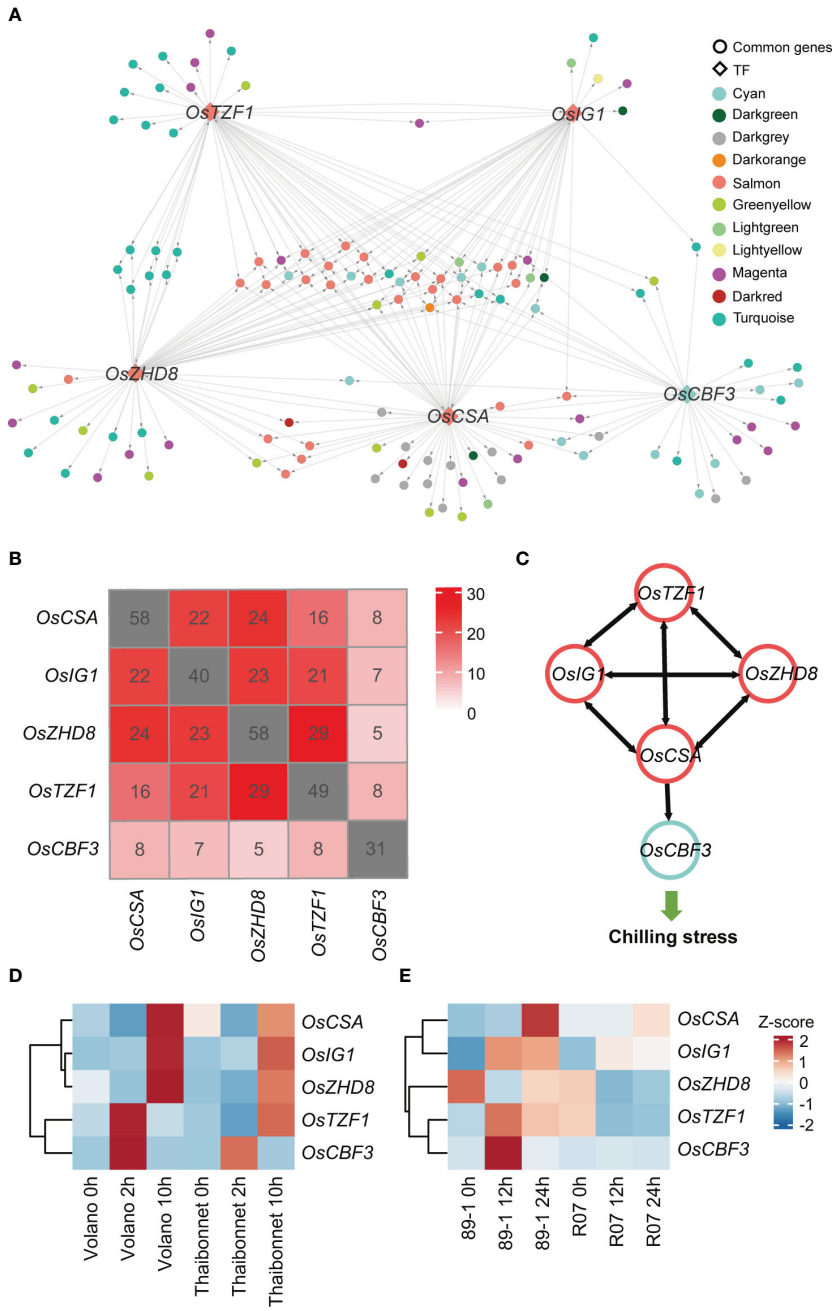

FIGURE 6
Identification of crucial transcription factors (TFs) and their target genes in a gene regulatory network and temporal expression profiles of five key TFs in different cultivars under chilling stress. **(A)** An overview of the transcriptional regulatory sub-network centered by five TFs. Each point represents a gene. Genes with regulatory relationships are linked with lines. The direction of gene regulation is indicated by gray arrow. TFs are represented by diamond frames, while other genes are represented by circles. Genes from different co-expression modules are shown in different colors, consistent with the colors in Figure 2. **(B)** Overlaps among the predicted target genes of five TF candidates in GRN. The numbers of predicted TF target genes are marked in gray squares. **(C)** Illustration of mutual regulation relationships among the five TFs. Gene regulation directions are indicated by black arrows. TFs from the salmon and cyan modules are marked using salmon and cyan circles, respectively. **(D)** The expression levels of five key TFs in other independent chilling-resistant Volano and chilling-susceptible Thaibonnet varieties of rice under 4°C for 0h, 2h, and 10h. **(E)** The expression levels of five key TFs in the chilling tolerance glutinous rice 89-1 and the susceptible indica rice R07. The red and blue colors indicate high- and low-expression levels, respectively.

regulators in chilling stress response. However, it is noted that roles of these TFs in low temperature remain to be further validated.

Plant hormones, such as BR, ETH, JA, and ABA, have been reported to play key roles in the chilling stress (He et al., 1990; Cao et al., 2012; Xiang et al., 2017; Shu et al., 2022). We found ABA was a crucial factor in response to chilling stress in DC90 versus 9311. Previous study showed that ABA response genes were regulated by *OsCBF3* to resist low temperature (Jia et al., 2022; Li et al., 2022). The chilling stress dramatically increases endogenous ABA level in rice, which results in a significant upregulation of genes involved in

ABA biosynthesis and signaling pathways (Xiang et al., 2017). The silencing of *ABI5*, which is composed of PYR/PYL/RCAR receptors in the core ABA signaling pathway, significantly reduces the cold resistance in both rice and banana (Song et al., 2022). *OsNAC5* stabilizes the *OsABI5* protein by inhibiting proteasome-mediated degradation to improve the cold resistance of rice (Li et al., 2024). In our data, the ABA pathway genes *OsNCED1*, *OsPP2C2/5/7*, and *OsbZIP77* showed higher expression levels at 12h under low temperature in DC90 than in 9311. Although *OsPYL/RCR10*, *OsAAO3;1*, and *OsbZIP46/69* all showed lower expression profiles in these two species under chilling stimulate, they were upregulated at 84h (recovery stage), suggesting that they might be some negative regulatory factors involved in chilling stress.

Although WGCNA is an effective method for analyzing gene co-expression networks, the regulatory relationships between co-expressing genes need to be explored. Here, we used a machine learning algorithm GENIE3, which was based on the inference of a collection of regression trees to predict regulatory networks. In previous studies, many nitrogen deficiency-responsive genes and TFs were predicted to function as key regulators within the network in response to nitrogen deficiency based on GENIE3 in rice (Ueda et al., 2020). In this study, we further used GENIE3 to evaluate the top 50 TFs as the candidates. Combining WGCNA and GENIE3 tow algorithms, five crucial TFs (*OsCBF3*, *OsZHD8*, *OsTZF1*, *OsCSA*, and *OsIG1*) associated with the low-temperature resistance in rice were predicted. *OsCBF3*/*DREB1A* has been proven to bind with multiple genes and TFs to regulate the cold resistance of downstream genes (Jia et al., 2022). *OsZHD8* can bind to the promoter of *OsDREB1B*, which is specifically induced by low temperature, and shows an increasing expression after ABA treatment in rice (Figueiredo et al., 2012), suggesting that it might have function on the chilling stress. Overexpression of *OsTZF1* causes ABA-induced growth inhibition of rice seedlings compared with WT, suggesting *OsTZF1* positively regulates ABA response (Zhang et al., 2012). Meanwhile, the high expression level of *OsTZF1* enhances resistance to hydrogen peroxide, salt, and drought stresses, suggesting that *OsTZF1* might be a multiple abiotic stress resistant regulators and probably play an important role in resisting chilling stress (Jan et al., 2013). The R2R3 MYB TF *OsCSA* can increase adaptations to adverse environments by balancing glucose and ABA homeostasis (Sun et al., 2021). *OsIG1* plays an important role in regulating rice floral organs development (Zhang et al., 2015), and its role in cold stress and ABA signaling pathways is currently unclear. Altogether, our results suggest the combination WGCNA and GENIE3 would be an efficient way to predict hub/key regulators in complicated networks.

In the original article, combining analysis of the differentially accumulated metabolites (DAMs) and DEGs, it has been predicted that galactinol, b-alanine, glutamate, naringenin, serotonin, ABA, and *OsNCED3* might be involved in the chilling tolerance variation of 9311 and DC90 (Cen et al., 2020). However, core TFs involved in regulating the biological processes of chilling stress remain unclear. In our study, crucial genes/TFs of low temperature tolerance were identified through WGCNA in combination with GENIE3 network based on DEGs. In addition, we identified a lot of TFs and constructed a potential TF regulatory network. Our results not only reveal common candidates (such as the ABA pathway, and *OsNCED3*), but also uncover more crucial TFs, which may reflect the application of different prediction methods. These two sets of results could be complemented to each other and will provide more candidate genes for rice breeding and deepen our understanding mechanisms underlying how the rice resists low temperature.

5 Conclusions

In this study, we performed a transcriptome analysis of rice seedlings in two cultivars under chilling stress at 6 time points. We identified 3,590 DEGs including chilling-responsive genes that were dynamically regulated under low temperature. Specifically, abscisic acid biosynthesis and signaling, coupled with transcription regulator activity, emerges as closely intertwined with the low-temperature resistance of rice. The integration analysis of hub gene networks has shed light on the key TFs triggered in response to chilling conditions. Through the correlation investigation of WGCNA and GRN, five TF candidates were predicted involved in the processes of chilling response. Our results provide invaluable gene resources for breeding climate resilient rice.

Data availability statement

The original contributions presented in the study are included in the article/Supplementary Material. Further inquiries can be directed to the corresponding author.

Author contributions

RZ: Conceptualization, Formal analysis, Methodology, Writing – original draft. XX: Formal analysis, Investigation, Writing – review & editing. XC: Writing – review & editing, Investigation. YW: Investigation, Writing – review & editing. MZ: Conceptualization, Funding acquisition, Methodology, Writing – review & editing.

Funding

The author(s) declare financial support was received for the research, authorship, and/or publication of this article. This work was supported by the Zhejiang Provincial Natural Science Foundation of China (LZ22C020001), the Fundamental Research Funds for the Central Universities (226-2024-00102), the 111 Project (Grant B14027), and the Hundred-Talent Program of Zhejiang University to MZ.

Acknowledgments

We thank colleagues and lab members for helpful comments and discussions.

Conflict of interest

The authors declare that the research was conducted in the absence of any commercial or financial relationships that could be construed as a potential conflict of interest.

Publisher's note

Supplementary material

The Supplementary Material for this article can be found online at: https://www.frontiersin.org/articles/10.3389/fpls.2024.1451403/full#supplementary-material

SUPPLEMENTARY FIGURE 1
GO enrichment for different modules selected before. Including **(A)** dark green, **(B)** turquoise, **(C)** magenta, **(D)** dark red, **(E)** dark gray, and **(F)** dark orange modules.

SUPPLEMENTARY FIGURE 2
Heatmap showing the expression patterns of DEGs related to BR pathways between DC90 and 9311 under 72h chilling treatment and 24h recovery. The color gradient indicates the normalized FPKM value (z-score) of genes [high expression (red) and low expression (blue)].

SUPPLEMENTARY FIGURE 3
Heatmap showing the expression patterns of DEGs related to CTK pathways between DC90 and 9311 under 72h chilling treatment and 24h recovery. The color gradient indicates the normalized FPKM value (z-score) of genes [high expression (red) and low expression (blue)].

SUPPLEMENTARY FIGURE 4
Heatmap showing the expression patterns of DEGs related to Eth pathways between DC90 and 9311 under 72h chilling treatment and 24h recovery. The color gradient indicates the normalized FPKM value (z-score) of genes [high expression (red) and low expression (blue)].

SUPPLEMENTARY FIGURE 5
Heatmap showing the expression patterns of DEGs related to GA pathways between DC90 and 9311 under 72h chilling treatment and 24h recovery. The color gradient indicates the normalized FPKM value (z-score) of genes [high expression (red) and low expression (blue)].

SUPPLEMENTARY FIGURE 6
Heatmap showing the expression patterns of DEGs related to IAA pathways between DC90 and 9311 under 72h chilling treatment and 24h recovery. The color gradient indicates the normalized FPKM value (z-score) of genes [high expression (red) and low expression (blue)].

SUPPLEMENTARY FIGURE 7
Heatmap showing the expression patterns of DEGs related to JA pathways between DC90 and 9311 under 72h chilling treatment and 24h recovery. The color gradient indicates the normalized FPKM value (z-score) of genes [high expression (red) and low expression (blue)].

References

Bolger, A. M., Lohse, M., and Usadel, B. (2014). Trimmomatic: a flexible trimmer for Illumina sequence data. *Bioinformatics* 30, 2114–2120. doi: 10.1093/bioinformatics/btu170

Cao, S. F., Cai, Y. T., Yang, Z. F., and Zheng, Y. H. (2012). MeJA induces chilling tolerance in loquat fruit by regulating proline and γ-aminobutyric acid contents. *Food Chem.* 133, 1466–1470. doi: 10.1016/j.foodchem.2012.02.035

Cen, W., Liu, J., Lu, S., Jia, P., Yu, K., Han, Y., et al. (2018). Comparative proteomic analysis of QTL CTS-12 derived from wild rice (Oryza rufipogon Griff.), in the regulation of cold acclimation and de-acclimation of rice (*Oryza sativa* L.) in response to severe chilling stress. *BMC Plant Biol.* 18, 163. doi: 10.1186/s12870-018-1381-7

Cen, W. J., Zhao, W. L., Ma, M. Q., Lu, S. Y., Liu, J. B., Cao, Y. Q., et al. (2020). The wild rice locus mediates ABA-dependent stomatal opening modulation to limit water loss under severe chilling stress. *Front. Plant Sci.* 11. doi: 10.3389/fpls.2020.575699

Chen, J., Zhang, L., Liu, Y., Shen, X., Guo, Y., Ma, X., et al. (2024). RNA-Seq-based WGCNA and association analysis reveal the key regulatory module and genes responding to salt stress in wheat roots. *Plants* 13, 274. doi: 10.3390/plants13020274

Chinnusamy, V., Zhu, J., and Zhu, J. K. (2006). Gene regulation during cold acclimation in plants. *Physiol. Plant* 126, 52–61. doi: 10.1111/j.1399-3054.2006.00596.x

Conway, J. R., Lex, A., and Gehlenborg, N. (2017). UpSetR: an R package for the visualization of intersecting sets and their properties. *Bioinformatics* 33, 2938–2940. doi: 10.1093/bioinformatics/btx364

Cui, Z., Xue, C., Mei, Q., and Xuan, Y. (2022). Malectin domain protein Kinase (MDPK) promotes rice resistance to sheath blight via IDD12, IDD13, and IDD14. *Int. J. Mol. Sci.* 23, 8214. doi: 10.3390/ijms23158214

Ding, Y., Shi, Y., and Yang, S. (2019). Advances and challenges in uncovering cold tolerance regulatory mechanisms in plants. *New Phytol.* 222, 1690–1704. doi: 10.1111/nph.15696

Figueiredo, D. D., Barros, P. M., Cordeiro, A. M., Serra, T. S., Lourenco, T., Chander, S., et al. (2012). Seven zinc-finger transcription factors are novel regulators of the stress responsive gene OsDREB1B. *J. Exp. Bot.* 63, 3643–3656. doi: 10.1093/jxb/ers035

Ginestet, C. (2011). ggplot2: Elegant graphics for data analysis. *J. R. Stat. Soc A.* 174, 245–245. doi: 10.1111/j.1467-985X.2010.00676_9.x

Gnanaraj, J. (2008). Minimally invasive appendicectomy using the cytoscope. *Trop. Doct.* 38, 14–15. doi: 10.1258/td.2007.060125

Guan, Y. L., Hwarari, D., Korboe, H. M., Ahmad, B., Cao, Y. W., Movahedi, A., et al. (2023). Low temperature stress-induced perception and molecular signaling pathways in plants. *Environ. Exp. Bot.* 207, 105190. doi: 10.1016/j.envexpbot.2022.105190

He, R. Y., Wang, X. S., and Wang, G. J. (1990). Effects of brassinolide (Br) on the growth and chilling resistance of maize. *Abstr. Pap. Am. Chem. S.* 200, 220–230. doi: 10.1021/bk-1991-0474.ch019

Hu, Y., Ma, M., Zhao, W., Niu, P., Li, R., and Luo, J. (2024). Identification of hub genes involved in GA-regulated coleoptile elongation under submerged germinations in rice. *J. Exp. Bot.* 75, 3862–3876. doi: 10.1093/jxb/erae144

Hubbard, T., Barker, D., Birney, E., Cameron, G., Chen, Y., Clark, L., et al. (2002). The Ensembl genome database project. *Nucleic Acids Res.* 30, 38–41. doi: 10.1093/nar/30.1.38

Jan, A., Maruyama, K., Todaka, D., Kidokoro, S., Abo, M., Yoshimura, E., et al. (2013). OsTZF1, a CCCH-tandem zinc finger protein, confers delayed senescence and stress tolerance in rice by regulating stress-related genes. *Plant Physiol.* 161, 1202–1216. doi: 10.1104/pp.112.205385

Jia, M., Meng, X., Song, X., Zhang, D., Kou, L., Zhang, J., et al. (2022). Chilling-induced phosphorylation of IPA1 by OsSAPK6 activates chilling tolerance responses in rice. *Cell Discovery* 8, 71. doi: 10.1038/s41421-022-00413-2

Kaufmann, K., Pajoro, A., and Angenent, G. C. (2010). Regulation of transcription in plants: mechanisms controlling developmental switches. *Nat. Rev. Genet.* 11, 830–842. doi: 10.1038/nrg2885

Kim, D., Paggi, J. M., Park, C., Bennett, C., and Salzberg, S. L. (2019). Graph-based genome alignment and genotyping with HISAT2 and HISAT-genotype. *Nat. Biotechnol.* 37, 907–915. doi: 10.1038/s41587-019-0201-4

Kuang, J. F., Wu, C. J., Guo, Y. F., Walther, D., Shan, W., Chen, J. Y., et al. (2021). Deciphering transcriptional regulators of banana fruit ripening by regulatory network analysis. *Plant Biotechnol. J.* 19, 477–489. doi: 10.1111/pbi.13477

Kumar, S., Shah, S. H., Vimala, Y., Jatav, H. S., Ahmad, P., Chen, Y. L., et al. (2022). Abscisic acid: metabolism, transport, crosstalk with other plant growth regulators, and its role in heavy metal stress mitigation. *Front. Plant Sci.* 13. doi: 10.3389/fpls.2022.972856

Langfelder, P., and Horvath, S. (2008). WGCNA: an R package for weighted correlation network analysis. *BMC Bioinf.* 9, 1–13. doi: 10.1186/1471-2105-9-559

Li, M., Duan, X., Gao, G., Liu, T., and Qi, H. (2022). Running title: ABA pathway meets CBF pathway at CmADC. *Hortic. Res.* 9, uhac002. doi: 10.1093/hr/uhac002

Li, M., Lin, L., Zhang, Y., and Sui, N. (2019). ZmMYB31, a R2R3-MYB transcription factor in maize, positively regulates the expression of CBF genes and enhances resistance to chilling and oxidative stress. *Mol. Biol. Res.* 46, 3937–3944. doi: 10.1007/s11033-019-04840-5

Li, R., Song, Y., Wang, X., Zheng, C., Liu, B., Zhang, H., et al. (2024). OsNAC5 orchestrates OsABI5 to fine-tune cold tolerance in rice. *J. Integr. Plant Biol.* 66, 660–682. doi: 10.1111/jipb.13585

Liao, Y., Smyth, G. K., and Shi, W. (2014). featureCounts: an efficient general purpose program for assigning sequence reads to genomic features. *Bioinformatics* 30, 923–930. doi: 10.1093/bioinformatics/btt656

Liu, J., Liu, J., He, M., Zhang, C., Liu, Y., Li, X., et al. (2023). OsMAPK6 positively regulates rice cold tolerance at seedling stage via phosphorylating and stabilizing OsICE1 and OsIPA1. *TAG. Theor. Appl. Genet.* 137, 10. doi: 10.1007/s00122-023-04506-8

Love, M. I., Huber, W., and Anders, S. (2014). Moderated estimation of fold change and dispersion for RNA-seq data with DESeq2. *Genome Biol.* 15, 1–21. doi: 10.1186/s13059-014-0550-8

Lukatkin, A. S. (2005). Initiation and development of chilling injury in leaves of chilling-sensitive plants. *Russ. J. Plant Physl.* 52, 542–546. doi: 10.1007/s11183-005-0080-z

Lukatkin, A. S., Brazaityte, A., Bobinas, C., and Duchovskis, P. (2012). Chilling injury in chilling-sensitive plants: a review. *Zemdirbyste* 99, 111–124. doi: 10.21273/HORTSCI.21.6.1329

Mao, D., and Chen, C. (2012). Colinearity and similar expression pattern of rice DREB1s reveal their functional conservation in the cold-responsive pathway. *PLoS One* 7, e47275. doi: 10.1371/journal.pone.0047275

Nawaz, M., Sun, J. F., Shabbir, S., Khattak, W. A., Ren, G. Q., Nie, X. J., et al. (2023). A review of plants strategies to resist biotic and abiotic environmental stressors. *Sci. Total Environ.* 900, 165832. doi: 10.1016/j.scitotenv.2023.165832

Nie, Y., Guo, L., Cui, F., Shen, Y., Ye, X., Deng, D., et al. (2022). Innovations and stepwise evolution of CBFs/DREB1s and their regulatory networks in angiosperms. *J. Integr. Plant Biol.* 64, 2111–2125. doi: 10.1111/jipb.13357

Seki, M., Narusaka, M., Abe, H., Kasuga, M., Yamaguchi-Shinozaki, K., Carninci, P., et al. (2001). Monitoring the expression pattern of 1300 Arabidopsis genes under drought and cold stresses by using a full-length cDNA microarray. *Plant Cell* 13, 61–72. doi: 10.1105/tpc.13.1.61

Shafi, S., Shafi, I., Zaffar, A., Zargar, S. M., Shikari, A. B., Ranjan, A., et al. (2023). The resilience of rice under water stress will be driven by better roots: Evidence from root phenotyping, physiological, and yield experiments. *Plant Stress* 10, 100211. doi: 10.1016/j.stress.2023.100211

Shu, P., Li, Y. J., Xiang, L. T., Sheng, J. P., and Shen, L. (2022). Ethylene enhances tolerance to chilling stress in tomato fruit partially through the synergistic regulation between antioxidant enzymes and ATP synthases. *Postharvest Biol. Tec.* 193, 112065. doi: 10.1016/j.postharvbio.2022.112065

Song, Z., Lai, X., Chen, H., Wang, L., Pang, X., Hao, Y., et al. (2022). Role of MaABI5-like in abscisic acid-induced cold tolerance of 'Fenjiao' banana fruit. *Hortic. Res.* 9, uhac130. doi: 10.1093/hr/uhac130

Sun, J., Zheng, T. H., Yu, J., Wu, T. T., Wang, X. H., Chen, G. M., et al. (2017). TSV, a putative plastidic oxidoreductase, protects rice chloroplasts from cold stress during development by interacting with plastidic thioredoxin Z. *New Phytol.* 215, 240–255. doi: 10.1111/nph.14482

Sun, L., Yuan, Z., Wang, D., Li, J., Shi, J., Hu, Y., et al. (2021). Carbon starved anther modulates sugar and ABA metabolism to protect rice seed germination and seedling fitness. *Plant Physiol.* 187, 2405–2418. doi: 10.1093/plphys/kiab391

Thomashow, M. F. (1999). Plant cold acclimation: Freezing tolerance genes and regulatory mechanisms. *Annu. Rev. Plant Biol.* 50, 571–599. doi: 10.1146/annurev.arplant.50.1.571

Ueda, Y., Ohtsuki, N., Kadota, K., Tezuka, A., Nagano, A. J., Kadowaki, T., et al. (2020). Gene regulatory network and its constituent transcription factors that control nitrogen-deficiency responses in rice. *New Phytol.* 227, 1434–1452. doi: 10.1111/nph.16627

Vân, A. H. T., and Geurts, P. (2018). dynGENIE3: dynamical GENIE3 for the inference of gene networks from time series expression data. *Sci. Rep.* 8, 3384. doi: 10.1038/s41598-018-21715-0

Wu, T. Z., Hu, E. Q., Xu, S. B., Chen, M. J., Guo, P. F., Dai, Z. H., et al. (2021). clusterProfiler 4.0: A universal enrichment tool for interpreting omics data. *Innovation-Amsterdam* 2, 100141. doi: 10.1016/j.xinn.2021.100141

Xiang, H. T., Wang, T. T., Zheng, D. F., Wang, L. Z., Feng, Y. J., Luo, Y., et al. (2017). ABA pretreatment enhances the chilling tolerance of a chilling-sensitive rice cultivar. *Braz. J. Bot.* 40, 853–860. doi: 10.1007/s40415-017-0409-9

Xie, G., Zou, X., Liang, Z., Zhang, K., Wu, D., Jin, H., et al. (2024). GBF family member PfGBF3 and NAC family member PfNAC2 regulate rosmarinic acid biosynthesis under high light. *Plant Physiol.* 195, 1728–1744. doi: 10.1093/plphys/kiae036

Xu, L. M., Zhou, L., Zeng, Y. W., Wang, F. M., Zhang, H. L., Shen, S. Q., et al. (2008). Identification and mapping of quantitative trait loci for cold tolerance at the booting stage in a rice near-isogenic line. *Plant Sci.* 174, 340–347. doi: 10.1016/j.plantsci.2007.12.003

Yin, Q., Qin, W., Zhou, Z., Wu, A. M., Deng, W., Li, Z., et al. (2024). Banana MaNAC1 activates secondary cell wall cellulose biosynthesis to enhance chilling resistance in fruit. *Plant Biol. J.* 22, 413–426. doi: 10.1111/pbi.14195

Zhang, J. R., Tang, W., Huang, Y. L., Niu, X. L., Zhao, Y., Han, Y., et al. (2015). Down-regulation of a LBD-like gene, OsIG1, leads to occurrence of unusual double ovules and developmental abnormalities of various floral organs and megagametophyte in rice. *J. Exp. Bot.* 66, 99–112. doi: 10.1093/jxb/eru396

Zhang, C., Zhang, F., Zhou, J., Fan, Z., Chen, F., Ma, H., et al. (2012). Overexpression of a phytochrome-regulated tandem zinc finger protein gene, OsTZF1, confers hypersensitivity to ABA and hyposensitivity to red light and far-red light in rice seedlings. *Plant Cell Rep.* 31, 1333–1343. doi: 10.1007/s00299-012-1252-x

Zhang, M., Zhao, R., Huang, K., Huang, S., Wang, H., Wei, Z., et al. (2022). The OsWRKY63-OsWRKY76-OsDREB1B module regulates chilling tolerance in rice. *Plant J.* 112, 383–398. doi: 10.1111/tpj.15950

Zhu, N., Cheng, S., Liu, X., Du, H., Dai, M., Zhou, D. X., et al. (2015). The R2R3-type MYB gene OsMYB91 has a function in coordinating plant growth and salt stress tolerance in rice. *Plant Sci.* 236, 146–156. doi: 10.1016/j.plantsci.2015.03.023

frontiers | Frontiers in Plant Science

TYPE Original Research
PUBLISHED 22 August 2024
DOI 10.3389/fpls.2024.1443681

OPEN ACCESS

EDITED BY
Zemin Wang,
Gansu Agricultural University, China

REVIEWED BY
Rinku Sharma,
Brigham and Women's Hospital,
United States
Attila Fábián,
Hungarian Research Network,
Hungary

*CORRESPONDENCE
Nepolean Thirunavukkarasu
nepolean@millets.res.in

RECEIVED 04 June 2024
ACCEPTED 29 July 2024
PUBLISHED 22 August 2024

CITATION
Singh S, Viswanath A, Chakraborty A, Narayanan N, Malipatil R, Jacob J, Mittal S, Satyavathi TC and Thirunavukkarasu N (2024) Identification of key genes and molecular pathways regulating heat stress tolerance in pearl millet to sustain productivity in challenging ecologies.
Front. Plant Sci. 15:1443681.
doi: 10.3389/fpls.2024.1443681

Identification of key genes and molecular pathways regulating heat stress tolerance in pearl millet to sustain productivity in challenging ecologies

Swati Singh[1], Aswini Viswanath[1], Animikha Chakraborty[1], Neha Narayanan[1], Renuka Malipatil[1], Jinu Jacob[1], Shikha Mittal[2], Tara C. Satyavathi[1] and Nepolean Thirunavukkarasu[1]*

[1]Genomics and Molecular Breeding Lab, Global Center of Excellence on Millets (Shree Anna), ICAR-Indian Institute of Millets Research, Hyderabad, India, [2]Department of Biotechnology and Bioinformatics, Jaypee University of Information Technology, Waknaghat, Solan, India

Pearl millet is a nutri-cereal that is mostly grown in harsh environments, making it an ideal crop to study heat tolerance mechanisms at the molecular level. Despite having a better-inbuilt tolerance to high temperatures than other crops, heat stress negatively affects the crop, posing a threat to productivity gain. Hence, to understand the heat-responsive genes, the leaf and root samples of two contrasting pearl millet inbreds, EGTB 1034 (heat tolerant) and EGTB 1091 (heat sensitive), were subjected to heat-treated conditions and generated genome-wide transcriptomes. We discovered 13,464 differentially expressed genes (DEGs), of which 6932 were down-regulated and 6532 up-regulated in leaf and root tissues. The pairwise analysis of the tissue-based transcriptome data of the two genotypes demonstrated distinctive genotype and tissue-specific expression of genes. The root exhibited a higher number of DEGs compared to the leaf, emphasizing different adaptive strategies of pearl millet. A large number of genes encoding ROS scavenging enzymes, WRKY, NAC, enzymes involved in nutrient uptake, protein kinases, photosynthetic enzymes, and heat shock proteins (HSPs) and several transcription factors (TFs) involved in cross-talking of temperature stress responsive mechanisms were activated in the stress conditions. Ribosomal proteins emerged as pivotal hub genes, highly interactive with key genes expressed and involved in heat stress response. The synthesis of secondary metabolites and metabolic pathways of pearl millet were significantly enriched under heat stress. Comparative synteny analysis of HSPs and TFs in the foxtail millet genome demonstrated greater collinearity with pearl millet compared to proso millet, rice, sorghum, and maize. In this study, 1906

unannotated DEGs were identified, providing insight into novel participants in the molecular response to heat stress. The identified genes hold promise for expediting varietal development for heat tolerance in pearl millet and similar crops, fostering resilience and enhancing grain yield in heat-prone environments.

KEYWORDS

abiotic stress, climate resilience, functional genes, heat stress, RNAseq, pearl millet, transcriptomes

Introduction

Pearl millet [*Pennisetum glaucum (L.R. Br)*] belongs to the Poaceae family. It is a crop widely grown in the arid and semi-arid regions of Sub-Saharan Africa and the Indian subcontinent, where other cereals fail to achieve an economic yield (Sun et al., 2020). India is the world's largest pearl millet producer, with a total cultivated area of 7.41 million hectares and a production output of 10.3 million tons in 2020-2021 (Indiastat, 2020). It is a hardy crop that can withstand the unpredictable effects of climate change. Climate change endangers agricultural production, raising serious worries about global food security. Temperature fluctuations are a significant component that significantly impacts crop growth and development. Climate models predict that the production of pearl millet in Sub-Saharan Africa will reduce from 17% to 7% by 2050 (Schlenker and David, 2010).

Heat stress is a major environmental threat that reduces crop productivity and results in yield reduction (Jagadish et al., 2021). In comparison to other crops, pearl millet has a high tolerance level to abiotic stresses such as heat, drought, salinity, and nutrient deficiency (Vadez et al., 2012), which allows it to produce higher yields under the same conditions and is critical in ensuring food and nutritional security in fluctuating climatic conditions. It is a climate-resilient crop that can survive high temperatures of up to 42°C; however, when exposed to temperatures exceeding 42°C, crop carbohydrate reserves are depleted, and plant starvation occurs (Djanaguiraman et al., 2009). Furthermore, it results in decreased growth due to a loss of cellular water content and an overall reduction in cell size. This crop struggles to survive under prolonged heat stress and suffers from adverse effects such as compromised cell membrane integrity, a significant drop in chlorophyll content, and a decrease in antioxidant enzymes, resulting in the accumulation of free radicals that cause cell damage and apoptosis (Hasanuzzaman et al., 2013). Therefore, it is imperative to develop heat-tolerant varieties that can endure changes caused by high temperatures in the production ecologies in which they are cultivated.

Studies have revealed that pearl millet has outperformed maize regarding morphological and physiological indices such as relative growth rate and net assimilation rate (NAR) at high temperatures (Ashraf and Hafeez, 2004). The molecular mechanism entails the activation of transcription factors (TFs), heat shock proteins (HSPs), metabolite synthesis, and other heat stress-related genes (He et al., 2023). The repository of genes in pearl millet distinguishes it from other crops. Mwadzingeni et al., 2016 described heat stress as a complicated process mediated by an intricate interplay of many genes and their regulated expression (Mwadzingeni et al., 2016). Transcriptome analysis has emerged as a valuable methodology to investigate gene expression and complex regulatory networks. Its application has been beneficial in unravelling the molecular mechanisms operative in crops when exposed to heat stress (Frey et al., 2015). Recent studies have effectively used transcriptome-based approaches in several crops to elucidate the molecular function of abiotic stress tolerance namely, maize (Qian et al., 2019), rice (Wang et al., 2019), wheat (Rangan et al., 2020), eggplant (Zhang et al., 2019) and pearl millet (Goud et al., 2022).

Pearl millet genotypes show a wide level of variation in heat tolerance when compared to other cereal crops. The present study was designed to mine the heat-stress-responsive genes from such genetic variation. Here, two pearl millet inbreds contrasting to heat tolerance behavior were used to discover DEGs through a genome-wide RNA-Seq approach. We discovered DEGs that encode important transcription factors, ion transporters, and metabolic pathway regulators from the leaf and root tissues. Our findings establish the groundwork for mining essential genes linked with heat tolerance in pearl millet and elucidating the molecular mechanisms operating in pearl millet in response to heat stress. It will also provide valuable insights into improving pearl millet productivity under heat-stress ecologies in the changing climate scenarios.

Materials and methods

Plant materials and treatment condition

The study used two contrasting pearl millet genotypes, namely EGTB 1034 (heat-tolerant) and EGTB 1091 (heat-sensitive), developed from the pearl millet breeding program at ICAR-IIMR,

Hyderabad. Several genotypes were systematically evaluated under heat stress in both pre-and post-flowering stages, and the above-contrasting genotypes were selected based on phenotypic performances for further characterization through transcriptomes. The seeds of these genotypes were grown in cups under a photoperiod of 16 hours of light and 8 hours of darkness at room temperature with 90% relative humidity. Heat stress was induced on seven-day-old seedlings in a controlled growth chamber with a constant temperature of 45°C for 24 hours, whereas, for control samples, the same procedure was performed at room temperature 30°C. Immediately after 24 hours, leaf and root samples were collected with three biological replicates from both control and heat-treated conditions of HTG and HSG and used for RNA sequencing, independently.

RNA extraction and library preparation

Total RNA from the leaf and root of the three biological replicates of both control and treated genotypes was extracted using TRIzol reagent (RNAiso-plus) (ThermoFisher Scientific, United States), following the protocol of the manufacturer and further purified using MN Nucleospin RNA clean up kit (Macherey-Nagel, Germany). RNA quality and integrity were checked in 1% agarose (Lonza, Belgium) and Nanodrop 2000 (Thermofisher Scientific, Massachusetts, USA). Furthermore, the samples with RNA integrity number ≥7 were processed for analysis (Hosseini et al., 2021). The libraries were constructed using the KAPA HyperPrep Kit for the cDNA Synthesis & Amplification module, and length assessment was carried out using a bioanalyzer (Agilent Technologies, Santa Clara, California, USA). Then, the RNA-Seq libraries were sequenced on the Illumina sequencing platform (NovaSeq 6000) using a paired-end approach.

Transcriptome sequencing analysis

Following RNA-Seq, a quality assessment of the reads was performed using FastQC (http://www.bioinformatics.babraham.ac.uk/projects/fastqc/), and adapter sequences and Illumina-specific sequences were removed using Trimmomatic (Version 0.36) (Bolger et al., 2014). The remaining cleaned reads were mapped to the reference genome of pearl millet (Table 1), obtained from the International Pearl Millet Genome Sequence Consortium (https://cegsb.icrisat.org/ipmgsc/genome.html) using the alignment tool Hisat2 ver. 2.0.4. Finally, the number of reads for each gene was counted using the featureCounts tool (version 2.0.0) (Liao et al., 2014).

Identification of differentially expressed genes

DEGs were identified using the R bioconductor package edgeR version 3.42.4 (Robinson et al., 2010). TMM (Trimmed Mean of M-values) normalization method was applied to account for library size and composition differences across samples. The genes with the threshold of log2 fold change (FC) cutoff ≥2 and adjusted p-value ≤0.01 were selected as significant DEGs for further analyses and interpretations.

Functional annotation of DEGs

To identify putative biological functions and pathways for the DEGs, the Gene Ontology (GO) and Kyoto Encyclopedia Of Genes And Genomes (KEGG) databases were searched for annotation using the Database for Annotation, Visualization and Integrated Discovery (DAVID, version 6.8) (https://david.ncifcrf.gov/summary.jsp) and SRplot (https://www.bioinformatics.com.cn) (Huang et al., 2007). This analysis provided all GO terms significantly enriched in DEGs compared to the genome background and filtered the DEGs corresponding to the biological functions. Significant GO and KEGG pathways were identified with the criterion of FDR-corrected p-value <0.05 (Yoav and Hochberg, 2000). Hyper-geometric statistical tests and Bonferroni correction methods were also applied (Sidak, 1967).

Enrichment analysis of transcription factors

To identify enriched TF families functioning between genotypes under stressed and control conditions, a TF enrichment analysis was conducted. The identified DEGs were used as input and compared against the *Setaria italica* TF database from PlantRegMap (Tian et al., 2020). The DEGs were screened against 2,410 TFs, classified into 56 families, with a stringency p-value ≤0.01.

Identifying the hub genes involved in the protein interaction network

Protein-Protein Interactions (PPI) are crucial to most biological processes, and understanding them is imperative for unravelling the molecular mechanisms underlying DEGs in transcriptomics. The DEGs obtained under heat stress were utilized to construct a network of PPIs. The STRING (Search Tool for the Retrieval of Interacting Genes and Proteins) database was employed and the required interaction score for the physical sub-network was set to default parameters to identify both validated and predicted protein-protein interactions to investigate protein functional relationships (http://string-db.org) (Szklarczyk et al., 2023). The resulting interactions were utilized to construct the PPIs network, which was then analyzed and visualized using Cytoscape v3.10.0 (https://cytoscape.org/) (Shannon et al., 2003). The gene network was examined using average path length to determine key global centrality parameters such as proximity and betweenness, centrality, and average degree. The PPIs network was designed to identify significant players or hub genes (nodes with the highest degree) involved in heat stress tolerance. The hub genes were identified and ranked based on degree using the Cytoscape plugin cytoHubba (Chin et al., 2014). The degree algorithm calculates the

10.3389/fpls.2024.1443681

TABLE 1 Summary of RNA-Seq data sets acquired from 24 samples of heat-tolerant and sensitive genotypes under heat stress conditions mapped to pearl millet reference genome.

Sample ID	Tissue	Conditions	Raw reads	Aligned reads	Alignment rate	Uniquely mapped reads (%)	Multi-mapped reads (%)
HTG_CL_R1	Leaf	Control	5.00E+07	42329687	82.46%	53.22%	29.24%
HTG_CR_R1	Root	Control	5.00E+07	32191133	68.98%	50.08%	18.90%
HTG_CL_R2	Leaf	Control	3.00E+07	20003729	71.83%	48.25%	23.58%
HTG_CR_R2	Root	Control	3.00E+07	24828065	71.27%	51.00%	20.27%
HTG_CL_R3	Leaf	Control	5.00E+07	38766968	79.55%	46.34%	33.21%
HTG_CR_R3	Root	Control	4.00E+07	27153552	65.32%	47.92%	17.40%
HTG_TL_R1	Leaf	45°C	1.00E+08	91657981	89.85%	59.38%	30.47%
HTG_TR_R1	Root	45°C	5.00E+07	38269304	80.23%	58.53%	21.70%
HTG_TL_R2	Leaf	45°C	3.00E+07	29098139	86.09%	52.71%	33.38%
HTG_TR_R2	Root	45°C	4.00E+07	30888850	73.58%	56.09%	17.49%
HTG_TL_R3	Leaf	45°C	2.00E+07	19022430	78.49%	44.54%	33.95%
HTG_TR_R3	Root	45°C	3.00E+07	27025054	79.26%	53.28%	25.98%
HSG_CL_R1	Leaf	Control	4.00E+07	33176962	80.45%	56.37%	24.08%
HSG_CR_R1	Root	Control	9.00E+07	57597229	67.19%	48.00%	19.19%
HSG_CL_R2	Leaf	Control	4.00E+07	31974747	83.28%	47.34%	35.94%
HSG_CR_R2	Root	Control	5.00E+07	37151752	75.21%	49.93%	25.28%
HSG_CL_R3	Leaf	Control	4.00E+07	19861195	55.31%	30.62%	24.69%
HSG_CR_R3	Root	Control	3.00E+07	15390775	50.47%	30.65%	19.82%
HSG_TL_R1	Leaf	45°C	5.00E+07	20934726	44.41%	30.02%	14.39%
HSG_TR_R1	Root	45°C	3.00E+07	13284437	49.38%	35.12%	14.26%
HSG_TL_R2	Leaf	45°C	3.00E+07	25434882	87.18%	62.90%	24.28%
HSG_TR_R2	Root	45°C	4.00E+07	21105953	53.31%	38.69%	14.62%
HSG_TL_R3	Leaf	45°C	4.00E+07	34398084	84.12%	59.18%	24.94%
HSG_TR_R3	Root	45°C	4.00E+07	28901096	81.13%	58.38%	22.75%

HTG, heat-tolerant genotype; HSG, heat-sensitive genotype; CL, control condition of leaf tissue; CR, control condition of root tissue; TL, treatment condition of leaf tissue; TR, treatment condition of root tissue and R1, R2, and R3- biological replicates

number of direct interactions of each gene in the PPI network. Hub genes were recognized based on the higher number of connections or degrees over other genes.

Results

Genome-wide transcriptome data statistics

Genome-wide transcriptome profiling was conducted in leaf and root tissues of HTG and HSG under control and heat-treated conditions to examine the transcriptome regulation of tissue-specific genes in response to heat stress. We extracted a total of one billion raw reads using Illumina sequencing technology, of which 760 million reads, after rigorous quality testing and data cleaning, were mapped to the pearl millet reference genome from established 24 RNA-Seq cDNA libraries. Over 72.43% of the high-quality reads were effectively mapped to the pearl millet reference genome, of which 48% were uniquely mapped, whereas 23% illustrated multiple genomics locations (Table 1).

Gene expression profile analysis of HTG and HSG under heat stress

The expressed genes were generated and discovered using a stringent log2 FC ≥2 threshold and p-value <0.01 to comprehend their biological function better. Table 2 presents statistics of the DEGs between the twelve possible combinations. A thorough examination of tissue-specific comparisons between control and stress conditions in both genotypes produced 13,464 DEGs, of which 6,932 showed down-regulation and 6,532 showed up-

10.3389/fpls.2024.1443681

TABLE 2 Pairwise comparison of differentially expressed genes (DEGs) in heat-tolerant and heat-sensitive genotypes under different heat stress conditions.

S. No	Combinations	Total DEGs	Down-regulated DEGs	Up-regulated DEGs
1	HTG_CL *vs* HTG_TL	1265	921	344
2	HSG_CL *vs* HSG_TL	82	77	5
3	HTG_CL *vs* HSG_CL	148	92	56
4	HTG_TL *vs* HSG_TL	1084	575	509
5	HTG_CR *vs* HTG_TR	516	378	138
6	HSG_CR *vs* HSG_TR	996	989	7
7	HTG_CR *vs* HSG_CR	2081	407	1674
8	HTG_TR *vs* HSG_TR	330	133	197
9	HTG_CL *vs* HTG_CR	231	104	127
10	HTG_TL *vs* HTG_TR	2817	1607	1210
11	HSG_CL *vs* HSG_CR	951	71	880
12	HSG_TL *vs* HSG_TR	2963	1578	1385

HTG, heat-tolerant genotype; HSG, heat-sensitive genotype; CL, control condition of leaf tissue; CR, control condition of root tissue; TL, treatment condition of leaf tissue; TR, treatment condition of root tissue.

regulation. In the leaf category, it was found that 1,665 genes were down-regulated, and 914 genes were up-regulated out of a total of 2,579 genes identified. Comparatively, 2,016 genes were induced in the root category, while 1,907 genes were suppressed among the 3,923 genes examined. The comparison between leaf and root tissues revealed that the most DEGs, with 3,360 showing lower expression and 3,602 displaying higher expression, out of 6,962 genes studied. In addition, tissue-specific evaluation of HTG and HSG revealed that 489 and 15 genes were commonly up-regulated and down-regulated, respectively (Figure 1).

Identification of heat-responsive DEGs in leaf

The leaf transcriptome analysis identified 2,579 expressed transcripts, with 1,665 showing down-regulation and 914 showing up-regulation (Table 2). The Venn diagram (Figure 1) represents the total DEGs identified in the leaf tissues of both genotypes under control and treated conditions. Significant expression patterns were observed in various comparisons. For instance, in HTG_CL vs HSG_CL, 92 genes were down-regulated, and 56 genes were up-regulated. Similarly, in HTG_CL vs HTG_TL, we found 921 suppressed and 344 induced genes. Moreover, in HSG_CL vs HSG_TL, 77 genes showed lower expression while only five genes were over-expressed, and in HTG_TL vs HSG_TL, 575 genes were down-regulated while 509 were up-regulated.

The comparisons indicate a trend where genes responsible for various mechanisms and pathways in pearl millet leaves tend to experience suppression under stress conditions. The sensitive genotype showed a significant increase in down-regulated DEGs, suggesting its heightened vulnerability to heat stress. This implies that the HSG genotype is more sensitive to the negative impacts of high temperatures than the HTG genotype.

On comparing the transcript abundance profile among all four combinations, we identified that *HATPase domain-containing protein, SHSP, protein kinases, lipoxygenase, chlorophyll a-b binding protein*, and *BHLH* were significantly up-regulated. In contrast, *stachyose synthase, BURP, lipase_3, lipase_GDSL domain-containing protein, cytochrome C* and *b559, BZIP, dirigent protein*, and *lipoxygenase* showed significant down-regulation. Four of the top 10 highest up-regulated genes were expressed in HTG_TL *vs* HSG_TL, and of the top 10 down-regulated genes, HSG_CL *vs* HSG_TL included five highly-expressed genes. The significant up-regulation and down-regulation of expressed genes in the leaf are summarized in Table 2. Among all the genes expressed, lipase was

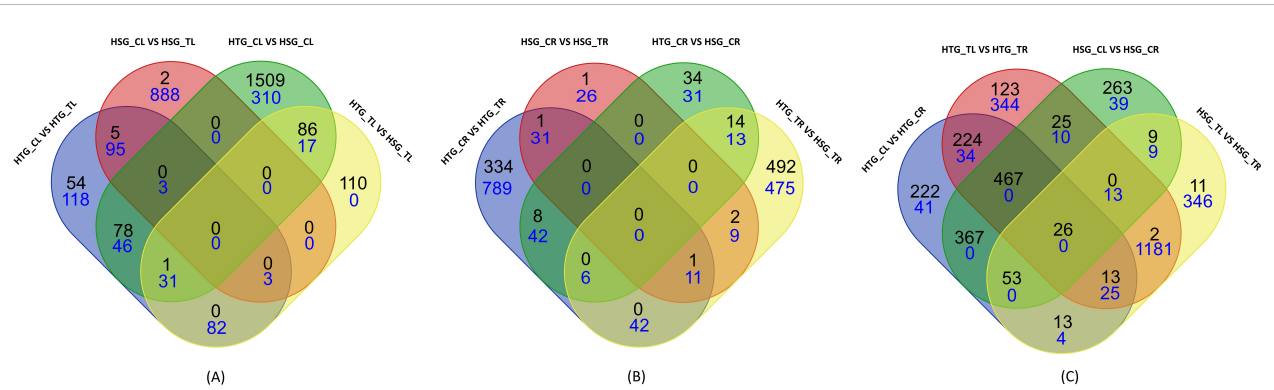

FIGURE 1
Up- (black) and down-regulated (blue) DEGs across comparisons in **(A)** leaf, **(B)** root, and **(C)** leaf vs root under heat stress treatments.

expressed in all the combinations except HSG_CL *vs* HSG_TL, which was down-regulated (-11.5 FC) in the sensitive genotype. The comparison between tolerant and sensitive genotypes under control conditions revealed down-regulation of *Receptor-like serine/threonine-protein kinase*, *AP2/ERF domain-containing protein*, and *ABC transporter*. In contrast, there was a significant up-regulation, ranging from -11 to 14-fold, of *Lipase_3 domain-containing protein, NAD(P)H dehydrogenase*, and *Laccase*. P*eroxidase*, *jmjC protein* (chromatin remodeling and histone modification), *WRKY*, *24.1kDa HSP, LEA protein* (prevents protein aggregation under stress), *chitinase, elongation factor, NAC*, and *DNA helicase* were induced several folds. On the other hand, *NAD(P)H dehydrogenase, AAI domain-containing protein, bidirectional sugar transporter SWEET, FE2OG dioxygenase, phytocyanin*, and *ABC transporter* genes were down-regulated across most of the combinations.

Chlorophyll a-b binding protein involved in photosynthetic activity was highly up-regulated in the tolerant genotype under treatment conditions. *Peroxidase* and *thioredoxin* enzymes belonging to the hydrogen peroxide catabolic process were more repressed in HSG. The *lipoxygenase* that plays a role in fatty acid biosynthesis and lipid oxidation was down-regulated across all combinations except HTG_TL *vs* HSG_TL, where it was five-fold induced. Genes involved in glutathione metabolic processes, such as *glutathione synthetase* and *glutathione transferase*, were mostly repressed in the treated sensitive genotype. *Cytochrome b599* and *photosystem I* and *II* are cellular components of the chloroplast thylakoid membrane and were mostly down-regulated in the stressed HSG. In contrast, these genes displayed less suppression in the tolerant genotype than in the sensitive genotype. Extracellular region enzymes *expansin*, involved in cell wall organization, was up-regulated threefold in HTG_TL *vs* HSG_TL. In contrast, *L-ascorbate oxidase* was down-regulated threefold in HTG_CL *vs* HTG_TL. *Bidirectional sugar transporter SWEET* was down-regulated several folds in the HTG_TL *vs* HSG_TL and up-regulated in the HTG_CL *vs* HTG_TL. *Amino acid permease* involved in the transmembrane transporter activity of amino acid, *alpha-amylase* and *PsbP* domain-containing protein, which is part of PSII, was more down-regulated in the sensitive genotype than in the tolerant genotype under heat stress.

Identification of heat-responsive DEGs in root

Transcriptome analysis of all comparisons of root samples identified 3923 genes, of which 2016 and 1907 genes were induced and repressed, respectively (Figure 1). The Venn diagram represents commonly up-regulated and down-regulated genes under control and stress conditions in the roots of HTG and HSG. While analyzing the expression dynamics, on comparing HTG control with treatment, we found that 138 genes were up-regulated, and 378 genes were down-regulated. We observed more down-regulated genes (989) and fewer induced genes (Ashraf and Hafeez, 2004) in the control *vs* treatment of sensitive genotype. Comparing the control conditions of both genotypes, it was observed that 1674 genes were up-regulated while 407 genes were down-regulated. When comparing the treatment conditions of both genotypes, 197 genes showed over-expression, while 133 transcripts showed under-expression (Table 2).

In contrast to the leaf samples, the root tissues showed a higher number of up-regulated DEGs (2016). This up-regulation of genes in the roots under heat stress conditions suggests a different molecular response than the leaves. The HSG exhibited a notable number of down-regulated DEGs in the roots, indicating a suppression of gene expression, specifically in this genotype under heat stress.

From the present study, we identified DEGs encoding *peroxidase, protein kinase* and *AAI domain-containing proteins* that were significantly expressed across all combinations. *Aldehyde oxygenase, involved in lipid biosynthesis, bidirectional sugar transporter SWEET*, and *Fe2OG dioxygenase* domain-containing protein, was up-regulated in the HTG combinations, whereas in the sensitive genotype, these genes were down-regulated.

In the sensitive genotypes treatment condition, it was revealed that *17.9kDa HSP, chlorophyll a-b binding protein, PSII, RuBisCO, thioredoxin, malate dehydrogenase, potassium transporter, ABC transporter, copper transporter, glutamine synthetase, glutathione transferase, nitrate reductase, PsbP protein, Clp protease, temperature-induced lipocalin (TIL)* that protects chloroplasts from ion toxicity, *PSI, phosphate transporter, MAPK, MYB, RING-type E3 ubiquitin transferase* and *zinc finger proteins* were down-regulated several folds. Enzymes *lipase* and *lipoxygenase, laccase* and *stachyose synthase*, and the *fructose bisphosphate aldolase* that participates in carbohydrate degradation in the glycolysis cycle were primarily down-regulated in the sensitive genotypes. Under control conditions, comparison between genotypes revealed suppressed expression of *Glutathione S-transferase, Protein kinase*, and *Sucrose synthase*. Conversely, there was up-regulation of *terpene synthase*, which is involved in the synthesis of secondary metabolites, as well as *Phosphoenolpyruvate carboxykinase* and *Fructose-bisphosphate aldolase*, both of which are involved in carbohydrate biosynthesis. In the treatment comparison of both the genotypes, *stromal 70kDa HSP* was down-regulated, in contrast to *calcium-binding protein 60*, which was induced two-fold. *Xyloglucan endotransglucosylase/hydrolase* was down-regulated across all the combinations, but the level of expression was found more suppressed (-6 folds) in the sensitive genotype in comparison to the tolerant. The results from the present study align with the comparative transcriptomic research conducted on *Agrostis species*, which revealed the activation of root antioxidant enzymes, genes involved in respiration, HSPs, and transcription factors aided tolerant genotype to adapt better to heat stress by maintaining growth and development (Huang, Bingru et al., 2012).

Comparison of heat-responsive DEGs in leaf *vs* root

Leaf and root stress treatments were compared to identify the tissue-specific expression of genes involved in transcriptional regulation of both pearl millet genotype's responses to heat stress.

The comparative transcriptomic analysis between leaf and root tissues revealed 6,962 expressed genes, with 3,602 showing up-regulation and 3,360 displaying down-regulation (Figure 1). Under control conditions, the comparison indicated 127 up-regulated genes and 104 down-regulated in the tolerant genotype, whereas 880 genes were induced and 71 genes were suppressed in the sensitive genotype. Under heat stress, HTG exhibited 1,210 up-regulated genes, while 1607 genes were down-regulated in the root. Meanwhile, 1385 genes were up-regulated, and 1,578 genes were down-regulated in the HSG (Table 2). The analysis of expression dynamics demonstrated distinct transcriptional responses to heat stress in the different tissues of both genotypes, highlighting their divergent molecular mechanisms in coping with environmental challenges.

AP2/ERF, auxin response factor, WRKY, NAC, lipoxygenase, lipase-GDSL, calmodulin-binding protein, PIP26, PIP11, respiratory burst oxidase, ring-type E3 ubiquitin transferase, sucrose synthase, terpene synthase, patatin, cytokinin dehydrogenase, bidirectional sugar transporter SWEET, and calcium uniporter showed induced expression across all the comparisons except in control condition of the tolerant genotype. In comparing leaf and root tissues under control conditions, the tolerant genotype showed enhanced expression of *dirigent protein* and *Photosystem I P700*. Conversely, in the sensitive genotype, *protein kinase*, *peroxidas*e, and *the bidirectional sugar transporter SWEET* were significantly down-regulated. Some of the genes *Burp, laccase, lipase, BZIP, potassium transporter, protein kinase, peroxidase, and glutathione transferase* displayed distinct expression patterns across all combinations of HTG under control and stress conditions. Notably, *FAD-binding protein, xyloglucan endotransglucosylase/hydrolase*, and *BHLH* expression were positively regulated, indicating they were significantly more active in tolerant genotype's roots.

Genes such as *PEPC, chlorophyll a-b binding protein, cytochrome p450, fructose-bisphosphate aldolase, B-box zinc finger, ferredoxin–NADP reductase, PsbP, PSI, PSII, RNA helicase, Ring-CH-type domain-containing protein, MYB, sHsp17.0A, superoxide dismutase, stromal HSP70, thioredoxin, HSF protein, glutathione peroxidase, copper transporter*, and *CP12 domain-containing protein* conversely demonstrated suppression of transcription and notable decrease in the expression levels. Furthermore, *zeaxanthin epoxidase, zinc finger protein, RAP domain-containing protein, HATPase, GrpE protein, elongation factor*, and *catalase* expression were down-regulated several folds in the root tissues.

Functional annotation and pathways enrichment of expressed genes

GO enrichment analysis was conducted to identify and describe putative DEGs between tolerant and sensitive genotypes under heat stress. A complete set of all DEGs was aligned against the DAVID GO database, resulting in the classification of annotated genes to three fundamental GO components: cellular component (CC) and molecular functions (MF) biological process (BP). Annotated genes included 452 for 19 CC, 331 for 22 MF, and 251 for 36 BP. The most substantially over-represented GO terms for the up-regulated genes were chloroplast thylakoid membrane, heme binding, and hydrogen peroxide catabolic process in the CC, MF, and BP categories, respectively. Similarly, for down-regulated genes, chloroplast, peroxidase activity, and hydrogen peroxide catabolic process were prevalent in each component.

The GO classification of expressed genes in different tissue-specific categories for both genotypes is represented in Supplementary Figure S1. In the leaf, out of 2552 genes analyzed, 1259 were sorted into three functional categories: 610 in BP, accounting for 48.5%, 644 in CC, making up 51.2%, and 870 in MF, representing 69.1%. For root tissues, the analysis revealed that out of 3885 genes studied, 1628 were classified as follows: 777 (47.7%) in BP, 858 (52.7%) in CC, and 1100 (67.6%) in MF. While comparing leaf versus root categories with a total of 6879 genes, 2569 were distributed across three classes: 1218 (47.4%) in BP, 1361 (53%) in CC, and 1777 (69.2%) in MF.

In our study, KEGG analysis was used to assign biological pathways to the identified expressed genes. The comparative study of the tolerant and sensitive genotypes under both control and stressed conditions suggested a significant enrichment of genes that regulate metabolic and biosynthesis of secondary metabolites pathways. Under control conditions, the protein modification pathway in leaves and the carotenoid biosynthesis pathway in roots were enriched in the tolerant compared to the sensitive genotype. Under stressed conditions, tissue-specific differences in pathway enrichment were observed. In leaf tissues of the tolerant genotype, genes associated with photosynthesis, cysteine and methionine metabolism, and phenylpropanoid biosynthesis pathways were significantly enriched, whereas, in roots, the isoquinoline alkaloid biosynthesis pathway was enriched. When comparing control and stressed conditions within the tolerant genotype, genes involved in photosynthesis, linoleic acid metabolism, and carotenoid biosynthesis pathways were expressed in leaf tissues, while in roots, genes involved in the biosynthesis of amino acids and starch and sucrose metabolism pathways were expressed (Figure 2). The pathway enrichment analysis revealed that 1,172 of the expressed genes in the tolerant genotype were associated with 17 significant pathways. Additionally, metabolic pathways, biosynthesis of secondary metabolites, and photosynthetic pathways were highly enriched in both overexpressed and underexpressed genes (Figure 2). These findings provide valuable insights into the specific functions, processes, and pathways associated with the heat stress response in pearl millet.

We successfully annotated a subset of the DEGs, revealing valuable information about their molecular functions, biological processes, and cellular components. The analysis also highlighted the presence of significant number of 1906 uncharacterized proteins, indicating potential novel genes associated with the heat stress response in pearl millet. A considerable proportion of the 60 transcripts remained unannotated, highlighting the need for future investigations to unravel their roles and functions. The identification of a substantial number of DEGs across various comparisons underscores the significant impact of heat stress on gene expression. It highlights the intricate molecular mechanisms underlying the plant's response to heat stress.

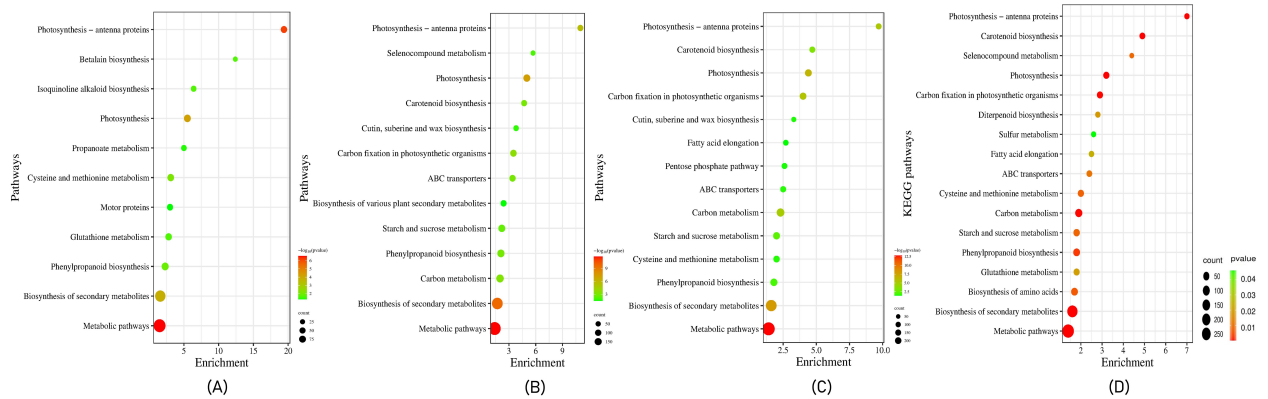

FIGURE 2
Biological pathways enrichment of the DEGs in **(A)** the leaves and roots of tolerant *vs* sensitive genotypes under heat stress conditions. **(B)** tolerant genotype leaf *vs* root **(C)** sensitive genotypes leaf *vs* root and **(D)** top 17 biological pathways enrichment of the DEGs in the leaves and roots of pearl millet genotypes under heat stress conditions. The size of the dot represents the number of the DEGs involved in each pathway. The color of the dot represents the p-value of each pathway; the pathways with p value ≤ 0.05 were significantly enriched pathways.

Enrichment analysis of TFs under heat stress

To better understand the molecular mechanisms underlying the response to heat stress in pearl millet, TF enrichment analysis was performed on DEGs from HTG and HSG under both control and stressed conditions. This analysis revealed several TF families with significant enrichment, suggesting their potential regulatory roles under heat stress. The top five enriched TFs and their associated GO terms from each comparison category are summarized in Table 3. The comparisons included HTG *vs* HSG under both control and stressed conditions, as well as HTG and HSG stressed *vs* control conditions.

The significantly enriched TF families included *bZIP, MYB, bHLH, G2-like*, and *NAC*. The *bZIP* family was prominently enriched across all comparisons. In the tolerant *vs* sensitive genotype under stress, the *bZIP* family had 48 target genes, with GO terms indicating its involvement in responses to abiotic stresses. Additionally, the G2-like family, with 39 target genes, along with *MYB* and *NAC* families, with 15 and 25 target genes respectively, were significantly enriched and predominantly found in the tolerant genotype under heat stress. These TFs are involved in various biological processes and molecular functions related to transcription regulation, abiotic stress responses, and developmental processes. These findings suggest the crucial role of these TF families in gene regulation under heat stress in pearl millet, offering valuable targets for further functional studies to elucidate their roles in stress response and plant development.

Network analysis of core heat stress-responsive genes: hub genes, functional enrichment, and molecular insights

The PPI network of core heat stress-responsive genes comprised 260 nodes and 3336 edges, forming two distinct clusters– one large and one small. The genes in the larger clusters were most significantly enriched in functions related to ribosomes, metabolic pathways, carbon metabolism and biosynthesis of secondary metabolites. The genes in smaller clusters were predominantly enriched in starch and sucrose metabolism along with metabolic pathways.

Key hub genes exhibiting high connectivity (degree >70) included *KOW domain-containing proteins*, various *ribosomal proteins* (such as *uS12, bL36*, and *bL17*), *S5 DRBM domain-containing proteins, elongation factor Tu (EF Tu)*, and several uncharacterized proteins. These hub genes interacted with other crucial proteins, such as *BAG domain-containing protein, Superoxide dismutase, PsbP domain-containing protein, HATPase_c, WRKY, ERF, Fes1 domain-containing protein, Pyruvate kinase, Acyl carrier protein, chlorophyll a-b binding protein, Thioredoxin domain-containing protein*, and *EF Ts*.

In this study, one notable hub gene, namely the *KOW domain-containing protein*, is a nuclear RNA binding protein essential for plants' innate immunity against various biotic and abiotic stresses (Aksaas et al., 2011). We observed 39 genes related to ribosomal proteins, including S5 DRBM domain-containing protein, exhibited high connectivity ranging from 32 to 91 degrees (Figure 3). The results indicated that heat stress caused detrimental effects on the expression of ribosomal proteins of the large subunit genes due to their decreased stability. Ribosomal proteins are involved in the selective synthesis of important proteins in response to heat stress. These ribosomal proteins modulate protein accumulation under stress conditions and their regulation reduces energy consumption.

Another significant hub gene, *EF Tu* with a degree of 71, is a highly conserved GTP-binding protein essential for translation in many species, including prokaryotes and eukaryotes (Xifeng et al., 2018). Studies in spring wheat showed its accumulation in response to heat stress, with higher levels correlating with improved heat tolerance (Bukovnik et al., 2009). Notably, the recombinant maize pre-EF-Tu was stable at 45°C and acted as a molecular chaperone, reserving protein stability under heat stress by preventing thermal protein aggregation (Rao et al., 2004).

10.3389/fpls.2024.1443681

TABLE 3 Enriched transcription factors in tolerant and sensitive genotypes under control and stress conditions.

Category	TF	Gene Input	Target Genes	p-value	q-value(BH)	Gene ontology
HTG *vs* HSG control	CPP	649	57	6.84E-04	1.65E-01	GO:0009934 regulation of meristem structural organization GO:0048444 floral organ morphogenesis GO:0051302 regulation of cell division GO:0005634 nucleus GO:0016021 integral component of membrane
	bZIP	649	27	1.85E-03	2.23E-01	GO:0045893 positive regulation of transcription, DNA-templated GO:0005634 nucleus GO:0003700 transcription factor activity, sequence-specific DNA binding GO:0043565 sequence-specific DNA binding
	MYB	649	20	3.00E-03	2.39E-01	GO:0006355 regulation of transcription, DNA-templated GO:0005634 nucleus GO:0003677 DNA binding
	GRAS	649	146	4.82E-03	2.39E-01	GO:0006355 regulation of transcription, DNA-templated GO:0009723 response to ethylene GO:0009737 response to abscisic acid GO:0009867 jasmonic acid mediated signaling pathway GO:0009938 negative regulation of gibberellic acid mediated signaling pathway GO:0010187 negative regulation of seed germination GO:0010218 response to far red light GO:0042176 regulation of protein catabolic process GO:0042538 hyperosmotic salinity response GO:2000033 regulation of seed dormancy process GO:2000377 regulation of reactive oxygen species metabolic process GO:0005634 nucleus GO:0003700 transcription factor activity, sequence-specific DNA binding GO:0044212 transcription regulatory region DNA binding
	bHLH	649	15	4.97E-03	2.39E-01	GO:0009637 response to blue light GO:0005634 nucleus GO:0046983 protein dimerization activity
HTG *vs* HSG stressed	bZIP	363	18	2.93E-03	4.69E-01	GO:0006355 regulation of transcription, DNA-templated GO:0009737 response to abscisic acid GO:0005829 cytosol GO:0003700 transcription factor activity, sequence-specific DNA binding GO:0043565 sequence-specific DNA binding GO:0044212 transcription regulatory region DNA binding
	bZIP	363	16	6.23E-03	4.69E-01	GO:0045893 positive regulation of transcription, DNA-templated GO:0005634 nucleus GO:0003700 transcription factor activity, sequence-specific DNA binding GO:0043565 sequence-specific DNA binding
	MYB	363	15	1.13E-02	4.69E-01	GO:0003677 DNA binding
	G2-like	363	14	2.77E-02	4.81E-01	GO:0006355 regulation of transcription, DNA-templated GO:0005634 nucleus GO:0003677 DNA binding
	bZIP	363	14	3.41E-02	5.07E-01	

(Continued)

TABLE 3 Continued

Category	TF	Gene Input	Target Genes	p-value	q-value(BH)	Gene ontology
						GO:0009409 response to cold GO:0009414 response to water deprivation GO:0009651 response to salt stress GO:0009737 response to abscisic acid GO:0009739 response to gibberellin GO:0010152 pollen maturation GO:0010187 negative regulation of seed germination GO:0010200 response to chitin GO:0045893 positive regulation of transcription, DNA-templated GO:0048316 seed development GO:0005634 nucleus GO:0003700 transcription factor activity, sequence-specific DNA binding GO:0043565 sequence-specific DNA binding
HTG stressed *vs* control	G2-like	483	25	3.52E-03	4.44E-01	GO:0006355 regulation of transcription, DNA-templated GO:0005634 nucleus GO:0003677 DNA binding
	bZIP	483	12	4.57E-03	4.44E-01	GO:0006355 regulation of transcription, DNA-templated GO:0003700 transcription factor activity, sequence-specific DNA binding GO:0043565 sequence-specific DNA binding
	NAC	483	15	5.84E-03	4.44E-01	GO:0006355 regulation of transcription, DNA-templated GO:0009753 response to jasmonic acid GO:0045995 regulation of embryonic development GO:0048317 seed morphogenesis GO:0080060 integument development GO:0005634 nucleus GO:0044212 transcription regulatory region DNA binding
	NAC	483	10	7.62E-03	4.44E-01	GO:0006355 regulation of transcription, DNA-templated GO:0010072 primary shoot apical meristem specification GO:0010160 formation of organ boundary GO:0010223 secondary shoot formation GO:0048366 leaf development GO:0048504 regulation of timing of organ formation GO:0005634 nucleus GO:0003677 DNA binding
	bHLH	483	11	1.32E-02	4.61E-01	GO:0009637 response to blue light GO:0005634 nucleus GO:0046983 protein dimerization activity
HSG stressed *vs* control	bZIP	338	9	8.06E-04	1.42E-01	GO:0006355 regulation of transcription, DNA-templated GO:0007231 osmosensory signaling pathway GO:0008272 sulfate transport GO:0009294 DNA mediated transformation GO:0009652 thigmotropism GO:0009970 cellular response to sulfate starvation GO:0045596 negative regulation of cell differentiation GO:0051170 nuclear import GO:0005634 nucleus GO:0005829 cytosol GO:0003682 chromatin binding GO:0003700 transcription factor activity, sequence-specific DNA binding GO:0043565 sequence-specific DNA binding

(Continued)

TABLE 3 Continued

Category	TF	Gene Input	Target Genes	p-value	q-value(BH)	Gene ontology
						GO:0043621 protein self-association GO:0051019 mitogen-activated protein kinase binding
	ARF	338	5	1.67E-03	1.42E-01	GO:0006355 regulation of transcription, DNA-templated GO:0009734 auxin-activated signaling pathway GO:0009908 flower development GO:0005634 nucleus GO:0003677 DNA binding GO:0005515 protein binding
	CPP	338	32	2.33E-03	1.42E-01	GO:0009934 regulation of meristem structural organization GO:0048444 floral organ morphogenesis GO:0051302 regulation of cell division GO:0005634 nucleus GO:0016021 integral component of membrane
	GRAS	338	83	2.41E-03	1.42E-01	GO:0006355 regulation of transcription, DNA-templated GO:0009723 response to ethylene GO:0009737 response to abscisic acid GO:0009867 jasmonic acid mediated signaling pathway GO:0009938 negative regulation of gibberellic acid mediated signaling pathway GO:0010187 negative regulation of seed germination GO:0010218 response to far red light GO:0042176 regulation of protein catabolic process GO:0042538 hyperosmotic salinity response GO:2000033 regulation of seed dormancy process GO:2000377 regulation of reactive oxygen species metabolic process GO:0005634 nucleus GO:0003700 transcription factor activity, sequence-specific DNA binding GO:0044212 transcription regulatory region DNA binding
	bZIP	338	16	3.08E-03	1.46E-01	GO:0045893 positive regulation of transcription, DNA-templated GO:0005634 nucleus GO:0003700 transcription factor activity, sequence-specific DNA binding GO:0043565 sequence-specific DNA binding

CPP, cystein-rich polycomb-like protein; bZIP, Basic leucine zipper; MYB, myeloblastosis viral oncogene homolog; G2-like, Golden2-Like; NAC, NAM, ATAF, and CUC; bHLH, basic/helix-loop-helix; ARF, Auxin response factors; and GRAS, Gibberellic acid; Repressor of GA and Scarecrow).

Genes associated with *HATPase*, photosynthesis, carbon metabolism and TFs including *WRKY* and *ERF* interacted with the hub genes. *BAG domain-containg protein*, recruited molecular chaperones using their domains under stress conditions to target proteins and changed their function by altering the protein conformation (Ding et al., 2020). BAG proteins regulate various physiological processes such as apoptosis, tumor induction, stress response and cell cycle. BAGs also regulate HSP chaperone proteins (positively or negatively) and form complexes with various transcription factors. At the transcriptional level, BAG family genes in plants have key roles in the PCD processes which range from growth, and tolerance to fungi to abiotic stress tolerance.

Comparative analysis of tolerant *vs* sensitive genotypes under heat stress conditions revealed a primary cluster and two sub-clusters, where hub genes in the primary cluster (degree >10) were predominantly associated with respiration and photosynthetic pathways. The two sub-clusters were enriched for transcription factors, such as NAC, and stress-responsive proteins, including small heat shock proteins (sHSPs). In the leaf *vs* root comparison of the tolerant genotype, hub genes identified were elongation factor Tu (EF Tu) with a degree of 53 and several uncharacterized ribosomal proteins. Conversely, in the sensitive genotype, hub genes comprised S5 DRBM domain-containing proteins, EF Tu, and other uncharacterized proteins, with degrees ranging from 20 to 42 (Figure 3). PPI network highlighted the intricate interplay among various proteins involved in the heat-stress response and explained potential mechanisms underlying heat tolerance in pearl millet.

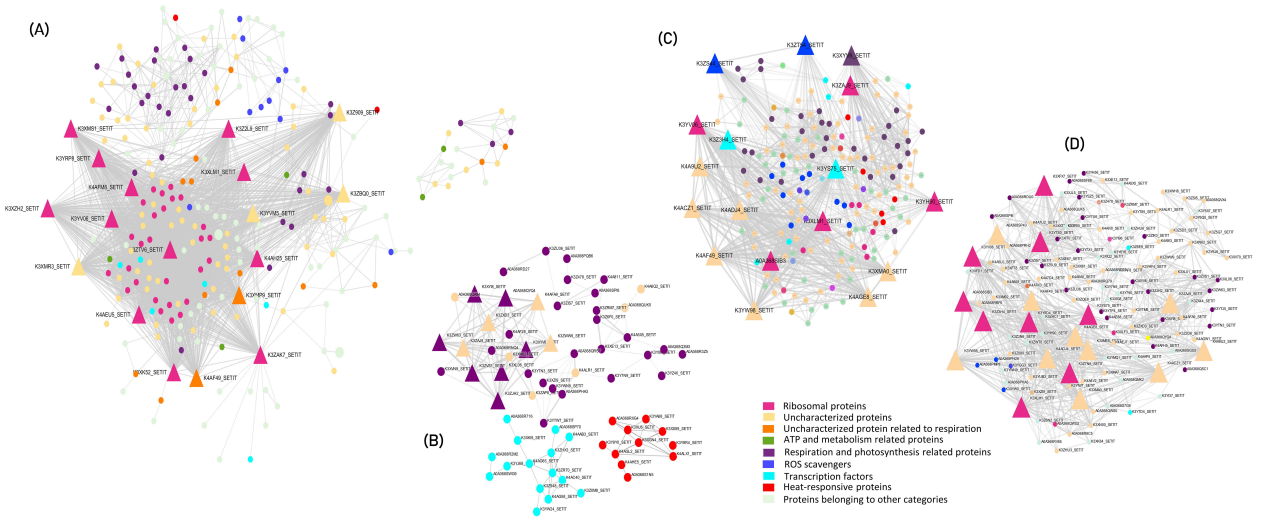

FIGURE 3
Protein-Protein Interaction network of **(A)** overall genes expressed in response to heat stress **(B)** DEGs in leaf and root of tolerant *vs* sensitive genotype **(C)** DEGs in the leaf *vs* root of tolerant genotype and **(D)** DEGs in the leaf *vs* root of sensitive genotype. Triangular nodes represent the hub genes identified and circular nodes represent the crucial genes involved in heat stress responsive mechanisms.

Unveiling the evolutionary significance of heat shock proteins and transcription factors across related crop species under heat stress

Our transcriptome results highlighted the crucial involvement of HSPs and TFs in the heat stress response of pearl millet. Therefore, 15 HSP and 179 TF-related genes identified in pearl millet were searched against rice, maize, proso millet, sorghum and foxtail millet genomes using BLAST for the identification of orthologous genes. Foxtail millet showed the maximum gene homology, sharing 11 HSP-related genes with pearl millet, followed by proso millet, rice, maize, and sorghum (Chandel et al., 2013; Nagaraju et al., 2015; Singh et al., 2016; Li and Howell, 2021; Barthakur and Bharadwaj, 2022). TF-related genes also showed maximum homology, with foxtail millet sharing 137 genes, followed by proso millet, sorghum, rice and maize (Chandel et al., 2013; Nagaraju et al., 2015; Singh et al., 2016; Li and Howell, 2021; Barthakur and Bharadwaj, 2022). Annotations were assigned to the identified orthologues to understand their functionality in the respective species.

Our analysis revealed that several genes had more than one orthologous sequence across different crops. Specifically, in proso millet, out of the total of 132 identified genes associated with TF, 109 genes had more than one ortholog sequence. Similarly, out of the 10 identified genes related to HSP, 7 genes had more than one ortholog sequence. (Figure 4). All crops except sorghum had 2 genes associated with HSP, while sorghum had only one gene with more than one ortholog. Rice, sorghum, foxtail millet, and maize had 48, 43, 45, and 58 TFs, respectively, had more than one ortholog sequence.

Foxtail millet showed the highest similarity to HSPs and TFs by capturing 13 and 184 ortholog sequences from 15 HSPs and 179 TFs, respectively (Figure 4). In proso millet, 18 ortholog sequences were identified for 10 HSPs. Out of these, 13 sequences showed more than 85% similarity and three sequences showed more than 70% similarity to pearl millet HSPs. Similarly, 285 ortholog sequences were identified for 132 TFs, of which 91 sequences showed more than 85% similarity and 81 sequences showed more than 70% similarity to pearl millet TFs.

In the study, it was found that Sorghum had nine ortholog sequences for eight HSPs. Out of these, six sequences showed more than 85% similarity and three sequences showed more than 70% similarity. On the other hand, 172 ortholog sequences were identified for TFs, of which 32 sequences showed more than 85% similarity and 44 sequences showed more than 70% similarity (Figure 4). The comparison between pearl millet and maize resulted in the identification of 11 ortholog sequences, which were mapped to nine genes related to HSP. Additionally, 205 ortholog sequences were detected for 125 genes related to TF. Our research explained the conservation and diversity of HSPs and TFs engaged in the response to heat stress among different crop species.

Discussion

Our results provide an understanding of the transcriptional responses of pearl millet to heat stress in leaf and root tissues. We discovered a total of 13,464 DEGs across all comparisons using comprehensive analysis, revealing the considerable influence of heat stress on gene expression patterns in different tissues of pearl millet. Figure 5 illustrates the expression pattern of DEGs across all the pairwise combinations of HTG and HSG.

Uniquely expressed genes and their regulation associated with photosynthesis and CO_2 assimilation

Photosynthesis, photochemical reactions, chlorophyll biosynthesis, NADPH and ATP synthesis, and respiration are all

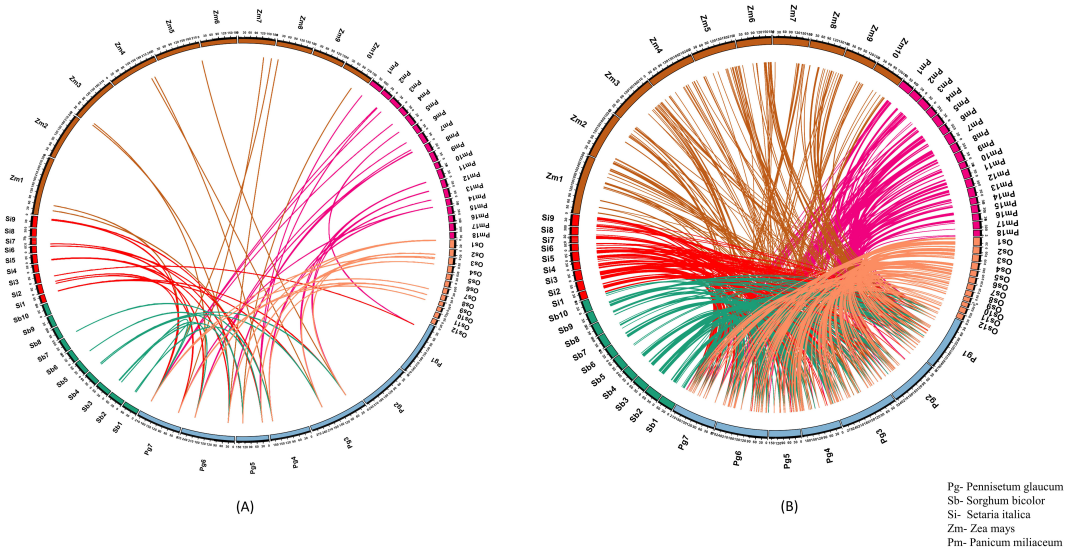

FIGURE 4
Comparative synteny plot demonstrating the orthologous genes related to **(A)** HSPs and **(B)** TFs in pearl millet to rice, maize, proso millet, sorghum and foxtail millet. The numeric values in the plot represent the chromosome number.

vital physiological processes in plants that help them adapt to heat stress. However, photosynthesis becomes susceptible at high temperatures, with its components, particularly PS II, being extremely sensitive (Ashraf and Harris, 2013). This susceptibility reduces photosynthetic efficiency, limiting plant development. Our study discovered 347 genes associated with respiration and photosynthesis pathways, including 90 uncharacterized proteins. Heat stress drastically reduced the expression of genes involved in CO_2 assimilation and photosynthesis in the sensitive than tolerant genotype (Figure 5).

Several vital genes involved in electron transport, chlorophyll production, and carbohydrate metabolism, including *chlorophyll-*

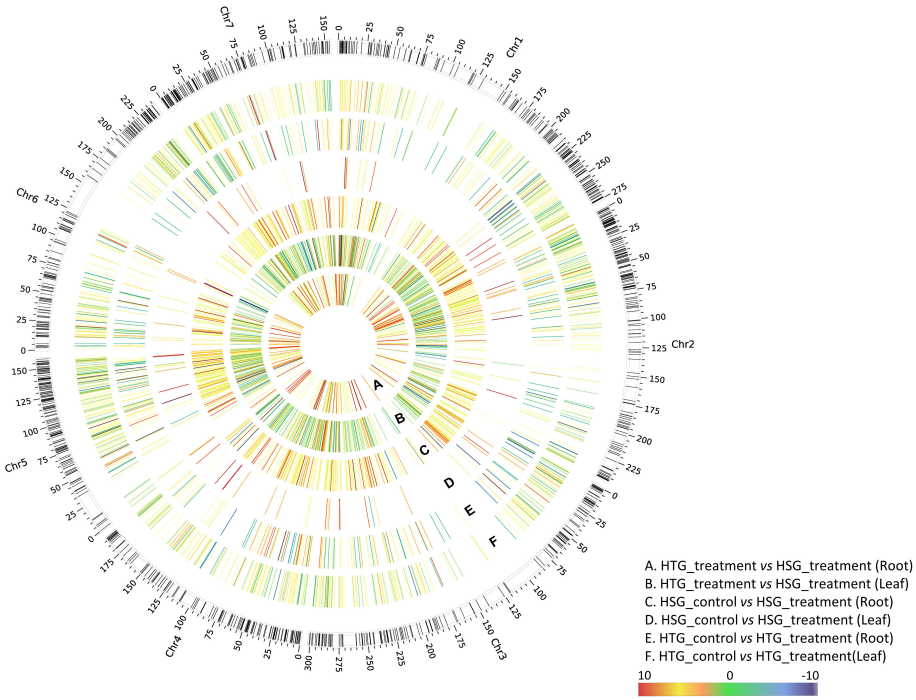

FIGURE 5
Circos plot represents differential expression pattern of heat-responsive genes in the HTG and HSG under control and treatment conditions. The outermost ring shows pearl millet chromosomes. The six rings namely, **(A–F)**, explain the expression pattern of genes across different pairwise comparisons of HTG and HSG.

binding a/b proteins, PS I and *PS II components, PsbP domain-containing protein, 2-hydroxy-acid oxidase, cytochrome P450, phosphoenolpyruvate carboxykinase (PEPC), phosphoglucomutase, stachyose synthase, phosphoribulokinase (PRK), malate dehydrogenase, phosphoglycerate kinase* and *ferredoxins*, were significantly more down-regulated under heat stress in the sensitive over the tolerant genotype (Table 4). Xu and Huang also reported that in response to drought, heat and combined stress, chlorophyll-binding proteins were down-regulated in both the tolerant and sensitive *Kentucky bluegrass* genotypes, but the level of expression in the tolerant was less suppressed than the sensitive genotype (Xu and Bingru, 2012).

Genes encoding *phytocyanins* are pivotal in facilitating electron transfer exhibited induced expression in treated heat-tolerant genotypes. This upregulation suggests a potential role for *phytocyanins* in aiding stress adaptation mechanisms. The *Rieske* protein of cytochrome b6/f complex is a component of the photosynthetic electron transport chain in the chloroplast and was induced in the leaves of *Pinellia ternate* under heat stress (Zhu et al., 2013). The leaves of HTG recorded *Rieske* protein down-regulation to 2 folds. In contrast, the HSG was suppressed to -11 folds, indicating that the tolerant genotype under stress conditions adapts by conserving energy to cope with the adverse effects.

Under heat stress conditions, a significant decrease in gene expression related to photosynthesis and respiration pathways was evident. This decline was more pronounced in the sensitive genotype compared to the tolerant genotype (Table 4). This disparity suggests a higher susceptibility of sensitive genotypes to heat stress, resulting in more pronounced transcriptional suppression and a consequent reduction in respiratory processes. Heat affects the production of ATP and NADPH from the light reactions, and these, in turn, significantly affect the photosynthetic enzymes such as *RuBisCO*, *carbonic anhydrase* and *PRK*. *ATP synthase* α *subunit* expression was over-expressed in HTG and suppressed in HSG, which aligns with a study on *T. aestivum*, where *ATP synthase* α *subunit* activity was reduced in heat-sensitive and increased in the tolerant genotype

TABLE 4 Expression pattern of selected differentially expressed genes operating in important functional pathways under heat stress.

Category	Gene	HTG_Control *vs* HTG_Treatment	HSG_Control *vs* HSG_Treatment	HTG_Treatment *vs* HSG_Treatment
Nutrient/water uptake	*Bidirectional sugar transporter SWEET*	4.28 $^{R/}$4.02^{L}	-4.48 ^{R}	4.28 ^{R}
	Potassium transporter	-2.03 ^{R}	-5.17 ^{R}	3.30 ^{R}
	Phosphate transporter	–	-4.58 ^{R}	–
	Glutamine synthetase	–	-3.92 ^{R}	–
	ABC transporter	4.50 ^{L}	-6.97 ^{L}	-5.12 ^{R}
	Copper transporter	-2.13 ^{L}	-5.48 ^{R}	3.03 ^{L}
	Nitrate reductase	–	-5.27 ^{R}	-4.70 ^{L}
Photosynthesis and CO2 assimilation	*Chlorophyll a-b binding protein*	-2.70 ^{R}	-12.79 ^{R}	8.23 ^{L}
	PS-I	-3.56 ^{L}	-12.57 ^{R}	3.36 ^{L}
	PS-II	-3.54 ^{L}	-9.22 ^{R}	2.95 ^{L}
	PsbP	-2.22 ^{L}	-7.82 ^{R}	2.77 ^{L}
	PEPC	-3.19 ^{R}	-12.73 ^{R}	3.01 ^{R}
	Glyceraldehyde-3-phosphate dehydrogenase	3.60 ^{L}	-9.64 ^{R}	-4.38 ^{R}
	Rieske domain-containing protein	-2.36 ^{L}	-11.53 ^{R}	5.16 ^{L}
	Phosphoribulokinase	–	-5.65 ^{R}	–
	Phytocyanin	3.39 ^{L}	-7.07 ^{L}	-6.51 ^{R}
	Carbonic anhydrase	-2.41 ^{L}	-8.22 ^{R}	7.04 ^{L}
	RuBisCO	-2.11 ^{R}	-12.05 ^{R}	2.19 ^{L}
	ATP synthase subunit alpha	3.99 ^{L}	-10.98 ^{L}	-2.13 ^{L}
	Fructose-bisphosphate aldolase	-2.61 ^{R}	-12.55 ^{R}	-3.27 ^{R}

(Continued)

10.3389/fpls.2024.1443681

TABLE 4 Continued

Category	Gene	HTG_Control *vs* HTG_Treatment	HSG_Control *vs* HSG_Treatment	HTG_Treatment *vs* HSG_Treatment
Secondary metabolites/ ubiquitination genes	*Terpene cyclase*	-2.45 ^{R}	-9.36 ^{R}	2.99 ^{L}
	Clp	2.73 ^{L}	-3.13 ^{R}	–
	RING-type E3 ubiquitin transferase	-2.81 ^{R}	-5.03 ^{R}	-2.22 ^{L}
	Lipoxygenase (LOX)	-2.24 ^{R}	-10.25 ^{R}	-8.58 ^{L}
	Glyoxalase	–	-4.05 ^{R}	–
	Lipase_3	-3.02 ^{L}	-10.32 ^{L}	-2.28 ^{L}
Signal transduction	*Protein kinase*	-2.43 ^{L}	-6.02 ^{L}	9.06 ^{L}
	MAPK	-2.21 ^{L}	-4.46 ^{R}	–
	AAI domain-containing protein	3.90 ^{R}	-11.95 ^{R}	-4.34 ^{L}
	ARF	3.19 ^{L}	–	2.83 ^{L}
	MFS	3.05 ^{L}	-6.24 ^{R}	7.95 ^{L}
	Cyclic nucleotide-gated ion channel	–	-3.14 ^{R}	–
	Trehalose 6-phosphate phosphatase	3.32 ^{L}	–	-3.43 ^{L}
ROS-Signaling	*POD*	3.62 ^{L}	-6.75 ^{L}	6.90 ^{L}
	CAT	-2.04 ^{L}	-4.69 ^{R}	3.11 ^{L}
	Amine oxidase	2.34 ^{L}	–	-3.24 ^{L}
	Thioredoxin	-2.59 ^{L}	-9.03 ^{R}	2.37 ^{L}
	Laccase	-2.05 ^{R}	-5.32 ^{L}	-7.41 ^{L}
Transcription Factors	*BHLH*	2.29 ^{L}	-5.95 ^{R}	7.95 ^{L}
	MYB	–	-6.96 ^{R}	3.67 ^{L}
	NAC	5.79 ^{L}	-5.59 ^{R}	2.96 ^{L}
	WRKY	3.02 ^{L}	–	6.02 ^{L}
Heat Shock proteins	*sHSPs*	8.73 ^{L}	-5.02 ^{R}	-3.65 ^{L}
	HSP70	-2.07 ^{R}	–	-4.57 ^{R}
	HATPase	9.72 ^{L}	2.24 ^{L}	–

L- expression in leaf; R- expression in root

(Wang et al., 2015). *Carbonic anhydrase* in *G. max* and *Agrostis species* was increased in the tolerant species than the sensitive ones under heat stress, suggesting it should play an important role in imparting tolerance (Xu and Huang, 2010; Das et al., 2016). Most of the genes involved in the photosynthesis process and CO_2 assimilation under stress showed high connectivity with the significant hub genes (Figure 3).

The enzymes that play a key role in carbon flux in the Calvin cycle and in determining carbon assimilation, such as *PRK, glyceraldehyde 3-phosphate dehydrogenase (GAPDH) and fructose-bisphosphate aldolase (FBPA)*, were more suppressed in sensitive genotype than HTG (Figure 6). Previous studies have demonstrated the same results: *PRK* in rice, *A. stolonifera* and *A. scabra, GAPDH* in *A. stolonifera*, and *A. scabra* and *FBPA* in *G. max* and *M. sinensis* were suppressed under heat stress. Most of the genes involved in glycolysis and in the TCA cycle were down-regulated under heat stress in HSG, resulting in reduced respiratory electron transfer and oxidative phosphorylation in the sensitive than in the tolerant genotype. Similarly, genes involved in the Calvin cycle were also suppressed in the sensitive genotype. The tolerant genotype displayed less suppression of the above-mentioned genes in their leaves under heat stress conditions, indicating that respiratory carbon metabolism is significantly less inhibited under stress. This differential gene expression pattern favors the tolerant genotype, potentially aiding their adaptation to heat stress.

This observation aligns with previous findings (Kurimoto et al., 2004) and suggests that the genes responsible for glycolysis, the Calvin cycle, and the TCA cycle exhibit a more

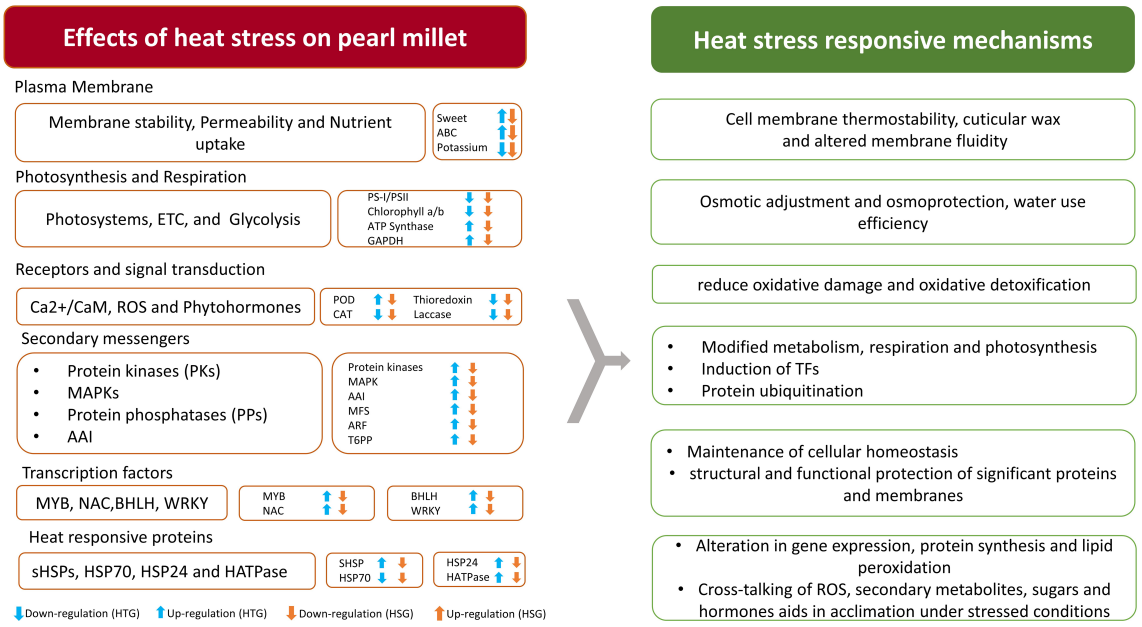

FIGURE 6
Elucidating the important genes operating in major pathways leading to heat stress tolerance in pearl millet.

resilient expression profile in the leaves of the tolerant genotype, contributing to their better adaptation to heat stress by conserving carbon resources. Reduction in respiratory and photosynthetic activity is correlated to a decrease in grain yield. At the cellular level, heat stress generates ROS that disrupt chloroplast membranes and the plasma membrane, leading to photosystem deactivation, reduced photosynthesis, and *RuBisCO* inactivation (Takahashi et al., 2007). This hampers the production and allocation of photo-assimilates, affecting grain's anthesis, filling, size, number, and maturity, ultimately reducing crop productivity. Genes associated with chloroplast, photosynthesis, photosystem II, plant-type cell wall, and chloroplast thylakoid membrane were considerably enriched based on GO enrichment.

Investigating the impacts of heat stress on nutrient and water uptake genes

Plant growth and development depend on adequate nutrient and water availability, primarily controlled by roots via mineral cycling and phytohormone signaling (Freschet et al., 2018; Kong et al., 2012). Heat stress dramatically impairs the synthesis of proteins involved in the uptake and transportation of nutrients. Our research discovered critical gene expressions that regulate amino acids, carbohydrates, and vital micronutrients (e.g., zinc, potassium, magnesium, boron) and macronutrients (e.g., phosphate, copper) transport across different parts of a plant (Fahad et al., 2017; Zelazny and Vert, 2014).

The *bidirectional sugar transporter SWEET* promotes carbohydrate transport across membranes, influencing plant resistance to osmotic stress (Darko et al., 2019). Klemens (2013) demonstrated that over-expression of *AtSWEET16* in *Arabidopsis* improved osmotic and cold tolerance (Klemens et al., 2013). The *SWEET* gene showed up-regulation in the leaf and root tissues of HTG. It is involved in the regulation of abiotic stresses such as drought and heat in different crops (Yuan and Wang, 2013). Sensitive genotype roots displayed diminished nutrient absorption under heat stress, associated with reduced expression of *phosphate transporter*, *bidirectional sugar transporter SWEET*, and *copper transporters* in contrast to their up-regulation under control conditions (Figure 6). Similarly, in the roots of HSG, *potassium transporters* and enzymes involved in nutritional assimilation, such as *nitrate reductase* and *glutamine synthetase*, exhibited suppressed expression under stress conditions (Table 4). Potassium fluxes are essentially required to regulate the transpiration process, so the down-regulation of potassium transporter may affect the plant's response to heat and oxidative stress (Mulet et al., 2023). Furthermore, *Rieske domain-containing proteins* (-11.5 FC) involved in metal ion binding and nitrate assimilation were significantly down-regulated, particularly in the heat-sensitive genotype (Molik et al., 2001).

The *ABC transporter domain-containing protein*, an integral membrane component involved in ATPase-coupled transmembrane transporter activity and ATP binding (Dahuja et al., 2021), was repressed in the roots of the heat-treated sensitive genotype and induced in the leaf of HTG. *ABC transporters* are involved in the regulation of various metabolisms, growth, development and environmental responses. ABC transporters in model plants such as *Arabidopsis* and rice have been identified to resist biotic and abiotic stress (Moon and Jung, 2014). The down-regulation of genes associated with nutrient uptake, primarily observed in the HSG combination, led to decreased nutrient uptake, resulting in reduced root and shoot biomass of sensitive than in tolerant genotype.

Aquaporin PIP2, a membrane channel protein in the roots of the tolerant genotype, contributed to ionic balance maintenance,

which is essential for water and solute transport, and showed enhanced expression, assisting heat tolerance by regulating water balance (Maurel et al., 2008; Giri et al., 2017). Previous studies suggested that PIPs have a role in modulating plant root's water intake and function in plant heat tolerance (Vandeleur et al., 2005). Obaid et al. (2016) discovered that over-expression of three AQP genes increased water utilization and induced heat tolerance in *Rhazya stricta* (Obaid et al., 2016). Efforts have been made over the last decade to understand the function of PIPs, and a few studies have demonstrated that PIP gene over-expression is favorable in imparting tolerance under heat-stress conditions. The GO study discovered novel genes involved in water channel function and cellular response to water scarcity, revealing the active engagement of diverse cellular components in nutrition and water intakes, such as chloroplast structures and sugar transporters. Kegg pathway analysis revealed that 39 genes participated significantly in carbon metabolism, aiding in combating heat stress by providing the energy required for the maintenance of metabolic and cellular responses.

Genotype-specific responses of secondary metabolites biosynthesis and protein ubiquitination pathways

Our findings revealed unique gene expression patterns associated with 19 pathways corresponding to tolerant and sensitive genotypes, spanning critical biological activities. Pathways involved in amino acid, carbohydrate, photosynthesis, glycan, lipid, phenyl-propanoid metabolism, protein ubiquitination, and secondary metabolite production were significantly enriched. Notably, genes implicated in protein ubiquitination/modification pathways in the tolerant genotype, including *caseinolytic protease (Clp)* and *ring type E3 ubiquitin transferase*, displayed induced expression in the tolerant than sensitive genotype. *Clp* are chaperones involved in protein disaggregation; these proteases are required to protect against oxidative stress (Pulido et al., 2017). The PPI network revealed 39 ribosomal proteins that interacted with the key genes involved in the cellular response to heat stress (Figure 3). The intricate network of interactions between ribosomal proteins and stress-responsive genes explains the complex mechanisms that plants use to adapt and thrive under stress conditions (Figure 6). These findings are congruent with earlier research emphasizing varying crop responses to heat stress. High-temperature treatment affects the physiological functions of ER, hence affecting the protein's synthesis, modification and proper folding.

Stress-modulated lipid metabolism, with *lipoxygenase* (LOX), *lipase_3, lipase_GDSL domain-containing* and *patatin* enzymes were significantly more down-regulated in sensitive genotypes, indicating repressed lipid metabolic pathways (Table 4). *LOX* is documented in several crops to catalyze the synthesis of plant's defense-related *9(S)-hydroperoxy-octa-deca-trienoic acid* (Göbel et al., 2001). In research on tomato seedlings, increased lipoxygenase activity was correlated with salt tolerance, and in pepper, the *CaLOX1* gene was reported to modulate the abiotic stress responses via activation of defense-related marker genes and scavenging of ROS (Lim et al., 2015). *Lipase_GDSL* plays an important role in plants' defensive mechanism. For example, *AtLTL1* encoding *lipase_GDSL* in *Arabidopsis* was recorded to enhance salt tolerance (Naranjo et al., 2006).

Secondary metabolites have multifaceted roles in plant-environment interactions and provide pigmentation to various plant parts. However, *terpene cyclase, terpene synthase*, involved in the synthesis of metabolites that assist in the regulation of homeostasis and plant's response to biotic and abiotic stress and *glyoxalase*, important in secondary metabolite biosynthesis, displayed less suppression in tolerant genotype while experiencing significant more down-regulation in sensitive genotype (Pérez-Llorca et al., 2023). Secondary metabolites in some plants function as osmolytes and growth precursors to help plants recover from heat stress.

Phenylpropanoids play a crucial role in lignin synthesis, particularly under high temperatures. This observation suggests a modulation in the production of compounds responsible for lignin synthesis, a key aspect of plant stress response, in the heat-tolerant genotype. The decrease in secondary metabolite biosynthesis in tolerant genotype at high temperatures might signify a strategic energy conservation response under high-temperature conditions. These changes in gene expression related to secondary metabolites and protein ubiquitination pathways point to a nuanced adaptive response to heat stress. These alterations emphasize the genotype-dependent regulation of significant stress adaptation pathways in pearl millet, reflecting the diverse strategies employed by different genotypes in coping with heat stress conditions. Kegg pathways represent the involvement of 180 genes in the biosynthesis of secondary metabolites which includes *3-ketoacyl-CoA synthase* displaying up-regulation and down-regulation in the control *vs* treatment comparison of tolerant and sensitive genotype, respectively.

Increased temperature alters gene expression in signal transduction pathways

Elevated temperatures promote significant changes in gene expression within signal transduction pathways in plants, particularly when subjected to abiotic stress such as heat. These changes activate sophisticated regulatory networks, which trigger innate defense mechanisms. *Protein kinases*, particularly *MAPKs*, are important in orchestrating physiological adaptations by transducing environmental stimuli to the nucleus, thereby protecting plants from diverse biotic and abiotic stresses (Morrison, 2012). Furthermore, the *Cysteine-rich receptor-like protein*, a member of the RLK family, is involved in plant immunology, stress response, and growth and development (Tanaka et al., 2012). Importantly, elevated temperatures cause an increase in calcium influx, which is one of the first cellular alterations that occurs after a heat shock.

In this study, we found a significant down-regulation of genes encoding *MAPK*, *protein kinase* (-5.7 to -10.2 times), *ABC1 domain-containing protein* associated with protein kinase activity, *calmodulin-binding protein 60*, and *cysteine-rich receptor-like protein* in the sensitive genotype (Table 4). Heat stress triggers

the *MAPK* signaling cascades in the plant system. *MAPK* is a master regulator that operates various physiological and cellular activities in response to heat stress. In *wheat*, *MAPK* triggers different genes that impart heat tolerance under terminal heat stress (Banerjee et al., 2020). This evidence indicates that heat stress has a more adverse impact on the expression of signaling genes in sensitive genotypes.

Integral membrane proteins, particularly *ABC transporter proteins* that use ATP as energy source, displayed reduced expression in most combinations except in tolerant genotype under stress conditions (Figure 6). However, membrane transport protein-encoding *MFS (Major facilitator superfamily)* genes, which facilitate compound transport across cell membranes using electrochemical gradients, were more down-regulated in various HSG combinations than in HTG, implying potential disruptions in membrane transport functions within leaves and subsequent effects on distinct cellular activities (Niño-González et al., 2019).

Further, *cyclic nucleotide-gated ion channels (CNGCs)*, which are involved in calcium signal transduction, expression was repressed in the roots of the heat-sensitive plants under stress, similar to the findings in *Arabidopsis* (Alqurashi et al., 2016). This down-regulation is consistent with previous findings in *Arabidopsis* seedlings, implying a negative impact on thermo-tolerance by increasing ROS enzyme activity (Gao et al., 2012). Additionally, the observed suppression of gene expression for *trehalose 6 phosphate phosphatase (T6PP)* in sensitive genotype under stress conditions suggests a plausible reduction in trehalose levels induced by heat stress, potentially disrupting carbohydrate transport mechanisms critical for stress tolerance (Lunn et al., 2006; Ruan, 2014). The tolerant genotype displayed induced expression of *T6PP* in leaf compared to HSG. *T6PP* acts as a sugar signal and induces the expression of genes associated with stress injury (Lyu et al., 2018).

Plant growth regulators, also known as phytohormones, are essential in reacting to abiotic stress, particularly heat stress. Recent studies reveal that hormones such as auxin, cytokinin, ethylene, and abscisic acid (ABA) are actively implicated in heat response. *ABA*, a crucial stress-related hormone, and its association with the up-regulation of *AAI (an abscisic acid-inducible protein)* across the combinations of the tolerant genotype imply its potential involvement in conferring heat stress tolerance (Table 4). ABA boosts tolerance by regulating the transcript level of HSPs and engaging in spatial and temporal interactions with ROS (Suzuki et al., 2016). *Auxin*, responsible for cell wall synthesis and nucleic acid metabolism, activates multiple genes involved in auxin-mediated signaling pathways, including *ARF, auxin efflux carriers*, and *short auxin-up RNA (SAUR)* (Fenqi et al., 2023). The research discovered a two-fold increase in *ARF* gene expression in the stressed leaves of the tolerant genotype. In the heat-sensitive genotype, the *SAUR 36* gene, which is related to leaf senescence and cell elongation suppression, was down-regulated (Jia et al., 2020).

Earlier findings revealed complex interactions between ethylene, ABA, and brassinosteroids in regulating heat stress responses. We identified the activation of *CASP* proteins and 19 undiscovered proteins associated with the brassinosteroids signaling pathway. Heat stress decreases cytokinin synthesis, influencing cell division and elongation, with down-regulation recorded in genes involved in cytokinin biosynthesis and *zeaxanthin epoxidase*, a key player in hormone synthesis (Hoang et al., 2020). The suppression was more pronounced in sensitive genotype under heat stress. These findings suggest that the tolerant genotype employs distinct adaptive mechanisms in response to heat stress compared to the sensitive genotype.

ROS scavenging: a key pathway for modulating heat stress response mechanisms

When exposed to high temperatures, plants overproduce ROS, a pivotal signaling component that causes oxidative stress by destroying the cell structure, particularly the membrane structure (Slimen et al., 2014). Plants have ROS scavenging strategies to mitigate the damage, essential for cellular recovery and redox equilibrium (Kotak et al., 2007). In this study, we noticed differences in the expression of ROS-scavenging enzymes in response to heat stress in both genotypes.

Several ROS scavenging genes namely, *superoxide dismutase (SOD), ascorbate peroxidase (APX), catalase (CAT), peroxidase (PRX), glutathione peroxidase (GPX), amine oxidase, amino oxidase, respiratory burst oxidase, thioredoxin, and glutaredoxin* activated under the stress condition (Figure 6**).** We discovered 52 *peroxidase-related* genes involved in suberin and lignin synthesis, stomatal closure control, and stress-induced heat shock protein (HSP) expression (Havaux, 1993). This enzyme is involved in scavenging ROS, which are produced in response to heat stress. *Peroxidase* gene expression was significantly suppressed in the HSG treated conditions, and in the leaf of tolerant genotype under stress, it displayed induced expression (Table 4). In the roots, *SOD*, which is important for dismutating superoxide radicals (O_{2^-}) into oxygen (O_2) and hydrogen peroxide (H_2O_2) and thereby preserving photosynthetic organelles, was down-regulated in HSG under stress (Zang et al., 2020). Over-expression of *SOD* in *Avicennia marina* and *Alfalfa* confers tolerance to abiotic stress (Rubio et al., 2002; Prashanth et al., 2008).

Amine oxidase, involved in quinone binding and amine metabolism, influences plant responses to environmental stress and demonstrated induced expression patterns across tolerant genotype combinations (Gholizadeh and Mirzaghaderi, 2020). *APX*, which regulates hydrogen peroxide levels under heat and oxidative stress, displayed varying expression patterns across the tissues in both genotypes. The expression of *APX* in *Arabidopsis* resulted in chloroplast protection during heat stress (Panchuk et al., 2002). DEGs encoding *APX* were primarily more down-regulated in the sensitive than the tolerant genotype, indicating that in response to heat stress, HTG over-produced ROS, resulting in increased APX activity. The down-regulation of these genes suggests a possible disruption of metabolic adjustments in the leaf and roots of *pearl millet* under heat stress, primarily in the sensitive genotype.

Genes related to ROS detoxification, including *thioredoxin* involved in ROS signaling, *respiratory burst oxidase*, *CAT, GPX*, and *laccase*, which contributes to oxidoreductase activity in the

apoplast, displayed down-regulation predominantly in the sensitive genotype under stress conditions (Mittler, 2017). This down-regulation indicates heightened oxidative stress in sensitive genotypes. In contrast, the tolerant genotype exhibited reduced oxidative stress despite the down-regulation of these genes. This observation aligns with recent studies that reported decreased expression of ROS-scavenging genes under heat stress. GO demonstrated a significant representation of 60 oxidative stress-related genes in the category of oxidoreductase activity, highlighting the importance of ROS buildup on plant responses.

Role of transcription factors in heat stress resilience

TFs are essential in regulating transcriptional responses to heat stress, and various TFs implicated in heat stress acclimation were found in multiple crops. Previous studies have reported the differences in the expression of different TF families, including *WRKY, NAC, AP2/ERF, MYB, EF, GATA, bZIP, MADS-box, DEAD-box ATP-dependent RNA helicase, zinc finger protein, C2H2*, and *C3H domain-containing protein*, highlighting their role in the heat stress response (Ward and Schroeder, 1994; Seki et al., 2003). Figure 7 represents the expression of different TFs across the combinations of HTG and HSG. Among the identified TFs, *MYB*, a significant player in chromosomal structure and stress interactions and is involved in the biosynthesis of secondary metabolites, exhibited distinct expression patterns (Samad et al., 2017). El-Kereamy et al., 2012 found that heat stress triggered the activation of *OsMYB55* (El-Kereamy et al., 2012). Overexpressing *OsMYB55* alleviated the adverse effects of high temperatures on grain yield by enhancing amino acid metabolism and improving rice's heat stress tolerance. Seventeen differentially expressed *MYB* genes displayed reduced activity (Table 4) primarily in leaf and root tissues of the sensitive genotype, but upregulation in the tolerant genotype, indicating a vital function in regulating transcription under heat stress conditions (Chakraborty et al., 2022).

The *C2H2* TF family and a single *C3H* gene, implicated in growth, development, and abiotic stress responses, showed different expression profiles (Thirunavukkarasu et al., 2017; Hu et al., 2019). *WRKY, NAC, AP2/ERF*, *BHLH* and *BURP* genes were significantly up-regulated in the tissues of the tolerant genotype (Table 3). In contrast, the expression of *bZIP, MADS-box, BHLH, DEAD-box ATP-dependent RNA helicase, EF*, and *zinc finger* proteins were drastically reduced in sensitive genotype leaf and root tissues. The role of *WRKY* in regulating gene expression during heat and drought stress is consistent with our findings, indicating their potential for improving heat stress tolerance in *Arabidopsis* and *rice* (Wu et al., 2009; He et al., 2016). Similarly, enhanced expression of *NAC* and *AP2/ERF* in the tolerant genotype supports the finding of the earlier research demonstrating their significance in imparting tolerance to multiple abiotic stresses across many crops (Sakuma et al., 2002; Nakano et al., 2006; Shiriga et al., 2014). The *AP2/ERF* family, comprising plant-specific TFs, possesses a conserved DNA-binding domain. This family contains DRE-binding proteins that activate stress-responsive genes by specifically binding to the dehydration-responsive element/C-repeat (DRE/CRT) in gene promoters (Sakuma et al., 2002; Nakano et al., 2006). The *AP2-ERF* super-family significantly influences plant growth, development, hormonal regulation, and responses to diverse environmental stresses, notably heat stress (Mizoi et al., 2012). *SNAC3* in rice enhances the tolerance to heat and drought stress by modulating the ROS balance (Xi et al., 2022). A study on *switchgrass* showed that *DEAD-box ATP-dependent RNA helicases* may function as RNA chaperons (Li et al., 2013).

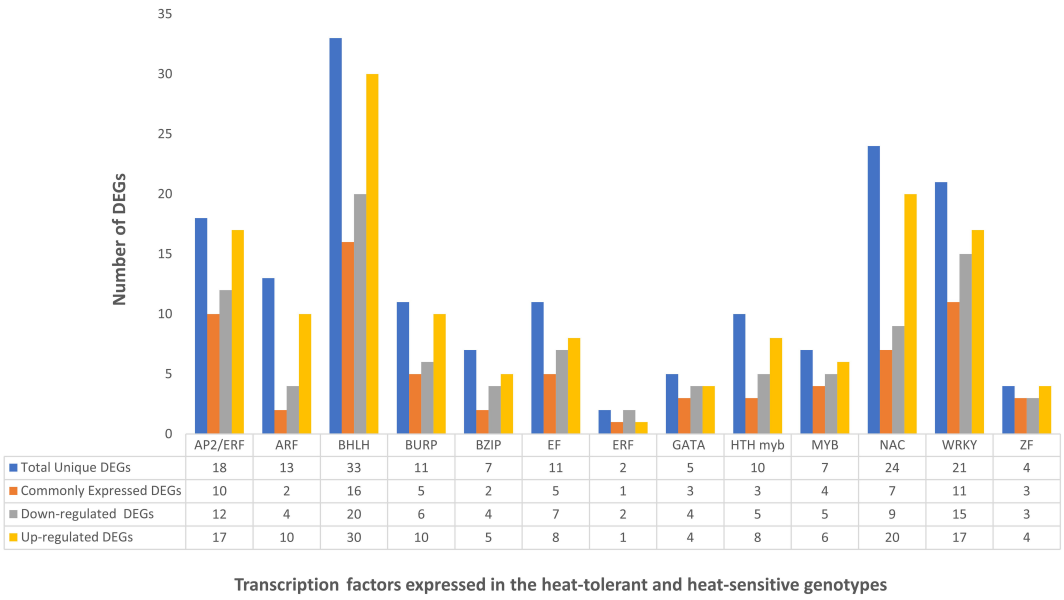

	AP2/ERF	ARF	BHLH	BURP	BZIP	EF	ERF	GATA	HTH myb	MYB	NAC	WRKY	ZF
Total Unique DEGs	18	13	33	11	7	11	2	5	10	7	24	21	4
Commonly Expressed DEGs	10	2	16	5	2	5	1	3	3	4	7	11	3
Down-regulated DEGs	12	4	20	6	4	7	2	4	5	5	9	15	3
Up-regulated DEGs	17	10	30	10	5	8	1	4	8	6	20	17	4

FIGURE 7
Expression of important transcription factors in the leaf and root tissues of heat-tolerant and heat-sensitive genotypes.

Moreover, the over-expression of *BURP* in the leaf of tolerant genotypes implies their participation in plant hormone signaling and adaptation to environmental stressors (Shu et al., 2018). In alignment with previous research, the down-regulation of *bZIP* and *zinc finger* protein expression in sensitive genotypes indicates that heat stress has a negative impact on growth and many signaling pathways. In the reproductive stage of *Arabidopsis*, *bZIP* regulates heat tolerance (Gao et al., 2022). *BHLH* play diverse roles in plant development and stress responses. The significant inhibition of *BHLH* gene expression in sensitive genotype's leaf and root tissues suggested that it plays an essential role in regulatory networks responding to heat stress. Studies revealing the drought-responsive behavior of *bHLH* genes, such as *MdbHLH130* in apples, and their participation in strengthening plant resistance highlight their potential significance in heat stress response pathways (Guo et al., 2021).

A study conducted on foxtail millet reveals the involvement of numerous *bHLH* genes in promoting drought tolerance, and *Fe2OG dioxygenases* are involved in various metabolic processes (Wang et al., 2018). Enrichment analysis of the TFs revealed that the TF-associated GO terms provide valuable insights into the underlying regulatory mechanisms and offer targets for further functional studies to elucidate their specific roles in plant stress response and development. Our research highlighted the conservation and diversity of TFs involved in heat stress response across various crops, and found that the foxtail millet is closely related to pearl millet TFs (Figure 4). The differential expression of TFs in both genotypes' leaf and root tissues suggests that they play an important role in regulatory pathways and transcriptome reconfiguration during heat stress in pearl millet. It implies that these TFs have a complicated interplay in the plant's response to heat stress, necessitating additional research into their precise regulatory roles.

The elevated response of heat shock proteins and heat shock factors in pearl millet under stressed conditions

Heat stress affects plant cell membrane integrity, alters protein structure, causes misfolding of native proteins, and promotes the accumulation of aberrant proteins. Plants have evolved different defense mechanisms in response to heat stress, including generating heat stress factors critical in regulating HSPs (Mittler et al., 2012). These HSPs function as molecular chaperones essential for maintaining cellular homeostasis. Several heat-related genes (Figure 6), including *HSP70, HSP24, HSP10kDa, sHsp17.6, sHSP domain-containing protein, sHsp17.0, HSF domain-containing protein*, and *HATPase_c domain-containing protein* were over-expressed. Figure 8 represents the expression pattern of HSPs and TFs across the pairwise comparisons of HTG and HSG. When exposed to heat, pearl millet synthesize stress proteins, specifically HSPs, which act as molecular chaperones, promoting protein folding and structural stability (Mukesh Sankar et al., 2021).

Our findings revealed significant up-regulation of *sHsp17.0, sHsp17.6, and sHSP* domain-containing proteins in the leaf and roots of the tolerant genotype (Table 4). The expression of *sHsp17.0* was prominently observed in root tissues of HTG under stressed conditions, and sHsp17.0 exhibited significant up-regulation in roots of treated conditions in the tolerant genotype (Figure 8). Several studies in *Arabidopsis, P. pastoris*, and woody plants have demonstrated that sHSPs confer heat and drought tolerance (Yang et al., 2017; Wang et al., 2017). Additionally, *sHSP* domain-containing proteins displayed up-regulation in the leaf and root tissues of HTG. The enhanced activity of HSP70, which is prevalent under stress, was significant, with *70kDa stromal HSPs* expressing in both HSG and HTG roots under stress, indicating a more significant transcriptional response in roots compared to leaves.

Stromal 70kDa HSP participates in transport pathways between the endoplasmic reticulum, mitochondria, and chloroplastic pre-protein intake. According to previous research on various plants, including *Hevea brasiliensis*, rice, tobacco, and wheat, *HSP70* plays an important role for cellular response to heat stress (Zhang et al., 2009; Wang et al., 2016; Wahab et al., 2020). HSPs in pearl millet, particularly *HSP70* and *HSP90*, have been studied for their role in heat and drought adaptation processes (Donald et al., 2015). It has been found that *HSP70* is involved in molecular chaperone activity under stress and plays a function in photo-protection and photosystem II repair (Schroda et al., 1999; Sung et al., 2001). *HATPase*, a member of the *HSP90* family, showed over-expression in tolerant genotype combinations, signifying its function in ATP binding and *ATPase* activity (Figure 8). Five genes related to *HATPase* were identified in soybean and rice, with the majority exhibiting up-regulation in the tolerant genotype combination (Schroda et al., 1999; Sung et al., 2001; Li et al., 2020). A comparative analysis of genes related to HSPs in pearl millet revealed orthologue sequences in rice, foxtail millet, sorghum, proso millet, and maize (Figure 4). This suggests that these genes are expressed in response to stress in various crops. The prevalence of HSPs, especially across HTG genotype combinations, highlights their crucial role in maintaining protein structure, ATP binding, and hydrolysis in response to heat stress and raising heat stress tolerance.

HSPs and heat-related genes are also regulated by heat shock transcription factors (HSFs), which orchestrate the plant's response to heat stress (Guo et al., 2016). Our findings revealed that HSF-related genes were up-regulated in tolerant genotypes and down-regulated in sensitive cultivars. Zhu et al., 2006 showed that over-expression of *GmHSFA1* in soybeans confers thermo-tolerance, possibly due to the activation of *sHSP and HSP70* (Zhu et al., 2006). This implies that they play an important role in tolerant genotype survival under heat-stress conditions. The PPI network reveals that the expression of HSP is related to different important TFs and HSF in response to heat stress (Figure 3). The prominent expression of HSPs and HSF-related genes in the tolerant genotype emphasizes their critical engagement in cellular and molecular processes during heat stress, which aligns with recent research across many crops. The pattern of HSP expression in pearl millet under stress conditions supports previous research on heat-induced HSPs, emphasizing their critical role in plants' response to heat stress.

Our research revealed substantial differences in the expression of genes involved in various physiological and biochemical processes, specifically in the tolerant genotype. We found significant differences in the expression of genes crucial in water, nutrient, and ion transport

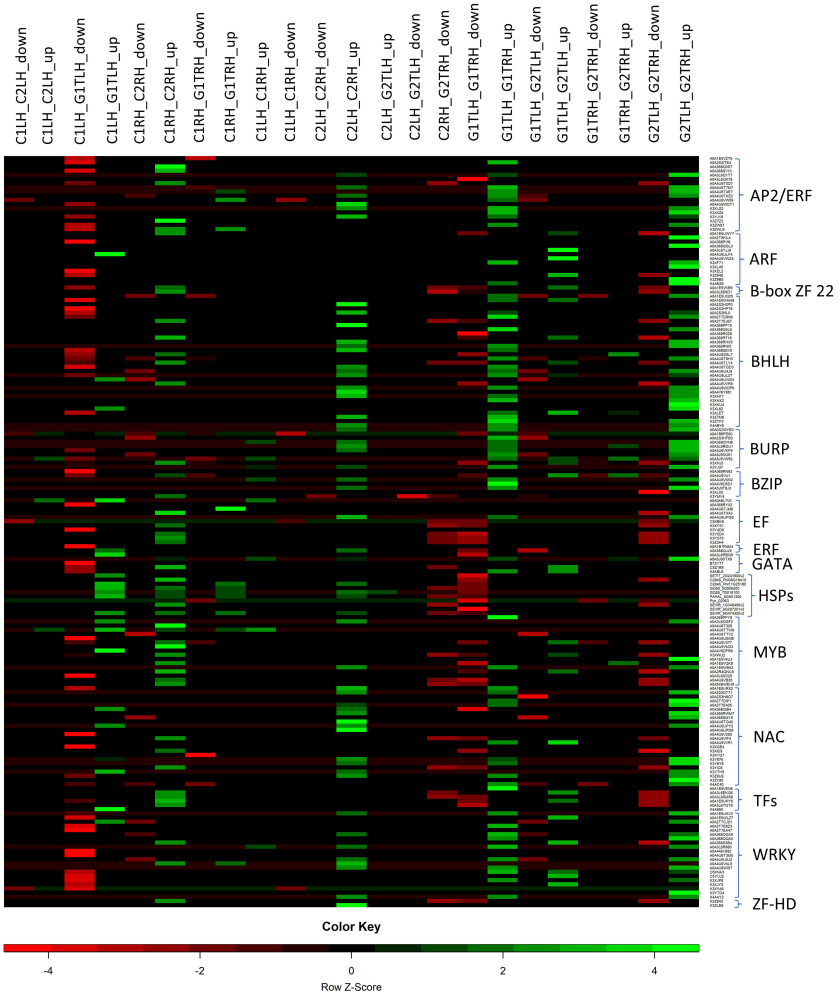

FIGURE 8
Heatmap of the selected TFs and HSPs operating under control and heat stress conditions in leaf, root and between leaf and root combinations of HTG and HSG. C1 and G1: HTG control and treatment conditions, C2 and G2: HSG control and treatment conditions, LH: leaf and RH: root, up: up-regulation and down: down-regulation.

(*bidirectional sugar transporter SWEET*, *ABC transporter domain-containing protein, PIP, potassium transporters*, *nitrate reductase* and *glutamine synthetase)*, cell wall maintenance (*expansin)*, photosynthesis (*RuBisCO*, *carbonic anhydrase* and *ATP synthase* α *subunit)*, transcription factors (*BZIP, BHLH, MYB, AP2/ERF, and BURP)*, signal transduction (*protein kinases, MAPK, ABA*, and *AAI)*, ROS scavenging (*SOD, peroxidases, GPX, and amine oxidase)*, HSPs (*SHSPs, HATPase, and HSP 10kDa)*, secondary metabolite biosynthesis (*LOX, Lipase_GDSL*, *terpene cyclase, terpene synthase*, and *3-ketoacyl-CoA synthase)* and protein modification pathways (*Clp* and *ring type E3 ubiquitin transferase)*, implying that pearl millet regulates the synthesis and expression of these genes to survive under heat stress.

Conclusions

A genome-wide transcriptome study was performed in two pearl millet genotypes (HTG and HSG) to examine the molecular mechanisms in response to heat stress. We comprehensively analyzed the leaf and root samples in three categories: between genotypes, within genotypes, and between tissues. These DEGs from pairwise comparisons of the treated and control samples provide substantial insight into the effects of heat stress on pearl millet.

The analysis of heat-responsive genes and hub genes revealed that protein processing in the endoplasmic reticulum is one of the critical pathways involved in heat stress. The protective impact of HSPs could be related to the chaperone mechanism network, in which multiple chaperones work together. Under stress, many structural proteins undergo adverse structural and functional modifications. As a result, refolding of denatured proteins and maintaining their function is crucial for cell survival in stress conditions. These findings could help in our understanding of the role of the genes implicated in heat tolerance.

We discovered a significant number of DEGs belonging to uncharacterized proteins, revealing possible new genes involved in

heat stress response in pearl millet. Our study provides fresh insights into the transcriptional modifications in different tissues of tolerant and sensitive genotypes, which aids in decoding the underlying mechanism to enhance crop resilience. This study will set the groundwork for identifying and utilizing key genes that are explicitly expressed in tissues to investigate the mechanisms of heat stress tolerance in pearl millet. These genes will also serve as appropriate molecular indicators for screening accessions for heat tolerance and speed up the variety of development programs in pearl millet and similar millet crops.

Data availability statement

The data presented in the study are deposited in the NCBI Sequence Read Archive database with accession number PRJNA1062049.

Author contributions

SS: Writing – review & editing, Writing – original draft, Visualization, Validation, Software, Resources, Methodology, Investigation, Formal analysis, Data curation, Conceptualization. AV: Writing – review & editing, Methodology. AC: Writing – review & editing, Data curation. NN: Writing – review & editing, Data curation. RM: Writing – review & editing, Resources. JJ: Writing – review & editing, Methodology. SM: Writing – review & editing, Visualization. TC: Writing – review & editing. NT: Writing – review & editing, Supervision, Funding acquisition, Conceptualization.

Funding

The author(s) declare that financial support was received for the research, authorship, and/or publication of this article. The experiment was funded by the Bill and Melinda Gates Foundation project (*INV-008187*), the ICAR-Indian Institute of Millets Research project (*CI/2018-23/120) and the Global Centre of Excellence on Millets (Shree Anna)*.

Conflict of interest

The authors declare that the research was conducted in the absence of any commercial or financial relationships that could be construed as a potential conflict of interest.

Publisher's note

Supplementary material

The Supplementary Material for this article can be found online at: https://www.frontiersin.org/articles/10.3389/fpls.2024.1443681/full#supplementary-material

References

Aksaas, K., Larsen, A. A. C. V., Rogne, M., Rosendal, K., Kvissel, A.-K., and Skålhegg, BjørnS. (2011). G-patch domain and KOW motifs-containing protein, GPKOW; a nuclear RNA-binding protein regulated by protein kinase A. *J. Mol. Signaling* 6, 1–14. doi: 10.1186/1750-2187-6-10

Alqurashi, M., Gehring, C., and Marondedze, C. (2016). Changes in the *Arabidopsis thaliana* proteome implicate cAMP in biotic and abiotic stress responses and changes in energy metabolism. *Int. J. Mol. Sci.* 17, 852. doi: 10.3390/ijms17060852

Ashraf, M., and Hafeez, M. (2004). Thermotolerance of pearl millet and maize at early growth stages: growth and nutrient relations. *Biol. Plantarum* 48, 81–86. doi: 10.1023/B:BIOP.0000024279.44013.61

Ashraf, M. H. P. J. C., and Harris, P. J. C. (2013). Photosynthesis under stressful environments: An overview. *Photosynthetica* 51, 163–190. doi: 10.1007/s11099-013-0021-6

Banerjee, G., Singh, D., and Sinha, A. K. (2020). Plant cell cycle regulators: Mitogen-activated protein kinase, a new regulating switch? *Plant Sci.* 294, 110660. doi: 10.1016/j.plantsci.2020.110660

Barthakur, S., and Bharadwaj, N. (2022). "Exploring genome-wide analysis of heat shock proteins (HSPs) in small millets as potential candidates for development of multistress tolerant crop plants," in *Omics of Climate Resilient Small Millets* (Singapore: Springer Nature Singapore), 337–355. doi: 10.1007/978-981-19-3907-5_17

Bolger, A. M., Lohse, M., and Usadel, B. (2014). Trimmomatic: a flexible trimmer for Illumina sequence data. *Bioinformatics* 30, 2114–2120. doi: 10.1093/bioinformatics/btu170

Bukovnik, Urška, Fu, J., Bennett, M., Prasad, P. V. V., and Ristic., Z. (2009). Heat tolerance and expression of protein synthesis elongation factors, EF-Tu and EF-1α, in spring wheat. *Funct. Plant Biol.* 36, 234–241. doi: 10.1071/FP08266

Chakraborty, A., Viswanath, A., Malipatil, R., Semalaiyappan, J., Shah, P., Ronanki, S., et al. (2022). Identification of candidate genes regulating drought tolerance in Pearl Millet. *Int. J. Mol. Sci.* 23, 6907. doi: 10.3390/ijms23136907

Chandel, G., Dubey, M., and Meena, X. X. X. R. (2013). Differential expression of heat shock proteins and heat stress transcription factor genes in rice exposed to different levels of heat stress. *J. Plant Biochem. Biotechnol.* 22, 277–285. doi: 10.1007/s13562-012-0156-8

Chin, C.-H., Chen, S.-H., Wu, H.-H., Ho, C.-W., Ko, M.-T., et al. (2014). cytoHubba: identifying hub objects and sub-networks from complex interactome. *BMC Syst. Biol.* 8, 1–7. doi: 10.1186/1752-0509-8-S4-S11

Dahuja, A., Kumar, R. R., Sakhare, A., Watts, A., Singh, B., Goswami, S., et al. (2021). Role of ATP-binding cassette transporters in maintaining plant homeostasis under abiotic and biotic stresses. *Physiologia Plantarum* 171, 785–801. doi: 10.1111/ppl.13302

Darko, E., Végh, Balázs, Khalil, R., Marček, T., Szalai, G., Pál, M., et al. (2019). Metabolic responses of wheat seedlings to osmotic stress induced by various osmolytes under iso-osmotic conditions. *PloS One.* 14, e0226151. doi: 10.137/journal.ponr.0226151

Das, A., Eldakak, M., Paudel, B., Kim, D.-W., Hemmati, H., Basu, C., et al. (2016). Leaf proteome analysis reveals prospective drought and heat stress response mechanisms in soybean. *BioMed. Res. Int.* 2016, 6021047. doi: 10.1155/2016/6021047

Ding, H., Mo, S., Qian, Y., Yuan, G., Wu, X., and Ge, C. (2020). Integrated proteome and transcriptome analyses revealed key factors involved in tomato *(Solanum lycopersicum)* under high temperature stress. *Food Energy Secur.* 9, e239. doi: 10.1002/fes3.239

Djanaguiraman, M., Sheeba, J.A., Devi, D.D., and Bangarusamy, U. (2009). Cotton leaf senescence can be delayed by nitrophenolate spray through enhanced antioxidant defense system. *J. Agron. Crop Sci.* 195, 213–224. doi: 10.1111/j.1439-037X.2009.00360.x

Donald, J., Tarafdar, A., Biswas, K., Sathyavathi, T. C., Padaria, J. C., and Kumar, P.A. (2015). Development and characterization of a high temperature stress responsive subtractive cDNA library in Pearl Millet (*Pennisetum glaucum* (L.) R. Br). *Indian J. Exp. Biol.* 53, 543-550.

El-Kereamy, A., Bi, Y.-M., Perrin, H., and Allen, G. (2012). Good, and Steven J. Rothstein. The rice *R2R3-MYB* transcription factor *OsMYB55* is involved in the tolerance to high temperature and modulates amino acid metabolism. *PloS One* 7, e52030. doi: 10.1371/journal.pone.0052030

Fahad, S., Bajwa, A. A., Nazir, U., Anjum, S. A., Farooq, A., Zohaib, A., et al. (2017). Crop production under drought and heat stress: plant responses and management options. *Front. Plant Sci.* 8, 1147. doi: 10.3389/fpls.2017.01147

Fenqi, C., Zhang, J., and Ha, X. (2023). and Huiling Ma. Genome-wide identification and expression analysis of the Auxin-Response factor (ARF) gene family in *Medicago sativa* under abiotic stress. *BMC Genomics* 24, 498. doi: 10.1186/s12864-023-09610-z

Freschet, G. T., Violle, C., Malo, Y., Bourget, M., and Florian, F. (2018). Allocation, morphology, physiology, architecture: The multiple facets of plant above-and below-ground responses to resource stress. *New Phytol.* 219, 1338–1352. doi: 10.1111/nph.15225

Frey, F. P., Urbany, C., Hüttel, B., Reinhardt, R., and Stich, B. (2015). Genome-wide expression profiling and phenotypic evaluation of European maize inbreds at seedling stage in response to heat stress. *BMC Genomics* 16, 1–15. doi: 10.1186/s12864-015-1282-1

Gao, F., Han, X., Wu, J., Zheng, S., Shang, Z., Sun, D., et al. (2012). A heat-activated calcium-permeable channel–Arabidopsis cyclic nucleotide-gated ion channel 6–is involved in heat shock responses. *Plant J.* 70, 1056–1069. doi: 10.1111/j.1365-313X.2012.04969.x

Gao, J., Wang, M.-J., Wang, J.-J., Lu, H.-P., and Jian-Xiang, L. (2022). bZIP17 regulates heat stress tolerance at reproductive stage in *Arabidopsis*. *Abiotech* 3, 1–11. doi: 10.1007/s42994-021-00062-1

Gholizadeh, F., and Mirzaghaderi, G. (2020). Genome-wide analysis of the polyamine oxidase gene family in wheat (*Triticum aestivum* L.) reveals involvement in temperature stress response. *PloS One* 15, e0236226. doi: 10.1371/journal.pone.0236226

Giri, A., Heckathorn, S., Mishra, S., and Krause, C. (2017). Heat stress decreases levels of nutrient-uptake and-assimilation proteins in tomato roots. *Plants* 6, 6. doi: 10.3390/plants6010006

Göbel, C., Feussner, I., Schmidt, A., Scheel, D., Sanchez-Serrano, J., Hamberg, M., et al. (2001). Oxylipin profiling reveals the preferential stimulation of the 9-lipoxygenase pathway in elicitor-treated potato cells. *J. Biol. Chem.* 276, 6267–6273. doi: 10.1074/jbc.M008606200

Goud,, Anjali, C., Satturu, V., Malipatil, R., Viswanath, A., Semalaiyappan, J., et al. (2022). Identification of iron and zinc responsive genes in pearl millet using genome-wide RNA-sequencing approach. *Front. Nutr.* 9, 884381. doi: 10.3389/fnut.2022.884381

Guo, M., Liu, J.-H., Ma, X., Luo, D.-X., Gong, Z.-H., and Lu., M.-H. (2016). The plant heat stress transcription factors (HSFs: structure, regulation, and function in response to abiotic stresses. *Front. Plant Sci.* 7, 114. doi: 10.3389/fpls.2016.00114

Guo, J., Sun, B., He, H., Zhang, Y., Tian, H., and Wang, B. (2021). Current understanding of bHLH transcription factors in plant abiotic stress tolerance. *Int. J. Mol. Sci.* 22, 4921. doi: 10.3390/ijms22094921

Hasanuzzaman, M., Nahar, K., Alam, Md M., Roychowdhury, R., and Fujita, M. (2013). Physiological, biochemical, and molecular mechanisms of heat stress tolerance in plants. *Int. J. Mol. Sci.* 14, 9643–9684. doi: 10.3390/ijms14059643

Havaux, M. (1993). Rapid photosynthetic adaptation to heat stress triggered in potato leaves by moderately elevated temperatures. *Plant Cell Environ.* 16, 461–467. doi: 10.1111/j.1365-3040.1993.tb00893.x

He, Y., Guan, H., Li, Bo, Zhang, S., Xu, Y., Yao, Y., et al. (2023). Transcriptome analysis reveals the dynamic and rapid transcriptional reprogramming involved in heat stress and identification of heat response genes in rice. *Int. J. Mol. Sci.* 24, 14802. doi: 10.3390/ijms241914802

He, G.-H., Xu, J.-Y., Wang, Y.-X., Liu, J.-M., Li, P.-S., Chen, M., et al. (2016). Drought-responsive WRKY transcription factor genes *TaWRKY1* and *TaWRKY33* from wheat confer drought and/or heat resistance in Arabidopsis. *BMC Plant Biol.* 16, 1–16. doi: 10.1186/s12870-016-0806-4

Hoang, M. H., Kim, H.-S., Zulfugarov, I. S., and Lee, C.-H. (2020). Down-regulation of zeaxanthin epoxidation in vascular plant leaves under normal and photooxidative stress conditions. *J. Plant Biol.* 63, 331–336. doi: 10.1007/s12374-020-09260-8

Hosseini,, Zahra, S., Ismaili, A., Nazarian-Firouzabadi, F., Fallahi, H., Nejad, A. R., et al. (2021). Dissecting the molecular responses of lentil to individual and combined drought and heat stresses by comparative transcriptomic analysis. *Genomics* 113, 693–705. doi: 10.1016/j.ygeno.2020.12.038

Hu, X., Zhu, L., Zhang, Y., Xu, L., Li, N., Zhang, X., et al. (2019). Genome-wide identification of C2H2 zinc-finger genes and their expression patterns under heat stress in tomato (*Solanum lycopersicum* L.). *PeerJ* 7, e7929. doi: 10.7717/peerj.7929

Huang, W., Sherman, B. T., Tan, Q., Collins, J. R., Alvord, W. G., Roayaei, J., et al. (2007). The DAVID Gene Functional Classification Tool: a novel biological module-centric algorithm to functionally analyze large gene lists. *Genome Biol.* 8, 1–16. doi: 10.1186/gb-2007-8-9-r183

Huang, B., Rachmilevitch, S., and Xu, J. (2012). Root carbon and protein metabolism associated with heat tolerance. *J. Exp. Bot.* 63, 3455–3465. doi: 10.1093/jxb/ers003

Indiastat. (2020). *Agricultural production* (New Delhi: Indiastat: Datanet India Pvt. Ltd) Available online at: http://www.Indiastat.com/searchresult.aspx (Accessed February 27, 2020).

Jagadish, S. V., Way, K. D. A., and Sharkey, T. D. (2021). Plant heat stress: Concepts directing future research. *Plant Cell Environ.* 44, 1992–2005. doi: 10.1111/pce.14050

Jia, S., Li, H., Jiang, Y., Tang, Y., Zhao, G., Zhang, Y., et al. (2020). Transcriptomic analysis of female panicles reveals gene expression responses to drought stress in maize (*Zea mays* L.). *Agronomy* 10, 313. doi: 10.3390/agronomy10020313

Klemens, A. W., Patzke, K., Deitmer, J., Spinner, L., Hir, R. Le, Bellini, C., et al. (2013). Overexpression of the vacuolar sugar carrier *AtSWEET16* modifies germination, growth, and stress tolerance in Arabidopsis. *Plant Physiol.* 163, 1338–1352. doi: 10.1104/pp.113.224972

Kong, X., Luo, Z., Dong, H., and Eneji, A. E. (2012). and Weijiang Li. Effects of non-uniform root zone salinity on water use, Na+ recirculation, and Na+ and H+ flux in cotton. *J. Exp. Bot.* 63, 2105–2116. doi: 10.1093/jxb/err420

Kotak, S., Larkindale, J., Lee, U., Koskull-Döring, P. v., Vierling, E., and Scharf, K.-D. (2007). Complexity of the heat stress response in plants. *Curr. Opin. Plant Biol.* 10, 310–316. doi: 10.1016/j.pbi.2007.04.011

Kurimoto, K., Day, D. A., Lambers, H., and Noguchi., Ko (, 2004). Effect of respiratory homeostasis on plant growth in cultivars of wheat and rice. *Plant Cell Environ.* 27, 853–862. doi: 10.1111/j.1365-3040.2004.01191.x

Li, Z., and Howell, S. H. (2021). Heat stress responses and thermotolerance in maize. *Int. J. Mol. Sci.* 22, 948. doi: 10.3390/ijms22020948

Li, J., Nadeem, M., Chen, L., Wang, M., Wan, M., Qiu, L., et al. (2020). Differential proteomic analysis of soybean anthers by iTRAQ under high-temperature stress. *J. Proteomics* 103968. doi: 10.1016/j.jprot.2020.103968

Li, Y.-F., Wang, Y., Tang, Y., Kakani, V. G., and Ramamurthy, M. (2013). Transcriptome analysis of heat stress response in switchgrass (*Panicum virgatum* L.). *BMC Plant Biol.* 13, 1–12. doi: 10.1186/1471-2229-13-153

Liao, Y., Smyth, G. K., and Shi, W. (2014). featureCounts: an efficient general purpose program for assigning sequence reads to genomic features. *Bioinformatics* 30, 923–930. doi: 10.1093/bioinformatics/btt656

Lim,, Woo, C., Han, S.-W., Hwang, In S., Kim, D. S., Hwang, B. K., et al. (2015). The pepper lipoxygenase *CaLOX1* plays a role in osmotic, drought and high salinity stress response. *Plant Cell Physiol.* 56, 930–942. doi: 10.1093/pcp/pcv020

Lunn, J. E., Feil, R., Hendriks, J. H. M., Gibon, Y., Morcuende, R., Osuna, D., et al. (2006). Sugar-induced increases in trehalose 6-phosphate are correlated with redox activation of ADPglucose pyrophosphorylase and higher rates of starch synthesis in *Arabidopsis thaliana*. *Biochem. J.* 397, 139–148. doi: 10.1042/BJ20060083

Lyu, J. Il, Park, Ji H., Kim, J.-K., Bae, C.-H., Jeong, W.-J., Min, S. R., et al. (2018). Enhanced tolerance to heat stress in transgenic tomato seeds and seedlings overexpressing a trehalose-6-phosphate synthase/phosphatase fusion gene. *Plant Biotechnol. Rep.* 12, 399–408. doi: 10.1007/s11816-018-0505-8

Maurel, C., Verdoucq, L., Luu, D.-T., and Santoni, Véronique (2008). Plant aquaporins: membrane channels with multiple integrated functions. *Annu. Rev. Plant Biol.* 59, 595–624. doi: 10.1146/annurev.arplant.59.032607.092734

Mittler, R. (2017). ROS are good. *Trends Plant Sci.* 22, 11–19. doi: 10.1016/j.tplants.2016.08.002

Mittler, R., Finka, A., and Goloubinoff, P. (2012). How do plants feel the heat. *Trends Biochem. Sci.* 37, 118–125. doi: 10.1016/j.tibs.2011.11.007

Mizoi, J., Shinozaki, K., and Yamaguchi-Shinozaki, K. (2012). AP2/ERF family transcription factors in plant abiotic stress responses. *Biochim. Biophys. Acta (BBA)-Gene Regul. Mech.* 1817, 86–96. doi: 10.1016/j.bbagrm.2011.08.004

Molik, S., Karnauchov, I., Weidlich, C., Herrmann, R. G., and Kloüsgen, R. B. (2001). The Rieske Fe/S Protein of the Cytochromeb 6/f Complex in Chloroplasts: Missing link in the evolution of protein transport pathways in chloroplasts? *J. Biol. Chem.* 276, 42761–42766. doi: 10.1074/jbc.M106690200

Moon, S., and Jung, K.-H. (2014). Genome-wide expression analysis of rice ABC transporter family across spatio-temporal samples and in response to abiotic stresses. *J. Plant Physiol.*, 1276–1288. doi: 10.1016/j.jplph.2014.05.006

Morrison, D. K. (2012). MAP kinase pathways. *Cold Spring Harbor Perspect. Biol.* 4, a011254. doi: 10.1101/cshperspect.a011254

Mukesh Sankar, S., Satyavathi, C.T., Barthakur, S., Singh, S. P., and Bharadwaj, C. (2021). Differential modulation of heat-inducible genes across diverse genotypes and molecular cloning of a sHSP from pearl millet (*Pennisetum glaucum* (L.) R. Br.). *Front. Plant Sci.* 12, 659893. doi: 10.3389/fpls.2021.659893

Mulet,, Jose, M., Porcel, R., and Yenush, L. (2023). Modulation of potassium transport to increase abiotic stress tolerance in plants. *J. Exp. Bot.* 74, 5989–6005. doi: 10.1093/jxb/erad333

Mwadzingeni, L., Shimelis, H., Dube, E., Laing, M. D., and Tsilo., T. J. (2016). Breeding wheat for drought tolerance: Progress and technologies. *J. Integr. Agric.* 15, 935–943. doi: 10.1016/S2095-3119(15)61102-9

Nagaraju, M., Reddy, P. S., Kumar, S.A., Srivastava, R. K., Kishor, P.B.K., and Manohar Rao, X. X. X. D. (2015). Genome-wide scanning and characterization of *Sorghum bicolor L.* heat shock transcription factors. *Curr. Genomics* 16, 279–291.

Nakano, T., Suzuki, K., Fujimura, T., and Shinshi, H. (2006). Genome-wide analysis of the ERF gene family in Arabidopsis and rice. *Plant Physiol.* 140, 411–432. doi: 10.1104/pp.105.073783

Naranjo, M. A., Forment, J., Roldan, M., Serrano, R., and Vicente, O. (2006). Overexpression of *Arabidopsis thaliana LTL1*, a salt-induced gene encoding a GDSL-motif lipase, increases salt tolerance in yeast and transgenic plants. *Plant Cell Environ.* 47, 1890–1900. doi: 10.1093/pcp/pcv020

Niño-González, María, Novo-Uzal, E., Richardson, D. N., Barros, P. M., and Duque, P. (2019). More transporters, more substrates: the Arabidopsis major facilitator superfamily revisited. *Mol. Plant* 12, 1182–1202. doi: 10.1016/j.molp.2019.07.003

Obaid, A. Y., Sabir, J. S. M., Atef, A., Liu, X., Edris, S., El-Domyati, F. M., et al. (2016). Analysis of transcriptional response to heat stress in *Rhazya stricta*. *BMC Plant Biol.* 16, 1–18. doi: 10.1186/s12870-016-0938-6

Panchuk, I. I., Volkov, R. A., and Schöffl, F. (2002). Heat stress-and heat shock transcription factor-dependent expression and activity of ascorbate peroxidase in Arabidopsis. *Plant Physiol.* 129, 838–853. doi: 10.1104/pp.001362

Pérez-Llorca, M., Pollmann, S., and Müller, M. (2023). Ethylene and jasmonates signaling network mediating secondary metabolites under abiotic stress. *Int. J. Mol. Sci.* 24, 5990. doi: 10.3390/ijms24065990

Prashanth, S. R., Sadhasivam, V., and Parida, A. (2008). and Ajay Parida. Over expression of cytosolic copper/zinc superoxide dismutase from a mangrove plant *Avicennia marina* in indica rice var Pusa Basmati-1 confers abiotic stress tolerance. *Transgenic Res.* 17, 281–291. doi: 10.1007/s11248-007-9099-6

Pulido, P., Llamas, E., and Rodriguez-Concepcion, M. (2017). Both Hsp70 chaperone and Clp protease plastidial systems are required for protection against oxidative stress. *Plant Signaling Behav.* 12, e1290039. doi: 10.1080/15592324.2017.1290039

Qian, Y., Ren, Q., Zhang, J., and Chen., L. (2019). Transcriptomic analysis of the maize (Zea mays L.). inbred line B73 response to heat stress at the seedling stage. *Gene* 692, 68–78. doi: 10.1016/j.gene.2018.12.062

Rangan, P., Furtado, A., and Robert, H. (2020). Transcriptome profiling of wheat genotypes under heat stress during grain-filling. *J. Cereal Sci.* 91, 102895. doi: 10.1016/j.jcs.2019.102895

Rao, D., Momcilovic, I., Kobayashi, S., Callegari, E., and Ristic, Z. (2004). Chaperone activity of recombinant maize chloroplast protein synthesis elongation factor, EF-Tu. *Eur. J. Biochem.* 271, 3684–3692. doi: 10.1111/j.1432-1033.2004.04309.x

Robinson, M. D., McCarthy, D. J., and Smyth, G. K. (2010). edgeR: a Bioconductor package for differential expression analysis of digital gene expression data. *Bioinformatics* 26, 139–140. doi: 10.1093/bioinformatics/btp616

Ruan, Y.-L. (2014). Sucrose metabolism: gateway to diverse carbon use and sugar signaling. *Annu. Rev. Plant Biol.* 65, 33–67. doi: 10.1146/annurev-arplant-050213-040251

Rubio, M. C., González, E. M., Minchin, F. R., Webb, K.J., Arrese-Igor, C., Ramos, J., et al. (2002). Effects of water stress on antioxidant enzymes of leaves and nodules of transgenic alfalfa overexpressing superoxide dismutases. *Physiologia Plantarum* 115, 531–540. doi: 10.1034/j.1399-3054.2002.1150407.x

Sakuma, Y., Liu, Q., Dubouzet, J. G., Abe, H., Shinozaki, K., and Kazuko Yamaguchi-, S. (2002). DNA-binding specificity of the ERF/AP2 domain of Arabidopsis DREBs, transcription factors involved in dehydration-and cold-inducible gene expression. *Biochem. Biophys. Res. Commun.* 290, 998–1009. doi: 10.1006/bbrc.2001.6299

Samad, A. F. A., Muhammad, S., Nazaruddin, N., and Izzat, A. (2017). Fauzi, Abdul MA Murad, Zamri Zainal, and Ismanizan Ismail. MicroRNA and transcription factor: key players in plant regulatory network. *Front. Plant Sci.* 8, 565. doi: 10.3389/fpls.2017.00565

Schlenker, W., and David, B. (2010). Lobell. Robust negative impacts of climate change on African agriculture. *Environ. Res. Lett.* 5, 014010. doi: 10.1088/1748-9326/5/1/014010

Schroda, M., Vallon, O., Wollman, Francis-André, and Beck, C. F. (1999). A chloroplast-targeted heat shock protein 70 (HSP70) contributes to the photoprotection and repair of photosystem II during and after photoinhibition. *Plant Cell* 11, 1165–1178. doi: 10.1105/tpc.11.6.1165

Seki, M., Kamei, A., Yamaguchi-Shinozaki, K., and Shinozaki, K. (2003). Molecular responses to drought, salinity and frost: common and different paths for plant protection. *Curr. Opin. Biotechnol.* 14, 194–199. doi: 10.1016/S0958-1669(03)00030-2

Shannon, P., Markiel, A., Ozier, O., Baliga, N. S., Wang, J. T., Ramage, D., et al. (2003). Cytoscape: a software environment for integrated models of biomolecular interaction networks. *Genome Res.* 13, 2498–2504. doi: 10.1101/gr.1239303

Shiriga, K., Sharma, R., Kumar, K., Yadav, S. K., Hossain, F., and Thirunavukkarasu, N. (2014). Genome-wide identification and expression pattern of drought-responsive members of the NAC family in maize. *Meta Gene* 2, 407–417. doi: 10.1016/j.mgene.2014.05.001

Shu, Y., Li, W., Zhao, J., Liu, Y., and Guo, C. (2018). Transcriptome sequencing and expression profiling of genes involved in the response to abiotic stress in Medicago ruthenica. *Genet. Mol. Biol.* 41, 638–648. doi: 10.1590/1678-4685-gmb-2017-0284

Sidak, Z. (1967). Rectangular confidence regions for the means of multivariate normal distributions. *J. Am. Stat. Assoc.* 62, 626–633. doi: 10.2307/2283989

Singh, R. K., Jaishankar, J., Muthamilarasan, M., Shweta, S., Dangi, A., and Prasad, M. (2016). Genome-wide analysis of heat shock proteins in C4 model, foxtail millet identifies potential candidates for crop improvement under abiotic stress. *Sci. Rep.* 6, 32641. doi: 10.1038/srep32641

Slimen, B., Najar, M. T., Ghram, A., Dabbebi, H., Mrad, M. B., and Manef, A. (2014). Reactive oxygen species, heat stress and oxidative-induced mitochondrial damage. A review *of hyperthermia*. *Int. J.* 30, 513–523. doi: 10.3109/02656736.2014.971446

Sun, M., Huang, D., Zhang, A., Khan, I., Yan, H., Wang, X., et al. (2020). Transcriptome analysis of heat stress and drought stress in pearl millet based on Pacbio full-length transcriptome sequencing. *BMC Plant Biol.* 20, 1–15. doi: 10.1186/s12870-020-02530-0

Sung, D. Y., Yul, D., Vierling, E., and Guy, C. L. (2001). Comprehensive expression profile analysis of the Arabidopsis Hsp70 gene family. *Plant Physiol.* 126, 789–800. doi: 10.1104/pp.126.2.789

Suzuki, N., Bassil, E., Hamilton, J. S., Inupakutika, M. A., Zandalinas, S. I., Tripathy, D., et al. (2016). ABA is required for plant acclimation to a combination of salt and heat stress. *PloS One*. 11, e0147625. doi: 10.1371/journal.pone.0147625

Szklarczyk, D., Kirsch, R., Koutrouli, M., Nastou, K., Mehryary, F., Hachilif, R., et al. (2023). The STRING database in 2023: protein–protein association networks and functional enrichment analyses for any sequenced genome of interest. *Nucleic Acids Res.* 51, D638–D646. doi: 10.1093/nar/gkac1000

Takahashi, S., Bauwe, H., and Badger, M. (2007). Impairment of the photorespiratory pathway accelerates photo-inhibition of photosystem II by suppression of repair but not acceleration of damage processes in Arabidopsis. *Plant Physiol.* 60, 487–494. doi: 10.1104/pp.107.097253

Tanaka, H., Osakabe, Y., Katsura, S., Mizuno, S., Maruyama, K., Kusakabe, K., et al. (2012). Abiotic stress-inducible receptor-like kinases negatively control ABA signaling in Arabidopsis. *Plant J.* 70, 599–613. doi: 10.1111/j.1365-313X.2012.04901.x

Thirunavukkarasu, N., Sharma, R., Singh, N., Shiriga, K., Mohan, S., Mittal, S., et al. (2017). Genomewide expression and functional interactions of genes under drought stress in maize. *Int. J. Genomics*. 2017, 2568706. doi: 10.1155/2017/2568706

Tian, F., Yang, D. C., Meng, Y. Q., Jin, J., and Gao, G. (2020). PlantRegMap: charting functional regulatory maps in plants. *Nucleic Acids Res.* 48, D1104–D1113. doi: 10.1093/nar/gkz972

Vadez, V., Hash, T., Bidinger, F. R., and Jana, Kholova (2012). II. 1.5 Phenotyping pearl millet for adaptation to drought. *Front. Physiol.* 3, 386. doi: 10.3389/fphys.2012.00386

Vandeleur, R., Niemietz, C., Tilbrook, J., and Tyerman, S. D. (2005). Roles of aquaporins in root responses to irrigation. *Plant Soil* 274, 141–161. doi: 10.1007/s11104-004-8070-z

Wahab, M. M. S., Srividhya, A., Shanthi, P., and Latha, X. X. X. P. (2020). Identification of differentially expressed genes under heat stress conditions in rice (*Oryza sativa L.*). *Mol. Biol. Rep.* 47, 1935–1948. doi: 10.1007/s11033-020-05291-z

Wang, X., Dinler, B. S., Vignjevic, M., Jacobsen, S., and Wollenweber, B. (2015). Physiological and proteome studies of responses to heat stress during grain filling in contrasting wheat cultivars. *Plant Sci.* 230, 33–50. doi: 10.1016/j.plantsci.2014.10.009

Wang, P., Wang, H., Wang, Y., Ren, F., and Liu, W. (2018). Analysis of bHLH genes from foxtail millet (*Setaria italica*) and their potential relevance to drought stress. *PloS One* 13, e0207344. doi: 10.1371/journal.pone.0207344

Wang, X., Yan, B., Shi, M., Zhou, W., Zekria, D., Wang, H., et al. (2016). Overexpression of a *Brassica campestris* HSP70 in tobacco confers enhanced tolerance to heat stress. *Protoplasma* 253, 637–645. doi: 10.1007/s00709-015-0867-5

Wang, Y., Zhang, Y., Zhang, Q., Cui, Y., Xiang, J., Chen, H., et al. (2019). Comparative transcriptome analysis of panicle development under heat stress in two rice (Oryza sativa L.). cultivars differing in heat tolerance. *PeerJ* 7, e7595. doi: 10.7717/peerj.7595

Wang, M., Zou, Z., Li, Q., Xin, H., Zhu, X., Chen, X., et al. (2017). Heterologous expression of three Camellia sinensis small heat shock protein genes confers temperature stress tolerance in yeast and. *Arabidopsis thaliana. Plant Cell Rep.* 36, 1125–1135. doi: 10.1007/s00299-017-2143-y

Ward, J. M., and Schroeder, J. I. (1994). Calcium-activated K+ channels and calcium-induced calcium release by slow vacuolar ion channels in guard cell vacuoles implicated in the control of stomatal closure. *Plant Cell* 6, 669–683. doi: 10.1105/tpc.6.5.669

Wu, X., Shiroto, Y., Kishitani, S., Ito, Y., and Toriyama, K. (2009). Enhanced heat and drought tolerance in transgenic rice seedlings overexpressing *OsWRKY11* under the control of HSP101 promoter. *Plant Cell Rep.* 28, 21–30. doi: 10.1007/s00299-008-0614-x

Xi, Y., Ling, Q., Zhou, Y., Liu, X., and Qian, Y. (2022). *ZmNAC074*, a maize stress-responsive NAC transcription factor, confers heat stress tolerance in transgenic Arabidopsis. *Front. Plant Sci.* 13, 986628. doi: 10.1016/j.bbagrm.2011.08.004

Xifeng, L., Cai, C., Wang, Z., Fan, B., Zhu, C., and Chen, Z. (2018). Plastid translation elongation factor Tu is prone to heat-induced aggregation despite its critical role in plant heat tolerance. *Plant Physiol.* 176, 3027–3045. doi: 10.1104/pp.17.01672

Xu, C., and Bingru, H. (2012). Comparative analysis of proteomic responses to single and simultaneous drought and heat stress for two Kentucky bluegrass cultivars. *Crop Sci.* 152, 1246–1260. doi: 10.2135/cropsci2011.10.0551

Xu, C., and Huang, B. (2010). Differential proteomic response to heat stress in thermal *Agrostis scabra* and heat-sensitive *Agrostis stolonifera*. *Physiologia Plantarum* 139, 192–204. doi: 10.1111/j.1399-3054.2010.01357.x

Yang, M., Zhang, Y., Zhang, H., Wang, H., Wei, T., Che, S., et al. (2017). Identification of MsHsp20 gene family in *Malus sieversii* and functional characterization of *MsHsp16. 9* in heat tolerance. *Front. Plant Sci.* 8, 1761. doi: 10.3389/fpls.2017.01761

Yoav, B., and Hochberg, Y. (2000). On the adaptive control of the false discovery rate in multiple testing with independent statistics. *J. Educ. Behav. Stat* 25, 60–83. doi: 10.3102/10769986025001060

Yuan, M., and Wang, S. (2013). Rice *MtN3/saliva/SWEET* family genes and their homologs in cellular organisms. *Mol. Plant* 6, 665–674. doi: 10.1093/mp/sst035

Zang, Yu, Jun, C., and Li, R. (2020). Shuai Shang, and Xuexi Tang. Genome-wide analysis of the superoxide dismutase (SOD) gene family in *Zostera marina* and expression profile analysis under temperature stress. *PeerJ* 8, e9063. doi: 10.7717/peerj.9063

Zelazny, E., and Vert, Grégory (2014). Plant nutrition: root transporters on the move. *Plant Physiol.* 166, 500–508. doi: 10.1104/pp.114.244475

Zhang, S., Zhang, A., Wu, X., Zhu, Z., Yang, Z., Zhu, Y., et al. (2019). Transcriptome analysis revealed expression of genes related to anthocyanin biosynthesis in eggplant (*Solanum melongena* L.). under high-temperature stress. *BMC Plant Biol.* 19, 1–13. doi: 10.1186/s12870-019-1960-2

Zhang, Z.-L., Zhu, J.-H., Zhang, Q.-Q., and Cai, Y.-B. (2009). Molecular characterization of an ethephon-induced *Hsp70* involved in high and low-temperature responses in *Hevea brasiliensis*. *Plant Physiol. Biochem.* 47, 954–959. doi: 10.1016/j.plaphy.2009.06.003

Zhu, B., Ye, C., Lü, H., Chen, X., Chai, G., Chen, J., et al. (2006). Identification and characterization of a novel heat shock transcription factor gene, *GmHsfA1*, in soybeans (*Glycine max*). *J. Plant Res.* 119, 247–256. doi: 10.1007/s10265-006-0267-1

Zhu, Y., Zhu, G., Guo, Q., Zhu, Z., Wang, C., and Liu, Z. (2013). A comparative proteomic analysis of *Pinellia ternata* leaves exposed to heat stress. *Int. J. Mol. Sci.* 14, 20614–20634. doi: 10.3390/ijms141020614

frontiers | Frontiers in Plant Science

TYPE Original Research
PUBLISHED 27 August 2024
DOI 10.3389/fpls.2024.1439972

OPEN ACCESS

EDITED BY
Yanbo Hu,
Northeast Forestry University, China

REVIEWED BY
Deguo Han,
Northeast Agricultural University, China
Ujjal Jyoti Phukan,
University of Arizona, United States

*CORRESPONDENCE
Yasir Majeed
yasirmajeed5453@gmail.com
Yu Zhang
zhangyu@catas.cn
Huaijun Si
hjsi@gsau.edu.cn

RECEIVED 28 May 2024
ACCEPTED 16 July 2024
PUBLISHED 27 August 2024

CITATION
Zhu X, Li W, Zhang N, Duan H, Jin H, Chen Z, Chen S, Zhou J, Wang Q, Tang J, Majeed Y, Zhang Y and Si H (2024) Identification of autophagy-related genes ATG18 subfamily genes in potato (*Solanum tuberosum* L.) and the role of *StATG18a* gene in heat stress. *Front. Plant Sci.* 15:1439972. doi: 10.3389/fpls.2024.1439972

Identification of autophagy-related genes ATG18 subfamily genes in potato (*Solanum tuberosum* L.) and the role of *StATG18a* gene in heat stress

Xi Zhu[1,2], Wei Li[1], Ning Zhang[3,4,5], Huimin Duan[1], Hui Jin[1], Zhuo Chen[1], Shu Chen[1], Jiannan Zhou[1], Qihua Wang[1], Jinghua Tang[1], Yasir Majeed[3,4,5]*, Yu Zhang[1]* and Huaijun Si[3,4,5]*

[1]Key Laboratory of Tropical Fruit Biology, Ministry of Agriculture and Rural Affairs/Key Laboratory of Hainan Province for Postharvest Physiology and Technology of Tropical Horticultural Products, South Subtropical Crops Research Institute, Chinese Academy of Tropical Agricultural Sciences, Zhanjiang, Guangdong, China, [2]National Key Laboratory for Tropical Crop Breeding, Sanya Research Institute, Chinese Academy of Tropical Agricultural Sciences, Sanya, China, [3]State Key Laboratory of Aridland Crop Science, Gansu Agricultural University, Lanzhou, China, [4]College of Life Science and Technology, Gansu Agricultural University, Lanzhou, China, [5]College of Agronomy, Gansu Agricultural University, Lanzhou, China

Autophagy is a highly conserved process in eukaryotes that is used to recycle the cellular components from the cytoplasm. It plays a crucial function in responding to both biotic and abiotic stress, as well as in the growth and development of plants. Autophagy-related genes (ATG) and their functions have been identified in numerous crop species. However, their specific tasks in potatoes (*Solanum tuberosum* L.), are still not well understood. This work is the first to identify and characterize the potato *StATG18* subfamily gene at the whole-genome level, resulting in a total of 6 potential *StATG18* subfamily genes. We analyzed the phylogenetic relationships, chromosome distribution and gene replication, conserved motifs and gene structure, interspecific collinearity relationship, and cis-regulatory elements of the ATG18 subfamily members using bioinformatics approaches. Furthermore, the quantitative real-time polymerase chain reaction (qRT-PCR) analysis suggested that *StATG18* subfamily genes exhibit differential expression in various tissues and organs of potato plants. When exposed to heat stress, their expression pattern was observed in the root, stem, and leaf. Based on a higher expression profile, the *StATG18a* gene was further analyzed under heat stress in potatoes. The subcellular localization analysis of StATG18a revealed its presence in both the cytoplasm and nucleus. In addition, *StATG18a* altered the growth indicators, physiological characteristics, and photosynthesis of potato plants under heat stresses. In conclusion, this work offers a thorough assessment of *StATG18* subfamily genes and provides essential recommendations for additional functional investigation of autophagy-associated genes in potato plants. Moreover, these results also contribute to our understanding of the potential mechanism and functional validation of the *StATG18a* gene's persistent tolerance to heat stress in potato plants.

KEYWORDS

autophagy, potato, StATG18a, physiological, photosynthesis, heat stress

1 Introduction

The potato (*Solanum tuberosum* L.) has its origins in the Andes Mountains of South America and flourishes in the low-temperature climate. According to Zheng et al. (2024), it is the third most consumed and stable crop in the world, following rice and wheat. With its remarkable adaptability and a greater percentage of edible biomass (~85%) compared to cereals (~50%), it is one of the most significant crops in the world (Lutaladio and Castaldi, 2009). Depending on the cultivar and season, the potato crop can flourish in soils with a pH range of 5–7.5 and produce a yield of 40–70 tons per hectare (Fuqiang et al., 2021). This crop has a short growth season and may be grown in various environmental conditions (Muhammad and Zoltan, 2022). The majority of cultivated plant varieties are susceptible to heat. Temperature is considered the main uncontrolled factor that affects the development and output of potatoes (Zhang et al., 2024). The average day temperature range of 14–22°C is excellent for the growth of most commercial potato cultivars, deviating from this range significantly reduces the yield (Siano et al., 2024). The primary aspects of climate change are the greenhouse effect and global warming, which significantly impact on ecology, the agriculture industry, and food security at both national and international levels by affecting agricultural productivity. The greenhouse effect and global warming impact on potato production is anticipated to distress world yield by 18–32% by 2050 (Anderson et al., 2020). High temperatures have diverse effects on the growth and development of potatoes. They have the ability to reduce the total leaf area, increase the number of flowers per branch, restrict root development, promote stem growth, and boost branching (Tang et al., 2018). Elevated temperatures cause damage to chloroplasts, which overall lowers the amount of chlorophyll significantly. Consequently, the rate of photosynthetic respiration and assimilate synthesis decreases, causing a shift in the distribution of assimilate from tubers to leaves. Heat stress leads to decreased tuber induction, formation, development, and expansion (Singh et al., 2020). In addition, it induces necrosis, decreases dry matter content, and leads to tuber deformities (Rudack et al., 2017).

Autophagy—"self-eating"—is one of the numerous mechanisms and cellular responses in agricultural plants engaged under extreme climatic conditions. The process is a highly conserved system in eukaryotes that involves the breakdown and recycling of many cytoplasmic components, including damaged nuclear fragments, malfunctioning complexes, proteins, and even entire organelles (Lal et al., 2022). Plants have been observed to exhibit three separate but non-exclusive forms of autophagy: macro-autophagy, micro-autophagy, and mega-autophagy (Marshall and Vierstra, 2018). Macro-autophagy is the process in which cellular loads are sequestered and appropriated by the double-membrane structures of autophagosomes. These structures then join with the vacuole for digestion and recycling. It frequently leads to the random degradation of bulk proteins and the identification of autophagy substrates through specialized receptors, selectively eliminating particular components (Schuck, 2020; Luong et al., 2022). On the other hand, the transportation of anthocyanin aggregates from the cytosol to the vacuole is an instance of the direct absorption of cytoplasmic substances into the vacuole by the inward folding or outward bulging of the tonoplast during micro-autophagy. The vacuolar membrane directly engulfs these components, causing them to eventually be released into the vacuolar lumen (Rubio-Tomás et al., 2023), Mega-autophagy is an extreme form of autophagy that occurs when the vacuolar membrane becomes permeable or ruptures.

Previous studies demonstrated that several autophagy-related genes have been discovered in different crop plants. Recently, ATG homologs have been discovered in plants as well as animals, whereas yeast (*Saccharomyces cerevisiae*) is the very first organism in which the ATG homolog was discovered (Rehman et al., 2021). Besides, in many plant species number of ATG homologs have been identified, such as in model algae Chlamydomonas (*Chlamydomonas reinhardtii*), (Pérez-Pérez and Crespo, 2010), *Arabidopsis* (*Arabidopsis thaliana*) (Kwon et al., 2010), wheat (*Triticum aestivum*) (Cui et al., 2018), rice (*Oryza sativa*) (Marshall and Vierstra, 2018), maize (*Zea mays*) (Pérez-Pérez and Crespo, 2010), tobacco (*Nicotiana tabacum*) (Zhou et al., 2015) and tomato (*Solanum lycopersicum*) (Zhou et al., 2014). The up-regulation of ATG homologue in crop plants enhanced the autophagic flux, boosted seed yield, and fortified deferred aging (Brimson et al., 2021). The expression of *ATG* genes in plants' response to abiotic stress may be controlled at the transcriptional level by certain transcription factors. Such as heat shock transcription factor SlHsfA1a (Wang et al., 2015), ethylene response factor SlERF5 (Zhu et al., 2018) and transcription factor SlWRKY33a/SlWRKY33b (Zhou et al., 2014) in tomato. Moreover, it has been shown that genes responsible for transcription factors play crucial roles in the response of other plants to abiotic stress, except for model plants and crops (Li et al., 2022b; Han et al., 2018, Han et al., 2020, Han et al., 2021; Han et al., 2023). Autophagy-related genes have been extensively investigated in many crops to understand their involvement in mitigating heat stress. Studies have shown that autophagy has a crucial role in alleviating heat stress, leading to the accumulation of autophagosomes in tomatoes, apples, and *Arabidopsis* (Kwon et al., 2010; Zhou et al., 2014; Huo et al., 2020). There was a suggestion that heat stress causes endoplasmic reticulum (ER) stress, which then triggers autophagy. ER stress occurs due to the buildup of unfolded proteins in the endoplasmic reticulum, resulting in the creation of protein aggregates (Yang et al., 2016). The *Arabidopsis AtATG5* and *AtATG7* genes displayed greater susceptibility to heat stress compared to wild-type plants, as seen by heightened wilting, increased electrolyte leakage, and reduced photosynthetic performance. Furthermore, the *AtATG7* gene exhibited an accumulation of insoluble protein aggregates that were tagged with ubiquitin (Zhou et al., 2013). Similarly, Zhou et al. (2014) conducted a study, which revealed that when tomatoes were subjected to heat stress, they observed comparable results in the virus-induced gene silencing (VIGS) of *SlATG5* and *SlATG7*. The temperature is progressively rising due to climate change, mostly caused by the greenhouse effect and global warming. Heat stress impacts all stages of crop plants and immediately decreases the yield and productivity. Developing heat-tolerant crop varieties is imperative to meet the rising food requirements of the expanding

population amidst the challenges presented by climate change. This is a novel investigation that identified the autophagy-related genes of subfamily *StATG18* in potato plants on the base of genome-wide identification through bioinformatics analysis. A comprehensive search approach included 6 putative *StATG18* subfamily genes comprising *StATG18a, StATG18b, StATG18c, StATG18d, StATG18f*, and *StATG18h*.

To further understand the functional, structural, and evolutionary characteristics of potato *StATG18* subfamily genes, we analyzed the phylogenetic relationship, chromosomal distribution, and gene duplication, analysis of conserved motifs and gene structure, interspecific collinearity relationship, and cis-regulatory elements in potatoes. An extensive investigation was carried out on differential expression analysis of the *StATG18* subfamily gene in various tissues and organs such as tuber, flower, petiole, stem, stolon, leaf, and root of potato plants and then under heat stress, differential expression analysis of roots, stems, and leaves of potato plants were also performed by using qRT-PCR analysis. Additionally, functional validation of the novel gene *StATG18a* response to heat stress will be provided in this article. This article will also provide a fresh perspective for researchers to understand the molecular, physiological, and biochemical processes of the *StATG18a* gene in potato plants under heat stress.

2 Materials and methods

2.1 Identification of *StATG18* subfamily genes in potato plants

The phylogenetic tree of potato *StATG18* subfamily genes with other species such as *Arabidopsis*, rice, and tomato has been constructed as shown in Supplementary Figure 1. It was discovered that the nucleotide sequences of the *StATG18* subfamily genes may be used to find the genes inside the potato genome using the BLAST database of potatoes (http://spuddb.uga.edu/blast.shtml). Similarly, another approach included using the term "autophagy" to search the potato genome database (http://spuddb.uga.edu/integrated_searches.shtml) to identify genes belonging to the StATG18 subfamily. Following the removal of unnecessary genes, a database of the NCBI conserved domain (https://www.ncbi.nlm.nih.gov/Structure/bwrpsb/bwrpsb.cgi) was used to search all possible potato *StATG18* subfamily genes for autophagy-related domains (Marchler-Bauer et al., 2014). (The Spud DB potato genome database was used to ascertain the chromosomal location, coding sequence (CDS), and genome length of the predicted *StATG18* subfamily genes. The ExPasy website (https://web.expasy.org/protparam/), which provides the ProtParam software (Gasteiger et al., 2003), (was utilized to predict and identify the StATG18 subfamily proteins, amino acid count, theoretical molecular weight (MW), isoelectric point (pI), and grand average of hydropathicity (GRAVY) as shown in Supplementary Table 1. The subcellular localization of *StATG18* subfamily genes was predicted using the Plant-mPLoc website (http://www.csbio.sjtu.edu.cn/bioinf/plant/), as described by Chou and Shen, 2010.

2.2 Multiple sequence alignments and phylogenetic analysis

The protein files of potato (DM v4.03/v4.04), *Arabidopsis thaliana* (TAIR10), rice (*Oryza sativa* v7.0), and tomato (ITAG4.0) were obtained by downloading them from the Rice Genome Annotation Project database, Phytozome v13 database, TAIR database, and Spud DB potato genome database (http://spuddb.uga.edu/). The StATG18 subfamily proteins were found to have multiple sequence alignment (MUSCLE) (Edgar, 2004). With 1,000 Bootstrap repetitions and other default settings (phylogenetic reconstruction, model/method P-distance, alternative types: amino acids, inter-site ratio uniform ratio, full omission for gap deletion data processing), MEGA-X was used to create a phylogenetic tree (Supplementary Figure 1) (Dereeper et al., 2010), using the neighbor-joining (NJ) method.

2.3 Chromosome localization and gene duplication analysis

The Circos software (http://circos.ca/software/download/) was utilized to identify a total of 6 *StATG18* subfamily genes on potato chromosomes (Krzywinski et al., 2009). The physical position of the chromosomes was determined using the Spud DB Potato Genome database (http://spuddb.uga.edu/). The specific genes and their locations may be found in Supplementary Table 1 and Supplementary Figure 2. Duplicate occurrences in *StATG18* subfamily genes were revealed by the default parameter analysis of adopting MCScanX (Multiple collinear scanning toolkit, MCScanX) (https://github.com/wyp1125/MCScanx) (Wang et al., 2012). The TBtools software (https://github.com/CJ-Chen/TBtools/releases) premeditates both non-synonym substitution (Ka) and synonym replacement (Ks), according to Chen et al. (2020). Emanuelsson et al. (2000) calculation formula was used to evaluate the divergence time of duplicated *StATG18* subfamily genes (Supplementary Table 2 and Supplementary Figure 2).

2.4 Conserved motifs and gene structure analysis

The Multiple "Em for Motif Elicitation" (MEME) tool v5.3.0 (http://meme-suite.org/meme-software/5.3.0/meme-5.3.0.tar.gz) was used to identify the conserved motifs of the putative StATG18 protein (Li et al., 2022a), (Supplementary Figure 3, Supplementary Table 3). The following were the established parameters: ten motifs were analyzed, ranging in length from six to two hundred residues. To further annotate all motifs, Inter Pro Scan (http://www.ebi.ac.uk/interpro/) was used (Blum et al., 2021), as shown in Supplementary Figure 4. Six *StATG18* subfamily genes genome sequences and CDS were taken from the potato genome database Spud DB, Using the gene structure display server (GSDS 2.0) (http://gsds.gao-lab.org/) (Hu et al., 2015). The CDS of *StATG18* subfamily genes were connected to the pertinent genomic DNA sequence. Consequently, the distribution of exons and introns in *StATG18* subfamily genes was also determined, as seen in Supplementary Figure 4.

2.5 Synteny analysis of *StATG18* family genes

The protein sequences of rice, potato, *Arabidopsis*, and tomato were absorbed using the previously described method (Supplementary Figure 5). A source of tomato protein sequence data was obtained by Phytozome v13 (https://phytozome-next.jgi.doe.gov/). Using the Makeblastdb program, the protein sequences of the *StATG18* subfamily genes of these four plants were assembled into a local database (Johnson et al., 2008). The protein sequences of the potato and the other three plants were then coherent using the Blastp software (Jacob et al., 2008). The linear connection was assembled using the MCScanX software (https://github.com/wyp1125/MCScanx) (Wang et al., 2012).

2.6 Cis-elements in the promoter of *StATG18* family genes

The Perl programming language retrieved the 2000 bps DNA sequence of the 5´ end non-coding region upstream of the *StATG18* subfamily genes with the start codon "ATG". Next, download the promoter region sequence using PlantCARE (http://bioinformatics.psb.ugent.be/webtools/plantcare/html/), examine each binding site, and forecast its possible function in the cis-regulatory elements displayed in Supplementary Table 4, Supplementary Figure 6 (Lescot et al., 2002).

2.7 Plant growth and heat treatment

In this study, the potato (*Solanum tuberosum* L.) variety 'Atlantic' (pH 5.8–6.0) was cultivated on MS medium containing 3% sucrose and 0.7% agar. A Biotron was used for the incubation, which had a temperature of 22°C, an 8-hour dark cycle, and a 16-hour photoperiod (2800 Lx). After four weeks, they were grown on MS media and given heat treatment (35°C) at different time intervals, such as 0 (control) 1, 2, 4, 8, 16, 24, and 48 h for three biological replicates and three technical replicates. Leaves stems, and roots of harvested plants were stored in liquid nitrogen at -80°C, and the *StATG18* subfamily genes were detected by quantitative reverse transcription-PCR (qRT-PCR). The sprouting tubers were grown to a developmental stage that allowed for the collection of leaves, flowers, petioles, stems, stolons, and roots to determine the differences in *StATG18* subfamily gene expressions across different tissues. The tubers were then gathered until they attained the mature stage. The samples were frozen in liquid nitrogen at -80°C before analyzing the relative expression level of *StATG18* subfamily genes (*StATG18a*, *StATG18b*, *StATG18c*, *StATG18d*, *StATG18f* and *StATG18*) by qRT-PCR.

2.8 RNA extraction and qRT-PCR analysis

Total RNA was extracted from the obtained samples using the TRIzol RNA Extraction kit (Invitrogen, Carlsbad, CA, USA). Using the First-Strand cDNA Synthesis Kit (TransGen Biotech, Beijing, China), the target genes' first-strand cDNA was created. A LightCycler 480 II real-time PCR machine (Roche, Rotkreuz, Switzerland) was utilized to perform quantitative polymerase chain reaction (qPCR). The reaction mixture consisted of 0.8 µL of 0.5 µM specific primers, 100 ng of cDNA, and 10 µL of SYBR Premix Ex Taq (2 ×) (Takara, Tokyo, Japan). After 3 min of initial incubation at 94°C, the reactions were subjected to 36 cycles of 94°C for 45 s, 59°C for 34 s, and 72°C for 1 min. The *Stef1a* was used as a reference gene for standardization, and relative expression was calculated using the $2^{-\Delta\Delta CT}$ method (Livak and Schmittgen, 2001). Supplementary Table 5 provides a list of primer sequences used in this study.

2.9 Construction and transformation of the plasmid

To create overexpressing *StATG18a* plants (OE plants), the encoding sequence of *StATG18a* was cloned into the pBI121-EGFP plasmid using a previously published method (Li et al., 2020). Transformation studies were conducted using *Agrobacterium tumefaciens* strains LBA4404 for overexpression. Using the previously reported method, potato plants were created to knockdown the expression of StATG*18a* by RNA interference (Ri plants) (Lu et al., 2019). Supplementary Table 5 provides a list of primer sequences used in this study. After being cultivated for about 48 hours at 28°C in LB medium with 50 mg of gentamicin and 50 mg of spectinomycin, plasmid-containing agrobacterium was recovered by centrifugation (5,000 rpm, 10 min) and re-suspended in MS medium (OD600 = 0.3). After being cultivated in Agrobacterium solution for 10 min, the sterile seedling stems (2 cm) were grown in MS medium (pH: 5.8) that included 7.4 g/L agar, 30 g/L sucrose, 0.5 mg/L 6-BA, 2.0 mg/L ZT, 0.2 mg/L GA3, and 1.0 mg/L IAA. The growth medium was then kept in the dark for 48–72 hours. The seedlings were then placed in a differentiation medium (MS, 7.4 g/L agar, 30 g/L sucrose, 300 mg/L Timentin, 100 mg/L kan, 0.5 mg/L 6-BA, 2.0 mg/L ZT, 0.2 mg/L GA3, and 1.0 mg/L IAA; PH: 5.8), and changed every two weeks. Once adventitious roots were induced, the resistant adventitious buds were moved to a root media that had been prepared (MS + 7.4 g/L agar + 30 g/L sucrose + 300 mg/L Timentin + 100 mg/L kan, pH=5.8).

2.10 Subcellular localization of the StATG18a protein

To find out the subcellular localization of the StATG18a protein in potato plants, the *StATG18a* (XM_006356959.2) was amplified using the primers (pBI121-EGFP), with forward primer (5'-

ATGGCCACTGTTTCCCCTCTCC-3') and reverse primer (5'-CGAGGCCTTTTCGGACTTC AGA-3') sequences. After being ligated into the pBI121-EGFP vector and mediated by the *Agrobacterium tumefaciens* strain (Gv3101), the recombinant plasmid pBI121-EGFP-StATG18a was created. The total RNA was then extracted for PCR examination. Tobacco epidermal cells are injected with the recombinant plasmid Gv3101 (Sparkes et al., 2006). These plants were maintained at 24°C for 12 hours in a dark greenhouse. After being treated for 48 hours, the plant's epidermal cells were extracted, and the stained piece was then cut apart. Leica TCA confocal scanning laser microscope (Leica, Weztlar, Germany) was used to detect the green fluorescent protein signals.

2.11 Phenotypic analysis between transgenic and non-transgenic (NT) potato plants

Again four-weeks-old seedlings of transfected and non-transfected potato plants were grown in MS media containing 8% sucrose. The seedlings were cultivated for 30 d to create potato tubers, and then the sprouting tubers were cultivated in pots (26.2 cm diameter, 24.8 cm height) supplemented with nutrition soil and vermiculite (1:1, v/v). To determine the growth indexes (plant height, total fresh and dry weights, as well as fresh and dry root weights) transgenic and non-transgenic potato plants were grown in pots for 6 weeks as a control, then potted plants (transgenic and non-transgenic) were grown for another six-weeks and subjected to heat stress for 48 hours before returning to normal temperature for 7 d. Similarly, again potted plants (transgenic and non-transgenic) were grown for another six weeks subjected to heat stress for 48 hours, and returned to normal temperature growth state for 14 d. The point where the soil surfaces meet the apex of the shoot was used to measure the height of the plant. The biomass was calculated by weighing all of the plant's fresh and dried components together. The entire plant was maintained in an oven at 70°C until consistent bulks were reached in order to determine the dry weight. In this experiment, there was a complete random disturbance of the triplicated treatments.

2.12 Determination of physiological and biochemical indicators

Four-week-old transgenic and non-transgenic potato plantlets were cultivated in MS media supplemented with 8% sucrose to encourage tuber formation. The sprouting tubers were cultivated in pots for six weeks with soil water content in the pots was 70–75%, soil water content was monitored at 10:00 and 16:00 every day using TDR-300 sensors (Spectrum R, Aurora, IL, USA). The leaves were subjected to heat treatment at different time intervals (0, 4, 8, 16, 24, and 48 h), after which they were collected and measured using methods previously reported for proline (Bates et al., 1973), malondialdehyde (MDA) (Heath and Packer, 1968) and hydrogen peroxide (H_2O_2) (Bouaziz et al., 2015), as well as superoxide dismutase (SOD), catalase (CAT), and peroxidase (POD) (Li, 2000). Each treatment was arranged in triplicate with a completely random configuration. A total of 270 pots (5 lines × 6 treatments × 3 replicates × 3 pots) were used in each repeat, with 3 pots per treatment and 1 plant per pot.

2.13 Measurements of gas exchange parameters

The third leaf from the top of the plant was detected between 9:30 and 11:30. The stomatal conductance, transpiration rate, and net photosynthetic rate were measured using a portable photosynthetic LI-6400XT system (Li-COR, Lincoln, NE, USA). A fixed photon flux density of 1500 $\mu mol \cdot m^{-2} \cdot s^{-1}$ was used. Relative humidity in the leaf chamber ranged from 60 to 70 percent. There was 400 µmol/mol of CO_2. Each treatment was set up in triplicate using a fully random design. There were 3 pots and 1 plant per pot in each repeat for every treatment, for a total of 270 pots (5 lines × 6 treatments × 3 replicates × 3 pots).

2.14 Statistical analysis

All statistical analyses were done using IBM SPSS 19.0 Statistical Software (IBM, Chicago, IL, USA) and GraphPad Prism Software (GraphPad, San Diego, CA, USA). The findings are shown as mean plus standard deviation. The program GraphPad Prism was used to design line charts and histograms. One-way ANOVA with the Tukey test, Dunnett's T3 for posthoc analysis, or two-way ANOVA adjusted by Sidak's multiple comparisons test was used for multiple comparisons.

3 Results

3.1 Genome-wide identification of the *StATG18* subfamily genes in potato

The availability of the nucleotide sequence facilitated the identification of all the genes belonging to the *StATG18* subfamily in potatoes. After a thorough search and validation of the entire potato genome, a total of 6 potential *StATG18* subfamily genes were identified. Members of the *STATG18* gene subfamily in potato plants were identified and classified, and Supplementary Table 1 displayed the physicochemical properties and characteristics of *STATG18* subfamily genes found in the potato genome. Using the Spud DB potato genome database, the anticipated chromosomal position, CDS, and genome length of the *StATG18* subfamily genes were determined. Supplementary Table 1 provided the following information, which was utilized to assess the identified *StATG18* subfamily genes: protein ID, gene ID, chromosomal position, strand type, amino acid length (AAL),MW, pI, GRAVY and subcellular localization. The maximum MW was given for *StATG18h* (95453.87), amino acid length (878), while the minimum was given for *StATG18b* (39707.58), amino acid length (365). Similarly, the maximum pI was observed for *StATG18f*a (8.44), whereas the minimum was 6.3 for *StATG18h*. The maximum

positive value for GRAVY was calculated for *StATG18b* (0.13) and the minimum negative values amounted to *StATG18f* (-0.283). The subcellular localization described that the *StATG18a* is localized in the cytoplasm as well as in the nucleus, *StATG18b, StATG18c*, and *StATG18d* are located only in the nucleus, while *StATG18f* is located in the nucleus as well as chloroplast and *StATG18h* is only located only in the chloroplast.

3.2 Polygenetic analysis of *StATG18* subfamily members in potato

An evolutionary tree was generated to analyze the phylogenetic relationship among members of the *StATG18* subfamily in potatoes and other species, including *Arabidopsis*, rice, and tomato, as depicted in Supplementary Figure 1. Phylogenetic analysis revealed that the StATG18 subfamily protein sequences were extremely comparable to their homologues (*Arabidopsis*, rice, and tomato) and it is evident from the observation that many internal branches have maximum bootstrap values that pairs of potentially orthologue proteins with comparable functions have been derived from a common ancestor in a statistically valid manner. The phylogenetic tree also showed that the potato *StATG18* subfamily genes were more closely related to tomatoes. The *StATG18* subfamily genes in potatoes (*StATG18a*, *StATG18b*, *StATG18c*, *StATG18f*, and *StATG18h*) have a one-to-one correspondence with their tomato counterparts (*SlATG18a*, *SlATG18b*, *SlATG18c*, *SlATG18f*, and *SlATG18h*), as seen in Supplementary Figure 1 with bootstrap values of 100. These proteins may play similar functions *in vivo*.

3.3 Chromosomal localization and gene replication analysis of *StATG18* subfamily genes

The physical map positions of the 6 *StATG18* subfamily genes on 12 chromosomes of the potatoes were displayed in Supplementary Figure 2. The distribution of these *StATG18* subfamily gene homologs throughout the chromosomes appeared to be irregular. The *StATG18* subfamily genes, such as *StATG18a* and *StATG18d* are located on chromosomes 8, *StATG18b* and *StATG18h* are situated on chromosome 7, *StATG18c* is positioned on chromosome 1, and *StATG18f* is found on chromosome 12. The duplicate chromosomal regions at different lengths were displayed by the red lines in Supplementary Figure 2. The red line connected the duplicate chromosomal portions on chromosome 8, which connected the *StATG18a* gene with *StATG18d.* Additionally, The Ka/Ks ratio is a useful indication for understanding the process of gene differentiation after replication. The *StATG18* subfamily genes, *StATG18a/StATG18d* have a Ka/Ks ratio of less than 1, indicating that these duplicates were selected for the following purification. Moreover, no replicator pair greater than one is found, indicating that positively selected replicators are absent from the potato *StATG18* subfamily genes. Supplementary Table 2 computes the time needed to replicate the event. The previous 17.76 million years of replication occurrences for the pair *StATG18a*/*StATG18d* were detected. As indicated in Supplementary Table 2, a Ka/Ks analysis and an estimation of the absolute dates for the duplication events between the duplicated *StATG18* subfamily genes in potatoes were noted.

3.4 Conserved motifs and gene structure analysis

A tool called MEME motif was utilized to perform conservative motif analysis of ATG18 subfamily proteins in potato, *Arabidopsis*, rice, and tomato, based on their amino acid sequences. Within *StATG18* subfamily members, the conserved motifs are numbered from 1 to 10. The highest number of conservative motifs were found in the *StATG18a* (7), *StATG18c* (7), and *StATG18d* (7) and minimum numbers were found in *StATG18b* (4), while the rest of the *StATG18* subfamily members have 5 numbers of conservative motifs shown in Supplementary Figure 3 and Supplementary Table 4. These analyses revealed that all StATG18 subfamily members in potato have similar motif composition to ATG18 subfamily members in *Arabidopsis*, rice, and tomato, with a high degree of homology. Similar amino acid conserved domain composition suggests that similar gene functions may exist. The distribution of these conserved motifs also indicates that *StATG18* subfamily genes are relatively conserved in the evolutionary process.

In comparing the exon-intron architectures of potato *StATG18* subfamily genes to those of *Arabidopsis*, rice, and tomato, it was found that the most of *StATG18* subfamily genes exhibited greater conservatism in terms of exon length and number. Additionally, a noticeable variation in exon-intron structure was seen when compared to those of *Arabidopsis* and rice. To investigate the structural variety of *StATG18* subfamily gene sequences, the quantity and length of introns and exons in *StATG18* subfamily genes were also measured. The 6 *StATG18* subfamily genes are categorized and compared to the ATG18 subfamily genes of rice, tomato, and *Arabidopsis*, as seen in Supplementary Figure 4. Furthermore, the exon numbers varied in each member of subfamily *StATG18*, such as *StATG18a*, and *StATG18d* containing 4 exons, *StATG18f*, and *StATG18h* have 7 exons, and *StATG18b* has 11 exons. The intron length of *StATG18* subfamily genes was given as *StATG18a* (3.8 Kb), *StATG18b* (4.8 Kb), *StATG18c* (2.6 Kb), *StATG18d* (2.7 Kb), *StATG18f* (1.9 Kb), and *StATG18h* (4.5 Kb). Certain *StATG18* subfamily genes revealed similarities in the length and number of exon-intron compositions with other plant species, which suggests that the potato, *Arabidopsis*, rice, and tomato ATG18 subfamily genes may be consistent in specific functions.

3.5 Synteny analysis and identification of cis-regulatory elements of *ATG18* subfamily members in potato

The study of gene evolution can offer a more thorough understanding of the roles of *StATG18* subfamily genes. As Supplementary Figure 5 illustrates a comparative synteny map among the genomes of potatoes, *Arabidopsis*, rice, and tomatoes. Three orthologous genes were identified in *StATG18* and *AtATG18*

10.3389/fpls.2024.1439972

subfamily members (Supplementary Figure 5). The chromosomes 1 of *Arabidopsis* and potato contain an orthologous gene (PGSC0003DMT400063510/AT1G54710.1), whereas chromosome 4 of *Arabidopsis thaliana* and chromosome 7 of potato contain an orthologous gene (PGSC0003DMT400028996/AT4G30510.1). There was a collinear relationship among *AtATG18f* (AT5G5 4730.1), *StATG18f* (PGSC0003DMT400065820) and *StATG18h* (PGSC0003DMT400049486) on chromosome 5 of *Arabidopsis Thaliana*. Three gene pairs in rice have a collinear relationship with potatoes. There is also a pair of orthologous genes on chromosome 1 of each rice and potato (PGSC0003DMT400063510/LOC_Os01g70780). A pair of orthologous genes between chromosome 1 of rice and chromosome 7 of potato (PGSC0003DMT400049486/LOC_Os01g57720) was also detected. Similarly, chromosome 2 of rice and chromosome 7 of potato also have a pair of orthologous genes (PGSC0003DMT400028996/LOC_Os02g54910). However, as shown in Supplementary Figure 5, the *ATG18* family members in tomatoes are collinear in all *ATG18* family members in potatoes.

To investigate the biological functions and regulatory networks of *StATG18* subfamily genes in potatoes, we obtained the promoter region sequence located 2000 bp upstream of these genes. We then analyzed the cis-acting elements using Plantcare website and identified 37 cis-acting elements. Most of them have roles linked to light responsiveness, hormones, metabolism, regulation, and stress. More specifically, eight light-responsive modules, four MYB binding sites, four components related to various stressors (cold, drought, and wound), three auxin-responsive elements, two gibberellin-responsive elements, one MeJA-responsive element, one salicylic and abscisic acid component each, and some cis-elements were involved in regulation as the metabolism of various substances were linked to the hormone-response elements. Furthermore, as Supplementary Figure 6 illustrates most cis-regulatory elements were specifically associated with endosperm expression, anaerobic induction, regulation of zein metabolism, differentiation of palisade mesophyll cells, circadian control, regulation of the cell cycle, flavonoid biosynthesis, and regulation that is specific to seeds. According to these results, *StATG18* subfamily genes could be involved in metabolic regulation, biochemical stimulation, growth and development of potatoes, hormone signaling transduction, and the regulation of different stress responses. Number statistics of different 37 cis-regulatory elements in promoter regions of potatoes for different genes (*StATG18a*, *StATG18b*, *StATG18c*, *StATG18d*, *StATG18f*, and *StATG18h*) of subfamily *StATG18* were given in Supplementary Table 5. In particular, the majority of the genes were found to be involved in metabolic control, hormone stimulation, light-responsiveness, stress-responsiveness, and metabolism, all of which define the important roles that *StATG18* subfamily genes play in signal transduction and evolutionary processes.

3.6 Different *StATG18* subfamily genes were recognized as differently expressed in various tissues and organs of potato plants under heat stress.

Using qRT-PCR analysis, the relative mRNA expression pattern showed distinct *StATG18* subfamily genes that were found in potato plants' tuber, flower, petiole, stem, stolon, leaf, and root, as shown in Figures 1A–F. The highest level of expression was seen in the roots for *StATG18a*, *StATG18b*, *StATG18c*, and *StATG18f*, while *StATG18d* showed the highest expression in the leaf, and *StATG18h* presented the highest expression in the flower, as shown in Figure 1. In addition, the *StATG18b* and *StATG18f*

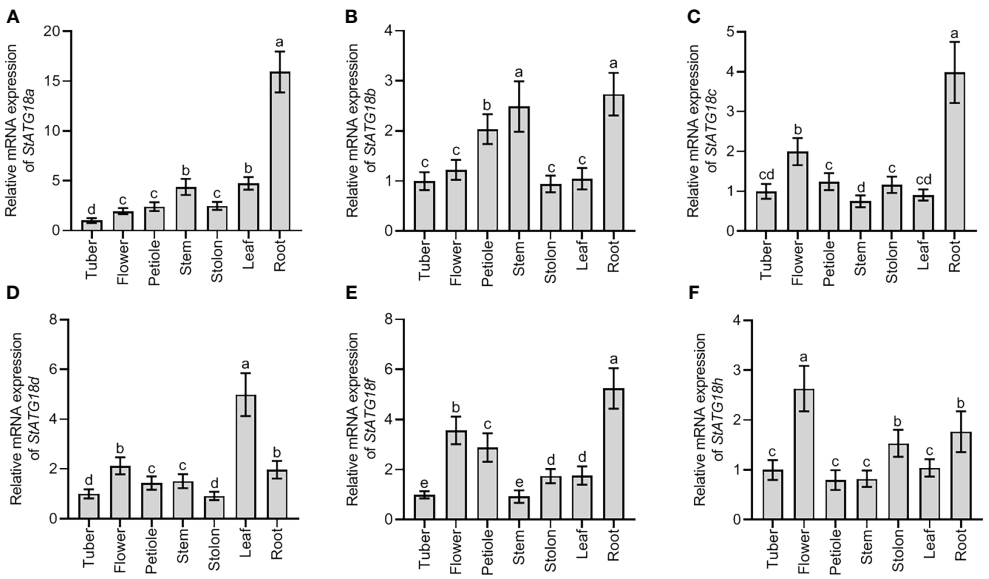

FIGURE 1
Expression profiles of *StATG18* subfamily genes in different tissues of potato. Transcript levels of **(A)** *StATG18a*, **(B)** *StATG18b*, **(C)** *StATG18c*, **(D)** *StATG18d*, **(E)** *StATG18f*, and **(F)** *StATG18h* at mRNA levels, in the tuber, flower, root, petiole, stem, leaf and root. Data were the means ± standard deviation. Different letters indicated significant differences between the two groups (p-value less than 0.05, calculated by one-way ANOVA, followed by LSD and Duncan or Dunnett's T3).

10.3389/fpls.2024.1439972

genes showed higher levels of expression in the stem and petiole, and in the flower and petiole, respectively. The findings suggest that the *StATG18* subfamily genes have a role in the growth and development of different tissues and organs in potatoes. Additionally, we inspected the relative mRNA expression profile of *StATG18* subfamily genes (*StATG18a, StATG18b, StATG18c, StATG18d, StATG18f*, and *StATG18h*) in roots, stems and leaves of potato plants under heat stress at different time intervals (0, 1, 2, 4, 8, 16, 24and 48 h), while (0 h) was considered as control group. Results from qRT-PCR analysis exhibited that the *StATG18a* in roots, stems, and leaves were up-regulated ($p < 0.05$) after heat treatment. In the same way, the rest of the *StATG18* subfamily genes (*StATG18b, StATG18c, StATG18d, StATG18f*, and *StATG18h*) showed up-regulation first and then down-regulation expression in roots, stems, and leaves after heat treatment at different time intervals showed in Figure 2.

3.7 Subcellular localization analysis of StATG18a

The protein localization of StATG18a was predicted using the Subcellular Plant-mPLoc website (http://www.csbio.sjtu.edu.cn/bioinf/plant-multi/), which predicted that the StATG18a protein is located in the nucleus. To govern the subcellular localization of StATG18a, The recombinant plasmid pBI121-EGFP-StATG18a was transformed into *Agrobacterium tumefaciens* GV3101 and then transiently transformed into tobacco. The green fluorescence from the EGFP vector expressed by pBI121-EGFP-StATG18a demonstrated that the StATG18a was observed in the cytoplasm as well as in the nucleus by confocal-scanned microscopy as shown in Figure 3. To confirm the localization of StATG18a, the EGFP empty vector or control vector was presented in the membrane, cytoplasm, and nucleus, while the pBI121-EGFP-StATG18a was detected in the cytoplasm and nucleus, which confirmed the presence of StATG18a in potato plants. Despite the *StATG18a* being discovered in potato plants, its role has not been specified to date, which is needed for further analyses under heat stress conditions.

3.8 *StATG18a* was involved in modulating potato growth

We created overexpressing *StATG18a* and knockdown potato plants to examine the effects of *StATG18a* on potato growth under heat stress. After screening stably transformed plants, their expression efficiency was confirmed by RT-qRCR, as seen in Figures 4A, B (***$p < 0.001$). We observed the phenotypes of transgenic and non-transgenic plants under normal and heat-stress conditions. Phenotypic analysis of transgenic and non-transgenic potato plants showed no significant difference under control conditions (Figure 4C1). After 48 hours of heat stress treatment, there was still no significant difference in phenotype, as shown in Figure 4C2. However, on the 7th and 14th d after heat treatment, we found that some leaves of non-transgenic and *StATG18a* knockdown plants turned yellow and began to wilt, while the leaves of overexpressing *StATG18a* transgenic plants remained normal and did not wilt, as shown in Figures 4C3, C4. There were no statistically significant changes in plant height for all potato plants after 7 and 14 d of heat stress treatment. However, transgenic potato plants (OE-2, OE-5, Ri-1, and Ri-4) showed significant differences in total fresh and dry weights, as well as root fresh and dry weights, as shown in Figures 4D–H. 7 d after heat treatment, the total fresh weight of overexpression plants (OE-2 and OE-5) exhibited an increase of 1.17 and 1.15 folds, respectively, compared to non-transgenic plants. In contrast, the total fresh weight of RNA interference-expressing plants (Ri-1 and Ri-4) decreased by 11% and 13%, respectively, when compared to the control group. Similarly, 14 d after heat treatment, the total fresh weight of overexpression plants (OE-2 and OE-5) showed an increase of 1.19-fold and 1.24-fold, respectively, relative to non-

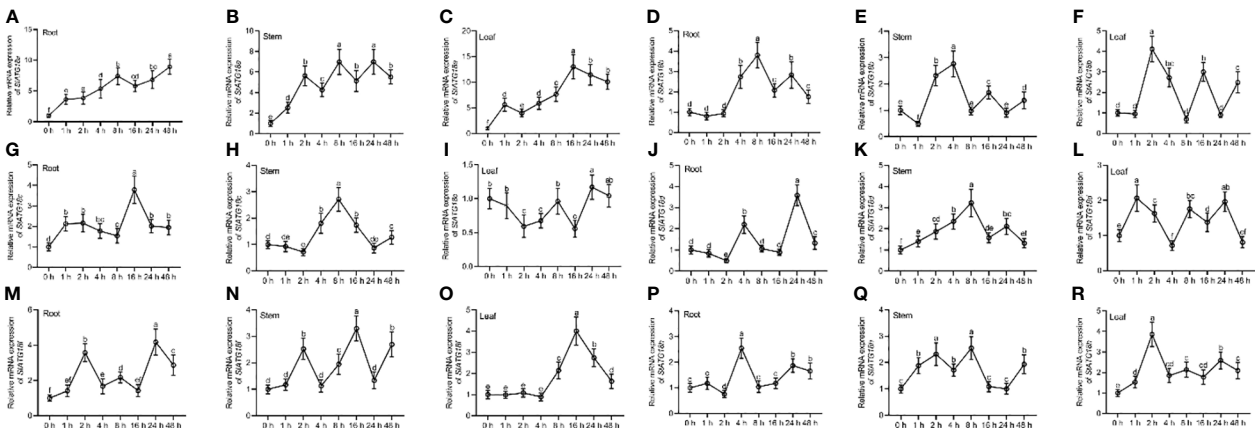

FIGURE 2
Expression profiles of *StATG18* subfamily genes in potato leaves, stem and roots in response to heat stress. Transcript levels of **(A–C)** *StATG18a*, **(D–F)** *StATG18b*, **(G–I)** *StATG18c*, **(J–L)** *StATG18d*, **(M–O)** *StATG18f* and **(P–R)** *StATG18h* in leaves, stems, and roots under heat stress treatment at different time intervals (0, 1, 2, 4, 8, 16, 24, and 48h). Data were the means ± standard deviation. Different letters indicated significant difference between two groups (*p*-value less than 0.05, calculated by one-way ANOVA, followed by LSD and Duncan or Dunnett's T3).

10.3389/fpls.2024.1439972

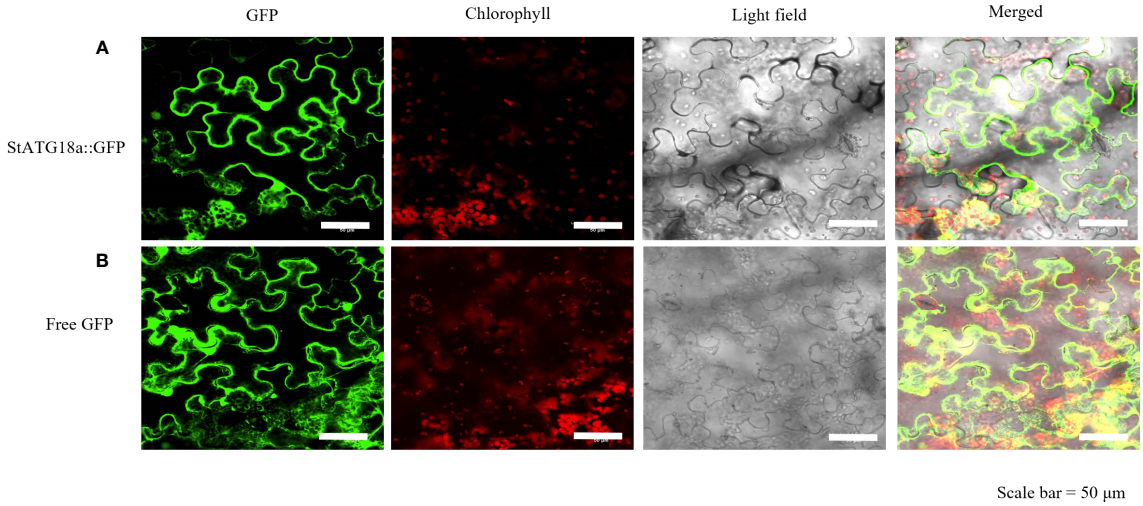

FIGURE 3
Subcellular localization of StATG18a-GFP fusion protein in *Nicotiana benthamiana* leaves. **(A)** Confocal scanning laser microscopy analysis of tobacco transformed with pBI121-EGFP-StATG18a. **(B)** The empty vector (GFP) served as a control. Bar = 50 μm.

transgenic plants. Concurrently, the total of fresh weight of RNA interference-expressing plants (Ri-1 and Ri-4) was reduced by 20% and 12%, respectively, compared to the control group. On the 7th d after the heat treatment period, the root fresh weight of overexpression plants (OE-2 and OE-5) was found to be 1.3-fold and 1.23-fold greater than that of non-transgenic plants, respectively. Conversely, the root fresh weight of RNA interference-expressing plants (Ri-1 and Ri-4) was diminished by 13% and 19%, respectively, in comparison to non-transgenic plants. Likewise, on the 14th d after the heat treatment period, the root fresh weight of overexpression plants (OE-2 and OE-5) was observed to be increased by 1.24-fold and 1.27-fold, respectively, relative to non-transgenic plants. However, the root fresh weight of RNA interference-expressing plants (Ri-1 and Ri-4) was reduced by 19% and 21%, respectively, when compared to non-transgenic plants. Furthermore, 7 d after heat treatment, the dry weight of overexpression plants (OE-2 and OE-5) was found to be increased by 26% and 30%, respectively, in comparison to non-transgenic plants. In contrast, the dry weight of RNA interference-expressing plants (Ri-1 and Ri-4) was decreased by 10% and 14%, respectively, relative to the non-transgenic lines. Besides, 14 d after heat treatment, the dry weight of overexpressing *StATG18a* plants (OE-2 and OE-5) was increased by 1.33 and 1.27 times greater than that of non-transgenic plants, respectively. In contrast, the dry weight of RNA interference-expressing plants (Ri-1 and Ri-4) was reduced by 21% and 19%, respectively, when compared to the non-transgenic potato lines. Correspondingly, 7 d after heat treatment, the root dry weight of overexpressing *StATG18a* plants (OE-2 and OE-5) exhibited an increase of 43% and 52%, respectively, relative to non-transgenic plants. The root dry weight of RNA interference-expressing plants (Ri-1 and Ri-4) was found to be decreased by 6% and 2% than those of non-transgenic potato plants, respectively. Similarly, 14 d after heat treatment, the root dry weight of overexpressing *StATG18a* plants (OE-2 and OE-5) was determined to be increased by 1.33-fold and 1.28-fold than those of non-transgenic plants, respectively. When compared to non-transgenic plants, the root dry weight of RNA interference-expressing plants (Ri-1 and Ri-4) was reduced by 20% and 16%, respectively. In summary, the *StATG18a* has been shown to mitigate the detrimental effects of heat stress and plays a crucial regulatory role in the growth and development of potatoes under such stress conditions.

3.9 *StATG18a* affected the physiological indexes of potato plants under heat stress conditions

Under normal conditions, compared with non-transgenic plants, the activities of SOD, CAT, and POD activities, as well as the amounts of H_2O_2, proline, and MDA, were not significantly changed in overexpressing *StATG18a* and knockdown potato plants as shown in Figure 5. Under heat stress conditions, the overexpression of *StATG18a* resulted in elevated levels of SOD activity (Figure 5A), CAT activity (Figure 5B), POD activity (Figure 5C), and proline content (Figure 5D). In contrast, the knockdown expression of *StATG18a* led to a reduction in the levels of SOD activity (Figure 5A), CAT activity (Figure 5B), POD activity (Figure 5C), and proline content (Figure 5D) as compared to the non-transgenic plants ($*p < 0.05$, $**p < 0.01$). Concurrently, we noticed a substantial decrease ($*p < 0.05$, $**p < 0.01$) in the contents of H_2O_2 (Figure 5E) and MDA (Figure 5F) in overexpression of *StATG18a* potato plants when subjected to heat stress, as compared to the non-transgenic plants. Meanwhile, we observed that the levels of H_2O_2 (Figure 5E) and MDA (Figure 5F) in potato plants overexpressing *StATG18a* were significantly reduced ($*p < 0.05$, $**p < 0.01$) during heat stress, as compared to the non-transgenic plants. However, we noticed the reverse results for the contents of H_2O_2 (Figure 5E) and MDA (Figure 5F) in the knockdown expression of *StATG18a* potato plants ($*p < 0.05$, $**p <$

10.3389/fpls.2024.1439972

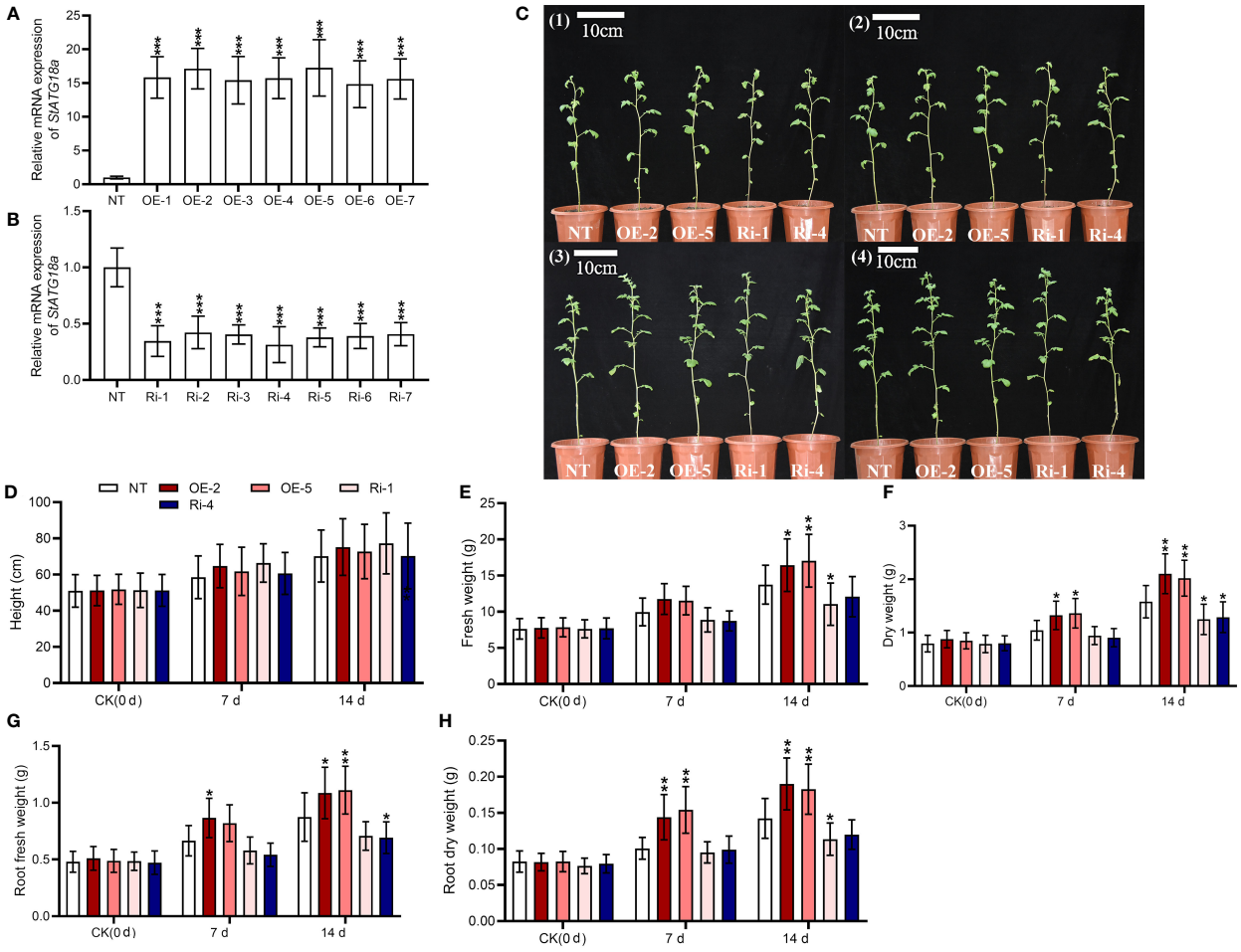

FIGURE 4
Effects of *StATG18a* on potato plant growth phenotypes. Transcript levels of *StATG18a* in **(A)** overexpressing *StATG18a* and **(B)** knock down potato plants (*p < 0.05, **p < 0.01, ***p< 0.001). One-Way ANOVA corrected by Dunnett (Figures 5A, B, n = 9). **(C1)** The phenotypes of transgenic and non-transgenic potato plants were grown normally for 6 weeks, **(C2)** The phenotypes of transgenic and non-transgenic potato plants treated with 35°C heat stress for 48 hours after 6 weeks of normal growth, **(C3)** The phenotypes of transgenic and non-transgenic potato plants that recovered 7 d after heat stress treatment, **(C4)** The phenotypes of transgenic and non-transgenic potato plants that recovered 14 d after heat stress treatment, and **(D)** plant height, **(E)** total fresh weights and **(F)** dry weights, as well as **(G)** root fresh weights and **(H)** dry weights were measured after the heat treatment at different time intervals (0 d, 7 d and 14 d), Bar = 10 cm. NT, non-transgenic plants; OE, pBI121-EGFP-StATG18a-transgenic plants (OE-2 and OE-5); Ri, pART-StATG18a-RNAi-transgenic plants (Ri-1 and Ri-4); Two-Way ANOVA amended by Tukey (Figures 4D–H, n = 9; *p < 0.05, **p< 0.01).

0.01) (Figures 5E, F). The research showed that when exposed to heat stress, transgenic lines with overexpressing *StATG18a* had less physiological harm compared to the non-transgenic potato lines. Conversely, lines with RNA interference expression had more physiological damage than the NT lines. Therefore, *StATG18a* influenced the physiological functions of potato plants in response to heat stress.

3.10 *StATG18a* affected the photosynthesis of potato plants under heat stress conditions

Moreover, we observed that net photosynthetic rate (Figure 6A), transpiration rate (Figure 6B), and stomatal conductance (Figure 6C) were not significantly changed by *StATG18a* overexpression and knockdown compared to non-transgenic plants under normal conditions ($p > 0.05$). However, we detected that compared with non-transgenic plants net photosynthetic rate (Figure 6A) of potato plants with high overexpression of *StATG18a* increased, and the transpiration rate (Figure 6B) and stomatal conductance (Figure 6C) decreased under heat stress. Meanwhile, *StATG18a* knockdown decreased net photosynthetic rate (Figure 6A), while transpiration rate (Figure 6B) and stomatal conductance were increased (Figure 6C) (*p < 0.05, **p < 0.01) under heat stress conditions. On 48h of treatment, the net photosynthetic rates of OE-2 and OE-5 were 1.47 and 1.68 times more than those of NT plants, respectively, while Ri-1 and Ri-4 were increased by 53% and 43% compared to NT plants, respectively. On the contrary, the transpiration rate and stomatal conductance for all plants were decreased, the rate of that decline was faster in OE-2 and OE-5, and values were, given as 30%–49%

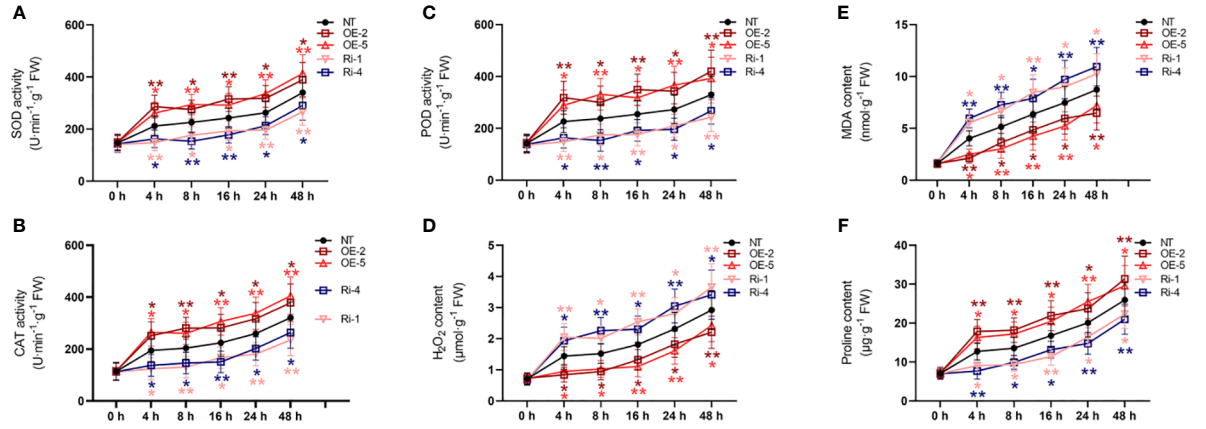

FIGURE 5
Effects of *StATG18a* on **(A)** SOD activity, **(B)** CAT activity, **(C)** POD activity, **(D)** H_2O_2 content, **(E)** MDA content, and **(F)** proline content. Potato plants (transgenic and non-transgenic) were treated with heat stress at different time intervals (0, 4, 8, 16, 24, and 48h), and examined the SOD, CAT, as well as POD activities, and H_2O_2 MDA as well as proline content. NT, non-transgenic plants; NT, non-transgenic plants; OE, pBI121-EGFP-StATG18a-transgenic plants (OE-2 and OE-5); Ri, pART-StATG18a-RNAi-transgenic plants (Ri-1 and Ri-4); Data were computed by means ± standard deviation; p-values (*p<0.05, **p<0.01) were calculated by ordinary two-way ANOVA, followed by Tukey's multiple comparisons tests (n = 9).

and 40%–53%, respectively, than those of NT plants, while Ri-1 and Ri-4 were increased by 1.5–1.76 and 1.46–1.62 times, respectively, compared to NT plants. It is evident from the above statement that the *StATG18a* plays a significant function in photosynthesis by regulating the net photosynthetic rate, transpiration rate, and stomatal conductance in potato plants under heat stress.

4 Discussion

The prospect of exceedingly hot weather is increasing due to global climate change, and its length is steadily getting longer. This has detrimental effects on crop growth and development, especially in China's north and northwest regions where temperatures can approach 35°C during the potato growing season. Heat Stress modifies the cellular processes, metabolism, physiology, photosynthesis, and phenotype of crop plants, which negatively impacts all stages of crop growth, development, yield, and productivity (Hasanuzzaman et al., 2013). The heat tolerance of cultivars may be assessed using these characteristics (Hastilestari et al., 2018). To overcome these problems, plants acquire several kinds of mechanisms and responses, one such mechanism is autophagy, which is regulated by several *ATGs* that have been discovered in many crop plants (Cao et al., 2021).

In this study, six putative genes belonging to the *StATG18* subfamily were identified by wide-genome analysis data of potatoes (Supplementary Table 1). In a previous study, a polygenetic analysis found 108 putative *TaATGs* from 13 different subfamilies in wheat. The subfamily *TaATG16* has 29 genes categorized based on conserved motifs and exon-intron composition. Moreover, 114 cis-elements were discovered which play a significant role in response to stress, light, and hormonal association (Yue et al., 2018). In our study, chromosomal localization and gene duplication were carried out to find the position of the member of the subfamily *StATG18* genes by phylogenetic investigation. Similarly, conservative motifs distribution and composition as well as intron-exon length and number were also analyzed in potatoes with other crop species, such as *Arabidopsis*, rice, and

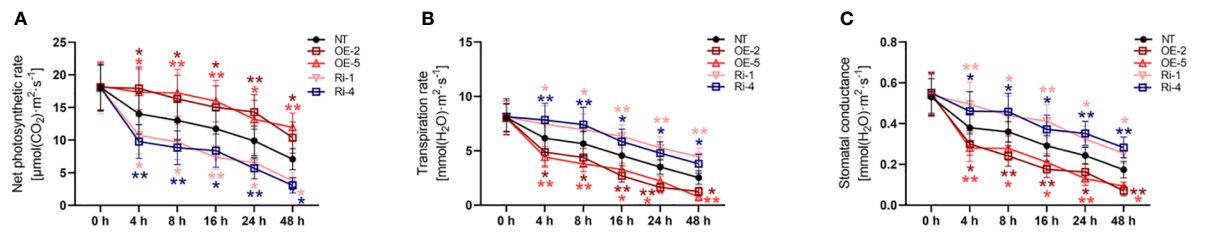

FIGURE 6
Effects of *StATG18a* on **(A)** net photosynthetic rate, **(B)** transpiration rate and **(C)** stomatal conductance under heat conditions.Potato tubers stimulated by transgenic and non-transgenic lines were monitored by cultivation with heat stress treatment at different time intervals (0h, 4h, 8h, 12h, 24h, and 48h). Analyses for heat stress **(A)** net photosynthetic rate, **(B)** transpiration rate, and **(C)** stomatal conductance. NT, non-transgenic plants; OE, pBI121-EGFP-StATG18a-transgenic plants (OE-2 and OE-5); Ri, pART-StATG18a-RNAi-transgenic plants (Ri-1 and Ri-4); Data were computed by means ± standard deviation; p-values (*p<0.05, **p<0.01) were estimated by ordinary two-way ANOVA, followed by Tukey's multiple comparisons tests (n = 9).

tomato. Finally, 37 cis-regulatory elements with different functions have been identified and the phylogenetic relationship between potato and other crop species was drawn by collinear analysis.

The qRT-PCR research demonstrated that the *StATG18* subfamily genes exhibited varying levels of expression in the different tissues (tuber, flower, petiole, stem, stolon, leaf, and root) of potato plants (Figure 1). It is hypothesized that these genes play a role in the growth and development of different tissues and organs in potato plants. Another research on autophagy-related genes of *Medicago truncatula* demonstrated that *MtATGs* have a potential role in the growth and development of plants. The expression profile of these genes was identified in various tested tissues and organs at various stages of seed development. Through microarray analysis, it is reported that the *MtATG* genes showed varied expression in roots, leaves, stems, and flowers in the late seed development stage (Benedito et al., 2008). Additionally, under heat stress, *StATG18* subfamily gene expression was also observed in roots, stems, and leaves of potato plants in our investigation (Figure 2). Furthermore, qRT-PCR analysis suggests that the *StATG18a* exhibited a high expression pattern in roots, stems, and leaves, after subjected to heat treatment, which was further analyzed for heat stress studies. Previous reports indicated that the results of qRT-PCR and RT-PCR showed that *TdATG8* is constitutively expressed in roots and leaves and it is increased in both tissues in response to osmotic stress and PEG-treated leaves and roots, respectively. It also exhibits 24–40 fold increases in *TdATG8* expression levels in roots and leaves under abiotic stress conditions (Kuzuoglu-Ozturk et al., 2012).

In a study, it was found that the subcellular localization investigation of GFP-SiATG8a determined the confirmation of *SiATG8a* protein in the cytoplasm as well as in the membrane in foxtail millet (*Setaria italica* L), while the GFP vector is used as a control (Li et al., 2015). In another investigation, the green fluorescence observation depicted the presence of MdHARBI1–GFP union protein in the nucleus of apples (*Malus domestica*), while GFP is used as a control vector, which was present in the nucleus, cytoplasm, and membrane (Huo et al., 2021). In our study, subcellular localization analysis validated the presence of StATG18a in the cytoplasm and nucleus. Through confocal scanning laser microscopy, the green fluorescence detected the protein of StATG18a in the cytoplasm and nucleus shown in Figure 3. The strong cytoplasmic and nuclear membrane signals from GFP-StATG18a further validated the presence of StATG18a in the cytoplasm and nucleus, whereas the empty or control vector the GFP was presented in the membrane, cytoplasm and the nucleus.

According to previous research reports, wild-type (WT) plants of apples were exposed to 48°C for 6 hours resulting in burned and wrinkled leaves. However, only the young leaves on top of transgenic plants showed indications of dehydration and burn, while mature leaves remained green and robust, and was found that heat stress prompted minor damage to *MdATG18a* overexpressing apple plants (Sun et al., 2018). High temperatures also caused leaf wilting and decreased leaf relative water content (RWC). Heat treatment reduced total chlorophyll concentrations, although the loss was less in transgenic plants compared to WT plants. Heat stress reduced the damage of phenotypes of transgenic apples, indicating that *MdATG18a* plays a vital role in heat stress response (Sun et al., 2018). Our phenotypic analysis of transgenic and non-transgenic potato plants showed that potato plants showed no significant differences in response to heat stress treatment and control conditions (Figures 4C1, C2). Compared with non-transgenic potato lines, the growth and progression of agronomic traits (such as total fresh and dry weight, root fresh and dry weight) of overexpressing *StATG18a* lines (including OE-2 and OE-5) were greatly improved 7 and 14 d after heat treatment. Most NT and knockdown potato plants were slow to recover from the effects of high temperature or their leaves turned yellow and wilted due to high-temperature burns (Figures 4C3, C4), but overexpressing *StATG18a* plants showed tolerance to high temperature and recovered relatively well, with few leaves wilting, which demonstrated the role of autophagy-related genes in potato plants under high-temperature stress.

Environmental stressors cause physiological changes in crop plants, and these changes are considerable enough to gauge a plant's tolerance and resilience to different biotic and abiotic stress scenarios (Tang and Bassham, 2022). Autophagy-related genes are essential for maintaining genome integrity in eukaryotic species. This idea is further supported by the existence of up-regulated genes linked to DNA repair and responses to stimuli that cause DNA damage (Feng and Klionsky, 2017). In a prior investigation, the role of ATGs concerning physiological markers including MDA, H_2O_2, and proline content, as well as POD, SOD, and CAT activity, was evaluated under various abiotic stress conditions. Under salt and drought stress conditions, a significant difference was seen in the levels of proline, MDA, and H_2O_2 as well as in antioxidant enzyme systems (Zhou et al., 2015). Physiological characteristics were examined in this work to evaluate the *StATG18a* gene's tolerance to heat stress. Because heat stress causes an increase in H_2O_2 and MDA concentration and alters the equilibrium of reactive oxygen species (ROS), the *StATG18a*-overexpression potato lines displayed a downward trend in these cases. Therefore, overexpression of *StATG18a* in OE-2 and OE-5 potato plants under heat stress resulted in an improved MDA (Figure 5E) and H_2O_2 (Figure 5D) content, whereas RNA interference expression lines (Ri-1 and Ri-4) displayed elevation in comparison to non-transgenic lines. Overall, the regulating role of overexpressing *StATG18a* potato plants under heat stress is confirmed by the considerable variation in physiological parameters.

Heat stress induces morphological and structural alterations in leaves, the primary organ engaged in transpiration and photosynthesis, resulting in wilting and changes to morphology, anatomy, physiology, and photosynthetic ability (Mathur et al., 2014). Plant photosynthesis is significantly influenced by several factors such as the rate of transpiration and the absorption of CO_2 by leaves, which are both regulated by stomatal behavior (Hu et al., 2018). In a previous report, after four hours of heat treatment, differences in stomatal morphology between overexpressing *MdATG18a* and WT plants were observed in apples. The stomatal aperture was reduced by a high temperature, although the OE lines had less shrinking overall (Huo et al., 2020). It also examined the gaseous exchange characteristics of the overexpressing *MdATG18a* plants following an 18-hour recovery from heat treatment to assess the extent of damage in this respect. No variation in Pn, Gs, Ci, or Tr was seen across plants of various

genotypes under normal temperature conditions. Pn was significantly reduced in plants of all genotypes; however, the two overexpressing *MdATG18a* lines' Pn differences were approximately 1.74 times larger because of the overexpression of the *MdATG18a* gene than those of the WT plants (Huo et al., 2020). In our study similar results were observed, maximum net photosynthesis, transpiration, and stomatal conductance was exposed in all potato lines (transgenic and non-transgenic) under normal conditions. After 4–48 h of heat treatment, the OE-2 and OE-5 transgenic potato lines indicated an upward trend in net photosynthetic rate (Figure 6A) compared to non-transgenic lines due to overexpression of *StATG18a* gene, while knockdown expression of *StATG18a* gene revealed contrary results. Transpiration rate (Figure 6B) and stomatal conductance (Figure 6C) were inhibited due to the overexpression of the *StATG18a* gene after heat stress treatment compared to non-transfected lines. It is very crucial to maintain water balance in plants under high temperatures and dry conditions to avoid wilting. Stomatal behavior directly regulates the rate of transpiration under heat or drought stress, it is very essential to preserve water loss under high temperatures to uphold water equilibrium in plants. Therefore, overexpression of *StATG18a* showed a stronger downward trend in transpiration rate and stomatal conductance to preserve water under heat stress, whereas knockdown expression induces heat stress by exceeding the transpiration rate by increasing stomatal conductance. These confirmations propose that the photosynthetic indices of overexpressing *StATG18a* potato lines OE-2, and OE-5 depicted enhanced progression under heat stress treatment, compared to non-transgenic lines.

5 Conclusion

In conclusion, we identified the *StATG18* subfamily genes in the potato genome. Firstly, a total of 6 putative subfamily *StATG18* members were systematically analyzed for the phylogenetic relationships, chromosome distribution and gene replication, conserved motifs, gene structure, interspecific collinearity relationship, and cis-regulatory elements. Secondly, the expression profile of *StATG18* subfamily genes by qRT-PCR demonstrated the differential expression level in different potato parts (leaf, flower, stem, root, stolon, petiole, and tuber). Additionally, the expression pattern of roots, stems, and leaves was also investigated under heat stress, which validated the high expression level of the *StATG18a* gene in leaves, stems, and roots of potato plants under heat treatment at different time intervals. Finally, our results showed the localization of StATG18a in the cytoplasm and nucleus by green florescence from EGFP expressed by pBI121-EGFP-StATG18a through subcellular localization analysis. Moreover, physiological and photosynthetic indices also depicted the highly significant differences in overexpressing *StATG18a* lines (OE-1 and OE-5), compared to non-transgenic potato lines under heat stress. Additionally, *StATG18a* modulated the growth of transgenic plants, as depicted after the 7^{th} and 14^{th} d of heat treatment the OE-1 and OE-5 potato plants showed less injury and wilting than those of non-transgenic plants. This study not only provides novel insight into *StATG18* subfamily members' characterization and functional identification of potato autophagy but also provides essential evidence about the *StATG18*a gene functional analysis under heat stress in potato plants.

Data availability statement

The datasets presented in this study can be found in online repositories. The names of the repository/repositories and accession number(s) can be found in the article/Supplementary Material.

Author contributions

XZ: Funding acquisition, Investigation, Methodology, Project administration, Software, Supervision, Visualization, Writing – original draft, Writing – review & editing. YM: Conceptualization, Methodology, Visualization, Writing – original draft, Writing – review & editing. WL: Formal analysis, Investigation, Methodology, Visualization, Writing – review & editing. NZ: Conceptualization, Investigation, Methodology, Visualization, Writing – review & editing. HD: Conceptualization, Investigation, Methodology, Visualization, Writing – review & editing. HJ: Conceptualization, Investigation, Project administration, Resources, Validation, Visualization, Writing – review & editing. ZC: Data curation, Investigation, Validation, Visualization, Writing – review & editing. SC: Investigation, Methodology, Validation, Visualization, Writing – review & editing. JZ: Data curation, Investigation, Validation, Visualization, Writing – review & editing. QW: Data curation, Investigation, Visualization, Writing – review & editing. JT: Conceptualization, Data curation, Visualization, Writing – review & editing. YZ: Conceptualization, Formal analysis, Funding acquisition, Investigation, Methodology, Project administration, Resources, Supervision, Validation, Visualization, Writing – original draft, Writing – review & editing. HS: Conceptualization, Data curation, Formal analysis, Investigation, Methodology, Supervision, Visualization, Writing – original draft, Writing – review & editing.

Funding

The author(s) declare financial support was received for the research, authorship, and/or publication of this article. This Research Program was financially supported by the National Natural Science Foundation of China (Grant No. 32360459), the Natural Science Foundation of Guangdong Province, China (Grant No. 2024 A1515010068), the Hainan Provincial Natural Science Foundation of China (Grant No. 322MS116, 323MS095), and Central Public-interest Scientific Institution Basal Research Fund for Chinese Academy of Tropical Agricultural Sciences (Grant No. 1630062024005).

Acknowledgments

We thank Rongkai Wang (Bioediates, Shaanxi, China) for providing the plasmids pBI121-EGFP, pHANNIBAL, and pART.

Conflict of interest

The authors declare that the research was conducted in the absence of any commercial or financial relationships that could be construed as a potential conflict of interest.

Publisher's note

All claims expressed in this article are solely those of the authors and do not necessarily represent those of their affiliated organizations, or those of the publisher, the editors and the reviewers. Any product that may be evaluated in this article, or claim that may be made by its manufacturer, is not guaranteed or endorsed by the publisher.

Supplementary material

The Supplementary Material for this article can be found online at: https://www.frontiersin.org/articles/10.3389/fpls.2024.1439972/full#supplementary-material

References

Anderson, R., Bayer, P. E., and Edwards, D. (2020). Climate change and the need for agricultural adaptation. *Curr. Opin. Plant Biol.* 56, 197–202. doi: 10.1016/j.pbi.2019.12.006

Bates, L. S., Waldren, R. P. A., and Teare, I. D. (1973). Rapid determination of free proline for water-stress studies. *Plant Soil* 39, 205–207. doi: 10.1007/BF00018060

Benedito, V. A., Torres-Jerez, I., Murray, J. D., Andriankaja, A., Allen, S., Kakar, K., et al. (2008). A gene expression atlas of the model legume Medicago truncatula. *Plant J.* 55, 504–513. doi: 10.1111/j.1365-313X.2008.03519.x

Blum, M., Chang, H. Y., Chuguransky, S., Grego, T., Kandasaamy, S., Mitchell, A., et al. (2021). The InterPro protein families and domains database: 20 years on. *Nucleic Acids Res.* 49, 344–354. doi: 10.1093/nar/gkaa977

Bouaziz, D., Charfeddine, M., Jbir, R., Saidi, M. N., Pirrello, J., Charfeddine, S., et al. (2015). Identification and functional characterization of ten AP2/ERF genes in potatoes. *Plant Cell Tissue Organ Cult.* 123, 155–172. doi: 10.1007/s11240-015-0823-2

Brimson, J. M., Prasanth, M. I., Malar, D. S., Sharika, R., Sivamaruthi, B. S., Kesika, P., et al. (2021). Role of herbal teas in regulating cellular homeostasis and autophagy and their implications in regulating overall health. *Nutrients* 13, 2162. doi: 10.3390/nu13072162

Cao, J. J., Liu, C. X., Shao, S. J., and Zhou, J. (2021). Molecular mechanisms of autophagy regulation in plants and their applications in agriculture. *Front. Plant Sci.* 11. doi: 10.3389/fpls.2020.618944

Chen, C., Chen, H., Zhang, Y., Thomas, H. R., Frank, M. H., He, Y., et al. (2020). TBtools: an integrative toolkit developed for interactive analyses of big biological data. *Mol. Plant* 13, 1194–1202. doi: 10.1016/j.molp.2020.06.009

Chou, K. C., and Shen, H. B. (2010). Plant–mPLoc: a top–down strategy to augment the power for predicting plant protein subcellular localization. *PLoS One* 5, e11335. doi: 10.1371/journal.pone.0011335

Cui, G., Sun, F., Gao, X., Xie, K., Zhang, C., Liu, S., et al. (2018). Proteomic analysis of melatonin-mediated osmotic tolerance by improving energy metabolism and autophagy in wheat (*Triticum aestivum* L.). *Planta* 248, 69–87. doi: 10.1007/s00425-018-2881-2

Dereeper, A., Audic, S., Claverie, J. M., and Blanc, G. (2010). Blast-explorer helps you build datasets for phylogenetic analysis. *BMC Evol. Biol.* 10, 8. doi: 10.1186/1471-2148-10-8

Edgar, R. C. (2004). MUSCLE: a multiple sequence alignment method with reduced time and space complexity. *BMC Bioinf.* 5, 113. doi: 10.1186/1471-2105-5-113

Emanuelsson, O., Nielsen, H., Brunak, S., and Von Heijne, G. (2000). Predicting subcellular localization of proteins based on their N-terminal amino acid sequence. *J. Mol. Biol.* 300, 1005–1016. doi: 10.1006/meth.2001.1262

Feng, Y. C., and Klionsky, D. J. (2017). Autophagy regulates DNA repair through SQSTM1/p62. *Autophagy* 13, 995–996. doi: 10.1080/15548627.2017.1317427

Fuqiang, L., Haoliang, D., Yucai, W., Xuan, L., Xietian, C., Lintao, L., et al. (2021). Potato growth, photosynthesis, yield, and quality response to regulated deficit drip irrigation under film mulching in A cold and arid environment. *Res. Sq.* 11, 1–16. doi: 10.1038/s41598-021-95340-9

Gasteiger, E., Gattiker, A., Hoogland, C., Ivanyi, I., Appel, R. D., and Bairoch, A. (2003). ExPASy: The proteomics server for in-depth protein knowledge and analysis. *Nucleic Acids Res.* 13), 3784–3788. doi: 10.1093/nar/gkg563

Han, D., Ding, H., Chai, L., Liu, W., Zhang, Z., Hou, Y., et al. (2018). Isolation and characterization of *MbWRKY1*, a WRKY transcription factor gene from *Malus baccata* (L.) Borkh involved in drought tolerance. *Can. J. @ Plant Sci.* 98, 1023–1034. doi: 10.1139/cjps-2017-0355

Han, D., Han, J., Xu, T., Li, X., Yao, C., Li, T., et al. (2021). Overexpression of *MbERF12*, an ERF gene from *Malus baccata* (L.) Borkh, increases cold and salt tolerance in *Arabidopsis thaliana* associated with ROS scavenging through ethylene signal transduction. *In Vitro Cell Dev. Biol. Plant* 57, 760–770. doi: 10.1016/j.plaphy.2023.01.048

Han, D., Zhou, Z., Du, M., Li, T., Wu, X., Yu, J., et al. (2020). Overexpression of a *Malus xiaojinensis* WRKY transcription factor gene (*MxWRKY55*) increased iron and high salinity stress tolerance in *Arabidopsis thaliana*. *In Vitro Cell Dev. Biol. Plant* 56, 600–609. doi: 10.1007/s11627-020-10129-1

Han, J., Li, X., Li, W., Yang, Q., Li, Z., Cheng, Z., et al. (2023). Isolation and preliminary functional analysis of FvICE1, involved in cold and drought tolerance in Fragaria vesca through overexpression and CRISPR/Cas9 technologies. *Plant Physiol Biochem* 196, 270–280. doi: 10.1016/j.plaphy.2023.01.048

Hasanuzzaman, M., Nahar, K., Alam, M. M., Roychowdhury, R., and Fujita, M. (2013). Physiological, biochemical, and molecular mechanisms of heat stress tolerance in plants. *Int. J. Mol. Sci.* 14, 9643–9684. doi: 10.3390/ijms14059643

Hastilestari, B. R., Lorenz, J., Reid, S., Hofmann, J., Pscheidt, D., Sonnewald, U., et al. (2018). Deciphering source and sink responses of potato plants (*Solanum tuberosum* L.) to elevated temperatures. *Plant Cell Environ.* 41, 2600–2616. doi: 10.1111/pce.13366

Heath, R. L., and Packer, L. (1968). Photoperoxidation in isolated chloroplasts: I. Kinetics and stoichiometry of fatty acid peroxidation. *Arch. Biochem. Biophys.* 125, 189–198. doi: 10.1016/0003-9861(68)90654-1

Hu, B., Jin, J., Guo, A. Y., Zhang, H., Luo, J., and Gao, G. (2015). GSDS 2.0: an upgraded gene feature visualization server. *Bioinformatics* 31, 1296–1297. doi: 10.1093/bioinformatics/btu817

Hu, L., Zhou, K., Li, Y., Chen, X., Liu, B., Li, C., et al. (2018). Exogenous Myo-inositol alleviates salinity-induced stress in Malus hupehensis Rehd. *Plant Physiol. Biochem.* 133, 116–126. doi: 10.1016/j.plaphy.2018.10.037

Huo, L., Guo, Z., Wang, P., Sun, X., Xu, K., and Ma, F. (2021). MdHARBI1, a MdATG8i-interacting protein, plays a positive role in plant thermotolerance. *Plant Sci.* 306, 110850. doi: 10.1016/j.plantsci.2021.110850

Huo, L., Sun, X., Guo, Z., Jia, X., Che, R., Sun, Y., et al. (2020). MdATG18a overexpression improves basal thermotolerance in transgenic apples by decreasing damage to chloroplasts. *Hortic. Res.* 7, 21. doi: 10.1038/s41438-020-0243-2

Jacob, A., Lancaster, J., Buhler, J., Harris, B., and Chamberlain, R. D. (2008). Mercury BLASTP: Accelerating protein sequence alignment. *ACM Trans. Reconfigurable Technol. Syst.* 1, 9. doi: 10.1145/1371579.1371581

Johnson, M., Zaretskaya, I., Raytselis, Y., Merezhuk, Y., McGinnis, S., and Madden, T. L. (2008). NCBI BLAST: a better web interface. *Nucleic Acids Res.* 36, W5–W9. doi: 10.1093/nar/gkn201

Krzywinski, M., Schein, J., Birol, I., Connors, J., Gascoyne, R., Horsman, D., et al. (2009). Circos: An information aesthetic for comparative genomics. *Genome Res.* 19, 1639–1645. doi: 10.1101/gr.092759.109

Kuzuoglu-Ozturk, D., Cebeci Yalcinkaya, O., Akpinar, B. A., Mitou, G., Korkmaz, G., Gozuacik, D., et al. (2012). Autophagy-related gene, *TdATG8*, in wild emmer wheat, plays a role in drought and osmotic stress response. *Planta* 236, 1081–1092. doi: 10.1007/s00425-012-1657-3

Kwon, S. I., Cho, H. J., Jung, J. H., Yoshimoto, K., Shirasu, K., and Park, O. K. (2010). The Rab GTPase RabG3b functions in autophagy and contributes to tracheary element differentiation in *Arabidopsis*. *Plant J.* 64, 151–164. doi: 10.1111/j.1365-313X.2010.04315.x

Lal, M. K., Tiwari, R. K., Kumar, A., Dey, A., Kumar, R., Kumar, D., et al. (2022). Mechanistic concept of physiological, biochemical, and molecular responses of the potato crop to heat and drought stress. *Plants* 11, 2857. doi: 10.3390/plants11212857

Lescot, M., Déhais, P., Thijs, G., Marchal, K., Moreau, Y., Van de Peer, Y., et al. (2002). PlantCARE, a database of plant cis-acting regulatory elements and a portal to tools for in silico analysis of promoter sequences. *Nucleic Acids Res.* 30, 325. doi: 10.1093/nar/30.1.325

Li, G., Cao, C., Yang, H., Wang, J., Wei, W., Zhu, D., et al. (2020). Molecular cloning and potential role of *DiSOC1s* in flowering regulation in *Davidia involucrata Baill Plant Physiol. Biochem.* 157, 453–459. doi: 10.1016/j.plaphy.2020.11.003

Li, H. (2000). "Determination of superoxide dismutase activity by the means of nitroblue tetrazolium," in *Principles and techniques of plant physiological biochemical experiments* (Higher Education Press, Beijing), 293. doi: 10.1006/bbrc.2000.2911

Li, J., Wang, Z., Qi, B., Zhang, J., and Yang, H. (2022a). MEMe: a mutually enhanced modeling method for efficient and effective human pose estimation. *Sensors (Basel).* 22, 632. doi: 10.3390/s22020632

Li, W. W., Ming, C., Li, Z., Jia-ming, L., Zhao-shi, X., Lian-cheng, L., et al. (2015). Overexpression of the autophagy-related gene SiATG8a from foxtail millet (*Setaria italica* L.) Confers tolerance to both nitrogen starvation and drought stress in *Arabidopsis. Biochem. Biophys. Res. Commun.* 468, 800–806. doi: 10.1016/j.bbrc.2015.11.035

Li, X., Liang, X., Li, W., Yao, A., Liu, W., Wang, Y., et al. (2022b). Isolation and functional analysis of *MbCBF2*, a Malus baccata (L.) Borkh CBF transcription factor gene, with functions in tolerance to cold and salt stress in transgenic *Arabidopsis thaliana. Intl. J. Mol. Sci.* 23, 9827. doi: 10.3390/ijms23179827

Livak, K. J., and Schmittgen, T. D. (2001). Analysis of relative gene expression data using real-time quantitative PCR and the $2^{-\Delta\Delta CT}$ method. *Methods* 25, 402–408. doi: 10.1006/meth.2001.1262

Lu, H., Klocko, A. L., Brunner, A. M., Ma, C., Magnuson, A. C., Howe, G. T., et al. (2019). RNA interference suppression of AGAMOUS and SEEDSTICK alters floral organ identity and impairs floral organ determinacy, ovule differentiation, and seed-hair development in Populus. *New Phytol.* 222, 923–937. doi: 10.1111/nph.15648

Luong, A. M., Koestel, J., Bhati, K. K., and Batoko, H. (2022). Cargo receptors and adaptors for selective autophagy in plant cells. *FEBS Lett.* 596, 2104–2132. doi: 10.1002/1873-3468.14412

Lutaladio, N., and Castaldi, L. (2009). Potato: The hidden treasure. *J. Food Compos. Anal.* 22, 491–493. doi: 10.1016/j.jfca.2009.05.002

Marchler-Bauer, A., Derbyshire, M. K., Gonzales, N. R., Lu, S., Chitsaz, F., Geer, L. Y., et al. (2014). CDD: NCBI's conserved domain database. *Nucleic Acids Res.* 43, D222–D226. doi: 10.1093/nar/gku1221

Marshall, R. S., and Vierstra, R. D. (2018). Autophagy: the master of bulk and selective recycling. *Annu. Rev. Plant Biol.* 69, 173–208. doi: 10.1146/annurev-arplant-042817-040606

Mathur, S., Agrawal, D., and Jajoo, A. (2014). Photosynthesis: response to high-temperature stress. *J. Photochem. Photobiol. B Biol.* 137, 116–126. doi: 10.1016/j.jphotobiol.2014.01.010

Muhammad, W. N., and Zoltan, T. (2022). Effect of drought stress on potato production: A review. *J. Agron.* 12, 635. doi: 10.3390/agronomy12030635

Pérez-Pérez, M. E., and Crespo, J. L. (2010). Autophagy in the model alga Chlamydomonas reinhardtii. *Autophagy* 6(4), 562–563. doi: 10.4161/auto.6.4.11822

Rehman, N. U., Zeng, P., Mo, Z., Guo, S., Liu, Y., Huang, Y., et al. (2021). Conserved and diversified mechanism of autophagy between plants and animals upon various stresses. *Antioxidants* 10, 1736. doi: 10.3390/antiox10111736

Rubio-Tomás, T., Sotiriou, A., and Tavernarakis, N. (2023). The interplay between selective types of (macro) autophagy: Mitophagy and xenophagy. *Int. Rev. Cell Mol. Biol.* 374, 129–157. doi: 10.1016/bs.ircmb.2022.10.003

Rudack, K., Seddig, S., Sprenger, H., Köhl, K., Uptmoor, R., and Ordon, F. (2017). Drought stress-induced changes in starch yield and physiological traits in potato. *J. Agron. Crop Sci.* 203, 494–505. doi: 10.1111/jac.12224

Schuck, S. (2020). Microautophagy–distinct molecular mechanisms that handle cargoes of many sizes. *J. Cell Sci.* 133, jcs246322. doi: 10.1242/jcs.246322

Siano, A. B., Roskruge, N., Kerckhoffs, H., and Sofkova-Bobcheva, S. (2024). Effects of abiotic stress associated with climate change on potato yield and tuber quality under a multi-environment trial in New Zealand. *Potato Res.*, 1–22. doi: 10.1007/s11540-024-09695-3

Singh, B., Kukreja, S., and Goutam, U. (2020). Impact of heat stress on potato (*Solanum tuberosum* L.): Present scenario and future opportunities. *J. Hortic. Sci. Biotech.* 95, 407–424. doi: 10.1080/14620316.2019.1700173

Sparkes, I. A., Runions, J., Kearns, A., and Hawes, C. (2006). Rapid, transient expression of fluorescent fusion proteins in tobacco plants and generation of stably transformed plants. *Nat. Prot.* 1, 2019–2025. doi: 10.1038/nprot.2006.286

Sun, X., Wang, P., Jia, X., Huo, L., Che, R., and Ma, F. (2018). Improvement of drought tolerance by overexpressing MdATG18a is mediated by a modified antioxidant system and activated autophagy in transgenic apples. *Plant Biotechnol. J.* 16, 545–557. doi: 10.1111/pbi.12794

Tang, J., and Bassham, C. D. (2022). Autophagy during drought: function, regulation, and potential application. *Plant J.* 109, 390–401. doi: 10.1111/tpj.15481

Tang, R., Niu, S., Zhang, G., Chen, G., Haroon, M., Yang, Q., et al. (2018). Physiological and growth responses of potato cultivars to heat stress. *Botany* 96, 897–912. doi: 10.1139/cjb-2018-0125

Wang, Y., Cai, S., Yin, L., Shi, K., Xia, X., Zhou, Y., et al. (2015). Tomato *HsfA1a* plays a critical role in plant drought tolerance by activating ATG genes and inducing autophagy. *Autophagy* 11, 2033–2047. doi: 10.1080/15548627.2015.1098798

Wang, Y., Tang, H., Debarry, J. D., Tan, X., Li, J., Wang, X., et al. (2012). MCScanX: a toolkit for detection and evolutionary analysis of gene synteny and collinearity. *Nucleic Acids Res.* 40, e49. doi: 10.1093/nar/gkr1293

Yang, X., Srivastava, R., Howell, S. H., and Bassham, D. C. (2016). Activation of autophagy by unfolded proteins during endoplasmic reticulum stress. *Plant J.* 85, 83–95. doi: 10.1111/tpj.13091

Yue, W., Nie, X., Cui, L., Zhi, Y., Zhang, T., Du, X., et al. (2018). Genome-wide sequence and expressional analysis of autophagy Gene family in bread wheat (*Triticum aestivum* L.). *J. Plant Physiol.* 229, 7–21. doi: 10.1016/j.jplph.2018.06.012

Zhang, S., Ye, H., Kong, L., Li, X., Chen, Y., Wang, S., et al. (2024). Multivariate analysis compares and evaluates heat tolerance of potato germplasm. *Plants* 13, 142. doi: 10.3390/plants13010142

Zheng, X., Li, M., Zhang, X., Chen, J., Ge, X., Li, S., et al. (2024). Unraveling the mechanism of potato (*Solanum tuberosum* L.) tuber sprouting using transcriptome and metabolome analyses. *Front. Plant Sci.* 14. doi: 10.3389/fpls.2023.1300067

Zhou, J., Wang, J., Cheng, Y., Chi, Y. J., Fan, B., Yu, J. Q., et al. (2013). NBR1-mediated selective autophagy targets insoluble ubiquitinated protein aggregates in plant stress responses. *PLoS Genet.* 9, e1003196. doi: 10.1371/journal.pgen.1003196

Zhou, J., Wang, J., Yu, J. Q., and Chen, Z. (2014). Role and regulation of autophagy in heat stress responses of tomato plants. *Front. Plant Sci.* 5. doi: 10.3389/fpls.2014.00174

Zhou, X. M., Zhao, P., Wang, W., Zou, J., Cheng, T. H., Peng, X. B., et al. (2015). A comprehensive, genome-wide analysis of autophagy-related genes identified in tobacco suggests a central role of autophagy in plant response to various environmental cues. *DNA Res.* 22, 245–257. doi: 10.1093/dnares/dsv012

Zhu, T., Zou, L., Li, Y., Yao, X., Xu, F., Deng, X., et al. (2018). Mitochondrial alternative oxidase-dependent autophagy involved in ethylene-mediated drought tolerance in *Solanum lycopersicum. Plant Biotechnol. J.* 16, 2063–2076. doi: 10.1111/pbi.12939

Frontiers in
Plant Science

Cultivates the science of plant biology and its applications

The most cited plant science journal, which advances our understanding of plant biology for sustainable food security, functional ecosystems and human health.

Discover the latest Research Topics

See more →

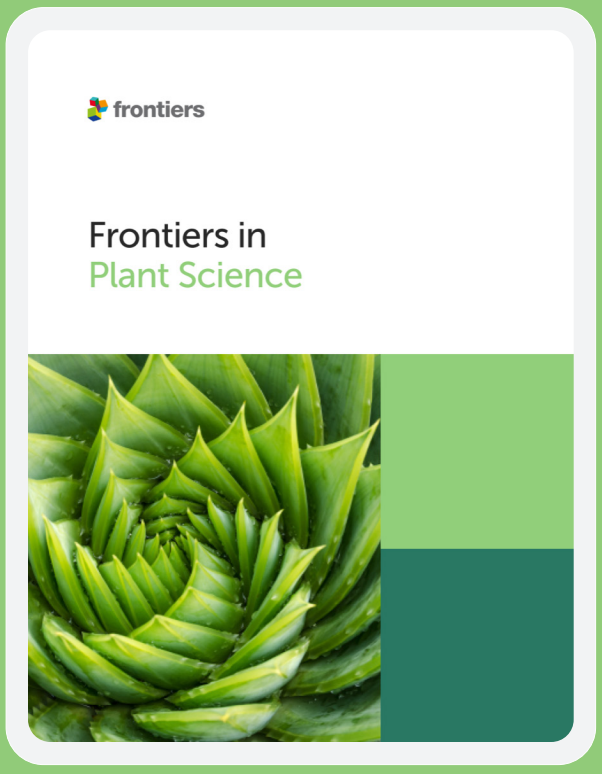

Frontiers

Avenue du Tribunal-Fédéral 34
1005 Lausanne, Switzerland
frontiersin.org

Contact us

+41 (0)21 510 17 00
frontiersin.org/about/contact